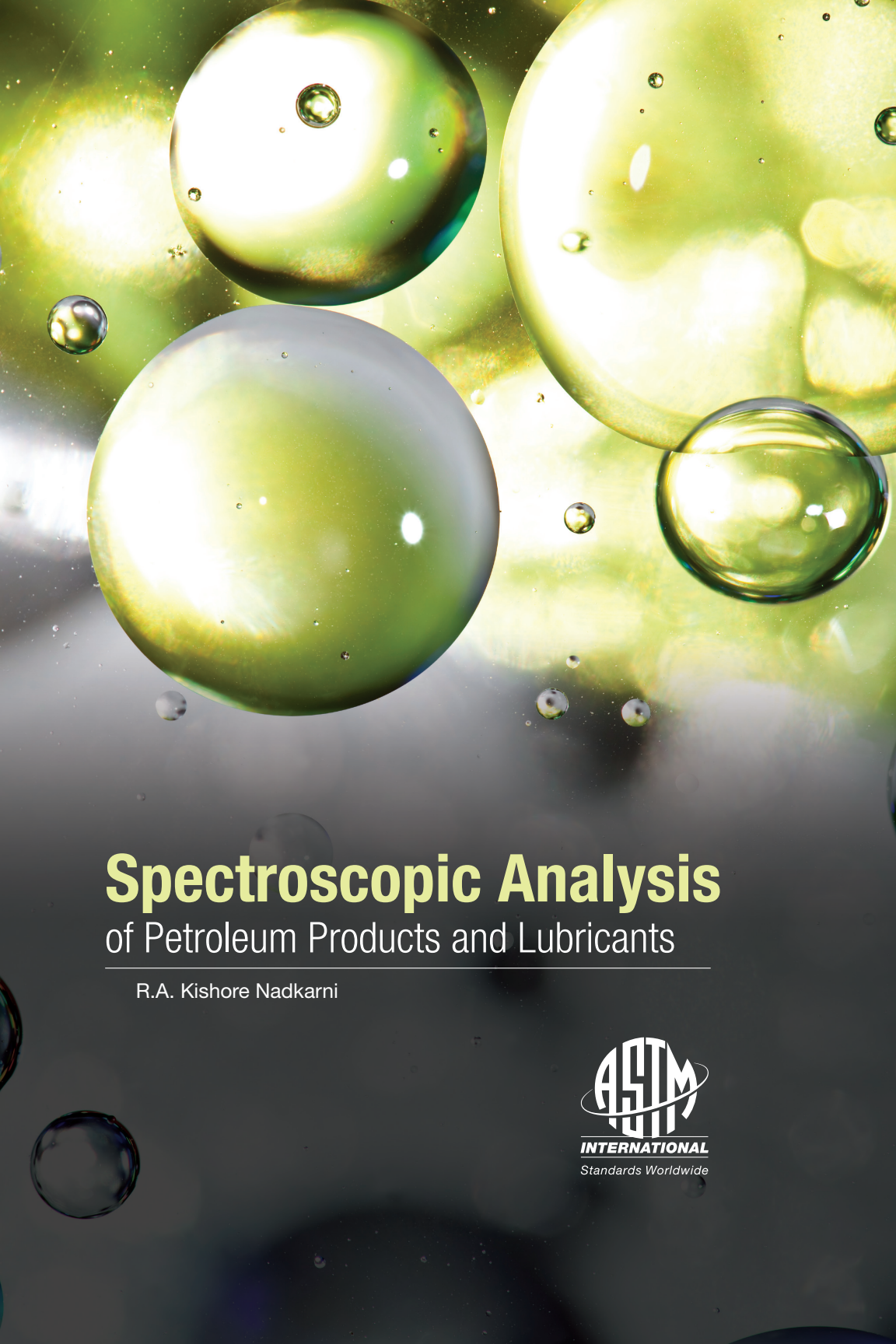

Spectroscopic Analysis

of Petroleum Products and Lubricants

R.A. Kishore Nadkarni

ASTM INTERNATIONAL
Standards Worldwide

Spectroscopic Analysis of Petroleum Products and Lubricants

R. A. Kishore Nadkarni

ASTM Stock Number: MONO9

ASTM International
100 Barr Harbor Drive
PO Box C700
West Conshohocken, PA 19428-2959

Printed in U.S.A.

Library of Congress Cataloging-in-Publication Data

Spectroscopic analysis of petroleum products and lubricants / R.A. Kishore Nadkarni.
p. cm.
"ASTM stock number: Mono 9."
Includes bibliographical references.
ISBN 978-0-8031-7020-9
1. Petroleum products—Analysis. 2. Lubricating oils—Analysis. 3. Spectrum analysis. 4. Petroleum—Spectra. I. Nadkarni, R. A.
TP691.S686 2011
665.5′38—dc23 2011012484

Printed in Bridgeport, NJ
August, 2011

Foreword

THIS PUBLICATION, ***Spectroscopic Analysis of Petroleum Products and Lubricants***, was sponsored by Committee D02 on Petroleum Products and Lubricants. The Editor is R. A. Kishore Nadkarni, Millennium Analytics, Inc., East Brunswick, NJ. This is Monograph 9 in ASTM's monograph series.

Contents

Part 1: Analytical Basics

1

Overview of Spectroscopic Analysis of Petroleum Products and Lubricants

R. A. Kishore Nadkarni[1]

FOR MORE THAN A CENTURY, ANALYTICAL CHEMISTRY HAS played a crucial role in the characterization of petroleum products and lubricants for their chemical and physical properties. Virtually all available well-known and many not-so-well-known analytical techniques have been used for this task. ASTM International Committee D02 on Petroleum Products and Lubricants has been a critical partner in standardizing such methodology, as evident from its compilation of nearly 600 analytical standards [1,2].

Although the analytical techniques may have been developed in universities and instrument vendors' laboratories, their applicability in the oil industry has progressed through the work done in the research and development laboratories of each of the large oil companies. There are some notable exceptions to this statement. Widely popular techniques and instruments such as apparent viscosity by cold cranking simulator (D5293) and by mini-rotary viscometer (D4684) were developed by Marvin Smith of Exxon Chemical Company in Linden, New Jersey; chemiluminiscent detection of nitrogen (D4629) and ultraviolet fluorescence (UV-Fl) detection for sulfur (D5453) were developed by Dr. Harry Druschel of Exxon Research and Development Laboratory in Baton Rouge, Louisiana; and ion chromatography by Drs. Hamish Small and colleagues of Dow Chemical Company in Midland, Michigan. All of these went on to become successful analytical instrumentation for companies such as Cannon, Antek, and Dionex, respectively.

Particularly in the elemental analysis area of petrochemicals, spectroscopy has played a crucial role, as evident from the proceedings of two ASTM symposiums in 1989 and 2004 [3,4]. The goal of publishing this monograph is to bring together the most widely used spectroscopic techniques used for analyzing petroleum products and lubricants. The words spectroscopy, spectrography, and spectrometry are sometimes used synonymously in the literature. The International Union of Pure and Applied Chemistry (IUPAC) defines spectrochemical analysis as a technique where wavelength is used to define a position within a spectrum to identify a specific element emitting light at that wavelength. If the emitted light is measured with the help of a photographic plate or a similar device, the technique is called spectrography. The term spectroscopy can be replaced by the more restrictive term spectrometry when intensities at one or more wavelengths are measured quantitatively with a spectrometer. Usually the measurements are taken with a photoelectric detector. Wavelength selection can be accomplished with a monochromator or an optical filter [5].

[1] *Millennium Analytics, Inc., East Brunswick, NJ*

A BRIEF HISTORY OF SPECTROSCOPY [6]

Spectroscopy can trace its beginnings to Sir Isaac Newton's observations of the prism spectrum of the sun, published in 1672. A Scottish scientist, Thomas Melville, reported in 1752 his observations on the spectra of mixtures of spirits with sea salts and the transition from bright yellow to the fainter color adjoining it when the flame contained salt. In 1800, astronomer F. W. Herschel discovered infrared radiation when he noted the differing sensations of heat while viewing the sun through combinations of colored glasses. A year later, J. W. Ritter revealed the presence of ultraviolet radiation.

A number of other workers over the years–Thomas Young in 1802, W. H. Wollaston in 1802, Josef Fraunhofer in 1817, and others–continued investigating the nature of light and attempting to isolate and identify the components of the spectrum. Perhaps the discovery of spectrochemical analysis can be attributed to the Scottish worker W. H. Fox Talbot, who from 1826 to 1834 observed flames colored by different salts using a crude but effective spectroscope. However, it was the work of Gustav Kirchoff (1859) and Robert Wilhelm Bunsen (1860) that gave one of the earliest examples of spectroscopic discoveries, which depended on the work in a completely different area. These two scientists formulated the laws of light absorption and emission in flames. Further advances included the work of A. J. Angstrom on improved diffraction gratings to measure wavelengths, and that of J. N. Lockyer and W. C. Roberts through observations of line lengths. However, after the early work of these scientists, little to no progress was made in using spectroscopy in practical chemical analysis. As late as 1910, H. Kayser stated, "There is little prospect that in the future qualitative analysis will apply spectroscopic methods to a large extent....I have come to the conclusion that quantitative spectroscopic analysis has shown itself to be impractical." In 1922, A. de Gramont wrote, "French chemists have an indolent dread of spectral analysis....has declared publicly that ever since Bunsen and Kirchoff, spectral analysis has been a deception and has made no progress from a practical point of view."

It was not until the 1950s that the spectroscopic technique which was to revolutionize metal analysis was promoted by an Australian, Sir Alan Walsh. Atomic absorption spectrophotometry (AAS), as it was called, did not have a smooth passage either. Walsh had to evangelize the technique by extensive traveling and lecturing in the United States, United Kingdom, South Africa, New Zealand, and Australia. Eventually, the simplicity of the technique and its revolutionary impact on classical analysis were recognized, making AAS a primary spectroscopic technique for metal analysis at one time. The rest is history!

Diverse techniques such as AAS, atomic fluorescence spectrometry (AFS), graphite furnace AAS (GF-AAS), cold vapor AAS (CV-AAS), ion chromatography (IC), inductively coupled plasma–atomic emission spectrometry (ICP-AES), gas chromatography (GC), liquid chromatography (LC), GC-mass spectrometry (MS), ICP-MS, isotope dilution MS (ID-MS), neutron activation analysis (NAA), nuclear magnetic resonance (NMR), and X-ray fluorescence (XRF), both wavelength-dispersive and energy-dispersive techniques, are discussed in this monograph as pertaining to their applications in the oil industry. Within the confines of the IUPAC definition of spectroscopic methods of analysis, it may be questioned why gas chromatographic methods are included in this book. Our rationale is that although chromatographic techniques are used for the separation of molecular

species, the ultimate identification and quantitation of the molecular composition is done by using spectroscopic measurement devices such as flame ionization detector (FID) and MS. Hence, it is important that the gas chromatographic techniques be included in this monograph along with other techniques generally considered "spectroscopic."

Thus, the goal of this monograph is to consolidate, in one volume, methodology that involves spectroscopic measurements as a primary or a final measurement tool. All the techniques described in this monograph fit this description.

Each topic is written by an author or authors who are acknowledged experts in their fields. Each chapter contains detailed discussion of the technical principles involved as well as the practical applications of these techniques to characterize petroleum products and lubricants.

The book is divided into three logical parts. Part A describes some of the fundamental considerations in spectroscopic analysis, such as calibration protocols, quality assurance and statistics, proficiency testing, and standard reference materials. Part B describes the analytical methodology of individual analytical techniques and the examples of their applications in the oil industry—AAS, GF-AAS, ICP-AES, ICP-MS, ID-MS, AFS, MS, WD-XRF, ED-XRF, MWD-XRF, NAA, NMR, NIR, FT-IR, IC, and GC-LC-AED. Part C describes special topics in spectroscopic analysis, such as the determination of sulfur and mercury and analysis of used oils, crude oil, and biofuels.

Chapter 2, written by Dr. Kishore Nadkarni (Millennium Analytics, Inc.), discusses the calibration protocols used for spectroscopic measurements of petroleum products. Calibration is a fundamental and usually the first step to be taken in any analysis. Calibration techniques for different analytical techniques such as AAS, ICP-AES, ICP-MS, GC, GC-MS, NAA, NMR, and XRF are described. Preparation and use of calibration standards in this context are discussed.

Chapter 3, written by Kishore Nadkarni, addresses the scope and application of quality assurance concepts in analysis of petroleum products and lubricants. This chapter includes various statistical protocols for qualifying the validity of data produced, statistical quality control, control charts, laboratory capability reviews, checklist for investigating the root causes of inconsistent results, use of standard reference materials, proficiency testing programs, representative sampling, rounding off test results, statistical tests for identifying data outliers, tests for demonstrating equivalency in precision and accuracy of different test methods to determine the same parameter, acceptability of intralaboratory and interlaboratory results of analysis of the same material, and rules for reducing testing frequency. Quality assurance instructions embedded in many individual spectroscopic test methods are also reviewed. Finally, an example is given of multielement spectroscopic analysis of the National Institute of Standards and Technology (NIST) lubricating oil Standard Reference Material (SRM), which was analyzed three different times in a company laboratory circuit—as a company product, as an ASTM ILCP sample, and as a NIST SRM. Excellent agreement between multiple sets of analysis testifies to the efficacy of good quality management and good laboratory practices, resulting in superior data quality in terms of precision and accuracy. Thus, quality assurance is a vital area in ensuring the correct preparation of products and delivery to meet customer product quality expectations.

Chapter 4, written by Dr. Jim Bover of ExxonMobil Biomedical Sciences, Inc., describes the proficiency testing services offered by ASTM International and how to interpret the statistical reports resulting from these interlaboratory cross-checks. This chapter discusses the techniques and approaches available to laboratories for evaluating their results relative to those of other laboratories participating in the testing program. It also discusses techniques for evaluating the performance of the test methods used across the participating laboratories. A number of examples from actual proficiency programs are included to illustrate how these techniques can be used.

Discussion of reference materials for calibration and quality assurance is the subject of **Chapter 5,** written by Kishore Nadkarni. Two examples are given of the development of an SRM by NIST for lubricating oil and by an oil company for a lubricant additive package. This is an important area in assuring the customers that the quality of data produced in the laboratory is reliable, accurate, and precise.

Chapter 6, written by Kishore Nadkarni, covers AAS as used in oil industry laboratories. AAS was perhaps the first widely used instrumental elemental analysis technique that made old-fashioned classical "wet" analysis obsolete throughout the industry. Until ICP-AES overtook it, there probably was no laboratory in the world that did not use an AAS instrument for determining metallic constituents in petroleum products and lubricants. Even today, despite the versatility of the ICP-AES technique, AAS is still widely used in smaller laboratories throughout the world because of its lower cost and ease of operation compared to ICP-AES, particularly in the less developed countries.

Offshoots of the original AAS technique include GF-AAS and CV-AAS. GF-AAS rivals ICP-AES in its sensitivity of detection; CV-AAS is useful for specific elements such as selenium, mercury, and arsenic, which are not usually easily determined by ICP-AES. In recent years, CV-AAS has received increased attention as a method of choice for ultra-trace determination of mercury in crude oils.

Dr. Paolo Tittarelli of SSC, Milan, Italy, describes the details of the GF-AAS technique and its applications in the oil industry in **Chapter 7.**

Standard test methods issued by ASTM D02 using AAS are listed in Table 1.

Chapter 8, by Dr. Bob Botto of ExxonMobil Refining and Supply Company in Baytown, Texas, describes ICP-AES and its use for elemental analysis in the oil industry. As noted previously, ICP-AES is a widely used popular spectroscopic technique for multielement analysis of many complex matrices. Samples generally have to be solubilized to be able to nebulize them into the argon plasma. However, normally that should not be a problem for most of the petroleum products or lubricants. A number of standard test methods have been issued by ASTM Committee D02 in this area (Table 2).

The analogous technique of ICP-MS is described in **Chapter 9** by Dr. David Hwang of Chevron Energy Technology Company, Richmond, California. ICP-MS extends the limits of detection of ICP-AES by a magnitude or more, and is also capable of speciation, which is important to distinguish between species such as those of selenium or mercury [7]. Given that ICP-MS is more of a research tool than a standardized method, ASTM has as yet not issued any standard for this technique for use in the oil industry.

TABLE 1—Analysis of Petroleum Products Using AAS	
ASTM Test Method Designation	**Analysis**
D3237	Lead in Gasoline by AAS
D3605	Trace Metals in Gas Turbine Fuels by AAS and FES
D3831	Manganese in Gasoline by AAS
D4628	Analysis of Ba, Ca, Mg, and Zn in Unused Lubricating Oils by AAS
D5056	Trace Metals in Petroleum Coke by AAS
D5184	Al and Si in Fuel Oils by Ashing, Fusion, ICP-AES, and AAS
D5863	Ni, V, Fe, and Na in Crude Oils and Residual Fuels by Flame AAS
D6732	Copper in Jet Fuels by Graphite Furnace AAS
D7622	Mercury in Crude Oil Using Combustion and Direct Cold Vapor Atomic Absorption Method with Zeeman Background Correction
D7623	Mercury in Crude Oil Using Combustion-Gold Amalgamation and Cold Vapor Atomic Absorption Method

TABLE 2—Analysis of Petroleum Products Using ICP-AES	
ASTM Test Method Designation	**Analysis**
D4951	Additive Elements in Lubricating Oils by ICP-AES
D5184	Al and Si in Fuel Oils by Ashing, Fusion, ICP-AES and AAS
D5185	Additive Elements, Wear Metals, and Contaminants in Used Lubricating Oils and Selected Elements in Base Oils by ICP-AES
D5600	Trace Elements in Petroleum Coke by ICP-AES
D5708	Ni, V, and Fe in Crude Oils and Residual Fuels by ICP-AES
D6595	Wear Metals and Contaminants in Used Lubricating Oils or Used Hydraulic Fluids by Rotating Disc Electrode AES
D6728	Contaminants in Gas Turbine and Diesel Engine Fuel by Rotating Disk Electrode AES
D7040	Low Levels of Phosphorus in ILSAC GF 4 and Similar Grade Engine Oils by ICP-AES
D7111	Trace Elements in Middle Distillate Fuels by ICP-AES
D7260	Optimization, Calibration, and Validation of ICP-AES for Elemental Analysis of Petroleum Products and Lubricants
D7303	Metals in Lubricating Greases by ICP-AES
D7691	Metals in Crude Oils by ICP-AES

Dr. Peter Stockwell describes the theory and applications of AFS in **Chapter 10.** Mercury and arsenic are determined in the petrochemical industry using this sensitive technique.

Chapter 11 describes the use of MS for determining organic species in petroleum products. This chapter is written by Drs. Todd Colin of Colin Consulting and Aaron Mendez of Petroleum Analyzer Company (PAC) in Houston, Texas. MS is a routine tool for chemical characterization in the research and development laboratories of all oil companies and universities. Although a highly specialized technique mainly used in research and development, a few standards have been written by ASTM Committee D02 in this area (Table 3).

Similar to AAS and ICP-AES techniques, another work-horse for elemental analysis of petroleum products and lubricants is XRF spectrometry. Wavelength, energy, and a new variation, monochromatic wavelength, dispersive XRF are described in **Chapter 12,** by Bruno Vrebos and Tim Glose of PANanalytical Instruments in Almelo, The Netherlands, and Westborough, Massachusetts, respectively; **Chapter 13,** by Dr. Mike Pohl of Horiba Instruments of Irvine, California, and Christelle Petiot of Oxford Instruments, Oxford, England; and **Chapter 14** by Drs. Zewu Chen and Fuzhong Wei of XOS, Albany, New York. All three techniques are particularly useful for determining sulfur in today's fuels, which cannot be easily done using AAS or ICP-AES. Particularly, with the regulation of sulfur content in gasolines and diesels by government regulatory agencies, XRF techniques have proved particularly useful. However, matrix interferences in oxygenated fuels need to be compensated for before sulfur in the samples can be accurately determined. A number of standard test methods for XRF use have been issued by ASTM Committee D02 (Table 4).

NAA is another highly sensitive method, described in **Chapter 15** by Kishore Nadkarni. For determining many metals and nonmetals in a variety of products, this technique is unrivalled in its sensitivity and its freedom from interferences. However, its use in the oil industry remains limited because of the need to have access to a nuclear reactor or another source of radiation for irradiating the samples. Determining oxygen in petroleum products is a particularly unique analysis that can only be done by NAA.

TABLE 3—Analysis of Petroleum Products Using MS

ASTM Test Method Designation	Analysis
D2425	Hydrocarbon Types in Middle Distillates by Mass Spectrometry
D2650	Chemical Composition of Gases by Mass Spectrometry
D2786	Hydrocarbon Types Analysis of Gas-Oil Saturates by High Ionizing Voltage Mass Spectrometry
D2789	Hydrocarbon Types in Low Olefinic Gasoline by Mass Spectrometry
D5769	Benzene, Toluene, and Total Aromatics in Finished Gasolines by GC/MS

TABLE 4—Analysis of Petroleum Products Using XRF	
ASTM Test Method Designation	**Analysis**
D2622	Sulfur in Petroleum Products by WD-XRF Spectrometry
D4294	Sulfur in Petroleum and Petroleum Products by ED-XRF Spectrometry
D4927	Elemental Analysis of Lubricant and Additive Components – Ba, Ca, P, S, and Zn by WD-XRF Spectroscopy
D5059	Lead in Gasoline by X-ray Spectroscopy
D6334	Sulfur in Gasoline by WD-XRF
D6376	Trace Elements in Petroleum Coke by WD-XRF Spectroscopy
D6443	Ca, Cl, Cu, Mg, P, S, and Zn in Unused Lubricating Oils and Additives by WD-XRF Spectrometry (Mathematical Correction Procedure)
D6445	Sulfur in Gasoline by ED-XRF Spectrometry
D6481	P, S, Ca, and Zn in Lubricating Oils by ED-XRF Spectroscopy
D7039	Sulfur in Gasoline and Diesel Fuel by Monochromatic WD-XRF Spectrometry
D7212	Low Sulfur Automotive Fuels by EDXRF Spectrometry using a Low-Background Proportional Counter
D7220	Sulfur in Automotive Fuels by Polarization XRF Spectrometry
D7343	Optimization, Sample Handling, Calibration, and Validation of XRF Spectrometry Methods for Elemental Analysis of Petroleum Products and Lubricants

The theory of NMR and its application in the petroleum industry are the subject of **Chapter 16,** written by Dr. John Edwards of Process NMR Associates in Danbury, Connecticut. Usually, this technique is more appropriate for research and development activities rather than for routine testing. However, there are a few standards issued by ASTM D02 Committee using NMR for the analysis of gasoline and aviation fuels. The chapter includes an extensive bibliography and gives examples of various types of NMR instrumentation for applications in the petroleum industry (Table 5).

Fourier transform–infrared (FT-IR) spectroscopy is another technique widely used in the industry for the detection or determination of organic species. This technique is discussed in **Chapter 17** by Dr. Jim Brown of ExxonMobil Research and Engineering Company of Clinton, New Jersey. FT-IR can also be used for "finger-printing" of organic species in samples to trace the provenance of the products. Five standards have been issued by ASTM Committee D02 in using FT-IR in petroleum analysis. Additionally, there are several standards where IR is used as a detection device for quantitation (Table 6).

TABLE 5—Analysis of Petroleum Products Using NMR	
ASTM Test Method Designation	**Analysis**
D3701	Hydrogen Content of Aviation Turbine Fuels by Low Resolution NMR Spectrometry
D4808	Hydrogen Content of Light Distillates, Middle Distillates, Gas Oils, and Residua by Low-Resolution NMR Spectroscopy
D5292	Aromatic Carbon Contents of Hydrocarbon Oils by High Resolution NMR Spectroscopy
D7171	Hydrogen Content of Middle Distillate Petroleum Products by Low-Resolution Pulsed Nuclear Magnetic Resonance Spectroscopy

Chapter 18, written by Kirk Chassional of Dionex Corp. in Sunnyvale, California, discusses the concept and use of IC. The development of this technique was revolutionary, changing the protocol for determining anions in samples [8]. Compared to the laborious wet chemistry methods of gravimetry, titrimetry, or colorimetry, and separations, with IC a number of common anions such as halides, nitrate, and sulfate could be simultaneously determined in less than 10 minutes. The effect of IC in the quantitative determination of anions was analogous to the effect of AAS in the determination of metallic constituents in the industrial samples. An entire analytical instrumentation industry (principal among the companies is Dionex) rose out of this invention. Two standards have recently been issued by ASTM D02 Committee for using IC in the petrochemical laboratories:

D7319	Total and Potential Sulfate and Inorganic Chloride in Fuel Ethanol by Direct Injection Suppressed Ion Chromatography
D7328	Total and Potential Inorganic Sulfate and Total Inorganic Chloride in Fuel Ethanol by Ion Chromatography Using Aqueous Sample Injection

Chapter 19, written by Dr. Frank Di Sanzo of ExxonMobil Research and Engineering Company of Clinton, New Jersey, discusses chromatographic techniques. Of the various chromatographic techniques, GC and GC-MS remain the most commonly used organic analysis techniques in the industry, whether pharmaceutical or petrochemical. The importance of chromatographic techniques can be judged by the fact that nearly 50 standard test methods have been issued by ASTM Committee D02 (Table 7).

There are also a few LC standards that have been issued by ASTM Committee D02 (Table 8).

Chapter 20 on the determination of sulfur, written by Kishore Nadkarni, covers the unique challenge in the petroleum industry for the determination of this important element and pollutant governed by regulatory agencies. Several spectroscopic methods are available for determining sulfur in gasoline and

TABLE 6—Analysis of Petroleum Products Using Infrared Spectroscopy

ASTM Test Method Designation	Analysis
D4053	Benzene in Motor and Aviation Gasoline by IR
D5845	MTBE, ETBE, TAME, DIPE, Methanol, Ethanol, and tert-Butanol in Gasoline by IR
D6122	Practice for the Validation of the Performance of Multivariate Process IR Spectrophotometers
D6277	Benzene in Spark Ignition Engine Fuels Using Mid-IR Spectroscopy
D7214	Oxidation of Used Lubricants by FT-IR Using Peak Area Increase Calculation
D7371	Biodiesel FAME Content in Diesel Fuel Oil Using mid-IR (FT-IR – ATR – PLS Method)
D7412	Condition Monitoring of Phosphate Antiwear Additives in In-Service Petroleum and Hydrocarbon Based Lubricants by Trend Analysis Using FT-IR
D7414	Condition Monitoring of Oxidation in In-Service Petroleum and Hydrocarbon Based Lubricants by Trend Analysis Using FT-IR
D7415	Condition Monitoring of Sulfate Byproducts in In-Service Petroleum and Hydrocarbon Based Lubricants by Trend Analysis Using FT-IR
D7418	Practice for Set-Up and Operation of Fourier Transform Infrared Spectrometers for In-Service Oil Condition Monitoring
E2412	Practice for Condition Monitoring of In-Service Lubricants by Trend Analysis Using FT-IR Spectrometry

diesel issued by ASTM Committee D02 [9] (Table 9). Most prominent among these are D2622 WD-XRF, D4294 ED-XRF, D5453 UV-Fl, and D7039 MWD-XRF. Several of the newly issued methods are not yet in wide use in the industry. More test methods are being written by specialized vendors of such instrumentations.

Other nonspectroscopic methods for sulfur determination are also available, but except for a very few, their use is declining (Table 10).

Chapter 21 discusses the test methods for determining trace amounts of mercury in crude oils in particular. This chapter, written by Kishore Nadkarni, also discusses current concerns about mercury emissions from the use of fossil fuels, both coal and crude oil. This emitted mercury during coal combustion or crude oil processing or both is harmful to both humans and aquatic organisms. Test methods to quantify mercury in such materials involve atomic

TABLE 7—Analysis of Petroleum Products Using GC	
ASTM Test Method Designation	**Analysis**
D1319	Hydrocarbon Types in Liquid Petroleum Products by Fluorescent Indicator Adsorption
D2007	Characteristic Groups in Rubber Extender and Processing Oils and Other Petroleum-Derived Oils by the Clay-Gel Absorption Chromatography
D2268	Analysis of High Purity n-Heptane and iso-Octane by Capillary GC
D2426	Butadiene Dimer and Styrene in Butadiene Concentrates by GC
D2427	C_2 through C_5 Hydrocarbons in Gasolines by GC
D2504	Noncondensable Gases in C_2 and Lighter Hydrocarbon Products by GC
D2505	Ethylene, Other Hydrocarbons, and Carbon Dioxide in High-Purity Ethylene by GC
D2549	Separation of Representative Aromatics and Nonaromatics Fractions of High-Boiling Oils by Elution Chromatography
D2593	Butadiene Purity and Hydrocarbon Impurities by GC
D2597	Analysis of Demethanized Hydrocarbon Liquid Mixtures Containing Nitrogen and Carbon Dioxide by GC
D2712	Hydrocarbon Traces in Propylene Concentrates by GC
D2887	Boiling Range Distribution of Petroleum Fractions by GC
D3524	Diesel Fuel Dilution in Used Diesel Engine Oils by GC
D3525	Gasoline Diluent in Used Gasoline Engines by GC
D3606	Benzene and Toluene in Finished Motor and Aviation Gasoline by GC
D3710	Boiling Range Distribution of Gasoline and Gasoline Fractions by GC
D4424	Butylene Analysis by GC
D4626	Practice for Calculation of GC Response Factors
D4815	MTBE, ETBE, TAME, DIPE, tertiary-Amyl Alcohol and C_1 through C_4 Alcohols in Gasoline by GC
D4864	Traces of Methanol in Propylene Concentrates by GC
D5134	Detailed Analysis of Petroleum Naphthas through an n-Nonane by Capillary GC
D5303	Trace Carbonyl Sulfide in Propylene by GC
D5307	Boiling Range Distribution of Crude Petroleum by GC
D5441	Analysis of MTBE by GC
D5442	Analysis of Petroleum Waxes by GC

TABLE 7—Analysis of Petroleum Products Using GC (Continued)	
ASTM Test Method Designation	**Analysis**
D5443	Paraffin, Naphthene, and Aromatic Hydrocarbon Type Analysis in Petroleum Distillates Through 200°C by Multi-Dimensional GC
D5501	Ethanol Content of Denatured Fuel Ethanol by GC
D5580	Benzene, Toluene, Ethylbenzene, p/m-Xylene, 0-Xylene, C_9 and Heavier Aromatics, and Total Aromatics in Finished Gasoline by GC
D5599	Oxygenates in Gasoline by GC and Oxygen Selective Flame Ionization Detection
D5623	Sulfur Compounds in Light Petroleum Liquids by GC and Sulfur Selective Detection
D5986	Oxygenates, Benzene, Toluene, C_8-C_{12} Aromatics and Total Aromatics in Finished Gasoline by GC/FT-IR
D6159	Hydrocarbon Impurities in Ethylene by GC
D6160	PCBs in Waste Materials by GC
D6293	Oxygenates and Paraffin, Olefin, Naphthene, Aromatic (O-PONA) Hydrocarbon Types in Low-Olefin Spark Ignition Engine Fuels by GC
D6296	Total Olefins in Spark Ignition Engine Fuels by Multi-Dimensional GC
D6352	Boiling Range Distribution of Petroleum Distillates in Boiling Range from 174 to 700°C by GC
D6417	Estimation of Engine Oil Volatility by Capillary GC
D6584	Free and Total Glycerin in B-100 Biodiesel Methyl Esters by GC
D6729	Individual Components in Spark Ignition Engine Fuels by 100 Metre Capillary High Resolution GC
D6730	Individual Components in Spark Ignition Engine Fuels by 100 Metre Capillary (with Precolumn) High Resolution GC
D6733	Individual Components in Spark Ignition Engine Fuels by 50-Metre Capillary High Resolution GC
D6839	Hydrocarbon Types, Oxygenated Compounds and Benzene in Spark Ignition Engine Fuels by GC
D7041	Total Sulfur in Light Hydrocarbons, Motor Fuels, and Oils by Online GC with Flame Photometric Detection
D7059	Methanol in Crude Oils by Multidimensional GC
D7096	Boiling Range Distribution of Gasoline by Wide Bore Capillary GC
D7169	Boiling Point Distribution of Samples with Residues such as Crude Oils and Atmospheric and Vacuum Residues by High Temperature GC

(*Continued*)

TABLE 7—Analysis of Petroleum Products Using GC (Continued)	
ASTM Test Method Designation	**Analysis**
D7213	Boiling Range Distribution of Petroleum Distillates in the Boiling Range from 100 to 615°C by GC
D7398	Boiling Range Distribution of FAME in the Boiling Range from 100 to 615°C by Gas Chromatography
D7423	Oxygenates in C_2 through C_5 Hydrocarbons by GC-FID
D7500	Boiling Range Distribution of Distillates and Lubricating Base Oils in Boiling Range from 100 to 735°C by GC

spectroscopic analysis, both AAS and AFS, with a prior step of gold amalgamation to isolate the trace amounts of mercury present in coal or crude oil. Two test methods using gold amalgamation followed by AAS based on commercially available instruments have been issued: D7622 and D7623.

Chapter 22 describes the analysis of used oils using various spectrometric techniques. Although precise results may not be required, it is important to assess the changes in residual oils in engine blocks by analyzing used oils. Generally, this is called "trend analysis" and comprises metal analysis by ICP-AES, base number by potentiometric titration, water by Karl Fischer titration, and FT-IR analysis for oxidation, sulfonation, nitration, and so on. This chapter, written by Kishore Nadkarni, covers some ASTM standards used for this analysis (Table 11).

Analysis of crude oils by spectroscopic techniques is described by Kishore Nadkarni in **Chapter 23**. Applications of AAS, ICP-AES, GF-AAS, ICP-MS, and XRF are described. A useful addition to the literature is the recent monograph on crude oils by Giles and Mills [10].

TABLE 8—Analysis of Petroleum Products Using LC	
ASTM Test Method Designation	**Analysis**
D3712	Analysis of Oil-Soluble Petroleum Sulfonates by Liquid Chromatography
D5186	Aromatic Content and PNA Content of Diesel Fuels and Aviation Turbine Fuels by SFC
D6379	Aromatic Hydrocarbon Types in Aviation Fuels and Petroleum Distillates – HPLC Method with RI Detection
D6550	Olefin Content of Gasolines by SFC
D6591	Aromatic Hydrocarbon Types in Middle Distillates – HPLC Method with RI Detection
D7347	Olefin Content of Denatured Ethanol by SFC
D7419	Total Aromatics and Total Saturates in Lube Basestocks by HPLC with Refractive Index Detection

TABLE 9—Determination of Sulfur in Petroleum Products Using Spectroscopic Techniques

ASTM Test Method Designation	Technique Used	Analysis
D2622	WD-XRF	Sulfur in Petroleum Products by WD-XRF Spectrometry
D4294	ED-XRF	Sulfur in Petroleum and Petroleum Products by ED-XRF Spectrometry
D4927	WD-XRF	Elemental Analysis of Lubricants and Additive Components – Ba, Ca, P, S, and Zn by WD-XRF Spectroscopy
D4951	ICP-AES	Additive Elements in Lubricating Oils by ICP-AES
D5185	ICP-AES	Additive Elements, Wear Metals, and Contaminants in Used Lubricating Oils and Selected Elements in Base Oils by ICP-AES
D5453	UV-Fl	Total Sulfur in Light Hydrocarbons, Spark Ignition Engine Fuel, Diesel Engine Fuel, and Engine Oil by UV-Fluorescence
D5623	GC	Sulfur Compounds in Light Petroleum Liquids by GC and Sulfur Selective Detection
D6334	WD-XRF	Sulfur in Gasoline by WD-XRF
D6376	WD-XRF	Trace Metals in Petroleum Coke by WD-XRF Spectroscopy
D6443	WD-XRF	Ca, Cl, Cu, Mg. P, S, and Zn in Unused Lubricating Oils and Additives by WD-XRF Spectrometry (Mathematical Correction Procedure)
D6445	ED-XRF	Sulfur in Gasoline by ED-XRF Spectrometry
D6481	ED-XRF	P, S, Ca, and Zn in Lubricating Oils by ED-XRF Spectroscopy
D6667	UV-Fl	Total Volatile Sulfur in Gaseous Hydrocarbons and Liquefied Petroleum Gases by UV Fluorescence
D7039	MWD-XRF	Sulfur in Gasoline and Diesel Fuel by Monochromatic WD-XRF Spectrometry
D7041	GC-FID	Total Sulfur in Light Hydrocarbons, Motor Fuels and Oils by Online GC with Flame Photometric Detection

(*Continued*)

TABLE 9—Determination of Sulfur in Petroleum Products Using Spectroscopic Techniques (Continued)

ASTM Test Method Designation	Technique Used	Analysis
D7212	ED-XRF	Low Sulfur in Automotive Fuels by ED-XRF Spectrometry Using a Low-Background Proportional Counter
D7220	ED-XRF	Sulfur in Automotive Fuels by Polarization XRF Spectrometry
D7343	XRF	Practice for Optimization, Sample Handling, Calibration, and Validation of XRF Spectrometry Methods for Elemental Analysis of Petroleum Products and Lubricants

TABLE 10—Determination of Sulfur in Petroleum Products Using Nonspectroscopic Techniques

ASTM Test Method Designation	Technique Used	Analysis
D129	Gravimetry	Sulfur in Petroleum Products (General Bomb Method)
D1266	Gravimetry	Sulfur in Petroleum Products (Lamp Method)
D1552	IR	Sulfur in Petroleum Products (High Temperature Method)
D2784	Titrimetry	Sulfur in LPG (Oxy-Hydrogen Burner or Lamp)
D3120	Microcoulometry	Trace Quantities of Sulfur in Light Liquid Petroleum Hydrocarbons by Oxidative Microcoulometry
D3227	Potentiometry	(Thiol Mercaptan) Sulfur in Gasoline, Kerosine, Aviation Turbine, and Distillate Fuels (Potentiometric Method)
D3246	Microcoulometry	Sulfur in Petroleum Gas by Oxidative Microcoulometry
D4045	Colorimetry	Sulfur in Petroleum Products by Hydrogeneolysis and Rateometric Colorimetry
D4952	Colorimetry	Qualitative Analysis for Active Sulfur Species in Fuels and Solvents (Doctor Test)
D6920	Electrochemistry	Total Sulfur in Naphthas, Distillates, RFG, Diesels, Biodiesels, and Motor Fuels by Oxidative Combustion and Electrochemical Detection

TABLE 11—Analysis of Used Oils Using Spectroscopic Techniques

ASTM Test Method Designation	Technique Used	Analysis
D5185	ICP-AES	Additive Elements, Wear Metals, and Contaminants in Used Lubricating Oils and Selected Elements in Base Oils by ICP-AES
D5384	Colorimetry	Chlorine in Used Petroleum Products (Field Test Kit method)
D6595	AES	Wear Metals and Contaminants in Used Lubricating Oils or Used Hydraulic Fluids by Rotating Disc Electrode AES
D7214	FT-IR	Oxidation of Used Lubricants by FT-IR Using Peak Area Increase Calculation
D7412	FT-IR	Condition Monitoring of Phosphate Antiwear Additives in In-Service Petroleum and Hydrocarbon Based Lubricants by Trend Analysis Using FT-IR
D7414	FT-IR	Condition Monitoring of Oxidation in In-Service Petroleum and Hydrocarbon Based Lubricants by Trend Analysis Using FT-IR
D7415	FT-IR	Condition Monitoring of Sulfate Byproducts in In-Service Petroleum and Hydrocarbon Based Lubricants by Trend Analysis Using FT-IR
D7416	Multi-part	Analysis of In-Service Lubricants Using a Particular Five Part Integrator
D7418	FT-IR	Practice for Set-Up and Operation of FT-IR Spectrometers for In-Service Oil Condition Monitoring

Given the recent surge in interest in biofuels, spectroscopic methods applied for their analysis are discussed in **Chapter 24** by Kishore Nadkarni. The field is at early stage, and research and development efforts are under way to standardize the appropriate test methods. A number of specifications for biofuel products contain several spectroscopic tests, but no information is currently available regarding their applicability or precision for biofuels (Table 12).

These test methods originally developed for petroleum products are being adapted for biofuels. Some of these test methods do not show the same precision estimates as those seen in the petroleum product analysis. The situation is gradually being corrected through interlaboratory studies for these new matrices. X-ray methods used for sulfur determination in biofuels may also suffer from interference caused by the presence of large amounts of oxygenates in

TABLE 12—Biofuel Specifications	
ASTM Standard	**Specification for**
D396	Fuel Oils
D975	Diesel Fuel Oils
D4806	Denatured Fuel Ethanol for Blending with Gasolines for Use as Automotive Spark-Ignition Engine Fuel
D4814	Automotive Spark-Ignition Engine Fuel
D5798	Fuel Ethanol (Ed75-Ed85) for Automotive Spark-Ignition Engines
D6751	Biodiesel Fuel Blend Stock (B 100) for Middle Distillate Fuels
D7467	Diesel Fuel Oil, Biodiesel Blend (B6 to B20)
D7544	Pyrolysis Liquid Biofuel
D7566	Aviation Turbine Fuel Containing Synthesized Hydrocarbons

TABLE 13—Research Reports of Spectroscopic Methods of Analysis of Petroleum Products			
Test Method	**Analysis**	**Spectroscopic Technique**	**ASTM Research Report Number**
D1319	Hydrocarbon Types in Liquid Petroleum Products	GC	1361
D2007	Characteristic Groups in Rubber Extender and Processing Oils and Other Petroleum-Derived Oils by Clay-Gel	GC	1193
D2593	Butadiene Purity and Hydrocarbon Impurities	GC	1004
D2622	Sulfur in Petroleum Products	WD-XRF	1428; 1547; 1622
D2887	Boiling Range Distribution of Petroleum Products	GC	1406
D3237	Lead in Gasoline	AAS	1376
D3606	Benzene and Toluene in Finished Motor and Aviation Gasoline	GC	1042
D3701	Hydrogen Content of Aviation Turbine Fuels	NMR	1186
D3831	Manganese in Gasoline	AAS	1500

TABLE 13—Research Reports of Spectroscopic Methods of Analysis of Petroleum Products (Continued)

Test Method	Analysis	Spectroscopic Technique	ASTM Research Report Number
D4294	Sulfur in Petroleum and Petroleum Products	ED-XRF	1635
D4815	MTBE, ETBE, TAME, DIPE, *tert*-Amyl Alcohol, and C_1 through C_4 Alcohols in Gasoline	GC	1296
D4864	Traces of Methanol in Propylene Concentrates	GC	1243
D4908	Hydrogen Content of Light Distillates, Middle Distillates, Gas Oils, and Residua	NMR	1186
D4927	Elemental Analysis of Lubricants and Additive Components	WD-XRF	1259
D4951	Additive Elements in Lubricating Oils	ICP-AES	1349; 1599
D5059	Lead in Gasoline	XRF	1283
D5134	Detailed Analysis of Petroleum Naphthas through an n-Nonane	GC	1265
D5184	Al and Si in Fuel Oils	AAS / ICP-AES	1281
D5185	Additive Elements, Wear Metals, and Contaminants in Used Lubricating Oils and Base Oils	ICP-AES	1282
D5303	Trace Carbonyl Sulfide in Propylene	GC	1298
D5307	Boiling Range Distribution in Crude Petroleum	GC	1295
D5384	Chlorine in Used Petroleum Products	Color	1368
D5441	Analysis of MTBE	GC	1306
D5442	Analysis of Petroleum Waxes	GC	1316
D5443	Paraffin, Naphthene, and Aromatic Hydrocarbon Type Analysis in Petroleum Distillates through 200°C	GC	1315
D5453	Total Sulfur in Light Hydrocarbons, Spark Ignition Engine Fuel, Diesel Engine Fuel, and Engine Oil	UV-FL	1307; 1456; 1465; 1475; 1547; 1633

(*Continued*)

TABLE 13—Research Reports of Spectroscopic Methods of Analysis of Petroleum Products (Continued)

Test Method	Analysis	Spectroscopic Technique	ASTM Research Report Number
D5501	Ethanol Content of Denatured Fuel Ethanol	GC	1266
D5580	Analysis of Finished Gasolines	GC	1329
D5599	Oxygenates in Gasoline	GC	1359
D5623	Sulfur Compounds in Light Petroleum Liquids	GC	1335
D5708	Ni, V, and Fe in Crude Oils and Related Fuels	ICP-AES	1351
D5769	Benzene, Toluene, and Total Aromatics in Finished Gasolines	GC / MS	1382
D5845	MTBE, ETBE, TAME, DIPE, Methanol, Ethanol, and *tert*-Butanol in Gasoline	FT-IR	1374
D5863	Ni, V, Fe, and Na in Crude Oils and Residual Fuels	AAS	1351
D5986	Aromatics in Finished Gasolines	GC / FT-IR	1399
D6159	Hydrocarbon Impurities in Ethylene	GC	1412
D6160	PCBs in Waste Materials	GC	1413
D6277	Benzene in Spark-Ignition Engine Fuels	FT-IR	1431
D6296	Total Olefins in Spark-Ignition Engine Fuels	GC	1433
D6352	Boiling Range Distribution of Petroleum Distillates in Boiling Range from 174 to 700°C	GC	1445
D6379	Aromatic Hydrocarbon Types in Aviation Fuels and Petroleum Distillates	HPLC	1446
D6417	Estimation of Engine Oil Volatility	GC	1451
D6443	Additive Elements in Unused Lubricating Oils and Additives	WD-XRF	1450
D6550	Olefin Content of Gasolines	SFC	1478
D6584	Free and Total Glycerin in B 100 Biodiesel Methyl Esters	GC	1603

TABLE 13—Research Reports of Spectroscopic Methods of Analysis of Petroleum Products (Continued)

Test Method	Analysis	Spectroscopic Technique	ASTM Research Report Number
D6591	Aromatic Hydrocarbon Types in Middle Distillates	HPLC	1503
D6595	Wear Metals and Contaminants in Used Lubricating Oils or Hydraulic Fluids	Rotrode AES	1487
D6667	Total Volatile Sulfur in Gaseous Hydrocarbons and Liquefied Petroleum Gases	UV-FL	1506
D6728	Contaminants in Gas Turbine and Diesel Engine Fuels	Rotrode AES	1514
D6729	Individual Components in Spark Ignition Engine Fuels	GC	1519
D6730	Individual Components in Spark-Ignition Engine Fuels	GC	1518
D6732	Copper in Jet Fuels	GF-AAS	1512
D6733	Individual Components in Spark-Ignition Engine Fuels	GC	1520
D6839	Hydrocarbon Types, Oxygenated Compounds, and Benzene in Spark-Ignition Engine Fuels	GC	1544
D7039	Sulfur in Gasoline and Diesel Fuel	MWD-XRF	1552
D7040	Low Levels of Phosphorus in ILSAC GF4 and Similar Grade Engine Oils	ICP-AES	1559
D7041	Total Sulfur in Light Hydrocarbons, Motor Fuels, and Oils	GC	1558
D7111	Trace Elements in Middle Distillate Fuels	ICP-AES	1569
D7171	Hydrogen Content of Middle Distillate Fuels	NMR	1557
D7212	Low Sulfur in Automotive Fuels	ED-XRF	1587
D7214	Oxidation of Used Lubricants	FT-IR	1623
D7220	Sulfur in Automotive Fuels	ED-XRF	1592
D7303	Metals in Lubricating Greases	ICP-AES	1608

(*Continued*)

TABLE 13—Research Reports of Spectroscopic Methods of Analysis of Petroleum Products (Continued)

Test Method	Analysis	Spectroscopic Technique	ASTM Research Report Number
D7319	Total and Potential Sulfate and Inorganic Chloride in Fuel Ethanol	IC	1614
D7328	Total and Potential Inorganic Sulfate and Total Inorganic Chloride in Fuel Ethanol	IC	1611
D7347	Olefin Content of Denatured Ethanol	SFC	1640
D7371	FAME Content in Diesel Fuel Oil	FT-IR	1624
D7412	Condition Monitoring of Phosphate Antiwear Additives in In-Service Petroleum and Hydrocarbon Based Lubricants	FT-IR	1667
D7414	Condition Monitoring of Oxidation in In-Service Petroleum and Hydrocarbon Based Lubricants	FT-IR	1668
D7416	Analysis of In-Service Lubricants	FT-IR	1646; 1669
D7419	Total Aromatics and Total Saturates in Lube Basestocks	HPLC	1632
D7622	Mercury in Crude Oils	CV-AAS	1692
D7623	Mercury in Crude Oils	CV-AAS	1692
D7691	Metals in Crude Oils	ICP-AES	1716

AAS: Atomic Absorption Spectroscopy
AES: Atomic Emission Spectroscopy
AS: Atomic Spectroscopy
ED-XRF: Energy Dispersive X-ray Fluorescence Spectroscopy
FES: Flame Emission Spectroscopy
FT-IR: Fourier Transform Infrared Spectroscopy
GC: Gas Chromatography
GC-FID: Gas Chromatography Flame Ionization Detection
GF-AAS: Graphite Furnace – Atomic Absorption Spectrometry
IC: Ion Chromatography
ICP-AES: Inductively Coupled Plasma – Atomic Emission Spectrometry
IR: Infrared Spectroscopy
MS: Mass Spectroscopy
MWD-XRF: Monochromatic Wavelength Dispersive X-ray Fluorescence Spectroscopy
NMR: Nuclear Magnetic Resonance Spectroscopy
UV-Fl: Ultraviolet Fluorescence
WD-XRF: Wavelength Dispersive X-ray Fluorescence Spectroscopy
XRF: X-ray Fluorescence Spectroscopy

these samples. Other spectroscopic methods used for biofuels include ICP-AES for trace metals, IC for sulfate and chloride content, UV-Fl for sulfur, and FT-IR and MS for molecular species. A few other test methods have been specifically developed for biofuels.

Finally, Table 13 lists the available ASTM research reports associated with pertinent spectroscopic methods used in the analysis of liquid fossil fuels. These research reports are a great source of information on the development of individual standards. When a research report is not available, that standard is not listed in the table. These reports are available from ASTM Headquarters.

We hope that this monograph proves to be of use and benefit to the researchers in the oil industry as well as students of analytical and fuels chemistry in colleges and universities.

ACKNOWLEDGMENTS

I want to thank Kathy Dernoga, publications manager at ASTM International, for supporting this project, and Christina Urso, editor at American Institute of Physics, for shepherding the book through its often frustrating ups and downs with the authors and the reviewers. Needless to say, I thank all the authors for diligently giving their best in their areas of expertise. All is well that ends well!

References

[1] Annual Book of ASTM Standards, Volumes 05.01, 05.02, 05.03, and 05.04, ASTM International, West Conshohocken, PA, 2008.

[2] Nadkarni, R. A., *Guide to ASTM Methods for the Analysis of Petroleum Products and Lubricants*, MNL44, 2nd edition, ASTM International, West Conshohocken, PA, 2007.

[3] Nadkarni, R. A., ed., *Modern Instrumental Methods of Elemental Analysis of Petroleum Products and Lubricants, ASTM STP 1109,* ASTM International, West Conshohocken, PA, 1989.

[4] Nadkarni, R. A., ed., *Elemental Analysis of Fuels and Lubricants: Recent Advances and Future Prospects, ASTM STP 1468,* ASTM International, West Conshohocken, PA, 2004.

[5] Irving, H. M. N. H., Freiser, H. and West, T. S., *IUPAC Compendium of Analytical Nomenclature – Definitive Rules 1977,* Pergamon Press, Oxford, 1978.

[6] Laitinen, H. A. and Ewing, G. W., eds., *A History of Analytical Chemistry,* American Chemical Society, Washington, D. C., 1977.

[7] McElroy, F. C., Mennito, A., Debrah, E. and Thomas, R., "Uses and Applications of ICP-MS in the Petrochemical Industry," *Spectroscopy,* Vol. 13(2), 1988, pp. 43–53.

[8] Small, H., Stevens, T. S. and Bauman, W. C., "Determination of Anions by Ion Chromatography," *Anal. Chem.,* Vol. 47, 1975, p. 1801.

[9] Nadkarni, R. A., "Determination of Trace Amounts of Sulfur in Petroleum Products and Lubricants: A Critical Review of Test Performance," *Amer. Lab.,* Vol. 32(22), 2000, pp. 16–25.

[10] Giles, H. N. and Mills, C. O., "Crude Oils: Their Sampling, Analysis, and Evaluation," MNL68, ASTM International, West Conshohocken, PA, 2010.

2

Calibration Protocols for Spectroscopic Measurements of Petroleum Products

R. A. Kishore Nadkarni[1]

INTRODUCTION

All apparatus and instruments used in a laboratory require some kind of calibration or verification before an instrument is used for producing reliable data. A perfect analysis needs a perfect calibration as a first step and perfect quality control as perhaps the last step in the sequence of analytical event. Often this cycle is depicted as [1]:

$$\text{Calibration} \rightarrow \text{Sample Analysis} \rightarrow \text{QC Analysis} \rightarrow \text{Calibration} \rightarrow \rightarrow \rightarrow \quad (1)$$

Quite often problems in analytical results can be traced to inadequate calibration practices. This is true whether the measurements are chemical or physical in nature.

The concept of calibration is basic to all measurements. Measurement is essentially a comparison process in which an unknown whose value is to be determined is compared with a known standard. The only purpose of calibration is to eliminate or minimize the bias in a measurement process. The precisions of calibrated and uncalibrated systems can be equivalent, but not necessarily the accuracy [2].

Some methods require little to no method calibration; others require only simple one-step calibration; yet others require elaborate calibration routines before the product is analyzed for its content. Fairly often it can be shown that the round-robin results by a cooperator are all biased with respect to those from other laboratories. Presumably, failing to follow good laboratory practices and instructions in the test methods can be a causal factor of such errors. A further consequence is an unnecessarily large reproducibility estimate or the data being dropped from the study as an outlier. Among other causes of such discrepancies could be different or inadequate calibration practices used in the laboratory. Most test methods spell out the calibration requirements but often do not quote the frequency required, letting the laboratories use good laboratory practices for this task. Thus, uniform practice for instrument calibration would be beneficial in standardizing the test procedures and obtaining consistent results across laboratories.

Terminology

The most commonly used phrases or words and their definitions related to this discussion of calibration are given in Table 1.

Calibration or Verification?

Although the words verification and calibration are often used synonymously, they indeed have different connotations. Verification pertains to checking that

[1] *Millennium Analytics, Inc., East Brunswick, New Jersey*

TABLE 1—Terminology for Calibration

Term	Explanation	Source
Calibration standard	A material with a certified value for a relevant property, issued by or traceable to a national organization such as NIST, and whose properties are known with sufficient accuracy to permit its use to evaluate the same property of another sample.	ASTM Standard Practice D6792
Certified reference material (CRM)	A reference material, one or more of whose property values are certified by a technically valid procedure, accompanied by a traceable certificate or other documentation that is issued by a certifying body.	ISO Guide 30
Check standard	A material having an assigned (known) value (reference value) used to determine the accuracy of the measurement system or instrument. This standard is not used to calibrate the measurement instrument or system.	ASTM Standard Practice D7171
Reference material (RM)	A material with accepted reference values accompanied by an uncertainty at a stated level of confidence for desired properties, which may be used for calibration or quality-control purposes in the laboratory.	ASTM Standard Practice D6792
Traceability	A property of the result of a measurement or the value of a standard whereby it can be related to stated references, usually national or international standards, through an unbroken chain of comparisons, all having stated uncertainties.	ASTM Standard Practice D6792

the instrument or a system is in a condition fit to use, and calibration involves standardization as in a measuring instrument by determining the deviation from a reference standard to ascertain the proper correction factors. In the ash D482 and sulfated-ash D874 tests, for example, no specific verification or calibration is done other than using appropriate thermometers for monitoring the temperature in the oven or furnace, and balance calibration. On the other hand, in the D4951 and D5185 ICP-AES methods for metals, the instrument is calibrated over several concentration ranges to check that the linearity is acceptable, and other additional checks are also required.

The overall program of calibration of equipment should be designed and operated to ensure that the measurements made in the testing laboratories are traceable (where the concept is applicable) to national standards of measurement and, where available, to international standards of measurement specified by such bodies.

Where the concept of traceability to national or international standards of measurement is not applicable, the testing laboratory should provide satisfactory evidence of correlation or accuracy of test results (e.g., by participating in a suitable program of interlaboratory comparison, or by primary and interference-free classical chemistry techniques such as gravimetry or titrimetry).

Different test methods require different calibration intervals. Thus, a decision about appropriate calibration frequency must be made on a case-by-case basis. It goes without saying, however, that the calibration practices are a must for all analytical testing and must be thoroughly documented regarding both the plan and the factual evidence that it is being followed. Some tests may require additional verifying with check standards. There is a tendency among many laboratories to do the bare-minimum calibrations, similar to their approach toward quality control requirements. This is not the way to achieve superior performance. Moreover, if an instrument is found to be out of calibration, and the situation cannot be immediately addressed, then the instrument shall be taken out of operation and tagged as such until the situation is corrected. Under no circumstances can data from that instrument be reported to the customers.

The performance of apparatus and equipment used in the laboratory but not calibrated in that laboratory (i.e., precalibrated, vendor supplied) should be verified by using a documented, technically valid procedure at periodic intervals.

Appropriate calibration standards must be used during analysis. A wide variety of such standards are available from commercial sources, National Institute of Science and Technology (NIST), and others. Many laboratories have capabilities of preparing reliable in-house standards. Calibration standards identical to the samples being analyzed would be ideal, but, failing that**,** at least some type of standard must be used to validate the analytical sequence. In physical measurements this is usually achievable, but it is often difficult or sometimes almost impossible in chemical measurements. Even the effects of small deviations from matrix match and analyte concentration level may need to be considered and evaluated on the basis of theoretical or experimental evidence or both. Sometimes using standard additions technique to calibrate the measurement system is a possibility. But because an artificially added analyte may not necessarily respond in the same manner as a naturally occurring analyte, this approach may not be always valid, particularly in molecular speciation work.

Many ASTM test methods either do not specify the calibration steps or do not give the frequency of calibration. In such cases, the incidence and the frequency are determined from laboratory experience or industry practice or both. ASTM Standard Practice for Quality System in Petroleum Products and Lubricants Testing Laboratories D6792-07 states that "procedures shall be established to ensure that measuring and testing equipment is calibrated, maintained properly, and is in statistical control. Items to consider when creating these procedures include:

- Records of Calibration and Maintenance
- Calibration and Maintenance Schedule.

TABLE 2—Classification of Analytical Instrumentation Used in Laboratories

Class I	Class II	Class III
Glassware	Colorimeter	AAS
Centrifuge	Pressure gages	ICP-AES
Cold or hot baths	Glassware, if critical in final analysis	XRF
Hot plates / ovens / furnaces	Microwave digestion ovens	Thermometers (E77)
Freezers	...	Balances (E319, E898)
Mixers / stirrers / shakers	...	ICP-MS
Refrigerators	...	MS
Sonic baths	...	FT-IR
Noncritical thermometers	...	NMR
Desiccators	...	...
Drying ovens	...	...

- Traceability to National or International Standards
- Requirements of the Test Method or Procedure,
- Customer Requirements, and
- Corrective Actions."

Based on the requirements of calibration involved and the importance of an instrument or an apparatus being calibrated, most laboratory apparatus and analytical instruments used can be (arguably) classified into three categories as Class I, II, and III, based on the extent of calibration needed in each case from minimal to extensive, and with increasing degree of importance or criticality (Table 2).

Class I apparatus include miscellaneous, unsophisticated equipment that may need no calibration or minimal verification such as motor speed or temperature maintained. Perhaps stirrers or some types of thermometers will fall in this category. Generally, these apparatus do not produce actual analytical data.

Class II apparatus include equipment that should be maintained, or possibly calibrated on a routine basis, and may have minimal verification requirements. This might include, for example, balances, temperature controllers, and gas flow meters. The data from Class II instruments usually is not sent to the customers.

Class III instruments include sophisticated instrumentation and equipment that should require scheduled full verification, calibration, or both as given in the standard ASTM protocols before the instrument is used for the sample analysis. These may be done either by the analysts or outside contractors or original equipment manufacturers (OEM). For all of these instruments ASTM standard methods are available which should be followed in operation. The data produced from these instruments could be given to the customers.

The four most commonly used accessories in most analytical testing are temperature-measuring devices (TMD), time-measuring devices, balances, and glassware.

TEMPERATURE-MEASURING DEVICES

These include liquid-in-glass mercury or alcohol thermometers and other electronic digital thermometers and thermocouple probes. With the increasing concern about mercury toxicity, such thermometers are being replaced in the laboratories as well as in ASTM test methods with electronic devices. These calibrated thermometers should have tags affixed to them indicating the date of current and next calibrations, correction factor, if any, and the name of the person calibrating them. ASTM standards E77 and E2251 describe calibration requirements for thermometers.

The critical TMDs are purchased from vendors with a certificate verifying that they are calibrated using ASTM standard methods and are traceable to NIST standards. One certified set of thermometers is purchased to be used exclusively for verifying other TMDs. Annually, the certified set of thermometers can be verified using the NIST traceable standards. This service is often contracted out. Over and above the annual recalibration of TMDs, some ASTM test methods specifically require additional calibration of thermometers as a part of the analytical procedure. Individual ASTM test methods should be consulted for details of required recalibrations. Many ASTM test methods do not, however, specify the frequency of calibration. The thermometers that are not used in analytical testing are considered noncritical and generally are not calibrated. Such thermometers are used, for example, in blending and synthesis.

TIMERS

Both stopwatches and electronic time-measuring devices can be calibrated once a year using the time signals as broadcast by NIST and received by calling the NIST phone number in Boulder, Colorado. The procedure is given in Appendix A3 of ASTM Standard Test Method D445. The timers used for general laboratory purposes are verified at two different intervals: 60 and 300 seconds. These verification data are recorded in laboratory notebooks. Any timer not meeting the verification standard is discarded. No other maintenance is expected on these timers.

MASS BALANCES

The procedure for calibration of laboratory electronic mass balances is described in ASTM standard E898 or E319. Balances are usually calibrated once a year using NIST traceable standard weights. Generally most laboratories contract this function to a vendor. Use of NIST mass standards maintains traceability.

A suggested calibration frequency for generic equipment used in elemental analysis is given in Table 3. In-house calibrations should follow reliable procedures and protocols recommended by NIST or other recognized standards writing bodies.

VOLUMETRIC GLASSWARE

Certified glassware should be used or be calibrated according to ASTM standards E542 or E288. This applies only to, e.g., burets, pipets, syringes, and volumetric flasks, and not to beakers that are generally not used for quantitative measurements.

TABLE 3—Suggested Calibration Frequency for Generic Laboratory Equipment

Instrument	Calibration Frequency	Possible Calibrator[a]
Pipets	Annual	In-house
Balances	Annual	In-house or vendor
Volumetric ware	Only Class A materials used	In-house
Thermometers	Annual	In-house or vendor
Stopwatches	Annual	In-house
Flowmeters	Annual	In-house or vendor
AAS	At the time of analysis	In-house
ICP-AES	At the time of analysis	In-house
ICP-MS	At the time of analysis	In-house
XRF	As necessary	In-house or manufacturer

[a] Other sources for calibration services are acceptable.

In all above cases, two requirements must be satisfied: (a) traceability to national standards, and (b) use of national standards methods of verification.

Calibration Standards

Calibration standards appropriate for the method and characterized with the accuracy demanded by the analysis to be performed must be used during analysis. Calibration materials consisting of materials closely resembling the test samples are needed for this purpose but may be difficult or impossible to prepare or obtain. The analyst may be forced to use surrogates added to the test sample or the method of standard additions of analyte to calibrate the measurement system.

Quantitative calibration standards should be prepared from constituents of known purity. Use should be made of primary calibration standards or certified reference materials specified or allowed in the test method. A wide variety of such standards are available from commercial sources, NIST, and so on. Many laboratories have capabilities of preparing reliable in-house standards. Calibration standards identical to the samples being analyzed would be ideal, but failing that, at least some type of standard must be used to validate the analytical sequence. In physical measurements this is usually achievable, but it is often difficult or sometimes almost impossible in chemical measurements. Even the effects of small deviations from matrix match and analyte concentration level may need to be considered and evaluated on the basis of theoretical or experimental evidence. Sometimes using standard additions technique to calibrate the measurement system is a possibility. But because an artificially added analyte may not necessarily respond in the same manner as a naturally occurring analyte, this approach may not be always valid, particularly in molecular speciation work [2].

If a laboratory wants to prepare in-house calibration standards, the appropriate values for reference materials should be produced following the certification protocol used by NIST or other standards issuing bodies, and should be traceable to national or international standard reference materials, if required or appropriate.

NIST uses seven models for value assignment of reference materials for chemical measurements: NIST-certified values are derived from certification at NIST using a single primary method with confirmation by other methods or using two independent critically evaluated methods or using one method at NIST and different methods by outside collaborating laboratories. NIST reference values are derived from the last of the two models mentioned, as well as values based on measurements by two or more laboratories using different methods in collaboration with NIST, or based on a method specific protocol, or NIST measurements using a single method or measurement by an outside collaborating laboratory using a single method, or based on selected data from interlaboratory studies. The last four means are used also for assigning NIST information values. See NIST Special Publication 260–136 for further details on this subject [3].

In addition to the oil-soluble organometallic compounds used to calibrate instruments such as atomic absorption spectrometry (AAS), inductively coupled plasma–atomic emission pectrometry (ICP-AES), or X-ray fluorescence (XRF), single-element or multielement calibration standards may also be prepared from materials similar to the samples being analyzed, provided the calibration standards to be used have previously been characterized by independent, primary (for example, gravimetric or volumetric) analytical techniques to establish the elemental concentration at mass percent levels.

REFERENCE MATERIALS

Reference materials (RM) can be classified as primary or secondary. The primary RMs are well-characterized, stable, homogenous materials produced in quantity, and with one or more physical or chemical property experimentally determined, within the stated measurement uncertainties. These are certified by a recognized standardization laboratory using the most accurate and reliable measurement techniques. The secondary RMs are working standards or quality control (QC) standards and may have undergone less rigorous evaluation for day-to-day use in the laboratory. Discussion on preparation and use of reference materials is included in Chapter 3 on calibration and quality control reference materials in this monograph. That chapter is important companion reading to this chapter.

CALIBRATION FREQUENCY

The calibration schedules will vary with the instrument type, some needing calibration before each set of analysis (e.g., AAS), others requiring calibration at less frequent periods (e.g. XRF). An important aspect of calibration is the decision on calibration intervals, i.e., the maximum period between successive recalibrations. Two basic and opposing considerations are involved: the risk of being out of tolerance at any time of use, and the cost in time and effort. The former should be the major concern because of the dilemma of what to do with the data obtained during the interval between the last known in and the first known out of calibration. An overly conservative approach could, however,

be prohibitively expensive. A realistic schedule should reduce the risk of the former without undue cost and disruption to work schedules. The factors that need to be considered in a realistic schedule include [2]:

- Accuracy requirement for the measured data
- Level of risk involved
- Experience of the laboratory in use of the equipment or methodology
- Experience of the measurement community
- Manufacturer's recommendations
- External requirements for acceptability of data
- Cost of calibration and quality control.

The best way to develop a specific calibration schedule is to start with a fairly frequent (too often) schedule, document the results of each calibration (actual readings versus calibrated readings), and start increasing the interval until a point is reached where one can determine that the accuracy desired is not being maintained. Apart from the techniques that require calibration with every analysis, such as AAS and ICP-AES, calibration should be triggered by quality control sample results or control chart rule being violated. To calibrate simply because it is time to calibrate is a waste of resources. In XRF analysis, if the quality control or the check sample goes out of control, drift correction is done. If the drift correction does not correct the problem, then calibration should be done.

The higher the accuracy required, the higher the initial cost of the equipment, the frequency of calibration, and the level of attention required. Hence, every effort should be made to use the highest level of uncertainty permissible. Repeatability or data compatibility or both are normally issues of greater concern than absolute accuracy. The ability to feel confident that the data taken today are comparable with the data taken at an earlier time or to be taken in the future is normally more critical. Stability, i.e., the ability of the device to produce the same reading at the same condition over an extended period of time, is another important concern. The absolute accuracy of a device may be low but its stability could be high. If so, the ability to compare results over time is greatly improved. The level of uncertainty of a measurement is also dependent on the total system, many of whose components have poorly defined long-term performance, with other components being very dependent on external conditions such as temperature and humidity.

An initial choice of calibration intervals may be made on the basis of previous knowledge or intuition. Based on the experience gained during its use, the intervals could be expanded if the methodology is always within tolerance at each recalibration, or it should be decreased if significant out-of-tolerance is observed. Control charts may be used to monitor the change of measured value of a stable test item correlated with the need to recalibrate. Many laboratories use a posted schedule of calibration that is followed by the analysts. This is fine, so long as intelligent judgment is used in adhering to this schedule. If the quality control sample or routine sample data produced by an instrument appear to be of doubtful quality, the first thing to check is the quality control and calibration of the instrument, irrespective of the calibration schedule.

There are some tests (e.g., ICP-AES) where calibration is an integral part of the analysis and ASTM test methods explicitly state the needed frequency. In all such cases this requirement must be met.

Calibration Documentation

All calibration records should be documented either in the instrument computer software or in manually prepared laboratory notebooks. This should include information such as date of last and next calibrations, the person who performed the calibration, method or procedure used for calibration, the material used for calibration, the values obtained during calibration, and the nature and traceability (if applicable) of the calibration standards. Records may be maintained electronically.

For instruments that require calibration, calibration and maintenance records may be combined.

CALIBRATION IN PHOTOMETRIC TEST METHODS

A number of test methods use flame emission or colorimetric measurements for quantitation of analytes, usually after reacting the matrix with a chromogenic reagent. Such instruments need to be calibrated using appropriate standards developed by reacting the pure metal analyte with the chromogenic reagent. The calibration curve of analyte concentration versus the photosignal (absorbance or transmittance) should follow the Beer-Lambert Law. The sample analysis should be carried out only in the linear range of the plot. If necessary, solutions with higher concentrations of metals should be diluted to bring them into the linear range of calibration.

Multiple standards, generally between three and six, are used for developing the calibration curve. The absorbance or transmittance of standard solutions is corrected by subtracting the signal of the blank solution. If a chemical procedure is used to develop the color, the same reagents and steps also need to be included in developing the blank color.

The test methods using such photometric methods include the following.

ASTM Test Method			
Number	**Analyte**	**Matrix**	**Measurement Technique**
D1091A	Phosphorus	Lube oils and additives	Colorimetry
D1318	Sodium	Fuel oils	Flame photometry
D1548	Vanadium	Fuel oils	Colorimetry
D1839	Amyl nitrate	Diesel	Spectrophotometry
D2784B	Sulfur	LPG	Titrimetry or photometry
D3231	Phosphorus	Gasoline	Spectrophotometry
D3340	Lithium / sodium	Greases	Flame photometry
D3348	Lead	Gasoline	Colorimetry
D4045	Sulfur	Petroleum	Rateometric colorimetry
D4046	Alkyl nitrate	Diesel	Spectrophotometry
D7041	Diesel	Sulfur	Flame photometry

CALIBRATION IN ATOMIC ABSORPTION SPECTROMETRY

A number of metals are determined by the popular technique AAS. In all cases the instrument needs to be calibrated before each set of analysis. Usually solutions of organometallic standards dissolved in solvents such as xylene, toluene, MIBK (methyl isobutyl ketone), and kerosine are used. Such standards are widely available from commercial sources or NIST. The concentration of metals in the standards for actual calibration is usually kept between 1 to 10 mg/kg, prepared by dilution from stock solutions. Although the purchased stock solutions of high metal concentrations can be preserved for long periods of time, the diluted working standards should not be kept for more than a day, since it is possible that there may be loss of analyte by adsorption on the container walls.

Similar to the photometric methods, a plot or correlation based on metal concentration versus absorbance is prepared and the metal concentration in the samples is calculated based on this factor. The analysis should be done only within the range of linear curve. If expected metal concentration is higher than the linear range, the sample should be diluted with appropriate solvent; otherwise results biased low will result.

The calibration curve may be manually plotted using concentration of metal in the working standards on the x-axis and corrected absorbance on the y-axis. Most AAS instruments have the capability of automatically constructing the calibration curve internally with the instrument software and displaying the curve on the instrument computer terminal, making actual manual plotting unnecessary. A curve with the best possible fit of the data within the available means should be used.

Most modern AAS instruments can store up to three or four calibration standards in memory. In such cases, follow the manufacturer's instructions, ensuring that the unknown sample's absorbance is in the linear part of the calibration range used.

Generally, stock solutions of standards contain 100 to 1,000 mg/kg metal concentration. For working standards, these are diluted with appropriate organic solvents to a level of up to about 10 mg/kg.

Generally three to six standards are used for establishing the calibration curve of metal concentration versus absorption signal. Often, though, one standard in the linear range is sufficient. A blank needs to be subtracted from the standard solutions' absorbance for compensating any contribution from the metals contaminating the standard solutions. If any chemical step is involved in final standard preparation, it should also be included in the blank solution preparation.

Calibration must be carried out before analyzing each group of samples and after finding any change in instrumental conditions, because instrument behavior can vary. Readings also may vary over short periods of time from such causes as buildup of deposits on the burner slot or in the nebulizer. Thus, a single standard should be aspirated from time to time during a series of samples to check whether the calibration has changed. A check after every fifth sample is recommended. The visual appearance of the flame also serves as a useful check to detect changes of condition.

Although the AAS methods are depicted as single-element analysis methods, they can be used to determine multiple elements in a single sample. In such

cases the sequence of operations in analyzing several samples should also be considered. Aspiration of a sample to determine the absorbance is very quick. Changing wavelength setting and lamps takes longer. Thus, it is most economical to make measurements at a single wavelength on a series of samples and standards before changing conditions. In such cases use of multielement calibration standards and multielement hollow cathode lamps would be useful.

Some of the test methods available for petroleum products and lubricants analysis using AAS include the following.

ASTM Test Method		
Number	**Analyte**	**Matrix**
D3237	Lead	Gasoline
D3605	Trace metals	Gas turbine fuels
D3831	Manganese	Gasoline
D4628	Additive metals	Lube oils and additives
D5056	Trace metals	Petroleum coke
D5184B	Aluminum and silicon	Fuels oils
D5863	Metals	Crude oils and residual fuels
D6732	Copper	Jet fuels

Although not strictly the AAS or ICP-AES type methods, D6595 and D6728 use rotating-disc electrode AES methods to determine wear metals and contaminants in used lubricating oils, used hydraulic fluids, and gas turbine and diesel engine fuels. The calibration operation range of such instruments for each element is established through the analysis of organometallic standards at known concentrations in the instrument manufacturing factory. A calibration curve for each element is established and correction factors are set to produce a linear response. Analyses of the test specimen must be performed within the linear range of the response. A minimum of a two-point routine standardization should be performed if the instrument fails the validation check or at the start of each working shift. A minimum of three analyses should be made using the blank and working standard.

CALIBRATION IN ICP-AES TEST METHODS

Given the capability of ICP-AES for simultaneous multielement capability, most laboratories use multielement standards for instrument calibration. Although such standards can be prepared in-house from pure organometallic standards, it is much more practical and convenient to use preblended, multielement organic standards available from many commercial sources. Most are available dissolved in base oil or other organic solvents at levels from 20 to 1000 mg/kg of individual elements. Custom-blended standards can also be obtained from these sources.

More than one multielement standard may be necessary to cover all elements of interest. It is imperative that concentrations are selected such that the emission intensities measured with the working standards can be measured precisely (i.e., the emission intensities are significantly greater than background), and these standards represent the linear region of the calibration curve. Frequently, the instrument manufacturer publishes guidelines for determining linear range.

Some commercially available organometallic standards are prepared from metal sulfonates, and therefore contain sulfur. Thus, for sulfur determination, a separate sulfur calibration standard can be required. Metal sulfonates can be used as a sulfur standard if the sulfur content is known or determined by an appropriate test method such as D1552. Petroleum additives can also be used as organometallic standards if their use does not adversely affect the precision nor introduce significant bias.

Some of the ICP-AES methods (e.g., D5184, D5600, and D7303) use aqueous solutions after decomposing the organic matrices, converting them into dilute acidic aqueous solutions. In such cases aqueous metal standards must be used. These are widely available from commercial sources, usually in 100 to 1000 mg/kg concentrations. They also can be prepared in-house by dissolving inorganic metal salts in dilute acids.

The linear range of all ICP-AES curves must be determined for the instrument being used. This is accomplished by running intermediate standards between the blank and the working standards and by running standards containing higher concentrations than the working standards. Analyses of test specimen solutions must be performed within the linear range of the calibration curve. At the beginning of the analysis of each set of test specimen solutions, a two-point calibration using the blank and the working standard is performed. A check standard is used to determine if each element is in calibration. When the results obtained with a check standard are within 5 % relative of the expected concentration for all elements, the analysis may be continued. Otherwise, any necessary adjustments to the instrument need to be made and the calibration repeated.

The calibration curves can be constructed differently, depending on the implementation of internal standard compensation. When analyte intensities are ratioed to internal standard intensities, the calibration curve, in effect, is a plot of intensity ratio for analyte versus the analyte concentration. When the internal standard compensation is handled by multiplying all results for a test specimen by the ratio of the actual internal standard concentration to the determined internal standard concentration, the calibration curve is, in effect, a plot of intensity for analyte minus intensity of the blank for the analyte versus analyte concentration. Although normally the calibration curves would be linear, sometimes inclusion of a second-order term can give a better fit, although in such cases it would require at least five standards for calibration.

Detailed discussion of calibration and all other pertinent protocols for use of ICP-AES for analyzing petroleum products and lubricants is given in ASTM Standard Practice D7260. Some of the test methods available for analysis of petroleum products and lubricants using ICP-AES include the following.

ASTM Test Methods		
Number	**Analyte**	**Matrix**
D4951	Additive metals	Additives and lubricants
D5184A	Aluminum and silicon	Fuel oils
D5185	Additive metals and contaminants	Base oils, lube oils, and used lube oils
D5600	Trace metals	Petroleum coke
D5708	Nickel, vanadium, and iron	Crude oils and residual fuels
D7040	Phosphorus	Lube oils
D7111	Trace elements	Middle distillate fuels
D7303	Metals	Lubricating greases
D7691	Metals	Crude oil

CALIBRATION IN NEUTRON ACTIVATION ANALYSIS

Neutron activation analysis (NAA) is like AAS, ICP-AES, or XRF based on comparison of measurements from the sample and a standard of an analyte of interest. In NAA standards are prepared from highly stable, pure metallic compounds, which are sealed in quartz ampoules along with similarly prepared samples. After irradiation, radioactivities from sample and standard are counted and the ratio allows one to calculate the concentration of the element of interest in the sample. It has been suggested to use certified reference material as the irradiation standard. The advantage of this approach is that the values of a great number of elements are known with a fair degree of uncertainty, elimination of effort to prepare a multielement calibration standard is eliminated, and any matrix difference between the sample and the standard is eliminated where possible [4].

CALIBRATION IN XRF TEST METHODS

Similar to ICP-AES, XRF has the capability of multielement analysis, even with a better precision. A large number of XRF test methods have been written for the determination of low levels of sulfur in fuels because of its importance in environmental and regulatory affairs.

Detailed discussion about the sample handling, calibration, and validation using XRF methods can be found in ASTM Standard Practice D7343. Some of the test methods utilizing XRF technique for the analysis of petroleum products and lubricants include the following.

ASTM Test Method			
Number	**Analyte**	**Matrix**	**XRF Type[a]**
D2622	Sulfur	Petroleum products	WD-XRF
D4294	Sulfur	Petroleum products	ED-XRF
D4927	Additive elements	Additives and lube oils	WD-XRF

Number	Analyte	Matrix	XRF Type[a]
D5059	Lead	Gasoline	WD-XRF
D6334	Sulfur	Gasoline	WD-XRF
D6443	Additive elements	Additives and lube oils	WD-XRF
D6445	Sulfur	Gasoline	ED-XRF
D6481	Additive elements	Lube oils	ED-XRF
D7039	Sulfur	Gasoline and diesel	MWD-XRF
D7212	Sulfur	Automotive fuels	ED-XRF
D7220	Sulfur	Automotive fuels	ED-XRF

[a]WD-XRF: wavelength dispersive X-ray fluorescence; ED-XRF: energy dispersive X-ray fluorescence; MWD-XRF: monochromatic wavelength dispersive X-ray fluorescence.

The calibration standards used in XRF analysis are similar to those used in ICP-AES analysis. Because for petroleum products analysis XRF usually is a solution analysis, the standards are prepared from pure organometallic compounds or organic sulfur compounds in base oil or other suitable organic solvents. Particular attention needs to be paid to the purity of the solvent used. Otherwise a blank correction may be necessary for the contaminants in the solvent.

Working calibration standards can be prepared by careful mass dilution of a certified organic compound with an analyte-free white oil or other suitable base material such as toluene, iso-octane, and xylene. The concentration of the unknown samples must lie within the calibration range that is used.

Some of the calibration standards suggested and widely used include:

1. Di-n-butyl sulfide, thiophene, 2-methyl thiophene for sulfur analysis.
2. Polysulfide oil: generally, nonyl polysulfides containing a known percentage of sulfur (as high as 50 m%) diluted in a hydrocarbon matrix. They exhibit excellent physical properties such as low viscosity, low volatility, and durable shelf life while being completely miscible in white oil. The sulfur content of the polysulfide oil concentrate is determined via mass dilution in sulfur-free white oil followed by a direct comparison analysis against NIST (or other primary standard body) reference materials.
3. Metal sulfonates, octoates, ethylhexanoates, or cyclohexanebutyrates for metal analysis such as barium, calcium, copper, magnesium, phosphorus, and zinc.

The calibration standards and check samples should be stored in glass bottles in a cool dark place until required. The glass bottles should be either dark or wrapped in opaque material and closed with glass stoppers, inert plastic lined screw caps, or other equally inert, impermeable enclosures. As soon as any sediment or change of concentration is observed, the standard should be discarded.

The calibration curve is established by determining the net intensity of the emitted radiation from the metal of interest in each of the standards. Usually five to ten calibration standards may be employed; these may be in the milligrams per kilogram or 0.x mass percent levels, depending on the level of the

analyte to be determined in the samples. Usually a calibration model is prepared by the software in the XRF instrument.

Respective X-ray cups are filled at least half full with the calibration standard solutions. No wrinkle or bulges should appear in the film, which must be flat. The filled cups with a vent hole punched in the top of the cell are placed in the X-ray beam to measure and record the net intensity (i.e., peak intensity minus background intensity) for the analyte signal. Although many XRF instruments can count for times even greater than 15 minutes, in petroleum products analysis a counting period up to 60 seconds may be used at each wavelength position. This is done for each of the calibration standards for each of the elements measured. A regression analysis is performed for each calibration element by plotting on a linear graph paper or using the instrument computer system. It is recommended that a multiple linear regression be performed for each calibration. The regression analysis will determine a slope and an intercept for each calibration element that will be used to determine elemental concentrations in the samples to be analyzed.

The initial calibration to obtain the slope, intercept, and interelement correlation factors is performed initially when the test method is set up, after any major instrumental maintenance is performed that could affect the calibration (for example, new X-ray tube installed, new crystal added, and so forth), and as deemed necessary by the operator (for example, triggered by quality-control sample results). Subsequently, recalibration is performed with a minimum of three standards containing each of the calibration elements at nominal concentrations across the respective calibration ranges to check the values of the slope and the intercept.

Immediately after the calibrations are completed, the sulfur concentration of one or more of the calibration check samples is determined. The difference between the two measured values should be within the repeatability of the test method being used. When this is not the case, the stability of the instrument and the repeatability of the sample preparation may be suspect, and corrective measures should be taken. The degree of matrix mismatch should also be considered when evaluating a calibration.

Using drift correction monitors to determine and correct instrument drift can be advantageous. Monitors are stable, solid disks or pellets containing all elements of interest in the test method used. Two disks are preferred to correct for both sensitivity and baseline drifts. The high-concentration drift monitor provides high-count rates, so that for each analyte, counting error is less than 0.25 % relative. The low-concentration drift monitor provides low-count rates, so that for each element, count rate is similar to that obtained with the calibration blank, or 0.0 mass % standard.

CALIBRATION IN INFRARED ANALYSIS

Although often used for qualitative analysis to identify molecular species, Fourier transform-infrared (FT-IR) spectroscopy can also be used for quantitation of these species. A number of ASTM standard practices are available for checking the performance of an IR or FT-IR spectrometer: e.g., D7418, E168, E932, E1252, and E1421.

Before any series of measurements, the spectrometer is standardized using the polystyrene test film. Most modern FT-IR instruments will automatically

perform this verification as a part of the start-up routine. Usually two performance tests are conducted:

1. An interferogram test is used to check the alignment. The central burst of the interferogram should be a sharp and stable negative peak.
2. A 100 % line test should give a level straight line at 100 % transmittance. In reality there is always some noise and the line is level with some scatter. This test is considered successful even if the line has a tilt at either or both ends, which at 5000 and 600 cm^{-1} falls between 99.5 and 100.5 % transmittance. A line falling above or below these values is considered a failed test and the nitrogen purge should be checked.

Quantitative IR analysis is conducted by measuring peak heights or peak areas and developing a calibration curve to relate these values to concentration. Quantitative analysis follows Beer-Lambert law. Increasingly, IR quantitative analysis is done using multivariate methods. Sometimes such multivariate methods are calibrated using surrogate mixtures, i.e., gravimetric mixtures of pure compounds. See Chapter 17 on IR analysis in this monograph for a detailed discussion of these calibration techniques.

CALIBRATION IN NMR ANALYSIS

Nuclear magnetic resonance (NMR) is used for identifying molecular species in complex petroleum products. ASTM has issued at least four standard methods in this area.

1. D3701 – Hydrogen Content of Aviation Turbine Fuels by Low Resolution Nuclear Magnetic Resonance Spectrometry.
2. D4808 – Hydrogen Content of Light Distillates, Middle Distillates, Gas Oils, and Residua by Low Resolution Nuclear Magnetic Resonance Spectrometry.
3. D5292 – Aromatic Carbon Contents of Hydrocarbon Oils by High Resolution Nuclear Magnetic Resonance Spectroscopy.
4. D7171 – Hydrogen Content of Middle Distillate Petroleum Products by Low Resolution Pulsed Nuclear Magnetic Resonance Spectroscopy.

In these methods, calibration of the instrument is achieved by using a pure hydrocarbon as a reference standard. Results from the integrator of the instrument are used as a means of comparing the theoretical hydrogen content of the standard with that of the sample.

CALIBRATION IN GC-MS METHODS

A widely used technique for the determination of organic compounds in petroleum products is gas chromatography (GC), often combined with mass spectrometry (MS), to identify and quantify organic components. See Chapter 19 of this monograph for a detailed discussion of this topic. A calibration curve is obtained by analyzing a known mixture of hydrocarbons covering the boiling range expected in the sample under the same chromatographic conditions as those used for samples. The calibration mixture is prepared by accurately weighed mixture of approximately equal mass quantities of n-hydrocarbons dissolved in a solvent such as carbon disulfide, etc. The mixture should cover the range from n-C_5 to C_{44} but does not need to include every carbon number. Calibration mixtures containing normal paraffins with the carbon numbers 5–12, 14–18, 20, 24, 28, 32, 36, 40, and 44 give a sufficient number of points to generate a reliable calibration curve.

The mass spectrometric part of the analyses follows a similar approach, where a mixture of organic components is analyzed under the same conditions as the sample and characteristic mass fragments are correlated to the concentration of hydrocarbon types. The average carbon numbers of the hydrocarbon types are calculated from the spectral data. The mixture spectrum obtained is resolved into individual constituents using simultaneous equations derived from the mass spectra of the pure compounds.

BLANK DETERMINATION

Although every attempt is made during an analysis to use pure reagents and maintain a clean working environment, often there will be contamination from an unknown quantity of the analyte of interest in an analytical sequence. To minimize such effects, a blank should always be subtracted from the sample and standard measurement responses. The blank sample in such cases should contain the same quantities of reagents or solvents added to the samples and undergo the same processing steps to mimic a sample treatment.

Referenced Standards

D445	Test Method for Kinematic Viscosity of Transparent and Opaque Liquids (and Calculation of Dynamic Viscosity)
D482	Test Method for Ash from Petroleum Products
D874	Test Method for Sulfated Ash from Lubricating Oils and Lubricants
D2622	Test Method for Sulfur in Petroleum Products by Wavelength Dispersive X-ray Fluorescence Spectrometry
D4294	Test Method for Sulfur in Petroleum and Petroleum Products by Energy Dispersive X-ray Spectrometry
D4951	Test Method for Determination of Additive Elements in Lubricating Oils by Inductively Coupled Plasma Atomic Emission Spectrometry
D5185	Test Method for Determination of Additive Elements, Wear Metals, and Contaminants in Used Lubricating Oils and Determination of Selected Elements in Base Oils by Inductively Coupled Plasma Atomic Emission Spectrometry
D6792	Practice for Quality System in Petroleum Products and Lubricants Testing Laboratories
D7171	Test Method for Hydrogen Content of Middle Distillate Petroleum Products by Low Resolution Pulsed Nuclear Magnetic Resonance Spectrometry
D7260	Practice for Optimization, Calibration, and Validation of Inductively Coupled Plasma Atomic Emission Spectrometry for Elemental Analysis of Petroleum Products and Lubricants
D7343	Practice for Optimization, Sample Handling, Calibration, and Validation of X-ray Fluorescence Spectrometry Methods for Elemental Analysis of Petroleum Products and Lubricants

D7691	Test Method for Determination of Metals in Crude Oils by ICP-AES
E77	Test Method for Inspection and Verification of Thermometers
E168	Practice for General Techniques of Infrared Quantitative Analysis
E287 / 288	Specification for Laboratory Glass Graduated Burets and Volumetric Flasks
E319	Practice for the Evaluation of Single Pan Mechanical Balances
E542	Practice for Calibration of Laboratory Volumetric Apparatus
E898	Test Method of Testing Top-Loading, Direct-Reading Laboratory Scales and Balances
E932	Practice for Describing and Measuring Performance of Dispersive Infrared Spectrometers
E1252	Practice for General Techniques for Qualitative Infrared Analysis
E1421	Practice for Describing and Measuring Performance of FT-IR Spectrometers
E1866	Guide to Establishing Spectrophotometer Performance Tests
E1944	Practice for Describing and Measuring Performance of Fourier Transform Near Infrared Spectrometers
E2251	Specification for Liquid-in-Glass ASTM Thermometers with Low Hazard Precision Liquids

References

[1] Nadkarni, R. A., "Zen and the Art (or Is It) Science of a Perfect Analysis," *J. ASTM Intl*., Vol. 2, No. 3, 2005, pp. 1–13.

[2] Taylor, J. K., *Quality Assurance of Chemical Measurements*, Lewis Publishers, Chelsea, MI, 1987.

[3] May, W., Parris, R., Beck, C., Fasset, J., Greenberg, R., Guenther, F, Kramer, G., Wise, S., Gills, T., Gettings, R. and MacDonald, B. "Definition of Forms and Models Used at NIST for Value-Assignment of Reference Materials for Chemical Measurements," *NIST Special Publication, 260-136,* 2000.

[4] Nadkarni, R. A., and Morrison, G. H., "Use of Standard Reference Materials as Multielement Irradiation Standards in Neutron Activation Analysis," *J. Radioanal. Chem*., Vol. 43, 1978, pp. 347–369.

3

Quality Assurance in Spectroscopic Analysis of Petroleum Products and Lubricants

R. A. Kishore Nadkarni[1]

INTRODUCTION

Quality assurance (QA) has been a fact of life in virtually all chemical processes and industries for many decades. Quality is an ingrained attitude, the results of which have a positive impact on all operations. Production of quality data does not occur automatically and is not guaranteed by following any one procedure or even several established procedures. It needs dedicated effort, careful attention to details, and practice of recognized principles of quality assurance.

Modern quality assurance is based on the premise that measurement can be established as a process that can be in a state of statistical control, achievable by applying the principles of quality control. The output of such a process can be described statistically and limits can be assigned for the confidence of single measurements. Hence, limits of uncertainty can be established for the data. Taylor [1] distinguishes between quality assurance and quality control. Quality assurance is a system of activities, the purpose of which is to provide to the producer and the user of a product or service the assurance that it meets defined standards of quality with a stated level of confidence. The QA system includes the separate but coordinated activities of quality control and quality assurance. Quality control is the overall system of activities designed to control the quality of a product or service so that it meets the needs of users. Inspection can play an important role in quality control. Inspection steps during sampling, calibration, and measurement can detect defects, malfunctions, or other problems that could jeopardize the analytical process and that should trigger corrective actions to rectify the causes and stabilize the system.

Similar to the measurements of chemical or physical properties, spectroscopic measurements should also be subjected to rigorous scrutiny for the validity and fitness for use of the data produced. As a part of the spectroscopic measurements themselves, there do exist certain protocols to validate the resulting data. These should be supplemented by additional statistical protocols used to review and maintain the statistical integrity of the spectroscopic data.

Table 1 gives the definitions of various statistical and other related terminology used in this chapter.

This chapter is divided into three main parts although sometimes these areas overlap with each other: (1) Overall laboratory quality control, (2) statistical quality control of spectroscopic data, and (3) data handling protocols.

[1] *Millennium Analytics, Inc., East Brunswick, New Jersey*

TABLE 1—Definition of Terminology Used in This Chapter

Term	Definition	Source
Accuracy	The closeness of agreement between a test result and an accepted reference value.	D6299
ANOVA	Analysis of variance: A procedure for dividing the total variation of a set of data into two or more parts, one of which estimates the error due to selecting and testing specimens and the other part or parts possible sources of added variation.	D6300
ARV	Accepted reference value: A value that serves as an agreed-upon reference for comparison and that is derived as (a) a theoretical or established value based on scientific principles, (b) an assigned value based on experimental work of some national or international organization, such as the U.S. National Institute of Standards and Technology (NIST), or (c) a consensus value, based on collaborative experimental work under the auspices of a scientific or engineering group.	D6299
Assignable cause	A factor that contributes to variation and that is feasible to detect and identify.	D6299
ATV	Assigned test value: The average of all results obtained in the several laboratories that are considered acceptable based on the reproducibility of the test method.	D3244
Bias	The difference between the population mean of the test results and an accepted reference value.	D6300
	A systematic error that contributes to the difference between a population mean of the measurements or test results and an accepted reference or true value.	D6299
Calibration	The determination of the value of the significant parameters by comparison with values indicated by a set of reference standards.	D6595
Calibration standard	A standard having an accepted reference value for use in calibrating a measurement instrument or system.	D6595
	A material with a certified value for a relevant property, issued by or traceable to a national organization such as NIST, and whose properties are known with sufficient accuracy to permit its use to evaluate the same property of another sample.	D6792
Certified reference material (CRM)	A reference material, one or more of whose property values are certified by a technically valid procedure, accompanied by a traceable certificate or other documentation which is issued by a certifying body.	D6792

(*Continued*)

TABLE 1—Definition of Terminology Used in This Chapter (Continued)

Term	Definition	Source
Check standard	A material having an assigned (known) value (reference value) used to determine the accuracy of the measurement instrument or system. This standard is not used to calibrate the measurement instrument or system.	D7171
Common cause	One of the generally numerous factors, individually of relatively small importance, that contributes to variation and that is not feasible to detect or control.	D6299
Control chart	An X-Y chart with results obtained on the Y axis versus the sequential observation period on the X axis, and with mean, 1, 2, and 3 sigma lines drawn on it, to check whether the measurements are in statistical control. The most commonly used control chart in the chemical industry is individuals (called X or I) chart, which is a modified Shewhart chart.	. . .
Control limits	Limits on a control chart that are used as criteria for signaling the need for action or for judging whether a set of data does or does not indicate a state of statistical control.	D6299
CpK	Process capability index, defined as minimum of either upper specification limit–average or average–lower specification limit divided by three sigma deviations. A CpK of $>$1.33 indicates a process that meets the specifications. A value of $<$1.00 CpK indicates the process is not adequate to meet specifications and the process or specifications must be changed.	. . .
Degrees of freedom	The divisor used in the calculation of variance. Usually, it is n–1, where n is the number of results.	D6300
Detection limit	A stated limiting value that designates the lowest concentration that can be determined with confidence and that is specific to the analytical procedure used.	D7111
EWMA	Exponentially weighted moving average control chart.	D6984
Fit for use	A product, system, or service that is suitable for its intended use.	D6624
GLP	Good laboratory practice: Guidelines for the management of laboratory experiments that are published by regulatory agencies or other recognized groups and are concerned with the organizational process and the conditions under which laboratory studies are planned, performed, monitored, recorded, and reported. An example would be the ASTM Standard Guide D6792.	D6046

TABLE 1—Definition of Terminology Used in This Chapter (Continued)

Term	Definition	Source
NIST	National Institute of Standards and Technology, Gaithersburg, MD; formerly known as National Bureau of Standards (NBS).	. . .
OOSC	Out-of-statistical-control data or chart. A process is called OOSC if the process fluctuates unpredictably, if there is a trend step-jump in the readings, if there is any change in the system of random variation, or if there is autocorrelation present in the readings.	. . .
Outlier	A result far enough in magnitude from other results to be considered not a part of the set.	D6300
PLOQ	Pooled limit of quantitation: Level of property or concentration of analyte above which the quantitative test results can be obtained with a specified degree of confidence.	D6259
Precision	The closeness of agreement between the test results obtained under prescribed conditions.	D6299
	The degree of agreement between two or more results on the same property of identical test material. Precision statements are quoted as repeatability or reproducibility (see below).	D6300
Precision ratio	An estimate of the relative magnitude of repeatability and reproducibility. The PR for a given standard test method can provide information on the relative significance between variation caused by different operators and laboratories compared to a single operator in a single laboratory performing the standard test method. Essentially it is ratio of reproducibility over repeatability of a test.	D6792
Proficiency testing	Determination of a laboratory's testing capability by evaluating its test results in interlaboratory exchange testing or cross-check programs.	D6792
Quality assurance	A system of activities, the purpose of which is to provide to the producer and user of a product, measurement, or service the assurance that it meets the defined standards of quality with a stated level of confidence; quality assurance includes quality planning and quality control.	D6792
Quality control	A planned system of activities whose purpose is to provide a level of quality that meets the needs of users.	D6792

(*Continued*)

TABLE 1—Definition of Terminology Used in This Chapter (Continued)

Term	Definition	Source
Quality control sample	A sample for use in quality assurance program to determine and monitor the precision and stability of a measurement system; a stable and homogenous material having physical or chemical properties, or both, similar to those of typical samples tested by the analytical measurement system. The material is properly stored to ensure sample integrity, and is available in sufficient quantity for repeated long-term testing.	D6792
Quality index	A mathematical formula that uses data from controlled parameters to calculate a value indicative of control performance.	D6984
Quality management	Management of quality assurance activities of a laboratory or site.	. . .
Reference material	A material with accepted reference value(s), accompanied by an uncertainty at a stated confidence level for desired properties, which may be used for calibration or quality control purposes in the laboratory. The RMs issued by NIST are called standard reference materials (SRM).	D6792
Relative bias	The difference between the population mean of the test results and an accepted reference value, which is the agreed-upon value obtained using an accepted reference method for measuring the same property.	D6300
Repeatability (r)	The quantitative expression of the random error associated with a single operator in a given laboratory obtaining repetitive results by applying the same test method with the same apparatus under constant operating conditions on identical test material within a short interval of time on the same day. It is defined as the difference between two such results at the 95 % confidence level.	D6300
Representative sample	A part of a homogenous material, or a part of the composited and mixed portions of a material, that carries all the true properties and physical characteristics of the whole material.	D4296
Reproducibility (R)	A quantitative expression of the random error associated with different operators from different laboratories, using different apparatus, each obtaining a single result by applying the same method on an identical test sample. It is defined as the 95 % confidence limit for the difference between two such single and independent results.	D6300
Run chart	A plot of data in chronological order without control limits.	. . .

TABLE 1—Definition of Terminology Used in This Chapter (Continued)

Term	Definition	Source
Site precision (R′)	The value below which the absolute difference between two individual test results obtained under site precision conditions may be expected to occur with a probability of approximately 95 %. It is defined as 2.77 times the standard deviation of results obtained under site precision conditions.	D6792
SOSC	State-of-statistical-control chart or data. Over time, a SOSC process should exhibit a mean value that does not change; variability that does not change; no existence of a pattern in the time sequence of the readings; and normal distribution of points that does not change.	. . .
Standard deviation	The most common measure of the dispersion of observed results expressed as the positive square root of the variance.	D6300
Standard reference material (SRM)	A term used by NIST for their CRMs.	. . .
Statistical quality assurance (SQA)	A system of activities to provide the producer and user of a product or service the assurance that it meets the defined quality standards with a stated level of confidence. Generally, the QC system used in a laboratory is termed SQA.	. . .
Statistical quality control (SQC)	The overall system of activities designed to control the quality of a product or service so that it meets the needs of users. Inspection can play an important role in quality control.	. . .
Test performance index (TPI)	An approximate measure of a laboratory's testing capability, defined as the ratio of test method reproducibility to site precision.	D6792
True value	The value toward which the average of single results obtained by N laboratories tends, when N becomes very large. Consequently, such a true value is associated with the particular test method employed. It is recognized that sometimes a true value may not be equal to the method average, if the method has a bias.	D3244
Variance	A measure of the dispersion of a series of accepted results about their average. It is equal to the sum of the squares of the deviation of each result from the average, divided by the number of degrees of freedom.	D6300

(*Continued*)

TABLE 1—Definition of Terminology Used in This Chapter (Continued)

Term	Definition	Source
X or I control charts	A chart of individual (I) values plotted in the form of a Shewhart X-bar chart for subgroup size n = 1. It is a widely used control chart in the chemical industry because due to the cost of testing, test turnaround time, and the time interval between independent samples, usually only a single measurement is made. In such cases I chart is the only practical choice.	. . .

PART I – LABORATORY QUALITY MANAGEMENT

Quality assurance must be viewed as an integral part of the complete analytical sequence, and not as an unnecessary added burden. It is surprising how many otherwise perfectly good, even ISO 9000 registered laboratories do not practice statistical quality assurance. A typical analytical sequence must be

Calibration Practices

Measuring and testing equipment used in the testing laboratory should be calibrated where appropriate before being put into service and thereafter according to an established program. The overall program of calibration of equipment should be designed and operated so as to ensure that the measurements made in the testing laboratory are traceable (where the concept is applicable) to national standards of measurement and, where available, to international standards of measurement specified by the International Committee of Weights and Measures. Where the concept of traceability to national or international standards of measurement is not applicable, the testing laboratory should provide satisfactory evidence of correlation or accuracy of the test results (for example, by participation in a suitable program of interlaboratory comparisons; see later section on proficiency testing), or by primary methods such as interference free classical chemistry techniques such and gravimetry or titrimetry.

Reference standards of measurement should be calibrated by a competent body that can provide traceability to a national or international standard of measurement. Where relevant, in-service testing equipment should be subjected to checks between regular recalibrations. Reference materials should where possible be traceable to the national or international standard reference material.

Different test methods require different types of calibrations; hence, decisions must be made on a case-by-case basis as to what is the most appropriate

calibration and its frequency. It goes without saying, however, that the calibration practices are a must for all analytical testing and must be thoroughly documented both regarding the plan and the factual evidence that it is followed. The calibration schedules will vary with the instrument type, some needing calibration before each set of analyses, others requiring calibration at less frequent intervals.

A new instrument should certainly be calibrated before putting it in use. Frequency of calibration thereafter will be dependent on the industry practices, SQA data, or written requirements of the standard test method. In the last case, where calibration is an integral part of the test method, calibrations must be done before samples are analyzed. Under no circumstances should the samples be analyzed if the instrument is found to be out of calibration.

Quality Control Samples

The sample selected for QC analyses should be homogeneous, stable, well characterized for the analyses of interest, available in sufficiently large quantities, and, hopefully, representative of the actual samples being analyzed. The material should be well characterized for the analyses of interest and have concentration values that are within the calibration range of the test method. It is not advisable to use the same sample for both calibration and quality control. If the concentration value for the species of interest is not known, replicate analyses should be performed to obtain such value. If the QC material is observed to be degrading or changing in physical or chemical characteristics, this should be immediately investigated and, if necessary, a replacement QC material should be prepared for use.

All routinely performed tests that result in quantitative data should have quality control samples analyzed as part of the complete analytical cycle. The frequency of SQA analysis will depend on the type of analysis and the instrument involved. Certainly at least one SQA standard should be analyzed with each lot of samples analyzed. Preferably one SQA standard should be analyzed before and after a series of analyses; even better, a few SQA samples should be interspersed with several real samples to continuously monitor the analytical data quality. A rule of thumb generally used is one SQA sample per five to ten samples.

Principal factors to consider for determining the frequency of testing include:

1. Frequency of use of the analytical measurement system
2. Criticality of the parameter being measured and business economics
3. Established system stability and precision performance based on past history
4. Regulatory requirements
5. Contractual provisions
6. Test method requirements.

Table 2 lists recommended minimal QC frequencies as a function of precision ratio (PR) and TPI. For those tests that are performed infrequently, say 25 samples spread over a month, at least one QC sample should be analyzed each time samples are analyzed. In some cases, the minimal QC frequency recommended in Table 2 may not be sufficient to ensure adequate statistical quality control, considering, for example, the significance of the use of such results. The TPI should be recalculated and reviewed at least annually. Adjustments to the QC frequency may be made based on the recalculated TPIs. Special

TABLE 2—Minimal QC Frequency as a Function of TPI			
TPI for Standard Test Methods with PR <4	**TPI for Standard Test Methods with PR =/> 4**	**Normal Quality Control Frequency**	**Approximate Percentage of QC Samples per Total Analyses**
Not determined	Not determined	10	9
< 0.8	< 1.6	10	9
0.8 – 1.2	1.6 – 2.4	20	5
1.2 – 2.0	2.4 – 4.0	35	3
> 2.0	> 4.0	40	2

treatment of QC samples to get a better result should be avoided because this seriously undermines the integrity of precision and bias estimates.

If the SQA sample indicates out-of-control results, immediate remedial action must be taken before analyzing further samples. Once the SQA frequency is established and the analysis appears to be in control over a long period of time, the QC frequency may be reduced.

Quality Control Charts

All QC data generated in the laboratory must be promptly plotted on a control chart, either manually or electronically. The charts used may be of any standard types available, such as I chart, $\bar{x}$ chart, moving average and moving range, exponentially weighted moving average (EWMA), or cumulated sums (CUSUM) charts. The person who performs the actual analyses should add the data points to the control charts immediately after completing the analyses, and verify that the test is under statistical control. Plotting a chart is not an end itself. The statistical behavior that data are indicating must be acted upon. There are a number of statistical run rules; at least three to four of the most-commonly used run rules should be followed (see below). If the run rules show out-of-control data, immediate remedial action must be taken to bring the analyses back in control. Periodically, the charts should be reviewed to identify the root causes of common out-of-statistical-control situations so that they can be remedied.

STATISTICAL RUN RULES

It is pointless to analyze the QC samples and plot the control charts if no attention is paid to the messages that the charts are giving. There are about 15 run rules in the literature used for identifying the OOSC data patterns [2]. Obviously it is impossible to use all of them on a routine basis. It is also undesirable because of overlapping rules and increased probability of false positives. The most commonly used four run rules that should be used for detecting OOSC behavior are given below. A laboratory may choose to use different run rules if there is a valid technical or business reason.

1. One data point beyond the action line.
2. Two out of three data points beyond the warning line.

3. Four out of five data points beyond the bias line.
4. Seven out of eight consecutive points on the same side of the mean.

The corrective actions taken must be recorded whenever an out-of-control data trend is recognized, and this documentation becomes a permanent record of the lab's quality history. When an OOSC situation has been identified:

1. Do not report the sample's data to the plant or the customer.
2. Take the particular instrument out of use.
3. Notify plant management of the status.
4. Trouble-shoot the problem to take corrective action.

When back in control, recheck last several retains to ascertain that all results are within the test repeatability limits.

Out-of-control situations may be detected by one or more analyses. In such cases it may be necessary to reanalyze the sample previously analyzed during the period between the last-in-control QC data point and the QC data point that triggered the out-of-statistical-control notice using retained samples and equipment known to be in control. If the new analysis shows a difference that is statistically different from the original results, and the difference exceeds the established site precision for that test, the laboratory should decide on what further action may be necessary.

Revision of Control Charts

Control charts should be revised only when the existing limits are no longer appropriate, but not simply because the existing page has been filled up. Revision is permitted in the following circumstances:

1. Sometimes, the trial control limits are set up based on fewer than 20 individual points or subgroups. Later, when 20 to 30 individual points or subgroups become available, the control chart can be reconstructed.
2. When the process has improved and this results in a special cause on the chart, the control chart can be reconstructed with narrower control limits.
3. When the control chart remains out of control for an extended period (20 or more subgroups), and all attempts to identify and eliminate the special cause have been exhausted, the control chart can be reconstructed with wider control limits.
4. When the existing QC material is used up and a new similar material is initiated, which may have a mean value somewhat different than the previous QC material, before completely switching to the new material, for some time period analyze both old and new QC samples to establish the traceability and ensure that the system is under control. The control limits for the new QC sample may be different from the old sample.

Laboratory Capability Review

Using the control charts or the SQA data, a laboratory should on some frequent basis—monthly or quarterly—calculate what the laboratory's precision is for individual tests. These sigmas compared with those given in, e.g., ASTM test methods, can give a clear picture as to how well a laboratory is performing against the industry standards. If the laboratory precision is significantly worse than the values suggested in the standard methods, an investigation should be launched to find the root cause for poor performance and devise corrective action to improve it. Such a periodic review should be a key feature of a

laboratory's continuous improvement program. For the purpose of this review, the term TPI is defined as:

ASTM Reproducibility / (Laboratory Standard Deviation X 2.77).

A laboratory precision worse than the published test method reproducibility may indicate poor performance. An investigation should be launched to determine the root cause for this performance so that corrective action can be undertaken if necessary. Such a periodic review should be a key feature of a laboratory's continuous quality improvement program. A guideline for relationship between the TPI value and the need to take action is summarized in Table 3.

CORRECTIVE AND PREVENTIVE ACTION

The need for corrective and preventive action may be indicated by one or more of the following unacceptable situations:

- Equipment out of calibration
- QC or check sample results out of control
- Test method performance by the laboratory does not meet performance criteria
- Product, material, or process out of specification data
- Outlier or unacceptable trend in an interlaboratory cross-check program
- Nonconformance identified in internal or external audit
- Nonconformance identified during review of laboratory data or records
- Customer complaint.

When any of these situations occur, the root cause should be investigated and identified. Several ways of handling such situations are described in Table 4, excerpted from ASTM Standard Guide D6728.

TABLE 3—Guidelines for Action Based on TPI Values

TPI for Test Methods with PR <4	TPI for Test Methods with PR >4	Recommended Quality Improvement Action
> 1.2	> 2.4	Indicates that the performance is probably satisfactory relative to ASTM published precision.
> 0.8 and < 1.2	> 1.6 and < 2.4	Indicates that the performance may be marginal relative to ASTM published precision; however, a method review could be necessary to improve its performance.
< 0.8	< 1.6	Suggests that the method as practiced at this site is not consistent with the ASTM published precision. Either laboratory method performance improvement is required, or the ASTM published precision does not reflect achievable precision. Existing interlaboratory proficiency testing performance (if available) should be reviewed to determine if the latter is plausible.

TABLE 4—A Checklist for Investigating the Root Cause of Unsatisfactory Analytical Performance
To identify why a laboratory's data may have been considered a statistical outlier and/or to improve the precision, the following action items are suggested. There may be additional ways to improve the performance.
1. Check the results for typos, calculation errors, and transcription errors.
2. Reanalyze the sample; check for repeatability.
3. Check the sample for homogeneity or contamination, and that a representative specimen has been analyzed.
4. Review the test method and ensure that the latest version of the ASTM test method is being used. Check the procedure step by step with the analyst.
5. Check the instrument calibration.
6. Check the statistical quality control chart to see if the problem has been developing earlier.
7. Check the quality of the reagents and standards used, and whether they are expired or contaminated.
8. Check the equipment for proper operation against vendor's operating manual.
9. Call the vendor for maintenance or repairs.
10. After the problem has been resolved, analyze a certified reference material if one is available, or the laboratory quality control sample to ascertain that the analytical operation is under control.
11. Provide training to new analysts and, if necessary, refresher training to the experienced analysts.
12. Document the incident and the lessons learned for use in future similar problems.

Reference Materials

Each laboratory should designate primary reference standards (e.g., CRS, calibrants) and secondary QC standards that it uses. In some cases, primary standards may be used as QC standards. These should be stored in a safe and environmentally stable atmosphere so that the RMs do not degrade. It is desirable to have such standards traceable to national bodies (such as NIST). Often when such primary RMs are not available, a laboratory may prepare its own standards following the certification protocol used by NIST (see below).

The primary calibration SRM values should be based on replicate analyses carried out on randomly selected aliquots of a stable homogeneous material of interest. The values should be corroborated by two independently based methods of known precision and accuracy and free from interference, one method used independently by two expert analysts, or different methods used in a round robin by expert analysts.

All of the analyses should be simultaneously accompanied by an analysis of known standard reference materials, or previously certified standards. In all the above cases, the resultant data should be statistically examined for outliers

and calculated for mean and variance values. Standards for routine quality control in the laboratory do not need such thorough study.

Generally, it is not advisable to use the same material both as a calibrant and a QC. The latter should be similar in matrix to the type of samples that are being analyzed, although this is not always feasible. When a commercially available RM is not available for QC purposes, it may be prepared by:

- Obtaining a large, stable, and homogeneous sample of a plant product, which is stable for long periods. The sample should be similar to the typical products tested.
- Analyzing this material for species of interest, while the analytical process is under statistical control, and ensuring that the instrument used is calibrated using primary SRM. At least 20 replicates spread over different days and by different analysts shall be obtained on the proposed QC sample. Collecting data in close proximity to each other and by "the best" analyst should be avoided.
- Based on the above replicate analyses, mean and standard deviation values should be assigned to this QC sample.
- The laboratory analysts should use the above secondary QC standard for the routine SQA program. Anytime the control chart indicates an out-of-control analysis, all aspects of the analytical process should be checked and the primary SRM, CRS, or certified standard should be analyzed if necessary. Remedial action should be taken appropriate to the findings.
- When the stock of the existing primary or QC standard becomes depleted, aliquots of these should be analyzed during certification of the new batch of standards, to maintain traceability. If an SRM or CRS is observed to be degrading or changing in physical or chemical characteristics, this should be immediately investigated and, if necessary, a replacement SRM or CRS should be prepared.

NIST refers to their CRMs as SRMs (standard reference materials). See NIST Special Publication 260-136 for details of NIST's certification program [3]. Also, see Chapter 5 on an update about the NIST SRMs for petroleum products and lubricants. Some of the SRMs in the petroleum products area issued by NIST that can be used in spectroscopic analysis are listed in Table 5. This information is extracted from reference [3]. Use of such standards is highly recommended in laboratories to understand the precision and accuracy that their laboratory can achieve.

Cross Checks and Proficiency Testing

Interlaboratory cross-checks help identify a particular laboratory's capability against those in the same industry. When a laboratory is less precise than others, cause of this must be searched and eliminated. In cases of quality complaints, cross-checks give better confidence regarding a customer's or supplier's data quality. Participation in a cross-check is not an end in itself. In the spirit of continuous improvement, it is critical to study the resultant data and act where necessary to eliminate the deficiencies in a lab's performance.

The cross-checks should be conducted on homogeneous and stable materials. Precautions must be taken to ensure that the material does not degrade or decompose between dispatch and receipt. Sufficient numbers of laboratories and samples should be included in a cross-check to be able to obtain statistically meaningful conclusions. ASTM recommends use of minimum five laboratories and more than ten different samples. As the number of laboratories/samples goes

TABLE 5—NIST SRMs for Spectroscopic Method of Analysis of Petroleum Products and Lubricants		
Base oil	1819	Sulfur
Crude oil	2721; 2722	Sulfur
	8505	Vanadium
Diesel fuel	1623; 1624; 2724; 2770; 8771	Sulfur
Di-n-butyl sulfide	2720	Sulfur
Fuel oil distillate	1624	Sulfur
Gas oil	8590	Sulfur
Gasolines – high octane	2298	Sulfur
	2286; 2287	Ethanol
Gasolines – RFG	2292; 2293	MTBE
	2294 – 2297; 2299	Sulfur
Kerosine	1616; 1617	Sulfur
Lubricating oil	1818	Chlorine
	1836	Nitrogen
Lubricating oil additive	1848	Sulfur, metals, etc.
Petroleum coke	2718; 2719	Sulfur
Reference fuel	1636 – 1638; 2712 – 2715	Lead
Residual fuel oil	1619 – 1623	Sulfur
	1634	Sulfur + trace elements
	1618; 2717	Vanadium + nickel

up, the number of samples/laboratories may be reduced, although this is not required if enough laboratories/samples are available. Obviously, the more samples and laboratories available, the stronger the resultant statistical conclusions. The obtained data should be analyzed for statistical outliers, which are deleted before calculating the intralaboratory repeatability and interlaboratory reproducibility. In addition to the data tables, graphical data representation is highly useful for a quick synopsis of a laboratory's performance in the cross-check.

All laboratories should take part in all cross-checks relevant to their areas of product manufacture. They should also participate in the ASTM industry-wide, interlaboratory cross-check program, if available.

Where a laboratory's performance is below that of the rest of the participating laboratories, the laboratory should take corrective actions to improve its precision and accuracy.

ASTM D02.CS 92 group has established an extensive proficiency testing program for petroleum products and lubricants since 1993. Currently approximately 2500 laboratories worldwide are taking part in 23 product programs. Nadkarni and Bover have described this program in detail [4]. These programs and the spectroscopic analysis included in them are listed in Table 6. Regular participation in interlaboratory proficiency testing programs, where appropriate samples are tested by multiple test facilities using a specified test protocol, should be

TABLE 6—ASTM D02 Committee's Proficiency Testing Programs

Material	Spectroscopic Tests Involved
#2 Diesel fuel	Sulfur: D2622; D4294; D5453
#6 Fuel oil	Wear metals: D5185
	Sulfur: D2622, D4294
	V, Ni, Fe, Na: D5708; D5863
Automatic transmission fluid	Metals: D4628; D4927; D4951; D5185
Automotive lubricant additive	Metals: D4628; D4927; D4951; D5185
Aviation turbine fuel	Sulfur: D2622; D4294; D5453
Base oil	Sulfur: D2611; D4294
Biodiesel	Metals: EN14538
	Phosphorus: D4951
	Sulfur: D5453
Crude oil	Ni, V, Fe: D5708; D5863
	Wear metals: D5185
	Sulfur: D2622; D4294
Fuel ethanol	Sulfur: D5453
Gear oil	Additive elements: D4951; D5185
	Sulfur: D4294
General gas oil	Sulfur: D2622; D4294
	V, Ni, Fe, Na: D5863; D5708
Hydraulic fluid oils	Elements: D4951; D5185
In-service diesel oil	Elements: D6481
	Wear metals: D5185; D6595
	FT-IR
In-service hydraulic fluids	Wear metals : D4951; D5185; D6595

TABLE 6—ASTM D02 Committee's Proficiency Testing Programs (Continued)	
Material	**Spectroscopic Tests Involved**
Lubricating oil	Additive elements: D4628; D4927; D4951; D5185
	Sulfur: D5453
Motor gasoline	Organics: D3606; D4053; D5580; D5769
	Sulfur: D2622; D4294; D5453; D7039
Reformulated gasoline	Organics: D3606; D5580; D5769
	Olefins: D6550
	Sulfur: D2622; D4294; D5453
Ultra low sulfur diesel	Sulfur: D2622; D5453; D7039; D7212

integrated into the laboratory's QC program. Proficiency test programs should be used as appropriate by the laboratory to demonstrate testing proficiency relative to other industry laboratories. Participation in such proficiency testing should not, however, be considered as a substitute for in-house quality control.

A guide for the analyses of data and interpretation of proficiency testing is available as ASTM Standard Guide D7372. A key learning of such review is calculation of TPI. Limits and actions needed to be taken based on TPIs are given in Table 3. If analytical performance is unsatisfactory, the root cause investigation tool given in Table 4 should be used.

PART 2 – STATISTICAL DATA HANDLING

Table 1 gave the definitions of various statistical and other related terminology used in this chapter. Table 7 lists the ASTM and other international standards relevant to the discussion that follows. Much of the discussion that follows in this section is based on some of these standards.

TABLE 7—Statistical Standards for Use in Data Analysis	
Standard	**Description**
D3244	Practice for Utilization of Test Data to Determine Conformance with Specifications
D3764	Practice for Validation of Process Stream Analyzers
D6122	Practice for Validation of Multivariate Process Infrared Spectrophotometers
D6259	Practice for Determination of a Pooled Limit of Quantitation
D6299	Practice for Applying Statistical Quality Assurance Techniques to Evaluate Analytical Measurement System Performance
D6300	Practice for Determination of Precision and Bias Data for Use in Test Methods for Petroleum Products and Lubricants

(*Continued*)

TABLE 7—Statistical Standards for Use in Data Analysis (Continued)

Standard	Description
D6617	Practice for Laboratory Bias Detection Using Single Test Result from Standard Material
D6708	Practice for Statistical Assessment and Improvement of the Expected Agreement Between Two Test Methods that Purport to Measure the Same Property of a Material
D6792	Guide for Quality System in Petroleum Products and Lubricants Testing Laboratories
D7372	Guide for Analysis and Interpretation of Proficiency Test Program Results
E29	Practice for Using Significant Digits in Test Data to Determine Conformance with Specifications
E177	Practice for Use of the Terms Precision and Bias in ASTM Test Methods
E178	Practice for Dealing with Outlying Observations
E456	Terminology Relating to Quality and Statistics
E548	Guide for General Criteria Used for Evaluating Laboratory Competence
E691	Practice for Conducting an Interlaboratory Study to Determine the Precision of a Test Method
E882	Guide for Accountability and Quality Control in the Chemical Analysis Laboratory
E994	Guide for Calibration and Testing Laboratory Accreditation Systems General Requirements for Operation and Recognition
E1301	Guide for Proficiency Testing by Interlaboratory Comparisons
E1323	Guide for Evaluating Laboratory Measurement Practices and the Statistical Analysis of the Resulting Data
E1329	Practice for Verification and Use of Control Charts in Spectrochemical Analysis
ISO 4259	Petroleum Products – Determination and Application of Precision Data in Relation to Methods of Test
ISO 9000 – 9004	Quality Management System Standards
ISO 17025	General Requirements for the Technical Competence of Testing and Calibration Laboratories
ASTM MNL 7	Manual on Presentation of Data Control Chart Analysis, 6th Ed.
ASTM STP 15D	ASTM Manual on Presentation of Data and Control Chart Analysis

Rounding of Test Results

Test data should be rounded off to significant digits per ASTM practices E29 and E380. The laboratory data reporting systems, whether manual or computer-based, should conform to these practices. Only a meaningful string of digits should be reported, and not what a calculator or a computer displays or prints out. The rounding off should not be done in a string of calculations, until the last step. The converted values should be rounded to the minimum number of significant digits that will maintain the required accuracy. In certain cases, the deviation from this practice to make use of convenient or whole numbers may be feasible, in which case the worst "approximate" must be used following the conversion. For example, when converting the integral values of units, consideration must be given to the implied or required precision of the integral value to be converted. For example, the value 4 mg/kg may be intended to represent 4, 4.0, 4.00, 4.000 or 4.0000 mg/kg., or even greater accuracy. Obviously, the converted value must be carried to a sufficient number of digits to maintain the accuracy implied or required in the original quantity.

Any digit that is necessary to define the specific value or quantity is said to be significant. When measured to the nearest 1 m, a distance may be recorded as 157 m; this number has three significant digits. If the measurement has been made to the nearest 0.1 m, the distance may have been 157.4 m; this number has four significant digits.

Zeros may be used either to indicate a specific value like any other digit, or to indicate the order of magnitude of a number.

The rounding-off method applies where it is the intent that a limited number of digits in an observed value or a calculated value are to be considered significant for purposes of determining conformance with specifications. With the rounding-off method, an observed value or a calculated value should be rounded off to the nearest unit in the designated place of figures stated in the standard, as, for example, "to the nearest 100 psi," "to the nearest 10 ohms," "to the nearest 0.1 percent." The rounded-off value should then be compared with the specified limit, and conformance or nonconformance with the specification based on this comparison. For example, the specification limits of 2.5 in. max., 2.50 in. max., 2.500 in. max. are taken to imply that, for purposes of determining conformance with specifications, an observed value or a calculated value should be rounded off to the nearest 0.1 in., 0.01 in., 0.001 in., respectively, and then compared with the specification limit.

The actual rounding-off procedure is as follows:

- When the digit next beyond the last place to be retained is less than 5, retain unchanged the digit in the last place retained, e.g., 6.44→6.4.
- When the digit next beyond the last place to be retained is greater than 5, increase by 1 the digit in the last place retained, e.g., 6.47→6.5.
- When the digit next beyond the last place to be retained is 5, and there are no digits beyond this 5, or only zeros, increase by 1 the digit in the last place retained if it is odd, leave the digit unchanged if it is even. Increase by 1 the digit in the last place retained, if there are digits beyond this 5, e.g., 6.35→6.4 or 6.65→6.6 or 6.651→6.7.
- This rounding-off procedure may be restated simply as follows: When rounding off a number to one having a specified number of significant digits, choose that which is nearest. If two choices are possible, as when the digits

dropped are exactly a 5 or a 5 followed only by zeros, choose that ending in an even digit. Table 8 gives examples of applying this rounding-off procedure.

In deciding whether a product is off-spec, consider the significant digits in the specification versus the laboratory analyses. For example, a saponification number of 45.3 is off-spec if the specification is 45.0, but not off-spec if it is 45, because the laboratory results would be rounded off to 45, assuming the laboratory precision is good only to two significant digits.

Also, see ASTM standard E29 for further details on rounding-off procedures.

Tests for Outliers

Before analyzing the data for any significance, the outliers in the data set need to be eliminated from the data set. Outliers are the individuals that statistically do not belong in a data set. They can result from causes such as blunders or malfunctions of the methodology, or from unusual contamination or losses. If outliers occur too often (> 25 % of the set), there may be deficiencies in the test. Possible outliers can be identified when data are plotted, or results are ranked, or control limits are exceeded. Only when a measurement system is well understood, and the variance is well established, or when a large body of data is available, is it possible to distinguish between extreme values and true outliers with a high degree of confidence. Whenever an outlier is suspected, an assignable cause should be looked for, e.g., miscalculation, use of wrong units, system malfunction, sample misidentification, contamination, transcription errors. Rules for data rejection

TABLE 8—Examples of Rounding-Off

Observed Value	Round Off to Nearest	Correct Rounded-Off Value
59,940 psi	100 psi	59,900 psi
59,950	100	60,000
59,960	100	60,000
56.4%	1%	56%
56.5	1	56
56.51	1	57
56.6	1	57
55.5	1	56
0.54%	0.1%	0.5%
0.55	0.1	0.6
0.56	0.1	0.6
0.406 ohm	0.01 ohm	0.41 ohm
0.405	0.01	0.40

should be used with caution, because in a well-behaved measurement system, an outlier should be a rare occurrence. The tests available for testing a suspected outlier, based on ranking the data and testing the extreme values for creditability, include Dixon, Grubbs, Cochran, and Youden tests. The Dixon test has the advantage that an estimate of the standard deviation is not needed to use it. The Cochran test is used when deciding whether a single estimate of a variance is extreme (i.e., excessively large) in comparison with a group with which it is expected to be comparable. Youden describes a test applicable to a group of laboratories to identify the ones that consistently report high or low results.

Tests for Equivalent Precision

After the outliers are removed, the method data sets can be compared with each other or against a set from standard test method to check which method has a better precision. The usual statistical tests used for this task are the Cochran test and the F-test. The Cochran test is used when deciding whether a single estimate of a variance is extreme (excessively large) in comparison with a group with which it is expected to be comparable. The F-test is used to compare the precision of the two sets of data, e.g., the results of two different analytical methods or the results from two different laboratories. F is the ratio of two variances, i.e., the squares of standard deviations. The value calculated for F is compared for its significance against the value in the F table, calculated from a Gaussian distribution corresponding to the number of degrees of freedom for the two sets of data. The data is expected to be Gaussian, but F itself has its own distribution.

Tests for Equivalent Accuracy

A second criterion applied to the data set is whether it has the same level of accuracy or bias as that obtained with the standard method. The statistical tests used for comparing accuracy of two methods when the reference materials with known values may or may not be available include Student's t-test, T-test, and paired t-test.

Student's t-test is used for small sample sets to compare the mean from a sample against a standard value and to judge the confidence in the significance of the comparison. It is also used to test the difference between the means of two sets of data. In the T-test, data from two different methods for the same analysis are compared for accuracy. The paired t-test is used when two methods of analysis analyze a set of samples with varying levels of analyte. It compares averages from two methods using paired observations.

Since these statistical tests are widely used and are fully described in standard statistical textbooks and in other literature, they will not be described in detail in this chapter.

Acceptability of Replicate Testing

Sometimes duplicate tests on a sample yield apparently different results, or tests run by the receiving laboratory may differ, casting doubt on the acceptability of the product in relation to its specification. Guidelines on interpreting such results are given in ASTM D 3244 and ISO 4259 standards.

Acceptability of Duplicate Intralaboratory Test Results

Most laboratories do not carry out more than one test on each product characteristic for routine quality control purposes. However, if the test result is off

specification, or if there is a dispute, more than one test may be run. In these abnormal circumstances, when multiple results are obtained in the same laboratory on the same sample, the consistency of the results must be checked against the repeatability of the method.

When only two results are obtained under repeatability conditions, and their difference is less than or equal to the repeatability, r, the test can be considered in control. The average of the two results shall be used as the estimated value of the property being testing. If the two results differ by more than repeatability, both shall be considered as suspect and at least three more results obtained. The difference between the most divergent results and the average of the remainder (including the first two) shall be calculated and compared with the repeatability. If the difference is less than or equal to r, all the results shall be accepted.

If the difference exceeds the repeatability, the most divergent result is rejected and the process repeated until an acceptable set of results is obtained. The average of all acceptable results shall be taken as the estimated value of the property. If two or more results from a total of not more than 20 have been rejected, the operating procedure and the apparatus shall be checked and a new series of tests made, if possible.

Acceptability of Interlaboratory Test Results in Quality Disputes

Many times the two analyses for the same test at the shipping point and the receiving point differ from each other. The following procedure should be used in such cases to decide which result truly represents the "true value."

When single results are obtained by two laboratories and their difference is less than or equal to the test's reproducibility, R, the two results shall be considered as acceptable and their average, rather than either one separately, shall be considered as the estimated value of the tested property.

If the two results differ by more than R, both are considered suspect. Each laboratory then obtains at least three other acceptable results by the procedure described above for repeatability. In this case, the difference between the average of all acceptable results of each laboratory is judged for conformity using a new value, R′, instead of R, given by:

$$R' = \sqrt{R^2 - (1 - \tfrac{1}{2K_1} - \tfrac{1}{2K_2}) \times r^2} \qquad (1)$$

where
R is the reproducibility of test method,
r is the repeatability of the test method,
K_1 is the number of results of the first laboratory,
K_2 is the number of results of the second laboratory.

If circumstances arise in which more than two laboratories supply single results, the difference between the most divergent result and the average of the remainder shall be compared with the reproducibility of the test method. If this difference is equal to or less than the reproducibility, all the results shall be regarded as acceptable and their average taken as the estimated value of the property.

If, however, the difference is greater than the reproducibility, the most divergent result is rejected and the procedure repeated until an acceptable set of results is obtained. The average of all acceptable results is taken as the estimated value of the property. If two or more results from a total of not more

than 20 have been rejected, the operating procedure and the apparatus should be checked and a new series of tests made, if possible.

Acceptability of Test Results Against Product Specifications

Many times a product, although shipped within test specifications, is reported as outside them by the receiver. If it is not possible for the supplier and the recipient to reach agreement about the quality of the product on the basis of their existing test results, then the following procedures should be adopted, based on ASTM standard D3244 and ISO standard 4259. Each laboratory shall reject its original results and obtain at least three other acceptable results on a check sample to ensure that the work has been carried out under repeatability conditions. The average of the supplier's results, $\bar{x}_s$ must be equal to or less than the upper specification limit, USL, or equal to or greater than the lower specification limit, LSL.

The product is accepted if the average of the receiver's results, $\bar{x}_R \leq$ USL or $\geq$ LSL. If the receiver's results, $\bar{x}_R >$ USL or $<$ LSL, the product is accepted if:

$$|\bar{x}_s - \bar{x}_R| \; < \; 0.84 \; R' \tag{2}$$

where R' is given by equation (1).

There is a possible dispute if $|\bar{x}_s - \bar{x}_R| > 0.84\,R'$, but it cannot be stated with confidence that the product does or does not comply with the specification limit; hence, resolution of the dispute may be by negotiation.

If $(\bar{x}_s + \bar{x}_R)/2 >$ USL or $<$ LSL, there is a dispute regardless of the difference $\bar{x}_s - \bar{x}_R$.

In case of dispute, the two laboratories shall contact each other and compare their operating procedure and apparatus. Following these investigations, a correlation test between the two laboratories shall be carried out on two check samples. The average of at least three acceptable results shall be computed in each laboratory, and these averages compared as indicated in Eqs (2) and (3).

If the disagreement remains, a third laboratory (neutral, expert, and accepted by the two parties) shall be invited to carry out the test using a third sample. This laboratory should obtain three acceptable results under repeatability conditions whose average is x_E. If the difference between the most divergent laboratory average and the average of the other two is less than or equal to R, then the product is accepted if:

$$(\bar{x}_s + \bar{x}_R + \bar{x}_E)/3 \; \leq \; \text{USL and/or} \; \geq \; \text{LSL} \tag{3}$$

The product is rejected if:

$$(\bar{x}_s + \bar{x}_R + \bar{x}_E)/3 \; \leq \; \text{USL or} \; < \; \text{LSL} \tag{4}$$

If the difference between the most divergent laboratory average and the average, $\bar{x}$, of the other two laboratory averages is greater than R, then:
The product is accepted if $\bar{x} \leq$ LSL and/or $\geq$ USL.
The product is rejected if $\bar{x} >$ USL or $<$ LSL.

Reduced Testing Frequency

In cases where production and testing have been in control for a long period, it may be appropriate to reduce the frequency of sample testing from every batch to "periodic." Decisions regarding such reduction should be made on a case-by-case basis.

A process may be considered in control when it has a Cpk of 1.33 or greater, or there are no "special events" indicated on the quality control charts in the previous 36 consecutive entries. If 36 data points are not available in a reasonable period of time, data from similar manufactured products and testing may be used to decide whether the process/testing is in control.

Additionally, the distribution of data points on the control chart around the mean value should be normal or nearly normal, and no statistical run-rules violation should have taken place.

Representative Sampling

When it is required to test the quality of a single batch of product that has been dispersed into several containers, it may not be necessary to sample and test the material from each container. The number of containers to be sampled is described in the ASTM D4057 protocol, which incorporates the following principles:

- Width of the product specification.
- Source and type of the material and whether or not more than one production batch may be represented in the lot.
- Previous experience with similar shipments, particularly with respect to the uniformity of quality from package to package.

Sample from a sufficient number of the individual packages to prepare a composite sample that will be representative of the entire lot or shipment. Select at random the individual packages to be sampled. The number of random packages will depend on several practical considerations. In most cases, the number to sample is the cube root of the total number of packages available. See the example in Table 9.

Other statistical protocols for further data analyses can be found in ASTM standards:

D6259, Practice for Determination of a Pooled Limit of Quantization, covers the determination of a lower quantitative limit for a test method for an analyte. In this practice the standard deviation of a test result, under repeatability conditions, at progressively higher levels of the analyte, is determined until the ratio of measured level to standard deviation becomes greater than ten and remains so.

D6299, Practice for Applying Statistical Quality Assurance Techniques to Evaluate Analytical Measurement System Performance, provides information for the design and operation of a program to monitor and control ongoing stability and precision and bias performance of selected analytical measurement systems using a collection of generally accepted statistical quality control procedures and tools.

D6300, Practice for Determination of Precision and Bias for Use in Test Methods for Petroleum Products and Lubricants, covers the necessary preparation and planning for the conduct of interlaboratory programs for the development of estimates of precision and bias. A software program, ADJD6300, performs the necessary computation prescribed by this practice.

D6617, Practice for Laboratory Bias Detection Using Single Test Result from Standard Material, covers a methodology for establishing an acceptable tolerance

TABLE 9—Minimum Number of Packages to Be Selected for Sampling

No. of Packages in Lot	No. of Packages to Be Sampled	No. of Packages in Lot	No. of Packages to Be Sampled
1 to 3	All	1322 to 1728	12
4 to 64	4	1729 to 2197	13
65 to 125	5	2198 to 2744	14
126 to 216	6	2745 to 3375	15
217 to 343	7	3376 to 4096	16
344 to 512	8	4097 to 4913	17
513 to 729	9	4914 to 5832	18
730 to 1000	10	5833 to 6859	19
1001 to 1321	11	6860 or over	20

zone for the difference between the result obtained from a single implementation of a test method on a check standard and its accepted reference value, based on user-specified Type I error, the user-established test method precision, the standard error of the accepted reference value, and a presumed hypothesis that the laboratory is performing the test method without bias.

D6708, Practice for Statistical Assessment and Improvement of the Expected Agreement Between Two Test Methods that Purport to Measure the Same Property of a Material, and deciding if a simple linear bias correction can further improve the expected agreement. It is intended for use with results collected from an interlaboratory study meeting the requirements of Practice D6300 or equivalent (e.g., ISO 4259). The interlaboratory study must be conducted on at least ten materials that span the intersecting scopes of the test methods, and results must be obtained from at least six laboratories using each method.

Detailed discussion of these statistical standards will not be included here, since they are documented in various statistical textbooks, and are familiar to the practitioners of this science.

PART 3 – QUALITY PROTOCOLS FOR TEST METHODS

Quality Components in Spectroscopic Methods

In almost all spectroscopic (and chromatographic) methods, quality parameters are built in either in the instrumentation and software or through mandatory steps in the analytical procedures. Most of the elemental analysis–atomic spectroscopic or XRF–have mandatory calibrations as a first step and quality control as an intermediate or as a last step in the analytical sequence of analysis. Generally, interferences, whether spectral or matrix related, are well known, and measures to overcome them have been documented, often as a mandatory step in the analysis. Three spectroscopic techniques are discussed here from this perspective: ICP-AES, XRF, and FT-IR. Further discussion of these aspects is given in the individual chapters on these specific techniques in this monograph.

Inductively Coupled Plasma – Atomic Emission Spectrometry

This is a widely used technique in the oil industry for the elemental analysis of a wide variety of products. From its start in an oil company laboratory in 1975, today virtually all oil analysis laboratories use this instrument. Its main strengths are high sensitivity for many elements of interest in the oil industry, relative freedom from interferences, linear calibration over a wide dynamic range, single- or multielement capability, and ability to calibrate the instrument based on elemental standards irrespective of their elemental chemical forms. Thus, the technique has become a method of choice in most of the oil industry laboratories for metal analysis of petroleum products and lubricants.

Much of the instrumentation is automatically controlled to use proper wavelengths. Peristaltic pumps are used to control the sample flow compensating for the viscosity differences between a sample and a calibration standard. Interelement spectral interferences are compensated for by computer correction of the raw data, which requires measurement of the interfering element at the wavelength of interest. Potential spectral overlap from concomitant elements may be estimated by measuring the signal arising from a high-purity single-element reference solution of the concomitant element. Potential interferences should be considered in the line selection process for polychromators. Other spectral interferences such as molecular band interferences and high background interferences also are compensated.

Physical interferences are the effects associated with the sample nebulization and transport processes. Such properties as change in viscosity and surface tension can cause significant inaccuracies, especially with samples that may contain high amounts of dissolved solids or acid concentrations, or both. Other physical effects include nebulizer transportation, suspended solids in the test specimen, and viscosity improver effects.

Chemical interferences include those due to molecular compound formation, selective volatilization, salt buildup in the nebulizer, and carbon buildup in the torch.

All effects mentioned here are well known and are taken care of during the ICP-AES analysis. A detailed discussion of such problems is given in the ASTM Standard Practice for Optimization, Calibration, and Validation of ICP-AES for Elemental Analysis of Petroleum Products and Lubricants (D7260), written by this author.

A number of ICP-AES methods have been issued by ASTM Committee D02 on Petroleum Products and Lubricants.

ASTM Test Method Designation	Analysis
D4951	Additive Elements in Lubricating Oils by ICP-AES
D5184	Al and Si in Fuel Oils by Ashing, Fusion, ICP-AES and AAS
D5185	Additive Elements, Wear Metals, and Contaminants in Used Lubricating Oils and Selected Elements in Base Oils by ICP-AES
D5600	Trace Elements in Petroleum Coke by ICP-AES
D5708	Ni, V, and Fe in Crude Oils and Residual Fuels by ICP-AES

ASTM Test Method Designation	Analysis
D6595	Wear Metals and Contaminants in Used Lubricating Oils or Used Hydraulic Fluids by Rotating Disc Electrode AES
D6728	Contaminants in Gas Turbine and Diesel Engine Fuel by Rotating Disk Electrode AES
D7040	Low Levels of Phosphorus in ILSAC GF 4 and Similar Grade Engine Oils by ICP-AES
D7111	Trace Elements in Middle Distillate Fuels by ICP-AES
D7260	Optimization, Calibration, and Validation of ICP-AES for Elemental Analysis of Petroleum Products and Lubricants
D7303	Metals in Lubricating Greases by ICP-AES
D7618	Metals in Crude Oils Using ICP-AES

Some of the common quality features of most of these ICP-AES methods include:

- Use of an internal standard to correct for the presence of viscosity index improvers in the samples.
- Use of a peristaltic pump to provide a constant flow of the solutions when there are differences in the viscosities of test specimen solutions and standard solutions, which can adversely affect the accuracy of the analysis. When severe viscosity effects are encountered, the test specimen and standard should be diluted 20-fold, while maintaining the same concentration of the internal standard.
- Judicious choice of analytical wavelength when spectral interferences cannot be avoided: the necessary corrections should be made using the computer software supplied by the instrument manufacturer.
- Use of a blank solution to correct for any contamination to the element of interest. When blank values are significant, correct for the blank or select alternative reagents that give insignificant blank values.
- Sufficient time should be allowed for solvent rinse between consecutive determinations to minimize the memory effects.
- Daily wavelength profiling.
- Daily 2 to 5 point calibration, followed by use of check standards to determine if each element is in calibration. If the results are not within 5 % relative, adjustments need to be made to the instrument and recalibration carried out.
- If a concentration of any analyte exceeds the linear calibration range, a diluted specimen should be reanalyzed.
- Analysis of the check standard every fifth test specimen analyzed. If any result is not within 5 % of the expected concentration, the instrument should be recalibrated and the test specimen should be reanalyzed back to the previous acceptable check standard analysis.
- Mandatory analysis of QA/QC samples with a set of analysis.

X-ray Fluorescence Analysis

Perhaps next to atomic absorption or emission spectroscopy, the most widely used technique for elemental analysis in oil industry is XRF, both wavelength- and energy-dispersive. See separate chapters on XRF in this monograph for a detailed discussion and applications of these techniques. The technique has the capability of simultaneous multielement nondestructive determination, parts-per-million level sensitivity for certain elements, and excellent precision and accuracy of ~1 %. There are, however, various interferences and the necessity of matching of samples and standards in this technique.

Because of numerous interelement matrix effects, standards identical in composition to the samples need to be used. Particle shape and size are also important, and determine the degree to which the incident X-ray beam is absorbed or scattered. Many of these interferences and matrix effects can be compensated by corrective techniques such as standard addition, internal standards, matrix dilution, thin film method, and mathematical corrections.

Several methods, particularly for sulfur determination, based on the XRF technique have been issued by ASTM Committee D02.

ASTM Test Method Designation	Technique Used	Analysis
D2622	WD-XRF	Sulfur in Petroleum Products by WD-XRF Spectrometry
D4294	ED-XRF	Sulfur in Petroleum and Petroleum Products by ED-XRF Spectrometry
D4927	WD-XRF	Elemental Analysis of Lubricants and Additive Components – Ba, Ca, P, S, and Zn by WD-XRF Spectroscopy
D6334	WD-XRF	Sulfur in Gasoline by WD-XRF
D6376	WD-XRF	Trace Metals in Petroleum Coke by WD-XRF Spectroscopy
D6443	WD-XRF	Ca, Cl, Cu, Mg, P, S, and Zn in Unused Lubricating Oils and Additives by WD-XRF Spectrometry (Mathematical Correction Procedure)
D6445	ED-XRF	Sulfur in Gasoline by ED-XRF Spectrometry
D6481	ED-XRF	P, S, Ca, and Zn in Lubricating Oils by ED-XRF Spectroscopy
D7039	M-WD-XRF	Sulfur in Gasoline and Diesel Fuel by Monochromatic WD-XRF Spectrometry
D7212	ED-XRF	Low Sulfur in Automotive Fuels by ED-XRF Spectrometry using a Low-Background Proportional Counter
D7220	ED-XRF	Sulfur in Automotive Fuels by Polarization XRF Spectrometry
D7343	XRF	Practice for Optimization, Sample Handling, Calibration, and Validation of XRF Spectrometry Methods for Elemental Analysis of Petroleum Products and Lubricants

Some of the principal measures taken to ensure the data quality in all of these XRF methods include:

- Standard and sample matrices must be well-matched or the matrix difference be accounted for. Matrix mismatch caused by carbon/hydrogen ratio difference between the samples and standards, or by the presence of other interfering heteroatoms or species can bias the results.
- Fuels containing large concentrations of ethanol or methanol having a high oxygen content can result in low sulfur results. This effect needs to be corrected.
- A drift correction monitor is used automatically by the software to implement the instrument stability.
- Verification of system control through the use of quality control samples and control charting is mandatory.
- Calibration is done with multiple standards to establish linearity.
- The check standards are used after calibration to check that the difference between two measured values is within the repeatability of the test method.
- Sufficient number of counts are taken to satisfy a percent relative standard deviation of at least 1 % or less.
- Blank measurements are carried out to take care of contamination from reagents if necessary.
- Background correction is carried out on all measurements to compensate for background Compton effects.

Further discussion of these essentials of quality management in XRF spectroscopy can be found in the ASTM Standard Practice D7343.

IR, NIR, and FT-IR

A technique widely used in the industry for the analysis of organics in the samples is infrared spectroscopy. It is more often used for qualitative identification of compounds; however, in recent years it is also being used for quantitation of these compounds. See the chapter on FT-IR in this monograph for a detailed discussion of this technique. Some of the standards issued by ASTM Committee D02 include the following IR, mainly FT-IR, methods:

ASTM Test Method Designation	Analysis
D4053	Benzene in Motor and Aviation Gasoline by IR
D5845	MTBE, ETBE, TAME, DIPE, Methanol, Ethanol, and ter-Butanol in Gasoline by IR
D5986	
D6122	Practice for the Validation of the Performance of Multivariate Process IR Spectrophotometers
D6277	Benzene in Spark Ignition Engine Fuels Using Mid-IR Spectroscopy
D7214	Oxidation of Used Lubricants by FT-IR Using Peak Area Increase Calculation

ASTM Test Method Designation	Analysis
D7371	Biodiesel FAME Content in Diesel Fuel Oil Using Mid-IR (FT-IR – ATR – PLS) Method
D7418	Set-up and Operation of FT-IR Spectrometers for In-Service Oil Condition Monitoring

Many of the standard operating procedures used in infrared spectroscopy have been defined in other ASTM standards:

E168	General Techniques of Infrared Quantitative Analysis
E932	Describing and Measuring Performance of Dispersive Infrared Spectrometers
E1252	General Techniques for Qualitative Infrared Analysis
E1421	Describing and Measuring Performance of FT-IR Spectrometers: Level Zero and Level One Tests
E2412	Condition Monitoring of Used Lubricants by Trend Analysis Using FT-IR Spectrometry.

Some of the quality parameters incorporated in these standards to ensure instrument performance and uniformity include level zero tests (energy spectrum test, 100 % line test, polystyrene test, interferogram test) and level one tests (energy spectrum test, 100 % line test, stability test, signal averaging test, polystyrene test, photometric jitter test, and nonphysical energy test).

Proof of the Pudding

Nadkarni has discussed the ways of achieving a "perfect" analysis, which involves excellence in every link of the analytical chain of operations: sampling, calibration, contamination control, use of valid test method, participation in professional testing, benchmarking, and statistical quality control operations [5]. The laboratories managed in this way demonstrate superiority in precision and accuracy of the results produced over the laboratories that do not practice such thorough quality management. An example of such analysis of NIST lubricating additive package SRM 1848 is demonstrated next. This was a material that has been analyzed under multiple circumstances. This case history is known because this author supplied this material to NIST to prepare the SRM 1848.

Originally, this material was analyzed in this author's group of laboratories.

At a later date, the same material was supplied to ASTM for use in their Interlaboratory Crosscheck Program. Along with other industry laboratories, the author's group of laboratories also analyzed this sample. However, in this instance, the laboratories did not know that it was the same sample they had analyzed six months earlier.

TABLE 10—Spectroscopic Analysis of Lube Additive SRM

Parameter	Company Group of Laboratories	ASTM	Company Group of Laboratories
Time frame of analysis	April 1996	October 1996	October 1996
No. of labs	24	59	14
Replicate analysis	4	1	1
Outliers in data set	. . .	140	8

The same material was donated to NIST, and eventually they designated it SRM 1848, and certified it for a number of parameters in it. NIST used some of the same methods employed by other laboratories in addition to certain other spectroscopic methods. These were:

- Boron – PGAA and ICP-AES
- Magnesium – XRF and ICP-AES
- Phosphorus – XRF and ICP-AES
- Sulfur – ID-TIMS
- Chlorine – XRF and PGAA
- Calcium – XRF and ICP-AES
- Zinc – PGAA and ICP-AES
- Hydrogen – PGAA, and

TABLE 11—Analysis of a Lube Additive in Multiple Cross Checks

Analysis	Product Specifications[a]	Case 1 Cross Check	ASTM Cross Check		NIST Certification
			Case 2	Case 3	
Boron, m%	0.12 – 0.13 – 0.14	0.137 ± 0.003	0.133 ± 0.0067	0.133 ± 0.003	0.136 ± 0.013
Calcium, m%	0.335 – 0.36 – 0.385	0.355 ± 0.009	0.357 ± 0.013	0.356 ± 0.009	0.345 ± 0.011
Magnesium, m%	0.76 – 0.82 – 0.88	0.818 ± 0.013	0.828 ± 0.024	0.826 ± 0.011	0.821 ± 0.058
Phosphorus, m%	0.72 – 0.78 – 0.84	0.794 ± 0.015	0.783 ± 0.025	0.776 ± 0.011	0.779 ± 0.036
Silicon, mg/kg	58 – 120	52 ± 12	47 ± 9	48 ± 6	50 ± 2
Sulfur, m%	2.2 (T)	2.28 ± 0.07	2.35 ± 0.08	2.34 ± 0.08	2.3270 ± 0.0043
Zinc, m%	0.81 – 0.86 – 0.91	0.859 ± 0.012	0.845 ± 0.028	0.842 ± 0.021	0.866 ± 0.034

[a]The values are given as minimum – target – maximum specifications.
(T) A typical value, not in the specifications.

TABLE 12—Alternate Spectroscopic Analysis of Metals in NIST SRM 1848					
Analysis	**All Methods**	**AAS**	**ICP-AES**	**WD-XRF**	**NIST Certification**
B, m%	0.137 (2.0 % RSD; n = 10)	0.139 (4.0 % RSD; n = 6)	0.139 (3.5 % RSD; n = 7)		0.136 ± 0.013
Ca, m%	0.355 (2.4 % RSD; n = 19)	0.357 (4.0 % RSD; n = 7)	0.351(1.3 % RSD; n = 7)	0.356 (2.7 % RSD; n = 9)	0.345 ± 0.011
Mg, m%	0.818 (1.6 % RSD; n = 15)	0.826 (4.6 % RSD; n = 8)	0.817 (1.6 % RSD; n = 9)		0.821 ± 0.058
P, m%	0.794 (1.9 % RSD; n = 16)		0.787 (3.6 % RSD; n = 7)	0.789 (2.5 % RSD; n = 10)	0.779 ± 0.036
Si, mg/kg	52 (22.3 % RSD; n = 11)	47 (18.9 % RSD; n = 4)	54 (21.9$ RSD; n = 9)		50 ± 2
S, m%	2.28 (3.1 % RSD; n = 11)		2.30 (0.46 % RSD; n = 2)	2.88 (3.7 % RSD; n = 10)	2.327 ± 0.0043
Zn, m%	0.859 (1.4 % RSD; n = 18)	0.870 (2.7 % RSD; n = 5)	0.857 (1.2 % RSD; n = 7)	0.855 (2.2 % RSD; n = 10)	0.866 ± 0.034

- Silicon – XRF
- (PGAA: Prompt gamma ray activation analysis; ID-TIMS: Isotope dilution thermal ionization mass spectrometry).

Table 10 gives the details of these three cross checks for spectroscopic parameters determined.

Table 11 shows the comparison of the company internal analysis (case 1) and ASTM cross-check results (case 2 and 3) versus the product specifications, and eventual NIST-certified values for spectroscopic analyses.

In this exercise, alternative spectroscopic methods were used by different laboratories. The results shown in Table 12 indicate, however, that all values by alternative methods are well within the reproducibility of each of the methods used.

Several conclusions drawn from these data sets include the following:

- The results from company laboratories in case 1 and case 2 are very close to each other, although the analyses were done six months apart, and the second time it was an unknown sample.
- All results from the company laboratories are well within the product specifications.
- Although there were only 8 statistical outliers in the data set from 14 company laboratories, ASTM identified 140 of them in the 59 industry laboratories.
- Most important, the repeatability and reproducibility values of the company laboratories both times were superior to those shown in the ASTM cross check.
- In all cases, the mean values calculated from each spectroscopic method were well within the overall percent relative standard deviations range for the seven elements analyzed. This shows that the elements analyzed by alternative methods AAS, WD-XRF, or ICP-AES give equivalent results based on the interlaboratory average value for each analysis technique.

These data show that consistent comprehensive technical quality management does pay dividends in maintaining superior quality in the long range.

References

[1] Taylor, J. K., *Quality Assurance of Chemical Measurements*, Lewis Publishers, Inc., Chelsea, MI, 1987.

[2] Nelson, L. S., "Statistical Outliers in Data Treatment," *J. Quality Technol.,* Vol. 17, No. 2, 1985, p. 114.

[3] May, W., Parris, R., Beck, C., Fasset, J., Greenberg, R., Guenther, F., Kramer, G., Wise, S., Gills, T., Colbert, J., Gettings, R. and MacDonald B., "Definitions of Forms and Modes Used at NIST for Value-Assignment of Reference Materials for Chemical Measurements," NIST Special Publication, 260–136, 2000.

[4] Nadkarni, R. A. and Bover, W. J., "Bias Management and Continuous Improvements through Committee's D02's Proficiency Testing," *ASTM Standardization News,* Vol. 32, No. 6, 2004, pp. 36–39.

[5] Nadkarni, R. A. "Zen and the Art (or Is It Science) of a Perfect Analysis," *J. ASTM Intl.*, Vol. 2, No. 3, ASTM International, West Conshohocken, PA, 2005, Paper ID JAI12964.

4

Analyzing and Interpreting Proficiency Test Program Data for Spectroscopic Analysis of Petroleum Products and Lubricants

W. James Bover[1]

INTRODUCTION

Background

Quality system standards for testing laboratories (ASTM D6792 and ISO 17025) require the use of processes to manage precision and bias. Several ASTM International standards guide users in the quality assurance and quality control (QA/QC) practices for managing precision and bias within a testing laboratory (e.g., D6299, D6617, E882 and E1323). Some deal specifically with laboratories servicing the petroleum products and lubricants industry. Many of these practices focus on within-laboratory precision (repeatability). Using certified reference standards and statistical quality control (SQC) techniques like control charts are two widely used tools employed to satisfy requirements to manage precision and bias within a laboratory.

Another important aspect of overall laboratory performance concerns the precision and bias of one laboratory relative to others or, said another way, concerns the between-laboratory precision. A related but different set of practices deals with monitoring laboratory performance relative to the published between-laboratory precision (reproducibility). A proficiency test program (PTP) is one of the primary tools for assessing laboratory performance relating to between-laboratory precision on a regular basis and with "real world" laboratories [1-5].

Although PTPs have been in use for a long time and supply participating laboratories with much useful information, participants often feel that they are on their own to analyze and interpret PTP reports beyond the simplest of reviews. Both E1301, *Standard Guide for Proficiency Testing by Interlaboratory Comparisons* (originally published in 1989), and D7372, *Standard Guide for Analysis and Interpretation of Proficiency Test Program Results* (initial version in 2007), provide guidance in these matters. The latter standard focuses specifically on the petroleum and lubricants industry and recognizes the role of that industry's proficiency test program.

This chapter deals with and expands on the concepts identified in D7372 and E1301. This chapter gives numerous examples extracted from ASTM International Committee D02's PTP. This chapter gives a description and rationale for PTPs in Section I, and addresses two important continuous improvement activities, one by the individual PTP participant in Section II and the other by the responsible ASTM subcommittees and other work groups in Section III. Although

[1] *ExxonMobil Biomedical Sciences, Inc., Annandale, New Jersey*

the techniques for investigating PTP results are discussed with respect to whether the participating laboratory or a responsible work group initiates an investigation, these techniques are available to all. The reason for the split is that more often a laboratory is interested only in how they are doing (as in Section II) versus how the test method is performing or how the entire PTP group is performing (as in Section III). For purposes of this chapter, when referring to *industry laboratories*, we mean the laboratories that analyze petroleum products and lubricants supporting facilities like refineries, lube oil blending plants, and terminals and activities like research and compliance with (government) regulations.

TERMINOLOGY

Definitions and terminology unique to this chapter or simply worth repeating are described here. Many of the terms and definitions from Chapter 3 are relevant here as well.

Bias – A systematic error that contributes to the difference between a population mean[2] of the measurements or test results and the accepted reference or true value (D6299, E456).

Bias, relative – The difference between the population mean of the test results and an accepted reference value, which is the agreed-upon value obtained using an accepted reference method for measuring the same property (D6300). In addition, relative bias is the systematic error that contributes to the difference between population means from measurements or test results using two test methods that purport to measure the same property.

Interlaboratory Crosscheck Program (ILCP) – ASTM International Proficiency Test Program sponsored by Committee D02 on Petroleum Products and Lubricants; see http://www.astm.org/STAQA/petroproducts.html (accessed April 6, 2011)

Petroleum Products – Designations for ILCP products used in this chapter:

ALA – automotive lubricant additives
GGO – general gas oil
ISDO – in-service diesel oil
Jet Fuel – aviation turbine fuel
Lube Oil – engine lubricating oil
Mogas – motor gasoline
RFG – reformulated gasoline
ULSD – ultra low sulfur diesel

Proficiency Testing – Determination of laboratory testing performance or capability by means of interlaboratory comparisons (D6299, E1301, ISO/IEC Guide 2).

uncertainty – An indication of the magnitude of error associated with a value that takes into account both systematic errors and random errors associated with the measurement or test process (E2655).

Z-Score – A standardized and dimensionless measure of the difference between an individual result in a dataset and the arithmetic mean of the dataset, re-expressed in units of standard deviation of the dataset. Z-score is the difference of an individual result minus the mean divided by the standard deviation for the dataset (D7372).

[2] *Population mean* is the value toward which the mean of results would converge, were an ever-larger number of results to be obtained under the same sampling conditions.

SECTION I – PROFICIENCY TEST PROGRAMS

A PTP is one in which identical samples are distributed to participating industry laboratories, where the samples are analyzed using standard test methods, and the results reported for statistical analysis. Other names for PTPs, such as cross-check, check-scheme, exchange group, and round robin programs, are used in some industries and regions. Participating in PTPs offers opportunities for engaging in continuous improvement activities. Many quality practitioners consider participation as essential for the right to participate in the marketplace.

Here are several key criteria associated with a successful PTP:

- Samples distributed in each PTP are representative of the products in commercial production.
- Samples are packaged and distributed in a manner to maintain homogeneity and stability with respect to the parameters measured by the participating laboratories.
- The PTP administrator or the standard test method procedures provide instructions on the proper handling and mixing of the test sample in order to achieve a representative sub-sample for analysis.
- The PTP provides adequate descriptions of the statistical treatments applied to laboratory results.
- The tests are blind in that there are no comparisons of results between laboratories before submission of results.
- There is a mechanism to provide feedback from the participants to the program sponsors and vice versa.

PTP Benefits

Several benefits derive from participating in PTPs, especially within the petroleum and lubricants industry [6]:

- Helps satisfy laboratory accreditation requirements
- Provides an SQC tool to compare individual performance versus other laboratories worldwide or region-wide
- Provides data for monitoring laboratory strengths and weaknesses across numerous test methods and products
- Provides means to determine measurement uncertainty when PTP data combine with internal site precision data from control charts
- Offers ability to compare results among several test methods measuring the same parameter or property of a material that is being tested
- Demonstrates testing capability to customers
- Helps ASTM work groups validate test method performance under real-world conditions
- Provides residual PTP materials that, along with the published statistical data, can serve as quasi-standards and are useful internal quality control samples (in combustion testing, these are known as “golden fuels”)
- Provides opportunity to establish analyst proficiency (i.e., consistency and comparability of data) when coupled with other tools or mechanisms.

ASTM D02 Interlaboratory Crosscheck Program

ASTM Committee D02 on Petroleum Products and Lubricants and Coordinating Subcommittee 92 on Interlaboratory Crosscheck Programs [7] sponsor a proficiency test program called the ILCP. The concept for this program dates back to 1989, and the first four product programs began in 1993. Table 1 shows

TABLE 1—ASTM D02 ILCP Programs													
			Annual Distribution Schedule										
Product Program	Initial Year	2010 # Participants	Jan	Feb	Mar	Apr	May	Jun	Jul	Aug	Sep	Oct	Nov	Dec
#2 Diesel	1993	407		X				X				X		
#6 Fuel Oil	1995	293	X				X				X			
Automatic Transmission Fluid	1995	40			X				X				X	
Automotive Lube Additives	1996	50		X				X				X		
Aviation Turbine (Jet) Fuel	1993	311			X				X				X	
Base Oils	2001	81						X						X
Biodiesel	2005	117				X				X			X	
Crude Oil	2000	181			X				X				X	
Engine Oil Lubricants	1993	212	X				X				X			
Fuel Ethanol	2007	92				X				X				X
Gear Oil	1995	36				X				X				X
General Gas Oils	2003	57			X				X				X	

(*Continued*)

TABLE 1—ASTM D02 ILCP Programs (Continued)

Product Program	Initial Year	2010 # Participants	Annual Distribution Schedule											
			Jan	Feb	Mar	Apr	May	Jun	Jul	Aug	Sep	Oct	Nov	Dec
Hydraulic Fluids / Oils	2006	49	X				X					X		
Industrial Gear Oil	1998	25			X						X			
In-Service Diesel Oil	2001	73			X				X				X	
In-Service Hydraulic Oil	2007	25					X			X			X	
Lubricating Grease	2000	66				X						X		
Motor Gasoline	1993	180				X				X				X
Petroleum Wax	2002	44		X				X				X		
Reformulated Gasoline	1995	143	X	X	X	X	X	X	X	X	X	X	X	X
Turbine Oil	1998	90				X						X		
Ultra Low Sulfur Diesel	2004	186	X	X	X	X	X	X	X	X	X	X	X	X

the 2009 status of the ILCP, which now includes 22 products ranging from crude oil to diesel fuel to gasoline to biodiesel and fuel ethanol. The distribution of a sample represents a cycle, and each product program has 2, 3, or 12 cycles per year, as demonstrated in Table 1. More than 2,700 laboratory units were participating (some laboratories participate in more than one product program) at the end of 2010. This is a truly global program, with participants from more than 70 countries in North and South America, Europe, Asia, Australia, and Africa. The ILCP satisfies the success criteria outlined in the previous section.

Eighteen of the ILCP product programs call out a number of spectroscopic-based standard test methods. These include those based on wavelength or energy dispersive X-ray fluorescence (WD-XRF, ED-XRF), inductively coupled plasma atomic emission spectroscopy (ICP-AES), atomic absorption spectroscopy (AAS), infrared spectroscopy, and gas chromatograph–mass spectrometry (GC-MS). Table 2 shows the distribution of these spectroscopic methods across the ILCP product programs.

Opportunities for Continuous Improvement

As mentioned earlier, a PTP offers a number of opportunities for process improvement [1,4]. Fig. 1 best illustrates this by highlighting the overall proficiency testing process as practiced by ASTM D02 for the ILCP. In the ILCP process, a supplier (i.e., refinery, plant, or other interested party with access to material) gives a representative sample to the contract distributor, who is responsible for homogenizing the bulk material and preparing the individual samples for distribution. The contactor distributes the samples by commercial carriers to the participating laboratories, which number from 20 to more than 400, depending on the specific product program, as noted in Table 1. The ILCP office at ASTM notifies the laboratories of the sample shipment and their corresponding lab identification code for that cycle and opens a website for the laboratories to report results. After the reporting period is closed, the ILCP office consolidates and analyzes results following agreed-upon statistical protocols, and prepares reports using standard formats. ASTM issues the final reports to the participating laboratories electronically as a downloadable Adobe PDF file via a link to the website.

All this activity is designed to provide both the participating laboratories and the responsible ASTM D02 subcommittees and workgroups with opportunities; Fig. 1 highlights these opportunities by the steps enclosed in the oval. True success happens only when the laboratory first analyzes and interprets the data by considering outliers, biases, and other performance indicators, and then taking appropriate actions to implement improvements. To do nothing is a waste of effort and a lost opportunity. The same goes for the responsible subcommittees and workgroups, who should consider between-laboratory statistical analyses for the current cycle as well as for previous cycles. After careful consideration of ILCP results and perhaps other independent data, the subcommittees should consider actions aimed at improving overall performance. Some of these actions could lead to revisions of the standard test methods.

The Toolkit

Before initiating any data analysis, one should first inventory their process toolkit to verify that they have the appropriate tools available to assist in their analysis and interpretation of proficiency testing results. Table 3 lists key components of such a toolkit along with references to more detailed discussions. This chapter discusses each of these tools.

TABLE 2—Spectroscopic-Based Test Methods in ILCP Product Programs

Test Method	Technique	Target Analytes	Motor Gasoline	Reformulated Gasoline	Fuel Ethanol	#2 Diesel Fuel	Ultra Low Sulfur Diesel	Biodiesel	Aviation Turbine Fuel	#6 Fuel Oil	General Gas Oil	Crude Oil	Lubricating Oil	Base Oil	Automotive Lubricant Additive	Automatic Transmission Fluid	Gear Oil	Hydraulic Fluid Oils	In-Service Diesel Oil	In-Service Hydraulic Fluids
D1552	IR	S							X	X			X		X	X				
D1840	UV	Naphth							X											
D2622	WD-XRF	S	X	X		X	X		X	X	X	X		X						
D4053	IR	Benzene	X																	
D4294	ED-XRF	S	X	X		X	X		X	X	X	X		X			X			
D4628	AAS	Metals											X		X	X				
D4927	WD-XRF	Metals, P, S											X							
D4951	ICP-AES	Metals, P, S						X					X		X	X	X	X		X
D5184	ICP-AES	Al,Si								X										
D5185	ICP-AES	Metals, P, S								X			X		X	X	X	X	X	X
D5453	UVF	S	X	X	X	X	X	X	X				X							
D5708	ICP-AES	Fe, Ni, V								X	X	X								
D5769	GC/MS	Benzene	X	X																
D5845	IR	oxygenates	X	X																
D5863	AAS	Fe, Ni, V								X	X	X								
D6443	WD-XRF	Metals, P, S											X							
D6481	ED-XRF	Elements											X							
D6595	RDE-AES	wear Metals																	X	X
D7039	WD-XRF	S	X	X		X	X													
D7212	ED-XRF	S					X													
EN14538	ICP-OES	Metals						X												

Statistical Tools and Evaluations

The following are some of the statistical tools available for analyzing PTP results [12,13].

ANDERSON-DARLING STATISTIC

Calculate the Anderson-Darling (AD) statistic in accordance with D6299 to determine if the data are normally distributed. If the data are distributed normally (i.e., AD < 1.0), then the equations that follow are applicable. When the AD > 1.0, suggesting that the data are not normally distributed, then the tools described next should be used with caution.

STANDARD ERROR OF THE MEAN

The standard error of the mean (SE) is used to assess the confidence interval for the sample means obtained from multiple cycles of a proficiency testing for a given test parameter.

$$SE = \left(\frac{s}{\sqrt{n}}\right) \tag{1}$$

where:
s = standard deviation for the PTP results (per cycle), and
n = number of valid results reported.

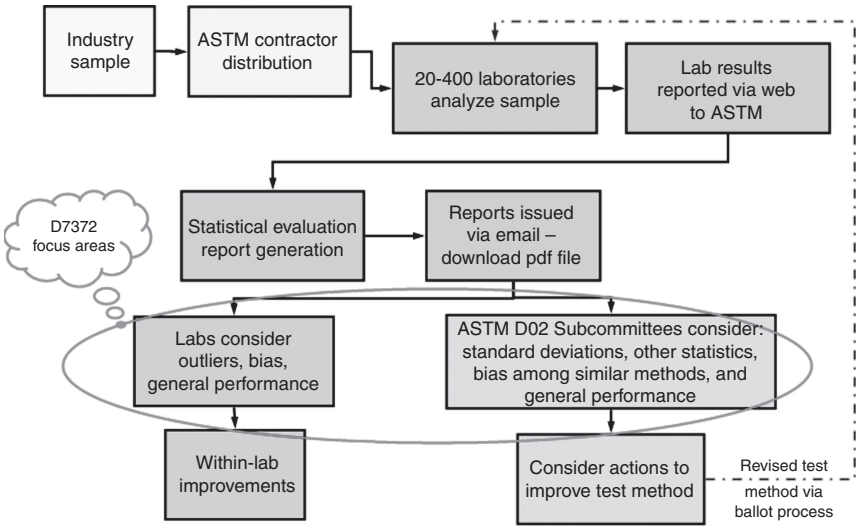

Fig. 1—Paradigm for continuous improvement in a proficiency test program [8,9].

Estimate the upper and lower 95 % confidence intervals for the mean using Eq 2. The "1.96 · SE" expression is also known as *expanded uncertainty* (see discussions in E2655).

$$95\,\%\text{ confidence limits} = \overline{X} \pm (1.96 \cdot \text{SE}) \tag{2}$$

Examples of the use of Eq 2 include the error bars shown in Fig. 13b and others.

POOLED STANDARD DEVIATION

Estimate the pooled standard deviation (s_{pooled}) for multiple proficiency test cycles for a given test method using Eq 3. This assumes a normal or near-normal distribution of data and that the precision is about the same for each cycle[3] in the pooled set.

$$s_{pooled} = \sqrt{\frac{\sum (n_i - 1) \cdot s_i^2}{(\sum n) - N}} \tag{3}$$

where:
n_i = number of labs providing data in single cycle (no outliers), s_i = standard deviation for single cycle, and N = number of proficiency testing cycles in dataset.

F-TEST – COMPARISON OF STANDARD DEVIATIONS FROM TWO TEST METHODS

Use the *F-test* in Eq 4 for comparing two standard deviations from any sources provided they be independently obtained. For purposes of this discussion,

[3] Either precision does not depend on level (concentration) or the concentration varies from cycle to cycle but in a narrow range.

TABLE 3—Toolkit for Analysis and Interpretation of PTP Results

Item	Reference/Comment
Anderson-Darling Statistic	AD is a test for normally distributed data as described in D6299.
Box and Whisker Graphs	These graphs provide a cross reference of test data generated by different test methods for the same parameter (e.g., sulfur by five different test methods).
Graphs	The ILCP reports contain scatter graphs of the results obtained for each test method, plotted in increasing order versus the corresponding laboratory identification code. Other graphs such as those plotting means, relative standard deviation, test performance index (TPI), and similar parameters are employed and discussed in this chapter.
Histograms	The ILCP reports contain histograms for datasets exceeding a minimum number of valid results. See discussion later in this chapter. Individuals using Excel or other graphics software tools can generate histograms, as well.
Laboratory Records	Supporting data, calculations, corresponding control charts, etc.
PTP Report	ILCP reports [10] are in Adobe PDF format[a] and are available to users via a web link.
Quality Control Charts	Control charting techniques as discussed in D6299 are available for use in analyzing proficiency test results.
Result Tables and Statistical Summary	Reports should list the results for each test method and should summarize the mean, standard deviation, AD statistic, and $TPI_{industry}$. Outliers should be identified (i.e., flagged).
Robust Statistics (Mean, Standard Deviation)	Each ILCP report has a brief discussion of robust statistics[b] in the Introduction Section. A reference source is included [11].
Root Cause Investigation Guide	Refer to the checklist found in the Section II paragraph on Flagged Data and Investigations. Similar checklist presented in all ILCP reports and in D7372, Appendix X1.
Statistics	Tools such as the standard error of the mean, *F-test*, *t-test*, and pooled standard deviation are discussed in Section I.
$TPI_{industry}$	The ILCP report provides a TPI (industry) capability index in the statistical summary for each set of test method results for which the robust reproducibility ($R_{these\ data}$) and the corresponding ASTM reproducibility (R_{ASTM}) are calculated.
Z-Score	Z-score is a dimensionless measure of the difference between an individual result and the arithmetic mean of the dataset, divided by its standard deviation.

[a]Because it is difficult or impossible to extract useable digital data from the ILCP reports in PDF format, the user may request data files in Excel format from the program administrators.
[b]Use of robust mean and robust standard deviation as data treatments is specific to the ASTM ILCP and is not necessarily the only way to minimize the effect of outliers on mean and standard deviation.

we use the *F-test* to determine if the precisions (standard deviations) for two datasets, from two test methods (X and Y) measuring the same parameter, are statistically indistinguishable (or conversely, that the differences are not statistically significant):

$$F = \left(\frac{s_Y}{s_X}\right)^2 \tag{4}$$

The degrees of freedom are $n_Y - 1$ and $n_X - 1$ for the numerator and denominator, respectively. When using Excel for these calculations, the probability or *p*-value (two-tailed) for this test is determined by

$$p = 2 \times \text{MIN}\left[\text{FDIST}(F, n_Y - 1, n_X - 1), 1 - \text{FDIST}\left(F, n_Y - 1, n_X - 1\right)\right] \tag{5}$$

If $p \leq 0.05$, then one concludes that the precision from test method X is different from (not equal to) that of test method Y with 95 % confidence. If $p \leq 0.10$ or $p \leq 0.01$, then s_X is different from s_Y with 90 % or 99 % confidence, respectively.

T-TEST – COMPARING MEANS FROM TWO TEST METHODS, STANDARD DEVIATIONS NOT EQUAL

Use the *t-test* in Eq 6 to determine if the means obtained from two test methods, X and Y, are distinguishable statistically. Statistically significant differences imply a bias of one method relative to the other, hence a relative bias.

$$t = \frac{\left|\overline{X} - \overline{Y}\right|}{\sqrt{\frac{s_X^2}{n_X} + \frac{s_Y^2}{n_Y}}} \tag{6}$$

It is necessary to use absolute value here for the difference in means when using Excel's TDIST function. The approximate degrees of freedom for this statistic is

$$df = \frac{\left(\frac{s_X^2}{n_X} + \frac{s_Y^2}{n_Y}\right)^2}{\frac{s_X^4}{n_X^2(n_X - 1)} + \frac{s_Y^4}{n_Y^2(n_Y - 1)}} \tag{7}$$

When using Excel for these calculations, the probability or *p*-value (two-tailed) for this test is determined by $p = \text{TDIST}(t,df,2)$.

Therefore, if $p < 0.05$, we conclude with 95 % confidence that the means are significantly distinguishable and there is a high probability of a bias.

T-TEST – COMPARING MEANS FROM TWO TEST METHODS, STANDARD DEVIATIONS EQUAL

If the standard deviations for the two test methods are equal, then use the *t-test* in Eq 8 to test for bias:

$$t = \frac{\left|\overline{X} - \overline{Y}\right|}{\sqrt{\frac{(n_X - 1)s_X^2 + (n_Y - 1)s_Y^2}{n_X + n_Y - 2}\left(\frac{1}{n_X} + \frac{1}{n_Y}\right)}} \tag{8}$$

where:
$df = n_X + n_Y - 2$ and $p = \text{TDIST}\ (t,df,2)$.

Therefore, if $p < 0.05$, we conclude with 95 % confidence that the means are statistically distinguishable and there is a high probability of a bias.

SECTION II – ANALYSIS AND INTERPRETATION BY LABORATORY STAFF

Objectives

Key objectives for laboratories participating in PTPs, once they receive the reports, include analyzing results, correcting errors, and, as appropriate, identifying opportunities for performance improvement. The following procedures and tools are readily available to participating laboratories.

- Administrative reviews
- Flagged data and investigations
- Data normality checks
- Histograms
- Bias (deviation from mean)
- Z-scores
- $TPI_{industry}$
- PTP and site precision comparisons

Administrative Reviews

Although this may appear trivial, it is important to verify that all results submitted by the laboratory match those recorded in the published PTP report. This review could identify cases where errors are made in handling the laboratory result, such as omitting a result from the report or introducing a transcription error. Other common error sources include results reported with incorrect units of measure (e.g., mg/kg versus mass %) and incorrect reporting resolution or significant figures (35.456 versus 35 or 0.03 versus 0.0259). In the ILCP, errors involving transcription, units of measure, and significant figures account for a large proportion of rejected results. One way for a laboratory to minimize such errors is to perform quality control checks on the report form before submission.

Flagged Data and Investigations

Most PTP reports identify and then highlight or flag individual results that exceed certain statistical outlier criteria. PTP reports should describe all flag codes and provide some guidance on how to interpret them. One of the most common flags is the one to reject a datum as an outlier based on known statistical criteria. A number of outlier tests are available, such as the Cochran test for within laboratories and the Hawkins test for between laboratories [D6300]. Other techniques like the GESD (Generalized Extreme Studentized Deviate) for multiple-outlier cases are available for use with control charts [14,15]. The ILCP uses the Z-score in the first stage of the robust mean estimate to identify outliers [10]. In general, outliers are rejected or trimmed from the dataset and the remaining data are used to recalculate the mean and standard deviation.

Other flags are those applied to data that exceed selected control limits. The ILCP flags individual results when they exceed the corresponding ASTM reproducibility (R_{ASTM}) control limits or exceed the corresponding PTP reproducibility ($R_{these\ data}$) control limits.

The following is a summary of some of the flags applied to ILCP results.

Code	Description
Rejected	Result rejected; initial absolute Z-score > 3 in first stage of $R_{these\ data}$ calculations
1	Lab data outside ±3 sigma range for the crosscheck dataset
2	Lab data outside ±3 sigma range for ASTM reproducibility
3	Lab Z-score is outside range -2 to $+2$
X	PI < 0.8; lab precision needs improvement

It is important to recognize statistical outliers, but it is even more important to take action to identify the root cause and to implement corrective or preventative measures. Each ILCP report references a checklist for investigating the root cause of unsatisfactory analytical performance. The published standard D7372 also presents a version of this checklist.

TABLE 4—Root Cause Investigation Guide	
1.	Check the results for typographical, calculation, and transcription errors.
2.	Re-analyze the sample; compare the new result to the site precision, or, if not available, compare to the test method repeatability.
3.	Check the proficiency test sample for homogeneity or contamination.
4.	Determine if the lab had taken a representative sample for analysis.
5.	Ensure that the laboratory followed the latest version of the standard test method.
6.	Verify that the analyst followed the procedure step-by-step without deviation.
7.	Verify instrument calibrations or standardizations.
8.	Examine the corresponding quality control chart and investigate if the flagged data are associated with any issues identified by the control chart.
9.	Check the reagents and standards to verify that they are of appropriate quality and grade and are not expired or contaminated.
10.	If the poor results appear linked to instrument or equipment performance, then perform maintenance or repairs following established guidelines.
11.	After resolving a problem, analyze a certified reference material, if one is available, or a quality control sample, to verify that the analytical operation is under statistical control.
12.	Train or retrain the analysts as appropriate.
13.	Document the incident and the lessons learned for future use if or when a similar problem occurs.
(Note: Not all steps may apply and there may be other ways to improve performance)	

Data Normality Checks

Typical statistical evaluations of proficiency testing results assume data are from normal distributions, so it is necessary to evaluate the data for normality. The AD statistic is used to test objectively for normality, and it is sensitive to inadequate data measurement resolution relative to the overall variation in the dataset. D6299 covers the calculation of the AD statistic, a goodness of fit test to determine if the data are from a normal distribution. The ILCP uses AD as the primary tool for testing for normal distributions. D6299 recommends the following criteria to evaluate the AD statistic and these should apply to PTP data as well:

AD < 1.0	Data are likely normally distributed and the participants should take action to address all data flags.
AD > 1.0	Data may not represent a normal distribution; participants should exercise caution in planning actions for flagged data.
AD $>>> 1$	This is strong evidence of inadequate variation in the dataset due to inadequate numerical resolution (could also arise from un-removed outliers or a perversely non-normal data distribution).

In addition, graphical tools are available for evaluating normality. For example, one can use a normal probability or normal deviate plot (a special case of a *q*-q plot) to visually assess the validity of the normality assumption. Refer to D6299 for guidance regarding preparing and interpreting normal probability plots and AD results. If the data are normally distributed, the normal probability plot should be approximately linear. Major deviations from linearity indicate non-normal distributions. The appearance of a series of steps in the plotted data rather than a smooth line indicates that the data (or measurement) resolution is too coarse relative to the precision of the test method. A few examples of these normal probability plots are shown in parallel with histograms in the following section.

Histograms

Plotting interlaboratory proficiency test data as histograms is a useful graphical tool for viewing data distribution and variability. The ILCP program plots histograms for all datasets where $n > 20$. For datasets with $n > 30$, the ILCP also includes the mean and the first and 99th percentile limits on the histogram. These limits are based on "*median ± 2.33 · Robust Standard Deviation*" for the sample, where ±2.33 are respectively the first and 99th percentiles of the standard normal distribution.

When histograms are available, proficiency test participants should review them and note unusual data distributions. Most important, participants should locate where their result falls within the histogram bins. Depending on the histogram, the location of data in certain bins could indicate a potential problem. It is more powerful to use a review of the histogram in parallel with reviews of the corresponding statistical data such as the Z-score, AD statistic, $TPI_{industry}$, and normal probability (or deviate) plot.

The histogram in Fig. 2a represents a case for 45 valid results (i.e., outliers rejected) at relatively low sulfur levels (1–4 mg/kg) for ILCP #2 diesel fuel sample DF21006. An AD of 0.76 indicates normally distributed data and the $TPI_{industry} = 0.82$ shows fair overall performance by the participants especially at the low sulfur levels. The linearity of the normal deviate plot along with the AD statistic and visual appearance of the histogram supports the conclusion of a normal distribution of data. The slight indication of steps in Fig. 2b suggests

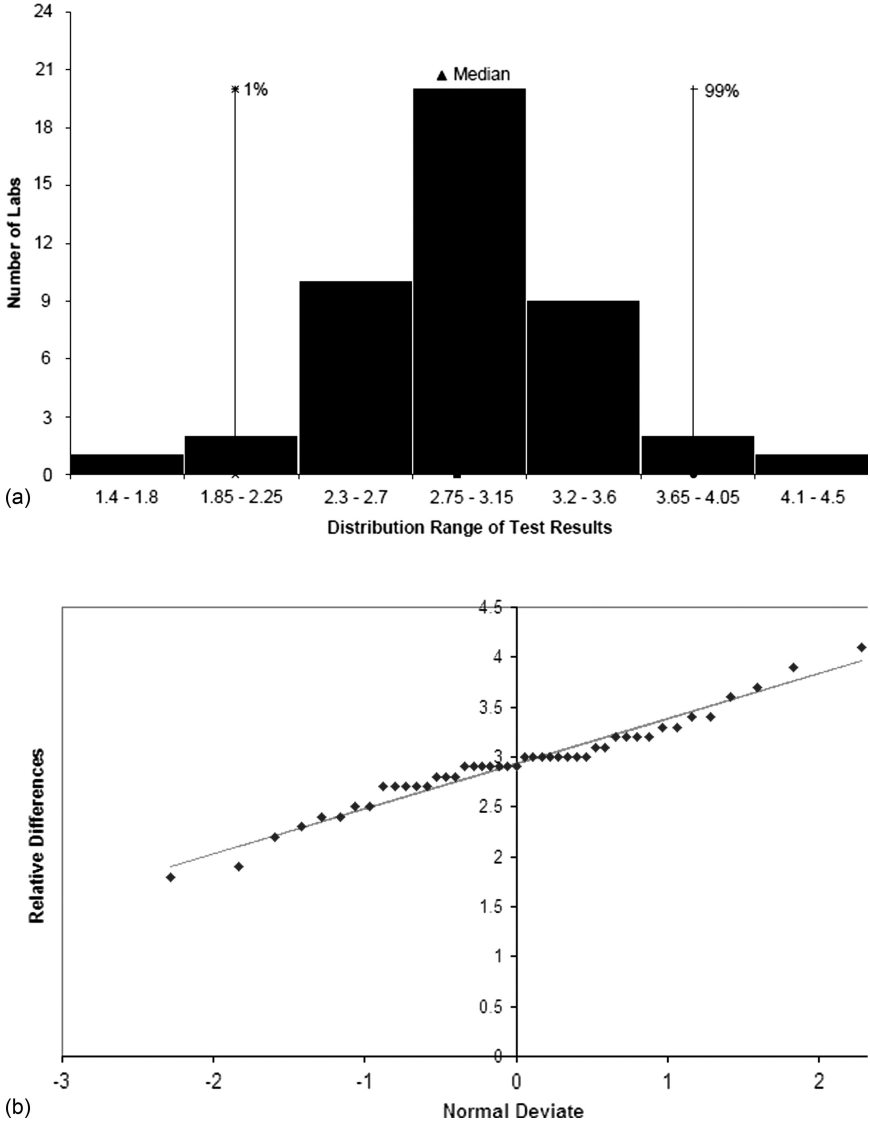

Fig. 2—(a) ILCP histogram for sulfur in #2 diesel by D7039. (b) Normal deviate plot for sulfur in #2 diesel by D7037.

that measurement resolution issues may be involved. Laboratories with flagged results or results out on the wings of the distribution should consider investigating for cause.

Fig. 3a shows the histogram for 4–8 mg/kg sulfur by D5453 for a diesel sample (DF20906). In this case, there are 154 valid results, the $TPI_{industry}$ = 1.32, and the AD = 0.93. The appearance of the histogram, the AD statistic, and the approximate linearity of the normal deviate plot in Fig. 3b suggest that the data are normally distributed. The appearance of minor steps in the normal deviate plot indicates that there may be some measurement resolution issues.

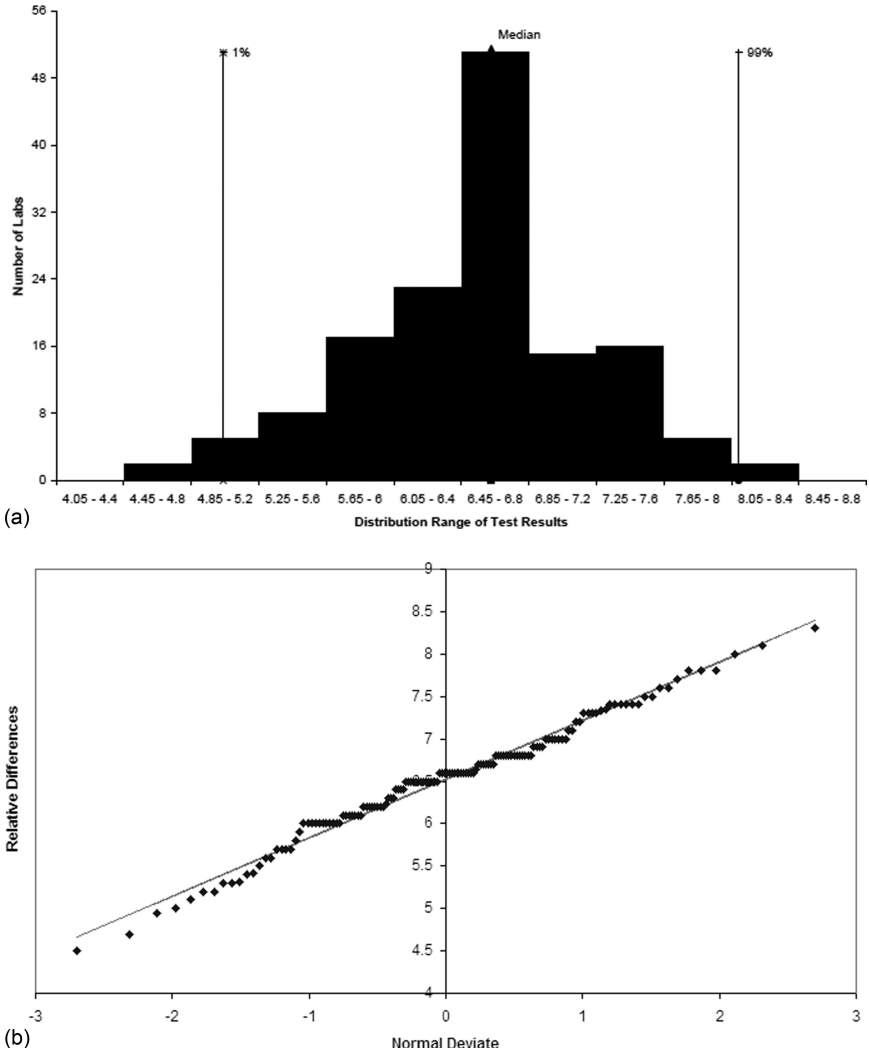

Fig. 3—(a) ILCP histogram for sulfur in #2 diesel by D5453. (b) Normal deviate plot for sulfur in #2 diesel by D5453.

This may be related to the application of D5453 at the low sulfur levels, which represents the lower operation range for this test method.

The histogram in Fig. 4a reflects the distribution for 70 valid results with a $TPI_{industry} = 0.99$ and AD = 1.07. The $TPI_{industry}$ indicates good overall performance by the participants. The histogram shows a small node or bump near the first percentile limit. The slightly high value for the AD and the indications of nonlinearity at the lower end of the normal deviate plot in Fig. 4b suggest non-normal behavior. This bimodality should be of concern to the participants, especially those with results in the lower node on the left side of the histogram.

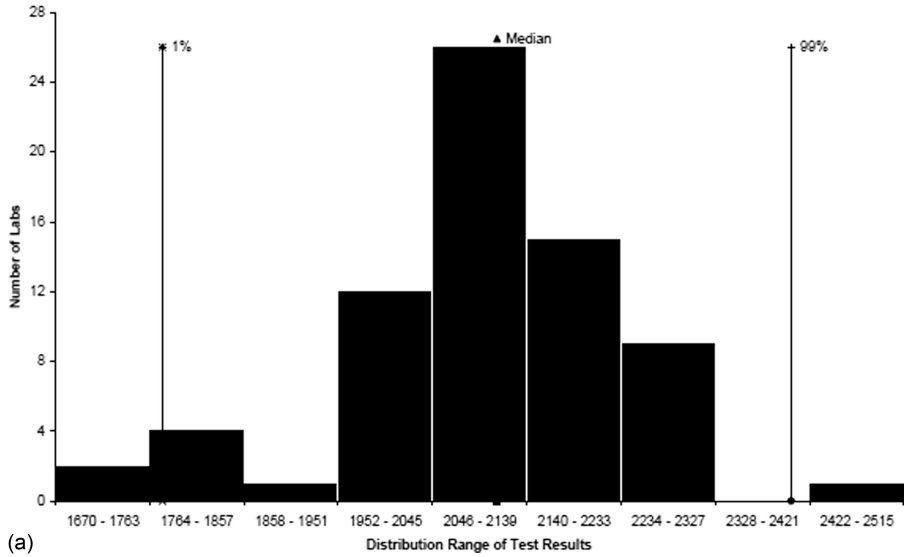

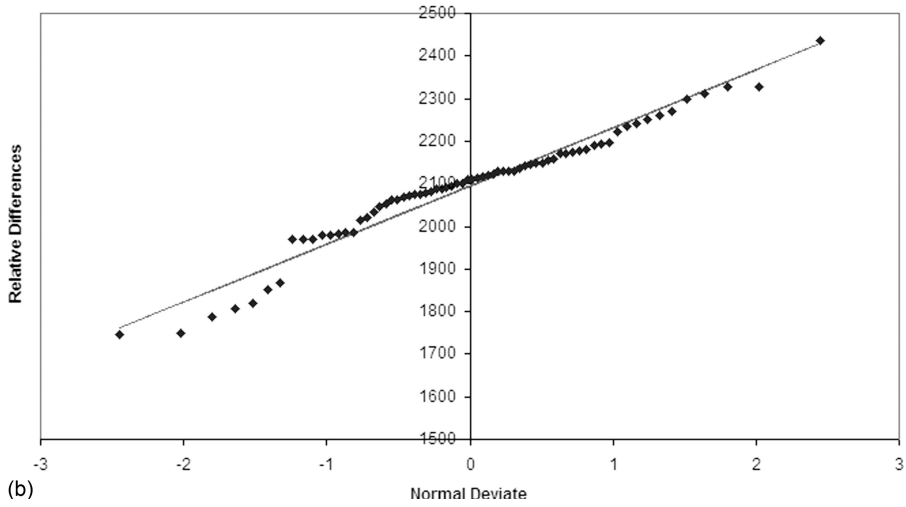

Fig. 4—(a) ILCP histogram for calcium in engine lube oil by D5185. (b) Normal deviate plot for calcium in engine lube oil by D5185.

Laboratories with results in the area of the lower node should investigate looking for root causes.

The histogram in Fig. 5a for sample DF20906 is a case for 49 valid results, $TPI_{industry} = 0.51$, and AD =2.04 for sulfur values down in the 3 to 12 mg/kg range, the lower operating range for the test method. The normal deviate plot in Fig. 5b shows a distinct step function indicative of measurement resolution problems for the method. The skewed shape of the histogram, the AD statistic,

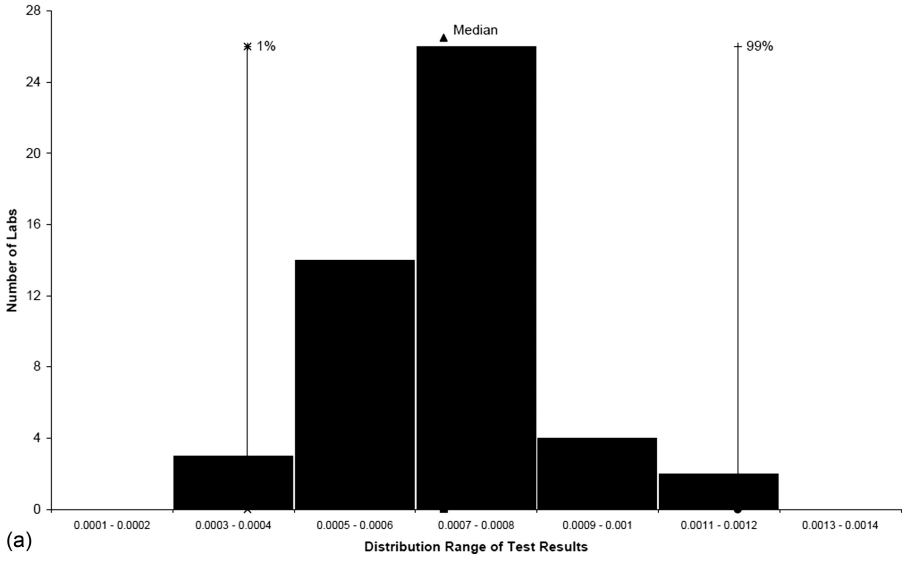

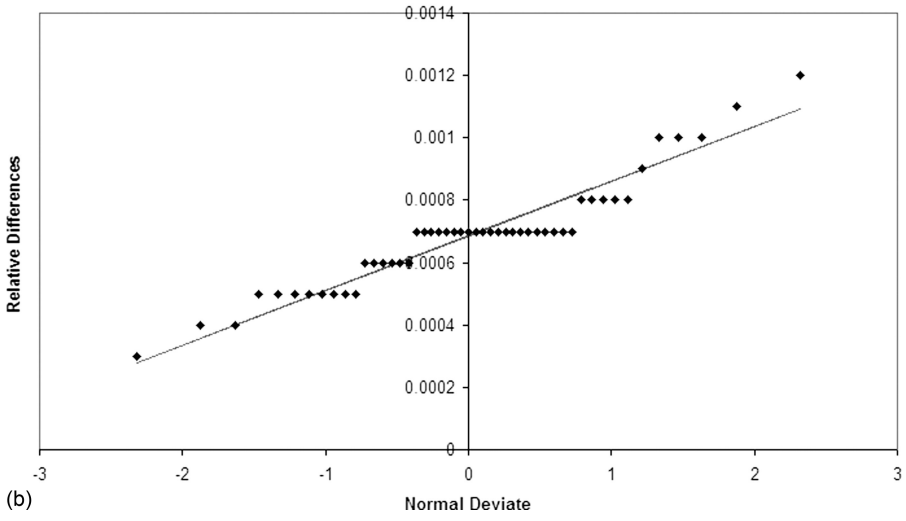

Fig. 5—(a) ILCP histogram for sulfur in #2 diesel fuel by D2622. (b) Normal deviate plot for sulfur in #2 diesel by D2622.

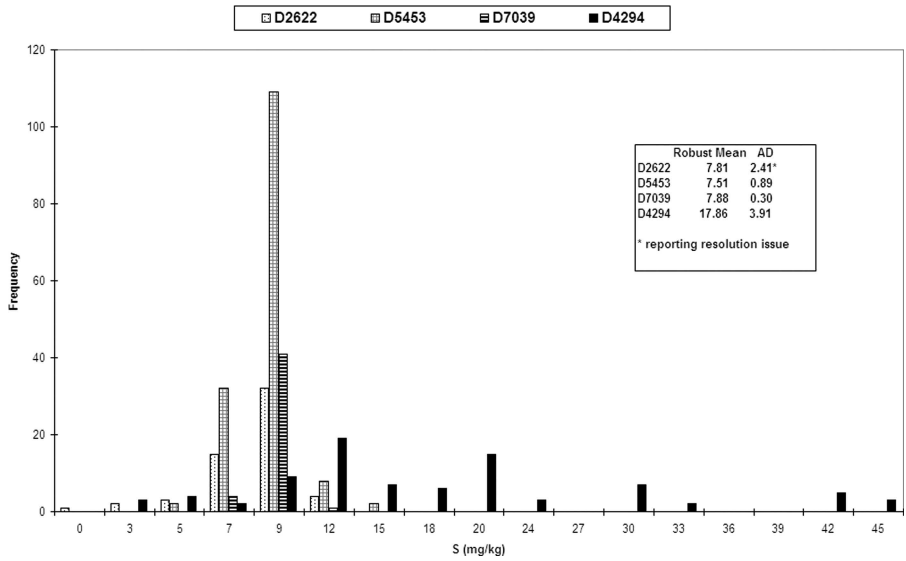

Fig. 6—Distribution of sulfur results in an ILCP #2 diesel fuel sample by four test methods.

and the normal deviate plot generally support a conclusion that the data are not normally distributed. Based on these statistics, laboratories should investigate rejected data and Z-score > 3 outliers, but other less critical flagged data may not require significant effort to find a root cause.

Laboratories may choose to develop histograms in support of their investigations. For example, an investigator can use a histogram to view the distribution of data derived from several test methods measuring the same parameter for a single crosscheck sample.

The histogram in Fig. 6 was generated in Excel using ILCP data from the DF20910 cycle for sulfur in #2 diesel fuel. In this case, where the mean sulfur level is approximately 7 mg/kg, the distribution of results for D2622, D5453, and D7039 is similar and as expected. The distribution for D4294, however, is very different. This observation along with evaluations presented later in this chapter suggests that D4294, as practiced by the laboratories in this PTP, appears to be less capable in this low sulfur range. In addition to Excel, several other software tools are available to the investigator for creating histograms.

Bias (Deviation from Mean)

A graphical technique for a laboratory to assist in evaluating proficiency test results is to plot the deviations from the mean for each result for each test cycle. D6299 mentions this in its approach in section 7.6 on proficiency testing, where participants are encouraged to plot their signed deviations from the consensus value (robust mean) on control charts. Laboratories would then apply the run rule strategy outlined in that standard to identify outliers and other issues such as long-term biases. The control chart preferred by the author is a chart of individual observations (called an I-Chart) with an exponentially weighted moving average (EWMA) overlaid on the data.

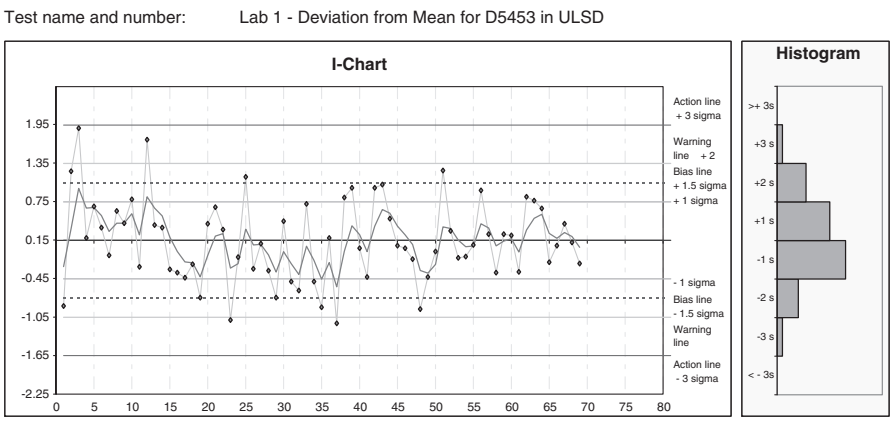

Fig. 7—Single lab deviations from the mean, for sulfur in ULSD by D5453 plotted on a control chart (I-Chart with EWMA).

Fig. 7 is a control chart for a single laboratory's deviations for determination of sulfur in ULSD by D5453. Using a control chart in this case is acceptable in that both the corresponding AD and normal deviate plot (not shown) indicate a normal distribution of data. This control chart shows reasonably good behavior for the laboratory in that data are within the designated control limits and the moving average (EWMA) generally moves about the mean, showing no indications of bias. Where the precision varies with analyte level or the data cover a large range, it may be more useful to plot the corresponding Z-scores rather than the raw deviations.

Another graphical approach for monitoring bias involves use of box and whisker graphs (discussed in detail in Section III). As is the case for reviewing histograms, laboratories should use the box and whisker graphs to observe where their particular result lies in the graph relative to the general distribution of results for the test method they used. We recommend investigating any data outside the whisker end, if those data were not flagged already for other causes. A review of the apparent distribution of results for each test method measuring the same parameter may provide valuable insight regarding overall biases between methods.

Another statistical but more complex approach to evaluate biases is described in D6617. This standard practice estimates whether or not a single test result is biased compared to the consensus value from the PTP program.

Z-Scores

Z-score (D7372) is defined as a standardized and dimensionless measure of the difference between an individual result and the corresponding arithmetic mean of a dataset, re-expressed in units of standard deviation (dividing the actual difference from the mean by the standard deviation):

$$Z_{score} = \frac{X_1 - \overline{X}}{s} \tag{9}$$

where $\overline{X}$ is the mean and s is the standard deviation.

Z-scores are calculated and presented along with laboratory results as part of the data summary tables in the ILCP reports. Several examples regarding how to use Z-scores to evaluate PTP results follow. Note that the objective of this and other tools is to identify potential issues, which can then be addressed to find solutions that will improve performance.

The sign and magnitude of the Z-score reflect the relative bias of the individual result versus the mean for the sample group. Note that the robust approach used by the ILCP eliminates the most egregious results (i.e., Z-scores >3 or <-3) in the first stage for determining the robust means and standard deviations. Z-scores in the 2 to 3 or -2 to -3 zones obviously represent somewhat greater differences (relative bias) than scores in the middle -2 to 2 zone. Therefore, laboratories should prioritize their investigations, concentrating first on results with Z-score >3 or <-3 and then on those >2 or <-2. This process of comparing and responding to Z-score values falling into different Z-score zones (e.g., 2 to 3 or -2 to -3), is similar to that used with control charts (D6299) with values falling in the various zones (e.g., between the mean and 1-sigma, 1 to 2 sigma).

When historical Z-scores are available, laboratories should plot the data to monitor for longer term trends and calculate the average Z-score for the inclusive period. Analysis of historical Z-scores is a means of evaluating laboratory performance over time to determine the in-statistical-control status of laboratory performance. The general expectation is for the average Z-score to be small and within ±1. Investigate cases where the average is >2 or <-2. As mentioned previously, one can plot and analyze Z-scores on a control chart and then take actions in accordance with the applicable run rules.

In 2008, as the ILCP prepared to reorganize the result tables in the ILCP reports to incorporate the most recent six historical Z-scores, there was no statistic to evaluate the means and standard deviations derived for the set of historical Z-scores. As a result, the ILCP program team developed a statistic, the precision indicator (PI), to assist laboratories in assessing Z-score trends. PI is a type of performance or capability index and is the ratio of the overall pooled standard deviation (across all laboratories for all reported historical Z-scores) to the individual laboratory Z-score standard deviation. The ILCP program team also adopted PI = 0.8 as the critical value for taking action. The critical value of 0.8 is similar to that used for TPI determinations as described in D6792 (§10.3.1.3) and D7372 (§6.1.7.1). If the resulting calculation produces a PI $<$ 0.8, then the laboratory should consider that their long-term precision for this test method most likely needs improvement. The following examples and discussions highlight the range of analyses and potential actions in dealing with Z-scores.

Fig. 8 represents Z-score results for two laboratories collected for nearly 4 years of monthly samples for sulfur in ULSD using D7039. In this case, a moving average (from Excel) that is similar to the EWMA shows how the averages move about the centerline. This is similar to plotting Z-scores on a quality control chart as mentioned previously. A review of the dispersion of Z-scores over time is different for the two laboratories. For the entire dataset, an *F-t*est shows that the standard deviations for all Z-scores for these two laboratories are statistically distinguishable. An examination of the chart for the most recent 12 cycles would suggest that the standard deviations should be similar. We

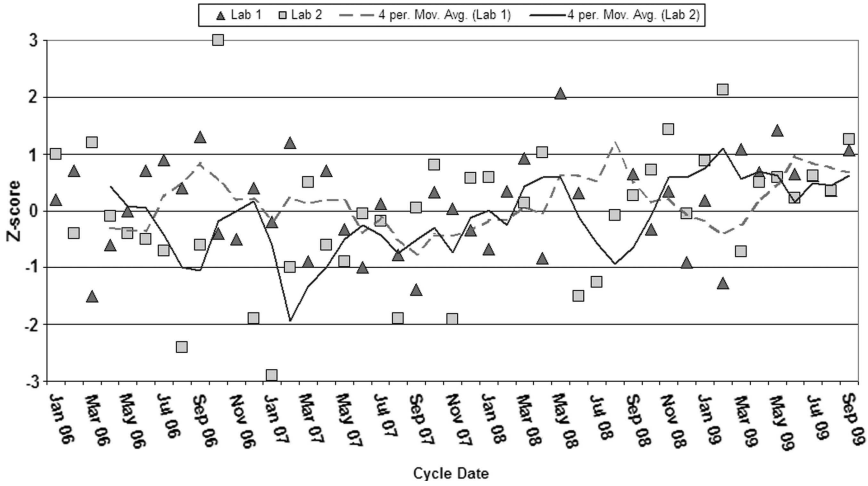

Fig. 8—Z-scores (with moving average) for determination of sulfur in ULSD by D7039, plotted sequentially by sample date.

substantiated this observation using the *F-test* and *t-test*, and the results show that the standard deviations and mean for the 12 most recent data are not statistically distinguishable. This means Lab 2 was able to improve performance over time eventually matching that for Lab 1.

As shown in Table 1, the ILCP designed some PTPs with 12 cycles per year, and so these programs generate copious data over relatively short periods. This is the case represented by Fig. 9, which covers sulfur in ULSD by D5453. A visual inspection of the chart indicates that the variability of the Z-scores seems to get worse over time, as highlighted by the two overlaid ovals. Analysis of these data shows that the standard deviation during the earlier period ($s = 0.71$) was noticeably better than the precision ($s = 1.06$) in the more recent period. Further, an *F-test* of this data revealed that the respective standard deviations are statistically distinguishable. Therefore, the real question for the laboratory would be, what happened to cause the Z-score precision to increase and how can they return to the previous precision level? Be aware, however, that the Z-scores might be getting worse because the standard deviations representing the performance of all participating laboratories might be getting better over time.

Fig. 10 shows sequential historical Z-scores plotted for two laboratories for determination of calcium in lube oil by D4951. This chart also shows the linear trend lines (from the Excel spreadsheet). For these cases, use the graphics along with the corresponding PIs to enhance the analysis. The story for Lab A is a good one in that the trend for Z-score over time shows improvement from scores in the -1 to -2 range to the 0 to -1 range. Because PI > 0.8, there is no indication that the laboratory precision needs improvement. Lab B has a PI < 0.8, so laboratory precision may be in need of improvement, as is obvious from the scatter of data in the graph. There does not appear to be any decrease in variability over the more recent cycles, although the corresponding trend

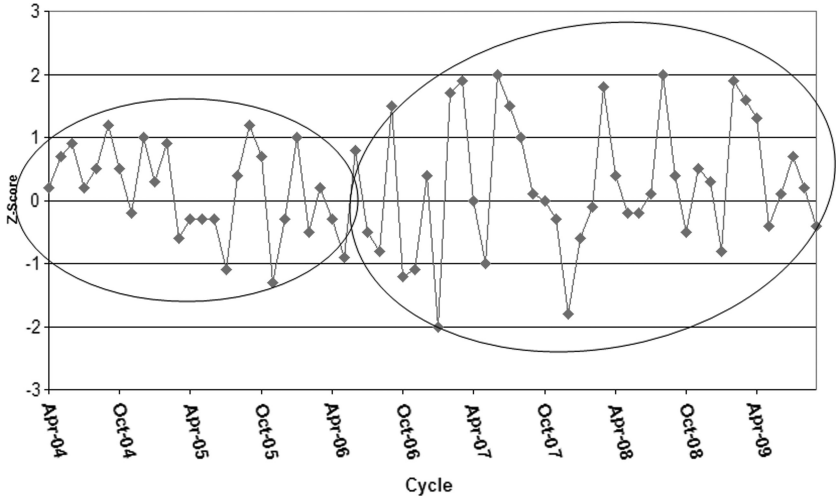

Fig. 9—Plot of Z-scores for single laboratory for sulfur in ULSD by D5453 covering multiyear period.

line is in the right direction. The differences in precision between Labs A and B in Fig. 10 are obvious even without referring to the PI scores.

TPI$_{Industry}$

The TPI, as defined in D6792 (§10), is a capability index that compares the published test method reproducibility to the site precision. TPI is a measure of the

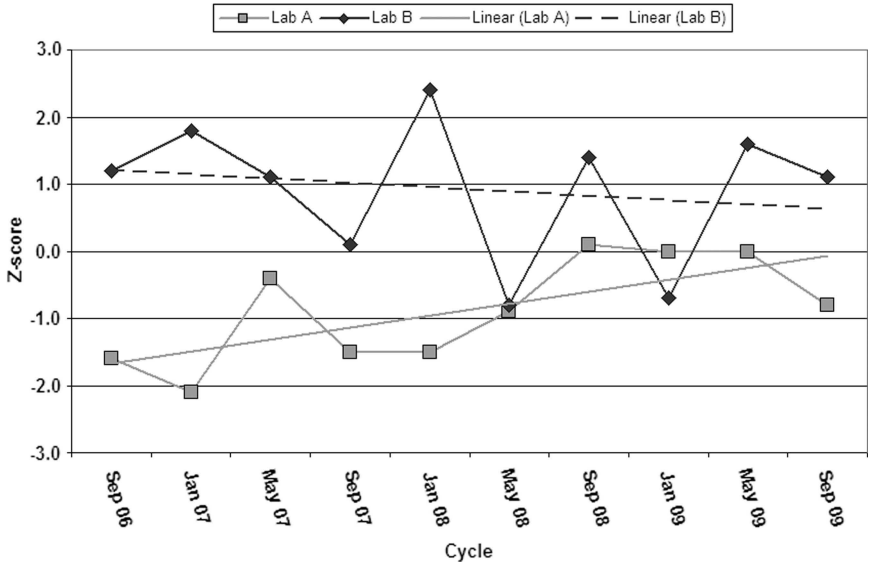

Fig. 10—Historical Z-scores for calcium in lube oil by D4951; PI = 1.07 and 0.79 for Labs A and B, respectively.

capability of the laboratory to meet the published precision of the test method. The author developed the TPI in the late 1980s to assist laboratories with interpretation of their quality control chart results [16,17]. When reviewing these early control charts, we observed that laboratories might have impressive-looking charts based on the precision estimates (i.e., the site precision) generated by the laboratory in the process of setting up the control limits. Impressive in this case means that results were always in control. When we calculated the corresponding expected ASTM reproducibility (R_{ASTM}) for the quality control sample, however, we often discovered that the site reproducibility ($R' = site\ precision \cdot 2.77$) was significantly different (greater) than the published R_{ASTM}. From this observation and coupled with knowledge of capability indices in general, we developed the TPI as the ratio of the two reproducibility estimates. We also developed action criteria. As the use of control charts spread, so did the use of the TPI tool. D6792 incorporated the TPI in 2002 along with guidance for interpreting the TPI and for determining when to take action.

$TPI_{industry}$ is similar to TPI, in that it is the ratio of the calculated ASTM reproducibility (R_{ASTM}) to the reproducibility observed for the ILCP dataset ($R_{these\ data}$). Thus, $TPI_{industry}$ is a measure of the capability of the participating laboratories with respect to the performance expected from the corresponding test method. The guidance in D6792 for interpretation of TPI results generally applies to the interpretation of $TPI_{industry}$. Table 5 shows the key action criteria for this statistic.

For situations where $TPI_{industry} < 0.8$ and a laboratory Z-score is very high (>2 or >3) or very low (<-2 or <-3), the laboratory needs to consider their contribution to the relatively poor performance by the industry group. Although influencing a large group of participants to improve overall performance is beyond the capability of a single laboratory, each laboratory should consider taking action as appropriate based on the guidance in Table 6.

Fig. 11 is a composite of sections of an ILCP report showing how a low TPI score and a high Z-score along with the scatter plot and histogram lead to similar conclusions. These data indicate that Lab 26 should investigate the cause of their contribution to poor precision and bias. Even though the

TABLE 5—Interpretation of $TPI_{Industry}$ and Associated Actions

$TPI_{industry}$	Implication
> 1.2	The performance of the group providing the data is probably satisfactory relative to the corresponding ASTM published precision. In the general case, the greater the $TPI_{industry}$ value above 1.2, the more significant the difference in reproducibility precisions.
0.8 to 1.2	The performance of the group providing the data may be marginal and each laboratory should consider reviewing the test method procedures to identify opportunities for improvement. (See Table 4.)
< 0.8	The performance of the test method as practiced by the group is not consistent with the ASTM published precision. Participants should look for opportunities to improve overall test method performance.

TABLE 6—Implications of Low $TPI_{Industry}$ and High Z-Score		
$TPI_{industry}$	Z-score	Implication
< 0.8	> 3.0 or <-3.0	The laboratory is likely a significant contributor to the group's poor reproducibility. The laboratory should investigate as described in Table 4.
< 0.8	2 to 3 or -2 to -3	There are more laboratories in this group and each should consider actions to improve precision. Use Table 4 as appropriate.

AD > 1.0 in this case, the other evidence is strong enough to support taking action to improve performance. See the next section for further discussions regarding analyses of $TPI_{industry}$ data by the responsible technical groups.

PTP and Site Precision Comparisons

Another opportunity to evaluate laboratory performance involves comparison of the PTP precision to the corresponding site precision. As mentioned previously, a laboratory generates site precision data as part of preparing and maintaining quality control charts (in accordance with D6299). When site precision is available, the laboratory can divide the corresponding PTP precision by the site precision. We would consider this ratio as another capability-type index similar to TPI. In general, a laboratory would aim to have this ratio > 1.0.

ASTM #2 Diesel Fuel
Sample ID: DF20906
June 2009
Sulfur - D4294
(mass %)

271

Current Data					Historic Z Scores									
Lab	Test Results	Robust Deviation	Z Score	Notes	0902	0810	0806	0802	0710	0706	Mean Z	Std Dev Z	Precision Indicator (PI)	Significant Difference
008	0.001	-0.0013	-0.8		R	1.0	1.7	-0.8	1.2	0.3	0.43	1.06	0.93	
011	**0.0106			R	NDS	NDS	2.0	NDS	0.0	NDS	1.00	1.41	N/A	N/A
012	0.002	-0.0003	-0.2		1.9	-0.1	-0.6	NDS	1.4	-0.3	0.35	1.03	0.96	
016	0.001	-0.0013	-0.8		2.0	NDS	-0.8	NDS	NDS	NDS	0.13	1.62	N/A	N/A
017	0.0012	-0.0011	-0.6		R	-2.2	0.4	NDS	NDS	NDS	-0.80	1.31	N/A	N/A
019	0.00	-0.0023	-1.4	2	-1.1	-0.6	NDS	NDS	NDS	NDS	-1.03	0.40	N/A	N/A
020	0.0014	-0.0009	-0.5		NDS	NDS	NDS	NDS	NDS	NDS	-0.50	0.00	N/A	N/A
022	0.0017	-0.0006	-0.4		NDS	NDS	NDS	NDS	NDS	NDS	-0.40	0.00	N/A	N/A
026	0.00782	0.0056	3.2	1, 2, 3	0.0	0.8	0.1	0.0	1.1	0.3	0.79	1.15	0.86	

Pooled Standard Deviation = 0.99

No. Valid Results	112
Robust Mean	0.0023
Robust Standard Deviation	0.0017
Reproducibility ASTM Standard	0.0014
Reproducibility These Test Data	0.0047
Anderson Darling	2.86
TPI	0.30

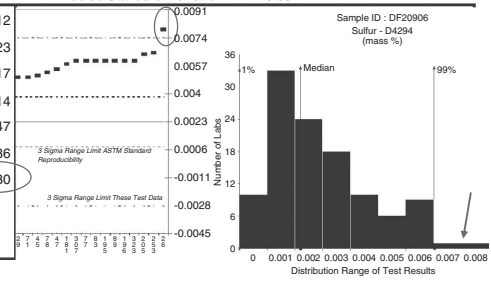

Fig. 11—Combined use of the ILCP result table, statistical summary, and graphs to identify opportunities for improvement.

SECTION III – ANALYSIS AND INTERPRETATION BY INDUSTRY GROUPS

This discussion is directed to the ASTM (or other standard developing organization) subcommittees or work groups that are responsible for developing and maintaining standard test methods. Another important group includes those responsible for company-wide laboratory quality assurance or those responsible for participation of a multilaboratory cluster in a proficiency test program. These groups generally have an interest in any observation related to a relative bias of one laboratory group versus the rest of the participants, the overall performance or capability of a test method as practiced by industry laboratories, and the relative bias of one method versus another for determining a given parameter. In addition, these groups are interested in the overall implications that PTPs may have with respect to improvements in precision over time [18]. The approaches discussed here are available to all interested parties, including PTP participants.

Techniques to investigate relative biases and test method capability (precision) are discussed here. Data normality was discussed previously, and those tools are applicable regardless of whether a laboratory or a work group uses them. All examples discussed here are from the ILCP.

Relative Bias

Bias is the systematic error that contributes to the difference between a population mean of the measurements or test results and the accepted reference or true value. The accepted reference or true value may be provided as a certified reference material (CRM) or as a consensus material from a PTP.

Some test methods used for analysis of petroleum products and lubricants have published bias statements based on analyses of CRMs. Knowing these biases, when they exist, is valuable for method developers and for those planning to adopt these test methods in their laboratories. The biases that may exist among the multiple test methods used to analyze the same parameter are also of significant interest. The between-method bias is just another component of the overall between-laboratory bias that we observe when laboratories use different test methods to evaluate the same parameter for product quality. So, this relative bias relates to the magnitude of difference in means by one or more test methods analyzing for the same test parameter. More specifically, relative bias, as used in this discussion, is the systematic error that contributes to the difference between population means from measurements or test results using two test methods that purport to measure the same property.

PTP results offer significant insight regarding relative bias. The techniques recommended for evaluating relative bias include graphical comparison of means, statistical evaluations to determine significance of bias, and combinations of statistical and graphical comparisons. The following sections demonstrate these approaches using examples from the ILCP.

BOX AND WHISKER PLOTS

Box and whisker plots are available in ILCP reports when data are generated for a given property by two or more different test methods. Box and whisker plots group test data by quartiles, with the center box representing the middle 50 % of test data centered on the median. The horizontal line within the box represents the median of the reported data. The whisker length is adjusted to

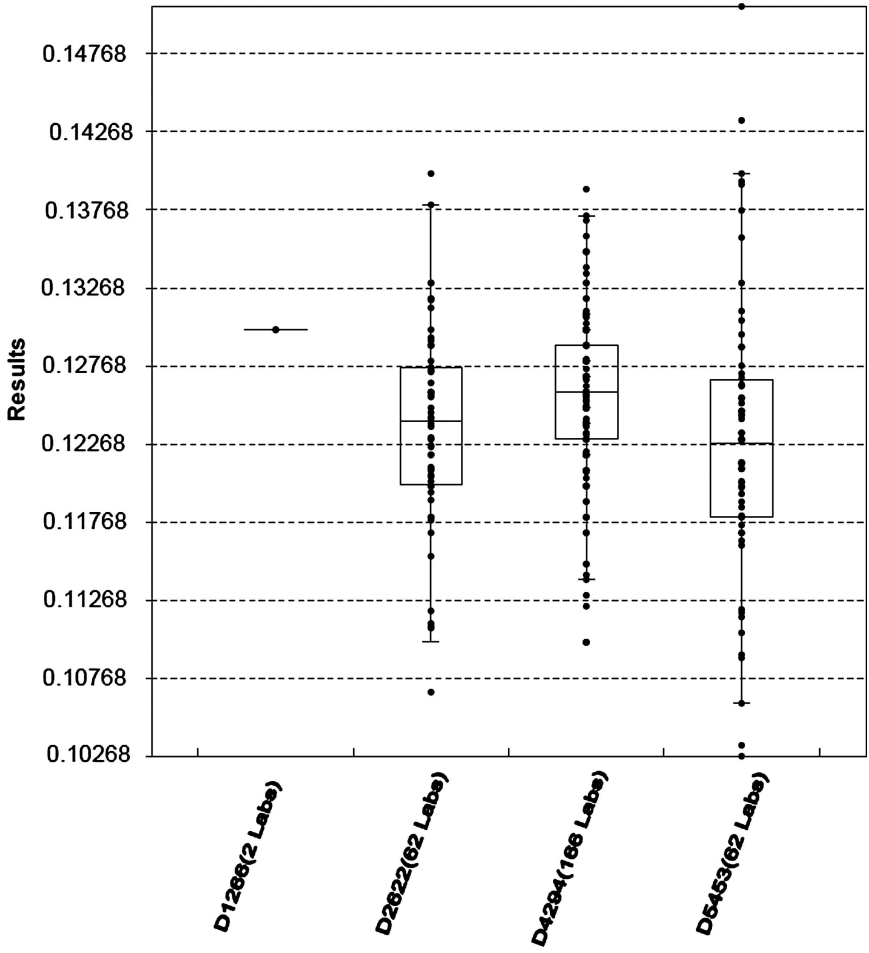

Fig. 12—Box and whisker plots for sulfur in jet fuel (03/2009 cycle); D1266 (2 labs), D2622 (62 labs), D4294 (166 labs), and D5453 (62 labs).

the last data point that falls within 1.5 times the difference between the upper and lower value of the center box. Data points above or below the whisker are included in the plot unless they are off the Y-axis scale.

The size (length) of the box and whisker is a measure of the precision of the proficiency test results. The position of one median relative to that in another box is a measure of the relative bias among the test methods involved. The box and whisker plots, however, do not estimate the significance of any bias observed. Further, these graphs represent the distribution of data only for one PTP cycle, so observed biases here may not be supported in subsequent cycles.

Fig. 12 shows the box and whisker plots for sulfur determinations in an ILCP jet fuel sample. The following discussion demonstrates how a laboratory or responsible work group might proceed with an investigation or analysis using these box and whisker graphs. The plots in Fig. 12 for a 2009 cycle have

mean sulfur levels of 1240 mg/kg (0.1240 mass %). The data distributions (precision) and the means (relative biases) among the three test methods (D2622, D4294, and D5453) appear to be similar. The data displayed for D1266 are largely ignored because there are only two data reported and the significance of the reported mean is uncertain.

For the results displayed in Fig. 12, it is difficult just from a review of the displayed plots to determine if the observed differences in means and precisions among the three test methods are significant. Analyses using *F-tests* and *t-tests* show that the means and precisions among the pairs are statistically significantly distinguishable, with the exception of the D2622 and D5453 pair, where the means are not statistically distinguishable. The individual laboratory should determine where their results fall within the graph and evaluate any implications.

MEAN ($\overline{X}$) GRAPHS

Perhaps the simplest graphical approach for evaluating long-term bias is to plot the means obtained for each test method on the same chart for multiple cycle results. This is more meaningful when results are available for numerous PTP cycles. In these cases, one might be able to observe whether there appears to be any significant relative biases among the methods. Fig. 13a shows the relative biases for four test methods analyzing for sulfur in RFG. The ovals on the chart are used only to highlight the four results for a specific cycle/sample. Based on this chart, one would readily conclude that there is a reasonable chance that D4294 results are biased high relative to the means reported by the other three methods. For the scale used in this plot the results for D2622, D5453 and D7039 are packed too closely to make any immediate conclusion regarding relative biases. Even with the scales exploded, it is still difficult to discern any bias. Although this is an easy plot to make, without also knowing the corresponding standard deviations it is difficult to know for sure if any of the observed differences are significant.

Perhaps a more effective graphical approach is to plot the means for one or more test methods versus another test method. This shows relative biases more directly, especially if error bars ($\overline{X} \pm 1.96 \cdot \mathrm{SE}$) are also used. We demonstrate this in Figs. 13b,13c for the same dataset. The overall bias for D4294 relative to D2622 is obvious in Fig. 13b, especially considering the distance that most the error bars are from the parity line (vertical error bars are for D4294 and horizontal bars are for D2622). We determined using the *t-test* that this relative bias is statistically significant at the 95 % confidence level and using the *F-test* that the precisions are statistically distinguishable, with D4294 having the larger precision.

In some cases, the graphical approach does not lead one to a clear conclusion regarding biases. For example, the plot in Fig. 13c seems to suggest that D5453 results may not be biased relative to D2622. In this case, we observe that the error bars are generally close to, or overlapping, the parity line. In this case, one should resort to using a *t-test* for clearer guidance. Such analyses show that the means for D5453 are not statistically significantly distinguishable from D2622.

From Fig. 14 it would appear that for the ILCP cycles observed, the means from D4294 are statistically significantly distinguishable from those using

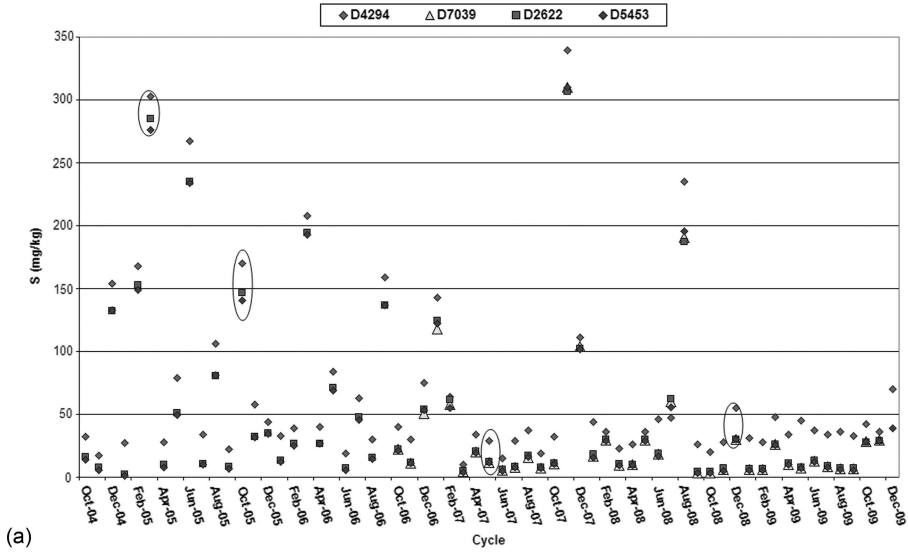

(a)

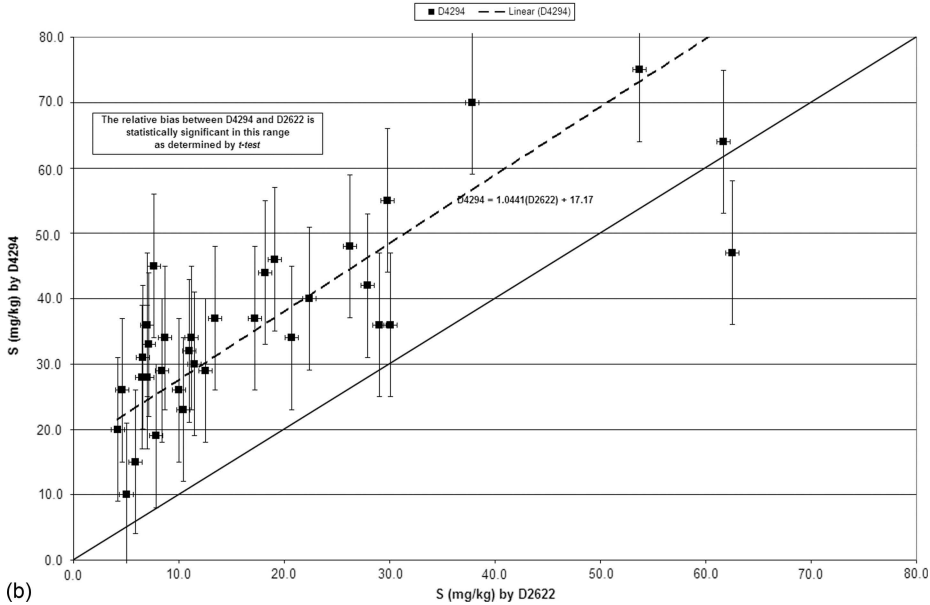

(b)

Fig. 13—(a) Plot of means by test methods by ILCP cycle for sulfur in RFG. (b) Plot of mean sulfur in RFG by D4294 versus D2622; each data point represents a program cycle. (c) Plot of mean sulfur in RFG by D5453 versus D2622. (Continued)

D2622. Statistical analyses to determine pooled standard deviations along with the *F-test* and *t-test* statistics show that the precision for D4294 is statistically significantly distinguishable compared to D2622. Further, the means for D4294 versus D2622 are not distinguishable at the 95 % confidence level; however, the difference appears to be statistically significant at the 90 % confidence level.

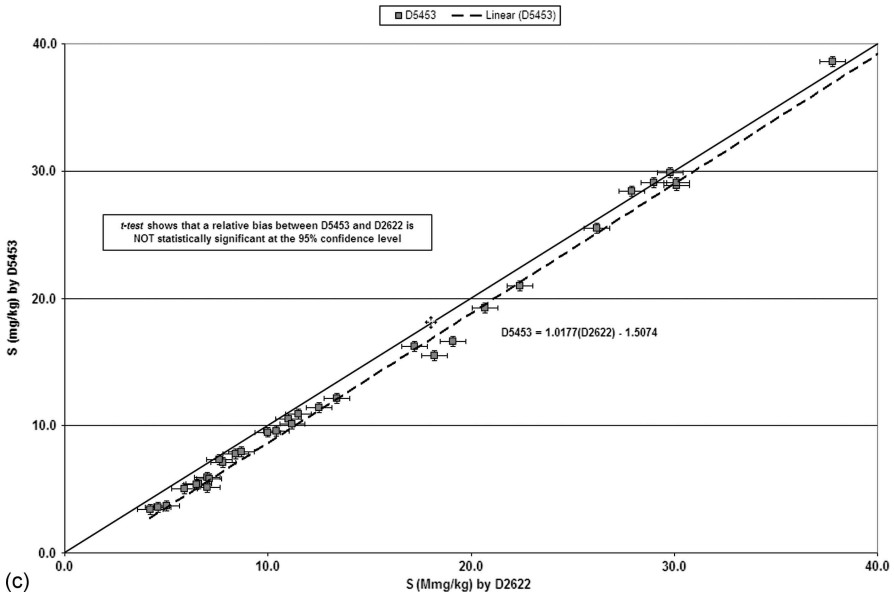

Fig. 13—(Continued)

Therefore, one would suggest that these observations are worth further investigations. Note that the approach used here is not quantitative because the standard deviations may vary with concentrations across the cycles.

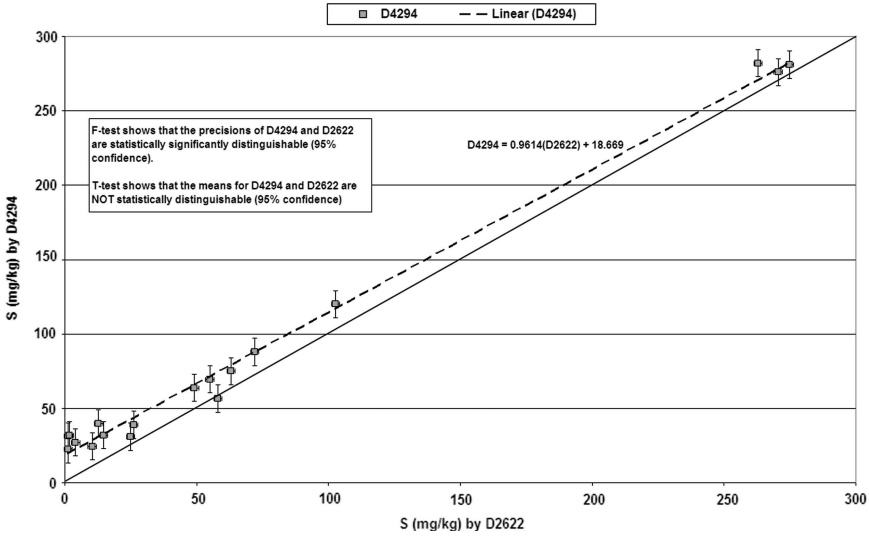

Fig. 14—Mean sulfur in mogas by D4294 versus D2622 covering numerous ILCP cycles.

Test Method Capability Trends

A laboratory or work group can assess the general capability of a test method by itself or relative to other methods using tools such as $TPI_{industry}$, relative standard deviation (or coefficient of variance), and the ratio of mean to standard deviation (quantitation index). We employ each tool with graphical analysis as well as statistical calculations to assess capability. It is important to note that we can determine the capability of one method versus another based on two data sources. One is to use the published reproducibility (R_{ASTM}), which provides the accepted or target values and the other is to use the data from a PTP ($R_{these\ data}$), which provides results as practiced by "real world" laboratories.

$TPI_{INDUSTRY}$

As discussed earlier, $TPI_{industry}$ is the ratio of R_{ASTM} to $R_{these\ data}$. This TPI is a capability index because it measures the relationship of the performance of the test method as practiced by an assortment of laboratories ($R_{these\ data}$) versus an expected performance (R_{ASTM}). This index helps determine how well the average laboratory performs the given test. Comparing TPI among test methods that purport to measure the same parameter (or property of a material that is being tested) provides interesting substance for debate. We recommend analyzing $TPI_{industry}$ both as a function of the proficiency test cycle (sequential results over time) and as a function of the mean result for the test cycle. Several examples are provided from the ILCP.

Figs. 15 and 16 are the graphs for $TPI_{industry}$ versus either the test cycle or the mean sulfur content, respectively, for sulfur in RFG. For the $TPI_{industry}$ versus test cycle chart, the linear trend line for D5453 shows an increasing trend, which means that overall, laboratory precision is improving over time and that interlaboratory variation is decreasing. The more recent data shows that the average

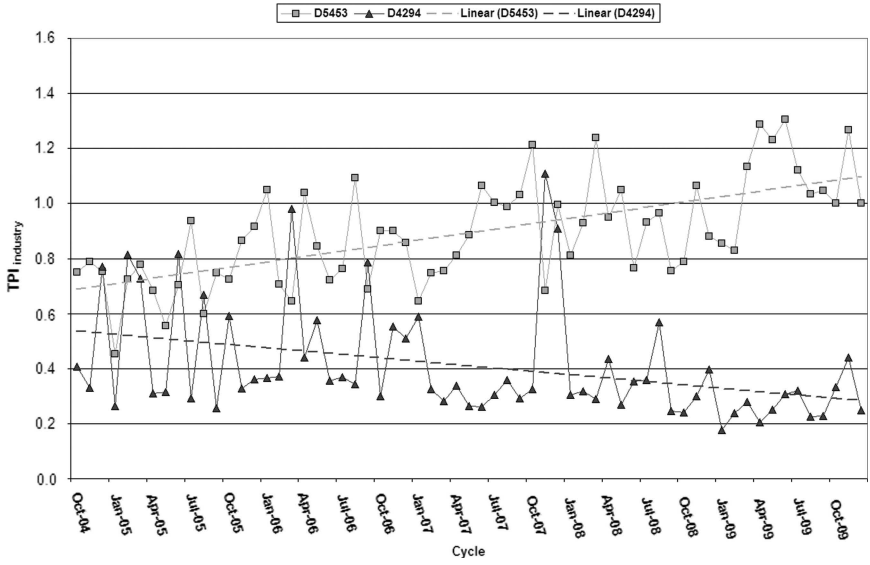

Fig. 15—$TPI_{industry}$ for sulfur in RFG by D5453 and D4294 by proficiency test cycle.

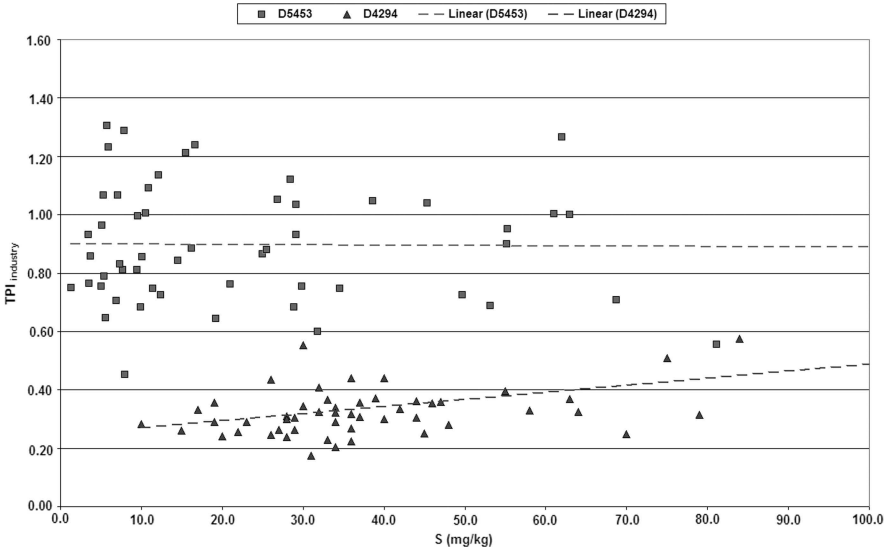

Fig. 16—$TPI_{industry}$ for sulfur in RFG by method versus mean sulfur.

$TPI_{industry}$ values are approaching 1.0, which indicates improving capability. The $TPI_{industry}$ trend for D4294 is decreasing, indicating deteriorating performance over time. Although not apparent from the chart, fewer laboratories are using this method. D4294 consistently posts the lowest $TPI_{industry}$ values, thus showing the poorest capability, as practiced by industry laboratories, for RFG and other products especially at low sulfur levels.

Fig. 16 shows the $TPI_{industry}$ data as a function of the corresponding reported mean sulfur level for a different dataset representing sulfur determinations in RFG. Although there is a fair scatter of $TPI_{industry}$ results across the range of mean sulfur levels shown, the general tendency for $TPI_{industry}$ for D5453 is in the 0.6 to 1.0 range. D4294, on the other hand, has relatively low values across this sulfur range. One could conclude that D4294, as practiced by the participating laboratories, is not very capable for sulfur measurements in RFG in the $<$100 mg/kg range.

RELATIVE STANDARD DEVIATION

Relative standard deviation (RSD) (or the coefficient of variation, CV) expressed as a decimal or as a percent, is an easy statistic to generate and interpret. Generally, one wants the percent relative standard deviation to be low, perhaps 10 % or lower. To establish a target, one can generate an expected percent RSD based on the published reproducibility. Several examples of plots and interpretation of RSD data from the ILCP follow.

Fig. 17 shows the relationship between RSD and the mean sulfur content of the sample across a number of products using D2622. The plots also show two expected RSD lines based on precision statements specifically for gasoline range and diesel range samples. This chart demonstrates that the capability of the test method (as practiced by industry laboratories) is relatively independent

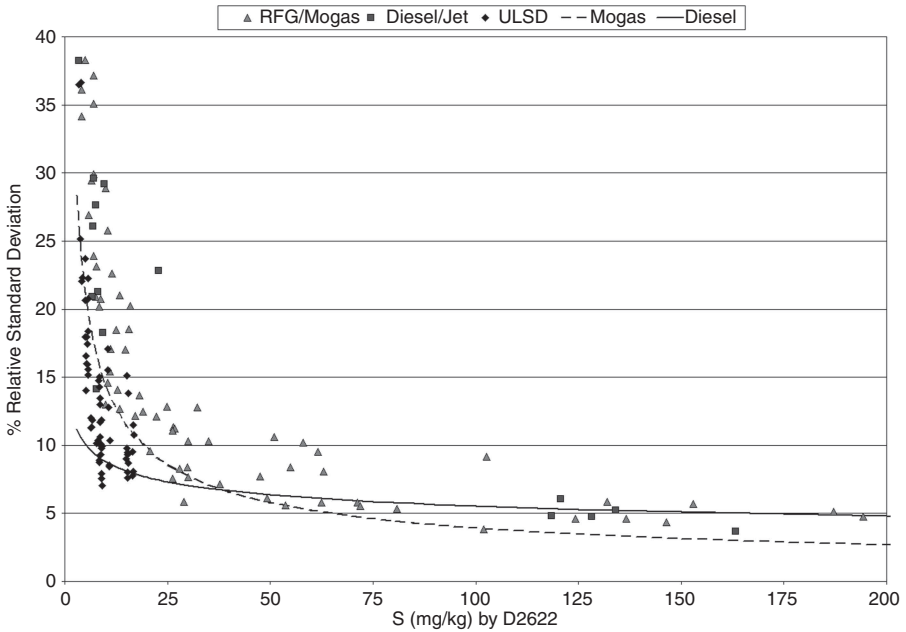

Fig. 17—Percent relative standard deviation for mean sulfur by D2622 by PTP product groups.

of product type across the concentration range studied for #2 diesel, jet fuel, mogas, and RFG. D2622 performance is slightly better (i.e., a lower RSD) for the ULSD product in the 5 to 15 mg/kg sulfur range. Further investigation would be needed to understand the reasons for such observations.

An analysis of D4294 capability from Fig. 18 shows that this method appears to be much less capable, especially at sulfur levels below 100 mg/kg. Here, capability seems to be independent of the product types included. More investigation is warranted, but reaching such conclusions is not the purpose of this chapter.

Fig. 19 shows good capability for D5453 across a range of ILCP products. Similar to the observations for D2622 (Fig. 17), the capability for D5453 appears to be slightly better for the ULSD product. These differences are just about as pronounced as they were for D2622 in the lowest sulfur range. Understanding the rationale supporting these differences would require further investigation by the responsible technical group.

RATIO OF MEAN TO STANDARD DEVIATION

Another measure of test method capability is the ratio of the mean to the standard deviation. Obviously, this is the reciprocal of the relative standard deviation. The reason for using the mean to standard deviation ratio relates to the use of a similar expression in evaluating limits of quantitation[4] (see

[4] The limit of quantitation is the point at which the ratio of mean concentration to repeatability standard deviation exceeds 10.

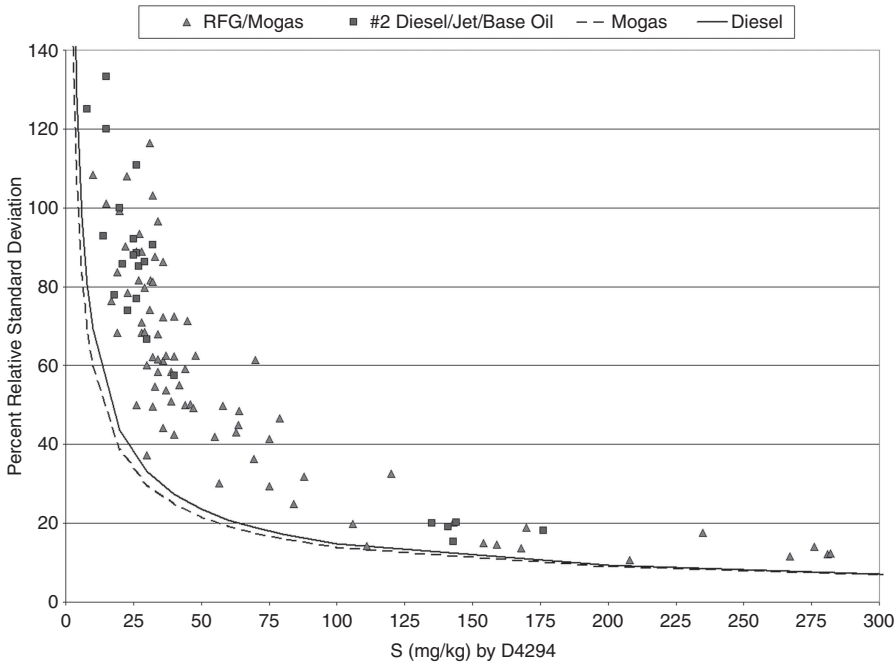

Fig. 18—Percent relative standard deviation for sulfur by D4294 by PTP product.

D6259). For purposes of discussion in this chapter, we call this ratio the quantitation index. This concept is especially important in evaluating test method performance at the lowest end of their operating ranges. Government regulations and manufacturing specifications are constantly pushing analytical techniques to pursue lower quantitation and detection limits.

Fig. 20 examines the performance of D5453 for sulfur determinations in the 0 to 15 mg/kg range, the lower end of its operating range. For these determinations, the capability of D5453 appears to be much better for ULSD product than for the others. The quantitation index for the ULSD product is in the 10 to 20 range compared to the 0 to 10 range for the other products. The base dataset for Fig. 20 is the same as used in Fig. 19. The next step would be to understand why this occurs, a task for the responsible technical group.

Influence of Uncontrolled Variables

An option available to the test method developers associated with a proficiency test program is the ability to request special information or data from the participants to enhance a special investigation. For example, one could request information regarding calibration practices or source of calibration standards. The requesting group would use this information in their investigation. Most investigations aim at improving performance of a specific test method used by a PTP.

One of the earliest tools used by the coordinating subcommittee responsible for the ILCP was to develop and issue lists of helpful steps that laboratories could take to improve performance. These lists, known as *Aids to Analysts*,

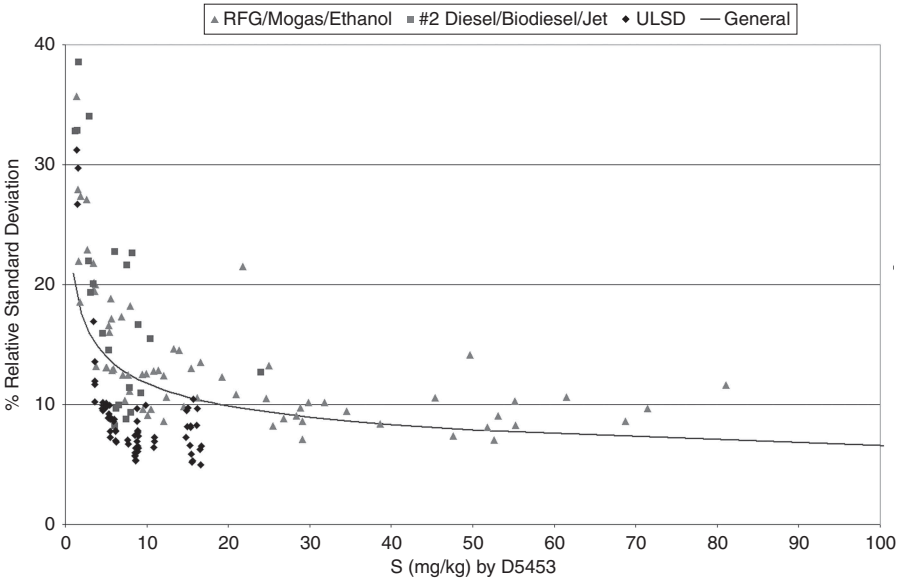

Fig. 19—Percent relative standard deviation for mean sulfur by D5453 by PTP product.

were distributed periodically to participants [19]. Some of these lists were incorporated into test methods as appendices (e.g., see D4628, D5453, and D5185).

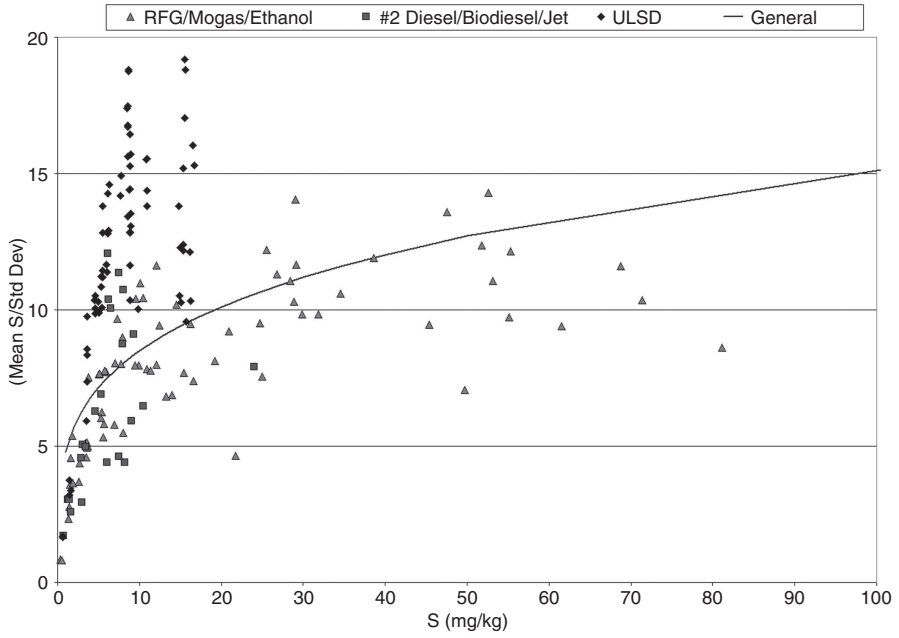

Fig. 20—Ratio of mean to standard deviation versus mean sulfur by D5453 by product.

Referenced Standards

Quality Assurance, Quality Control, and Statistics References	
D3244-07a	Standard Practice for Utilization of Test Data to Determine Conformance with Specifications
D6259-98 (Reapproved 2004)	Standard Practice for Determination of a Pooled Limit of Quantitation
D6299-08	Standard Practice for Applying Statistical Quality Assurance and Control Charting Techniques to Evaluate Analytical Measurement System Performance
D6300-08	Standard Practice for Determination of Precision and Bias Data for Use in Test Methods for Petroleum Products and Lubricants
D6617-08	Standard Practice for Laboratory Bias Detection Using Single Test Result from Standard Material
D6708-08	Standard Practice for Statistical Assessment and Improvement of Expected Agreement between Two Test Methods that Purport to Measure the Same Property of a Material
D6792-07	Standard Practice for Quality System in Petroleum Products and Lubricants Testing Laboratories
D7372-07	Standard Guide for Analysis and Interpretation of Proficiency Test Program Results
E177-08	Standard Practice for Use of the Terms Precision and Bias in ASTM Test Methods
E178-08	Standard Practice for Dealing with Outlying Observations
E456-08	Standard Terminology Relating to Quality and Statistics
E882-87 (Reapproved 2003)	Standard Guide for Accountability and Quality Control in the Chemical Analysis Laboratory
E1301-95 (Reapproved 2003)	Standard Guide for Proficiency Testing by Interlaboratory Comparisons
E1323-09	Standard Guide for Evaluating Laboratory Measurement Practices and the Statistical Analysis of the Resulting Data
E1329-00 (Reapproved 2005)	Standard Practice for Verification and Use of Control Charts in Spectrochemical Analysis
E2489-96	Standard Practice for Statistical Analysis of One-Sample and Two-Sample Interlaboratory Proficiency Testing Programs
E2554-07	Standard Practice for Estimating and Monitoring the Uncertainty of Test Results of a Test Method in a Single Laboratory Using a Control Sample Program

E2655-08	Standard Guide for Reporting Uncertainty of Test Results and Use of the Term Measurement Uncertainty in ASTM Test Methods
ISO 17025	General Requirements for the Competence of Testing and Calibration Laboratories
Spectroscopic Test Methods	
D1552-08	Standard Test Method for Sulfur in Petroleum Products (High-Temperature Method)
D1840-07	Standard Test Method for Naphthalene Hydrocarbons in Aviation Turbine Fuels by Ultraviolet Spectrophotometry
D2622-08	Standard Test Method for Sulfur in Petroleum Products by Wavelength Dispersive X-ray Fluorescence Spectrometry
D4053-04 (2009)	Standard Test Method for Benzene in Motor and Aviation Gasoline by Infrared Spectroscopy
D4294-08a	Standard Test Method for Sulfur in Petroleum and Petroleum Products by Energy Dispersive X-ray Fluorescence Spectrometry
D4628-05	Standard Test Method for Analysis of Barium, Calcium, Magnesium, and Zinc in Unused Lubricating Oils by Atomic Absorption Spectrometry
D4927-05	Standard Test Methods for Elemental Analysis of Lubricant and Additive Components—Barium, Calcium, Phosphorus, Sulfur, and Zinc by Wavelength-Dispersive X-ray Fluorescence Spectroscopy
D4951-09	Standard Test Method for Determination of Additive Elements in Lubricating Oils by Inductively Coupled Plasma Atomic Emission Spectrometry
D5184-01(2006)	Standard Test Methods for Determination of Aluminum and Silicon in Fuel Oils by Ashing, Fusion, Inductively Coupled Plasma Atomic Emission Spectrometry, and Atomic Absorption Spectrometry
D5185-09	Standard Test Method for Determination of Additive Elements, Wear Metals, and Contaminants in Used Lubricating Oils and Determination of Selected Elements in Base Oils by Inductively Coupled Plasma Atomic Emission Spectrometry (ICP-AES)
D5453-09	Standard Test Method for Determination of Total Sulfur in Light Hydrocarbons, Spark Ignition Engine Fuel, Diesel Engine Fuel, and Engine Oil by Ultraviolet Fluorescence
D5708-05	Standard Test Methods for Determination of Nickel, Vanadium, and Iron in Crude Oils and Residual Fuels by Inductively Coupled Plasma (ICP) Atomic Emission Spectrometry
D5769-04	Standard Test Method for Determination of Benzene, Toluene, and Total Aromatics in Finished Gasolines by Gas Chromatography/Mass Spectrometry
D5845-01(2006)	Standard Test Method for Determination of MTBE, ETBE, TAME, DIPE, Methanol, Ethanol and *tert*-Butanol in Gasoline by Infrared Spectroscopy
D5863-00a (2005)	Standard Test Methods for Determination of Nickel, Vanadium, Iron, and Sodium in Crude Oils and Residual Fuels by Flame Atomic Absorption Spectrometry

D6443-04	Test Method for Determination of Calcium, Chlorine, Copper, Magnesium, Phosphorus, Sulfur, and Zinc in Unused Lubricating Oils and Additives by Wavelength Dispersive X-ray Fluorescence Spectrometry (Mathematical Correction Procedure)
D6481-99 (2004)	Standard Test Method for Determination of Phosphorus, Sulfur, Calcium, and Zinc in Lubrication Oils by Energy Dispersive X-ray Fluorescence Spectroscopy
D6595-00 (2005)	Standard Test Method for Determination of Wear Metals and Contaminants in Used Lubricating Oils or Used Hydraulic Fluids by Rotating Disc Electrode Atomic Emission Spectrometry
D7039-07	Standard Test Method for Sulfur in Gasoline and Diesel Fuel by Monochromatic Wavelength Dispersive X-ray Fluorescence Spectrometry
D7212-07	Standard Test Method for Low Sulfur in Automotive Fuels by Energy-Dispersive X-ray Fluorescence Spectrometry Using a Low-Background Proportional Counter
Other Test Methods for Comparison	
D3120-08	Standard Test Method for Trace Quantities of Sulfur in Light Liquid Petroleum Hydrocarbons by Oxidative Microcoulometry

References

[1] Bover, W. J., "Tackling Interlaboratory Variability for the Global Marketplace," *ASTM Standardization News*, Vol. 22(6), 1994, pp. 56–63.

[2] Bover, W. J., "ASTM, the Petroleum Industry, and Quality Assurance–Good Partners Years Ago... Still Good Today," *ASTM Standardization News*, Vol. 26(4), 1988, pp. 29–33.

[3] Nadkarni, K., "Does Your Laboratory Measure Up? ASTM Program Helps Build Proficiency," *Lubes'N'Greases*, April 2001, p. 28.

[4] Tanguay, W., "Confirm Lab Quality with the Cross-Check Program," *Practicing Oil Anal.*, July–August 2002, p. 54.

[5] Bradley, D., "ASTM Proficiency Testing Programs: Statistical Quality Assurance Tool for Laboratories," *ASTM Standardization News*, Vol. 32(3), 2004, pp. 26–239.

[6] Nadkarni, R. A. and Bover, W. J., "Bias Management and Continuous Improvements through Committee's D02's Proficiency Testing," *ASTM Standardization News*, Vol. 32(6), 2004, pp. 36–39.

[7] Bover, W. J., Chair; Nadkarni, R. A., Vice-Chair Program Management; Schanerberger, E., Vice-Chair; Mammel, W., Vice-Chair Program Improvement; McKlindon, A., Program Manager, D02.92 Coordinating Subcommittee on Interlaboratory Cross-check Programs.

[8] Nadkarni, R. A. Bover, W. J. and Bradley, D. R., "Proficiency Test Programs–Impact on Analytical Test Methods used by the Petroleum Industry," *Eastern Analytical Symposium*, Somerset, NJ, 2006.

[9] Bover, W. J., "Relevant Global Standards: A Petroleum Industry Perspective–Continuous Improvement through Proficiency Testing and Training Programs," *International Forum on Process Analytical Technology*, Arlington, VA, Feb. 2006.

[10] ASTM ILCP Reports for product programs, available to participants and to D02 subcommittees and work groups; request from ASTM International at PTP@astm.org.

[11] Analytical Methods Committee of the Royal Society of Chemistry, "Robust Statistics: How Not to Reject Outliers," *Analyst*, Vol. 114, 1989, pp. 1693–1697.

[12] Box, G. E. P., Hunter, W. G. and Hunter, J. S., *Statistics for Experimenters, An Introduction to Design, Data Analysis and Model Building*, John Wiley & Sons, New York, 1978.

[13] Stanley R. M., "F and t-Tests for Custom Reports," committee correspondence, presented to ASTM D02.92, 2007.

[14] Rosner, B., "Percentage Points for a Generalized ESD Many-Outlier Procedure," *Techometrics*, Vol. 25, No. 2, May 1983, pp. 165–172.

[15] Walfish, S., "A Review of Statistical Outlier Methods," *Pharmaceutical Technol.*, Nov. 2006, pp. 82–88.

[16] Bover, W. J., Paszek, J. and Troxell, J. K., "Design of Interlaboratory Quality Control Program and New Quality Control Charts Based on Resistant Methods," Exxon Research and Engineering Company, internal communication, May 1990.

[17] Bover, W. J. and Stillman, J. E., "Statistical Quality Control for the Petroleum Laboratory: Using the Control-Performance Chart," Exxon Biomedical Sciences, Inc., internal communication, October 1992.

[18] Stanley, R. M. and Schaefer, R., "Statistical Performance of Methods for Measuring Sulfur Concentrations in Ultra Low Sulfur Diesel," *J. ASTM International*, Vol. 3, 2006 p. 30, Paper ID JAI 100294.

[19] *Aids to Analyst*, available from ASTM International at PTP@astm.org.

5

Calibration and Quality Control Standards and Reference Materials for Spectroscopic Analysis of Petrochemical Products

R. A. Kishore Nadkarni[1]

INTRODUCTION

Calibration and quality control form an integral part of all analyses, including spectroscopic analysis of petroleum products and lubricants. All apparatus and instruments used in a laboratory for such analysis require calibration or verification before an instrument can be used for producing reliable data. A perfect analysis needs a perfect calibration as a first step and perfect quality control as perhaps the last step in the sequence of analytical events. Often this cycle is depicted as [1]:

$$\text{Calibration} \rightarrow \text{Sample Analysis} \rightarrow \text{QC Analysis} \rightarrow \text{Calibration} \rightarrow \quad (1)$$

Appropriate calibration and quality control standards must be used during the analysis. A wide variety of such standards is available from commercial sources and National Institute of Standards and Technology (NIST), and many oil company laboratories prepare their own calibration or quality control reference materials. Calibration standards identical to the samples being analyzed would be ideal, but failing that, at least some type of standards must be used to validate the analytical sequence.

TERMINOLOGY

Some definitions of commonly used term in this area are described in Table 1.

REFERENCE MATERIALS

Three principal areas can be identified where the usage of reference materials is essential:

1. Method development and evaluation: For verification and evaluation of precision and accuracy of the test methods, for development of reference test methods, for evaluation of field test methods, and for validation of methods for a specific use.
2. Traceability of measurements: For developing secondary reference materials, for developing traceability protocols, and for direct field use.
3. Assurance of measurement compatibility: For direct calibration of methods and instruments in widely separated plants, or between customers and suppliers, and for intra- and interlaboratory quality assurance.

[1] *Millennium Analytics, Inc., East Brunswick, New Jersey*

TABLE 1—Terminology Used in Calibration and QC Reference Materials

Keyword	Description	Source
Calibration standard	Material with a certified value for a relevant property issued by or traceable to a national organization such as NIST, and whose properties are known with sufficient accuracy to permit its use to evaluate the same property of another sample.	D6792
Certified reference material (CRM)	Reference material one or more of whose property values are certified by a technically valid procedure, accompanied by a traceable certificate or other documentation that is issued by a certifying body.	ISO Guide 30
Check standard	A material having an assigned (known) value (reference value) used to determine the accuracy of the measurement system or instrument. This standard is not used to calibrate the measurement instrument or system.	D7171
Quality control standard	For use in quality assurance program to determine and monitor the precision and stability of a measurement system; a stable and homogenous material having physical or chemical properties, or both, similar to those of typical samples tested by the analytical measurement system. The material is properly stored to ensure sample integrity, and is available in sufficiently large quantity for repeated long-term testing.	D6299
Reference material	A material with accepted reference values, accompanied by an uncertainty at a stated level of confidence for desired properties, which may be used for calibration or quality control purposes in the laboratory. Sometimes these may be prepared "in-house" provided the reference values are established using accepted standard procedures.	D6792
Standard reference material	Certified reference materials that are issued by the National Institute of Standards and Technology, Gaithersburg, MD.	

ASTM Standard D6792: Guide for Quality System in Petroleum Products and Lubricant Testing Laboratories
ASTM Standard D7171: Test Method for Hydrogen Content of Middle Distillate Petroleum Products by Low-Resolution Pulsed Nuclear Magnetic Resonance Spectroscopy
ASTM Standard D6299: Practice for Applying Statistical Quality Assurance Techniques to Evaluate Analytical Measurement System Performance

CALIBRATION STANDARDS

Calibration standards appropriate for the method and characterized with the accuracy demanded by the analysis to be performed must be used during analysis. Quantitative calibration standards should be prepared from constituents of known purity. Use should be made of primary calibration standards or certified reference materials specified or allowed in the test method. Use of calibration standards almost identical to analysis samples is usually achievable in physical measurements but is often difficult or sometimes almost impossible in chemical measurements. Even the effects of small deviations from matrix match and analyte concentration level may need to be considered and evaluated on the basis of theoretical or experimental evidence or both. Sometimes the use of standard additions technique to calibrate the measurement system is a possibility. But because an artificially added analyte may not necessarily respond in the same manner as a naturally occurring analyte, this approach will not be always valid, particularly in molecular speciation work.

Where appropriate, values for reference materials should be produced following the certification protocol used by NIST or other standards-issuing bodies, and should be traceable to national or international standard reference materials, if required or appropriate.

It is not a good idea to use the same material both as a calibration and quality control standard. The latter should be similar in matrix to the types of samples being analyzed, although this is not always possible due to lack of availability of suitable certified materials. At least for quality control purposes, it is easy enough to obtain a reasonable large quantity of a plant product, analyze it by the tests of interest multiple times, and calculate the average and the variance values to initiate the control chart. The key here is not necessarily the accuracy of the results but how repeatable the analysis is.

In addition to the oil-soluble organometallic compounds used for the calibration of instruments such as atomic absorption spectrometry (AAS), inductively coupled plasma–atomic emission spectrometry (ICP-AES), or X-ray fluorescence (XRF), single- or multielement calibration standards may also be prepared from materials similar to the samples being analyzed, provided the calibration standards to be used have previously been characterized by independent, primary (for example, gravimetric or volumetric) analytical techniques to establish the elemental concentration at mass percent levels.

CALIBRATION REFERENCE MATERIAL

Calibration reference material (RM) can be classified as primary or secondary. The primary RMs are well-characterized, stable, homogenous materials produced in quantity, and with one or more physical or chemical properties experimentally determined, within the stated measurement uncertainties. These are certified by a recognized standardization laboratory using the most accurate and reliable measurement techniques. The secondary RMs are working standards or quality control standards and may have undergone less rigorous evaluation for day-to-day use in the laboratory.

The two most important considerations in preparing reference materials are their homogeneity and stability. Considerable time and money would be wasted if analytical certification measurements were done on reference materials that were later found to be inhomogeneous with respect to properties of interest.

Hence, several randomly selected representative aliquots should be analyzed first to ensure homogeneity. This testing does not need to produce the most accurate data, only relative measurements using precise analytical techniques such as X-ray fluorescence or neutron activation analysis, where applicable.

Similarly, if a reference material is found to be unstable over the period of its use, it would be of little benefit to the standardization community. It is not very practical, however, to check the stability over an inordinately extended period of time before issuing the reference material for general use. Hence, testing the stability of the material continues as part of ongoing quality control of reference materials.

Both stock and working standards need to be stored in a contamination-free environment, out of direct sunlight, and in clean containers, preferably amber glass bottles to safeguard against physical degradation. One way for checking for degradation is to measure the response of an aliquot of the standard by the same instrument under identical instrumental conditions over a period of time, and monitor it for changes. A list of suggested precautions to be taken in storage of reference materials is given in Table 2.

Shaking the bottle containing the standard is recommended before an aliquot is taken out of the bottle to ensure the uniformity of the blends. If stirring is necessary, a polytetrafluoroethylene (PTFE) coated magnetic stirrer is advisable for this purpose.

Often, when a suitable matrix CRM or SRM is not available from a national or international commercial source, well-equipped laboratories can prepare and certify a reference material for their own use. One advantage of such an

TABLE 2—Precautions to Be Taken for Storage and Use of Reference Materials

#	Precautions
1	Store only in the original containers in the dark and not subject to significant variations in temperature and humidity.
2	Do not heat the material in the original container for any reason.
3	Shake the material well before removing any material from the original container.
4	Never place any equipment such as glass rods, metal spatulas, etc. in the original container.
5	When preparing calibration standards, remove the necessary amount into a secondary container.
6	Any material removed from the original container should never be poured back into it.
7	When two thirds of the material has been used up, prepare additional material using standardized protocols and methods.
8	The long-term stability of some of the calibration standard materials may be unknown. If any changes in appearance or other characteristics are observed suggesting material instability, discard the rest of the material, and obtain a new batch of the material.

approach is that the RM can be very similar to the products that will be analyzed using this RM. An example of this would be certification of a lubricant additive containing barium and sulfur as principal components [Nadkarni, unpublished]. This material was analyzed multiple times on multiple days along with a blank and a NIST SRM using two independent primary methods for each element. Barium was analyzed using (a) ashing followed by barium sulfate precipitation, and (b) alkali fusion followed by barium sulfate precipitation. All final precipitates and residual filtrates were checked by XRF and ICP-AES for contaminants and incomplete precipitation. With each batch, 99.99 or 99.999 % pure barium sulfate or barium nitrate chemical compounds were assayed. Sulfur was analyzed using (a) alkali fusion followed by barium sulfate precipitation, and (b) Ditert tube combustion followed by redox titration. With each batch five nines pure barium sulfate and NIST fuel oil SRM were analyzed.

Materials available from ASTM Proficiency Testing Programs (PTP) may be used provided no obvious bias or unusual frequency distributions of results are observed. The consensus value is most likely the value closest to the true value of this material; however, the uncertainty attached to this mean value is dependent on the precision and the total number of participating laboratories. It has been observed that the variance on the mean value of such PTPs is very large, making such materials unsuitable for calibration work. They are, however, suited for use as quality control materials.

ANALYSIS OF CRMs

Because the CRMs will potentially be used for calibration and quality control of a large number of instruments and measurements, the values assigned to them need to be "accurate" values; i.e., they should be within the overall uncertainty of "true" values. Hence, the methods used in certifying the values must have a valid and well-described theoretical foundation, must have negligible systematic errors and a high level of precision, and must give "true" value with high reliability. These primary methods require skilled and experienced personnel, are time consuming and comparatively expensive to perform, and are perhaps uneconomical for routine field use. Three types of such methods may be used for certification:

1. Measurement by a method of known and demonstrated accuracy performed by two or more analysts independently. Frequently an accurately characterized backup method is used to provide assurance of correctness of data.
2. Measurement by two or more independent and reliable methods whose estimated inaccuracies are small relative to the required accuracy for certification. The basic principles of two techniques must be entirely different; e.g., copper determination by electrogravimetry and titrimetry is acceptable, but not by AAS and ICP-AES, because both latter methods are based on the atomic spectroscopic methods, one by absorption and the other by emission. The likelihood of two independent methods being biased by the same amount in the same direction is small. When the results by two methods agree, there is a good possibility that the results are accurate; three methods would almost guarantee it.
3. Measurement via a worldwide network of laboratories, using both methods of proven accuracy and using existing certified reference materials as controls. It has to be recognized, however, that the mean value of results from a large number of laboratories may not necessarily represent an accurate value when the repeatability and reproducibility are large.

The resultant data from the above analyses will be statistically examined for outliers, and calculated for mean and variance values. Because only limited quantities of primary reference standards are generally available, it is a good idea to prepare secondary quality control standards based on or traceable to the primary standards. These can be produced by obtaining a large, stable, and homogenous sample of a product. It should be similar to the products usually analyzed in the laboratory. Analyzing this new material for the species of interest while the analytical process is under statistical control and ensuring that the instrument used is calibrated using primary reference standards should be the basis of preparing a secondary or working reference standard. At least 20 replicates spread over different days and by different analysts, if possible, are obtained on the proposed QC standard. Based on these replicate analyses, the mean and the standard deviation values can be assigned to this material.

Sometimes, out of necessity, some values for reference materials are quoted based on only one technique that does not qualify it as a reference method for that analysis. Such values are usually labeled as "for information only" values. These can be later upgraded to certified values when subsequently additional techniques or laboratories produce reliable confirmatory data.

Further discussion of calibration standards and similar issues can be found in ASTM Standard Practice for Calibration Requirements for Elemental Analysis of Petroleum Products and Lubricants, currently in the ballot process in Committee D02.

SOURCES OF REFERENCE STANDARDS

NIST by far has been one of the biggest producers of reference materials both for calibration and quality control. Some of these are listed in Table 5. Several other mostly commercial organizations—Leco, Cannon, Alpha, VHG, Spex, Conostan, Accustandard, Spectrum Standards Inc., Analytical Services, Inc., Laboratory of Government Chemist U.K.—also provide such materials, although probably not with the rigor that NIST uses in their certification. Often once NIST issues an SRM, a body of literature data rapidly builds up, increasing the number of elements for which information is available. For example, fuel oil SRM 1634 was issued by NIST for seven elements, but Gladney et al. [2] list data on 22 elements from the literature for this popular SRM. SRM 1634 was replaced with SRM 1634a in 1982 again with seven trace elements certified.

A number of other NIST residual fuel oils (SRM 1619 through 1623) have been certified for sulfur but not for any other trace elements. These sulfur SRMs are potential trace element standards, if homogeneity with respect to trace elements can be demonstrated. Filby et al. [3] using neutron activation analysis showed that SRM 1634a is suitable as a standard for seven more trace elements in addition to those originally certified by NIST. Seven other trace elements appeared to be inhomogeneously distributed, however, and were probably present in mineral particulates (see Table 3). SRM 1619 is a convenient standard for vanadium and for low levels of nickel in oils, but SRM 1620a did not appear to be a suitable standard for any trace element investigated because of the high percent relative standard deviation for this material (see Table 4). It must be admitted, however, that part of the high variability may be due more to analytical uncertainty at such low concentration levels rather than to the inherent inhomogeneity of the material.

TABLE 3—Trace Element Analysis of Residual Fuel Oil NIST SRMs

Element	SRM 1634 Reference or Consensus Values[a]	X ± Std. Dev. (n)	SRM 1634a Reference or Information Values[b] (*)	X ± Std. Dev. (n)
Nickel	36 ± 4	33.0 ± 2.3 (9)	29 ± 1	26.3 ± 2.5 (12)
Vanadium	320 ± 15	301 ± 15 (3)	56 ± 2	58.5 ± 5.0 (9)
Iron	13.5 ± 1	27.5 ± 6.5 (9)	31	41.0 ± 7.2 (12)
Zinc	0.23 ± 0.05	1.0 ± 0.4 (8)	2.7 ± 0.2	2.89 ± 0.92 (12)
Arsenic	0.081 ± 0.026	0.062 ± 0.13 (9)	0.12	0.141 ± 0.017 (12)
Selenium	0.19 ± 0.02	0.151 ± 0.058 (9)	0.15 ± 0.02	0.19 ± 0.05 (12)
Sodium	11.9 ± 0.9	15.3 ± 1.9 (9)	87 ± 4	102 ± 16 (9)
Bromine	0.04 ± 0.009	0.33 ± 0.09 (8)	< 1	0.88 ± 0.19 (12)
Chromium	0.097 ± 0.002	0.22 ± 0.06 (8)	0.7	0.82 ± 0.11 (12)
Cobalt	0.31 ± 0.05	0.33 ± 0.06 (9)	0.3	0.50 ± 0.37 (12)
Antimony	0.011 ± 0.002	0.09 ± 0.11 (8)	–	0.034 ± 0.031 (9)

All values are in milligrams per kilogram. Additional results for rare earths and other elements are also given in this paper, but that information is not reprinted here because generally those data would not be of interest to petroleum chemists (excerpted from Ref [2]).
[a] NBS certified only for nickel, vanadium, and iron; other values are from Gladney and Burns [4].
[b] NBS certified or information values for SRM 1634a.

Nadkarni and Morrison used a novel way of using calibration standards in neutron activation analysis [5]. Instead of using pure metallic elements as irradiation standards, they advocate using well-characterized matrix standards for multielement analysis. The advantages are simplicity of operation, long shelf life, and elimination of errors inherent in the preparation of a large number of synthetic standards at the trace element levels. Examples of this approach were illustrated by analyzing geological materials using U.S. Geological Survey (USGS) diabase W-1 as the irradiation standard, and biological materials using NBS SRM 1571 orchard leaves as the irradiation standard. The results obtained using this approach matched very well with other literature values within the analytical uncertainty.

The protocols that NIST uses for certification of SRMs and CRMs are described in May et al. [6].

Kelly et al. [7] suggested a "designer" method for the preparation of NIST traceable fossil fuel standards with concentrations intermediate to SRM values for sulfur. Laboratories can mix and prepare standards for distillate fuels oil, residual fuel oil, and coal in almost any desired concentrations with uncertainties that are calculable and traceable to NIST-certified values. Because the sulfur content of all fossil fuel SRMs was certified at NIST with a high degree of accuracy and precision by isotope dilution thermal ionization mass spectrometry, in

TABLE 4—Trace Element Analysis of NIST Residual Fuel Oils SRMs

Element	SRM 1619	% RSD	SRM 1620a	% RSD
Nickel	12.0 ± 1.1 (12)	9	< 2 (6)	
Vanadium	42.6 ± 4.7 (6)	11	< 0.2 (6)	
Iron	23 ± 16 (12)	74	11 ± 7 (7)	62
Zinc	1.27 ± 0.35 (12)	28	0.7 ± 0.5 (11)	84
Cobalt	0.35 ± 0.04 (12)	11	0.08 ± 0.06 (12)	72
Chromium	0.38 ± 0.11 (12)	29	0.2 ± 0.07 (11)	39
Selenium	1.39 ± 0.67 (12)	48	2.0 ± 0.6 (12)	28
Antimony	0.03 ± 0.02 (10)	60	0.1 ± 0.14 (10)	148
Arsenic	0.094 ± 0.010 (12)	11	0.04 ± 0.01 (12)	24
Bromine	0.7 ± 0.9 (12)	127	0.6 ± 0.6 (12)	100
Sodium	27 ± 6 (9)	23	9.4 ± 2.9 (9)	31

Data excerpted from Ref [7]. All values are in milligrams per kilogram. The numbers in parentheses are the number of replicates analyzed.

almost all cases the total expanded uncertainties of the standards produced from binary mixtures are an order of magnitude smaller than the reproducibility of current methods used in the commercial laboratories. This method gives the SRM user a continuum of concentrations available for calibration and quality control test samples. Unlike calibrants prepared from high purity components, this method enables the SRM user to create a customized series of calibrants in the fossil fuel matrix of interest. This should reduce or eliminate biases that result from differences in matrix composition among standards and unknowns.

A partial list of SRMs available from NIST is given in Table 5. A large percentage of these SRMs are certified for sulfur given the importance of this element in environmental studies. The NIST catalog of SRMs (Special Publication 260) should be consulted for further information, price, and availability.

GENESIS OF AN SRM

Lubricating oil additive package SRM 1848 has been characterized for a large number of parameters by NIST. Additionally and separately, this material was also used for an Interlaboratory Crosscheck Program (ILCP) by ASTM D02 Committee on Petroleum Products and Lubricants. The chemical company that supplied this material to both these organizations had also conducted an independent and separate interlaboratory study for its internal plant laboratories. Some of the laboratories that participated in the internal crosscheck also participated in the ASTM crosscheck. It is interesting to compare the precision obtained in these three exercises of analyses of this SRM.

TABLE 5—A Partial List of NIST Reference Materials for Petrochemical Industry

NIST SRM #	Matrix	Certification
Sulfur		
2721	Crude oil	1.5832 ± 0.0044 m%
2722	Crude oil	0.21037 ± 0.0084 m%
2770	Distillate fuel oil	41.57 ± 0.39 mg/kg
1624 d	Distillate fuel oil	3,882 ± 20 mg/kg
2723 a	Diesel fuel oil	11.0 ± 1.1 mg/kg
2714 b	Diesel fuel oil	426.5 ± 5.7 mg/kg
1622 e	Residual fuel oil	2.1468 ± 0.0041 m%
1619 b	Residual fuel oil	0.6960 ± 0.007 m%
1621 e	Residual fuel oil	0.9480 ± 0.0057 m%
1623 c	Residual fuel oil	0.3806 ± 0.0024 m%
1620 c	Residual fuel oil	4.561 ± 0.015 m%
1634	Residual fuel oil	Sulfur and trace elements
2717 a	Residual fuel oil	2.9957 ± 0.0032 m%
1616 b	Kerosine	8.41 ± 0.12 mg/kg
1617 a	Kerosine	1730.7 ± 3.4 mg/kg
1819	Lubricating oil	Sulfur
1819 a	Base oils	Five levels from 0.04235 to 0.6135 m%
2710	Di-n-butyl sulfide	Sulfur
8771	Diesel fuel	Sulfur
8590	Gas oil	Sulfur
2294	Reformulated gasoline	0.00409 ± 0.00010 m%
2295	Reformulated gasoline	0.0308 ± 0.0002 m%
2296	Reformulated gasoline	0.00400 ± 0.00004 m%
2297	Reformulated gasoline	0.03037 ± 0.00015 m%
2299	Reformulated gasoline	0.00136 ± 0.00015 m%
2298	High octane gasoline	0.00047 ± 0.00013 m%
2286 and 2287	High octane gasolines	Sulfur

TABLE 5—A Partial List of NIST Reference Materials for Petrochemical Industry (Continued)		
NIST SRM #	**Matrix**	**Certification**
2719	Calcined petroleum coke	0.8877 ± 0.0010 m%
2718	Green petroleum coke	4.7032 ± 0.0079 m%
Mercury		
1919 b	Residual fuel oil	0.00346 ± 0.00074 ng/kg
2721	Light-sour crude oil	0.0417 ± 0.0057 ng/kg
2722	Heavy-sweet crude oil	0.129 ± 0.013 ng/kg
2724 b	Diesel fuel oil	0.000034 ± 0.000026 ng/kg
Vanadium/Nickel		
8505	Crude oil	Vanadium 390 mg/kg
2721	Crude oil	Vanadium
1618	Residual fuel oil	Vanadium 423; nickel 75 mg/kg
2717	Residual fuel oil	
1634 c	Fuel oil #6	Vanadium 28.19; nickel 17.54 mg/kg
Organics		
1829	Reference fuels	Alcohols
2292 to 2297; 2299	Reformulated gasolines	MTBE
2286; 2287; 2298; 1838	High octane gasolines	Ethanol
1837	Gasoline	Methanol and butanol
1839	Gasoline	Methanol
2288; 2289	Gasolines	t-Amyl-methyl ether
2290; 2291	Gasolines	Ethyl-t-butyl ether
2293	Gasoline	Methyl-t-butyl ether
Miscellaneous		
1580	Shale oil	
1582	Crude oil	
8507	Mineral oil	Water 76.8 mg/kg
1818	Lubricating oil	Chlorine
1083–1085	Used oils	Wear metals

(*Continued*)

TABLE 5—A Partial List of NIST Reference Materials for Petrochemical Industry (Continued)

NIST SRM #	Matrix	Certification
1836	Lubricating oil	Nitrogen
1636 to 1638	Reference fuels	Lead
2712	Reference fuel	Lead 11.4 mg/kg
2713	Reference fuel	Lead 19.4 mg/kg
2714	Reference fuel	Lead 28.1 mg/kg
2715	Reference fuel	Lead 784 mg/kg
1848	Lubricating oil additive	See Table 6
8506 a	Transformer oil	Water 39.7 mg/kg

NIST used prompt gamma ray activation analysis, ICP-AES, isotope dilution thermal ionization mass spectrometry (ID-MS), and X-ray fluorescence (XRF) for elemental analysis in addition to other ASTM test methods listed in Table 6 for base number, flash point, ash, sulfated ash, and kinematic viscosity determinations.

In the ASTM ILCP, 59 industry laboratories participated. Only a single aliquot was analyzed by each laboratory, so repeatability of analysis cannot be calculated. All laboratories used ASTM standard test methods for obtaining all the results. In addition to the ASTM tests mentioned in Table 6, elemental analysis was also conducted using ASTM standard test methods D4951, D5185 (ICP-AES), and D4927 (WD-XRF). In the company internal crosscheck, 24 laboratories participated using essentially the same test methods as previously mentioned.

Based on the data in Table 6, it can be concluded that the three data sets are in very good agreement with each other. Although there were only 8 statistical outliers in the company internal crosscheck, ASTM identified 140 of them in their larger crosscheck. Shown in Table 7 are the results obtained using alternative methods such as AAS, ICP-AES, and XRF for determination of metals. These data show that the alternate methods produced equivalent results based on the interlaboratory average for each analytical technique. Similarly, nitrogen content determined by three alternative methods—D3228, D4629, and D5261—also produced equivalent results. Overall, the reproducibility of the analyses was better than that given in the individual ASTM test methods. Thus, this SRM should prove to be an ideal candidate for calibration and quality control in oil additives laboratories.

PREPARATION OF A LUBE OIL CRM

The example described next shows how an organization can prepare and certify a CRM for internal use when a similar material may not be available from a national certifying body. A large quantity of a 5W30 lubricating oil sample has been prepared for use as a quality control standard in Linden and its associated contract laboratories. The oil was analyzed in replicate in four contract

TABLE 6—Analysis of NIST SRM 1848 Additive Package

Analysis	NIST Value	ASTM ILCP Values (ALA 9610)	Company ILS Values
Boron, m%	0.136 ± 0.013	0.133 ± 0.0067	0.137 ± 0.003
Magnesium, m%	0.821 ± 0.058	0.828 ± 0.024	0.818 ± 0.013
Phosphorus, m%	0.779 ± 0.036	0.783 ± 0.025	0.794 ± 0.015
Sulfur, m%	2.3270 ± 0.0043	2.35 ± 0.08	2.28 ± 0.07
Chlorine, m%	0.0934 ± 0.0046		0.077 ± 0.0063
Calcium, m%	0.345 ± 0.011	0.357 ± 0.009	0.355 ± 0.009
Zinc, m%	0.866 ± 0.034	0.845 ± 0.028	0.859 ± 0.012
Hydrogen, m%	12.3 ± 0.4		
Nitrogen, m%	0.57 ± 0.03	0.587 ± 0.034	0.575 ± 0.012
Silicon, mg/kg	50 ± 2	47 ± 9	52 ± 12
Base number, mg KOH/g (D2896)	56.7 ± 0.7	56.1 ± 0.6	55.8 ± 0.7
Base number, mg KOH/g (D4739)	49.6 ± 5.6		
PMCC flash point (D93)	173°C (*)	174 ± 5	173 ± 7
COC flash point (D92)	194°C (*)		
Kinematic viscosity @ 100°C (D445)	170 cSt (*)	170.2 ± 1.2	
Kinematic viscosity @ 40°C (D445)	4,000 cSt (*)	3,935 ± 51	4,153 ± 24
Ash, m% (D482)	5 (*)		
Acid number, mg KOH/g (D664)	21 (*)		
Sulfated ash, m% (D874)	6.1 (*)	6.17 ± 0.60	6.17 ± 0.36
Density @ 15°C, g/mL (D4052)		0.9549 ± 0.0012	0.9547 ± 0.0007
(*) Information Value			

laboratories for a number of commonly determined parameters by multiple test methods where possible. Overall, the agreement between the four laboratories has been excellent. Based on this interlaboratory study, values have been assigned to analytical parameters. The mean values obtained are consistent with the expected product specifications of this lube oil. Where possible, different test methods were used for analyzing the same parameter and gave similar

TABLE 7—Elemental Analysis of NIST SRM 1848 by Alternative Test Methods				
Analysis	**AAS**	**ICP-AES**	**WD-XRF**	**Others**
Method	**D4628**	**D4951**	**D4927**	. . .
Boron, m%	0.139 ± 0.0102	0.139 ± 0.0047	. . .	. . .
Calcium, m%	0.357 ± 0.022	0.351 ± 0.009	0.356 ± 0.010	. . .
Magnesium, m%	0.826 ± 0.013	0.817 ± 0.016	. . .	. . .
Phosphorus, m%	. . .	0.787 ± 0.014	0.789 ± 0.032	. . .
Silicon, mg/kg	47 ± 14.2	54 ± 5.8	. . .	. . .
Sulfur, m%		2.30 ± 0.029	2.28 ± 0.055	. . .
Zinc, m%	0.870 ± 0.021	0.857 ± 0.009	0.855 ± 0.020	. . .
Nitrogen, m%	. . .	. . .	. . .	0.580 ± 0.022 (D 4629)
				0.574 ± 0.024 (D 5291)
				0.567 ± 0.013 (D 3228)

TABLE 8—Analytical Cross Check for 5W30 Lube Oil						
LAB/ANALYSIS	**ASTM METHOD**	**Lab # 1**	**Lab # 2**	**Lab # 3**	**Lab # 4**	**MEAN ± STD. DVN. (# of LABS)**
API gravity	D287			33.8 ± 0.13	33.9 ± 0.08	33.9 ± 0.07 (2)
Ash, m%	D482	0.636 ± 0.0089	0.658 ± 0.014	0.65 ± 0.005	0.596 ± 0.035	0.635 ± 0.028 (4)
BF viscosity @ −40°C, cP	D2983		88,180 ± 2502	67,540 ± 1521	75,620 ± 1644	77,113 ± 10401 (3)
Calcium, mg/kg	D5185			1,827 ± 26[a]	1,864 ± 9.3	
	D6443	1,840 ± 7.1	1,837 ± 9			
	D4951	1,770 ± 10[b]	1,840 ± 53[a]			1,830 ± 32 (6)
CCS @ −25°C, mPas	D5293		2,406 ± 42	2,330 ± 34	2,450 ± 14 (a)	2,395 ± 61 (3)
CCS @ −30°C, mPas	D5293		4,527 ± 47	4,620 ± 46	4,496 ± 90	4,548 ± 65 (3)
Chlorine, mg/kg	D6443		23.6 ± 2.3	28.8 ± 2.9		
	D808	26.4 ± 1.3			< 50	26.3 ± 2.6 (3)
Flash point (PMCC), °C	D93		203 ± 1.3	201 ± 2.7	204 ± 0.5	202.7 ± 1.5 (3)
Kin. viscosity @ 40°C, cSt	D445		59.90 ± 0.14	60.10 ± 0.06	60.06 ± 0.11	60.02 ± 0.11 (6)
Kin. viscosity @ 100°C, cSt	D445		10.33 ± 0.05	10.33 ± 0.71[a]	10.34 ± 0.03	10.33 ± 0.006 (3)
MRV @ −35°C, cP	D4684		18352 ± 134	18286 ± 120	18540 ± 182	18393 ± 132 (3)
Yield stress	D4684		No	No	No	No
Molybdenum, mg/kg	D5185	53.7 ± 1.01			54 ± 0.71	54 ± 0.2 (4)
Nitrogen, mg/kg	D4629	553 ± 24	636 ± 7.2	608 ± 7.7	704.4 ± 20.5	625 ± 63 (4)

(*Continued*)

TABLE 8—Analytical Cross Check for 5W30 Lube Oil (Continued)

LAB/ANALYSIS	ASTM METHOD	Lab # 1	Lab # 2	Lab # 3	Lab # 4	MEAN ± STD. DVN. (# of LABS)
Noack, m%	D5800 B			14.8 ± 0.4	14.6 ± 0.12	14.7 ± 0.3 (2)
Phosphorus, mg/kg	D5185			931.6 ± 2.7	995.4 ± 6.0	
	D4951	955.6 ± 8.9	940 ± 35.6			
	D6443	927.8 ± 10.1	967.6 ± 4.8			952 ± 25 (6)
Pour point, °C	D97		− 39.6 ± 1.3	− 42.0 ± 0.0	− 42.0 ± 0.0	
	D5950			− 44.0 ± 1.4		− 41.7 ± 1.6 (5)
	D5985		− 41.0 ± 0.0			
Ramsbottom carbon, m%	D524			0.846 ± 0.55[a]	0.834 ± 0.02[a]	0.84 ± 0.009 (2)
SASH, m%	D874	0.764 ± 0.0089	0.768 ± 0.018	0.778 ± 0.011	0.806 ± 0.015	0.779 ± 0.019 (4)
Sulfur, m%	D5185	0.2488 ± 0.0022		0.2648 ± 0.0076	0.2326 ± 0.0026	
	D6443	0.2558 ± 0.0019	0.2520 ± 0.001			0.2508 ± 0.0118 (8)
TAN, mg KOH/g	D664		1.83 ± 0.26[a]	1.75 ± 0.06	1.66 ± 0.04	1.75 ± 0.09 (3)
TBN, mg KOH/g	D2896		6.20 ± 0.17	6.40 ± 0.12	6.39 ± 0.17	6.33 ± 0.11 (3)
Zinc, m%	D4951	0.1035 ± 0.0044				
	D5185	0.1026 ± 0.0009	0.1063 ± 0.0006	0.1025 ± 0.008	0.1059 ± 0.0005	0.1035 ± 0.0024 (6)
	D6443	0.009994 ± 0.0007				

[a] Precision significantly different based on F-test at 95 % confidence limits.
[b] Mean significantly different based on t-test at 95 % confidence limits.

TABLE 9—Analytical Consensus Values versus Product Specifications of 5W30 Lube Oil

Analysis	ASTM Test Methods	Nominal Target	Assigned Value
API gravity	D287	33.6	33.9 ± 0.07
Ash, m%	D482	. . .	0.64 ± 0.03
BF Viscosity @ −40°C, Cp	D2983	. . .	77,113 ± 8972
Calcium, mg/kg	D4951; D5185; D6443	1,950	1,830 ± 32
Chlorine, mg/kg	D6443	150	26 ± 3
CCS @ −25°C, mPas	D5293	2,546	2,395 ± 61
CCS @ −30°C, mPas	D5293	4,801	4,548 ± 65
Flash point (PMCC), °C	D93	227	203 ± 1.5
Kin. viscosity @ 40°C, cSt	D445	60.37	60.02 ± 0.11
Kin. viscosity @ 100°C, cSt	D445	10.31	10.33 ± 0.006
MRV @ −35°C, cp	D4684	20,900	18,393 ± 132
Molybdenum, mg/kg	D5185	53	54 ± 0.2
Nitrogen, mg/kg	D4629	681	625 ± 63
Noack loss, m%	D5800 B	14.6	14.7 ± 0.3
Pour point, °C	D97; D5950; D5985	–42	−42 ± 1.6
Phosphorus, mg/kg	D4951; D5185; D6443	925	952 ± 25
Ramsbottom carbon, m%	D524	0.84	0.84 ± 0.009
SASH, m%	D874	0.8	0.78 ± 0.02
Sulfur, m%	D5185; D6443	0.3106	0.2508 ± 0.0118
TAN, mg KOH/g	D664	1.5	1.75 ± 0.09
TBN, mg KOH/g	D2896	6.6	6.33 ± 0.11
Zinc, m%	D4951; D5185; D6443	0.1012	0.1035 ± 0.0024

results, e.g., elemental analysis and pour point. The precisions obtained in a majority of analyses in this study were at least equal to or better than those given in the ASTM standard test methods.

The sample was analyzed on different days for five replicates for various product specification parameters. For all analyses, ASTM standard test methods were used.

Between the four laboratories, about 20 replicate analyses for most of the parameters were obtained. The individual data from each laboratory are included in Table 2. Because there were no statistical outliers under Dixon test, all data are pooled together for calculating the mean values in this table.

In Table 8 the precisions for all analyses obtained by the individual laboratories are summarized. Overall, the precisions obtained for each type of analysis are similar for each laboratory. In some cases, however, the precision of one of the laboratories is significantly different from those of others based on F-test at 95 % confidence limits. However, although the precision of a laboratory may be different than that of other laboratories, in reality it is better than that of other laboratories. Table 9 compares the agreement between the product specifications and the consensus values obtained from four laboratories.

COMPARISON OF TEST METHODS

Sometimes different ASTM test methods were used for the elemental analysis of this lube oil. It is interesting to compare the results obtained by different methods (Table 10). Two ICP-AES and two XRF methods were used. Where the data are available, different test methods produced essentially equivalent average results. In some cases, however, the precisions obtained by each method were not necessarily identical, e.g., ICP versus XRF ASTM methods for analysis of calcium, phosphorus, sulfur, and zinc. In all cases, the XRF results were more precise than the ICP results. Three different pour point methods—manual D97 and automatic D5950 and D5985—produced closely matching results.

COMPARISON OF PRECISIONS IN LABORATORIES VERSUS ASTM METHODS

Table 11 summarizes the repeatability (r) and the reproducibility (R) obtained for various analyses and compares them against the expected precisions given in the ASTM test methods. Where only one laboratory used a particular method, obviously only repeatability can be compared.

- The precisions were about the same in this study and in ASTM methods for the determination of API gravity (D287), PMCC flash point (D93), CCS @ −25°C (D5293), kinematic viscosity @ 40°C (D445), and Noack volatility (D5800 B).

TABLE 10—Multitechnique Elemental Analysis of 5W30 Lube Oil Standard

Analysis	D4951 (ICP)	D5185 (ICP)	D6443 (XRF)	D4927 (XRF)
Calcium, m%	0.1840 ± 0.0053	0.1846 ± 0.0027	0.1837 ± 0.0009	0.1840 ± 0.0011
Chlorine, mg/kg	...	...	26.0 ± 3.7	26.4 ± 1.3[a]
Molybdenum, mg/kg	...	54.0 ± 0.7	...	...
Phosphorus, mg/kg	940 ± 36	964 ± 34	968 ± 5	956 ± 9
Sulfur, m%	...	0.249 ± 0.018	0.252 ± 0.001	0.249 ± 0.002
Zinc, m%	0.1035 ± 0.0044	0.1042 ± 0.0019	0.1063 ± 0.0006	0.1026 ± 0.0009

[a] This test method does not determine chlorine in its ASTM format; however, the laboratories have reported results by this method.

TABLE 11—Precision of the ILS versus ASTM Test Methods						
			Repeatability		Reproducibility	
Analysis	ASTM Test Method	Concentration	ILS	ASTM	ILS	ASTM
API gravity	D287	33.9 ± 0.07, °	0.29	0.20	0.33	0.50
Ash	D482	0.64 ± 0.03, m%	0.044	0.007	0.078	0.024
BF viscosity @ −40°C	D2983	77,113 ± 8972, cp	5,233	6,120	24,852	18,318
Calcium	D4951	0.1840 ± 0.0053, m%	0.015	0.007		
	D5185	1,846 ± 27 mg/kg	48.9	74.8	73.8	264.4
	D6443	0.1837 ± 0.0009, m%	0.0026	0.020		
CCS @ −25°C	D5293	2,395 ± 59 mPas	83	62	163	175
CCS @ −30°C	D5293	4,548 ± 81 mPas	169	118	224	332
Chlorine	D6443	26 ± 3.7 mg/kg	5.9	4	10.3	20
Flash point PMCC	D93	202.6 ± 2.2°C	4.2	5	6.1	10
Kin. viscosity @ 40°C	D445	60.03 ± 0.11 cSt	0.29	0.16	0.31	0.46
Kin. viscosity @ 100°C	D445	10.33 ± 0.006 cSt	0.11	0.026	0.017	0.076
MRV @−35°C	D4684	18,393 ± 132 Cp	402	2416	366	6,550
Nitrogen	D4629	656 ± 52.9 mg/kg	39.1	5.15	146.5	22.8
Noack loss	D5800 B	14.7 ± 0.3 m%	0.72	0.364	0.75	0.997

(*Continued*)

TABLE 11—Precision of the ILS versus ASTM Test Methods (Continued)						
			Repeatability		Reproducibility	
Analysis	ASTM Test Method	Concentration	ILS	ASTM	ILS	ASTM
Phosphorus	D4951	940 ± 35.6 mg/kg	98.6	24.8		
	D5185	964 ± 34 mg/g	12.1	70.0	94.2	133.5
	D6443	967.6 ± 4.8 mg/kg	13.3	41.2		
Pour point	D97	− 41.2 ± 1.4°C	0.62	3.0	3.9	6
	D5950	− 44 ± 1.4°C	3.9	3.9		
	D5985	− 41 ± 0.0°C	0	2.3		
Ramsbottom carbon	D524	0.84 ± 0.009, m%	0.79	0.07	0.025	0.13
SASH	D874	0.78 ± 0.02, m%	0.037	0.050	0.055	0.118
Sulfur	D5185	0.249 ± 0.018, m%	0.014	0.028	0.050	0.042
	D6443	0.2520 ± 0.001, m%	0.0028	0.0069		
TAN	D664	1.75 ± 0.09 mg KOH/g	0.14	0.102	0.25	0.48
TBN	D2896	6.33 ± 0.11 mg KOH/g	0.43	0.189	0.31	0.44
Zinc	D4951	0.1035 ± 0.0044, m%	0.012	0.012		
	D5185	0.1042 ± 0.0019, m%	0.0018	0.0068	0.0053	0.017
	D6443	0.1063 ± 0.0006, m%	0.0017	0.0025		

- The laboratory precisions (r and R) obtained were superior than those given in ASTM methods D5185 for calcium; D6443 for calcium, chlorine, phosphorus, sulfur, and zinc; D5293 for CCS @ −30°C; D4684 MRV; D874 SASH; and D97 pour point.
- The laboratory precisions were not as good as given in ASTM methods in the cases of r of D4951 for calcium and phosphorus; r and R of D4629 for nitrogen; R of D664 for TAN; r of D2896 for TBN; and r and R of D482 ash methods. In this last case, however, the precisions are not exactly comparable since the precisions given in the method relate to different levels of ash than that found in this work.
- In three cases the laboratory r was inferior but R was as good or better than given in ASTM methods D445 for kinematic viscosity @ 100°C ; D524 for Ramsbottom carbon; and D6443 for chlorine.
- Three laboratories obtained varying results for D2983 Brookfield Viscosity @ −40°C. Although each laboratory's precision was close to that allowed in the method, the overall agreement between the laboratories, i.e. reproducibility, was quite poor. It is not clear why this is so because as far as we know all three laboratories are properly running this test.

Thus, although there are a few cases where the laboratory precision was poorer than expected in the ASTM standards, generally the precisions obtained in this study were equal to or better than those given in the ASTM test methods. This can only be attributed to good laboratory quality management practices such as following the test method correctly and doing appropriate calibrations and quality control during analysis. In any case this material is serving a useful role as a laboratory QC reference material in several company laboratories.

References

[1] Nadkarni, R. A., "Zen and the Art (or Is It Science) of a Perfect Analysis," *J. ASTM Intl.*, Vol. 293, ASTM International, West Conshohocken, PA, 2005, Paper ID 12964.

[2] Gladney, E. S., Burns, C. E., Perrin, D. R., Roelandis, I. and Gills, T. E., "Comprehensive Values for NBS Standard Reference Materials," National Bureau of Standards, Spec. Publ. No. 260-88, 1984.

[3] Filby, R. H., Van Berkel, G. J., Bragg, A. E., Joubert, A., Robinson, W. E. and Grimm, C. A., "Evaluation of Residual Fuel Oil Standard Reference Materials as Trace Element Standards," *J. Radioanal. Chem.*, Vol. 91, 1985, pp. 361–368.

[4] Gladney, E. S. and Burns, C. E., "Analysis of NBS Geological Standards," *Geostandards Newsletter*, Vol. 7, 1983.

[5] Nadkarni, R. A. and Morrison, G. H., "Use of Standard Reference Materials as Multielement Irradiation Standards in Neutron Activation Analysis," *J. Radioanal. Chem.*, Vol. 43, 1978, pp. 347–369.

[6] May, W., Parris, R., Beck, C., Fassett, J., Greenberg, R., Guenther, F., Kramer, G., Wise, S., Gills, T., Colbert, J., Gettings, R. and MacDonald, B., "Definition of Terms and Modes Used at NIST for Value-Assignment of Reference Materials for Chemical Measurements," NIST Special Publication, 260-136, 2000.

[7] Kelly, W. R., MacDonald, B. S. and Leigh, S. D., "A Method for the Preparation of NIST Traceable Fossil Fuel Standards with Concentrations Intermediate to SRM Values," *J. ASTM Intl.*, Vol. 4, No. 2, ASTM International, West Conshohocken, PA, 2007, Paper ID 1100748.

Part 2: Analytical Technology

6

Atomic Absorption Spectrometry in the Analysis of Petroleum Products and Lubricants

R. A. Kishore Nadkarni[1]

An analytical revolution in the area of metals determination took place in the mid-fifties when Sir Alan Walsh of CSIRO, Melbourne, Australia, invented the technique of atomic absorption spectrometry (AAS) [1]. Until then, metals had to be determined by the tedious, labor-intensive, and time-consuming techniques of wet chemistry separations and gravimetric, titrimetric, or colorimetric measurements.

A number of books [2–8] and reviews [9–18] have been published on this topic. Since the technique was first introduced in the mid-fifties, tens of thousands of AAS instruments have been sold, and perhaps thousands of publications have appeared describing the fundamentals or the applications of this technique to various matrix products, including petroleum products and lubricants. It has essentially evolved into a "cookbook" type of analysis. Many modern instruments are fully automated. Once the material is in solution, the actual analysis takes less than a minute, although this time depends on the number of elements determined in each sample. Other than refractory oxide-forming elements, the detection limits for AAS are less than a part per million for most metals.

Use of electrothermal or graphite furnace AAS is described in the next chapter in this monograph.

A simple schematic representation of AAS can be shown as (see Fig. 1):

HOLLOW CATHODE LAMP → NEBULIZER → FLAME → DETECTOR → MONOCHROMATOR → PHOTOMULTIPLIER → RECORDER → PRINTER TUBE DETECTOR GRAPHICS

The basic AAS instrument consists of a suitable light source emitting a light spectrum directed at the atomizer through single- or double-beam optics. The light emitted by the source is obtained from the same excited atoms that are measured in the atomizer. The light leaving the atomizer passes through a simple monochromator to a detector. The measured intensity is electronically converted into analytical concentration of the element being measured. Quantitative measurements in AAS are based on Beer's Law. However, for most elements, particularly at high concentrations, the relationship between concentration and absorbance deviates from Beer's Law and is not linear. Usually two or more calibration standards spanning the sample concentration and a blank are used for

[1] *Millennium Analytics, INC. East Brunswick, New Jersey*

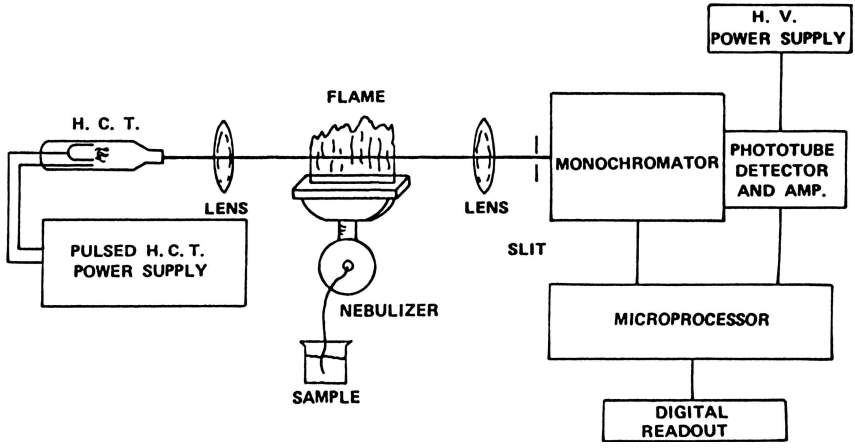

Fig. 1—Schematic diagram of an atomic absorption spectrometer.

preparing the calibration curve. After initial calibration, a check standard at mid-range of calibration should be analyzed.

The ground-state atom absorbs the light energy of a specific wavelength as it enters the excited state. As the number of atoms in the light path increases, the amount of the light absorbed also increases. By measuring the light absorbed, a quantitative determination of the amount of the analyte present can be calculated.

Two types of AAS instruments use either single beam or double beam. In the first type, the light source emits a spectrum specific to the element of which it is made, which is focused through the sample cell into the monochromator. The light source is electronically modulated to differentiate between the light from the source and the emission from the sample cell. In a double-beam AA spectrometer, the light from the source lamp is divided into a sample beam that is focused through the sample cell, and a reference beam that is directed around the sample cell. In a double-beam system, the readout represents the ratio of the sample and the reference beams. Therefore, fluctuations in the source intensity do not become fluctuations in the instrument readout, and the baseline is much more stable. Both types use the light sources that emit element specific spectra.

In AAS, the sample solution, whether aqueous or nonaqueous, is vaporized into a flame, and the elements are atomized at high temperatures. The elemental concentration is determined by absorption of the analyte atoms of a characteristic wavelength emitted from a light source, typically a hollow cathode lamp that consists of a tungsten anode and a cylindrical cathode made of the analyte metal, encased in a gas-tight chamber. Usually a separate lamp is needed for each element; however, multielement lamps are in quite common use. The detector is usually a photomultiplier tube. A monochromator separates the elemental lines and the light source is modulated to discriminate against the continuum light emitted by the atomization source.

More than 70 elements can be determined by AAS, usually with a precision of 1 to 3 % and with detection limits of the order of sub-mg/kg levels, and with

little or no atomic spectral interference. There could, however, be molecular spectral, ionization, chemical, and matrix interferences. Both aqueous as well as organic solvent solutions can be analyzed so long as the calibration standards are prepared in the same solvent media.

INTERFERENCES

Generally, the AAS method is considered a technique with few interferences. The several types of interferences possible are chemical, ionization, matrix, emission, spectral, and background absorption interferences [3,5]. Because these interferences are well-defined, it is easy to eliminate or compensate for them.

Chemical Interferences—If the sample for analysis contains a thermally stable compound with the analyte that is not totally decomposed by the energy of the flame, a chemical interference exists. It can normally be overcome or controlled by using a higher temperature flame or adding a releasing agent to the sample and standard solutions.

Ionization Interferences—When the flame has enough energy to cause the removal of an electron from the atom, creating an ion, ionization interference can occur. It can be controlled by adding an excess of an easily ionized element to both samples and standards. Normally, alkali metals that have very low ionization potentials are used.

Matrix Interferences—These can cause either a suppression or enhancement of the analyte signal. Matrix interferences occur when the physical characteristics—viscosity, burning characteristics, surface tension—of the sample and standard differ considerably. To compensate for the matrix interferences, the matrix components in the sample and standard should be matched as closely as possible. Matrix interferences can also be controlled by diluting the sample solution until the effect of dissolved salts or acids is negligible. Sometimes, the method of standard addition is used to overcome this interference. See below.

Emission Interferences—At high analyte concentrations, the atomic absorption analysis for highly emissive elements sometimes exhibits poor analytical precision, if the emission signal falls within the spectral bandpass being used. This interference can be compensated for by decreasing the slit width, increasing the lamp current, diluting the sample, or using a cooler flame.

Spectral Interferences—When an absorbing wavelength of an element present in the sample but not being determined falls within the bandwidth of the absorption line of the element of interest, a spectral interference can occur. An interference by other atoms can occur when there is a sufficient overlapping between radiation and emitted by the excited atoms and other absorbing atoms. Usually the bandwidth is much wider than the width of the emission and absorption lines. Thus, interferences by other atoms are fortunately quite limited in AAS. The interference can result in erroneously high results. This can be overcome by using a smaller slit or selecting an alternate wavelength.

Background Absorption Interferences—There are two causes of background absorption: light scattering by particles in the flame and molecular absorption of light from the lamp by molecules in the flame. This interference cannot be corrected with standard addition method. The most common way to compensate for background absorption is to use a background corrector that uses a continuum source.

Standard Addition Method—One way of dealing with some of the interferences in the AAS methods is to use a technique called standard addition [4]. The International Union of Pure and Applied Chemistry (IUPAC) rule defines this technique as the "Analyte Addition Method"; however, "standard addition method" is well known and is widely used by the practitioners of AAS; hence, there is no need to adopt the IUPAC rule. It takes longer time than the direct analysis, but when only a few samples need to be analyzed, or when the samples differ from each other in the matrix, or when the samples suffer from unidentified matrix interferences, this method can be used. The method of standard addition is carried out by (1) dividing the sample into several—at least four—aliquots, (2) adding to all but the first aliquot increasing amount of analyte, (3) diluting all to the same final volume, (4) measuring the absorbance, and (5) plotting the absorbance against the amount of analyte added. The amount of the analyte present in the sample is obtained by extrapolation beyond the zero addition. The method of standard addition is less accurate than direct comparison; but when matrix interferences are encountered, it is necessary to use standard addition.

SAMPLE INTRODUCTION

Atomic absorption spectrometry can handle both aqueous and nonaqueous samples, but because AAS is a method for the analysis of liquids, if the sample to be analyzed is a solid or semisolid, it needs to be brought into solution first. Some of the techniques used for such sample preparation include, from simplest to more elaborate:

1. Dilution of hydrocarbon liquid samples with organic solvents such as xylene, toluene, methyl isobutyl ketone (MIBK), or kerosine.
2. Oxidation of organic liquid or solid samples in an oxygen-pressurized stainless steel bomb, which converts the elements present to inorganic compounds. The contents are diluted with water or dilute acid for measurement [19].
3. Incineration of organic samples with or without sulfuric acid followed by the dissolution of the residue in a mixture of acids or fusing with alkalis and further dissolution in an acid mixture.
4. Dissolution in sealed polytetrafluoroethylene bombs with acids, heated for several hours at ~150°C, and then dilution with water for measurement [20].
5. Dissolution in a microwave oven in a mixture of acids in a very short period of time [21].
6. Gold amalgamation before cold vapor measurement for mercury determination [22].
7. Hydride formation of certain volatile elements—e.g., selenium, arsenic, antimony—and direct measurement by AAS [23].
8. Incineration of organic samples by low-temperature plasma. It takes, however, several days to complete the oxidation. The residue is dissolved in a mixture of acids prior to AAS determination.

CALIBRATION STANDARDS

All AAS measurements of samples are preceded by calibration of the instrument with elemental standards. Such calibration needs to be undertaken every time the flame is lit because each time the flame conditions cannot be precisely replicated and there will be small differences in the intensity of elemental lines

with each flame condition. Such standards could be aqueous or organic solvent based. Aqueous metallic standards are used when samples are converted to aqueous acid forms, and organometallic standards in organic solvents are used where samples are simply dissolved or diluted in base oil or organic solvents. Generally the calibration standards today are commercially available, prepared in suitable concentrations. Either single-element or multielement standards are available.

The elements usually determined in petroleum products and lubricants are listed in Table 1 along with their recommended wavelengths, flam conditions, range of analysis, and detection limits.

TABLE 1—AAS Determination of Selected Metals in Petroleum Products and Lubricants

Metal	Wavelength, nm	Flame	Range, mg/kg	Detection Limit, mg/kg
Aluminum	393.1; 309.2	Nitrous oxide + acetylene	5–50	0.02
Arsenic	193.7	Air + acetylene	0.1–10	0.2
Barium	553.6	Nitrous oxide + acetylene	1–20	0.01
Boron	249.8	Nitrous Oxide + acetylene	1–50	2
Calcium	422.7	Air + acetylene	0.1–10	0.002
Chromium	357.9	Air + acetylene	0.5–10	0.005
Copper	324.8	Air + acetylene	0.1–10	0.001
Iron	248.3; 372.0	Air + acetylene	0.1–10	0.01
Lead	217.0; 283.3	Air + acetylene	1–20	0.02
Magnesium	285.2	Air + acetylene	0.1–2	0.0001
Manganese	279.2	Air + acetylene	0.1–10	0.005
Molybdenum	313.3	Air + acetylene	5–20	0.02
Nickel	232.0; 341.5	Air + acetylene	0.5–10	0.02
Potassium	766.5	Air + acetylene	1–10	0.004
Selenium	196.1	Air + acetylene	0.1–1	0.3
Silicon	251.6	Nitrous oxide + acetylene	1–50	0.2
Sodium	589.6	Air + acetylene	0.1–1	0.001
Vanadium	318.4	Nitrous oxide + acetylene	1–100	0.08
Zinc	213.9; 398.8	Air + acetylene	0.1–2	0.003

BURNER SYSTEM

A duel option burner system consists of both a flow spoiler and an impact bead for optimal operation under different analytical conditions. Equivalent precision is obtained with the air-acetylene flame using the flow spoiler or the impact bead. For nitrous oxide-acetylene flame, however, noticeably poorer precision is obtained when using the impact bead.

FLAME SOURCES

Usually, AAS instruments use flame as the atomization source. An air-acetylene (C_2H_2) flame is used for most elements; the nitrous oxide (N_2O)-C_2H_2 flame reaches higher temperature (2,300°C for air-C_2H_2 versus 3,000°C for N_2O-C_2H_2), and is used for atomizing the more refractory oxide-forming metals. Flame conditions used in AAS are summarized in Table 2.

Of several possible combinations (Table 2), air-C_2H_2 and N_2O-C_2H_2 are the most commonly used flames as atomization sources in AAS. More than 30 elements can be determined with the air-C_2H_2 flame. The N_2O-C_2H_2 flame is the hottest of the flames used and produces a maximum temperature of 3,000°C. It can atomize refractory elements such as aluminum, silicon, vanadium, titanium, and others, all forming highly refractory oxide molecules in the flame. Although the N_2O-C_2H_2 flame can be used for the determination of more than 65 elements, in practice it is used only where the air-C_2H_2 flame is ineffective.

HOLLOW CATHODE LAMPS

A typical hollow cathode lamp consists of a quartz envelope containing a cathode, made of the element to be determined and a suitable anode. The sealed envelope is filled with an inert gas such as argon or neon at a low pressure. When a high voltage—up to 600 volts—is applied across the electrodes, positively charged gas ions bombard the cathode and dislodge atoms of the element used in the cathode. These atoms are subsequently excited and the spectrum of the chemical element is emitted. Hollow cathode lamps are preferred as the light

TABLE 2—Flame Conditions in AAS

Fuel	Oxidant	Temperature, °C	Burning Velocity, cm/s
Natural gas	Air	1,700–1,900	55
Propane	Air	1,925	82
Propane	Oxygen	2,800	
Hydrogen	Air	2,100	320
Acetylene	Air	2,300	160
Hydrogen	Oxygen	2,550–2,700	915
Acetylene	Nitrous oxide	2,955	180
Acetylene	Oxygen	3,050	1130

sources because they generate a very narrow line, about one tenth of the elemental absorption line width. Usually these lamps are stable and can be used for several thousand determinations. By combining two or more elements of interest into one cathode, multielement hollow cathode lamps are produced. For chemical elements that do not have close resonance lines and are metallurgically compatible, multielement hollow cathode lamps save the analyst considerable time not having to switch the lamps and recalibrate the instrument to determine multiple elements in the same sample.

Failure of hollow cathode lamps occurs when the fill gas is gradually captured on the inner surfaces of the lamp, and finally, the lamp can no longer be lighted. Higher lamp current accelerates the gas depletion and cathode sputtering and should be avoided. It is a compromise between obtaining good sensitivity for the elements being determined and prolonging the lamp life.

Although hollow cathode lamps are an excellent, bright, and stable line source for most elements, for some volatile elements, where low intensity and short lamp life time are a problem, electrode-less discharge lamps can be used. The latter are typically more intense than hollow cathode lamps, and thus offer better precision and lower detection limits for some elements.

NEBULIZERS

Liquid sample is introduced into a burner through the nebulizer [3] by the venturi action of the nebulizer oxidant. In its passage through the nebulizer, the liquid stream is broken into a droplet spray. During nebulization, some liquids are broken into a finer mist than others. For example, MIBK is more efficiently converted into a fine droplet size than water. The nebulizer draws the solution up a tube of narrow diameter or capillary. High-viscosity fluids flow through the capillaries at a slower rate than the low-viscosity fluids. Hence, it is important to keep the viscosities of the samples and standards solutions similar to avoid the possibility of physical interference problems.

Nebulizer capillaries readily become clogged by particulate material, and they sometimes corrode. It is very important to keep the particulate materials out of the nebulizers even though it may require a time-consuming filtration step.

MONOCHROMATORS

A monochromator isolates a single atomic resonance line from the line spectrum emitted by the hollow cathode lamp, excluding all other wavelengths. A typical resolution in AAS for this discrimination is 0.1-nm bandpass. The light emitted by the spectral source is focused onto a narrow entrance slit. From this, the light diverges until it reaches the first mirror, where it is collimated into a parallel beam and directed toward the grating.

DETECTORS

A photomultiplier is used as a detector device in AAS because of its sensitivity over the range of wavelength used in AAS. The photomultiplier produces an electrical signal that is proportional to the intensity of the light at the wavelength that has been isolated by the monochromator. This electrical signal is then amplified and is used to provide a quantitative measure of absorption.

READOUTS

The readout system of an AAS consists of a way to convert the electrical signal from the photomultiplier to a meter, a digital display, or a graphic printout. All modern instruments are capable of directly converting the signal to a metal concentration after inputting the sample weight taken for analysis, and a previously prepared calibration curve.

COLD VAPOR AAS

Cold vapor AAS (CVAAS) is used for the high-sensitivity determination of mercury and certain metallic hydride-forming elements such as arsenic, antimony, selenium, tellurium, bismuth, and tin. In this technique, the gaseous hydrides of these metals are chemically generated by adding a reducing agent such as sodium borohydride. The gaseous hydrides and hydrogen produced by the reaction are then swept by an argon purge into a heated quartz cell. When the sample vapor is atomized in the cell, a peak signal is produced, the height of which is proportional to the amount of analyte in the sample.

The detection limits for hydride generation AAS are far better than those by conventional AAS. See Table 3

APPLICATION OF AAS IN OIL INDUSTRY

There are hundreds of publications on the applications of AAS in the petroleum products area. See Refs [2–18] for comprehensive reviews of this subject. AAS is truly a workhorse of the metal analysis of petroleum products to the point that "cookbook" methods are available for almost all elements that are amenable to AAS determination. Inherent limitations of AAS such as sample preparation and limited dynamic range can be overcome on a technique based on peristaltic pumps performing on-line multiple calibration from a single bulk standard and fast automatic on-line dilution of over-range samples [13].

A large number of publications have appeared applying AAS technique for the determination of metals in petroleum products and lubricants. It is beyond

TABLE 3—Detection Limits of CVAAS versus Flame AAS

Element	Flame Detection Limits, μg/mL	Hydride Detection Limits, μg/mL
Antimony	45	0.15
Arsenic	150	0.03
Bismuth	30	0.03
Mercury, μg/L	300	0.009
Selenium	100	0.03
Tellurium	30	0.03
Tin	150	0.5

(Excerpted from Jenniss et al. [4]).

TABLE 4—Examples of Application of AAS in the Petrochemical Field

Product	Element	References
Crude oil – Venezuela	Cd, Pb, and Ni	24
Crude oils	Cu, Mg, Na, Sn, Cd, Zn, Al	25
Gasoline	Pb	26–33
Lube oils, additives	Sb	34
Lube oils	Ba	35
Lube oils, additives	Ba, Ca, Zn	36
Lube oils, additives	Several elements	37
Lube oils, additives	Ti	38
Petroleum products	Hg	39
Petroleum products	As and Se	39, 40
Petroleum products	Trace metals	41
Petroleum Products	Ca and Zn	42

the scope of this chapter to cite all these references; however, a few examples are given here in Table 4 to demonstrate the applicability of this technique for petroleum products and lubricants analysis field, and which will go to support the extensive use of this technique in the petrochemical analysis field. Several books and reviews exist [2–9].

Samples that are wet-ashed and brought into aqueous solution can be analyzed by standard AAS methods. Other petroleum samples such as lubricating oils and additives can be diluted with suitable organic solvents such as xylene, MIBK, or kerosine before measurements. In the latter case, organometallic standards have to be used for calibration.

Viscosity plays an important role in the accuracy of oil analysis by AAS. Viscosity differences between the samples and the calibration standards have been reported to lead to errors of up to 40 % for iron [30].

Simultaneous multielement flame AAS has been used to determine cadmium, lead, and nickel in burned and unburned Venezuelan crude oils. Better than 1 % precision was obtained [24].

Lead–For the determination of lead, gasoline is usually diluted with isooctane, MIBK, or acetone [26]. Some methods extract lead into an aqueous solution using iodine monochloride [27] or a hydrochloric acid-nitric acid (HCl-HNO_3) mixture [28]. A chemical dependency has been observed in the determination of lead. Tetraethyl and tetramethyl lead solutions give different absorptions. This effect can be overcome by the addition of iodine and a quaternary ammonium salt to all samples and standards. Lead determinations have been automated to analyze more than 75 samples each day [29]. Lead is also

determined by using mixtures emulsified by addition of a surfactant and a water-miscible organic solvent such as ethanol or iso-propanol [31].

Silicon—Lubricating oil, fuel additive, or lube additive sample can be dissolved in xylene, with addition of potassium naphthenate as an ionization suppressor and aspirated in a acetylene + nitrous oxide flame in the AAS instrument. Silicon is determined at 251.6-nm wavelength. The precision of the method is ~1.5 % RSD at a silicon concentration of ~ 5,000 ppm.

Wear Metals—Until the advent of ICP-AES, AAS was widely used for the determination of wear metals in used oils. Sampling is a serious problem with wear metals analysis. This subject is discussed in a separate chapter on used oil analysis in this monograph. An extensive review of wear metals, principally by using AAS, of pre-1980 publications is given by Schyra et al. [9]. Several papers have compared ICP-AES with AAS [43–45] methods for wear metal analysis and found them equivalent. A round robin of 27 laboratories using these methods found excellent data agreement [45].

In this author's laboratory, a number of metals in lubricating oils and lubricating additive packages have been determined using AAS. An example of such analysis and the experimental conditions used are given in Table 5. In all cases, the sample was diluted with reagent-grade xylene. In a few cases, for high viscosity materials such as poly-iso-butylenes, the sample was ashed at 750°C with sulphuric acid, and the residue was dissolved in dilute mineral acid before aspirating into the flame. In all cases a blank was carried through the entire analytical sequence. Ionization suppressant was added where necessary. Organometallic standards in xylene were used for calibration, and each set of analyses was accompanied by a quality control sample producing data to construct a statistical quality control chart.

The results given in Table 5 show good agreement with the product specifications of this material. The elements boron, calcium, magnesium, and zinc are the chemical constituents of this lubricant; silicon is added as an anti-foamant, and other trace elements such as aluminum, barium, copper, iron, and sodium

TABLE 5—Analysis of a Lubricant Product Using AAS

Element	Flame Used	Wave-length, nm	Slit Width, nm	Found (n = 5)	Product Specifications
Al, ppm	$N_2O + C_2H_2$	309.3	0.7	51 ± 10	...
B, m%	$N_2O + C_2H_2$	249.8	0.2	0.13 ± 0.02	0.12–0.13–0.14
Ba, ppm	$N_2O + C_2H_2$	553.6	0.5	< 20	...
Ca, m%	Air + C_2H_2	422.7	0.2	0.35 ± 0.01	0.335–0.36–0.385
Cu, ppm	$N_2O + C_2H_2$	324.8	0.2	11 ± 3	...
Fe, ppm	Air + C_2H_2	248.3	0.2–0.3	7 ± 1	...
Mg, m%	Air + C_2H_2	285.2	0.2–0.5	0.82 ± 0.02	0.76–0.82–0.88
Na, ppm	Air + C_2H_2	589.0	0.4	29 ± 4	...
Si, ppm	$N_2O + C_2H_2$	251.6	0.2–0.3	54 ± 6	58–20
Zn, m%	Air + C_2H_2	213.9	0.5	0.87 ± 0.02	0.81–0.86–0.91

are present as contaminants from raw materials used in blending or commingling during blending and processing of the product.

ASTM TEST METHODS

Several test methods have been written by D02 Committee based on the use of AAS for metal analysis in petroleum products and lubricants.

In the ASTM D3237-02 test method, the gasoline sample is diluted with MIBK and the alkyl lead compounds are stabilized by reaction with iodine and a quaternary ammonium salt, followed by AAS determination of lead. Determination of trace metals such as lead, sodium, calcium, and vanadium in gas turbine fuels is the subject of the ASTM D3605-00(05) test method. Certain organometallic compounds (e.g., methylcyclopentadienyl manganese tricarbonyl) are added as anti-knock agents to gasoline. ASTM test method D3831-01(06) describes the determination of manganese in such gasoline samples by AAS after reacting the sample with bromine and diluting with MIBK.

A widely used test method for the determination of additive elements—barium, calcium, magnesium, and zinc—in lubricating oils is described in ASTM test method D4628-05. Oils that contain viscosity index (VI) improvers may give low results unless calibration standards also contain VI improvers. The results by this method are found equivalent to those obtained by using ASTM D4927 X-ray fluorescence or D4951 inductively coupled plasma atomic emission spectrometry test methods. Trace metals in petroleum coke are determined by ASTM test method D5056-04 after ashing the sample, fusion of the ash with lithium borate, dissolution of the melt in HCl, and AAS measurement of aluminum, calcium, iron, nickel, silicon, sodium, and vanadium. Aluminum and silicon in fuel oils are determined by ASTM test method D5184-01(06) following the same procedure as in D5056. The method also alternatively allows use of inductively coupled plasma for this determination. Crude oils and residual fuels are analyzed for nickel, vanadium, iron, and sodium content by either ashing or direct dilution with an organic solvent, and AAS determination in

TABLE 6—ASTM Test Methods for AAS Analysis of Petroleum Products and Lubricants

ASTM Test Method	Analysis
D3237	Lead in gasoline by AAS
D3605	Trace metals in gas turbine fuels by AAS and flame emission spectrometry (FES)
D3831	Manganese in gasoline by AAS
D4628	Analysis of Ba, Ca, Mg, and Zn in unused lubricating oils by AAS
D5056	Trace metals in petroleum coke by AAS
D5184	Al and Si in fuel oils by ashing, fusion, ICP-AES, and AAS
D5863	Ni, V, Fe, and Na in crude oils and residual fuels by flame AAS
D6732	Copper in jet fuels by graphite furnace AAS

TABLE 7—ASTM Proficiency Testing Using AAS Methods		
Product	**ASTM Test Method**	**Analysis**
#6 Fuel oil	D5184	Aluminum and silicon
	D5863	Vanadium, nickel, iron, and sodium
Automotive transmission fluid	D4628	Additive elements
Automotive lubricant additive	D4628	Additive elements
Crude oil	D5863	Nickel, vanadium, and iron
Lubricating oil	D4628	Additive elements
General gas oils	D5863	Vanadium, nickel, and iron

ASTM test method D5863-00a(05). GF-AAS is used in ASTM test method D6732-04 for the analysis of parts-per-billion amounts of copper in jet fuels.

ASTM PROFICIENCY TESTING

For the last 10 years, ASTM D02 Committee on Petroleum Products and Lubricants has initiated a large program on proficiency testing of various petroleum products and lubricants among nearly 2,500 worldwide oil industry laboratories [46]. Some of the AAS methods are used in this testing (Table 7).

TABLE 8—Alternate Spectroscopic Analysis of Metals in NIST SRM 1848					
Analysis	**All Methods**	**AAS**	**ICP-AES**	**WD-XRF**	**NIST Certification**
Boron, m%	0.137 (2.0 % RSD; n = 10)	0.139 (4.0 % RSD; n = 6)	0.139 (3.5 % RSD; n = 7)		0.136 ± 0.013
Calcium, m%	0.355 (2.4 % RSD; n = 19)	0.357 (4.0 % RSD; n = 7	0.351 (1.3 % RSD; n = 7)	0.356 (2.7 % RSD; n = 9)	0.345 ± 0.011
Magnesium, m%	0.818 (1.6 % RSD; n = 15)	0.826 (4.6 % RSD; n = 8)	0.817 (1.6 % RSD; n = 9)		0.821 ± 0.058
Silicon mg/kg	52 (22.3 % RSD; n = 11)	47 (18.9 % RSD; n = 4)	54 (21.9 % RSD; n = 9)		50 ± 2
Zinc, m%	0.859 (1.4 % RSD; n = 18)	0.87 (2.7 % RSD; n = 5)	0.857 (1.2 % RSD; n = 7)	0.855 (2.2 % RSD; n = 10)	0.866 ± 0.034

TABLE 9—Comparison of Results from ASTM Lubricant Additive ALA 0802 ILCP Cross Check

Element	AAS (D4628)	ICP-AES (D4951)	ICP-AES (D5185)
Boron, m%		0.0315 ± 0.0017 (22)	0.0321 ± 0.0024 (13)
Calcium, m%	1.353 ± 0.011 (8)	1.363 ± 0.022 (24)	1.334 ± 0.033 (13)
Magnesium, m%	0.258 ± 0.002 (7)	0.258 ± 0.009 (23)	0.2596 ± 0.0066 (13)
Phosphorus, m%		0.6953 ± 0.0104 (23)	0.6976 ± 0.024 (12)
Zinc, m%	0.7702 ± 0.0104 (8)	0.7605 ± 0.0105 (23)	0.7544 ± 0.0197 (12)

Results are given as mean ± standard deviation (number of valid results).

INTERTECHNIQUE COMPARISON

A number of studies have compared the three most widely used techniques—AAS, ICP-AES, and XRF—for metal analysis in lube oils and have found them equivalent. Table 8 gives an example of the analysis of an automotive lube additive for the analysis of National Institute of Standards and Technology (NIST) Standard Reference Material (SRM) 1848. The results by all three methods are in excellent agreement with each other as well as with the values certified by NIST.

Table 9 gives examples of the intertechnique equivalency based on the analysis of a lubricating additive and a lubricating oil (Table 10) from the ASTM ILCP proficiency testing program mentioned previously. Again, the agreement between the three methods is excellent within the precision of the test methods.

Note the smaller number of laboratories using AAS compared with a much larger number of laboratories using ICP-AES. The first technique is declining while the second one is being used more and more.

CONCLUSION

Finally, Table 11 compares the detection limits of most commonly used alternative atomic spectroscopic methods, and Table 12 compares the advantages and disadvantages of these methods. It is clear that AAS has reasonable detection limits for most elements of interest in the petroleum field, but ETAAS and ICP-AES are better at sub-ppm levels of elements. A major drawback of AAS or ETAAS is its single-element capability compared to ICP-AES, DCP-AES, or XRF. The precision of the results is superior for AAS, followed by ICP-AES, and ETAAS in the last place.

If only a limited number of elements are to be determined, and cost of purchase and maintenance, and ease of operations, is a factor in the decision, then AAS is a very competitive tool for the determination of metals in petroleum products and lubricants.

Finally, in Table 13, suggestions to improve the precision and accuracy of metal analysis in lubricants using AAS are listed. These suggestions are based on practical laboratory experience, and we hope that they will be a useful guide for the practitioners of this technique.

TABLE 10—Comparison of Results from ASTM Lubricating Oil LU 0801 ILCP Cross Check					
ELEMENT	**AAS (D4628)**	**ICP-AES (D4951)**	**ICP-AES (D5185)**	**WD-XRF (D4927B)**	**ED-XRF (D6481)**
Calcium, m%	0.2128 ± 0.0130 (9)	0.2061 ± 0.0110 (67)	0.2048 ± 0.0129 (63)	0.2197 ± 0.0077 (17)	0.1981 ± 0.0092 (9)
Phosphorus, m%		0.0760 ± 0.0039 (69)	0.0744 ± 0.0054 (67)	0.0806 ± 0.0045 (16)	0.0761 ± 0.0084 (6)
Zinc, m%	0.0912 ± 0.0087 (9)	0.0858 ± 0.0051 (70)	0.0840 ± 0.0052 (65)	0.0890 ± 0.0036 (16)	0.0861 ± 0.0037 (10)
Results are given as mean ± standard deviation (number of valid results).					

TABLE 11—Detection Limits of Selected Elements by Atomic Spectroscopic Methods

Element	Flame AAS	Flame AES	Electrothermal AAS	ICP-AES	DCP-AES	AFS
Ag	0.9	2	0.001	0.2	2	0.1
Al	20	3	0.01	0.2	2	0.6
As	0.02	2000	0.08	2	45	0.1
B	700	50	15	0.1	5	2000
Ba	8	1	0.04	0.01	2	2
Ca	0.5	0.1	0.01	0.001	0.2	0.08
Co	2	5	0.008	0.1	1	2
Cr	2	1	0.004	0.08	1	1
Cu	1	3	0.005	0.04	2	0.03
Fe	3	10	0.01	0.09	3	3
Hg	0.001	150	0.2	1	75	0.003
K	1	0.01	0.004	30	0.3	0.8
Li	0.3	0.001	0.01	0.02	1	0.4
Mg	0.1	1	0.0002	0.003	0.2	0.1
Mn	0.8	1	0.0005	0.01	0.5	0.4
Mo	10	10	0.02	0.2	0.5	12
Na	0.2	0.01	0.004	0.1	0.05	0.1

(*Continued*)

TABLE 11—Detection Limits of Selected Elements by Atomic Spectroscopic Methods (Continued)

Element	Flame AAS	Flame AES	Electrothermal AAS	ICP-AES	DCP-AES	AFS
Ni	2	10	0.05	0.2	2	2
P	. . .	100	0.3	15	75	. . .
Pb	10	0.2	0.007	1	23	10
S	. . .	1600	10	30	. . .	. . .
Se	0.02	. . .	0.05	1	45	0.06
Si	20	. . .	0.005	2	15	300
V	20	7	0.1	0.06	8	30
Zn	0.8	1000	0.0006	0.1	2	0.0002

All values are in nanograms per millilitre.
Excerpted from Ref [13].

TABLE 12—Comparison of Atomic Spectroscopic Techniques				
Parameter	**AAS**	**ET-AAS**	**AFS**	**ICP-AES**
Advantages				
Maintenance	Moderate	Moderate	Moderate	High
Dynamic range	Narrow	Narrow	Narrow	Wide
Number of elements	~70	~70	~70	~70
Detection limit	PPM	Sub-PPM	PPM	Sub-PPM
Analysis time	Few minutes	>AAS	Few minutes	Few minutes
Sample volume	Few mL	μL	Few mL	Few mL
Precision, % RSD	1–2	5	1–2	2–5
Application in oil industry	Widely used	Limited use	Very limited use	Very widely used
Drawbacks				
Cost	Moderate	Moderate	Moderate	High
Element capability	Single	Single	Single	Multielement
Interferences	Chemical ionization	Chemical	Chemical	Spectral and matrix
Excerpted from Refs [13,47].				

TABLE 13—Practical Hints for Improved AAS Measurements	
Area	**Improvement Suggestion**
Sampling	Employ adequate mixing and sampling procedures, especially for heavy oils. Heat such oils sufficiently to obtain good fluidity, and then shake vigorously on a shaking machine.
Burner	Disassemble and clean the burner on a maintenance schedule that is appropriate for the frequency and the type of use. Monitor for deposit formation on the burner head and clean when necessary.
Nebulizer	Inspect the nebulizer tubing daily for kinks or cracks, and replace if necessary.
	Measure the nebulizer uptake rate daily to check for plugging. Clean the nebulizer if the rate is not normal.
Carbon buildup	Adjust the gas flow rates when using the nitrous oxide / acetylene flame to minimize the carbon buildup on the burner. Clean off the carbon regularly during analysis with a sharp instrument. Carbon buildup can be particularly troublesome when nebulizing the nonaqueous solutions.
Gases	Prevent leakage of acetone from the acetylene gas tank by monitoring the pressure. Replace the tank when the pressure reaches 50 psi.
Hollow cathode lamps	Check the alignment of the hollow cathode lamps before analysis, following the manufacturer's instructions.
Glassware	Clean all glassware to prevent contamination. Soak the glassware in warm dilute (5 %) nitric acid for several hours, and then rinse thoroughly with deionized water.
Blank solution	Always run a blank with all solvents and other reagents added to the standards and the samples.
Reagents	Use pure analyte-free solvents. Verify that the solvents are indeed free of the analyte.
Sample composition	If the oils contain VI improvers, calibration standards also need to contain VI improvers. Alternatively, a large sample dilution will eliminate this effect.
	Match the matrix of standard solution to sample solutions as closely as possible.
	If ionization suppressant is necessary to add, do so for both samples and standards, in the same concentration levels. Maintain these concentrations when the samples are diluted.
Calibration standards	Low-level working calibration standards should be prepared fresh daily from higher concentration stock solution standards.
Calibration	Standardize the instrument each time the flame is ignited. Carry out calibration before each group of samples to be analyzed, or after change in any instrumental conditions.

TABLE 13—Practical Hints for Improved AAS Measurements (Continued)

Area	Improvement Suggestion
	Keep all absorbances within the linear and calibrations ranges. Dilute the sample solutions gravimetrically, if necessary.
Check standards	A single standard should be aspirated from time to time during a series of samples to check whether the calibration has changed. A check after every fifth sample is recommended.
Flame	The visual appearance of the flame serves as an useful indicator to detect change of conditions, perhaps as a buildup of carbon in the nebulizer or burner.
	To avoid flame transport problems, add a metal-free base oil of about 4 cSt @ 100 °C to both samples and calibration standards. A 100 neutral base oil is suitable.
Background correction	Whenever possible, employ background subtraction to obtain more reliable results.
Instrument	Verify the linearity of the concentration / absorbance response for each analyte following the instrument manufacturer's instructions. Perform all determinations within this range. Prepare the standard solutions with concentrations at the top of the linear range.
Standard addition	This technique may be employed for samples known to have elemental or other interferences.
Bracketing technique	For best results, use a bracketing technique for calibration involving taking absorbance readings for the calibration solutions before and after each of the sample solution measurements.
Multielement analysis	Because checking the absorbance of a sample is very quick once the instrument is calibrated for that analyte, but changing the wavelength settings and hollow cathode lamps takes longer, it is economical to make measurements at a single wavelength on a series of samples and standards for an analyte before changing the conditions for the measurement of another analyte.
Quality control	Establish and implement a QC protocol that can aid in achieving the required data quality. At a minimum, a QC sample should be analyzed with each set of samples analyzed. It is also important to plot this data on a QC chart.

References

[1] Walsh, A., *Spectrochim. Acta*, Vol. 7, 1955, p. 108.

[2] Hofstader, R. A., Milner, O. I. and Runnels, J. H., "Analysis of Petroleum for Trace Metals," American Chemical Society, Washington, D.C., Adv. Chem. Series, No. 156, 1976.

[3] Van Loon, J. C., *Atomic Absorption Spectroscopy: Selected Methods*, Academic Press, New York, 1980.

[4] Jenniss, S. W., Katz, S. A. and Lynch, R. W., *Applications of Atomic Spectroscopy to Regulatory Compliance Monitoring*, 2nd Ed., Wiley-VCH, New York, 1983.

[5] Christian, G. D. and Feldman, F. J., *Atomic Absorption Spectrometry: Applications in Agriculture, Biology, and Medicine*, Wiley-Interscience, New York, 1970.
[6] Pinta, M., *Modern Methods for Trace Element Analysis*, Ann Arbor Science, Ann Arbor, MI, 1978.
[7] Weberling, R. P. and Cosgrove, J. F., "Flame Emission and Absorption Methods," in *Trace Analysis: Physical Methods*, ed. Morrison, G. H., Interscience Publishers, New York, 1965, pp. 245–269.
[8] Amos, M. D., Bennett, P. A., Matousek, J. P., Parker, C. R., Rothery, E., Rowe, C. J. and Sanders, J. B., *Basic Atomic Absorption Spectroscopy: A Modern Introduction*, Varian Techtron, Springvale, Australia, 1975.
[9] Sychra, V., Lang, I. and Sebor, G. "Analysis of Petroleum and Petroleum Products by Atomic Absorption Spectroscopy and Related Techniques," *Progr. Anal. Atom. Spectroscopy*, Vol. 4, 1981, pp. 341–426.
[10] de al Guardia, M. and Salvador, A., *Atomic Spectroscopy,* Vol. 5, 1984, p. 150.
[11] Varnes, A. W., "Applications of Atomic Spectroscopy in the Petrochemical Industry," *Spectroscopy,* Vol. 1, No. 11, 1986, pp. 28–33.
[12] Routh, M. W., "A Comparison of Atomic Spectroscopic Techniques: Atomic Absorption, Inductively Coupled Plasma, and Direct Current Plasma," *Spectroscopy,* Vol. 2, No. 2, 1987, pp. 45–51.
[13] Parsons, M. L., Major, S. and Forester, A. R., "Trace Element Determination by Atomic Spectroscopic Methods – State of the Art," *Appl. Spectroscopy,* Vol. 37, No. 5, 1983, pp. 411–418.
[14] Browner, R. F. and Boorn, A. W., "Sample Introduction: The Achilles' Heel of Atomic Spectroscopy?" *Anal. Chem.,* Vol. 56, No. 7, 1984, pp. 786A–798A.
[15] Browner, R. F. and Boorn, A. W., "Sample Introduction Techniques for Atomic Spectroscopy," *Anal. Chem.,* Vol. 56, No. 7, 1984, pp. 875A–888A.
[16] Slavin, W., "Flames, Furnaces, Plasmas: How Do We Choose?" *Anal. Chem.,* Vol. 58, No. 4, 1986, pp. 589A–597A.
[17] Walsh, A., "Atomic Absorption Spectroscopy: Stagnant or Pregnant?" *Anal. Chem.,* Vol. 46, No. 8, 1974, pp. 698A–708A.
[18] Winefordner, J. D., Fitzgerald, P. T. and Omenetto, N., "Review of Multielement Atomic Spectroscopic Methods," *Appl. Spectroscopy*, Vol. 29, No. 2, 1975, pp. 369–384.
[19] Nadkarni, R. A., "Determination of Volatile Elements in Coal and Other Organic Materials by Oxygen Bomb Combustion," *Amer. Lab.,* Vol. 13, No. 8, 1981, pp. 22–29.
[20] Nadkarni, R. A., "Analytical Techniques for Characterization of Oil Shales," in *Geochemistry and Chemistry of Oil Shales*, ed. Miknis, F. P. and McKay, J. F., *Amer. Chem. Soc. Symp. Series,* Vol. 230, 1983, pp. 477–492.
[21] Nadkarni, R. A., "Applications of Microwave Oven Sample Dissolution in Analysis," *Anal. Chem.,* Vol. 56, 1984, pp. 2233–2237.
[22] Fox, B. S., Mason, K. J. and McElroy, F. C., "Determination of Total Mercury in Crude Oil by Combustion Cold Vapor Atomic Absorption Spectrometry," *J. ASTM Intl.,* Vol. 2, No. 6, ASTM International, West Conshohocken, PA, 2005, Paper ID 13089.
[23] Nadkarni, R. A., "Applications of Hydride Generation Atomic Absorption Spectrometry to Coal Analysis," *Anal. Chim. Acta,* Vol. 135, 1982, pp. 363–368.
[24] Sheldon, J., Lee, Y. I., Hammond, J. L., Noble, C. O., Beck, J. N. and Profit, C. E., "Determination of Selected Metals by Simultaneous Multielement Flame AAS in Burned and Unburned Venezuelan Crude Oil," *Amer. Environ. Lab.,* Vol. 10, No. 6, 1998, p. 4.
[25] Arakting, Y. E., Chakrabarti, C. L. and Maines, I. S., "Determination of Cobalt, Magnesium, Sodium, Tin, Cadmium, Zinc, and Aluminum in Crude Oils," *Spectroscopy Lett.,* Vol. 7, 1974, p. 97.
[26] McCorriston, L. L. and Ritchie, R. K., *Anal. Chem.,* Vol. 47, 1975, p. 1137.
[27] Coleman, M. F. M., *J. Chem. Educ.,* Vol. 62, 1985, p. 261.

[28] Bowen, B. C. and Foote, H., Institute of Petroleum Report IP 74-010, London.
[29] Heistand, R. N. and Shaner, W. C., *At. Abs. Newsletter,* Vol. 13, 1974, p. 65.
[30] Ibrahim, R. J. and Sabbah, S., *At. Abs. Newsletter,* Vol. 14, 1975, p. 131.
[31] Cardarelli, E., Cifani, M., Mecozzi, M. and Schi, G., *Talanta,* Vol. 33, 1986, p. 279.
[32] Aznarez, J., Vidal, J. C. and Carciner, R., *J. Anal. At. Spectro.,* Vol. 2, 1987, p. 55.
[33] Kashiki, M., Yamazoe, S. and Oshima, S., "Determination of Lead in Gasoline by Atomic Absorption Spectrophotometry," *Anal. Chim. Acta,* Vol. 53, 1971, p. 95.
[34] Supp, G. R., "Determination of Antimony in Petroleum Additives Using Atomic Absorption Spectrophotometry," *At. Abs. Newsletter,* Vol. 11, 1972, 12.
[35] Holding, S. T. and Roeson, J. J., "The Determination of Barium in Unused Lubricating Oils by Means of Atomic Absorption Spectrophotometry," *Analyst,* Vol. 100, 1975, p. 465.
[36] Peterson, G. E. and Kahn, H. L., "Ba, Ca, and Zn in Additives and Lube Oils," *At. Abs. Newsletter*, Vol. 9, 1970, p. 61.
[37] Barnett, W. B., Kahn, H. L. and Peterson, G. E., "Rapid Determination of Several Elements in a Single Lubricating Oil Sample by AAS," *At. Abs. Newsletter,* Vol. 10, 1971, p. 106.
[38] Saba, C. S. and Eisentraut, K. J., "Determination of Titanium in Aircraft Lubricating Oils by Atomic Absorption Spectrophotometry," *Anal. Chem.,* Vol. 49, 1977, p. 455.
[39] Meyer, G. A., *Anal. Chem.,* Vol. 59, 1987, 1345A.
[40] Walker, H. H., Runnels, J. H. and Merryfield, R., *Anal. Chem.,* Vol. 48, 1976, 2056.
[41] Vigler, M. S. and Gaylor, V. E., "Trace Metals Analysis in Petroleum Products by Atomic Absorption," *Appl. Spectr.,* Vol. 28, 1974, p. 342.
[42] Holding, S. T. and Matthews, P. H. D., "The Use of a Mixed-Solvent System for the Determination of Calcium and Zinc in Petroleum Products by Atomic Absorption Spectrophotometry," *Analyst,* Vol. 97, 1972, p. 189.
[43] McKenzie, T., Varian Technical Note No. AA-10 (1981).
[44] Varnes, A. W. and Andrews, T. E. *Jarrell-Ash Plasma Newsletter,* Vol. 191, 1978, p. 12.
[45] Allied Analytical Systems ICP Application Note, 1985.
[46] Nadkarni, R. A. and Bover, W. J., "Bias Management and Continuous Improvements through Committee D02's Proficiency Testing," *ASTM Standardization News,* Vol. 32, No. 6, 2004, pp. 36–39.
[47] Nadkarni, R. A., "A Review of Modern Instrumental Methods of Elemental Analysis of Petroleum Related Materials. Part II – Analytical Techniques," ASTM STP 1109, ASTM International, West Conshohocken, PA, 1991, pp. 19–51.

7

Graphite Furnace Atomic Absorption Spectrometry for the Analysis of Petroleum Products and Lubricants

Paolo Tittarelli[1]

INTRODUCTION

Since the pioneering work carried out by Boris V. L'Vov [1], graphite furnace atomic absorption spectrometry (GFAAS) represents a powerful tool for the determination of trace elements at ppb concentrations [2].

GFAAS differs from flame AAS (FAAS) in only one component of the spectrometer, i.e., the atomizer. In FAAS the atomization temperature is reached using a flame (see Chapter 6 on FAAS for detailed description). In GFAAS, the atomization temperature is reached using a graphite device heated to the high atomization temperature by Joule effect.

The technique is often referred to as electrothermal AAS (ETAAS). However, as only graphite atomizers are used in commercially available spectrometers, the acronym GFAAS is commonly employed to identify this specific approach to atomic absorption analysis.

Graphite furnaces have been available since the beginning of 1970s. Since then, atomic absorption spectrometers equipped with both flame and graphite furnace atomizers represented the "workhorse" of the laboratory for trace (ppm) and ultra trace (ppb) elemental analysis. From the early 1980s, AA spectrometers specifically designed for GF atomizers have been available for use when the workload of trace analysis is relevant and requires sample splitting between ppm (FAAS) and ppb (GFAAS) levels.

A variety of applications have been developed during the years. A book dedicated to GFAAS procedures only was published in 1992 [3].

INSTRUMENTATION

The instrumental setup employed for GFAAS is almost identical to that used for flame measurements (see Chapter 6 on FAAS). Hence the optical path (lamp, atomizer, dispersing system, detector) is the same.

The original atomizer developed by L'Vov was a graphite cuvet with a tip capable of holding a few millilitres of sample solution. However, the actual atomizers are quite similar to the design developed by Massmann [4], i.e., a graphite tube with a sampling hole, about 10 to 20 mm length and 3 to 5 mm internal diameter in modern instruments. The tube is heated by end-side or lateral graphite contacts. Tubes with an internal platform are available to enable the element vaporization in a hot environment. The sample is injected in the tube through a small hole. An inert gas flows outside the tube to protect graphite from oxidation

[1] *Stazione Sperimentale per i Combustibili, Milan, Italy*

and inside the tube to allow the removal of the matrix. Gas flow is stopped during the atomization to increase the residence time of the analyte atoms in the tube.

In GFAAS, the atomic vapor deriving from sample decomposition is contained and restricted in the specific volume of the graphite tube; in FAAS the sample is diluted in a large volume of oxidizing and fuel gases. Taking into account the volume of liquid sample injected in a graphite furnace and the furnace volume, and the corresponding sample and gas volumes in FAAS, the ratio between these two "dilution" factors explains the much higher sensitivity of GFAAS (about one-hundred times better).

The residence time of atomic vapors is about 1 to 5 s in GFAAS; in FAAS the residence time of the atoms in the optical path is a few milliseconds because of the high velocity of the gas mixture flowing through the burner slit.

Further differences between GFAAS and FAAS, as well as ICP-AES and ICP-MS, concern the measurement of atomic absorption (or emission for ICP-AES). In GFAAS the sample aliquot injected in the furnace is vaporized by a heating cycle that can last about 60 s; in FAAS the measurement is performed when the sample flowing through the burner reaches a stable state (within a few seconds). Therefore, the analytical output of GFAAS (number of samples/time) is much lower than that of FAAS.

In FAAS, the most relevant analytical parameters are the flame temperature and the oxidizing or reducing environment. The whole thermal treatment of the sample (solvent evaporation, decomposition of the matrix, vaporization of atomic species) occurs within few milliseconds.

In GFAAS, the temperature, heating rate, and hold time of the furnace can be controlled with much greater selectivity. Hence thermal cycles can be developed specifically for each combination of matrix and analyte.

The thermal cycle can be divided into the following steps:

- Drying, i.e., solvent evaporation. The temperature of this step is tuned according to the type of solvent, and the time according to the volume injected in the graphite furnace.
- Decomposition, better defined as *pyrolysis* in petroleum products analysis. The temperature is set according to the element being analyzed and to the thermal properties of the sample, the time according to the complete decomposition of the sample. Sometimes, two decomposition steps are employed, the first to completely decompose the matrix, the second to reach the optimum decomposition of the element species. Usually the maximum temperature without element loss is chosen to reduce vapor-phase interference of the matrix.
- Atomization. The temperature is set according to the element and the time according to the complete atomization of the element. The gas flow is applied to obtain the highest residence time of atoms in the tube. Usually the minimum temperature with complete vaporization is chosen to increase the lifetime of the tube.
- Cleaning. The maximum temperature is set, with standard or even higher gas flow, to remove all residues of sample decomposition.

Decomposition and atomization temperatures are specific for each element, and may vary for each GF type because of the different design (e.g., length, diameter, graphite thickness). Length and diameter of the tube affect the analytical conditions, because the tube volume is inversely proportional to the concentration of

the atomic vapors. Actual tubes show a length of about 1.5 to 2 cm and an internal diameter of about 3 to 5 mm. Graphite thickness affects the heating rate of the tube. Furthermore, side heating of the tube enables a more uniform heating in comparison to end-side heating.

Over the years, GFAA spectrometers capable of measuring the atomic absorption of different elements simultaneously have been developed. These instruments are equipped with various lamps and with a specific optical arrangement to enable simultaneous reading of atomic absorption at different wavelengths using solid state detectors.

When measuring various elements at the same time, thermal properties of these elements should be considered. Elements with similar properties (pyrolysis and atomization temperature) can be handled without problems. Problems arise when elements with very different properties are analyzed simultaneously. In this case, the lowest pyrolysis temperature should be chosen to avoid the loss of the most volatile element, and the highest atomization temperature to enable the atomization of the most stable element. Also using matrix modifiers should be considered, because only elements analyzed with the same modifier can be measured at the same time.

INTERFERENCES

Some problems associated with GFAAS are:

- Element loss before the measurement of atomic absorption occurs. The element can be lost as atomic vapor exiting the measurement volume or as molecular species.
- Spectral interferences that can affect the accurate measurement of specific absorption.

Interferences in GFAAS analysis are more severe than those encountered in FAAS. These interferences are due to the element volatility and to the matrix.

The element loss represents the most serious drawback for the current use of GFAAS in standardized test methods. Clearly the loss is related to the volatility of the element and its species.

As far as the elemental properties are concerned, the elements can be roughly divided into four groups:

- volatile elements (e.g., lead, cadmium, zinc, arsenic, antimony)
- stable elements (e.g., iron, copper, chromium, nickel)
- elements with high boiling point (e.g., titanium, vanadium)
- elements with very high boiling point (e.g., rhenium, zirconium).

Beside the thermal properties of the element itself, the thermal properties of the respective compounds must be taken into account. Halides are extremely volatile; the element can be lost as chloride or fluoride before the atomization occurs. Extensive work was carried out to demonstrate the behavior of several halides [5,6]. The presence of halides in the sample can hinder the complete recovery of the element. Also the treatment of samples with hydrochloric or hydrofluoric acids (HCl or HF) can affect the accuracy of the measurements.

Sulfates and nitrates generally decompose to the corresponding element oxide plus sulfur and nitrogen oxides. The element oxides are then reduced to elemental species onto the graphite surface of the furnace and vaporized during the atomization step. The chemical treatment of samples, nitric acid (HNO_3) and sulfuric acid (H_2SO_4) should be preferred to HCl and HF. Oxides

are usually as thermally stable as the corresponding element. Oxide species represent the ideal source of atomic vapors during the atomization step.

The risk of element loss during the thermal treatment preceding the atomization step is particularly evident for volatile elements, i.e., elements with boiling temperature below 1,500°C. The element can be lost as atomic vapor before the measurement occurs or, more frequently, as volatile molecular species during the decomposition/pyrolysis step. In particular, chlorides of volatile elements also show low boiling points. In the presence of an excess of chloride in the matrix, for instance, due to sample treatment with hydrochloric acid, the analyte can be lost via vaporization before the atomization/measurement takes place.

Matrix modifiers are currently employed to overcome element loss during the thermal steps preceding the atomization. The aim is to "trap" the volatile element into species stable at high temperature without element release. Some modifiers are developed for specific elements and matrices; others can be considered "fit-for-all-purposes." For instance, lead and magnesium added at microgram levels can allow the complete recovery of elements like cadmium, zinc, lead, arsenic, and selenium.

Spectral interference can be caused by the presence of specific molecular species, generally di- and triatomic molecules, or by the presence of a continuum nonspecific absorption during the atomization step. These species show absorption spectra constituted by a series of bands located in the whole ultraviolet range. For most of diatomic molecules, the most relevant molecular absorption occurs at short wavelengths (below 250 nm). For instance, sulfur species such as CS, SO, and SO_2 show intense absorption in the range of 190 to 250 nm. Quite often, the evolution of these species during the atomization step occurs very quickly. The elements affected by the appearance of molecular absorption are those having analytical lines at short wavelengths, like cadmium, lead, arsenic, antimony, and selenium. The higher the wavelength of the analytical lines, the lower the risk of presence of molecular species interfering during the atomization step. This is the case with manganese, aluminum, copper, and chromium.

Continuum absorption is caused by the evolution of decomposition residues from the sample matrix and from particle scattering. The evolution affects the whole absorption range involved in GFAAS analysis. A typical example is given by the evolution of by-products formed during the pyrolysis of petroleum products.

In the graphite furnace, pyrolysis of petroleum products such as crude oil occurs from about 350°C and continues up to 900 to 1,000°C [7]. The concentration of these products in the tube is related to the type of sample. Fuel and residual oils (especially those with high density and high carbon/hydrogen ratio) exhibit an intense absorption because most of the by-products form at high temperature, whereas products from gasoline to diesel fuel show a limited residual evolution during the atomization step.

INSTRUMENTAL CONDITIONS

Correction of Nonspecific Absorption

The presence of molecular species during the atomization step can interfere with the absorption measurement. The correction of nonspecific absorption due to the presence of molecular species or scattering can be performed using a deuterium lamp or using the Zeeman effect. Deuterium correction is effective when molecular absorption is constant within the slit width. In structured

absorption bands, the deuterium approach fails to distinguish correctly atomic from total absorption.

The Zeeman effect occurs when a magnetic field is applied to atomic vapors. The effect is the splitting of atomic absorption or emission lines into a series of polarized π and σ components with a shift from the original frequency proportional to the magnetic field applied (higher shift for σ components). The π component is usually employed to measure total absorption; σ components are used to measure the nonspecific absorption. The measurement of nonspecific absorption is quite accurate because it occurs at very short distance from the analytical line.

The number of π and σ components may vary according to the element and the radiation (transition) involved. For instance, the sodium line at 589.6 nm originates two π and two σ components, while the line at 589.0 originates two π and four σ components. In the specific case of alkaline-earth elements, only one π and only two σ components of the resonance lines are originated (see Rossi chapter in reference 3 for a detailed description of Zeeman effect). The magnetic field can be applied to the radiation source (lamp) or to the atomizer, the latter case being adopted in commercial instruments.

The determination of trace elements is affected by molecular absorption based on the wavelength of the analytical line. Chromium, copper, and vanadium are less prone to spectral interferences than elements like cadmium, zinc, and arsenic because their analytical lines are located above 300 nm. For the former elements, a deuterium-based correction can be effective in removing nonspecific absorption. For analytical lines at short wavelengths, the use of Zeeman-corrected absorption is recommended unless molecular absorption of matrix components is negligible.

PROCEDURES

FAAS instrumental conditions and procedures have been developed during the years. As a result, "cookbooks" for GFAAS are available as well. Table 1 lists some hints that can be useful to perform GFAAS measurements.

Wavelength

As already mentioned, the same wavelengths are used for FAAS and GFAAS (see Table 2 of Chapter 22).

Pyrolysis and Atomization Temperature

The temperatures can vary from furnace to furnace depending on tube size and shape. Refer to the instrument "cookbook" to identify the correct thermal conditions of each element.

Calibration

As for FAAS, the linear dynamic range of GFAAS is very limited (only one order of magnitude). The calibration in GFAAS is performed in the same way as in FAAS. There are, however, some differences between the two techniques. In GFAAS, a transient atomization occurs, with a profile that follows the formation and disappearance of the atomic species. The shape of the atomization peak is affected by the thermal properties of the element. Peak profiles of volatile elements show almost symmetrical behavior, and peak profiles of low volatile/refractory elements show evident tailing. As a consequence, the peak area of

TABLE 1—Practical Hints for GFAAS Measurements	
Sample injection	Verify the cleanliness of the pipet tip. Thorough cleaning with the solvent used for sample dilution, when automatic sampler is used.
	Verify the complete dispensing of aliquot.
Sample injection	Verify the uniform loading of the aliquot in the tube. Aqueous solutions form a droplet located in the injection site; organic solutions spread along the wall or platform.
	The same behavior should be observed for standards and samples.
Matrix modifier	Loaded on the same surface of the sample for maximum efficiency.
Drying temperature	The drying should proceed without sample spattering till the end of the step.
Pyrolysis temperature	Maximum temperature without loss of atomic vapors. Slightly increase the temperature in case of excessive evolution of molecular vapors during the atomization step.
Atomization temperature	Minimum temperature to enable complete atomization in order to increase tube life. Slightly modify the temperature to reduce overlapping with nonspecific absorption.
	The fastest heating rate to avoid excessive peak broadening.
Furnace cleaning	Required when decomposition products are still present in the tube.
Graphite contacts	Verify cleanliness of the contacts to ensure full transmission of power.
Furnace windows	Inspection and cleaning to remove dirt and decomposition products (a major contribution to poor precision).
Furnace cooling	Check water flow to avoid excessive heating of the furnace.
Gas flow	Check symmetric flow when tubes wear unevenly (effect on peak shape).
Characteristic mass	Verify to evaluate the correct performance of the system.
Atomic absorption	Verify the shape of peak profile that can be affected by the fast appearance of nonspecific absorption.
Poor accuracy of measurements	Verify that the behavior of pyrolysis and atomization temperature are equivalent for standards and samples.

transient atomization must be measured, and not the peak height. When peak tailing is present, it is possible to increase the atomization time to get the full atomization of the analyte. As a discrete volume of sample is vaporized in each cycle, the calibration can be expressed as a function of mass versus peak absorbance.

Sample Analysis

GFAAS offers a distinct advantage over FAAS. The sample volume can be optimized for analysis according to the element concentration. When the

concentration falls outside the calibration range, the sample volume can be decreased. When the element concentration is too low, a higher volume can be injected. In the latter case, it is necessary to check that higher volumes do not alter the atomization process (excessive background absorption, incomplete sample decomposition, tailing of the atomization peak). Modern instruments provide automatic correction for the sample volume.

Detection Limit

Detection limits for GFAAS are reported in Chapter 22 (Table 2). However, as different injected volumes can be set in GFAAS (higher volume → lower detection limit), it is necessary to indicate the volume used to determine the detection limit. The "characteristic mass" is used in GFAAS to evaluate the sensitivity of the measurements. The characteristic mass is the mass of element corresponding to 0.0044 absorbance (1 % absorption). This mass is not really associated with the detection limit, because the detection limit is derived from the signal to noise ratio and gives an indication about the precision of the measurement, whereas the characteristic mass shows the sensitivity of the measurement and is a good indicator of the instrumental performance. The characteristic mass of each element is reported in the cookbooks as a reference.

Autosampler

The use of an autosampler to inject sample aliquots into the furnace represents a substantial improvement in measurement precision over manual introduction. Furthermore, computer-programmed autosamplers can perform a variety of functions, such as sample dilution, calibration, matrix modifier addition, and analyte addition.

Solvents

Solvents used in GFAAS do not differ from those employed in FAAS. Xylene is often used for fuel and residual oils because of its excellent power to dissolve asphaltenes, and methyl isobutyl ketone (MIBK) is more suitable for dilution of lubricating oils. Specific temperatures are set in the drying step to remove quantitatively each type of solvent. Each solvent, however, shows specific behavior toward the graphite surface of the tube, such as wetting and reactions with carbon [8].

Standard Reference Materials

Standard reference materials (SRMs) of petroleum products with element content at the micrograms per kilogram level are not readily available for GFAAS use. This is due to the poor stability of petroleum products when the content of the trace element is very low. To overcome this problem, SRMs with higher element concentration are used after dilution to reach the usual working range of GFAAS. A typical example is given by standard reference fuel oils, with element concentration suitable for FAAS, but used in GFAAS after (multiple) dilution. Although this approach introduces additional variability, it represents the only way to check GFAAS analytical results for accuracy.

APPLICATIONS

Products

The analysis of volatile elements, lead, for example, can be handled by the use of a matrix modifier capable of trapping the trace element and releasing it only at high temperature, when the petroleum product is removed from the tube.

Gasoline and Diesel Fuel

Several papers have been published on light fractions analysis with the aim of avoiding element loss [9] or improving the stability of sample solutions. Concerning the latter case, extensive studies have been carried out to stabilize the sample solutions by the preparation of emulsions [10–12]. The behavior of the emulsions is very similar to that of aqueous solutions. Hence, the calibration can be performed using aqueous standards. The emulsions can be prepared easily and are very stable.

Fuel Oils and Vacuum Distillates

Nickel and vanadium are the elements commonly analyzed in these products. FAAS shows sufficient sensitivity when nickel and vanadium content is greater than 5 mg/kg. For specific products, when the content is lower than the range of an FAAS method, GFAAS can be employed down to very low element concentrations. In this case, there are some aspects to consider that affect an accurate determination of the element. For instance, care must be taken to ensure the complete atomization of nickel and vanadium.

Waxy distillates can be analyzed for nickel, vanadium, copper, iron content, as well as any other crude fraction, when the content of these elements is too low for FAAS.

In general, although copper and iron do not pose particular problems, nickel and vanadium show a tendency to be "trapped" in decomposition products of asphaltenes during the pyrolysis step, with possible formation of the corresponding carbides. These carbides are very stable and decompose at very high temperature, barely attainable by graphite furnaces. As an example of this behavior, Fig. 1

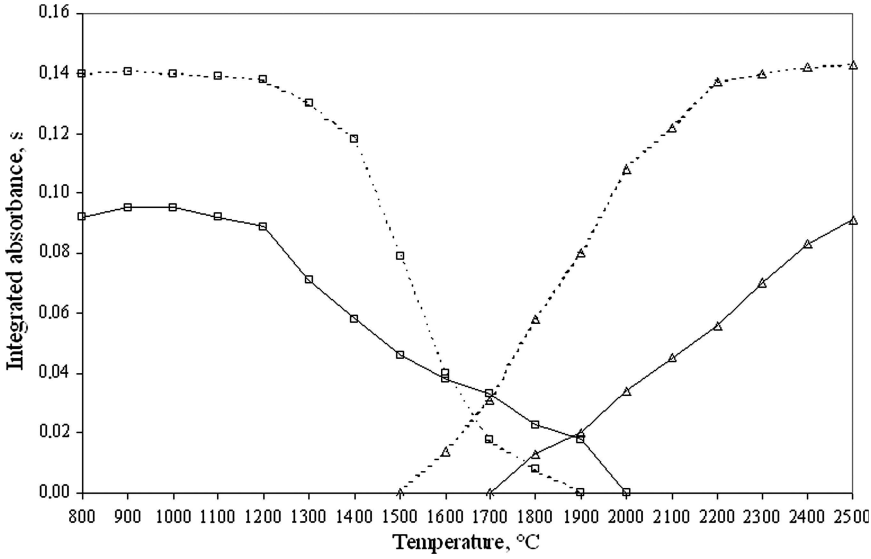

Fig. 1—Pyrolysis and atomization curves of nickel in fuel oil. □ pyrolysis curve, Δ atomization curve. Solid line: argon as internal gas at 500 °C; dotted line: air as internal gas (from Ref [13]).

shows the pyrolysis and atomization of nickel in a fuel oil with nickel content of about 1 mg/kg, diluted with xylene.

The pyrolysis curve (□) shows that the release of nickel atoms proceeds to very high temperature, as the element is trapped in pyrolysis products with formation of the very stable carbide (full line curves). Consequently, the evolution of nickel atoms (Δ) increases slowly but steadily by increasing the atomization temperature. This behavior indicates that the direct determination of nickel, but also that of vanadium, is hindered by some incomplete atomization of the element. The tailing of the peak profile is very evident, even at maximum temperature.

Pyrolysis and atomization curves are quite different from those obtained with aqueous solutions. In aqueous solution, the atomization occurs by decomposition of the oxide formed during the pyrolysis step. Adding an intermediate ashing step at about 500°C, with a low flow of air to oxidize and remove the pyrolysis products, allows the restoration of conditions similar to those found in aqueous solution, with complete atomization of nickel (dotted line curves). However, using an ashing step with air as alternative internal gas should be performed under careful control of the graphite tube, to avoid an excessive oxidation of the furnace.

Lubricating Oils

Wear elements in lubricating oils can be handled after dilution with an appropriate solvent (usually MIBK). The sample can be analyzed before and after filtration, to measure the presence of a dissolved or suspended element.

Biofuels

The use of GFAAS for biofuel analysis is related to the properties defined in technical specifications. Some elements in biodiesel (sodium, potassium, magnesium, calcium) are measured by FAAS because the specification limits are quite high and can be handled by this technique. Phosphorus is measured by ICP-AES because GFAAS does not show adequate sensitivity for this element.

Ethanol is analyzed for sulfur, phosphorus, and copper content. Also in this case, the phosphorus limit is too low to handle this element, which can be determined by ICP-AES. Copper can be determined by GFAAS, but also by ICP-AES, because the technique can exploit its great sensitivity for this element. The procedure for copper analysis is similar to that developed for jet fuel analysis, i.e., direct determination without dilution.

Table 2 summarizes a list of papers on petroleum products and lubricants by GFAAS. Further references can be found in the publications listed in the table.

Standard Test Methods

The number of GFAAS standard test methods is still quite limited. Despite the wide availability of GFAAS instruments, there is a general feeling, at least in petroleum products analysis, that the possible loss of volatile elements in the vaporization step affects the accuracy of the procedure. Nevertheless, GFAAS is employed in many laboratories as a useful procedure for in-house methods.

ISO 8691:1994, *Petroleum products – Low levels of vanadium in liquid fuels – Determination by flameless atomic absorption spectrometry after ashing*.

This test method requires the ashing of the oil sample, followed by ash dissolution and vanadium determination in aqueous medium. The procedure is

TABLE 2—References for Trace Element Analysis of Crude Oils and Petroleum Products

Product	Elements and References
Gasoline	Antimony, arsenic, selenium [12]
	Arsenic, lead [14]
	Cadmium, chromium, copper, lead, nickel [15]
	Cobalt, iron, manganese, zinc [19]
	Copper, iron, lead, nickel [11]
	Lead, nickel [16]
	Molybdenum, vanadium [17]
Naphtha	Nickel, vanadium [18]
Diesel fuel	Cadmium, chromium, copper, lead, nickel [15]
	Cobalt, iron, manganese, zinc [19]
	Lead, nickel [16]
	Vanadium [20]
Kerosine	Antimony, arsenic, selenium [12]
	Cadmium, lead [10]
Organic solutions	Cadmium, lead [21]
Petroleum	Copper, iron, vanadium [22]
	Nickel [23]
Crude oil	Vanadium [24]
Crude oil fractions	Lead [9]
Heavy ends	Nickel [13]
Asphaltene	Vanadium [20]
Lubricating oil	Antimony, tin [25]

time consuming, unless batches of samples are treated at the same time. Possible contamination can occur during the sample treatment.

ASTM D7632-02, *Standard Test Method for Determination of Copper in Jet Fuels by Graphite Furnace Atomic Absorption Spectrometry*.

IP 478/02 *Determination of copper in aviation turbine fuels by graphite furnace atomic absorption spectrometry*.

ASTM D7632 and IP 478 are equivalent. Both methods enable the direct determination of copper with satisfactory precision at the concentrations required by the technical specifications.

EN 15488:2007, *Ethanol as a blending component for petrol – Determination of copper content – Graphite Furnace atomic absorption method*.

EN 15488 has been developed by CEN for ethanol analysis using IP 478 as the source. As for IP 478, ethanol is analyzed directly, in this case after a calibration in ethanol. The main difference EN 15488 and D7632 or IP 478 deals with is the drying step of the thermal program, because ethanol is very volatile and it is quite difficult to dose onto the graphite platform with adequate repeatability.

As already mentioned, EN 15837:2009, *Ethanol as a blending component for petrol - Determination of phosphorus, copper and sulfur content - Inductively coupled plasma optical emission spectrometric direct method* shows slightly better precision than EN 15488, but allows the contemporaneous determination of all elements listed in ethanol specification EN 15376.

It is quite surprising that the "emulsion" approach, which shows clear advantages as far as sample preparation and stability are concerned, has not yet been developed as an international standard test method.

TRENDS AND DEVELOPMENTS

Although not strictly related to petroleum products analysis, it is useful to note that GFAAS shows a greater capacity to handle solids and slurries, in comparison to FAAS and ICP, because the thermal treatment can be extended to enable the full decomposition of the solid sample or of the slurry [26]. The complete recovery of the element in slurry analysis is affected by the species and element type in the slurry sample. Treating the slurry with diluted nitric acid enables the extraction of several trace elements. Then, the slurry analysis becomes the analysis of a trace element in the presence of high content of solid particles (see Tittarelli chapter in Ref [3]).

The capability of handling a large variety of samples is also exploited in the coupling of a graphite furnace to ICP or ICP-MS. In this coupling, the furnace behaves as an electrothermal vaporizer (ETV) to originate vapor species that are detected by ICP or ICP-MS. Hence, the electrothermal vaporizer is considered a "tool" for ICP-MS measurements. The ETV enables also some sort of "thermal" resolution, i.e., the selective vaporization of elements according to their thermal properties [27].

As already mentioned in describing GFAAS applications, two major aspects hinder the extensive use of GFAAS for standard test methods. One aspect is related to the possible loss of volatile elements. Although using matrix modifiers, coupled with graphite platform atomization and Zeeman correction of nonspecific absorption, shows good results in handling this problem, the risk of element loss still represents a sort of "shadow" for GFAAS. Various approaches, not connected to the use of modifiers, have been proposed to overcome this problem.

The filter furnace, developed by Katskov [28,29], shows accurate results when volatile elements are analyzed [20,30], including gasoline and diesel samples [15,19]. In the filter furnace, the sample is loaded onto a collector made of carbon fiber, the fiber is heated by the graphite tube, and the sample vapors are forced to flow to a porous graphite filter. The atomic species are detected in an environment almost free from molecular species (Fig. 2). The technique shows fast heating cycles, treatment of large sample sizes, and very low nonspecific absorption. However, filter furnaces are not available commercially yet.

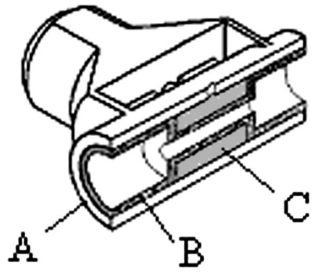

Fig. 2—Transverse heated filter furnace: A) tube, B) filter, C) collector (from Ref [19]).

For accurate measurements in the presence of interfering atomic or molecular species, new instruments have recently been introduced. Based on high resolution AA spectrometers, these instruments employ a continuum light source (xenon) and a high-resolution dispersing system with an echelle monochromator [31]. Using a solid-state detector, it is possible to follow the atomization process within a range of about 4 nm. This approach is very useful in method development, because it enables the identification and quantification of atomic and molecular lines overlapping the analytical line, especially when trace elements are analyzed in the presence of high concentration of salts. The technique has been applied successfully to the analysis of petroleum products [23,24].

CONCLUSIONS

Although a mature, perhaps aged technique, GFAAS is still used widely for ultra-trace analysis. The continuous interest in such technique is also demonstrated by numerous GFAAS applications presented in symposia and conferences [32].

The perspectives for the development of GFAAS standard test methods regard the determination of trace elements when a few elements are analyzed, when a limited working range is needed, and when element loss can be ignored, because of the thermal stability of the element or the use of specific matrix modifiers. Conventional GFAAS is less appealing in comparison to ICP-AES or ICP-MS when these requirements are not fulfilled.

References

[1] L'Vov, B. V., "The Analytical Use of Atomic Absorption Spectra," *Spectrochim. Acta*, Vol. 17, 1961, pp. 761–770.

[2] L'Vov, B. V., *Atomic Absorption Spectrochemical Analysis*, Hilger, London, 1970.

[3] Minoia, C. and Caroli, S., *Applications of Zeeman Graphite Furnace Atomic Absorption Spectrometry in the Chemical Laboratory and in Toxicology*, Pergamon, Oxford, 1992.

[4] Massmann, H., "The Comparison of Atomic Absorption and Atomic Fluorescence in the Graphite Cuvette," *Spectrochim. Acta* Part B, Vol. 23, 1968, pp. 215–226.

[5] Daminelli, G., Katskov, D. A., Mofolo, R. M. and Tittarelli, P., "Atomic and Molecular Spectra of Vapours Evolved in a Graphite Furnace. Part 1. Alkali Halides," *Spectrochim. Acta* Part B, Vol. 54, 1999, pp. 669–682.

[6] Katskov, D. A., Mofolo, R. M. and Tittarelli, P., "Atomic and Molecular Spectra of Vapours Evolved in a Graphite Furnace. Part 4: Alkaline Earth Chlorides," *Spectrochim, Acta* Part B, Vol. 56, 2001, pp. 57–67.

[7] Tittarelli, P., Lancia, R. and Zerlia, T., "Simultaneous Molecular and Atomic Spectrometry with Electrothermal Atomization and Diode Array Detection," *Anal. Chem.*, Vol. 57, 1985, pp. 2002–2005.

[8] Tserovsky, E. and Arpadjan, S., "Behaviour of Various Organic Solvents and Analytes in Electrothermal Atomic Absorption Spectrometry," *J. Anal. Atomic Spectrometry*, Vol. 6, 1991, pp. 487–491.

[9] Kowalewska, Z., Bulska, E. and Hulanicki, A., "Organic Palladium and Palladium-Magnesium Chemical Modifiers in Direct Determination of Lead in Fractions from Distillation of Crude Oil by Electrothermal Atomic Absorption Analysis," *Spectrochim. Acta* Part B, Vol. 54, 1999, pp. 835–843.

[10] Silva, I. A., de Campos, R. C. and Curtius, A. J. "Determination of Lead and Copper in Kerosene by Electrothermal Atomic Absorption Spectrometry: Stabilization of Metals in Organic Media by a Three-Component Solution," *J. Anal. Atomic Spectrometry*, Vol. 8, 1993, pp. 749–754.

[11] de Campos, R. C., Santos, H. R. and Grinberg, P., "Determination of Copper, Iron, Lead, Nickel in Gasoline by Electrothermal Atomic Absorption Spectrometry Using Three-Component Solutions," *Spectrochim. Acta* Part B, Vol. 57, 2002, pp. 15–28.

[12] Aucelio, R. Q. and Curtius, A. J., "Evaluation of Electrothermal Atomic Absorption Spectrometry for Trace Determination of Sb, As and Se in Gasoline and Kerosene Using Microemulsion Sample Introduction and Two Approaches for Chemical Modification," *J. Anal. Atomic Spectrometry*, Vol. 17, 2002, pp. 242–247.

[13] Anselmi, A. and Tittarelli, P., "Determination of Nickel in Petroleum Heavy Ends by Electrothermal Atomic Absorption Spectrometry," *La Rivista dei Combustibili*, Vol. 48, 1994, pp. 435–441.

[14] Aneva, Z. and Iacheva, M., "Simultaneous Extraction and Determination of Traces of Lead and Arsenic in Petrol by Electrothermal Atomic Absorption Spectrometry," *Anal. Chim. Acta*, Vol. 167, 1985, pp. 371–374.

[15] Anselmi, A., Tittarelli, P. and Katskov, D. A., "Determination of Trace Elements in Automotive Fuels by Filter Furnace Atomic Absorption Spectrometry," *Spectrochim. Acta* Part B, Vol. 57, 2002, pp. 403–411.

[16] Reyes, M. N. M. and Campos, R. C., "Graphite Furnace Atomic Absorption Spectrometric Determination of Ni and Pb in Diesel and Gasoline Samples Stabilized as Microemulsion using Conventional and Permanent Modifiers," *Spectrochim. Acta* Part B, Vol. 60, 2005, pp. 615–624.

[17] dos Santos, D. S. S., Texeira, A. P., Korn, M. G. A. and Texeira, L. S. G., "Determination of Mo and V in Multiphase Gasoline Emulsions by Electrothermal Atomic Absorption Spectrometry," *Spectrochim. Acta* Part B, Vol. 61, 2006, pp. 592–595.

[18] Meeravali, N. N. and Kumar, S. J., "The Utility of a W-Ir Permanent Chemical Modifier for the Determination of Ni and V in Emulsified Oils and Naphtha by Transverse Heated Electrothermal Atomic Absorption Spectrometry," *J. Atomic Absorp. Spectrometry*, Vol. 16, 2001, pp. 527–532.

[19] Tittarelli, P., Priola, M., Ricchiuto, S., Katskov, D. and Ngobeni, P. "Fuel Analysis by Filter Furnace Electrothermal Atomic Absorption Spectrometry," *J. ASTM Intl.*, ASTM International, West Conshohocken, PA, July/August 2005, Vol. 2, No. 7.

[20] Aucélio, R. Q., Doyle, A., Pizzorno, B. S., Tristão, M. L. and Campos, R. C., "Electrothermal Atomic Absorption Spectrometric Method for the Determination of Vanadium in Diesel and Asphaltene Prepared as Detergentless Microemulsions," *Microchem. J.*, Vol. 78, 2004, pp. 21–26.

[21] Mbileni, C., Ngobeni, P., Katskov, D. A. and Panichev, N., "Determination of Lead and Cadmium in Organic Solutions by Electrothermal Atomic Absorption Spectrometry with a Transverse Heated Filter Atomizer," *J. Anal. Atomic Spectrometry*, Vol. 17, 2002, pp. 236–241.

[22] Pedrini Brandão, G., de Campos, R. C., Ribeiro de Castro, E. V. and de Jesus, H. C. "Determination of Copper, Iron and Vanadium in Petroleum by Direct Sampling Electrothermal Atomic Absorption Spectrometry," *Spectrochim. Acta* Part B, Vol. 62, 2007, pp. 962–969.

[23] Vale, M. G. R., Damin, I. C. F., Klassen, A., Silva, M. M., Welz, B., Silva, A. F., Lepri, F. G., Borges, D. L. G. and Heitmann, U., "Method Development for the Determination of Nickel in Petroleum using Line-Source and High-Resolution Continuum-Source Graphite Furnace Atomic Absorption Spectrometry," *Microchem. J.*, Vol. 77, 2004, pp. 131–140.

[24] Lepri, F. G., Welz, B., Borges, D. L. G., Silva, A. F., Vale, M. G. R. and Heitmann, U., "Speciation Analysis of Volatile and Non-volatile Vanadium Compounds in Brazilian Crude Oils using High-Resolution Continuum Source Graphite Furnace Atomic Absorption Spectrometry," *Anal. Chim. Acta*, Vol. 558, 2006, pp. 195–200.

[25] Aucélio, R. Q., Curtius, A. J. and Welz, B., "Sequential Determination of Sb and Sn in Used Lubricating Oil by Electrothermal Atomic Absorption Spectrometry using Ru as a Permanent Modifier and Microemulsion Sample Introduction," *J. Anal. Absorp. Spectrometry*, Vol. 15, 2000, pp. 1389–1393.

[26] Kurfürst, U., *Solid Sample Analysis – Direct and Slurry Sampling using GF-AAS and ETV-ICP*, Springer-Verlag, Berlin, 1998.

[27] Kántor, T., Maestre, S. and de Loos-Vollebregt, M. T. C., "Studies on Transport Phenomena in Electrothermal Vaporization Sample Introduction Applied to Inductively Coupled Plasma for Optical Emission and Mass Spectrometry," *Spectrochim. Acta* Part B, Vol. 60, 2005, pp. 1323–1333.

[28] Katskov, D. A., Marais, P. J. J. G. and Tittarelli, P., "Design, Operation and Analytical Characteristics of the Filter Furnace, a New Atomizer for Electrothermal Atomic Absorption Spectrometry," *Spectrochim. Acta* Part B, Vol. 51, 1996, pp. 1169–1189.

[29] Katskov, D. A., Marais, P. J. J. G. and Ngobeni, P., "Transverse Heated Filter Atomizer for Electrothermal Atomic Absorption Spectrometry," *Spectrochim. Acta* Part B, Vol. 53, 1998, pp. 671–682.

[30] Marais, P. J. J. G, Panichev, N. A. and Katskov, D. A., "Performance of the Transverse Heated Filter Atomizer for the Atomic Absorption Determination of Mercury," *J. Anal. Atomic Spectrometry*, Vol. 15, 2000, pp. 1595–1598.

[31] Welz, B., Becker-Ross, H., Florek, S. and Heitmann, U., *High-Resolution Continuum Source AAS: The Better Way to Do Atomic Absorption Spectrometry*, Wiley-VCH, Weinheim, 2005.

[32] *Tenth Rio Symposium on Atomic Spectrometry, Book of Abstracts*, Salvador, Brazil, 7–12 September 2008.

8

Inductively Coupled Plasma Atomic Emission Spectrometry in the Petroleum Industry with Emphasis on Organic Solution Analysis

Robert I. Botto[1]

INTRODUCTION

One of the most important advantages of inductively coupled plasma atomic emission spectrometry (ICP-AES) is that it can analyze aqueous and organic solutions. This makes it an ideal technique for the petroleum/petrochemical industry, which generates a wide variety of aqueous and organic sample types. With proper solvent selection, the heavy end of the barrel as well as the light fractions of crude, and crude oil itself, can be analyzed. ICP-AES has been a well-established technique in the petroleum analysis laboratory since the 1970s. The author's laboratory at ExxonMobil (then Exxon Research and Engineering Company) in Baytown, Texas, ordered one of the first commercial ICP-AES instruments and took delivery in early 1976. This Jarrell-Ash (now Thermo Fisher Scientific, Inc.) direct-reading arc spectrometer fitted with an ICP source was the first ICP-AES installed in the petroleum industry. It served us well for nearly 25 years [1].

From the early 1990s onward, ICP-AES has been reinforced with inductively coupled plasma mass spectrometry (ICP-MS). Now both techniques serve side by side in many petroleum industry laboratories, including the author's own. Table 1 references some milestones in the development of ICP-AES and ICP-MS for organic solutions. One of the first organic solvents used for ICP-AES, mixed xylenes, is still widely used today. Petroleum/petrochemical applications of ICP depend on the use of organic solvents for dissolution of many samples. The first part of this work focuses on solvent selection and instrumentation for organic ICP-AES.

ORGANIC ICP-AES: SOLVENT SELECTION

Organic ICP-AES permits the analysis of petroleum crudes and fractions by direct aspiration of samples diluted in appropriate solvents or in "neat" form. Lengthy dry ashing or sulfated ashing procedures are avoided, along with losses and contamination from destructive sample preparations. Solvent dilutions are easy to automate for high throughput analysis. There are disadvantages that can be minimized. Instrument setup and return to aqueous service can be inconvenient. There is a loss in sensitivity when samples are diluted. Spectral and matrix interferences particular to the organic matrix may exert influence on the results if they are not addressed.

[1] *Analytical Services Laboratory, ExxonMobil Refining and Supply, Baytown, Texas*

TABLE 1—Milestones in Organic ICP Analysis

- First direct ICP analysis of oil diluted in gasoline by Pforr and Aribot in 1970 [2]
- Early work on USAF jet lubes in Fassel's laboratory, 1976 [3]
- Xylene plasma started in author's laboratory, mid-1976
- Organic ICP becomes routine in Petrochemical industry, 1977–84 [4-6]
- Organic liquid chromatography ICP-AES, 1981 [7]
- Organic aerosols and ICP effects studied, 1980–87 [8-13]
- Ar-O_2 organic ICP-MS with xylene solvent, 1986 [14]
- Air-ICP-AES used for analysis of organic solvents, 1986 [15]
- Ar-O_2 ICP-AES with ultrasonic nebulizer for volatile liquids, 1991 [16-18]
- Universal calibration for organic ICP-AES achieved with ultrasonic nebulizer/membrane desolvator, 1996 [19]
- Ar-O_2 ICP-MS with direct injection nebulization, 1996 [20-24]
- Ar-O_2 ICP-MS and ICP-AES with low flow nebulization, 2001 [25]
- Organic ICP-MS with collision/reaction cell technology [26]

"Like dissolves like" is the common wisdom of solvent selection. The solvent must solubilize the entire sample, if possible, and form stable solutions. Petroleum samples consist of varying amounts of saturates (paraffins, isoparaffins), olefins, aromatics, and "polars" or asphaltenes (molecules typically containing atoms such as oxygen, sulfur, halogens, or nitrogen in addition to carbon and hydrogen). Polars tend to concentrate in the high molecular weight fractions of crude oils along with metals. The polarity of each of these components of crude oil is different. Solutes and solvents should have similar polarity to form the most stable solutions. Normal paraffins, for example, would not be good solvents for crudes containing significant amounts of polars. Aging and oxidation of oils can increase the polar fraction leading to solvent incompatibility. Lube oil additives can be significantly more polar than basestock because of functional groups. Decomposition products in used lubes can be highly polar (e.g., organic acids). Solvent polarity index (Table 2) is a convenient way to predict solute/solvent compatibility.

Not all solvents are practical for ICP-AES. If a solvent is too volatile, it will tend to overload the plasma with vapor and destabilize or even extinguish it. Solvent-limiting aspiration rate (millilitres per minute) can be defined as the maximum rate of sample introduction into a medium-power argon ICP (1.2 to 1.8 kW) through a conventional pneumatic nebulizer (such as a concentric or cross flow) with a sustainable plasma. As expected, solvent-limiting aspiration rate is a strong function of boiling point, as shown in Table 3. Kreuning and Maessen [13] studied solvent plasma loading as a function of solvent saturation vapor pressure. Out of that study general guidelines were developed to predict solvent tolerance of the ICP with pneumatic nebulization: alkanes and cycloalkanes with carbon number greater than 8, aromatics with more than 7 carbons, all alcohols except methanol, all chlorohydrocarbons except CH_3Cl, ketones with more than 3 carbons, esters with more than 2 carbons, and ethers with more than 4 carbons.

In addition, solvent volatility affects the physical characteristics of the aerosol introduced into the ICP. Table 4 shows the relationship between saturation vapor pressure and the minimum percent aerosol component of the total mass of solvent reaching the ICP. With highly volatile solvents, the stream reaching the

TABLE 2—Solvent Polarity Index: A Scale for Relative Polarity

Solvent	Index Value	Typical Solutes
heptane	0.1	Paraffin wax
octane, decane		
isoparaffins		White spirit
kerosine		
cyclohexane	0.2	Petroleum distillates
decalin		
carbon tetrachloride	1.6	
toluene	2.4	
o-xylene	2.5	Automotive lubes
benzene	2.7	
1,2,3,4-tetrahydro-naphthalene		
chlorobenzene	2.7	Crudes
nitrobenzene		
ethyl ether	2.8	
dichloromethane	3.1	Petroleum resids
2-propanol (IPA)	4.0	
tetrahydrofuran	4.0	Coal liquids
trichloromethane (chloroform)	4.1	Shale oils
4-methyl-2-pentanone (MIBK)	4.2	
ethyl acetate	4.4	Jet engine lubes
1,4-dioxane	4.8	Hydraulic fluids
2-butanone (MEK)	4.8	
acetone	5.1	
methanol	5.1	
pyridine	5.3	Coal liquid distillation "bottoms"
dimethyl sulfoxide (DMSO)	7.2	
water	10.2	

TABLE 3—Solvent B. P. and Limiting Aspiration Rate[a]

Solvent	B. P., Degrees C	Limiting Aspiration Rate (ml/min)
ethyl ether	35	<0.1
dichloromethane	40	2.0
acetone	56	0.1
trichloromethane (chloroform)	61	3.0
methanol	65	0.1
tetrahydrofuran	65	<0.1
ethyl acetate	77	1.5
2-butanone (MEK)	80	
benzene	80	<0.1
cyclohexane	81	<0.1
2-propanol (IPA)	82	3.0
heptane	98	0.2
water	100	
1,4-dioxane	101	
toluene	111	1.0
pyridine	116	1.0
4-methyl-2-pentanone (MIBK)	117	3.0
carbon tetrachloride	121	<5.0
octane	125	0.5
chlorobenzene	132	3.0
p-xylene	138	4.0
m-xylene	139	4.0
o-xylene	144	4.0
decane	174	2.0
decahydronaphthalene	186	
dimethyl sulfoxide (DMSO)	189	2.0
1,2,3,4-tetrahydronaphthalene	207	
nitrobenzene	211	>5.0

[a] Data from Ref [9]

TABLE 4—Saturation Vapor Pressure and Aerosol Contribution[a]

Solvent	P_{sat} (mm Hg), 20 Degrees C	Minimum % Aerosol
ethyl ether	435	3
trichloromethane (chloroform)	155	4
methanol	93.3	31
carbon tetrachloride	86.7	8
cyclohexane	77.8	10
n-heptane	35.5	19
toluene	21.7	23
water	17.5	66
m-xylene	6.10	55

[a] Data from Ref [13]

plasma is mostly vapor, containing little liquid in the form of aerosol droplets. Aerosols created by volatile solvents evaporate in the spray chamber/conditioning chamber after exiting the nebulizer. Aerosol droplet size may decrease significantly within fractions of a second [9]. Smaller droplets are more likely to be carried into the ICP rather than to be eliminated by the walls or baffles of the spray chamber. Thus solvent volatility can affect sample transport efficiency into the ICP, explaining signal enhancements observed for organic over aqueous solutions.

Other solvent physical properties such as density, viscosity, and interfacial tension affect sample transport efficiency and, thus, sensitivity. The following empirical equation was developed by Nukiyama and Tanasawa to express the Sauter (volume to surface area ratio) mean droplet diameter of "primary" aerosol particles created by pneumatic nebulization [9]:

$$\text{Primary median droplet diameter, (Sauter) um} = 585/V(\sigma/\rho)^{0.5} + 597[\eta/(\sigma * \rho)^{0.5}]^{0.45} * [10^3 * Q_L/Q_G]^{1.5} \quad (1)$$

where:

V = linear velocity of gas flow in m/s,
σ = interfacial tension in dynes/cm,
ρ = liquid density in g/cm^3,
η = liquid viscosity in poise,
Q_L, Q_G = volume flow rates of liquid and gas (cm^3/s).

The equation was developed for a particular nebulizer and is not valid for general application. It illustrates, however, the qualitative effect of variations in the solution physical properties. Particle size will vary in proportion to interfacial

tension and viscosity, and inversely proportional to density. Larger particle sizes tend to translate to lower transport efficiency and sensitivity, so higher interfacial tension, viscosity, and density all work against high sensitivity.

Solvents selected for ICP analysis must be free of metal contaminants and available in bulk quantities. They must not attack the components of the sample introduction system. Low toxicity solvents are preferred. Those with irritating odors (like pyridine) may not be acceptable. Solvents having a definite composition are to be preferred over variable mixtures, for example, p-xylene versus mixed xylenes. Solvents most commonly used for organic solution ICP analysis include xylenes, methyl isobutyl ketone (MIBK), 2-propanol, kerosine, 2,2,4-trimethylpentane (isooctane), and 1,2,3,4-tetrahydronaphthalene (tetralin). Oxygenated solvents like MIBK are often blended with hydrocarbons to increase the solvent polarity index. Tetralin is a particularly useful solvent for petroleum ICP and it warrants a special discussion.

ORGANIC ICP-AES: INSTRUMENTATION

Sample Introduction System

The sample introduction system for organic ICP-AES typically consists of a pumping device, a nebulizer attached to a spray chamber (with or without a conditioning apparatus), connected to the injection tube of the ICP torch. The pumping device may draw from an automatic sample changer. Peristaltic pumps are most commonly used, but piston drive (high pressure liquid chromatography [HPLC] type) pumps, syringe drive pumps, and gas displacement pumps are sometimes used. Sample pumping is needed to minimize self-aspiration rate changes due to varying solution physical parameters. Peristaltic pump tubing must be solvent resistant. Viton™ type rubber tubing is best for most organic solvents. Transfer tubing must be polyethylene or fluorocarbon. To minimize pulsations, using ten or more rollers in the pump head is best. Making a "Y" tube from two pieces of pump tubing and using two pump channels to pump a single stream will also decrease pulsations. Multistream pumps can be used with switching valves to alternately introduce sample and blank or check standards. Flow injection equipment may take the place of the pump.

Table 5 shows the effect of using a peristaltic pump on the precision and accuracy of an analysis of heavy fuel oil diluted 10, 20, and 50 times in tetralin. Results from the three dilutions are much tighter and more accurate with the pump. For solvents that attack Viton™ gas, displacement pumping can be used. A gas displacement pump uses pumped air to displace sample from a dispensing vessel, as shown in Fig. 1.

Pneumatic nebulizers are normally used for organic ICP. Here are the most popular types [27]:

- Cross-flow type—gas and sample streams impact at a 90 degree angle.
- Glass concentric—liquid stream emerges surrounded by supersonic gas jet.
- Babington or "V" groove type—nonclogging type is best for samples containing particles.
- Burgener parallel path—resistant to particle clogging as sample capillary widens where it approaches orifice and gas stream.
- Low flow or micro—excellent for limiting sample aspiration rate (10 to 500 μL/min) but easily clogged by particles. They are self aspirating because peristaltic pump tubing is not available for lowest flow rates. A miniaturized version of the concentric nebulizer is available.

TABLE 5—Analysis of NIST Fuel Oil 1634 With (W) and Without (W/O) a Peristaltic Pump (ug/g)

	Dilution = 10		Dilution = 20		Dilution = 50		% RSD		
Element	W/O	W	W/O	W	W/O	W	W/O	W	NIST Cert.
Fe	13.3	13.4	14.1	13.8	15.2	14.7	5.5	3.9	13.5 +/– 1.0
Ni	32.6	34.5	36.2	34.1	40.9	38.5	9.3	5.6	36 +/– 4
V	285	292	305	298	326	310	5.5	2.5	320 +/– 15
Mn	0.12	0.10	0.12	0.11	(0.11)	(0.13)	–	–	(0.12)
Zn	0.67	0.35	1.06	0.31	2.15	(0.42)	48	13	0.23 +/– 0.05

Ultrasonic nebulizers (USN) are easily applied to organic ICP provided desolvation (flash heating and condensation of the aerosol) is employed to remove solvent load to the plasma (Fig. 2). USNs are highly efficient (approximately 30 % versus 3 % for conventional pneumatic nebulizers). Even aqueous aspiration can extinguish an ICP without the desolvation step. Desolvation will remove volatile metal species that condense with the solvent vapor. Direct injection nebulizers use very low flow rates to form an aerosol at the base of the ICP. They are ideal for interfacing a liquid chromatograph with the ICP. Because they do not require desolvation, there is no loss of volatile element species. Heated nebulizers have been constructed for introducing waxes and heavy oils without dilution or fouling.

Spray chambers of various designs are available to condition the aerosol before injection into the ICP. Large droplets that would cause signal instability are removed by impaction or settling in the spray chamber, and the aerosol may be conditioned at a temperature advantageous for the analysis. The most common spray chamber designs in use are the Scott type (cylindrical tube within a cylindrical body) and the cyclonic type. An advantage of the cyclonic

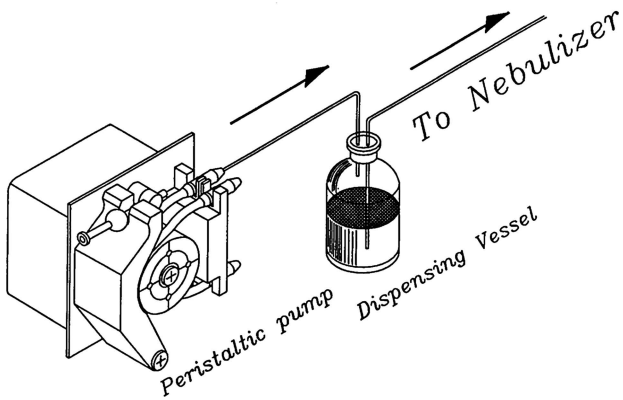

Fig. 1—Gas displacement pump for solvents that attack Viton™.

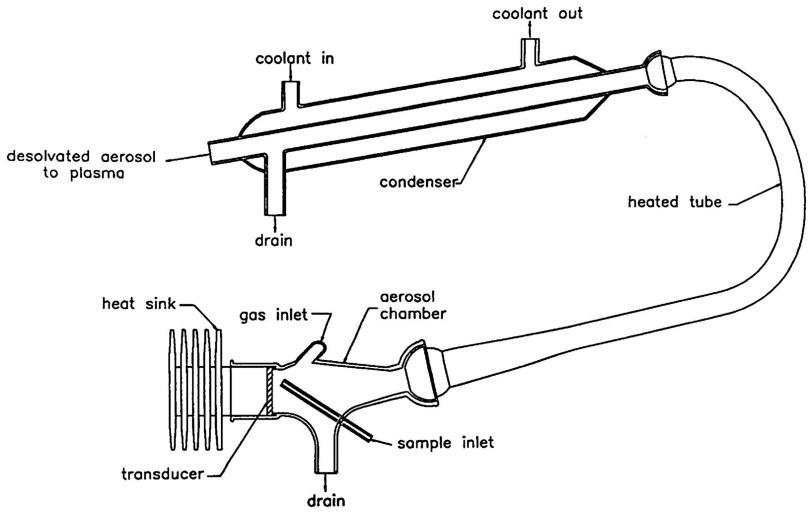

Fig. 2—Ultrasonic nebulizer (USN) with desolvation (heated tube for flash evaporation and condenser unit).

type is the possibility of a very small interior volume for fast washout and minimum memory effects. Spray chamber thermostatting, even if at room temperature, is generally recommended for increased long-term calibration stability. It compensates for evaporative cooling from aerosol production and for changes in room temperature. A chilled spray chamber is useful for minimizing solvent loading of the ICP. The temperature must be adjustable for various solvents because some freeze at moderate temperatures (p-xylene, for example: 14°C). A heated spray chamber can be used for organic ICP to partially desolvate the aerosol stream. It must be followed by a condensor apparatus to collect vaporized solvent.

The waste from organic ICP analysis must be handled safely to prevent operator exposure and accidental ignition. The author has used a carboy fitted with a side outlet connected to another vessel and equilibrated with the laboratory atmosphere through a charcoal filter. The carboy is filled with water up to the level of the outlet. Organic solvent waste is allowed to flow in underneath the water and float up and out the outlet to be collected in the smaller vessel for disposal. Small snorkel-type fume hoods are useful to remove sample vapors from the sample introduction/sample handling area at the ICP instrument.

ICP torches may be one piece or demountable. For organic ICP, the demountable torch is preferred because of ease of replacement of the injector tube if it is fouled with carbon deposits. Orifice tip diameter may be a critical parameter for good operability. One millimetre injector tips are generally recommended for organics, but it is advisable to try more than one size.

Using oxygen is highly recommended for organic ICP. It helps prevent carbon deposits on torch parts, reduces spectral emission background from molecular carbon species, and may permit higher ICP vapor loading [28]. Oxygen can be blended with the auxiliary argon flow or the main coolant argon flow. The flow rate required is low (0 to 100 mL/min), so a micrometer valve or

sensitive control device is needed. The argon and oxygen streams should be premixed in a buffer bottle upstream of the ICP torch. Commercial systems for oxygen mixing are available for most ICP instruments. Mass flow controllers are also recommended for the nebulizer (aerosol carrier) argon and auxiliary argon streams.

Spectrometer Considerations

Flexible line selection and background correction are highly desirable for organic solution ICP-AES. Line selection should be optimized for organic solution analysis. Alternate lines for aqueous solution analysis should be provided for elements where there is a distinct difference in sensitivity or dynamic range. Alkali elements (atomic lines) typically have a decreased sensitivity in the organic matrix due to the higher plasma power used for these solutions. Unfortunately, alternate line selection is limited for alkalis. Detector array systems present the best combination of speed and versatility for organic ICP-AES. Certain instrument manufacturers produce ICP-AES systems designed for organic solution analysis with line selection optimized as well.

The axial and radial ICP view options are both useful in organic ICP-AES. Table 6 shows detection limits obtained for solutions of 90 % tetralin/10 % p-xylene for a number of elements, and a few alternate lines using both axial and radial observation with various oxygen flow settings. In general, the best detection limits are obtained with axial viewing, even for UV lines. Radial viewing is not bad and may yield superior dynamic range performance particularly with high concentrations of alkalis and alkaline earths. The use of oxygen is recommended as noted above. However, it degrades the sensitivity of measurements in the deeper UV (<220 nm, affecting, e.g., arsenic and phosphorus). The deeper into the UV, the greater the signal suppression effect from oxygen becomes. Axial versus radial performance with respect to precision for the same sample matrix is shown in Table 7. Optimum sensitivity and precision are linked for most elements as expected, but for sodium the best sensitivity is obtained with axial viewing and the best precision with radial viewing. Optimized viewing and oxygen conditions are likely to produce the best results, as shown in Table 8. Although it may be inconvenient to adjust oxygen flow rate and recalibrate during a single analysis run, it is usually easy or even automatic to switch between axial and radial viewing if both are offered with the ICP-AES instrument.

ICP-AES ANALYSIS PROCEDURE FOR ORGANIC SOLUTIONS

Instrument Setup and Operating Conditions

Setting aside a nebulizer and spray chamber for organic solutions is recommended. If the same sample introduction system must be used for aqueous and organic solutions, a rinse with 2-propanol has been used effectively as a go-between. The oxygen flow usually must be off when starting the plasma. The torch is usually mounted 1 to 2 mm lower for organic ICP to accommodate the higher power. Typical operating conditions for organic ICP are given in Table 9. The plasma is started and aerosol is introduced slowly and carefully. The oxygen flow is then adjusted to eliminate the “green” (common appearance as viewed through a glass filter) carbon emission from the base and sheathing the plasma. The aerosol carrier (nebulizer) flow is then adjusted to bring the top of the “bullet” of carbon emission 5 to 10 mm above the top of the load coil.

TABLE 6—ICP-AES Axial/Radial Detection Limits						
90% Tetralin/10% p-Xylene – three sigma, ug/g						
Element	Wavelength nm	Axial View No O_2	Radial View No O_2	Axial View O_2 = 10 ml/min	Radial View O_2 = 10 ml/min	Axial View O_2 = 40 ml/min
Al	396.1	0.056	0.079	0.028	0.057	0.017*
As	189.0	0.019*	0.4	0.027	0.81	0.042
As	193.7	0.027*	0.14	0.043	0.19	0.03
Cd	214.4	0.0009*	0.003	0.0012	0.0054	0.0012
Fe	259.9	0.0027	0.0051	0.0042	0.0057	0.0024*
Hg	184.9	0.0036*	0.46	0.014	1.03	0.019
Mn	257.6	0.0003	0.0009	0.0003	0.0012	0.00016*
Mo	204.5	0.0048*	0.031	0.0087	0.033	0.0078
Na	589.5	0.088	0.053	0.13	0.049	0.032*
Ni	231.6	0.032	0.017	0.048	0.018	0.013*
P	178.2	0.037*	3.98	0.057	16.5	0.077
P	213.6	0.017*	0.071	0.029	0.055	0.028
Pb	220.3	0.032*	0.17	0.069	0.16	0.039
Sb	206.8	0.012	0.094	0.033	0.14	0.011*
Sn	189.9	0.016*	2.44	0.036	0.43	0.037
Ti	323.4	0.0024	0.0054	0.0024	0.0093	0.0015*
V	311.0	0.006	0.011	0.0042*	0.017	0.0045
Zn	206.2	0.0015*	0.0048	0.0033	0.0075	0.0018
* Indicates lowest value						

TABLE 7—Axial/Radial ICP-AES Short-Term Precision						
90% Tetralin/10% p-Xylene, 10 determinations, % RSD						
Element (ug/g)	**Wavelength nm**	**Axial View No O_2**	**Radial View No O_2**	**Axial View O_2 = 10**	**Radial View O_2 = 10**	**Axial View O_2 = 40**
Al (1.0)	396.1	1.1*	3.6	1.8	4.2	1.4
As (0.5)	189.0	0.92*	30	2.2	46	4.0
As (0.5)	193.7	2.2*	9.7	2.6	6.1	3.1
Cd (0.5)	214.4	0.53	0.81	1.7	1.3	0.49*
Fe (5.0)	259.9	0.31	0.80	0.62	0.58	0.26*
Hg (0.2)	184.9	1.4*	60	1.9	60	3.6
Mn (0.5)	257.6	0.36	0.63	0.64	0.52	0.34*
Mo (0.5)	204.5	0.58	2.0	0.63	2.7	0.45*
Na (0.5)	589.5	3.3	2.2*	14	3.5	4.3
Ni (0.5)	231.6	0.82*	1.8	1.3	1.6	1.7
P (5.0)	178.2	0.57*	50	0.64	49	1.5
P (5.0)	213.6	0.42	0.85	0.73	0.82	0.34*
Pb (0.5)	220.3	1.7*	13	4.4	16	2.7
Sb (0.5)	206.8	1.7	8.0	1.5*	9.5	1.7
Sn (0.5)	189.9	1.5*	41	3.4	58	6.3
Ti (0.5)	323.4	0.72	0.83	0.89	1.3	0.66*
V (0.5)	311.0	0.98	1.7	0.74*	2.0	0.90
Zn (0.5)	206.2	0.26	0.72	1.0	1.3	0.21*
* Indicates lowest value						

TABLE 8—ICP-AES Analysis of NIST Heavy Fuel Oil 1634B

1:20 dilutions in 90% tetralin/10% p-xylene (ug/g)

Element	Wavelength nm	Axial View (sigma)* O_2 = 40 ml/min	Axial View (sigma)* No O_2	Preferred Conditions	NIST Certified
Na	589.5	56.5 (0.95)	58.6 (0.79)	56.5	(90)
V	311.0	52.1 (0.35)	55.1 (0.37)	55.1	55.4 +/– 1.1
Mn	257.6	0.173 (0.01)	0.140 (0.006)	0.173	0.23 +/– 0.03
Fe	259.9	17.7 (0.07)	17.3 (0.05)	17.7	31.6 +/– 2.0
Ni	231.6	27.4 (0.16)	26.9 (0.16)	27.4	28 +/– 2
Zn	206.2	2.93 (0.12)	2.66 (0.019)	2.66	3.0 +/– 0.2
As	189.0	0.22 (0.28)	0.09 (0.12)	0.09	0.12 +/– 0.02
Pb	220.3	1.65 (0.27)	1.83 (0.21)	1.83	(2.8)

* Four replicate determinations

TABLE 9—Typical ICP-AES Operating Conditions: For Organic Solutions

RF Power:	
1.5–1.8 kW Forward, 2–10 W Reflected	
Flow Rates:	
Ar Outer	16–24 l/min
Ar Intermediate	0–2 l/min
Oxygen Outer	25–75 ml/min
Ar Aerosol	600–900 ml/min
Sample	1–3 ml/min
Observation Zone:	
5–8 mm above the tip of the "bullet"	

Optimization/Calibration

Calibration standards for organic ICP consist of oil-soluble metals in solution. They are available from several commercial sources as well as the National Institute of Standards and Technology (NIST). Standards from other sources are usually traceable to NIST. Calibration solutions should contain equivalent concentrations of oil (the same concentration as sample dilutions if possible)

in the appropriate solvent. Internal standard elements, if used, are also included. Metal-free base oil is often used for matrix matching and is available from commercial sources. Certain metal-organic compounds used as standards may have very limited solubility and stability when diluted in certain solvents.

Some manufacturers also recommend including a stabilizer when preparing dilute metal-organic standards. The stability of diluted organic solution standards should be investigated for quality assurance, and working standards should be prepared fresh prior to use. A complete set of calibration standards will include a calibration blank, one or more "high" standards containing all elements of interest at "high" concentration, solutions of elements at "upper limit" concentrations to test calibration linearity, single high purity element solutions for spectral interference evaluation, and optical alignment and optimization solutions, if needed.

Using an atom/ion line intensity ratio as a reference greatly assists in reproducing optimum analysis conditions on a day-to-day basis. An atom line (I) with a wavelength > 250 nm is paired with an ion line (II) with wavelength < 300 nm. Examples are Cu (I) 325 nm/Mn (II) 258 nm or Mg (I) 285 nm/Mg (II) 280 nm. The latter ratio has been used to ensure that the plasma is "robust" enough to minimize matrix interferences [29]. A minimum value can be set (a minimum ratio of 10.0 is used for aqueous systems) that will also serve for organic ICP. The atom/ion intensity ratio is usually adjusted by making minor changes in the aerosol carrier flow rate. To determine optimum conditions for a particular application, determine detection limits or other figures of merit as a function of the atom/ion intensity ratio and select the best value. Determine a two-sigma tolerance precision for the selected value and set a minimum intensity specification (counts) for the atom line. Before every calibration, set the atom/ion intensity ratio at the preselected value. Three consecutive measurements must fall within the tolerance range and meet the minimum intensity specification. The atom/ion intensity ratio thus defines the "compromise" conditions for multielement analysis and provides a means to reproduce them after making changes [30,31].

Spectral interference calibration can be performed after the atom/ion intensity ratio has been set. Calibrate the instrument for all of the elements of interest and analyze high-purity single-element reference solutions for each element. Compile a list of interelement correction factors after making sure that trace contaminants in the reference solutions are not masquerading as spectral interferences. Enter the verified interelement correction factors into software. It has been shown that using the atom/ion intensity reference for reproducing analysis conditions will greatly improve the long-term stability of interference calibrations [32].

Analysis Procedure

Once the atom/ion intensity ratio has been set and the ICP-AES calibrated, the analysis of samples diluted in the appropriate solvent can proceed. Samples should be "matrix matched" with the calibration reference solutions containing approximately the same amount of oil and solvent. It is important to ensure that the samples are completely dissolved before analysis, and that solutions are free of particulates that could clog the sample introduction equipment. Sample analyses should be interspersed with analyses of the calibration blank.

The blank analyses serve two purposes–to verify that sample concentrations have been washed out to background levels and to permit corrections for background drift. If concentrations are not sufficiently washed out, an additional blank analysis may be performed. A "check" standard containing all the elements in the analytical program at concentrations within their respective calibration ranges should be analyzed after every six to twelve samples to check for calibration drift. If results fall outside specified limits, the atom/ion intensity ratio should be checked and reset if necessary. Often this is all that is needed to re-establish an accurate calibration. If resetting the atom/ion intensity ratio has not brought all of the elements back into their respective calibration limits, the ICP-AES should be recalibrated. Alternately, if calibration drift is minor, mathematical correction may be an option.

INTERFERENCES IN ORGANIC ICP-AES

Spectral Interferences

Potential spectral interferences in organic ICP arise from increased background from carbon particle emission and molecular band emission from carbon, CN, OH, and other species created in the plasma from sample decomposition and reaction with entrained air, in addition to the atomic emission of carbon and other elements in the samples. The organic ICP is highly structured, with carbon emission concentrated in the "bullet" surrounded by a zone of high-intensity atomic emission and sheathed by an exterior zone containing emission from CN and other molecules [33]. Using oxygen minimizes the effects of carbon particle, carbon, and other molecular emission. Spectral resolution, the judicious choice of analytical lines, and background wavelengths also work toward minimizing spectral and background effects [34]. Of course the organic ICP exhibits the same atomic spectral line and wing overlaps as the aqueous ICP if interfering element combinations are present in the plasma.

Organic Matrix Interferences

Potential matrix interferences in the organic ICP arise from energy changes in the plasma (thermochemical effects) or differences in analyte transport efficiency (physical effects). Thermochemical effects are usually due to changes in organic mass loading of the ICP due to sample volatility, or to changes in the chemical composition of the samples. Physical effects are usually related to variations in solute concentration or physical properties or both. In general, a mismatch between samples and standards translates as matrix interference. Internal standards (IS) are most commonly used to minimize matrix interferences. They add, however, to the complexity of the analysis procedure and are not 100 % effective. Rigorous matching of samples and standards is the generally accepted protocol with or without IS.

The author performed a study aimed at identifying the source of organic matrix interferences and finding a way to prevent or minimize them by using a better choice of dilution solvent without resorting to internal standards [12]. Xylene was chosen as the baseline solvent for comparison. The results of the study revealed that thermochemistry can be a dominant cause of matrix interference, particularly in the analysis of xylene solutions. Xylene atomization consumes 10 to 20 % of the total plasma power under typical operating conditions. When an oil sample is diluted in xylene, it alters the bulk composition of the

solution as well as its physical properties. Solutions having higher hydrogen/carbon ratios have higher excitation energies and consume additional plasma power. Variations in plasma power consumption of a few watts may influence analyte excitation significantly. Tetralin was identified as a superior choice of solvent because it consumes significantly less power from the plasma. Consequently, the tetralin plasma runs hotter than the xylene plasma, even with the increased plasma power normally employed for organic solutions. Thus, the effect of a few watts of change is less in the tetralin plasma. Chilling the spray chamber is an effective means of minimizing matrix interference and improving operability for volatile samples. A chilled spray chamber may not improve the matrix interference situation for heavy petroleum samples diluted in xylene.

Tetralin is a superior solvent for ICP analysis of lubricating oils, middle distillates, and heavy fuel oils. It is more effective in solubilizing polar materials in residual oils than kerosine, for example. The power of tetralin to reduce or eliminate matrix interferences is shown by comparing Figs. 3 and 4. Here ICP-AES analyses of six elements at identical concentrations in solutions also containing 2.0, 5.0, 10.0 and 20.0 % of a lubricating oil base (75 Neutral) in xylene (Fig. 3) and tetralin (Fig. 4) were performed using xylene or tetralin calibration standards containing negligible oil. Spectral lines of the elements were chosen to encompass a range of excitation energies from "soft" or low energy (silver and copper) through medium energy (calcium and titanium) to "hard" or high energy (cadmium and zinc) lines. The wide spread of results observed for the xylene solutions (Fig. 3) illustrates strong matrix interference and large potential for error. The lack of deviation for the tetralin solutions (Fig. 4) demonstrates the virtual elimination of the matrix interferences for these solute concentrations. As a result, the analysis of heavy oils in tetralin may be performed accurately without an internal standard and without precise solute concentration matching (Table 10). A subsequent study using conventional and low flow torches also demonstrated the superiority of tetralin over xylene [35].

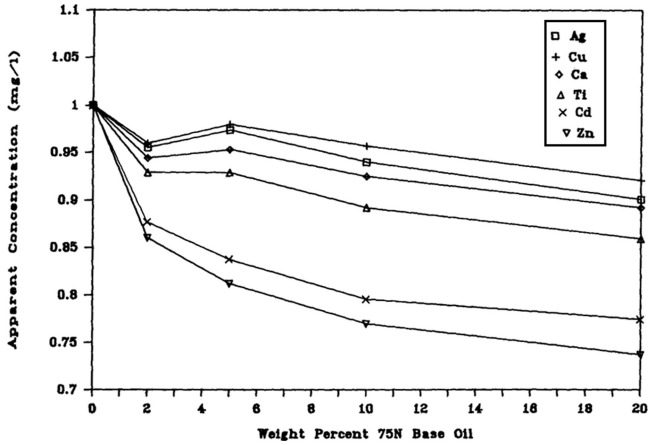

Fig. 3—Effect of 75N base oil in p-xylene.

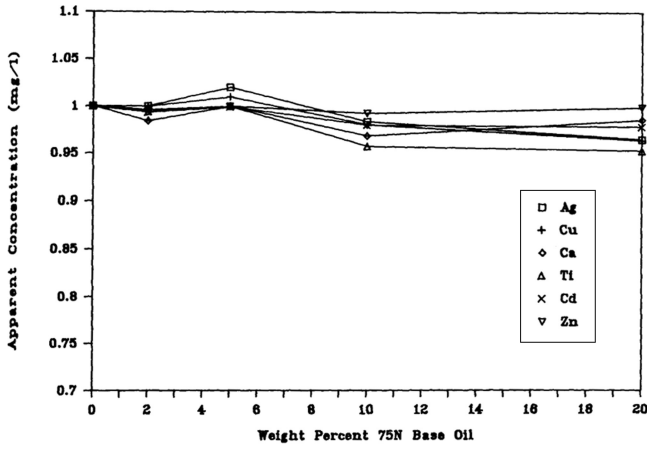

Fig. 4—Effect of 75N base oil in tetralin.

Wisely chosen IS can compensate for residual matrix effects as well as for variations in the sample introduction system. Thus precision and accuracy of the results can be improved. However, poorly chosen IS can create more errors than they compensate for. More than one IS would be required to compensate for the matrix effects affecting the six elements in Fig. 3, for example. The optimum choice of IS is one that is closely matched in excitation characteristics with the analyte. Multielement analysis will usually require more than one IS. Match ion (II) line IS with ion line of analyte and match the sum of the excitation energies [36]. Match atom (I) line IS with atom line of analyte by excitation energies. Atom and ion lines of a single element may serve as two IS [37].

PETROLEUM ANALYSIS BY ORGANIC ICP-AES

ICP Methods for the Petroleum Industry – Role of ASTM

Numerous ICP analysis methods exist for petroleum and petrochemical products that are not accessible to the world at large. Each petrochemical company has its own compendium of proprietary methods for analysis of their products. ASTM Committee D02 has performed a service to the analytical community by encouraging the publication of methods that otherwise might never see the light of day. A list of current ASTM methods under D02 for petroleum products and lubricants using ICP-AES is given in Table 11. Nadkarni has reviewed many ASTM methods related to fuels and lubricants, including ICP-AES methods [38].

ASTM D7260 presents a very useful overview of ICP-AES analysis strategy for obtaining accurate and precise results for petroleum products and lubricants using solvent dilution and sample digestion for analysis as aqueous solutions [39]. Analysis equipment capabilities, wavelength selection, background correction, spectral line overlap, and matrix interferences are discussed. It is recommended that the analyst consult this publication before setting up an ASTM ICP petrochemical application. The method is a compendium of recommendations based on recent work in the industry compiled by ASTM Committee D02. The writing of ASTM methods for ICP-AES has lagged the industry implementation of

TABLE 10—ICP-AES Analysis of NIST Fuel Oil 1634A										
1:50, 1:20, 1:10, 1:5 Dilutions in Tetralin and Xylenes (ug/g)										
	Tetralin Dilutions (4)*			Xylenes Dilutions (4)*			Wet Ashing (50)*			
Element	Mean	Sigma	%RSD	Mean	Sigma	%RSD	Mean	Sigma	%RSD	NIST Certified
Al	7.9	0.3	3.2	7.4	0.5	6.7	8.5	2.3	26	–
Ba	3.03	0.07	2.4	2.92	0.08	2.6	3.6	0.2	4.6	–
Ca	13.0	0.3	2.1	13.8	0.5	3.6	18.6	2.3	4.5	(16)
Fe	20.5	0.5	2.3	18.0	1.1	6.0	24	3.2	13	(31)
Mg	1.67	0.04	2.2	1.49	0.09	6.1	2.07	0.16	7.8	–
Mn	0.15	0.02	11	0.12	0.01	5.9	0.18	0.03	18	0.19 +/– 0.02
Na	56	1.5	2.6	57	2.6	4.5	73	8.6	12	87 +/– 4
Ni	27	1.2	4.3	26	0.7	2.6	25	1.5	2.7	29 +/– 1
Pb	2.09	0.06	3.1	1.74	0.08	4.7	2.42	0.19	7.8	2.80 +/– 0.08
V	55	2.7	5.0	50	3.2	6.4	54	2.2	4.0	56 +/– 2
Zn	2.52	0.09	3.4	1.98	0.18	9.2	2.6	0.5	19	2.7 +/– 0.2
* Calibration standards contained 1% lube base oil										

TABLE 11—ICP-AES Methods under ASTM D02 Committee (Petroleum Products and Lubricants)

- D4951, STM Determination of Additive Elements in Lubricating Oils by Inductively Coupled Plasma Atomic Emission Spectrometry
- D5184, STM Determination of Aluminum and Silicon in Fuel Oils by Ashing, Fusion, Inductively Coupled Plasma Atomic Emission Spectrometry, and Atomic Absorption Spectrometry
- D5185, STM Determination of Additive Elements, Wear Metals, and Contaminants in Used Lubricating Oils and Determination of Selected Elements in Base Oils by Inductively Coupled Plasma Atomic Emission Spectrometry (ICP-AES)
- D5600, STM Trace Metals in Petroleum Coke by Inductively Coupled Plasma Atomic Emission Spectrometry (ICP-AES)
- D5708, STM Determination of Nickel, Vanadium, and Iron in Crude Oils and Residual Fuels by Inductively Coupled Plasma (ICP) Atomic Emission Spectrometry
- D7040, STM Determination of Low Levels of Phosphorus in ILSAC GF 4 and Similar Grade Engine Oils by Inductively Coupled Plasma Atomic Emission Spectrometry
- D7111, STM Determination of Trace Elements in Middle Distillate Fuels by Inductively Coupled Plasma Atomic Emission Spectrometry (ICP-AES)
- D7151 (D27, Insulating Liq) Determination of Elements in Insulating Oils by Inductively Coupled Plasma Atomic Emission Spectrometry (ICP-AES)
- D7260, Standard Practice for Optimization, Calibration, and Validation of Inductively Coupled Plasma-Atomic Emission Spectrometry (ICP-AES) for Elemental Analysis of Petroleum Products and Lubricants

these techniques by 15 to 20 years [40]. As a result, the ASTM methods that are now in use draw on two decades of laboratory experience.

Analysis of New and Used Lubricating Oils

The analysis of additive elements in new lubricating oils by direct solvent dilution is one of the earliest applications of ICP-AES in the petroleum industry [5,6,41]. Our laboratory attempted to set up this analysis in 1976—indeed our instrument purchase was justified on the basis of improved analysis of lubes from our lube compounding plant. The analysis could not be made to be sufficiently accurate or convenient at that time because of severe matrix interferences and the inconvenience of switching between the aqueous and organic plasma. In time, advances in methodology, including the use of internal standards that were eventually incorporated into the industry standard ASTM D4951 [42], overcame these difficulties and served to promote the use of ICP in the petroleum industry.

Using ASTM D4951-06, additive elements such as boron, calcium, copper, magnesium, phosphorus, and zinc are determined by dilution of the lube oil in mixed xylenes, o-xylene, or kerosine with the required addition of an internal standard element such as cobalt, cadmium, or yttrium. Matrix interferences arising from the presence of viscosity index (VI) improvers in the lube oils can cause results to be in error by as much as 20 % [43]. VI improvers are long-chain, oil-soluble polymers that help maintain a desirable viscosity range of the lube oil over a wide range of engine operating temperatures. The polymers usually incorporate dispersant functionality as well. These specially engineered

molecules are product specific. Oils containing different and varying concentrations of VI improvers will differ significantly in physical properties, resulting in matrix-induced errors. Differences in sample dilution and mismatch between samples and calibration standards also contribute to bias. Use of the internal standard element and appropriate and consistent sample dilution (approximately 20 to 100 or 1 to 5 mass % sample is recommended [43]), together with the matching concentrations of base oil in the calibration standards, yields accurate and precise results. ASTM D7040, Standard Test Method for Determination of Low Levels of Phosphorous in ILSAC GF 4 and Similar Grade Engine Oils by Inductively Coupled Plasma Atomic Emission Spectrometry, requires an internal standard and a peristaltic pump for sample introduction to minimize matrix effects [44]. Phosphorus is an additive in these types of automotive lubes, but is also a potential catalyst poison in the automobile exhaust systems. The dilution solvents specified in ASTM D7040 are the same as for ASTM D4951.

The analysis of used lubes for wear metals by ICP-AES presents all of the challenges of variable oil matrix and physical properties of the new lubes and adds another, even more difficult challenge—particles. Wear metals from engine components are typically present, mainly as particles in used lubes. The particle size range can be less than a micrometre to several tens of micrometres. The ICP cannot efficiently atomize particles larger than a few micrometres. Larger particles also tend to settle out of the aerosol before they reach the plasma [45,46]. Unfortunately, it is these larger wear-metal particles that are the harbingers of catastrophic engine wear and the ones of greatest interest, particularly for aircraft [47]. ASTM method D5185 recognizes the limitations of ICP-AES in the determination of wear metals in used lubes [48], but responds to the automobile industry's need for a rapid survey technique that is focused on routine maintenance and not on predicting catastrophic engine failure. For automobile "engine trend analysis" predicting component failure, the method of choice is still rotating electrode spark emission because it can detect the larger wear particles [47].

ASTM D5185 combines the determination of lube additive elements, wear elements, and oil contaminants such as might occur from a cooling system leak into one 22-element method. Care is taken to homogenize the sample immediately before analysis using ultrasonication or vortex mixing. The sample is then diluted by a factor of ten in xylenes or other suitable solvent and introduced into the ICP through a peristaltic pump to minimize viscosity effects. The use of an internal standard is declared to be optional. A nebulizer designed to accommodate particles such as a Babington-type is specified. Wear-metals analysis programs often generate large numbers of samples, and the method lends itself to being fully automated using robotic sample preparation [49].

A "particle size independent" method has been developed for a total metals analysis of the used lubes and hydraulic (synthetic ester based) fluids for aircraft or other critical or heavy duty use engines [47,50]. A small quantity of a mixture of acids is used to dissolve the particles, and the aqueous digest is homogenized with the oil and diluted in the solvent for introduction into the ICP. Thus the particle size independent methods for used oils represent a cross between organic and aqueous sample introduction strategies. The methods have been used successfully to predict aircraft engine malfunction for the U.S.

Air Force [47,51]. An additional novelty in used oil analysis is the introduction of the samples without solvent dilution using a heated Babington nebulizer and inverted spray chamber and ICP torch [52].

Analysis of Middle-Distillate Fuels and Other Petroleum Products by Organic ICP

ASTM D7111 is a general method for determination of metals in middle distillate fuels (turbine diesel, marine and naval fuels) using direct dilution in kerosine with an internal standard element (yttrium is recommended) to correct for minor matrix effects [53]. Contaminants in turbine fuels can cause corrosion and fouling of engine parts. Metals contained in particulates may or may not be determined, depending on particle size. A Babington-type nebulizer is specified. It is noted that elements present in volatile species such as silicon will generate results higher than the true value.

Electrical insulating oils are similar to lighter lube oils in terms of base stock properties. Because of the rigorous purity needed to obtain the desired electrical properties, the additives used are different and their levels typically quite low. Contaminants in insulating oils can cause insulation performance breakdown and reflect problems in the equipment. ASTM D7151 uses direct dilution in kerosine with an internal standard element to determine contaminant elements in insulating oils [54]. As with turbine fuels and used motor lubes, particulates may be present and may or may not be reflected in the results. Sample filtration may be used to produce a "dissolved metals" result, and digestion of the particulates may be used to determine "total metals."

ICP-AES ANALYSIS OF CRUDE OILS AND RESIDUAL FUELS

Refined heavy oils represent the residuum from crude oil distillation–the "bottoms" or "resids" from the atmospheric or vacuum pipestill. Other heavy oils may result from polymeric reactions in high-temperature processing. The ultimate is solid petroleum coke. Heavy crude oils may be processed directly from wells or thermal/extraction processes. Refined heavy oils may be reprocessed in the refinery to lighter materials, or they may end up as products such as asphalt, petroleum coke, heavy fuel oil, or wax. Heavy oils may contain up to percent levels of nickel and vanadium in stable relict porphyrin structures. Asphaltenes (pentane insolubles) in heavy oils contribute to high levels of polar compounds containing sulfur, nitrogen, and oxygen. Resids may contain crude contaminants such as salts, corrosion products, or oil field additives. Some thermal polymers and cracking residuals contain catalyst fines. Heavy crude oils often contain an emulsified aqueous phase (brine) as well as entrained solids. They may also contain oil field additives, corrosion products, heavy waxes, and formation clay.

The overall challenge in the ICP analysis of heavy oils is to accurately characterize (without contamination or loss) a representative sample of a potentially heterogeneous semisolid or solid hydrocarbon type material that might be multiphase and contain high levels of polar components. Direct dilution is the approach often considered first because it involves the least amount of effort. The significant problems associated with the direct analysis of crude oils and residual fuels by ICP-AES are matrix effects resulting from the widely different physical properties of the samples and the limited solubility of polar

components. Matrix effects can be minimized through the judicious use of internal standards and peristaltic pumping as noted previously. Using tetralin as a solvent helps solubilize polar components. Brenner et al. published a method based on the use of scandium as an internal standard, tetralin as the solvent, a V-groove (high solids) nebulizer, and a fast sequential ICP-AES [55]. It was concluded that accurate results could be obtained with 1:10 dilutions using a two-point calibration despite the wide range of vanadium and iron levels encountered in the samples. Even with solutions containing 35 % heavy oil, measured intensities were decreased by only 10 to 20 %. ASTM D5708 Test Method A for direct determination of nickel, iron, and vanadium in crude oils and residual fuels by organic ICP recommends the high solids nebulizer, 1:10 solvent dilution, and tetralin among the recommended solvents [56]. No internal standard is required, consistent with recommendations of the author's study [12].

Choice of Sample Preparation Technique

Many heavy oil samples require some form of destructive sample preparation for complete solubilization. Available sample preparation techniques include the industry classic "sulfated ashing," high-temperature dry ashing, microwave digestion, various open and contained wet digestions, ash fusion, and Soxhlet extraction [57]. Sulfated ashing involves the complete destruction of all of the organic material, with dissolution of the inorganic residue using sulfuric acid as an ashing aid to tie up potentially volatile metals (e.g., cadmium, lead, sodium) as relatively involatile sulfates. A low sample dilution is possible. Sulfated ashing is time consuming, however, and sample contamination is possible. Highly volatile species (e.g., mercury, antimony, selenium) are lost in the furnace ashing step. A typical procedure mixes 20 g of sample with 5 mL of concentrated sulfuric acid in an open quartz beaker while coking the mixture on a "high" hot plate in a fume hood. The residue after acid fumes have disappeared is ashed in a muffle furnace at 540°C. Afterward, the residue is taken up with dilute acids. If aluminum and silicon are to be determined and volatile species are not a concern, the sample can be "dry ashed" (without addition of sulfuric acid) at high temperature and the ash digested in an acid mixture containing hydrogen fluoride or fused with lithium tetraborate or a similar salt [58].

Microwave digestion uses mineral acids, heat, and optionally pressure for complete destruction of the organic material. An enclosed system under pressure minimizes losses of volatile species, and the procedure is relatively fast and convenient. The procedure is limited to small sample sizes (usually less than 0.3 g), however, if pressure digestion vessels are to be used. High sample dilution and potential contamination from the vessels are drawbacks for trace analysis of heavy oils. A typical procedure digests 0.2 to 0.25 g of sample in a capped quartz vial also containing 4 mL of concentrated nitric acid and 1 mL of 35 % hydrogen peroxide. The vial is sealed inside a fluorocarbon pressure digestion vessel also containing 10 mL of water and 2 mL of 35 % hydrogen peroxide in the bottom. The digestion program takes the temperature of the vessel contents to 220°C in 30 minutes and holds it at that temperature for another 30 minutes. The reagents used need to be of the highest purity available.

TABLE 12—ICP-AES Lower Limits (three sigma) for Heavy Oils (ug/g)

Element	Sulfated Ashing Dilution = 2.5	Microwave Digestion Dilution = 200	Tetralin Dilution Dilution = 20
Ca	0.07	6	0.4
Cu	0.04	4	0.1
Fe	0.002	0.2	0.04
Mg	0.002	0.2	0.004
Na	0.1	8	1
Ni	0.004	0.4	0.4
V	0.03	3	0.2

The author's methods for calibration and analysis of aqueous solutions by ICP-AES have been published [30–32, 34]. Matrix-related effects are present in aqueous ICP just as they are in organic ICP. Mineral acid content of samples and standards must be carefully matched to avoid "acid matrix effects." Differences in dissolved solids content can also cause matrix interferences. Multiple internal standards are often required to correct for differences in acid and dissolved solids content. The author has demonstrated that it is possible to correct for these effects without using internal standards by using a hydrogen emission line at 486.133 nm (H-beta) [59].

Comparisons between direct dilution, sulfated ashing, and microwave digestion for ICP analysis of heavy oils conducted in the author's laboratory generally favor the classic sulfated ashing technique as the most sensitive and reliable method for all elements except those that are partially lost [60]. Direct dilution fails to include particulates, and microwave digestion is compromised by high dilution and reagent/vessel contamination. Table 12 shows lower limits for several key elements using the three sample preparation methods. The time-consuming sulfated ashing method is clearly the most sensitive. Table 13 shows the analysis precision achieved with ten replicate tetralin dilutions of NIST 1634c and ten replicate dilutions of a sample of refined heavy oil (deasphalted oil). The deasphalted oil was also spiked, and the recoveries and precision are also shown in the table. Sodium determinations in the NIST material are very imprecise (23 % RSD) compared to the precision of the deasphalted oil spikes (4.3 % RSD). This is probably due to the presence of sodium-bearing particulates in the NIST material.

Heavy oils containing solids can foul ICP sample introduction equipment and render direct dilution methods inaccurate or worse. Procedures for separation of "toluene insolubles" similar to ASTM D893 [61] for liquid heavy oils or ASTM D4072 [62] for tar and pitch can be used to separate solids from heavy crudes and residual oils that cannot be filtered or centrifuged without solvent dilution. The heavy oil solutions and recovered solids may be analyzed separately. Sulfated ashing can be employed as a "total" analysis. Thus the element

TABLE 13—ICP-AES Analysis of Heavy Oil by Tetralin Dilution

10 replicate dilutions (Dilution = 20)			
	Ni (ug/g)	V (ug/g)	Na (ug/g)
NIST Residual Fuel Oil 1634c			
Mean	17.9	27.6	23.2
Sigma	0.96	1.0	5.2
% RSD	5.4	3.7	23
NIST Certified value	17.54 +/− 0.21	28.19 +/− 0.40	(Approx. 37)
Deasphalted oil (100 ug/g spike)			
Mean	7.67 (104)	16.3 (107)	<3 (88)
Sigma	0.09 (3.6)	0.15 (5.3)	(3.8)
% RSD	1.1 (3.4)	0.95 (5.0)	(4.3)
% Spike Recovery	96	91	88

distribution between the solids and the oil can be examined. It often reflects the chemistry of the crude, as illustrated in Table 14.

Heavy oils can be analyzed by ICP as oil/water emulsions. Crude oils are often microemulsions in nature containing a small quantity of brine intimately mixed with the oil. Oil-in-water microemulsions containing a low percentage of oil can be prepared that are stable and resemble "aqueous" type samples having a nearly transparent appearance. All involve combining oil plus or minus matrix modifier with surfactant and water [63]. Acids can be incorporated into the mix to dissolve wear metals and other particles.

ICP-AES versus ICP-MS for Analysis of Heavy Oils

ICP-MS is becoming increasingly more integrated into petroleum/petrochemical industry laboratories as the technique matures. ICP-MS is particularly promising for ultratrace analysis of heavy oils and crudes [64]. For the foreseeable future, ICP-AES will continue to be the workhorse for nickel, vanadium, and the other more abundant elements in oils, however [65]. The greater sensitivity of ICP-MS should permit the determination of lower concentrations in heavy oils prepared by sulfated ashing and direct dilutions. Quadrupole ICP-MS instruments without collision/reaction cells will display interferences from carbon, hydrogen, nitrogen, and oxygen molecular species in the m/e 24 to 54 range particularly. Even so, high sensitivity is realized in the higher mass range for elements like mercury and lead. Adding a collision/reaction cell or interface greatly improves ICP-MS performance in the low mass range, rendering the technique useful for virtually the entire periodic table [26]. ICP-AES and ICP-MS will complement one another in any case and can be used as a cross check for many elements. Fig. 5 compares detection limits for ICP-AES with ICP-MS with and without a collision interface. The superior performance of the collision interface technology is evident.

TABLE 14—Element Distribution in Heavy Crude

Distribution between oil (toluene) and solids (toluene insolubles) reflects element species chemistry

Results from heavy crude samples: Crude 1 - low naphthenic acids, Crude 2 - high naphthenic acids

Element	% in Solids (Crude 1,2)	% in Toluene (Crude 1,2)
Ca	100, 6	0, 94
K	95, 100	5, 0
As	61, 100	39, 0
Zn	14, 52	86, 48
Ni	1, 1	99, 99

Fig. 6 compares results from ICP-AES (sulfated ashing) with results from direct analysis of the same crude sample using tetralin dilution ICP-MS with and without a collision interface. Higher results by ICP-AES (arsenic, molybdenum, tin, lead) may be due to the presence of particulates containing the elements. High results by ICP-MS without the collision interface (vanadium, iron) are probably due to molecular ion interferences.

ASTM ICP Methods for Grease, Fuel Oils, and Petroleum Coke

Lubricating greases are complex and challenging materials to analyze. Commercial greases may contain thickening agents (clays and lithium soaps with boron-complexing agent), together with rust inhibitors, antiwear additives (such as zinc dithiophosphate), extreme pressure additives (bismuth, molybdenum, lead), and contaminants [66]. Used greases contain all of these plus wear metals acquired from the machinery. The components of grease, together with the

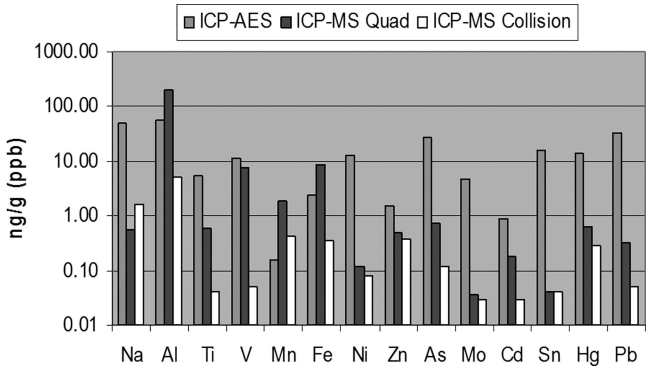

Fig. 5—ICP-AES and ICP-MS three sigma detection limits in tetralin.

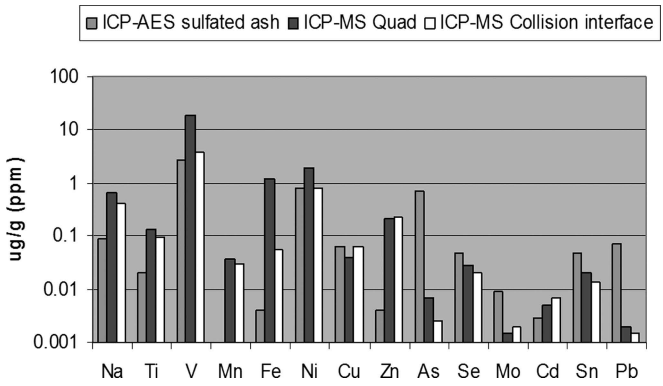

Fig. 6—Results from ICP-AES sulfated ashing versus ICP-MS (tetralin dilution) for heavy crude samples.

contaminants, are all contained in a matrix of heavy oil. Unfortunately, there is no common solvent that will dissolve all the components of grease. Therefore, destructive sample preparation is required for ICP analysis. Fox published a detailed study of sample preparation methodology for the ICP analysis of petroleum grease [67]. His study concluded that closed-vessel microwave digestion using 0.1-g samples and nitric acid is the method most likely to produce solutions containing complete recovery of the elemental components. ASTM D7303, the standard test method for determination of metals in lubricating greases by ICP-AES, allows the analyst to choose between sulfated ashing and closed vessel microwave digestion [68].

ASTM D5184 is the standard for the determination of aluminum and silicon in fuel oils using ICP-AES [69]. These elements are derived from catalyst "fines" entrained in the oil during processing and can contribute to engine wear. The method is based on dry ashing the sample in a muffle furnace at 550°C and fusing the ash with a mixture of 90 % lithium tetraborate and 10 % lithium fluoride flux at 925°C. The ashing and fusion are performed in a platinum dish, and the fusion pellet containing the ash is dissolved in a mixture of dilute tartaric acid and hydrochloric acid for final analysis. The ICP-AES determinations are made with blanks and standards matched to the sample solutions with respect to content of flux and acids.

The standard test method for petroleum coke, ASTM D5600, also uses the technique of ash fusion to solubilize the residue from ashing the coke [70]. Petroleum coke is rather refractory and must be ashed at the relatively high furnace temperature of 700°C. Coke samples are ashed in platinum dishes, and the resultant ash is fused with pure lithium tetraborate at 1000°C. The cooled fusion pellet is dissolved into dilute hydrochloric acid and the ICP-AES measurements are made with matrix-matched blanks and standards as with ASTM D5184.

ICP-AES ANALYSIS OF VOLATILE NAPHTHAS AND PETROCHEMICALS

Naphthas represent the most volatile liquid petroleum fraction (C_4-C_{15} hydrocarbons, boiling point range 15° to 221°C). Trace metals in naphthas are of

critical importance in refining/chemicals production. For example, reforming catalysts are vulnerable to being poisoned by various elements in naphtha feeds. Volatile hydrocarbons are challenging materials to analyze by ICP. They overload the plasma with vapor, tending to extinguish it. At a minimum, they cause exceptionally high molecular background emission degrading sensitivity. Two basic approaches are used to accommodate volatile hydrocarbons in the common low-power ICP. The first approach is to remove the hydrocarbon matrix as much as possible while retaining the analyte elements. The second approach is to use very low sample introduction rates to minimize the influence of the volatile hydrocarbons on the ICP. The author has explored both approaches with substantial success.

Analysis of Volatile Hydrocarbons using the Ultrasonic Nebulizer

Volatile hydrocarbons may be vaporized and condensed at moderate temperatures. Therefore, one method of removal involves using flash evaporation and condensation in the desolvation section of a USN. The USN makes the direct analysis of many volatile hydrocarbons and solvents by ICP-AES practical. The USN desolvator (Fig. 2) removes the bulk of the organic vapor (approximately 90 % of C_4-C_{10} hydrocarbons). Oxygen may be added to the nebulizer gas flow to further reduce the influence of the remaining organic vapor on the spectral background. Using the USN, it is possible to introduce hydrocarbons such as toluene directly into the ICP with flow rates approximately equivalent to aqueous. The detection limits achieved are approximately equivalent to aqueous USN detection limits (3 to 10 times better than pneumatic nebulization) [17]. Thus the "ultrasonic advantage" may be extended from aqueous samples to certain organic solvents and hydrocarbons.

Analyzing highly volatile solvents or hydrocarbons requires a second stage of desolvation. A microporous membrane added to the outlet of the USN condensor has been used to further remove the residual solvent vapor and boost the overall efficiency of the desolvation to 99 % or greater. Fig. 7 shows the overall USN microporous membrane desolvator (USN-MMD) system. With an 80-cm MMD, liquids as volatile as hexanes and heptanes (b.p. 66° to 98°C) could be analyzed directly [18]. Using a 140-cm membrane (commercialized version), pentanes (b.p. 35° to 36°C) could be aspirated directly into the ICP through the USN-MMD [19]. Typical operating conditions for the 140-mm MMD are shown in Table 15. The reduction in background emission and improvement in sensitivity with the MMD is shown using the nickel line at 231.60 nm as an example (Fig. 8). A comparison of detection limits achieved for various elements in hexanes, pentanes, and water (Fig. 9) clearly demonstrates that the "ultrasonic advantage" has been extended to highly volatile hydrocarbons using the USN-MMD sample introduction system.

Virtually complete matrix removal for ICP sample introduction available with the USN-MMD makes "universal calibration" practical. Universal calibration is a single analytical calibration valid for multiple solvent systems and sample types. It is ideal for nonroutine environments where sample matrix types vary in an unpredictable manner. The requirements for universal calibration are:

- Constant volumetric sample flow (pumped)
- Negligible matrix effects due to residual solvent loading

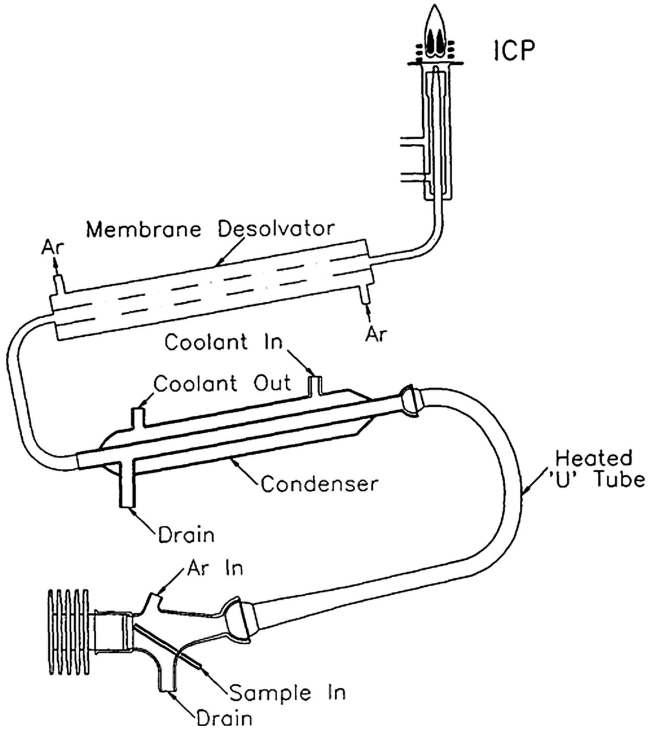

Fig. 7—Ultrasonic nebulizer (USN) with desolvation and microporous membrane.

- Nebulization efficiencies of the solvents/samples relative to the calibration standard must be known or measured.

With the USN-MMD, universal calibration should be achievable for virtually all organic liquids. There is no volatility limitation because heavier liquids may be diluted into lighter solvents. Table 16 shows an analysis of hexanes, pentanes, toluene, and gasoline spiked with 1 μg/mL of 19 elements referenced to 1 μg/mL of the elements in hexanes. The 11 % positive bias for pentanes relative to hexanes is no doubt due to a higher nebulization efficiency, which could not be measured easily. Approximately the same amount of negative bias was observed for the toluene results, and a measured nebulization efficiency for toluene of 90.6 % relative to hexanes is in good agreement with that observation. Elements using spectral lines in the UV exhibit a particular suppression, probably due to absorbance from residual aromatic structures in the tail flame of the plasma or the gas envelope surrounding it. The mean and percent RSD values in parentheses exclude these elements. Gasoline exhibits behavior similar to toluene but with a slightly lower nebulization efficiency (about 86 % relative to hexanes). Clearly, correcting for differences in nebulization efficiency using an internal standard would result in accurate analyses for most elements in these four sample matrices. Results from an analysis of gasoline spiked at 20 ng/mL (raw and corrected for nebulization efficiency) and calibrated using hexanes are shown in Table 17. Detection limits calculated from ten replicates are in the sub-nanogram per millilitre range for many elements.

TABLE 15—Typical Operating Conditions: For 140 mm MMD/USN/ICP-AES	
RF Power:	
1.5-1.6 kW Forward, <2 W Reflected, Automatic Control	
Flow Rates:	
Ar Outer	16 l/min
Ar Intermediate	1 l/min
Ar Aerosol	700 ml/min
Oxygen Outer	40–60 ml/min
MMD Sweep Ar In	1.1–1.3 l/min
MMD Ar/Solvent Out	Maximum
Sample Introduction	1.5–2.0 ml/min
Temperature Settings:	
USN Desolvator	140 degrees C
USN Chiller	−8 degrees C
Membrane Heater	160 degrees C

A significant limitation of the USN with or without the MMD is that the desolvation function efficiently removes volatile element species such as tetraethyllead (TEL) along with the organic matrix [71]. To determine TEL in gasoline, it is necessary to convert the lead to an involatile (inorganic) form for introduction into the ICP. Gasoline samples diluted in toluene may be reacted with a 1 % solution of elemental bromine in chloroform (1 mL per 80 g of sample solution). The bromine solution is added and allowed to stand 1 minute before adding 0.5 g of a commercial metal organic solution stabilizer (such as Conostan), which discharges the excess bromine. Blanks and standards are prepared in a similar manner. Results for TEL in various aviation fuels analyzed using USN ICP-AES compared well with X-ray fluorescence [17].

Analysis of Volatile Hydrocarbons using Low Flow Nebulization

Low flow rate nebulizers represent an alternative to desolvation for limiting the amount of organic material that reaches the ICP. With sample flow rates of about a few microlitres to a few tens of microlitres per minute, the plasma may be sustained even with very volatile hydrocarbons, and volatile analytes such as compounds of arsenic, selenium, silicon, and mercury may be retained. Two major types of low flow nebulizers, direct injection (DIN and direct injection high efficiency [DIHEN]) and pneumatic (PFA or microconcentric type), are in common use. The DIN is inherently delicate and technically challenging to

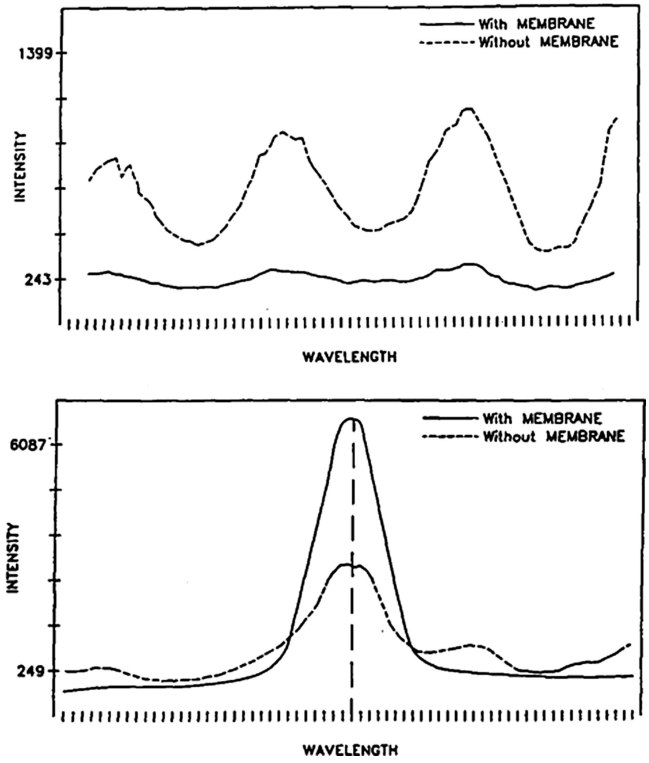

Fig. 8—Wavelength scan comparing background at nickel 231.60 nm with and without membrane (top) and the same with a 1-ppm solution of nickel in toluene (bottom).

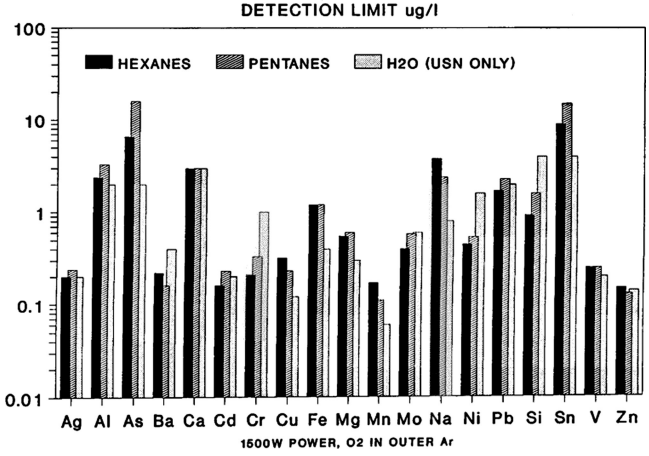

Fig. 9—Comparison of three sigma detection limits for hexanes and pentanes using the 140-mm membrane with water using the USN only.

TABLE 16—Analysis of Four Organic Liquids Containing 1 ug/ml of Various Elements—1500W Power, Calibrated Using Hexanes

Element	Hexanes	Pentanes	Toluene	Gasoline
Ag	1.00	1.01	0.93	0.84
Al	1.00	1.07	0.90	0.84
As*	1.00	1.16	0.80	0.71
Ba	1.00	1.19	0.83	0.89
Ca	1.00	1.17	0.88	0.88
Cd	1.00	0.98	0.92	0.81
Cr*	1.00	1.16	0.79	0.81
Cu	1.00	1.11	0.88	0.83
Fe	1.00	1.16	0.84	0.89
Mg	1.00	1.17	0.83	0.89
Mn	1.00	1.15	0.84	0.88
Mo*	1.00	1.17	0.79	0.79
Na	1.00	1.11	0.93	0.87
Ni	1.00	1.16	0.83	0.89
Pb	1.00	1.05	0.89	0.82
Si	1.00	1.02	0.90	0.81
Sn*	1.00	1.13	0.76	0.69
V	1.00	1.15	0.83	0.89
Zn	1.00	0.98	0.90	0.80
MEAN % RSD	1.00 –	1.11 6.3	0.86 (0.88) 6.0 (4.4)	0.83 (0.86) 7.1 (4.1)
NEB. EFF. MEASURED	1.00	–	0.906	–
MATRIX EFF.	NONE	NONE (?)	UV (<210 nm)	UV (<210 nm)
* UV LINE				

operate. Excellent results may be obtained, however, with a well-tuned DIN. The author has operated DIN systems for several years with ICP-AES and ICP-MS [24]. DIN ICP-AES suffers from high spectral background due to the organic sample load. For arsenic, selenium, and phosphorus, three critical volatile elements that the DIN is needed for, detection limits in hydrocarbons are degraded relative to aqueous detection limits [72]. The ICP-MS quadrupole instruments suffer from interferences due to matrix and argon molecular ion

TABLE 17—Analysis of Gasoline at 20 ng/ml Spike Concentration 1500W Power, Calibrated Using Hexanes

Element	20 ng/ml Spike* Raw Data	20 ng/ml Spike* Matrix Correction	Percent RSD* 20 ng/ml	DET. LIM.** ng/ml
Ag	16.9	20.1	12	3
Al	20.4	24.3	4.9	2
As	11.6	16.3	60	20
Ba	22.6	25.3	1.9	0.40
Ca	23.8	27.0	–	1
Cd	17.0	21.0	1.7	0.3
Cr	18.5	22.8	4.7	0.4
Cu	21.5	25.9	5.7	0.8
Fe	21.9	24.6	2.1	0.2
Mg	21.6	24.2	2.1	0.3
Mn	20.2	22.9	1.8	0.05
Mo	17.7	22.4	6.2	1
Na	20.6	23.6	3.0	0.5
Ni	21.1	24.8	2.3	0.2
Pb	16.7	20.3	3.6	0.8
Si	18.8	23.2	2.1	0.6
Sn	17.4	25.2	97	25
V	20.8	23.4	1.8	0.06
Zn	14.2	17.8	2.8	0.2
MEAN	19.2	22.9		

*From 10 Exposures of 10 s Duration
**From 10 Analyses of Unspiked Gasoline: 3 $\sigma/\sqrt{10}$

species, but the new collision cell technology for removing these interferences has the potential of making DIN/DIHEN ICP-MS for hydrocarbons a much more promising technique.

A new generation of low-flow nebulizers having a rugged PFA polymer construction is now available. They were developed primarily for aqueous ICP-MS but are finding application in organic ICP-AES and ICP-MS [73]. Flow rates available range from 20 to 500 μL/min and they are typically used with a

TABLE 18—ICP-AES Three Sigma Detection Limits (ng/ml)

Three solvents compared					
		Aqueous	Tetralin	Toluene	Conditions
Element	Wavelength nm	Bergener Trace nebulizer		PFA20/ PC-3	R = Radial, A = Axial
Al	396.1	39	57	53	R, O_2
Cd	214.4	0.8	0.9	1.2	A, No O_2
Fe	259.9	0.9	2.4	3.3	A, O_2
Mn	257.6	0.2	0.2	0.3	A, O_2
Mo	204.5	1.9	4.8	7.2	A, No O_2
Na	589.5	42	49	56	R, O_2
Ni	231.6	1.6	13	6.6	A, O_2
P	178.2	13	37	29	A, No O_2
Pb	220.3	10	32	20	A, No O_2
Sn	189.9	7.5	16	22	A, No O_2
Ti	323.4	5.6	5.4	48	R, No O_2
V	311.0	13	11	26	R, No O_2
Zn	206.2	0.8	1.5	1.2	A, No O_2

cyclonic spray chamber. A commercially available Peltier cooled spray chamber conditioning interface (PC-3) enables the aerosol temperature to be lowered to −15°C. Naphthas containing hydrocarbons as volatile as pentanes can be diluted in toluene and introduced directly into the ICP using the PFA 20 μL/min model (PFA20) with low-temperature aerosol conditioning. Table 18 shows limits of detection for ICP-AES obtained using the PFA20 compared with aqueous and tetralin detection limits using a parallel path nebulizer. Radial or axial ICP observations with or without added oxygen in the nebulizer gas flow are specified in the right column. Despite the tiny 20 μL/min sample flow, the detection limits for many elements are comparable across the board because of the very high nebulization efficiency of the PFA20.

Silicon in Naphtha

Silicon compounds (silicones) have been a worrisome fuel contaminant in recent years. The author recalls being given in 1996 a spark plug fouled with what looked like white sand taken from a commercial automobile fleet engine. Our analysis revealed pure silicon dioxide and the "silicon crisis" of 1996 was under way. Gasoline contaminated by silicon had been distributed widely over the Houston area as a result of a bulk lot of fuel-grade naphtha contaminated

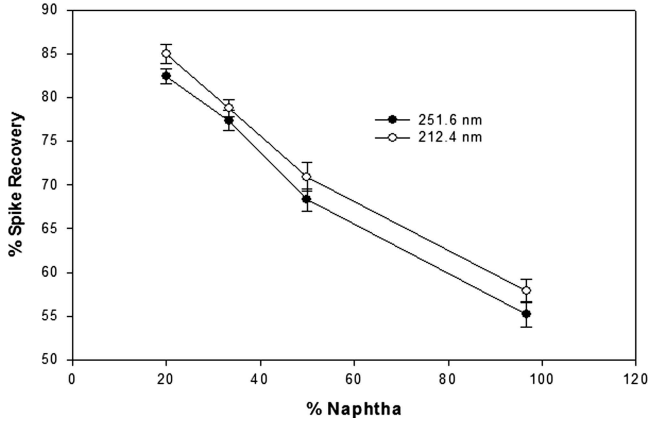

Fig. 10—Matrix effect of varying amounts of naphtha in toluene on results of silicon analysis by ICP-AES.

with silicones sold to a distributor (not ExxonMobil). In response to this crisis, methods for determination of silicon in naphtha were investigated, and at the time our laboratory used the USN ICP-AES as the best available technique. The method was not quantitative, however, and was useful only as a survey technique because of the volatility of the silicones and their tendency to be rejected by the USN desolvation system.

Using normal sample uptake rates of 0.1 to 2 mL/min, naphthas extinguish the ICP even when diluted five to ten times in tetralin or xylenes. Using the PFA20, some success was achieved by diluting naphthas in xylenes. Adding the PC-3, and chilling the aerosol to −15°C, permitted operationally stable ICP analysis of naphthas diluted in toluene [73]. The amount of naphtha in the toluene solutions was found to strongly affect the silicon measurements, however. Fig. 10 shows signal suppression of two silicon lines as a function of naphtha content in toluene solutions relative to silicon in toluene standards. The magnitude of this matrix effect is large enough to introduce significant error with minor variations in dilution factor. Differences in the relative volatility of the naphtha samples also affected the silicon recoveries since the term "naphtha" describes a wide boiling point range of hydrocarbons. A study was made to find an internal standard element and spectral line that behaved similarly to silicon, and molybdenum (204.5 nm) was found to compensate adequately at a spike level of 3.0 μg/ml. Fig. 11 shows the analysis in Fig. 10 replotted with the molybdenum reference. A further improvement in precision was obtained using oxygen admixed with the arsenic coolant flow (Table 19).

Silicon in naphtha analyses have been performed in our laboratory for several years using the molybdenum internal standard technique, and accuracy has been verified using standard spikes. Spike recoveries from 55 naphtha samples are summarized in Table 20. A detection limit of 0.006 μg/mL (without dilution factor) silicon in toluene was measured using 251.6 nm.

Organo-silicon compounds differ widely in volatility from tetramethylsilane (TMS) with a boiling point of 26.5°C to nonvolatile silicones with molecular

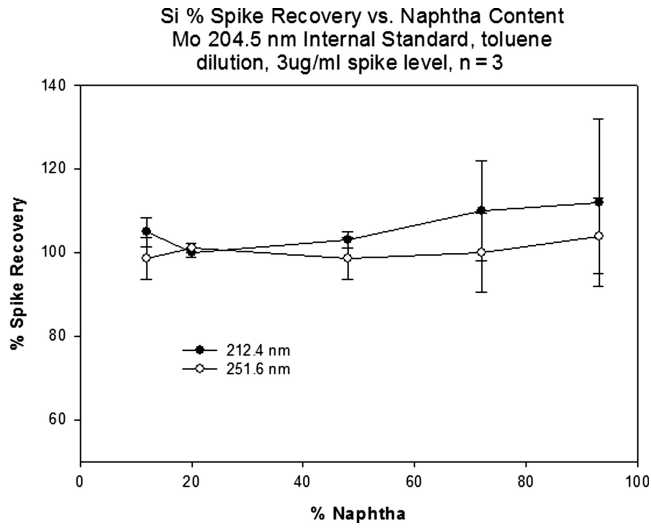

Fig. 11—Naphtha matrix effect compensated by use of molybdenum 204.5-nm internal standard.

weights in the thousands. Two compounds were selected to investigate the effect of Si compound volatility on method accuracy: TMS and hexamethyldisiloxane (HMS) with a boiling point of 101°C. Table 21 shows the spike recoveries of the two compounds relative to a nonvolatile Si standard in toluene (and 20 % naphtha in toluene) obtained using the molybdenum internal standard. There is clearly an enhancement for both compounds because of volatility with similar values obtained for the two silicon lines. TMS shows the greater

TABLE 19—Si % Spike Recovery vs. Naphtha Content

With and without oxygen addition

Mo 204.5 nm internal standard, toluene dilution, 3 ug/ml spike level, n = 6

	With 35 ml/min O_2		Without O_2	
% Naphtha	Mean	Sigma	Mean	Sigma
12.0	102	5.3	115	4.2
20.0	100	1.1	94	2.1
48.0	101	4.2	96	17
72.0	105	11	103	22
93.0	111	14	98	7.0
Overall (30)	103.8	9.1	101.2	14

TABLE 20—Si in Naphtha by ICP-AES Spike Recoveries		
1.00 ug/g spike level		
	Si 212.4 nm	**Si 251.6 nm**
N	55 (5 rejected)	55 (5 rejected)
Mean % Recovery	101.6	101.2
% RSD	9.6	10.9
Three sigma detection limit (ug/g)	0.02	0.006

enhancement as expected, but even in this extreme case the total effect is less than a factor of three.

Silicon determinations in naphtha have been performed recently using ICP-MS with a collision gas interface (hydrogen) and an ICP operated at "cool plasma" conditions (750 W versus 1200 to 1600 W normal ICP power level) using the PFA20 nebulizer and chilled spray chamber [26]. A detection limit of 0.6 ng/mL was achieved with this system. The volatility enhancement effect with TMS was observed with the ICP-MS as expected.

CONCLUSIONS

ICP-AES is well established in analytical laboratories throughout the petroleum/petrochemicals industry, and ASTM has contributed much to the success of the technique by providing key standard methods for routine analysis of a wide

TABLE 21—Effect of Volatile Si Compounds			
Samples spiked with tetramethylsilane (TMS), b.p. 26.5 degrees C or hexamethyldisiloxane (HMS), b.p. 101 degrees C - Mo internal standard			
	% Spike Recovery		
Toluene (neat)	**Si 212.4 nm**	**Si 251.6 nm**	**Sigma (n)**
TMS	175	174	4.8 (6)
HMS	146	139	6.9 (6)
20% Naphtha in Toluene			
TMS	214	214	26 (8)
HMS	176	177	6.6 (8)

variety of oils and products. The early days of ICP-AES were filled with challenges and frustration, particularly when analyzing oils and volatile hydrocarbons directly. In recent years, innovative low-flow nebulizers and other sample introduction equipment combined with advances in plasma generators and spectrometer design and the use of oxygen admixed with the Ar gas streams have brought even these difficult analyses into the realm of the easy and routine. ICP-AES is now supplemented by ICP-MS in many petroleum laboratories, but the utility, ease, and speed of ICP-AES is likely to ensure that it remains the cornerstone of the trace metals analysis laboratory for many years to come.

ACKNOWLEDGMENT

The author is grateful to his wife Kathy for providing a technical review and editing of the manuscript.

References

[1] Botto, R. I., "Updating a Vintage ICP Atomic-Emission Spectrometer," *Talanta*, Vol. 37, 1990, pp. 157–166.

[2] Pforr, G. and Aribot, O., *Z., Chem*., Vol. 10, 1970, p. 78.

[3] Fassel, V. A., Peterson, C. A., Abercrombie, F. N. and Kniseley, R. N., *Anal. Chem*., Vol. 48, 1976, p. 516.

[4] Ward, A. F. and Marciello, L., *Jarrell-Ash Plasma Newsletter*, Vol. 1, No. 4, 1978, p. 10.

[5] Merryfield, R. N. and Loyd, R. C., *Anal. Chem*., Vol. 51, 1979, p. 1965.

[6] Brown, R. J., *Spectrochim. Acta*, Vol. 38B, 1983, p. 283.

[7] Hausler, D. W. and Taylor, L. T., *Anal. Chem*., Vol. 53, 1981, p. 1223.

[8] Boorn, A. W., Cresser, M. S. and Browner, R. F., *Spectrochim. Acta*, Vol. 35B, 1980, p. 823.

[9] Boorn, A. W. and Browner, R. F., *Anal. Chem*., Vol. 54, 1982, p. 1402.

[10] Maessen, F. J. M. J., Seeverens, P. J. H. and Kreuning, G., *Spectrochim. Acta*, Vol. 39B, 1984, p. 1171.

[11] Blades, M. W. and Caughlin, B. L., *Spectrochim. Acta*, Vol. 40B, 1985, p. 579.

[12] Botto, R. I., "Matrix Interferences in the Analysis of Organic Solutions by Inductively Coupled Plasma–Atomic Emission Spectrometry," *Spectrochim. Acta*, Vol. 42B, 1987, pp. 181–199.

[13] Kreuning, G. and Maessen, F. J. M. J., *Spectrochim. Acta*, Vol. 42B, 1987, p. 677.

[14] Hausler, D., *Spectrochim. Acta*, Vol. 42B, 1987, p. 63.

[15] Meyer, G. A., *Spectrochim. Acta*, Vol. 42B, 1987, p. 201.

[16] Botto, R. I., "Applications of Ultrasonic Nebulization in the Analysis of Petroleum and Petrochemicals by ICP-AES," 1992 Winter Conference on Plasma Spectrochemistry, San Diego CA, January 1992.

[17] Botto, R. I., "Applications of Ultrasonic Nebulization in the Analysis of Petroleum and Petrochemicals by Inductively Coupled Plasma Atomic Emission Spectrometry," *J. Anal. At. Spectrom*., Vol. 8, 1993, pp. 51–57.

[18] Botto, R. I. and Zhu, J. J., "Use of an Ultrasonic Nebulizer with Membrane Desolvation for Analysis of Volatile Solvents by Inductively Coupled Plasma Atomic Emission Spectrometry," *J. Anal. At. Spectrom*., Vol. 9, 1994, pp. 905–912.

[19] Botto, R. I. and Zhu, J. J., "Universal Calibration for Analysis of Organic Solutions by Inductively Coupled Plasma Atomic Emission Spectrometry," *J. Anal. At. Spectrom*., Vol. 11, 1996, pp. 675–681.

[20] Botto, R. I., "Volatile Species in Volatile Organic Matrix: Direct Determination by ICP-AES and ICP-MS," 1996 Winter Conference on Plasma Spectrochemistry, Ft. Lauderdale, FL, January 1996.
[21] Botto, R. I., "Analysis of Volatile Petrochemicals using ICP-AES and ICP-MS," 1998 Winter Conference on Plasma Spectrochemistry, Scottsdale, AZ, January 1998.
[22] McElroy, F. C., Mennito, A., Debrah, E. and Thomas, R., "Uses and Applications of ICP-MS in the Petroleum Industry," *Spectroscopy*, Vol. 13, 1998, p. 43.
[23] Botto, R. I., "Analysis of Trace Elements in a Variety of Petrochemical Products using Direct Injection ICP-MS," 2000 Winter Conference on Plasma Spectrochemistry, Ft. Lauderdale, FL, January 2000.
[24] Botto, R. I., "Trace Element Analysis of Petroleum Naphthas and Tars using Direct Injection ICP-MS," *Can. J. Anal. Sci. Spectrosc*., Vol. 47, 2002, pp. 1–13.
[25] Botto, R. I., "Plasma Spectrochemical Analysis of Petroleum Naphthas Using Low Flow Sample Introduction Equipment," 2004 Winter Conference on Plasma Spectrochemistry, Ft. Lauderdale, FL, January 2004.
[26] Talbot, J. and Botto, R., "Silicon in Naphthas: a Near Cold Plasma Approach for Sub-PPB Detection Limits on an ICP-MS," FACCS, Reno, NV, 2008.
[27] Gaines, P., *Spectroscopy*, Vol. 20, No. 1, 2005.
[28] Botto, R. I., "Analysis of Organic Solutions using the Argon/Oxygen ICP," 2002 Winter Conference on Plasma Spectrochemistry, Scottsdale, AZ, January 2002.
[29] Romero, X., Poussel, E. and Mermet, J. M., *Spectrochim. Acta*, Vol. 52B, 1997, p. 495.
[30] Botto, R. I., "Interference Correction for Simultaneous Multielement Determinations by Inductively Coupled Plasma," in *Developments in Atomic Plasma Spectrochemical Analysis*, R. M. Barnes, Ed., 1981, pp. 141–166.
[31] Botto, R. I., "Quality Assurance in Operating a Multielement ICP Emission Spectrometer," *Spectrochim. Acta*, Vol. 39B, 1984, pp. 95–113.
[32] Botto, R. I., "Long Term Stability of Spectral Interference Calibrations for Inductively Coupled Plasma Atomic Emission Spectrometry," *Anal. Chem*., Vol. 54, 1982, pp. 1654–1659.
[33] Hauser, P. C. and Blades, M. W., *Appl. Spectrosc*., Vol. 42, 1988, p. 595.
[34] Botto, R. I., "Multielement Analysis of Fossil Fuels and Related Materials by ICP-AES," *Spectrochim. Acta Rev*., Vol. 14, 1991, pp. 141–159.
[35] Brenner, I. B. and Dorfman, E., *Microchemical Journal*, Vol. 52, 1995, p. 81.
[36] Lopez-Molinero, A., Caballero, A. V. and Castillo, J. R., *Spectrochim. Acta*, Vol. 49B, 1994, p. 677.
[37] Al-Ammar, A. A., Gupta, R. K. and Barnes, R. M., *J. Anal. At. Spectrom*., Vol. 14, 1999, p. 801.
[38] Nadkarni, R. A., "Elemental Analysis," in *Fuels and Lubricants Handbook: Technology, Properties, Performance, and Testing*, G. E. Totten, S. R. Westbrook, and R. J. Shah, Eds., ASTM International, West Conshohocken, PA, 2007, pp. 207–216.
[39] ASTM D7260-06, ASTM International, West Conshohocken, PA, 2006.
[40] Nadkarni, R. A., *ICP Information Newsletter*, Vol. 30, 2005, p. 1059.
[41] Fassel, V. A., Peterson, C. A., Abercrombie, F. N. and Kniseley, R. N., *Anal. Chem*., Vol. 48, 1976, p. 516.
[42] ASTM D4951-06, ASTM International, West Conshohocken, PA, 2006.
[43] Bansal, J. G. and McElroy, F. C., SAE Paper 932694, Fuels and Lubricants Meeting, Philadelphia, PA, October 18-21, 1993.
[44] ASTM D7040-04, ASTM International, West Conshohocken, PA, 2004.
[45] Browner, R. F., Boorn, A. W. and Smith, D. D., *Anal. Chem*., Vol. 54, 1982, p. 1411.
[46] Saba, C. S. and Rhine, W. E., *Anal. Chem.,* Vol. 53, 1981, p. 1099.

[47] Eisentraut, K. J., Neuman, R. W., Saba, C. S., Kauffman, R. E., and Rhine, W. E., *Anal. Chem*., Vol. 56, 1984, p. 1086 A.
[48] ASTMD 5185-05, ASTM International, West Conshohocken, PA, 2005.
[49] Granchi, M. P., Biggerstaff, J. A., Hilliard, L. J. and Grey, P., *Spectrochim. Acta,* Vol. 42B, 1987, p. 169.
[50] Kauffman, R. E., Saba, C. S., Rhine, W. E. and Eisentraut, K. J., *Anal. Chem*., Vol. 54, 1982, p. 975.
[51] Hancock, D. O. and Synovec, R. E., *Appl. Spectrosc*., Vol. 43, 1989, p. 202.
[52] Algeo, J. D., Heine, D. R., Phillips, H. A., Hoek, F. B. G., Schneider, M. R., Freelin, J. M. and Denton, M. B., *Spectrochim. Acta*, Vol. 40B, 1985, p. 1447.
[53] ASTM D7111-05, ASTM International, West Conshohocken, PA, 2005.
[54] ASTM D7151-05, ASTM International, West Conshohocken, PA, 2005.
[55] Brenner, I. B., Zander, A. T. and Shkolnik, J., *ICP Information Newsletter*, Vol. 20, 1995, pp. 738.
[56] ASTM D5708-05, ASTM International, West Conshohocken, PA, 2005.
[57] Botto, R. I. "Sample Preparation for Crude Oil, Petroleum Products and Polymers," Chapter 23 in *Comprehensive Analytical Chemistry*, D. Barcelo, Ed., Volume XLI, *Sample Preparation for Trace Element Analysis*, Z. Mester and R. Sturgeon, Eds., Elsevier, Amsterdam, 2003.
[58] Botto, R. I., "Coal Ash Element Analysis by ICPES Using an Automatic Fusion Device," in *Developments in Atomic Plasma Spectrochemical Analysis*, R. M. Barnes, Ed., 1981, pp. 506–522.
[59] Botto, R. I. "Method for Correcting for Acid and Salt Matrix Interferences in ICP-AES," *Spectrochim. Acta*, Vol. 40B, 1985, pp. 397–412.
[60] Botto, R. I., "Analysis of Heavy Oils for Trace Metals Using Plasma Spectrochemistry," ICP Winter Conference on Plasma Spectrochemistry, Temecula, CA, January 2008.
[61] ASTM D893-05a, ASTM International, West Conshohocken, PA, 2005.
[62] ASTM D4072-98 (Reapproved 2008), ASTM International, West Conshohocken, PA, 2008.
[63] Lord, C. J., *Anal. Chem*., Vol. 63, 1991, pp. 1594.
[64] Dreyfus, S., Pecheyran, C., Magnier, C., Prinzhofer, A., Lienemann, C. P. and Donard, O. F. X., "Direct Trace and Ultra-Trace Metals Determination in Crude Oil and Fractions by ICP-MS," in *Elemental Analysis of Fuels and Lubricants: Recent Advances and Future Prospects ASTM STP 1468*, R. A. Nadkarni, Ed., ASTM International, West Conshohocken, PA, 2005, pp. 51–58.
[65] Lienemann, C. P., Dreyfus, S., Pecheyran, C. and Donard, O. F. X., *Oil & Gas Science and Technology – Rev. IFP*, Vol. 62, 2007, pp. 69.
[66] Nadkarni, R. A., "Multielement Analysis of Lubricating Greases with ICP-AES," *J. ASTM Intl*., Vol. 6, No. 8, ASTM International, West Conshohocken, PA, 2009, Paper ID JAI102241.
[67] Fox, B. S., *J. ASTM Intl*., Vol. 2, ASTM International, West Conshohocken, PA, 2002, Paper ID JAI12966.
[68] ASTM D7303-06, ASTM International, West Conshohocken, PA, 2006.
[69] ASTM D5184-01 (Reapproved 2006), ASTM International, West Conshohocken, PA, 2006.
[70] ASTM D5600-04, ASTM International, West Conshohocken, PA, 2004.
[71] Olsen, S. D., Westerlund, S. and Visser, R. G., *Analyst*, Vol. 122, 1997, pp. 1229.
[72] Avery, T. W., Chakrabarty, C. and Thompson, J. J., *Appl. Spectrosc*., Vol. 44, 1990, pp. 1690.
[73] Botto, R. I., "Determination of Elemental Bad Actors (As, Hg and Si) in Petrochemical Samples Using ICP-AES and ICP-MS," 2006 Winter Conference on Plasma Spectrochemistry, Tucson, AZ, January 2006.

9

Applications of ICP-MS in the Petroleum Industry

J. David Hwang[1]

INTRODUCTION

One of the key responsibilities of modern analytical scientists is "solving problems," or "troubleshooting." As a matter of fact, this is one of the most attractive reasons for entering the field of analytical chemistry. "Problems" can arise in research, development, production, technical services, regulatory requirements (such as the [ASTM International], American Society for Testing and Materials U.S. Environmental Protection Agency [EPA], or U.S. Food and Drug Administration [FDA]), litigation, and many other areas [1]. The role of the analytical chemist in industry, quality assurance, methods and technical development, troubleshooting (also called "firefighting"), research or science resource, and miscellaneous analytical roles are described in an extremely interesting report entitled "Analytical Chemistry in Industry" [2]. Many problems in the petroleum industry, such as corrosion, incompatible formulation, failure of an engine, contamination of feedstock, or catalyst poisons, in general, can be traced back to some physical or chemically related problem of the system. As Botto stated in his 2006 Winter Conference on Plasma Spectrochemistry Symposium report [3]: "In the application of plasma spectrochemistry to 'real world' materials and problems, almost nothing can top the petroleum and petrochemical industry for its ability to generate tough analytical challenges on a daily basis. ICP spectrochemists working in the industry 'get down and get dirty' with some of the nastiest and most complex sample matrices on Earth." Hence, a symposium has been dedicated to petroleum materials and petroleum applications in the Winter Conference on Plasma Spectrochemistry since 2006.

The key to successful solutions for most problems is working closely with the appropriate engineers or scientists. Engineers and other application-oriented personnel are often the first to encounter defects, failures, or other problems. When this occurs, consultation with project-related personnel is an essential first step in the problem-solving or troubleshooting process. By virtue of his or her knowledge of analytical techniques, the analytical chemist (or scientist) should be able to define the problem, identify possible causes, and determine what type of information is needed. The analytical techniques that appear most applicable to the problem should also be determined. The experimental design and sampling plan are made. Measurements are taken and data are generated, processed, and interpreted. Last but not the least, the analytical chemist meets with the project-related engineer or other personnel to discuss data and solve the problem [4]. In all cases, the essence of the analytical process of problem solving and the analytical approach are shown in Tables 1 and 2 [5].

[1] *Chevron Energy Technology Company, Richmond, California*

With the large number of analytical techniques available, it is often difficult to identify the best method or methods for a given problem. The goal of this review is to introduce one of the most powerful and popular elemental analysis techniques, namely inductively coupled plasma–mass spectrometry (ICP-MS), and its applications in the petroleum industry. Alternative techniques such as atomic absorption spectrometer (AAS) and inductively coupled plasma–atomic emission spectroscopy (ICP-AES) just don't have the sensitivity for most elements or high-throughput capability of ICP-MS. Applications of ICP-MS to petroleum and related samples are discussed, and this review will by no means provide an all-inclusive bibliography. It is not my purpose to discuss the theory, principles and mechanisms, and instrumentation pertaining to all cases, because these topics have been adequately described elsewhere. Table 3 lists books that contain significant information or at least one chapter on ICP-MS. For discussion of these new analytical techniques or recent advances of existing analytical techniques, the reader should refer to both fundamental (published once every 2 years in even years) and application (published once every 2 years in odd years) reviews as well as the A-pages portion in every issue of the *Analytical Chemistry Journal* (published by the American Chemical Society). The fundamental review on ICP-MS since 2002 provides a comprehensive review on ICP-MS [6–9]. Several fundamental reviews on atomic spectroscopy [10–13] and atomic mass spectrometry [14–16] included significant developments in instrumentation, methodology, and applications of ICP-MS. Reviews of ICP-MS are routinely included in reviews in inorganic mass spectrometry [17–18], and more extensive reviews [18–22] dealing with ICP-MS have been published. The *Journal of Analytical Atomic Spectrometry* (JAAS), published by the Royal Society of Chemistry, which was founded in 1986, contains a very useful pragmatic section entitled Atomic Spectrometry Update (ASU). Typical ASUs include reports or reviews on Instrumentation, Atomization and Excitation; Environmental Analysis; Atomic Emission Spectrometry; Atomic Mass Spectrometry and X-ray Fluorescence (XRF) Spectrometry; Industrial Analysis: Metals; Chemicals, and Advanced Materials; and Clinical and Biological Materials, Foods, and Beverages. JAAS has become a major journal in the atomic spectrometry field and a good reference for many applications. The *ICP Information Newsletter*, of course, continues to provide important information on current trends in ICP atomic spectrometry, as well as abstracts of atomic spectrometry papers presented at major national and international meetings. This newsletter is edited by Professor Ramon M. Barnes, who retired from University of Massachusetts. Additionally, books in the series *Chemical Analysis: A Series of Monographs on Analytical Chemistry and Its Applications*, which are edited by Professor J. D. Winefordner, who retired from University of Florida (published by Wiley), are also a valuable resource for the introduction of new analytical techniques and applications. An ASTM symposium, Elemental Analysis of Fuels and Lubricants: Recent Advances and Future Prospects, held in Tampa, Florida, on December 6–8, 2004, contained several ICP-MS presentations. The symposium was sponsored by ASTM Committee D02 on Petroleum Products and Lubricants. A book, STP 1468, with some of the symposium papers, was published in 2006 by ASTM [23]. Many conferences are being held throughout the year, but only one remains that focuses on ICP-MS: the Winter

TABLE 1—The Analytical Process of Problem Solving

1. Definition of the problem
2. Selection of method(s)
3. Experimental design and sampling (random, unbiased, and representative)
4. Elimination of interference(s)
5. Performance of the experiment and/or measurement
6. Data processing and interpretation
7. Solution to the problem

Conference on Plasma Spectrochemistry. It's held in the United States and Asia on even years and Europe in odd years. A short course entitled "Analysis of petrochemical products and industrial materials by plasma spectrochemistry" is an excellent course for any scientists who are new or want to learn more about organics ICP and ICP-MS.

As regulatory requirements become more stringent and the necessity to determine many elements at low concentration levels (particularly at lower parts-per-billion [ppb] or parts-per-trillion [ppt] levels) has increased, the ICP-MS has successfully evolved as a powerful analytical tool for ultratrace elemental analyses. For the scientist and laboratory personnel who would like to get more information with the same or a smaller amount of a sample in either the same period of time or less, ICP-MS has become one of the most important analytical techniques for elemental determinations. The number of ICP-MS systems installed and used worldwide reached 5,000 (by 2004) since the first ICP-MS system was introduced in 1983 [24]. This is not surprising, given the ever-increasing needs for trace and ultratrace analysis of environmental and high-tech materials.

The growth in the number of ICP-related publications increased from fewer than 100 in 1980 to more than 3,000 in 1990. Some 2,000 papers containing "ICP-MS" were published from October 2005 to October 2007 according to SciFinder® Scholar 2007. Judged on the basis of the number of commercial instruments sold, their growth in usage and publications, and their acceptance by the scientific community, the ICP-MS undoubtedly has had the greatest impact to date as an analytical tool for elemental determination. Fassel [25] had clearly stated the need for an ideal method for elemental analysis. It is very close to what ICP-MS can do. Numerous other factors such as physical testing versus chemical analysis, surface analysis versus bulk analysis, nondestructive versus destructive, total element versus speciation, and invasive versus noninvasive should also be considered in determining the analytical technique to be used for your applications or for solving problems [1,26,27].

HISTORICAL DEVELOPMENT OF ICP-MS

The historical development of the use of ICP discharge in atomic optical spectroscopy was described by Hwang's review article entitled "Application of ICP-AES to Analysis of Solutions" in 1995 [28]. Another important elemental analysis technique using ICP discharge, namely mass spectrometry, was developed in the 1980s. Conventional inorganic mass spectrometry is an established method for elemental analysis [29]. Basic characteristics are the direct analysis of solids using RF spark, dc arc, laser, and so forth as an ion source; the high detection power and selectivity; the multielement capability and wide element coverage;

TABLE 2—The Analytical Approach

1. Defining the problem at hand.
2. Ensuring that the samples available are representative of the problem.
3. Interacting with the client to obtain his or her knowledge of the problem and to understand the requirements to be met by the solution in terms of needed accuracy and timing.
4. Developing an analytical plan involving the sequence and number of methods and instrumental studies to be undertaken.
5. Completing the work using the highest level of expertise and remembering the chemical theories relating to the work.
6. Communicating answers, newer data, including the precision and reliability of all numbers, and specifying any cautions or constraints on the best use of the answer.
7. Interpreting the information and results in a clear, consistent, meaningful report that can be used to help solve the problem.

and the capability to obtain isotope abundance information. Solutions cannot, however, be directly analyzed. Gray [30] was the first to show the feasibility using a dc capillary arc source and a quadrupole mass filter to develop a plasma source MS. The challenge to interface an atmospheric pressure plasma into a high-vacuum MS is much tougher than developing a gas chromatograph/mass spectrometer (GC-MS) and similar to (if not tougher than) developing a liquid chromatograph/mass spectrometer (LC-MS). This was finally accomplished by the use of a differentially pumping vacuum system containing electrostatic ion lens to extract a small fraction of the plasma gas through a pinhole sampling orifice. The first explorations of an ICP discharge as ion source were described by Gray and coworkers [31,32] and Houk and coworkers [33,34]. The pioneering work on ICP-MS was conducted primarily in three research laboratories: the Ames Laboratory at Iowa State University [33–35]; the laboratories in Sciex, in Canada [36]; and the University of Surrey, the British Geological Survey and VG Instruments [31–32, 37–39].

Since the first ICP-MS paper was published in 1980 [35], it is incredible to conceive that the first commercial ICP-MS was introduced just 3 years later at the 1983 Pittsburgh Conference, and that the first benchtop ICP-MS was introduced only 11 years after that. ICP-MS has rapidly expanded worldwide to become the method of choice for fast, ultratrace level elemental analysis. The rapid development of ICP-MS is the result of at least six unique capabilities for element analysis.

1. The detection limit of ICP-MS for direct analysis of solution samples is in the range of 1 to 100 pg/mL for most elements. These detection limits are 100 to 1,000 times superior to those that can be routinely achieved by either ICP-AES or ICP-AFS.
2. ICP-AES can detect only about 80 of the elements on the periodic table. ICP-MS, however, can detect almost all elements across the periodic table using atomic mass rather than optical wavelengths.
3. Mass spectra of the elements are very simple and unique. Spectral interferences are much less severe in ICP-MS than in ICP-AES. Also, because mass spectral peak widths are instrumentally limited, many mass spectral interferences can be eliminated if high-resolution, double-sector instruments are used.

TABLE 3—Books Related to ICP-MS

Title	Authors/Editors	Publisher	Year
Inductively Coupled Plasma Emission Spectroscopy Part I	Boumans, P. W. J. M.	Wiley	1987
Inorganic Mass Spectrometry	Adams, F., Gijbels, R., and Van Grieken, R.	Wiley-Interscience	1988
Applications of Inductively Coupled Plasma Mass Spectrometry	Date, A. R., and Gray, A. L.	Blackie, Glasgow	1989
Applications of Plasma Source Mass Spectrometry	Holland, G., and Eaton, A. N.	Royal Society of Chemistry	1991
Inductively Coupled Plasmas in Analytical Atomic Spectrometry, 2nd ed.	Montaser, A., and Golightly, D. W.	VCH	1992
Inductively Coupled and Microwave Induced Plasma Sources for Mass Spectrometry	Micromeritics, E. H., Giglio, J. J., Castillano, T. M., and Caruso, J. A.	Royal Society of Chemistry	1995
Atomic Spectroscopy, 2nd ed.	Robinson, J. W.	Marcel Dekker	1996
Inductively Coupled Plasma Mass Spectrometry	Montaser, A.	Wiley-VCH	1998
Flow Analysis with Atomic Spectrometry Detectors: Analytical Spectroscopy Library, Vol. 9	Sanz-Medel, A., Ed.	Elsevier	1999
ICP Spectrometry and Its Applications	Hill, S. J., Ed.	Sheffield Academic Press	1999
Plasma Source Mass Spectrometry: New Developments and Applications (Proceedings of the Durham Conference)	Holland, G., and Tanner, S. D., Eds.	Royal Society of Chemistry	1999
Elemental Speciation, New Approaches for Trace Element Analysis; Vol. 33 of Wilson & Wilson's Comprehensive Analytical Chemistry	Caruso, J. A., Sutton, K. L., and Ackley, K. L., Eds.	Elsevier	2000
Direct Sample Introduction Techniques for Inductively Coupled Plasma Mass Spectrometry; Vol. 34 of Wilson & Wilson's Comprehensive Analytical Chemistry	Beauchemin, D., Gregoire, D. C., Gunther, D., Karanassios, V., Mermet, J.-M., and Wood, T. J.	Elsevier	2000
Inorganic Mass Spectrometry: Fundamentals and Applications	Barshick, C. M., Duckworth, D. C., and Smith, D. H., Eds.	Marcel Dekker	2000

TABLE 3—Books Related to ICP-MS (Continued)

Title	Authors/Editors	Publisher	Year
Inductively Coupled Plasma-Mass Spectrometry: Practices and Techniques	Taylor, H. E.	Academic Press	2001
Applications of Inorganic Mass Spectrometry; Wiley-Interscience Series on Mass Spectrometry	De Laeter, J. R.	Wiley	2001
Plasma Source Mass Spectrometry: The New Millennium (Proceedings of the Durham Conference)	Holland, G., and Tanner, S. D., Eds.	Royal Society of Chemistry	2001
Elemental Speciation, New Approaches for Trace Element Analysis; Vol. XXXIII of Wilson & Wilson's Comprehensive Analytical Chemistry	Caruso, J. A., Sutton, K. L., and Ackley, K. L., Eds.	Elsevier	2000
Direct Sample Introduction Techniques for Inductively Coupled Plasma Mass Spectrometry; Vol. XXXIV of Wilson & Wilson's Comprehensive Analytical Chemistry	Beauchemin, D., Gregoire, D. C., Gunther, D. V., Karanassios, V., Mermet, J. M., and Wood, T. J.	Elsevier	2000
Analytical Methods for Environmental Monitoring	Taylor, F., Cartwright, M., and Ahmad, R.	Prentice Hall	2000
Applications of Inorganic Mass Spectrometry; Wiley-Interscience Series on Mass Spectrometry	de Laeter, J. R.	Wiley-Interscience	2001
Analytical Atomic Spectrometry with Flames and Plasmas	Broekaert, J. A. C.	Wiley-VCH	2001
Laser Ablation-ICP MS in the Earth Sciences	Silvester, P., Ed.	Mineralogical Association of Canada	2001
Inductively Coupled Plasma-Mass Spectrometry: Practices and Techniques	Taylor, H. E.	Academic Press	2001
Plasma Source Mass Spectrometry - The New Millennium (Proceedings of the Durham Conference)	Holland, G., and Tanner, S. D., Eds.	Royal Society of Chemistry	2001
Hyphenated Techniques in Speciation Analysis	Szpunar, J., and Lobinski, R., Eds.	Royal Society of Chemistry	2004
Methods for Environmental Trace Analysis	Dean, J. R.	Wiley	2003

(*Continued*)

TABLE 3—Books Related to ICP-MS (Continued)

Title	Authors/Editors	Publisher	Year
Acceleration and Automation of Solid Sample Treatment; Techniques and Instrumentation in Analytical Chemistry 24	Luque, M. D., DeCastro, J. L., and Luque, G.	Elsevier	2002
Handbook of Elemental Speciation: Techniques and Methodology	Cornelis, R., Caruso, J., Crews, H., and Heumann, K., Eds	Wiley	2003
Sample Preparation for Trace Element Analysis; Comprehensive Analytical Chemistry Series XLI	Mester, Z., and Sturgeon, R., Eds.	Elsevier	2003
Atomic Spectroscopy in Elemental Analysis; Analytical Chemistry Series	Cullen, M., Ed.	Blackwell Publishing	2004
A Practical Guide to ICP-MS	Thomas, R.	Marcel Dekker Inc.	2004
Applications of Inorganic Mass Spectrometry	de Laeter, J. R.	Wiley	2001
Encyclopedia of Analytical Science, 2nd ed.	Worsfold, P., Townshend, A., and Poole, C., Eds.	Elsevier Ltd.	2005
Practical Inductively Coupled Plasma Spectroscopy	Dean, J. R.	Wiley	2005
Handbook of Elemental Speciation II: Species in the Environment, Food, Medicine and Occupational Health	Cornelis, R., Caruso, J., Crews, H., and Heumann, K., Eds.	Wiley	2005
Inductively Coupled Plasma Mass Spectrometry Handbook	Nelms, S. M., Ed.	Blackwell Publishing	2005

4. Inherent in the ICP-MS technique is the ability to measure elemental isotope ratios. Thus it can be exploited not only in the fields where such information is needed (e.g., nuclear industry, mining, geology), but also in using the isotope dilution technique to solve and study analytical problems.
5. The advancement of all different sample introduction techniques makes ICP-MS more versatile to deal with all kinds of samples.
6. The ease of "interfacing" with many separation instruments extends ICP-MS from elemental analysis to elemental speciation analysis, which is extremely important to environmental, toxicological, biological, pharmaceutical, and many other studies.

The first step in ICP-MS analysis is the introduction of the sample. This has been achieved through a variety of means. The most common method is the use of a nebulizer. This is a device which converts liquids into an aerosol. The aerosol is swept into the plasma to create ions. Nebulizers work best with

simple liquid samples (i.e., solutions). There have been, however, instances of their use with more complex materials such as slurry. Many varieties of nebulizers have been coupled to ICP-MS, including concentric, cross-flow, Babington, and ultrasonic nebulizer (USN) types. The aerosol generated is often treated to limit it to only the smallest droplets, commonly by means of a double pass or cyclonic spray chamber. Use of an autosampler makes this easier and faster. Less commonly, laser ablation (LA) has been used as a means of sample introduction. In this method, a laser is focused on the sample and creates a plume of ablated material that can be swept into the plasma. This is particularly useful for solid samples, though it can be difficult to create standards. This is one of the leading challenges in quantitative analysis. Other methods of sample introduction are also used. Electrothermal vaporization (ETV) and in torch vaporization (ITV) use hot surfaces (graphite or metal, generally) to vaporize samples for introduction. These can use very small amounts of liquids, solids, or slurries. Other methods like vapor (e.g., hydride or cold vapor) generation are also known.

Polyatomic interferences were a major problem for the analysis of some elements by ICP-MS. The recent advent of collision/reaction cell technology has revolutionized quadrupole ICP-MS (QICP-MS). Through collision or reaction with appropriate gases in a cell before the analyzer quadrupole, interferences such as $^{40}Ar_2^+$ can be almost completely eliminated while leaving the analyte ions (^{80}Se in this case) relatively unaffected. With each new model of ICP-MS instrument, which typically decreased in size, came better detection limits, equipped with collision/reaction cell, more user-friendly software, better price and accessibility to maintenance, and easier interfacing with separation instruments for elemental speciation works.

However, some intrinsic limitations still remain with these QICP-MS, particularly when transient or time-dependent signals (such as those generated by LA, ETV, flow injection (FI) and chromatographic separation) are used to analyze a large number of isotopes. Time-of-flight mass spectrometry (TOF-MS) is an inherently simple type of mass spectrometer with high transmission efficiency. With TOF-MS, all ions are extracted simultaneously for mass analysis, resulting in complete elimination of changes in nebulization efficiency, variation in the plasma (plasma flicker), and the sampling of inhomogeneous plasma zones. The precision of isotopic ratios measurements using TOF-MS is therefore dictated mainly by fundamental noise effects rather than by the time-dependent signal fluctuations encountered with QICP-MS. Thus its precision can easily achieve below 0.05 % for isotopic ratio measurements. The other unique advantages of ICP-TOF-MS are the high data acquisition rate achievable over the whole mass spectrum in less than 50 μs, complete elemental coverage in micro-volume, and rapid transient signal. Hieftje and coworkers [40] have given an excellent overview of the applications of ICP-TOF-MS, as a detector for chromatography and capillary electrophoresis (CE) for elemental speciation studies. Benkhedda et al. [41] demonstrated that the combination of ICP-TOF-MS with FI on-line preconcentration provides a very useful technique for simultaneous determination of lead at trace levels and lead isotopic ratios in natural water samples. Winefordner's and Holcomb's research groups [42,43] have successfully used ETV-ICP-MS for the elemental analysis on petroleum products such as fresh and used lubricant oils. Bings [44] demonstrated

the use of LA with ICP-TOF-MS to perform a rapid simultaneous elemental analysis in lubricant oil samples.

Multicollector (MC) arrays have long been used in thermal ionization mass spectrometry (TIMS). For an ICP source without a thermalized beam, double-focusing ion optics is required to correct for both chromatic and angular aberrations of the beam. Walder and Freedman [45] were the first to describe the use of such an instrument, and MC-ICP-MS has since established itself as a valuable addition to TIMS and QICP-MS techniques. From its birth through geological and nuclear applications, environmental, archaeological, biological, medical, and forensic scientists are now recognizing what isotopic ratio analysis can offer. Milgram et al. [46] have described the interfacing of the ICP to ion trap mass spectrometer of the Fourier transform ion cyclotron resonance (FT-ICR) ion trap design. Though the truly interference-free analysis may be ultimately realized with the developing FT-ICR ICP-MS, the price is prohibitively expensive. Approximately 85 % of all ICP-MS sold are QICP-MS, and sector and TOFs make up 13 % and 1 %, respectively. These newly developed ICP-MS instruments equipped with these sample introduction devices qualify ICP-MS as an ideal method for elemental analysis (as shown in Table 4) derived from what Fassel had stated earlier [25].

OCCURRENCE AND SIGNIFICANCE OF TRACE METALS IN THE PETROLEUM INDUSTRY

Although petroleum consists predominantly of hydrocarbons, many elements play a vital role in petroleum production and finished products. Almost all elements in the periodic table are found in petroleum products, varying from percent levels for carbon, hydrogen, nitrogen, and sulfur to parts per million (ppm), ppb, and ppt levels for metals. The natural presence of elements in crude oil is ascribed to its marine animal and plant origin. Metals such as nickel, iron, vanadium, and sodium and nonmetals like sulfur and nitrogen in crude oils have an adverse affect on the refinery and processing operations, generally acting as catalyst poisons. Vanadium and sodium in fuel oils produce deleterious effects on refractory linings, metal surfaces of modern furnace, boilers, and turbines. Data on metals and sulfur concentration in fuel oils are also important for evaluating emissions for oil-fired power plants. Organometallic compounds of calcium, zinc,

TABLE 4—Ideal Requirements for Methods of Elemental Analysis

1. Applicable to all elements and all isotopes
2. Simultaneous or rapid sequential multielement determination capability at the major, minor, trace, and ultratrace concentration levels without change of operating conditions
3. No interelement interference effects
4. Applicable to the analysis of microlitre- or microgram-sized samples
5. Applicable to the analysis of solids, liquids, slurry, and gases for both organic and aqueous matrix with minimal preliminary sample preparation or manipulation
6. Capable of providing rapid analyses; amenable to process control
7. Easy to be interfaced with different separation analyzer(s) for speciation analysis
8. Acceptable precision and accuracy

and other metals are added as useful additives to petroleum products such as lubricant oils [47]. Wear metals like iron, lead, silver, copper, and chromium in used lubricant oils are often determined as indicators of possible or incipient bearing damage. Spectrometric oil analysis was first applied in the early 1940s in an effort to detect wear in diesel locomotive engines by the railroad industry. In the early 1960s, the U.S. Air Force adopted spectrometric oil analysis to monitor the wearing in turbojet aircraft engines [48].

For geochemical identification, nickel and vanadium determinations have been performed using ICP-AES [49]. However, this technique does not allow the detection of ppb or sub-ppb levels. Manganese, molybdenum, barium, iron, copper, and cadmium occur at ppb or sub-ppb levels; these can be used as potential "new" bio-geochemical markers to help us understand more in the formation and migration of the oil. The lead isotopic ratios in crude oil and fractions (maltenes and asphaltenes) have also been used as geochemical markers that can be applied to petroleum exploration and development needs. For catalyst poison and environmental pollution, ppb levels of arsenic, silicon, lead, and mercury analyses in oil and on different locations on plant sites are required [50–53]. These needs led to the development and use of ICP-MS in the petroleum industry.

CRUDE OILS

Dreyfus et al. [54] developed a direct-dilution (with xylene) ICP-MS method to determine trace metals (e.g., argon, arsenic, barium, cadmium, copper, mercury, molybdenum, lead, and tin) and isotopes in crude oils and their fractions as new geochemical markers to provide information on petroleum origins, maturity, biodegradation, oil/water interactions, and dating. As an example, barium was identified as a tracer for biochemical degradation from sulfate-reducing bacteria. Efficient introduction of organics requires addition of oxygen for complete combustion of the sample; carbon deposit on cones (interface) and extraction lenses was minimized by optimization of the argon to oxygen ratio in the plasma. As expected, these elements were found to be highly concentrated in the asphaltenic fraction.

Duyck et al. [55] used an ICP-MS method for the determination of trace elements in crude oil after sample dissolution in toluene and subsequent ultrasonic nebulization. Carbon buildup at the interface and ion lenses was minimized by optimization of the argon to oxygen ratio in the plasma and by the desolvation of the USN. The standard addition technique combining with internal standardization was capable of correcting the signal suppression, especially in solutions containing high asphaltenes. Comparison with microwave-assisted acid decomposition showed good agreement, validating the proposed method and emphasizing its applicability for routine analysis of crude oil and other toluene-soluble petroleum products. Dreyfus et al. [56] used an ICP-MS method to directly measure lead isotopic ratios in crude oils. Sample introduction entails mixing of an ultrasonic nebulizer-produced dry aerosol with an organic aerosol. Two introduction systems, an USN and a Scott-type spray chamber, were fitted to a specially-designed dual inlet torch. This configuration allowed simultaneous introduction of organic solutions and aqueous solutions in the plasma, and permitted mass bias correction of lead isotopic ratios using the certified lead isotope standard National Institute of Standards and

Technology (NIST) Standard Reference Material (SRM) 981. The isotopic measurements of crude oils of geochemistry interest exhibited good accuracy and reproducibility, demonstrating the convenience of this technique for petroleum geochemistry. This study supplies new isotopic information for the reconstruction of petroleum system history.

Dreyfus et al. [57] applied the oil-in-water microemulsion formation technique for introducing crude oils directly into an ICP-MS to greatly simplify the determination of trace metals in oil. The advantages of this method include rapid multielement detection, ease of sample preparation, long-term sample stability, and low detection limits. Accuracy and precision are approximate ±3 %. Oils that contain metals in the concentration range of 0.1 to several hundred ppm can be analyzed routinely. The upper end of this range can be extended by simple aqueous dilution of the microemulsion. Because the sample solutions are composed primarily of water, there is no carbon buildup on the mass spectrometer interface. Other petroleum-based materials such as gasoline, diesel fuels, lubricating oils, residual oils, and asphaltenes can also be analyzed with this method. Al-Swaidan et al. [58] used a similar microemulsion technique combining with a standard addition technique to determine lead, copper, cadmium, zinc, iron, and cobalt by ICP-MS in Saudi Arabian crude oil from four different producing fields. The same approach was also used to determine lead and cadmium in Saudi Arabian Petroleum products [59]. The results were used to trace the sources of the metals and possible environmental impact and health risks.

Akinlua and coworkers [60] reported a rare earth elements (REEs) profile of crude oils from the offshore shallow water and onshore fields in the Niger Delta, analyzed by ICP-MS. The oil samples were prepared by acid digestion into colorless aqueous solution before ICP-MS analysis. The concentrations of the detected REEs—lanthanum, cesium, praseodymium, neodymium, samarium, europium, gadolinium, dysprosium, erbium, and ytterbium—ranged from 0.01 to 1.58 ppb with an average of 0.98 ppb (relative standard deviation [RSD or % RSD] < 5) for the oil samples analyzed. Light REEs (LREEs) were identified in all the oil samples, and heavy rare earth elements (HREEs) were identified in offshore oil samples only. LREEs patterns constructed from chondrite-normalized values for the oils show some similarities among the oils, which suggests common origin of the oils and that the REEs got into the oils from a similar source. This indicates that REEs would be a useful tool in oil-oil correlation. Statistical evaluation of these oils by cluster analysis using the REEs as variables clearly discriminated according to their geographic sources. Biodegradation has a pronounced effect on the concentrations of REEs in oils. Therefore, REEs contents of oils are useful in oil classification. In a separate study, Yasnygina et al. [61] analyzed all REEs and other metals in the Baikalian crude oil using an ICP-MS. The comparison of the results showed that the REEs concentrations in this sample were about two orders of magnitude higher than in crude oils deposits from Siberia or the Russian Far East. The concentration of REEs in the Baikalian crude oil were four orders of magnitude lower than those in the sediments of the Lake Baikal, but their distribution patterns were rather similar. The Baikalian crude oil is characterized by low nickel and vanadium values, indicating that this crude oil resulted from processes in an oxidizing environment or by vanadium loss during biodegradation.

The unique features of microwave digestion have made it a popular tool for samples that require pretreatment before ICP-MS analysis [62–64]. The advantages of microwave dissolution include faster digestion that results from the high temperature and pressure attained inside the sealed containers. Using closed vessels also makes it possible to eliminate uncontrolled trace element losses of volatile species that are present in a sample or that are formed during sample dissolution. It is well known that significant amounts of elements such as arsenic, boron, chromium, mercury, antimony, selenium, and tin are lost at relative mild temperature with some open-vessel acid dissolution procedures [65–66]. Another advantage of microwave dissolution is to have better control of potential contamination in blank as compared to open vessel procedures. This is due to less contamination from laboratory environment, cleaner containers, and smaller quantity of reagents. The author has developed and used several microwave digestion methods to prepare different petroleum products before ICP-AES and ICP-MS analyses since 1997 [67].

Xie et al. [68] reported the use of microwave digestion in conjunction with ICP-MS to accurately determine trace elements in crude oil. In the other application, a wet ashing method was used to prepare Saudi Arabian crude oils before ICP-MS analysis [69]. The procedure consists of treatment with concentrated H_2SO_4, drying, and ashing, followed by dissolution in HNO_3, filtration, and preparation of standard aqueous solutions. An oxygen-bomb combustion method was used to decompose crude oil before determination of antimony and selenium by ICP-MS [70]. By a decomposition procedure, organic antimonious and selenious compounds were completely converted into the corresponding inorganic species, which were absorbed by a 0.01 M nitric acid and 1 % hydrogen peroxide solution. Botto [71] described the difficulties on analyzing heavy oils using ICP-AES and ICP-MS. Heavy oils include distillation residues and naturally heavy crude oils. Direct dilution is the most convenient approach to prepare these samples. But it is often difficult to solubilize the whole sample. Direct introduction of these sample solutions may have transport interference problems (due to differences in physical properties [e.g., viscosity and surface tension] of the samples and calibration standards), background problems (caused by organic nature of the sample, which may result in spectral interference), matrix effects (arising from the complexity of hydrocarbons and other contents), and standardization (calibration) problems (resulting from different types of organometallic compounds present in the sample). The analysis after digestion removes almost all the effects of direct organic introduction because digestion usually converts all organometallic compounds into an inorganic form. The determination of metals performed after total destruction of organic matter is still the most reliable procedure for determining metals in the heavy oil.

Accurate mercury measurements in petroleum products are needed to assess the contribution to the global mercury cycle and to comply with reporting regulations for toxic elements [72]. Kelly et al. [73] used a closed-system combustion (Carius tube) to prepare four different liquid petroleum (including two crude oil) SRMs and determine mercury by isotope dilution cold-vapor ICP-MS (ID-CV-ICP-MS). Samples of approximate 0.3 g were spiked with stable 201 mercury and wet ashed in a closed system (Carius tube) using 6 g of high-purity nitric acid. Three different types of commercial oils were measured: two Texas crude oils, SRM 2721 (41.7 ± 5.7 pg/g) and SRM 2722 (129 ± 13 pg/g), a

low-sulfur diesel fuel, SRM 2724b (34 ± 26 pg/g) and a low-sulfur residual fuel oil, SRM 1619b (3.5 ± 0.74 ng/g) (mean value and 95 % confidence interval [CI]). The mercury values for the crude oils and the diesel fuel are the lowest values ever reported for these matrixes. The method detection limit, which is ultimately limited by method blank uncertainty, is approximately 10 pg/g for a 0.3-g sample. In a previous study of mercury determination, Osborne [74] applied the ETV-ICP-MS technique for quantifying solution and suspended mercurials in petroleum. It was also evaluated as a potentially useful tool for the analysis and screening of crudes and naphthas. Crudes and naphthas can contain hazardous concentrations of mercury capable of causing the embrittlement of aluminum piping and heat exchange equipment. ETV was used to atomize the sample at 2,650°C. The aerosol of this untreated sample was channeled via an argon-gas stream into an ICP-MS. The study centers on C5-32 alkanes and reveals trends relevant to the analysis of mixed nonpolar unknowns. The system produces useful sensitivities in the C5-14 range with a detection limit of 3 ppb in pentane. For mixtures C15 and higher there was advanced equipment wear and suppression of the analyte signal. This suppression is attributed to changes in the sample transport efficiency and destabilization of the plasma, due to a greater energy release for the longer chains. The formation efficiencies of the monovalent ion were considered, and several compounds were investigated. No statistical difference between the burning of diethyldithiocarbamate mercury as found in Conostan® standards and elemental mercury as standards was found.

Duyck et al. [75] reviewed the determination of trace elements in crude oil and heavy molecule mass fractions (saturates, aromatics, resins, and asphaltenes) by ICP-MS, ICP-OES, and AAS. Metal occurrences, forms, and distributions are examined as well as their implications in terms of reservoir geochemical oil refining and environment. The particular analytical challenges for the determination of metals in these complex matrixes by spectrochemical techniques were discussed. Sample preparation based on ashing, microwave-assisted digestion, and combustion decomposition procedures is noted as robust and long used. However, the introduction of nonaqueous solvents and microemulsions into ICP is cited as a new trend for achieving rapid and accurate analysis. Separation procedures for operationally defined fractions in crude oil are more systematically applied for the observation of metal distributions and their implications. Chemical speciation is of growing interest, achieved by the coupling of high efficiency separation techniques (e.g., high performance liquid chromatography [HPLC], gas chromatography [GC], ion chromatography [IC], capillary electrophoresis [CE], and supercritical fluid extraction [SFE]) to ICP-MS instrumentation, which allows the simultaneous determination of multiple organometallic species of geochemical and environmental importance. Several other applications and studies were performed using ICP-MS to determine metals in crude oils [76–82].

UPSTREAM EXPLORATION, EXPLOITATION, AND OIL FIELD PRODUCTIONS

Lienemann et al. [83] evaluated the use of ICP-AES and ICP-MS for trace metals determination in exploration, but also in exploitation activities for corrective actions during oil production and refining. Two techniques provide a very large

concentration range of metal compounds to be determined on a routine basis: ICP-AES is preferred for trace element analysis whereas ICP-MS is particularly convenient for ultratrace metals analysis. Direct introduction of petroleum product in the plasma requires a methodical approach in order to minimize matrix effects and quenching/extinguishing of the plasma. In this study, three different sample introduction modes have been investigated depending on the elements of interest and the matrix analyzed. A classical pneumatic nebulizer and a USN were compared for ICP-AES. These introduction modes were compared with a microflow pneumatic concentric nebulizer associated with a chilled spray chamber used with ICP-MS. Classical pneumatic nebulization with ICP-AES leads to ppm-range limits of quantification in the petroleum product and five times higher with gasoline due to the important dilution factor. The use of a USN coupled with ICP-AES reduces the limits of quantification in gasoline to the 50 ppb range, but further study of matrix effects with such an introduction system must be done. The initial important dilution factor allows the introduction of light matrices without further dilution, but requires the use of a standard addition method, which is time-consuming.

Lienemann [84] presented a brief introduction to the problems posed by trace metals in the petroleum industry and reviewed three main techniques available for trace metals determination with their recent developments. Different introduction modes, used for graphite furnace atomic absorption spectrometry (GFAAS), ICP-AES, and ICP-MS, are discussed and compared in terms of detection limits. Applications are various and apply to all kinds of petroleum products, from bioethanol to the more common gasoline and diesel, and also to heavier products such as bitumen. This also included a review of the main chromatographic techniques coupled with ICP-MS that demonstrates the promise of these techniques for the future in terms of elemental speciation in petroleum products.

Dreyfus [85] described the need to investigate the occurrence of potential new biogeochemical markers using ultratrace ICP-MS metal determination to improve our understanding of the formation and migration of hydrocarbons from an inorganic or bioinorganic aspect. Both trace metal contents and isotope signatures in crude oil provide unique information that would affect the chemical/physical processes of hydrocarbons during their generation, migration, accumulation, and production in a petroleum system. Trace metals can be used in oil-oil or oil-source correlation to identify the depositional environments of source rocks as well as the quantification of biodegradation. The distribution of organic and inorganic metal species also provides very useful information on oil-solids-water interactions and oil-drilling fluids-completion fluids interaction. Understanding these processes is critical to resolving hydrocarbon production and refinery fouling issues.

Kimura et al. [86] reviewed the recent advancements and applications of ICP-MS and LA-ICP-MS for petroleum samples and petrology. Bernsted [87] studied the use of ICP-MS to determine trace heavy metals in American Petroleum Institute (API) Class G oilwell cement. Bryukhanova and coworkers [88] developed an ICP-MS method to determine trace elements in petroleum and applied it in geochemical studies of oil seepage in Lake Baikal. Grousset et al. [89] described anthropogenic versus lithogenic origins of trace elements in water column particles using ICP-MS to determine the heavy metal distribution.

Most trace element enrichments were more likely to be related to anthropogenic input, rather than to biological cycling. Isotopic composition of lead, determined by ICP-MS, showed that the proportion of anthropogenic lead derived from European gasoline consumption was 50–100%.

Filby and Olsen [90] compared trace element determination in petroleum geochemistry using ICP-MS and instrumental neutron activation analysis (INAA). Samples used are crude oils, oil fractions and source rock bitumens. Results for a wide variety of crude oil types show good agreement for many elements for which the two techniques are suited and which are geochemically important (e.g., nickel, vanadium, iron, selenium, and arsenic). For other elements, the two techniques are complementary (e.g., boron, beryllium, cadmium, bromine). The advantages and disadvantages of INAA and ICP-MS in geochemical exploration programs are reviewed and practical examples presented. Olsen [91] used the same approach to study a suite of geochemical petroleum prospecting samples from a wide geographic area and a variety of depositional environments. Good correlation between the two techniques was obtained for vanadium, nickel, and cobalt ($r = 0.95$ to 0.90). The correlation decreased in the order: zinc ($r = 0.87$), iron, antimony, selenium, uranium, titanium, lanthanum, arsenic, barium, manganese, and tungsten ($r = 0.18$). The contribution of trace elements to oils from produced waters, drilling fluids, biodegradation, and migration was suggested by some of the samples for which there was disagreement. Laboratory experiments confirmed that barite contributed manganese, iron, gallium, and lead to oil samples that had not been filtered. If formation water and produced water was not removed from the oil, the water contribution of elements (e.g., arsenic and bromine) was superimposed onto the organically bound contents in the oils. In such instances, it appears that these elements are not useful in fingerprinting and classifying oils. However, when the formation water contribution is removed, elements (e.g., arsenic) were geochemically significant. It was important to water wash and filter oil samples before analyzing for geochemical exploration purposes. Metals such as zinc, cadmium, and lead are picked up by oils migrating through ore bodies of these metals. Prior to examining the contributions of water, barite, and migration, oils could only be classified using their vanadium, nickel, and cobalt contents. The new understanding acquired from this work has made it possible to identify and eliminate samples with severe contamination. Application of multivariate statistics to the vanadium, nickel, cobalt, molybdenum, arsenic, antimony, iron, manganese, zinc, and bismuth data for the oils enabled appropriate oils can be correlated with each other.

Anderson et al. [92] developed ICP-AES and ICP-MS methods to determine organic phosphorus in oil production waters after preconcentration on silica-immobilized C18-minicolumns. Analytical results were presented for the optimization of analytical methods for the determination of phosphorus in phosphino-polycarboxylates (PPCA), used frequently as scale inhibitors during oil production. Because of the complex matrix of production waters (brines) and their high concentration in inorganic phosphorus, the separation of organic phosphorus before determination was carried out using silica-immobilized C18-minicolumns. The developed methodology was applied successfully to samples from the offshore wells in the Campos basin, Brazil. Assessment of the PPCA inhibitor was possible at lower concentrations than achieved by current

analytical methods, resulting in benefits such as reduced cost of chemicals, postponed oil production, and lower environmental impact.

GASOLINE, DIESEL, NAPHTHA, AND OTHER PETROLEUM FUELS

The presence of metallic and metalloid species in automotive fuels is undesirable, except in the form of additives to improve specific characteristics of the fuel. Metallic or metalloid elements may derive from raw products such as nickel and vanadium in petroleum-based fuel or phosphorus in biodiesel, or they may be introduced during production and storage, such as copper, iron, nickel, and zinc in case of petroleum-based fuel and alcohol or sodium and potassium in the case of biodiesel. Korn et al. [93] reviewed analytical methods that were developed for metal and metalloid quantification in automotive fuel. The presence of some elements can be undesirable in gasoline, not only by the possibility of damage of the motor parts and poor performance of the fuel, but also because of the pollution caused by the release of toxic metals to the atmosphere by the combustion of the fuel.

Saint'Pierre et al. [94] developed an ETV-ICP-MS technique with an emulsion sample introduction to determine copper, manganese, nickel, and tin in gasoline. An ICP-MS coupling of ETV minimizes the problems related to the introduction of organic solvents into the plasma. Also, sample preparation as oil-in-water emulsions reduces problems related to gasoline analysis. Samples were prepared by forming a 10-fold diluted emulsion with a surfactant (Triton® X-100), after treatment with concentrated nitric acid. The sample emulsion was preconcentrated in the graphite tube by repeated pipeting and drying. External calibration was used with aqueous standards in a purified gasoline emulsion. A better improved method with standard addition and isotope dilution was developed to determine cadmium, copper, iron, lead and thallium in gasoline [95]. The use of 10 mg palladium in solution as matrix modifier allowed the determination of all studied analytes together, at 800°C pyrolysis and 2,100°C vaporization temperatures. The limits of detection for the analytes in gasoline, by standard addition or by isotope dilution, were better than 5 μg/L. The measured concentrations for all analytes by standard addition and by isotope dilution calibration techniques were mostly in agreement. The precisions for both calibrations were also similar and adequate. Agreement was also found with concentration results for iron and copper obtained by electrothermal atomic absorption spectrometry (ETAAS), without using a matrix modifier. Kowalewska et al. [96] evaluated five different sample preparation procedures for copper determination in a wide range of petroleum products from crude oil distillation using flame atomic absorption spectrometry (FAAS), ETAAS, and ICP-MS:

1. Mineralization with sulfuric acid in an open system,
2. Mineralization in a closed microwave system,
3. Combustion in hydrogen-oxygen flame in the Wickbold's apparatus,
4. Matrix evaporation followed by acid dissolution, and
5. Acidic extraction.

All the above procedures led to the transfer of the analyte into an aqueous solution for the analysis measurement step. Use of FAAS was limited to the analysis of the heaviest petroleum products of high Cu content. In ICP-MS,

the use of internal standard (i.e., rhodium or indium) was required to eliminate the matrix effects in the analysis of extractants and the concentrated solutions of mineralized heavy petroleum products. Reimer and Miyazaki [97] reported a microemulsion ICP-MS method to determine nickel and vanadium in gasoline and crude oil to improve the sensitivity without the addition of oxygen. Nakamoto et al. [98] compared four different sample preparation approaches for metal analysis in crude oil and petroleum fractions by ICP-MS. Samples were supplied in the form of burnt gas with the addition of oxygen, in the form of microemulsion with the use of a surfactant, in the form of an aqueous solution with an aid of oxidizing agents, and in the form of a mixture of gases by vaporization.

Historically, the biggest environmental concern and the main source of anthropogenic sulfur emissions is the combustion of sulfur-containing petroleum products and fossil fuels. The presence of sulfur compounds in crude oil and petroleum products is not desirable (except those that are added as performance enhancers). Some sulfur compounds may corrode various metallic parts of internal combustion engines. Sulfur oxides form during the combustion of sulfur containing petroleum compounds or fossil fuels (including coal) can adversely affect catalysts and can also be converted to sulfuric acid to cause corrosion. Consequently, industrial sulfur emissions and the sulfur contents in motor fuels are strictly controlled by most state and national governmental environmental pollution control agencies (e.g., 1990 Clean Air Act). A legal limit of 50 ppm for sulfur in gasoline and diesel fuel is mandated according to the EU directive 98/70/EC. On January 1, 2004, the first phase of the EPA low-sulfur gasoline regulations was effective. In 2006, specifications for gasoline content changed from the previous 500 ppm sulfur ceiling for the Reformulated Gasoline Program outside of California to a required 30 ppm annual average and a per-gallon cap of 80 ppm for most gasoline. This led to the need of sensitive, fast, and accurate analytical methods to determine total sulfur and different sulfur species. Nadkarni [99] compared all standard test methods of sulfur determination published by ASTM D02 Committee on Petroleum Products and Lubricants. Not surprisingly, ICP-MS and hyphenated ICP-MS (e.g., GC-ICP-MS) along with isotope dilution technique have been used quite extensively for sensitive (sub-ppb) and accurate measurements of total sulfur and sulfur species.

Evans and Wolff-Briche [100] used a novel ID-ICP-MS method for establishing high accuracy reference values for sulfur in fossil fuels. The European Community planned to reduce the permitted content of sulfur in fossil fuels. In the case of diesel fuel, the 1993 limit of 2000 μg/g was to be reduced to 50 μg/g by 2003. The new approach will readily meet the needs set by these new legal limits. Samples were prepared by closed-vessel microwave digestion to ensure retention of the volatile sulfur compounds in solution and spike equilibration. The natural and spiked isotopic ratios of $^{32}S/^{34}S$ were then measured using a Finnigan® MAT Element magnetic sector ICP-MS operating in medium resolution (R = 3,000) mode to avoid the spectral interference of oxygen on the sulfur isotopes. The natural isotopic compositions of sulfur vary in nature and so must be measured in each sample. The isotopic components of silicon are well characterized and have minimal natural variation. Hence, the silicon is used, as a novel approach, to correct for the effects of mass bias. The new ID-ICP-MS

method shows excellent agreement with the certified values for NIST 2724b of 427 ± 7 μg/g compared to reference values of 428 ± 4 μg/g. There is also good agreement with industry standard methods of analyses for low-sulfur diesel. Samples taken from UK retail outlets sold as low-sulfur diesel (<50 μg/g) differ from the target sulfur content by up to 15 μg/g. This deviation is comparable to the range in results for recognized routine methods and highlights how improved reference values at these concentrations will aid both the producer and legislator.

Heilmann et al. [101] applied an ID-ICP-MS with direct injection of isotope-diluted samples into the plasma, using a direct injection high-efficiency nebulizer (DIHEN), for accurate sulfur determinations in sulfur-free premium gasoline, gas oil, diesel fuel, and heating oil. For direct injection, a microemulsion consisting of the corresponding organic sample and an aqueous ^{34}S-enriched spike solution was prepared with additions of tetrahydronaphthalene and Triton® X-100. The ICP-MS parameters were optimized with respect to high sulfur ion intensities, low mass-bias values, and high precision of $^{32}S/^{34}S$ ratio measurements. For validation of the DIHEN-ICP-IDMS method, two certified gas oil reference materials (Bureau Communautaire de References [BCR] 107 and BCR 672) were analyzed. For comparison, a wet-chemistry ID-ICP-MS method was applied with microwave-assisted digestion using decomposition of samples in a closed quartz vessel inserted into a normal microwave system. The results from both ID-ICP-MS methods agreed well with the certified values of the reference materials and also with each other for analyses of other samples. However, the standard deviation of DIHEN-ICP-IDMS was about a factor of two higher compared with those of wet-chemistry ID-ICP-MS, mainly due to the inhomogeneity of the microemulsion, which causes additional plasma instabilities. Detection limits of 4 and 18 μg/g were obtained for ID-ICP-MS in connection with microwave-assisted digestion and DIHEN-ICP-IDMS, respectively, with a sulfur background of the used Milli-Q® water as the main limiting factor for both methods.

Another study demonstrated the use of LA sample introduction with ID-ICP-MS to accurately determine sulfur in different petroleum fuels such as sulfur-free premium gasoline, diesel fuel, and heating oil [102]. Two certified gas oil reference materials were analyzed for method validation. Two different ^{34}S-enriched spike compounds, namely, elementary sulfur dissolved in xylene and dibenzothiophene in hexane, were synthesized and tested for their usefulness in this isotope dilution technique. The isotope-diluted sample was adsorbed on a filter-paper-like material, which was fixed in a special holder for irradiation by the laser beam. Under these conditions, no time-dependent spike/analyte fractionation was observed for the dibenzothiophene spike during the laser ablation process. This means that the measured $^{34}S/^{32}S$ isotope ratio of the isotope-diluted sample remained constant, which is a necessary precondition for accurate results with the isotope dilution technique. A comparison of LA-ICP-IDMS results with the certified values of the gas oil reference materials and with results obtained from ID-ICP-MS analyses with wet sample digestion demonstrated the accuracy of the new LA-ICP-IDMS method in the concentration range of 9.2 μg/g ("sulfur-free" premium gasoline) to 10.4 mg/g (gas oil reference material BCR 107). The detection limit for sulfur by LA-ICP-IDMS is 0.04 μg/g and the analysis time is only about 10 minutes, which therefore also

qualifies this method for accurate determinations of low sulfur contents in petroleum products on a routine level.

Recent regulations focusing on the low-sulfur gasoline require analytical methods able to provide specific information on sulfur containing compounds present in petroleum products at the ng/g range. Bouyssiere et al. [103] used a GC-ICP-MS to analyze six sulfur-containing compounds in petroleum sample. The online coupling of capillary GC with ICP-collision cell-MS was proposed for the speciation of sulfur in hydrocarbon matrices. The technique showed an absolute detection limit 0.5 pg for a 1 μL sample injected in the splitless mode. This is about two orders of magnitude lower than other currently used techniques.

Heilmann and Heumann [104] developed a species-specific isotope dilution GC-ICP-MS method for the determination of thiophene derivates in petroleum products. A species-specific isotope dilution uses a spike with isotopically labeled species. This technique would improve precision and accuracy in the quantitative results because species loss, transformation, or degradation during storage and sample preparation steps can be recognized and corrected. A species-specific isotope dilution technique for accurate determination of sulfur species in low- and high-boiling petroleum products was developed by coupling capillary gas chromatograph with QICP-MS (GC-ICP-IDMS). For the isotope dilution step, ^{34}S-labeled thiophene, dibenzothiophene, and mixed dibenzothiophene/4-methyldibenzothiophene spike compounds were synthesized on the milligram scale from elemental ^{34}S-enriched sulfur. Thiophene was found in gasoline, sulfur-free gasoline, and naphtha. By analyzing NIST SRM 2296, the accuracy of species-specific GC-ICP-IDMS demonstrated excellent agreement with the certified value. The detection limit was always limited by the background noise of the isotope chromatograms and was determined for thiophene to be 7 pg absolute. This corresponds to 7 ng sulfur/g sample under the experimental conditions used. Dibenzothiophene and 4-methyldibenzothiophene were determined in different high-boiling petroleum products like gas oil, diesel fuel, and heating oil. In this case, a large concentration range from <0.04 to $>2{,}000$ μg/g was covered for both sulfur species. In parallel GC-ICP-MS and GC-EI-MS experiments (EI-MS electron impact ionization mass spectrometry) the substantial influence of co-eluting hydrocarbons on the ICP-MS sulfur signal was demonstrated. This can significantly affect results obtained by external calibration but not those obtained by the isotope dilution technique. Heilmann and Heumann [105] then applied a species-unspecific isotope dilution GC-ICP-MS method for possible routine quantification of sulfur species in petroleum products. To guarantee a stable and continuous addition of the spike into the GC-ICP-MS system, a special dosing unit was designed and the synthesis of a ^{34}S-labeled dimethyldisulfide spike from ^{34}S-enriched elemental sulfur in the milligram range was developed. The sample was mixed with an internal standard for spike mass flow calibration. From the mass flow chromatogram obtained by species-unspecific GC-ICP-IDMS, determination of all separated sulfur species and of the total sulfur content was possible without any matrix influence by co-eluting hydrocarbons. The accuracy of the developed method was evaluated by determining SRM-2296, which had three certified sulfur species, and by comparing results obtained by species-specific GC-ICP-IDMS. The total sulfur concentration determined for all separated species agreed well with the sulfur content in the original samples, which demonstrated that all sulfur species were

covered. Structural characterization of sulfur species was carried out by corresponding sulfur standards and by applying electron ionization ion trap mass spectrometry. The low detection limit of 9 ng sulfur per g sample, independent of results on coeluting hydrocarbons, and the robust instrumental design of the continuous spike flow dosing unit qualifies this species-unspecific GC-ICP-IDMS method for accurate and sensitive sulfur multispecies determinations, also on a routine basis. In addition, fingerprints of sulfur species in crude oil and petroleum products can be used for the exploration of oil fields [106, 107] or for the investigation of environmental contamination sources [108, 109].

Airborne lead is a cumulative neurotoxin inhaled and ingested by humans, adversely affecting the mental and physical health of children, and causing damage to the reproductive organs, elevated blood pressure, hypertension, and other cardiovascular conditions in adults. It was reported that 80 % of airborne lead comes from combustion of leaded gasoline. Lead was banned from house paint in 1978. U.S. food canners quit using lead solder in 1991. A 25-year phaseout of lead in gasoline reached its goal in 1995. Chaudhary-Webb et al. [110] measured lead isotopic ratios with ICP-MS, using ETV for pottery, whole blood, and leaded gasoline from residents of a small town in Mexico. Comparison was made of the isotopic ratios $^{208}Pb/^{204}Pb$, $^{207}Pb/^{204}Pb$, and $^{208}Pb/^{204}Pb$ in ceramic cookware (pottery), leaded gasoline, and related whole blood specimens. It's apparent from the similarity of the two ratios that the predominant source of lead is the ceramic cookware and not gasoline. Martinez et al. [111] conducted a separate study to measure $^{206}Pb/^{207}Pb$ ratios in dry deposit samples from the metropolitan zone of Mexico Valley by ICP-MS. The $^{206}Pb/^{207}Pb$ ratios were then correlated with some contemporary environmental material such as gasoline and urban dust as possible pollution sources. The possible origin of lead in gasoline used before 1960 will be discussed. O'Conner et al. [112] used a low-pressure ICP sustained at 6 W, with 7 mL/min of helium and 1.8 mL/min of isobutene, to determine tetraethyllead (TEL) in fuel. In the case of lead speciation, Kim et al. [113] designed and used a heated transfer line to interface a capillary GC to an ICP-MS for the analysis of alkyllead species in fuel. The interface required only a simple modification to the conventional ICP-MS torch and the construction of a heated transfer line. Botto [114–115] used direct injection nebulization (DIN) for introducing a wide range of petroleum hydrocarbon types into the ICP-MS. DIN-ICP-MS proved to be a sensitive and rapid analytical technique for determination of trace elements in petroleum, including those in volatile forms. Bettinelli et al. [116] used an acid solubilization of the samples in a microwave oven before ICP-MS analysis for trace elements in fuel oils. SRM 1634b and SRM 1619 were used for the method validation and showed good accuracy and precision for approximately 20 elements.

BIODIESEL, BIOETHANOL, AND OTHER BIOFUEL PRODUCTS

As a result of concerns on the dependence of fossil fuel, lower oil supplies, and stronger demand as well as an awareness of the environmental impacts of petroleum fuels usage, alternative fuels like biofuels have become increasingly popular. Lachas et al. [117] compared several sample preparations (including wet ashing and microwave extraction) for trace element analysis in milligram sample sizes of biomass samples using ICP-MS. The accuracy and sensitivity of the measurements improved when the dilution rate decreased from 5,000 to

1,000 and to 500. Baernthaler et al. [118] developed a reliable and appropriate ashing method to accurately determine major (aluminum, calcium, iron, potassium, manganese, phosphorus, silicon, and titanium) and minor (arsenic, barium, cadmium, cobalt, chromium, copper, mercury, manganese, molybdenum, nickel, lead, antimony, thallium, vanadium, and zinc) ash-forming elements in solid biofuels using an ICP-MS. Wood and bark, straw, and olive residues were analyzed using several digestion and analytical methods. The digestion methods included wet decomposition in closed vessels with different acid mixtures as well as dry-ashing techniques. Analytical techniques included FAAS, GFAAS, CV-AAS, ICP-OES, ICP-MS, and XRF as well as direct mercury determination. Digestion with $H_2O_2/HNO_3/HF$ followed by neutralization with H_3BO_3 was validated for major element analyses, and digestion with $H_2O_2/HNO_3/HF$ was validated for minor element analyses. The validation results show that the applied digestion methods can be recommended for solid biofuel analyses. For the determination of the elements investigated in solid biofuels, the following approaches can be recommended: FAAS for calcium, iron, potassium, magnesium, sodium, silicon, manganese, zinc; ICP-AES for aluminum, calcium, iron, potassium, magnesium, sodium, phosphorus, silicon, titanium, manganese, zinc, barium, chromium, copper, nickel, vanadium; GFAAS for cadmium, chromium, copper, nickel, lead; ICP-MS for phosphorus, titanium, arsenic, barium, cadmium, cobalt, chromium, copper, manganese, molybdenum, nickel, lead, antimony, vanadium, and zinc and direct determination as well as CV-AAS for mercury.

In a recent study, Saint'Pierre et al. [119] used an ID ETV-ICP-MS to determine silver, cadmium, copper, lead, and thallium in fuel alcohol samples. The ID proved to be a robust, fast, and simple calibration technique for the analysis of fuel ethanol. Later on, Saint'Pierre et al. [120] developed a flow injection system coupling to an ultrasonic nebulizer for direct introduction of fuel ethanol for trace element analysis by ICP-MS. External calibration against aqueous solutions, matrix matching, and ID were compared. Both ID and calibration with aqueous solutions promoted speed, good precision, sensitivity, and agreement with the results obtained by ETV-ICP-MS. Woods and Fryer [121] used an ICP-MS fitted with an octapole reaction system (ORS) to directly measure the inorganic contents of several biodiesel materials. Following sample preparation by dilution in kerosine, the biofuel was analyzed directly. The ORS effectively removed matrix and plasma-based spectral interferences to enable measurement of all important analytes, including sulfur, at levels below those possible by ICP-AES. At the 2008 Winter Plasma Conference on Plasma Spectrochemistry, Saint'Pierre et al. [122] presented the use of many sample preparation and sample introduction systems with an ICP-MS for the analysis of biofuels and petroleum fuels.

LUBRICANTS

Analyzing used motor oil reveals a great deal about how the engine is operating. Parts that wear in the engine will deposit traces in the oil that can be detected with ICP-MS. Oil analysis can help to determine whether parts are failing. In addition, it can determine the amount of the original oil additives remaining, and tell how much service life the oil has remaining.

Langer and Holcombe [42] described a method for the direct analysis of petroleum products, including new and used lubricating oils, for trace metals

using ETV-ICP-MS. ETV is a technique which has the unique capability of introducing samples into an ICP-MS for multi-element detection which cannot be nebulized directly (e.g., solids, slurries, and viscous liquids). Escobar's previous work [43] has shown the feasibility of ETV-ICP-MS for the analysis of trace metals in lubricating oils. However, this method requires the dilution of the oil sample with xylene and the generation of calibration curves using organometallic standards in base oil. This research explores the potential for the direct analysis of lubricating oils, which requires neither dilution of the sample nor the use of base oil standards. An additional goal of this method is the use of aqueous standards for calibration. Bings [44] used the combination of direct LA with an ICP-TOF-MS for rapid simultaneous determination of silver, manganese, aluminum, titanium, chromium, iron, nickel, cobalt, copper, silver, and lead in lubricant oil samples.

HYPHENATED ICP-MS FOR SPECIATION ANALYSIS IN PETROLEUM AND PETROCHEMICAL APPLICATIONS

"Speciation" is the specific form of an element as defined by its isotopic composition, oxidation state and complex or molecular structure, or both. "Speciation analysis" describes the identification and quantification of individual species in a sample. ICP-MS offers superior sensitivity and selectivity for most elements. It is a robust detector that can be interfaced to common chromatographic separation techniques. As speciation analysis slowly enters authority's regulations (e.g., USEPA method 6800 for chromium and mercury speciation), precise and accurate quantitative species determination becomes routine analysis [123].

A growing trend in the world of elemental analysis has revolved around the speciation of certain metals such as chromium and arsenic. One of the primary techniques to achieve this is to use an ICP-MS in combination with an HPLC. From a clinical standard point, there are many advantages in knowing the specific species present within a patient's body. For example, one species of chromium, known as Cr(III), or trivalent chromium, is needed by the body and causes no ill effects; however, Cr(VI), or hexavalent chromium, is very toxic to the body. Cr(VI) will not only cause cancer and other serious medical issues to the exposed individual, but also can cause genetic mutations to occur within the person, meaning that any offspring produced can potentially be affected. Size exclusion chromatography (SEC) is used to separate molecules/species according to their effective size. Molecules/species that are smaller than the pore size of the stationary phase are retained for a certain period of time and elute later than the larger molecules/species. Del Paggio et al. [124] used ambient- and high-temperature SEC-ICP-MS to characterize metal-containing molecules in various feedstock and hydrotreated atmospheric tower bottoms. The result suggests the presence of a dissociative equilibrium among certain fractions of the heavier molecules present. The hydrodemetalization of feedstock studied proceeded most rapidly for the small molecules present in the feed. Under appropriate process conditions, thermal degradation of large metal-containing structures was observed to liberate small metalloporphyrin-like subunits. Carey et al. [125] investigated the feasibility of using supercritical fluid chromatograph (SFC) with ICP-MS to determine organomercury and organolead compounds in fuel samples. The accuracy of the SFC-ICP-MS single-ion monitoring technique was demonstrated by analysis of a NIST SRM 2715, giving a concentration of

785 ± 9.71 ppm of TEL, with the SFC-ICP-MS system, compared with the certified value of 784 ± 4.00 ppm at the 95% confidence level.

Robert and Spinks [126] developed a micellar electrokinetic capillary chromatograph (MECC) method and applied it to the separation of petroporphyrin model compounds (e.g., in petroleum analyses). The MECC technique offers several advantages over a similar HPLC separation, including smaller required mobile phase and sample volumes, milder aqueous-based solvents, and less expensive columns. Furthermore, the peak capacity of the MECC separation was large because less hydrophobic, neutral species can migrate in the 6 to 30 minute separation time window, suggesting that the technique when coupled to an ICP-MS detection system might prove extremely useful for metal speciation studies. Rodriguez et al. [127] applied microcolumn multicapillary GC-ICP-MS to the analysis of several organometallic (mercury, tin, lead) compounds in environmental samples. The results were validated with certified reference materials for tin (BCR477, PACS-2) and mercury (DORM-1, TORT-1).

The combination of HPLC with ICP-MS provides a powerful and sensitive technique for on-line elemental speciation analysis because of its simplicity, robustness, high reliability, and reproducibility. HPLC has the advantage to work at ambient temperature, and thus the method is not limited by the volatility or the thermal stability of the analytes. Moreover, fully automated HPLC-ICP-MS systems working in both isocratic and gradient elution modes are now available on the market. Paszek et al. [128] described how ICP-MS has been successfully used to measure ppb levels of selenium in refinery effluent streams. It demonstrated how hyphenated ICP-MS techniques assisted in development of bioremediation options for selenium removal in wastewater treatment plants. McElroy [129] showed the superior selectivity and sensitivity for sulfur, vanadium, and nickel elemental speciation using HPLC-ICP-MS. A new method for the speciation analysis of selenite (Se-IV), selenate (Se-VI), and selenocyanate (SeCN-) is described, and the first results are presented on the distribution of these species in wastewater samples from a Brazilian oil refinery plant [130]. The method is based on the ion chromatographic separation of these species followed by online detection of ^{77}Se, ^{78}Se, and ^{82}Se using QICP-MS. No certified reference materials were available for this study. However, results on spiked wastewater samples showed acceptable recoveries (80 to 110 %) and repeatabilities (RSD < 5 %), which validated this method for its intended purpose. Once optimized, the method was applied to wastewater samples from an oil refinery plant. In all samples analyzed, selenocyanate was by far the most abundant selenium species reaching concentrations of up to 90 μg/L. Selenite was detected only in one sample, and selenate could not be identified in any of the samples analyzed. Total concentrations of selenium in most samples, assessed by hydride generation ICP-MS and by solution ICP-AES, exceeded those obtained from speciation analysis, indicating the presence of other selenium species not observed by the methodology used in this study. In a similar study, McElroy [129] also applied IC-ICP-MS for selenium speciation (e.g., selenite, selenate, and selenocyanate) in refinery waste streams.

A speciation method for sulfur in petroleum liquids by GC-ICP-MS was developed [131]. The detection limit was approximately 0.05 pg with an ICP-MS detector. This took into account the GC split ratios, which were two or three orders of magnitude superior to those with GC–flame photometric detection (FPD) and GC–atomic emission detection (AED) and equivalent or ten times

superior to those with GC-pulsed FPD and GC–sulfur chemiluminescence detection (SCD). The detector response for sulfur is considered to be essentially equimolar for all sulfur species. However, in practice, the sensitivity decreased slightly for a species with a high boiling point. It was speculated that the reason for the low sensitivity was not an inefficient ionization in ICP, but discrimination at the GC injection port or decomposition in the GC column. The present method was successfully applied to petroleum liquids such as naphtha, gasoline, kerosine, and light oil. These results were also compared with those by GC-AED and GC-SCD, and showed satisfactory agreement. Although the quenching effects by concomitant hydrocarbons were found to be slightly larger than those observed with SCD, the present method was superior in sensitivity to other conventional methods, and was expected to contribute to the development of low-sulfur gasoline for automobiles and fuels for fuel cells. Hwang

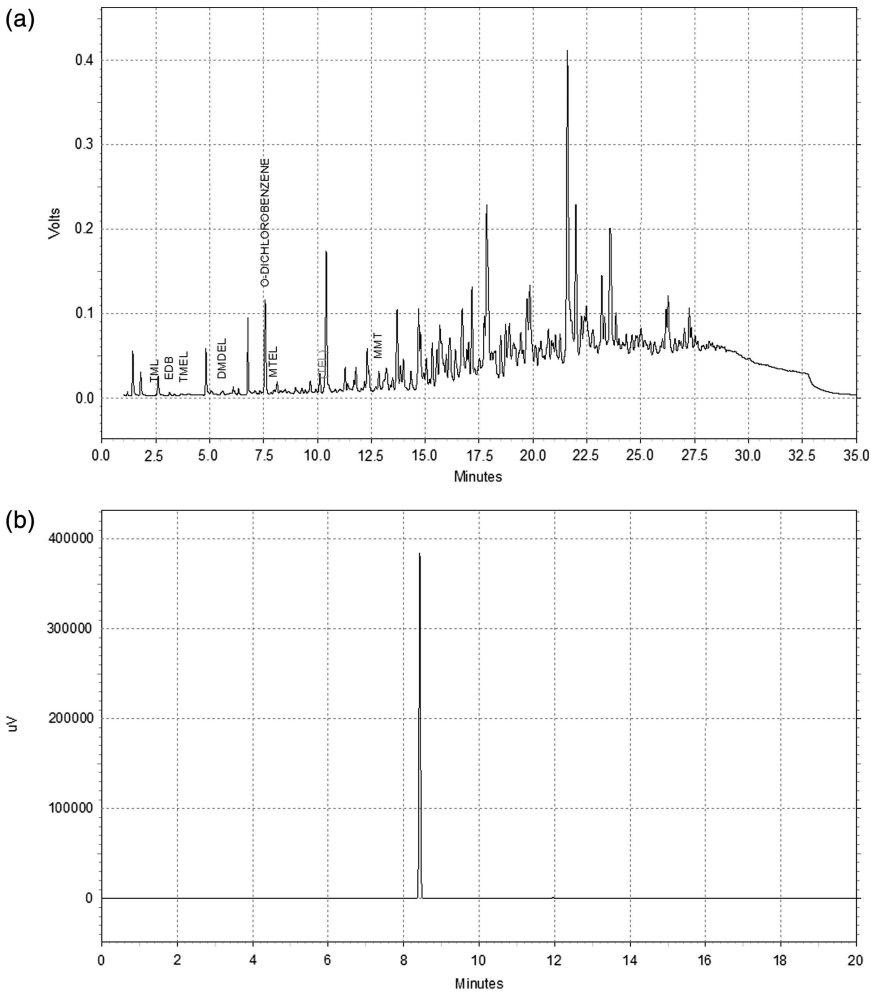

Fig. 1—(a) Pb analysis of a sample by GC-ICP-MS; (b) Pb analysis of a sample by GC-ECD.

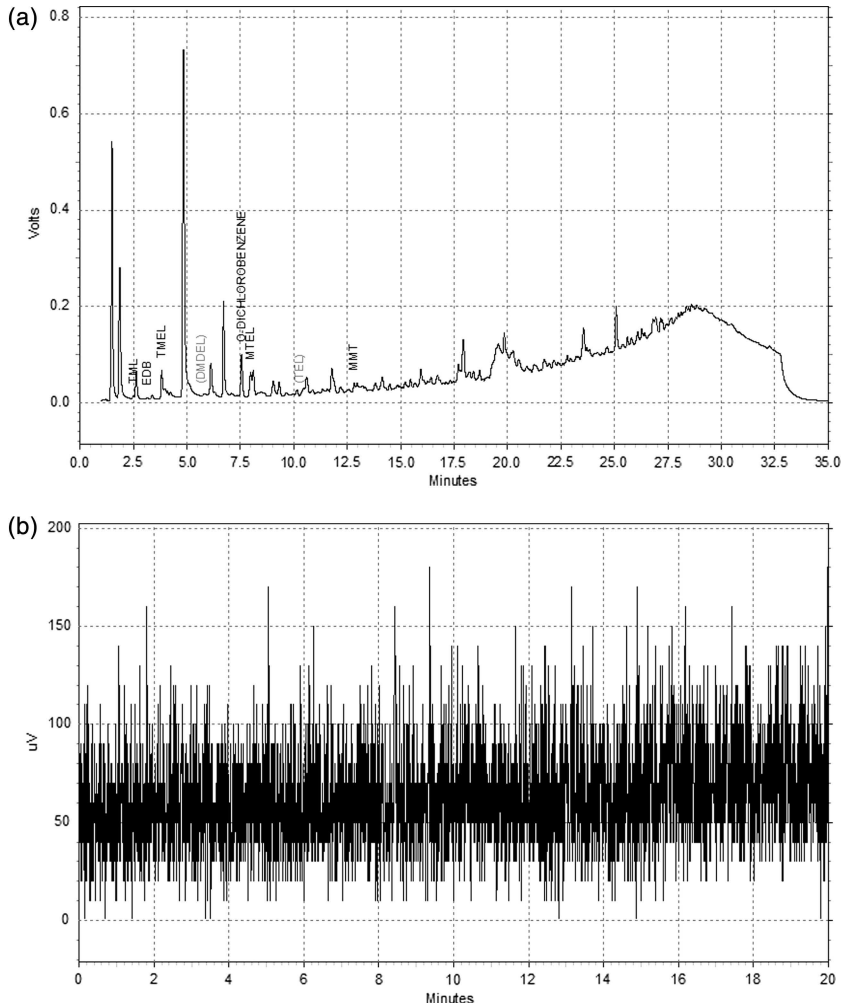

Fig. 2—(a) Pb analysis of an extracted hydrocarbon sample by GC-ECD; (b) Pb analysis of an extracted hydrocarbon sample by GC-ICP-MS.

[132,133] used a home-built high temperature interface (up to 450°C) to determine lead speciation in several environmental samples. As shown in Fig. 1, GC-ICP-MS has a clear advantage over the conventional GC detectors. Fig. 1a shows lead analysis of a sample by GC-ICP-MS. Only one component in the mixture contains lead and is identified as TEL. GC-ECD analysis of hydrocarbon (Fig. 1b) extracted from a monitoring well might be the source of groundwater contamination. Interpretation of the chromatogram is confounded by interference from oxygen-containing species. Fig. 2a shows GC–electron capture detection (ECD) analysis of hydrocarbon extracted from a refinery groundwater well in which the absence of lead in the sample cannot be demonstrated. Lead analysis of the same sample by GC-ICP-MS is shown in Fig. 2b. It shows unequivocally that there is no TEL (<1 ppb) in the sample.

FOSSIL FUELS AND OTHER PETROLEUM PRODUCTS

Varnes [134] compared different atomic spectroscopic techniques including AAS, ICP-AES, and XRF as well as several sample preparation techniques in the applications of the petroleum industry. Varnes describes interfacing an LC to an ICP, and examines some promising innovative techniques such as laser-enhanced ionization, ICP-MS detection, and total-reflection X-ray fluorescence. McElroy et al. [135] discussed the use and applications of ICP-MS in the petrochemical industry. Conventional methods of determining trace elementss in petrochemical samples involve time-consuming sample preparation and approaches followed by AA or ICP-AES detection. ICP-MS was demonstrated to be an effective technique for the analysis of ultratrace levels, trace elements, and elemental species in petrochemical analyses of oil-based samples simply by dilution with a suitable solvent. The combination of an extremely low chilling temperature spray–chamber with the addition of oxygen means that carbon-based spectral interferences can be reduced.

Li et al. [136] reported determination of ultratrace REEs in petroleum by ICP-MS. The sample preparation methods for the petroleum from different areas were tested and concentrated sulfuric acid was finally chosen as a carbonization agent. Interference from matrix elements was studied and Re was used as an internal standard to compensate the drift of the signals. In a recent study, Kulkarni et al. [137] developed a robust microwave-assisted acid digestion procedure followed by ICP-MS to quantify REEs in fluidized-bed catalytic cracking (FCC) catalysts. High temperature (200°C), high pressure (200 psig), acid digestion (HNO_3, HF, and H_3BO_3) with 20-minute dwell time effectively solubilized REEs from six fresh catalysts and a spent catalyst. This method was also employed to measure 27 non-REEs, including sodium, magnesium, aluminum, silicon, potassium, scandium, titanium, vanadium, chromium, manganese, iron, cobalt, nickel, zinc, gallium, arsenic, selenium, rubidium, strontium, zirconium, molybdenum, cadmium, cesium, barium, lead, and uranium. Complete extraction of several REEs (yttrium, lanthanum, cerium, praseodymium, neodymium, terbium, dysprosium, and erbium) required HF indicating that they were closely associated with the aluminosilicate structure of the zeolite FCC catalysts. Interlaboratory comparison using ICP-AES and instrumental neutron activation analysis (INAA) demonstrated the applicability of the newly developed analytical method for accurate analysis of REEs in FCC catalysts.

A microwave procedure for the digestion of the NIST 1634b "residual fuel oil" in closed pressurized vessels before ICP-MS analysis was developed in an attempt to facilitate routine analysis and obtain reproducible conditions or comparable results [138]. The influence of sample size, reagent component and volume, microwave power, and duration of heating on the digestion procedure was studied. Pressure and temperature inside the reaction vessels were monitored to determine the progression of the reaction and to develop optimal conditions. A nine-step heating program requiring 36.5 minutes with microwave power not exceeding 450 W in the pulsed mode was found suitable for the digestion of approximately 250 mg fuel oil with a mixture of nitric acid (5.0 mL) and hydrogen peroxide (2.0 mL). The experimental results were in good agreement with the certified and recommended concentrations for eight elements (aluminum, arsenic, cobalt, chromium, nickel, lead, vanadium, and zinc) in solutions obtained after one digestion step. An additional digestion step, consisting of

intermediate cooling and venting stages, was required for the accurate determination of iron. No agreement was reached for calcium and barium even after two-step digestion. The proposed method of digestion provided precise results with RSDs generally less than 5 % for most of the elements determined. In a separate study, Woodland et al. [139] used microwave digestion to prepare oil samples before analysis of platinum group and REEs. The platinum group elements (PGEs) consist of osmium, iridium, ruthenium, platinum, and palladium. Rhenium is also considered along with this group because of similarities in its chemical behavior. The PGEs are capable of exhibiting both siderophile and organophile behavior and thus offer great potential for tracing the sources of oils in sedimentary basins. This organophile behavior may cause significant PGE enrichment in oils over typical crustal values, rendering the PGE signature of an oil robust to chemical effects during its migration from source to trap. Hence the PGE signatures of the oil-source would be preserved despite migration of the oil through overlying crustal rocks. This in itself could prove to be a useful exploration fingerprinting tool.

The decomposition of a sample by the high-pressure oxygen combustion method and the preconcentration process using chelating resin (Chelex® 100) were studied for the determination of REEs in petroleum by ICP-MS [140]. In the decomposition procedure, a 1-g petroleum sample was burnt in 3 MPa of oxygen in a stainless vessel with 5 mL of 5 % HNO_3 + 1 % H_2O_2 absorbing solution. In the preconcentration process, the pH of absorbing solution after the combustion was adjusted at 4 with an ammonia solution and then stirred after the addition of 1 g of chelating resin (Chelex® 100). REEs ions adsorbed on the resin were eluted with 2 mol/L HNO_3. The solution was transferred to a 10-mL volumetric flask, and REEs were measured by ICP-MS.

As stated previously, ICP-MS has been used quite extensively to determine lead isotopes and its isotopic ratios in gasoline. Yoshinaga et al. [141] determined lead concentration and isotopic composition of prehistoric, historic, and contemporary Japanese bones, and deciduous teeth from contemporary Japanese children born from 1985 to 1988 by ICP-MS. Exposure to lead of the foreign origin was particularly evidently recorded in people born before the leaded gasoline ban. The history of human lead contamination in Japan is discussed based on the present results and other previously published data. In an environmental pollution study, Cocherie et al. [142] used ICP-MS to directly determine lead isotopic ratios in rainwater from the French Massif Central. The precision of ICP-MS data is sufficient to solve environmental problems to trace the origin of lead pollution present in rainwater from gasoline, a natural and an industrial component, and an unknown lead-enriched radiogenic component.

Another study demonstrated the feasibility of performing lead isotopic ratios by ICP-MS for studying the lead origin in hair of children living in polluted areas [143]. The analysis of ^{204}Pb, ^{206}Pb, ^{207}Pb, and ^{208}Pb isotopic ratios for environmental lead markers (lead gasoline, airborne particulate matter, house window dust) and hair of children was undertaken by the routine QICP-MS. Hair samples were collected from 10-year-old children living in Krakow, Poland, in 1995, and 35 randomly selected children, aged 11; both sexes were included in the current study. The associations of the lead in these environmental sources and lead in the hair of children were discussed. The relationships of the lead isotopic ratios and other parameters related to environmental

pollution are also analyzed. The analysis of the distribution of the $^{207}Pb/^{208}Pb$ ratio in the hair of children provided some evidence of the fact that hair lead of approximately 20 % of the investigated population could arise from gasoline, while the Pb from airborne dust and remaining sources can be attributed to approximately 80 % of the population.

Yu et al. [144] used an ID-ETV-ICP-MS to accurately determine sulfur in fossil fuels. The determination of sulfur by solution nebulization ICP-MS is difficult because of interferences from oxygen dimer ions. The large $^{16}O_2^+$ ion current from the solvent water is a serious interference at ^{32}S, the most abundant of the four isotopes, and precludes its measurement. The isotopic composition of sulfur varies in nature as a consequence of natural mass fractionation; therefore, high accuracy IDMS determination of sulfur requires that the ratio of $^{32}S/^{34}S$ be measured, for the two isotopes represent more than 99 % of natural sulfur. In this work, ETV was used to generate a water-free aerosol of the sample. Nonsolvent sources of oxygen were investigated and the spectral background was minimized. Further reduction of the oxygen dimer was achieved by using nitrogen as an oxygen scavenger in the argon plasma. The isotopic ratio of $^{32}S/^{34}S$ was used for the determination of sulfur by IDMS. Sulfur in two fossil fuel reference materials was measured, and the results were in good agreement (within 0.3 %) with those obtained by the more precise TIMS method.

Begak et al. [145] applied ICP-MS, Fourier transform infrared spectroscopy (FTIR), and γ-spectrometry to analyze heavy metals and radionuclides in petroleum refining sludges. Zhang et al. [146] determined organic and inorganic components in emission particulates from diesel engine by the use of ICP-MS, IC, and several other analytical methods. In a separate diesel engine emission study [147], the trace metal concentrations were determined by ICP-MS and used as an indicator of oil consumption. This study reports the results of detailed chemical analysis of trace metal in the particulate matter (PM) emitted from a single-cylinder heavy-duty diesel engine. Two techniques were used to make the trace metal concentration measurements. PM was captured on filters and trace metals were quantified with an ICP-MS, and also an aerosol time-of-flight mass spectrometer (ATOF-MS) was used to perform particle size and composition measurements in real time.

Hausler and Carlson [148] reviewed the use of ICP-MS and LC-ICP-MS as a geological exploration tool, and in monitoring of potential pollutants during refining. Kahen et al. [149] studied the use of a DIHEN with ICP-MS to analyze petroleum samples dissolved in volatile organic solvents. To minimize solvent loading, the solution uptake rate is reduced to 10 μL/minute. This is far less than the level (85 μL/min) commonly used for aqueous sample introduction with the DIHEN, and oxygen is added to the nebulizer gas flow and outer flow of the ICP. Factorial design is applied to study the effect of nebulizer tip position within the torch and the nebulizer and intermediate gas flow rates on the precision and the net signal intensity of the elements tested for multielemental analysis. Cluster analysis and principal component analysis are performed to distinguish the behavior of different isotopes, oxide species, and doubly charged ions. An acidified microemulsion procedure for petroleum sample pretreatment and sequential injection (SI) system were used for ICP-MS analysis [150]. The method was applied for the determination of lead and vanadium in Saudi Arabian Petroleum and its products. The results obtained are discussed

in relation to the possible environmental and health hazardous. Amorim et al. [151] reviewed and evaluated analytical methods based on atomic spectrometric techniques, particularly FAAS, electrothermal (ET) AAS, ICP-AES, and ICP-MS, for metal analysis in petroleum. Vanadium is recognized worldwide as the most abundant metallic constituent in petroleum. It is causing undesired side effects in the refining process, and corrosion in oil-fired power plants. In addition, an overview is provided of the sample pretreatment and preparation procedures for vanadium determination in petroleum and petroleum products. Also included are the most recent studies about speciation and fractionation analysis using atomic spectrometric techniques.

SUMMARY

Since the first ICP-MS paper was published in 1980, the first commercial ICP-MS instrument was introduced just 3 years later at the Pittsburgh Conference in 1983, and then the first benchtop ICP-MS was introduced 11 years after that. With each new model of ICP-MS instrument, which typically decreased in size, came improved detection limits and better price, more user-friendly software, and better accessibility to different sample introduction devices and different separation instruments. ICP-MS has been widely used in almost all industries (except petroleum), and its applications have continued to increase. Until the fundamental problems of petroleum samples are resolved, the use of ICP-MS in the petroleum industry will continue to lack the robustness required as a routine analyzer. However, ICP-MS is a very powerful tool for troubleshooting and conducting research and development in the petroleum industry. The superior detection limits with multielemental and multi-isotope capability may open a new dimension of research work to identify new "markers" or tracers for upstream exploration. For example, fingerprints of elemental species in crude oil and petroleum products can be used for the exploration of oil fields or for the investigation of environmental contamination sources. The use of hyphenated ICP-MS (e.g., SEC-ICP-MS) may lead us to explore the frontiers of unconventional resources and the new findings of additive chemistry information in lubricant, additives, and tribology studies.

ACKNOWLEDGMENT

The author would like to thank David Leong and Jeremy Weisser for their review of the manuscript.

References

[1] Tyson J., *Analysis: What Analytical Chemists Do,* Royal Society of Chemistry, London, 1988., pp. 1–12.

[2] Kaiser, M. A. and Ullman, A. H., "Analytical Chemistry in Industry," *Anal. Chem.,* Vol. 60, 1988, p. 823A.

[3] Botto, R. I., *ICP Information Newslett*, Vol. 31, No. 8, 2006, p. 823.

[4] Lucchesi, C. A., "The Analytical Chemist as Problem Solver," in *The Best of American Laboratory*, International Scientific Communications, Inc., Fairfield, CT, 1983, pp. 16–20.

[5] Hwang, J. D. and Wang, W. J., "Application of ICP-AES to Analysis of Solutions," *Applied Spectroscopy Reviews*, Vol. 30, No. 4, 1995, p. 234.

[6] Beauchemin, D., "Inductively Coupled Plasma Mass Spectrometry," *Anal. Chem.,* Vol. 76, 2004, pp. 3395–3416.
[7] Beauchemin, D., "Inductively Coupled Plasma Mass Spectrometry," *Anal. Chem.,* Vol. 78, 2006, pp. 4111–4136.
[8] Beauchemin, D., "Inductively Coupled Plasma Mass Spectrometry," *Anal. Chem.,* Vol. 80, 2008, pp. 4455–4486.
[9] Beauchemin, D., "Inductively Coupled Plasma Mass Spectrometry," *Anal. Chem.,* Vol. 82, 2010, pp. 4786–4810.
[10] Bings, N. H., Bogaerts, A. and Broekaert, J. A. C., "Atomic Spectroscopy," *Anal. Chem.,* Vol. 76, 2004, p. 3313.
[11] Bings, N. H., Bogaerts, A. and Broekaert, J. A. C., "Atomic Spectroscopy," *Anal. Chem.,* Vol. 78, 2006, p. 3917.
[12] Bings, N. H., Bogaerts, A. and Broekaert, J. A. C., "Atomic Spectroscopy," *Anal. Chem.,* Vol. 80, 2008, p. 4317.
[13] Bings, N. H., Bogaerts, A. and Broekaert, J. A. C., "Atomic Spectroscopy," *Anal. Chem.,* Vol. 80, 2010, pp. 4653–4681.
[14] Koppenaal, D. W, "Atomic Mass Spectrometry," *Anal. Chem.,* Vol. 60, 1988, p. 113R.
[15] Koppenaal, D. W., "Atomic Mass Spectrometry," *Anal. Chem.,* Vol. 62, 1990, p. 303R.
[16] Koppenaal, D. W., "Atomic Mass Spectrometry," *Anal. Chem.,* Vol. 64, 1992, p. 320R.
[17] Bacon, J. R., Linge, K. L., Parrish, R. R. and Van Vaeck, L., "Atomic Spectrometry Update: Atomic Mass Spectrometry," *J. Anal. At. Spectrom.,* Vol. 21, 2006, pp. 785–818.
[18] Bacon, J. R., Linge, K. L., Parrish, R. R. and Van Vaeck, L., "Atomic Spectrometry Update: Atomic Mass Spectrometry," *J. Anal. At. Spectrom*., Vol. 22, 2007, pp. 973–1006.
[19] Cottingham, K., "ICPMS: Many Laboratories Are Turning to ICPMS Because of Its Speed, Sensitivity, and Multielement Capability," *Anal. Chem*., Vol. 76, 2004, pp. 35A–38A.
[20] Douglas D. J. and Houk, R. S., "Inductively-Coupled Plasma Mass Spectrometry (ICP-MS)," *Prog. Anal. At. Spectrosc.,* Vol. 8, 1985, pp. 1–18.
[21] Olesik, J. W., "Elemental Analysis Using ICP-OES and ICP/MS: An Evaluation and Assessment of Remaining Problems," *Anal. Chem.,* Vol. 63, 1991, pp. 12A–1821A.
[22] Hieftje, G. M. and Vickers G. H., "Developments in Plasma-Source Mass Spectrometry," *Anal. Chim. Acta,* Vol. 216, 1989, p. 1–24.
[23] Nadkarni, R. A., *Elemental Analysis of Fuels and Lubricants: Recent Advances and Future Prospects,* STP 1468, ASTM International, West Conshohocken, PA, 2005.
[24] Thomas, R., *A Practical Guide to ICP-MS: A Tutorial for Beginners,* RC Press, Boca Raton, FL, 2008.
[25] Fassel, V. A., "There Must Be An Easier Way," *Spectrochim. Acta,* Vol. 40B, 1985, p. 1281.
[26] ASM Handbook Committee, Metals Handbook, Ninth Edition, Vol. 10, *Materials Characterization*, American Society for Metals, Metals Park, OH, 1986.
[27] Sibilia, J. P., Ed., *A Guide to Materials Characterization and Chemical Analysis,* VCH Publishers, New York, 1988.
[28] Hwang, J. D. and Wang, W. J., "Application of ICP-AES to Analysis of Solutions," *Applied Spectroscopy Reviews*, Vol. 30(4), 1995, pp. 231–350.
[29] Adams, F., Gijbels, R. and Van Grieken, R., Eds., *Inorganic Mass Spectrometry*, Wiley, New York, 1988.
[30] Gray, A. L., "Mass-Spectrometric Analysis of Solutions Using an Atmospheric Pressure Ion Source," *Analyst,* Vol. 100, 1975, pp. 289.
[31] Gray, A. L. and Date, A. R., in *Dynamic Mass Spectrometry*, D. Price and J. F. J. Todd, Eds., Vol. 6, Ch. 20, p. 252, Heydon, London, 1981.

[32] Date, A. R. and Gray, A. L., "Plasma Source Mass Spectrometry Using an Inductively Coupled Plasma and a High Resolution Quadrupole Mass Filter," *Analyst,* Vol. 106, 1981, p. 1255.

[33] Houk, R. S., Fassel, V. A. and Svec, H. J., in *Dynamic Mass Spectrometry*, D. Price and J. F. J. Todd, Eds., Vol. 6, Ch. 19, p. 234, Heydon, London, 1981.

[34] Houk, R. S., Svec, H. I. and Fassel, V. A., "Mass Spectrometric Evidence for Suprathermal Ionization in an Inductively Coupled Argon Plasma," *Appl. Spectrosc.,* Vol. 35, 1981, p. 380.

[35] Houk, R. S., Fassel, V. A., Flesch, G. D., Svec, H. J., Gray, A. L. and Taylor, C. E., "Inductively Coupled Argon Plasma as an Ion Source for Mass Spectrometric Determination of Trace Elements," *Anal. Chem.,* Vol. 52, 1980, p. 2283.

[36] Douglas, D. J., Quan, E. S. K. and Smith, R. G., "Elemental Analysis with an Atmospheric Pressure Plasma (MIP, ICP)/Quadrupole Mass Spectrometer System," *Spectrochim. Acta,* Vol. 38B, 1983, p. 39.

[37] Date, A. R. and Gray, A. L., "Development Progress in Plasma Source Mass Spectrometry," *Analyst*, Vol. 108, 1983, p. 159.

[38] Date, A. R. and Gray, A. L, "Isotope Ratio Measurements on Solution Samples Using a Plasma Ion Source," *Int. J. Mass Spectrom. Ion Phys.,* Vol. 48, 1983, p. 357.

[39] Gray, A. L. and Date, A. R., "Inductively Coupled Plasma Source Mass Spectrometry Using Continuum Flow Ion Extraction," *Analyst,* Vol. l08, 1983, p. 1033.

[40] Leach A. M., McClenathan, D. M. and Hieftje, G. M., "Plasma Source TOF-MS: A Powerful Tool for Elemental Speciation," in *Handbook of Elemental Speciation: Techniques and Methodology,* Eds. R. Cornelis, J. Caruso, H. Crews, and K. Heumann, John Wiley & Sons, New York, 2004, p. 313.

[41] Benkhedda, K. Infante, H. G. and Adams, F. C., "Determination of Total Lead and Lead Isotope Ratios in Natural Waters by ICP-TOF-MS after Flow Injection Online Pre-concentration," *Anal. Chim. Acta,* Vol. 506, 2004, p. 137.

[42] Langer, D. L. and Holcombe, J. A., "Direct Method for the Analysis of Trace Metals in New and Used Lubricating Oils," *Book of Abstracts*, 218th ACS National Meeting, New Orleans, Aug. 22–26, 1999.

[43] Escobar, M. P., Smith, B. W. and Winefordner, J. D., "Determination of Metalloorganic Species in Lubricating Oil by Electrothermal Vaporization Inductively Coupled Plasma Mass Spectrometry," *Anal. Chim. Acta,* Vol. 320, 1996, pp. 11–17.

[44] Bings, N. H., "Direct Determination of Metals in Lubricating Oils by Laser Ablation Coupled to ICP Time-of-Flight MS," *J. Anal. At. Spectrom.,* Vol. 17, 2002, p. 759.

[45] Walder, A. J. and Freedman, P. A., "Isotopic Ratio Measurement using a Double Focusing Magnetic Sector Mass Analyzer with an ICP as an Ion Source," *J. Anal. At. Spectrom.,* Vol. 7, 1992, p. 571.

[46] Milgram, K. E., White, F. M., Goodner, K. L., Watson, C. H., Koppenaal, D. W., Barinaga, C. J., Smith B. H., Winefordner, J. D., Marshall, A. G., Houk, R. S. and Eyler, J. R., "High-Resolution ICP Fourier-Transform Ion-Cyclotrone Resolution Mass Spectrometry," *Anal. Chem.,* Vol. 69, No. 18, 1997, p. 3714.

[47] Mortier R. M. and Orszulik, S. T., eds., *Chemistry and Technology of Lubricant,* Blackie Academic & Professional, London, UK, 1997.

[48] Sychra, V., Lang, I. and Sebor, G., *Prog. Analyt. Atom. Spectrosc.,* Vol. 4, 1981, pp. 341–426.

[49] Lopez, L. and Monaco, S. L., "Geochemical Implications of Trace Elements and Sulfur in the Saturate, Aromatic and Resin Fractions of Crude Oil from the Mara and Mara Oesta Fields," *Venezuela Fuel,* Vol. 83, 2004, pp. 365–374.

[50] Kellberg, L., Zeuthen, P. and Jakobsen, H. J., "Deactivation of HDT Catalyst by Formation of Silica Gels from Silicone Oil," *J Catal.,* Vol. 143, 1993, pp. 45–51.

[51] Didillon, B., Cosyns, J., Cameron, C., Uzio, D., Sarrazin, P. and Boitiaux, J. P., "Industrial Evaluation of Selective Hydrogenation Catalyst Poisoning," *Stud. Surf. Sci. Catal.,* Vol. 111, 1997, pp. 447–454.

[52] Souza, R. M., Da Silveira, C. L. P. and Aucelio, R. Q., "Determination of Refractory Elements in Used Lubricating Oil by ICP-OES Employing Emulsified Sample Introduction and Calibration with Inorganic Standards," *Anal. Sci.,* Vol. 20, 2004, pp. 351–355.

[53] Speight, J. G., *Handbook of Petroleum Analysis,* Wiley-Interscience, New York, 2001.

[54] Dreyfus, S., Pecheyran, C., Magnier, C., Prinzhofer, A., Lienemann, C. P. and Donard, O. F. X., "Direct Trace and Ultra-trace Metals Determination in Crude Oil and Fractions by Inductively Coupled Plasma Mass Spectrometry," ASTM STP 1468 (Elemental Analysis of Fuels and Lubricants), ASTM International, West Conshohocken, PA, 2005, pp. 51–58.

[55] Duyck, C., Miekeley, N., Porto, S., Carmem L. and Szatmari, P., "Trace Element Determination in Crude Oil and its Fractions by Inductively Coupled Plasma Mass Spectrometry using Ultrasonic Nebulization of Toluene Solutions," *Spectrochim. Acta,* Vol. 57B, No. 12, 2002, pp. 1979–1990.

[56] Dreyfus, S., Pecheyran, C., Lienemann, C. P., Magnier, C., Prinzhofer, A. and Donard, O. F. X., "Determination of Lead Isotope Ratios in Crude Oils with Q-ICP/MS," *J. Anal. At. Spectrom.,* Vol. 22, No. 4, 2007, pp. 351–360.

[57] Dreyfus, S., Pecheyran, C., Lienemann, C. P., Magnier, C., Prinzhofer, A. and Donard, O. F. X., "Determination of Trace Metals in Crude Oil by Inductively Coupled Plasma Mass Spectrometry with Micro-emulsion Sample Introduction," *Anal. Chem.,* Vol. 63, No. 15, 1991, pp. 1594–1599.

[58] Al-Swaidan, H. M., "Simultaneous Multi-element Analysis of Saudi Arabian Petroleum by Microemulsion Inductively Coupled Plasma Mass Spectrometry (ICP/MS)," *Anal. Lett.,* Vol. 27, No. 1, 1994, pp. 145–152.

[59] Al-Swaidan, H. M., "Micro-emulsion Determination of Lead and Cadmium in Saudi Arabian Petroleum Products by Inductively Coupled Plasma Mass Spectrometry (ICP/MS)," *Sci. Total Environ.,* Vol. 145, No. 1–2, 1994, pp. 157–161.

[60] Akinlua, A., Torto, N. and Ajayi, T. R., "Determination of Rare Earth Elements in Niger Delta Crude Oils by Inductively Coupled Plasma-Mass Spectrometry," *Fuel,* Vol. 87, No. 8-9, 2008, pp. 1469–1477.

[61] Yasnygina, T. A., Malykh, Yu. M., Rasskazov, S. V., Primina, S. P., Zemskaya, T. I. and Khlystov, O. M., "The ICP-MS Determination of Rare Earths and Other Metals in Baikal Crude Oil: Comparison with Crude Oils in Siberia and the Russian Far East," *Dokl. Earth Sci.,* Vol. 411, No. 8, 2006, pp. 1237–1240.

[62] Kingston, H. M. and Jassie, L. B., *Introduction to Microwave Sample Preparation-Theory and Practice,* American Chemical Society, Washington, D.C., 1988.

[63] Kingston, H. M. and Haswell, S. J., *Microwave-Enhanced Chemistry-Fundamentals, Sample Preparation, and Applications,* American Chemical Society, Washington, D.C., 1997.

[64] Ivanova, J., Djingova, R., Korhammer, S. and Markert, B., "On the Microwave Digestion of Soils and Sediments for Determination of Lanthanides and Some Toxic and Essential Elements by Inductively Coupled Plasma Source Mass Spectrometry," *Talanta,* Vol. 54, No. 4, 2001, pp. 567–574.

[65] Zief, M. and Mitchell, J. W., *Contamination Control in Trace Element Analysis,* John Wiley & Sons, New York, 1976.

[66] Eisentraut, K. J., Newman, R. W., Saba, C. S., Kauffman, R. E. and Rhine, W. E., "Spectrometric Oil Analysis: Detecting Engine Failures Before They Occur," *Anal. Chem.,* Vol. 56, 1984, p. 1087A.

[67] Hwang, J. D., Horton, M. and Leong, D., "The Use of Microwave Digestion and ICP-AES to Determine Elements in Petroleum Samples," ASTM STP 1468 (*Elemental*

Analysis of Fuels and Lubricants), ASTM International, West Conshohocken, PA, 2005, pp. 33–41.

[68] Xie, H., Li, L., Hu, H. and Li, A., "The Determination of Trace Metal Elements in Crude Oil by ICP-MS," *Shiyou Xuebao, Shiyou Jiagong*, Vol. 21, No. 4, 2005, pp. 86–90.

[69] Al-Swaidan, H. M., "Trace Metal Determination by Wet Ashing ICP/MS in Saudi Arabian Crude Oils," *Anal. Lett.,* Vol. 23, No. 7, 1990, pp. 1345–1356.

[70] Nakamoto, Y. and Tomiyama, T., "Highly Sensitive Determination of Antimony and Selenium in Crude Oils by Oxygen-Bomb Combustion/ICP-MS," *Bunseki Kagaku*, Vol. 46, No. 8, 1997, pp. 665–668.

[71] Botto, R. I. "Analysis of Heavy Oils for Trace Metals Using Plasma Spectrochemistry," *Winter Conference on Plasma Spectrochemistry* Paper IL S02, Temecula, CA, 2008.

[72] Wilhelm, S. M., Liang, L., Cussen, D. and Kirchgessner, D., "Mercury in Crude Oil Processed in the United States," *Environ. Sci. Technol.,* Vol. 41, No. 13, 2007, p. 4509.

[73] Kelly, W. R., Long, S. E. and Mann, J. L., "Determination of Mercury in SRM Crude Oils and Refined Products by Isotope Dilution Cold Vapor ICP-MS using Closed-System Combustion," *Anal. Bioanal. Chem.,* Vol. 376, No. 5, 2003, pp. 753–758.

[74] Osborne, S. P., "Quantitation of Mercury in Petroleum by ETV-ICP-MS," *Appl. Spectrosc.,* Vol. 44, No. 6, 1990, p. 1044–1046.

[75] Duyck, C., Miekeley, N., Porto S., Carmem L., Aucelio, R. Q., Campos, R. C., Grinberg, P., Brandao, P. and Geisamanda P., "The Determination of Trace Elements in Crude Oil and its Heavy Fractions by Atomic Spectrometry," *Spectrochim. Acta*, Vol. 62B, No. 9, 2007, pp. 939–951.

[76] Al-Swaidan, H. M., "Trace Determination of Vanadium and Nickel in Saudi Arabian Petroleum and Petroleum Products by Microemulsion ICP-MS," *At. Spectrosc*., Vol. 14, No. 6, 1993, pp. 170–173.

[77] Liu, X., Chen, J. and Wang, X., "Determination of Vanadium, Cobalt, Nickel and Lead in Crude Oil Standard Reference Material by Inductively Coupled Plasma-Mass Spectrometry," *Fenxi Huaxue,* Vol. 24, No. 6, 1996, pp. 669–672.

[78] Al-Gadi, A. A. and Al-Swaidan, H. M., "Determination of Vanadium in Saudi Arabian Crude Oil by Inductively Coupled Plasma-Mass Spectrometry (ICP/MS)," *Anal. Lett.,* Vol. 23, No. 9, 1990, pp. 1757–1764.

[79] Al Swaidan, H. M., "Simultaneous Determination of Trace Metals in Saudi Arabian Crude Oil Products by Inductively Coupled Plasma Mass Spectrometry (ICP/MS)," *Anal. Lett.,* Vol. 21, No. 8, 1998, pp. 1487–1497.

[80] Al-Swaidan, H. M., "The Determination of Lead, Nickel and Vanadium in Saudi Arabian Crude Oil by Sequential Injection Analysis/Inductively Coupled Plasma Mass Spectrometry," *Talanta*, Vol. 43, No. 8, 1996, pp. 1313–1319.

[81] Al-Swaidan, H. M., "Determination of Lead and Nickel in Saudi Arabian Crude Oils by ICP/MS using MIBK for Sample Pretreatment," *Anal. Lett.,* Vol. 25, No. 11, 1992, pp. 2157–2163.

[82] Veshev, S. A., Stepanov, K. I. and Vasil'eva, T. N., "Determination of a Wide Range of Trace Elements in Petroleum Fields," *Geokhimiya,* Vol. 10, 2000, pp. 1132–1136.

[83] Lienemann, C. P., Dreyfus, S., Pecheyran, C. and Donard, O. F. X., "Trace Metal Analysis in Petroleum Products: Sample Introduction Evaluation in ICP-OES and Comparison with an ICP-MS Approach," *Oil & Gas Science and Technology*, Vol. 62, No. 1, 2007, pp. 69–77.

[84] Lienemann, C. P., "Analysis of Trace Metals in Petroleum Products, State of the Art," *Oil & Gas Science and Technology*, Vol. 60, No. 6, 2005, pp. 951–965.

[85] Dreyfus, S. "Applications of Plasma Spectrochemistry to Petroleum Exploration and Development," *Winter Conference on Plasma Spectrochemistry* Paper IL 25, Temecula, CA, 2008.

[86] Kimura, J., Takaku, Y. and Yoshida, T., "Recent Advancement of Inductively Coupled Plasma Source Mass Spectrometry (ICP-MS) and Application to Petrology," *Chikyu Kagaku,* Vol. 50, No. 4, 1996, pp. 277–302.

[87] Bernsted, J., "Use of Inductively Coupled Plasma Mass Spectrometry (ICPMS) for Heavy Metal Trace Analysis of API Class G Oilwell Cement," *Cem. Concr. Res.,* Vol. 23, No. 4, 1993, pp. 993–994.

[88] Bryukhanova, N. N., Lomonosov, I. S., Tauson, V. L., Troshin, Yu. P., Afonina, T. E., Lozhkin, V. I., Sandimirova, G. P. and Kuznetsov, K. E., "Improved Method for Determination of Trace Elements in Petroleum (first data on the trace element composition of Lake Baikal petroleum)," *Prikladnaya Geokhimiya,* Vol. 4, 2003, pp. 68–75.

[89] Grousset, F. E., Quetel, C. R., Thomas, B., Donard, O. F. X., Lambert, C. E., Guillard, F. and Monaco, A., "Anthropogenic vs. Lithogenic Origins of Trace Elements (As, Cd, Pb, Rb, Sb, Sc, Sn, Zn) in Water Column Particles: Northwestern Mediterranean Sea," *Mar. Chem.,* Vol. 48, No. 3-4, 1995, pp. 291–310.

[90] Filby, R. H. and Olsen, S. D., "A Comparison of Instrumental Neutron Activation Analysis and Inductively Coupled Plasma-Mass Spectrometry for Trace Element Determination in Petroleum Geochemistry," *J. Radioanal. Nucl. Chem.,* Vol. 180, No. 2, 1994, pp. 285–294.

[91] Olsen, S. D., "Determination of Trace Elements in Petroleum Exploration Samples by Inductively Coupled Plasma Mass Spectrometry and Instrumental Neutron Activation Analysis," *Analyst,* Vol. 120, No. 5, 1995, pp. 1379–1390.

[92] Anderson R. A., Miekeley, N., Carmem L. P., Bezerra, M. and Carmem, M., "Determination of Organic Phosphorus in Oil Production Waters by ICP-AES and ICP-MS after Preconcentration on Silica-Immobilized C18," *Quimica Nova*, Vol. 21, No. 5, 1988, pp. 584–589.

[93] Korn, M. G. A., Sodre dos Santos, D. S., Welz, B., Vale, M. G. R., Teixeira, A. P., Lima, D. C. and Ferreira, S. L. C., "Atomic Spectrometric Methods for the Determination of Metals and Metalloids in Automotive Fuels - A Review," *Talanta,* Vol. 73, No. 1, 2007, pp. 1–11.

[94] Saint'Pierre, T. D., Dias, L. F., Pozebon, D., Aucelio, R. Q., Curtius, A. J. and Welz, B., "Determination of Cu, Mn, Ni and Sn in Gasoline by Electrothermal Vaporization Inductively Coupled Plasma Mass Spectrometry, and Emulsion Sample Introduction," *Spectrochim. Acta*, Vol. 57B, No. 12, 2002, pp. 1991–2001.

[95] Saint'Pierre, T. D., Dias, L. F., Maia, S. M. and Curtius, A. J., "Determination of Cd, Cu, Fe, Pb and Tl in Gasoline as Emulsion by Electrothermal Vaporization Inductively Coupled Plasma Mass Spectrometry with Analyte Addition and Isotope," *Spectrochim. Acta,* Vol. 59B, No. 4, 2004, pp. 551–558.

[96] Kowalewska, Z., Ruszczynska, A. and Bulska, E., "Cu Determination in Crude Oil Distillation Products by Atomic Absorption and Inductively Coupled Plasma Mass Spectrometry after Analyte Transfer to Aqueous Solution," *Spectrochim. Acta*, Vol. 60B, No. 3, 2005, pp. 351–359.

[97] Reimer, R. A. and Miyazaki, A., "Determination of Nickel and Vanadium in Commercial Gasolines and Crude Oil Reference Materials by Inductively Coupled Plasma Mass Spectrometry with Micro-emulsion Sample Introduction," *Anal. Sci.,* Vol. 9, No. 1, 1993, pp. 157–159.

[98] Nakamoto, Y. and Tokuyama R., "Metal Microanalysis in Petroleum Fractions by ICP-MS," *Idemitsu Giho,* Vol. 41, No. 5, 1998, pp. 457–463.

[99] Nadkarni, R. A. K., "Trace Levels of Sulfur in the Fuels of the Future: Analytical Perspective," ASTM STP 1468 (Elemental Analysis of Fuels and Lubricants), ASTM International, West Conshohocken, PA, 2005, pp. 85–97.

[100] Evans, P., Wolff-Briche, C. and Fairman, B., "High Accuracy Analysis of Low Level Sulfur in Diesel Fuel by Isotope Dilution High Resolution ICP-MS, using Silicon for

Mass Bias Correction of Natural Isotope Ratios," *J. Anal. At. Spectrom.,* Vol. 16, No. 9, 2001, pp. 964–969.

[101] Heilmann, J., Boulyga, S. F. and Heumann, K. G., "Accurate Determination of Sulfur in Gasoline and Related Fuel Samples using Isotope Dilution ICP-MS with Direct Sample Injection and Microwave-Assisted Digestion," *Anal. Bioanal. Chem.,* Vol. 380, No. 2, 2004, pp. 190–197.

[102] Boulyga, S. F., Heilmann, J. and Heumann, K. G., "Isotope Dilution ICP-MS with Laser-assisted Sample Introduction for Direct Determination of Sulfur in Petroleum Products," *Anal. Bioanal. Chem.,* Vol. 382(8), 2005, pp. 1808–1814.

[103] Bouyssiere, B., Leonhard, P., Proefrock, D., Baco, F., Lopez, G. C., Wilbur, S. and Prange, A., "Investigation of the Sulfur Speciation in Petroleum Products by Capillary Gas Chromatography with ICP-Collision Cell-MS Detection," *J. Anal. At. Spectrom.,* Vol. 19, No. 5, 2004, pp. 700–702.

[104] Heilmann, J. and Heumann, K. G., "Development of a Species-Specific Isotope Dilution GC-ICP-MS Method for the Determination of Thiophene Derivates in Petroleum Products," *Anal. Bioanal. Chem.,* Vol. 390, No. 2, 2008, pp. 643–653.

[105] Heilmann, J. and Heumann, K. G., "Development of a Species-Unspecific Isotope Dilution GC-ICPMS Method for Possible Routine Quantification of Sulfur Species in Petroleum Products," *Anal. Chem.,* Vol. 80, No. 6, 2008, pp. 1952–1961.

[106] Lopez, L. and Monaco, S. L., "Geochemical Implications of Trace Elements and Sulfur in the Saturate, Aromatic and Resin Fractions of Crude Oil from the Mara and Mara Oeste Fields, Venezuela," *Venez. Fuel,* Vol. 83, 2004, pp. 365–374.

[107] Hegazi, A. H., Andersson, J. T., Abu-Elgheit, M. A. and El-Gayar, M. S., "Utilization of GC/AED for Investigating the Effect of Maturity on the Distribution of Thiophenic Compounds in Egyptian Crude Oils," *Polycyclic Aromat. Compd.*, Vol. 24, 2004, pp. 123–134.

[108] Kahen, K., Strubinger, A., Chirinos, J. R. and Montaser, A., "Direct Injection High Efficiency Nebulizer-Inductively Coupled Plasma Mass Spectrometry for Analysis of Petroleum Samples," *Spectrochim. Acta*, Vol. 58B, No. 3, 2003, pp. 397–413.

[109] Andersson, J. T., Hegazi, A. H. and Roberz, B., *Anal. Bioanal. Chem.,* Vol. 386, 2006, pp. 891–905.

[110] Chaudhary-Webb, M., Paschal, D. C., Elliott, W. C., Hopkins, H. P., Ghazi, A. M., Ting, B. C. and Romieu, I., "ICP-MS Determination of Lead Isotope Ratios in Whole Blood, Pottery, and Leaded Gasoline: Lead Sources in Mexico City," *At. Spectrosc.,* Vol. 19, No. 5, 1998, pp. 156–163.

[111] Martinez, T., Lartigue, J., Juarez, F., Avila-Perez, P., Marquez, C., Zarazua, G. and Tejeda, S., "206Pb/207Pb Ratios in Dry Deposit Samples from the Metropolitan Zone of Mexico Valley," *J. Radioanal. Nucl. Chem.,* Vol. 273, No. 3, 2007, pp. 577–582.

[112] O'Conner, G., Ebdon, L. and Evans, E. H., "Qualitative and Quantitative Determination of Tetraethyllead in Fuel using Low Pressure ICP-MS," *J. Anal. At. Spectrom.,* Vol. 14, No. 9, 1999, pp. 1303–1306.

[113] Kim, A. W., Foulkes, M. E., Ebdon, L., Hill, S. J., Patience, R. L., Barwise, A. G. and Rowland, S. J., "Construction of a Capillary Gas Chromatography Inductively Coupled Plasma Mass Spectrometry Transfer Line and Application of the Technique to the Analysis for Alkyllead Species in Fuel," *J. Anal. At. Spectrom.,* Vol. 7, No. 7, 1992, pp. 1147–1149.

[114] Botto, R. I., "Determination of Elemental 'Bad Actors' (As, Hg and Si) in Petrochemical Samples Using ICP-AES and ICP-MS," Paper W 07, *Winter Conference on Plasma Spectrochemistry*, Tucson, AZ, 2006.

[115] Botto, R. I., "Trace Element Analysis of Petroleum Naphthas and Tars using Direct Injection ICP-MS," *Can. J. Anal. Sci. Spectros.,* Vol. 47, No. 1, 2002, pp. 1–13.

[116] Bettinelli, M., Spezia, S., Baroni, U. and Bizzarri, G., "Determination of Trace Elements in Fuel Oils by Inductively Coupled Plasma Mass Spectrometry after Acid Mineralization of the Sample in a Microwave Oven," *J. Anal. At. Spectrom*., Vol. 10, No. 8, 1995, pp. 555–560.

[117] Lachas, H., Richaud, R., Herod, A. A., Dugwell, D. R. and Kandiyoti, R., "Determination of Trace Elements by Inductively Coupled Plasma Mass Spectrometry of Biomass and Fuel Oil Reference Materials using Milligram Sample Sizes," *Rapid Commun. Mass Spectrom.,* Vol. 14, No. 5, 2000, pp. 335–343.

[118] Baernthaler, G., Zischka, M., Haraldsson, C. and Obernberger, I., "Determination of Major and Minor Ash-Forming Elements in Solid Biofuels," *Biomass Bioenergy*, Vol. 30, No. 11, 2006, pp. 983–997.

[119] Saint'Pierre, T. D., Tormen, L., Frescura, V. L. A. and Curtius, A. J., "The Development of a Method for the Determination of Trace Elements in Fuel Alcohol by ETV-ICP-MS using Isotope Dilution Calibration," *Talanta,* Vol. 68, No. 3, 2006, pp. 957–962.

[120] Saint'Pierre, T. D., Tormen, L., Frescura, V. L. A. and Curtius, A. J., "The Direct Analysis of Fuel Ethanol by ICP-MS using a Flow Injection System Coupled to an Ultrasonic Nebulizer for Sample Introduction," *J. Anal. At. Spectrom*., Vol. 21, No. 11, 2006, pp. 1340–1344.

[121] Woods, G. D. and Fryer, F. I., "Direct Elemental Analysis of Biodiesel by Inductively Coupled Plasma-Mass Spectrometry," *Anal. Bioanal. Chem*., Vol. 389, No. 3, 2007, pp. 753–761.

[122] Saint'Pierre, T. D., Tormen, L., Frescura, L. A. and Curtius, A. J., "The Direct Analysis of Fuel Ethanol by ICP-MS using a Flow Injection System Coupled to an Ultrasonic Nebulizer for Sample Introduction," IL 23 in *Winter Conference on Plasma Spectrochemistry,* Temecula, CA, 2008.

[123] Kingston, H. M., Huo, D., Lu, Y. and Chalk, S., "Accuracy in Species Analysis: Speciated Isotope Dilution Mass Spectrometry (SIDMS) Exemplified by the Evaluation of Chromium Species," *Spectrochim. Acta,* Vol. 53B, 1998, pp. 299–309.

[124] Paggio, A. A. del., Kamla, G. J., Forster, A. R. and Shepherd, M. A., "Characterization of Metal-Containing Molecules in Various Hydrotreated Atmospheric Tower Bottoms," *American Chemical Society, National Meeting*, Washington, D.C., August 26–31, 1990.

[125] Carey, J. M., Vela, N. P. and Caruso, J. A., "Multi-element Detection for Supercritical Fluid Chromatography by Inductively Coupled Plasma Mass Spectrometry," *J. Anal. At. Spectrom.,* Vol. 7, No. 8, 1992, pp. 1173–1181.

[126] Robert, J. M. and Spinks, C. D., "Separation of Metalated Petroporphyrin Models using Micellar Electrokinetic Capillary Chromatography," *J. Liq. Chromatogr.,* Vol. 20, No. 18, 1997, pp. 2979–2995.

[127] Rodriguez, I., Mounicou, S., Lobinski, R., Sidelnikov, V., Patrushev, Y. and Yamanaka, M., "Species-Selective Analysis by Microcolumn Multicapillary Gas Chromatography with Inductively Coupled Plasma Mass Spectrometric Detection," *Anal. Chem.,* Vol. 71, No. 20, 1999, pp. 4534–4543.

[128] Paszek, J., Mason, K. J., Mennito, A. S. and McElroy, F. C., "Advances in ICP-MS Technologies for Characterization and Ultra-trace Speciation as a Tool for the Petroleum Industry," *J. ASTM Intl.,* Vol. 2, No. 9, ASTM International, West Conshohocken, PA, 2005.

[129] McElroy, F. C., "Petroleum Analysis with Plasma Spectrometry," short course SA-08, *Winter Conference on Plasma Spectrochemistry,* Scotsdale, AZ, 1998.

[130] Miekeley, N., Pereira, R. C., Casartelli, E. A., Almeida, A. C. and Carvalho, M. de F. B., "Inorganic Speciation Analysis of Selenium by Ion Chromatography-Inductively Coupled Plasma-Mass Spectrometry and its Application to Effluents from a Petroleum Refinery," *Spectrochim. Acta,* Vol. 60B (5), 2005, pp. 633–641.

[131] Tao, H., Nakazato, T., Akasaka, M. and Satoh, S., "Speciation of Sulfur in Petroleum Liquids by Gas Chromatography/Inductively Coupled Plasma Mass Spectrometry," *Bunseki Kagaku*, Vol. 56, No. 5, 2007, pp. 333–347.

[132] Hwang, J. D., "Advances in ICP-AES and ICP-MS Technologies for Material Characterization in Petroleum Industry," Paper IL 10, *Winter Conference on Plasma Spectrochemistry,* Tucson, AZ, 2006.

[133] Hwang, J. D., "Trace Elemental Speciation by GC-ICP-MS," *Taiwan EPA Conference,* Tamsui, Taiwan, 1999.

[134] Varnes, A. W., "Applications of Atomic Spectroscopy in the Petrochemical Industry," *Spectroscopy,* Vol. 1, No. 11, 1986, pp. 28–33.

[135] McElroy, F., Mennito, A., Debrah, E. and Thomas, R., "Uses and Applications of Inductively Coupled Plasma Mass Spectrometry in the Petrochemical Industry," *Spectroscopy*, Vol. 13, No. 2, 1998, pp. 42–53.

[136] Li, J., Wu, L. and Ji, C., "Determination of Ultra-trace Rare Earth Elements in Petroleum by ICP-MS," *Yankuang Ceshi,* Vol. 17, No. 4, 1998, pp. 290–295.

[137] Kulkarni, P., Chellam, S. and Mittlefehldt, D. W., "Microwave-Assisted Extraction of Rare Earth Elements from Petroleum Refining Catalysts and Ambient Fine Aerosols prior to Inductively Coupled Plasma-Mass Spectrometry," *Anal. Chim. Acta,* Vol. 581, No. 2, 2007, pp. 247–259.

[138] Wondimu, T., Goessler, W. and Irgolic, K. J., "Microwave Digestion of 'Residual Fuel Oil' (NIST SRM 1634b) for the Determination of Trace Elements by Inductively Coupled Plasma-Mass Spectrometry," *Fresenius J. Anal. Chem.,* Vol. 367, No. 1, 2000, pp. 35–42.

[139] Woodland, S. J., Ottley, C. J., Pearson, D. G. and Swarbrick, R. E., "Microwave Digestion of Oils for Analysis of Platinum Group and Rare Earth Elements by ICP-MS," in *Plasma Source Mass Spectrometry: the New Millennium,* Royal Chemistry Society, Cambridge, UK.

[140] Takeda, K. and Arikawa, Y., "Determination of Rare Earth Elements in Petroleum by ICP-MS," *Bunseki Kagaku*, Vol. 54, No. 10, 2005, pp. 939–944.

[141] Yoshinaga, J., Yoneda, M., Morita, M. and Suzuki, T., "Lead in Prehistoric, Historic and Contemporary Japanese: Stable Isotopic Study by ICP Mass Spectrometry," *Appl. Geochem.,* Vol. 13, No. 3, 1998, pp. 403–413.

[142] Cocherie, A., Negrel, P., Roy, S. and Guerrot, C., "Direct Determination of Lead Isotope Ratios in Rainwater using Inductively Coupled Plasma Mass Spectrometry," *J. Anal. At. Spectrom,* Vol. 13(9), 1998, pp. 1069–1073.

[143] Barton, H., Zachwieja, Z., D'Ilio, S. and Caroli, S., "Application of Routine Estimation of Pb Isotopic Ratios by Inductively Coupled Plasma Mass Spectrometry for Studying the Pb Origin in Hair of Children Living in Polluted Areas: A Pilot Study," *Microchem. J.,* Vol. 67, No. 1–3, 2000, pp. 21–30.

[144] Yu, L. L., Kelly, W. R., Fassett, J. D. and Vocke, R. D., "Determination of Sulfur in Fossil Fuels by Isotope Dilution Electrothermal Vaporization Inductively Coupled Plasma Mass Spectrometry," *J. Anal. At. Spectrom.,* Vol. 16, No. 2, 2001, pp. 140–145.

[145] Begak, O. Y., Syroezhko, A. M. and Mendeleev, D. I., "Comparative Analysis of Petroleum Sludges of the Chernomortransneft Open-End Joint-Stock Company using a Set of Instrumental Methods of Analysis," *Khimicheskaya Promyshlennost,* Vol. 80, No. 2, 2003, pp. 79–86.

[146] Zhang, Y., Song, C., Cheng, C., Fan, G., Huang, Q. and Liu, P., "Analysis of Organic and Inorganic Components in Emission Particulates from Diesel Engine," *Ranshao Kexue Yu Jishu,* Vol. 10(3), 2004, pp. 197–201.

[147] Okada, S., Kweon, C. B., Stetter, J. C., Foster, D. E., Shafer, M. M., Christensen, C. G., Schauer, J. J., Schmidt, A. M., Silverberg, A. M. and Gross, D. S., "Measurement of Trace Metal Composition in Diesel Engine Particulate and its Potential for

Determining Oil Consumption: ICPMS (inductively coupled plasma mass spectrometer) and ATOFMS (Aerosol Time of Flight Mass Spectrometer) Measurements," Society of Automotive Engineers, SP-1737(CI Engine Combustion Processes & Performance with Alternative Fuels), 2003, pp. 59–72.

[148] Hausler, D. and Carlson, R., "Application of Plasma Spectrometry in the Petroleum Industry," *Spectrochim. Acta Reviews,* Vol. 14, No. 1-2, 1991, pp. 125–140.

[149] Kahen, K., Strubinger, A., Chirinos, J. R. and Montaser, A., "Direct Injection High Efficiency Nebulizer-Inductively Coupled Mass Spectrometry for Analysis of Petroleum Samples," *Spectrochim. Acta,* Part B, Vol. 58B, No. 3, 2003, pp. 397–413.

[150] Al-Swaidan, H. M. and Al-Gadi, A. A., "Detection of Lead and Vanadium as Trace Pollutants in Saudi Arabian Petroleum and its Products by SIA/ICP/MS," *J. Saudi Chem. Soc.,* Vol. 6, No. 1, 2002, pp. 1–6.

[151] Amorim, A. C., Welz, B., Costa, C. S., Lepri, F. G., Vale, M. G. R. and Ferreira, S. L. C., "Determination of Vanadium in Petroleum and Petroleum Products using Atomic Spectrometric Techniques," *Talanta,* Vol. 72, No. 2, 2007, pp. 349–359.

10

Atomic Fluorescence Spectrometry: An Ideal Facilitator for Determining Mercury and Arsenic in the Petrochemical Industry

Peter B. Stockwell[1]

INTRODUCTION

The author, in association with academic and industrial partners, has been developing analytical procedures and instrumentation using atomic fluorescence spectroscopy (AFS) to determine mercury at very low levels, especially in difficult matrices such as petrochemicals, for several years.

Speciation of the element forms is also important, and a system based on capillary gas chromatography (GC) AFS for mercury speciation in liquid condensates is described. Practical application of these analytical tools is presented.

References are also made to other applications of these powerful analytical techniques, which, in the hands of skilled analysts, give valid analytical results, traceable to international standards.

The presence of volatile arsenic compounds in natural gas was first identified as a problem in the late 1980s, when solid arsenic-containing residues in gas lines were leading to severe blocking of tubing and valves in a Mexican gas field. Delgado-Morales and coworkers [1,2] identified the residues as trialkyl sulfides, and Irgolic et al. [3] identified the source of these residues in the presence of volatile alkylarsines in the natural gas. Trimethylarsine (TMAs) was found to be the major volatile arsenic species, contributing 55–80 % of the total volatile arsenic in this natural gas, besides mixed methyl-ethyl-trialkylarsines and trietylarsine. It was not until almost 10 years later that Bouyssiere et al. [4] published a scientific paper on the identification of trialkylarsines in natural gas condensates. The major compound here was found to be triphenylarsine (TPhAs) along with triethylarsine and other, not further identified species.

Besides the issue of residue buildup, three major problematic areas have been identified regarding volatile arsenicals in natural gas: (a) environmental pollution caused by distribution of arsenic into the atmosphere through gas burning; (b) health and safety issues for workers in close contact with unprocessed gas during exploration and handling; and (c) the poisoning of catalysts during gas processing.

Currently, for the oil and gas producing industry, the major issue is to determine the total arsenic load in the natural gas and related products, i.e., the total arsenic burden in the combined gaseous and liquid (condensate) phases. Therefore it is necessary to determine the arsenic load in both the gaseous and the gas condensate phases.

[1] *P S Analytical Ltd., Kent, United Kingdom*

Krupp and coworkers described the measurement of trimethylarsine in natural gas and its portioning into the various phases in some detail [5].

Mercury occurs naturally in trace amounts in natural gas and natural gas condensate [6–9]; although it is difficult to generalize, the typical mercury concentration in natural gas and natural gas condensate is between 1 and 200 μg m^{-3}. Mercury in natural gas condensate could be present in various forms (elemental, organometallic, and inorganic salt), depending on the origin of the condensates [10]. Knowledge of the total mercury content and the different species present in natural gas condensate is extremely important. First, mercury in most forms is highly toxic and, particularly when present as the organomercury species, is a cause of great environmental concern. Second, the damage caused to industrial plants, particularly petrochemical plants, by the presence of mercury species can be financially crippling, especially when unscheduled shutdowns are forced.

The implication of the effect of mercury in natural gas was not reported until 1973, when a catastrophic failure of an aluminum heat exchanger occurred at the Skikda liquefied natural gas plant in Algeria [9–11]. Subsequent investigations determined that mercury corrosion caused the failure. The source of mercury, however, was debated [9,12]. After similar plant failures in both western and far eastern gas fields, the full mercury problem was realized together with the multimillion pound cost implications.

A recent paper defined the problem: "At present it is not well known in which chemical forms mercury is present in natural gases and gas condensates and, in addition, methods for the determination of total mercury concentrations must be regarded to be of unproven reliability due to lack of adequate standard reference materials and poor accuracy" [13]. Although a number of workers have recently addressed this problem in terms of the speciation [14,15], there is still a need for the development of reliable quantitative approaches to total mercury determination in such samples.

ATOMIC FLUORESCENCE SPECTROMETRY INSTRUMENTATION

Atomic fluorescence is a spectroscopic process based on the absorption of radiation of a certain wavelength by an atomic vapor and subsequent radiational deactivation of the excited atoms toward the detection device. Both the adsorption and the subsequent atomic emission processes occur at wavelengths that are characteristic of the atomic species present. AFS is a very sensitive and selective method for determining a number of environmentally and biomedically important elements such as mercury, arsenic, selenium, bismuth, antimony, tellurium, lead, and cadmium.

The main types of atomic fluorescence are (a) resonance fluorescence, (b) direct line fluorescence, and (c) stepwise line fluorescence. Resonance fluorescence occurs when atoms absorb and re-emit radiation of the same wavelength; this is the predominant form of fluorescence measured by analytical chemists. These wavelengths can be different. Direct line fluorescence is obscured when an atom is excited from the ground state to a higher excited electronic state and then undergoes a direct radiational transition to a metastable level above the ground state. Stepwise line fluorescence occurs when the upper energy levels of the exciting and the fluorescence line are different. The excited

atoms may undergo deactivation, usually by collisions, to a lower excited state rather than return directly to the ground state.

The intensity of the fluorescence radiation depends on a number of factors: (a) the intensity of the excitation source, (b) the concentrations of the atoms, i.e., the atomizer, (c) the quantitative efficiency of the process (i.e., the ratio of the energy emitted in the fluorescence to the energy absorbed per unit time), and (d) the extent of any self-absorption in the atomizer. The fluorescence radiation is linearly dependent on the source radiation and the fluorescence quantum efficiency of the transition as long as saturation is avoided. If the atomic concentration is low, the fluorescence signal varies linearly against the total atomic concentration.

Atomic fluorescence, however, can suffer from some disadvantages, for example, quenching and interferences. Quenching occurs when excited atoms collide with other molecules in the atomization sources. Those processes are discussed in more detail by two good reviews [16,17], but the benefits in the hands of experienced technicians far outweigh these disadvantages.

As with other techniques, interferences are of two major types. Spectral interferences occur when lines in the source overlap lines in the matrix elements in the atomizer. Chemical interferences result from various chemical processes during atomization that reduce the population of free atoms. The basic layout of an AFS instrument is shown in Fig. 1; it is similar to atomic absorption spectrometry (AAS) except that the light source and detectors are placed at right angles.

A number of excitation sources have been used in AFS, primarily spectral line sources and continuous sources. Because the intensity of the fluorescence radiation is proportional to the exciting radiation, sources with a high radiance are required to achieve good sensitivity and wide linear dynamic range. The source should be simple and easy to use, have good short-term and long-term stability, and require a minimum of maintenance to obtain optimum performance. To determine the hydride-forming elements, specifically arsenic, the boosted discharge hollow cathode lamp (BDHCL) meets this requirement. These are commercially available, and this has contributed significantly to the availability of commercial AFS instruments. To determine mercury, a low-pressure mercury discharge lamp provides a simple, intense source. Most atomizers used for AFS are similar to those used in AAS or atomic emission spectrometry (AES). The basic requirement is for an efficient and rapid production of free atoms with minimal background noise, long residence time for the analyte in the optical path, and low quenching properties. In addition, ease of handling and economic cost of operations are also important. Quenching is very

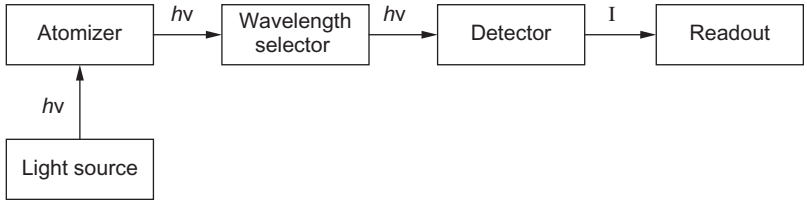

Fig. 1—Schematic diagram of an AFS instrument.

important in AFS, and to increase the sensitivity of the instrumentation, steps must be taken to minimize this effect.

For determining mercury, the atomizer is of less importance because mercury is atomic at room temperature, but for the hydride-forming elements, the design of the atomizer is of great importance. Mercury has a significant vapor pressure at room temperature, and it therefore can be measured without additional thermal energy. Mercury vapor produced by reduction of the metal from its compounds with a suitable reductant (sodium borohydride or tin (II) chloride) is swept out of the reaction vessel using an argon carrier gas and introduced into the optical beam where the mercury atoms can be excited by a suitable source, i.e., a mercury lamp. Corns et al. [18] have investigated different types of diffusion flame atomizers, primarily for arsenic measurements. They concluded that the AFS signals were optimal using an argon hydrogen flame. The atomization in the flame is not due to thermal decomposition but to free radicals in the flame.

In most AFS systems, wavelength selection is achieved using a filter located between the source and the detector. Representative schematic optical arrangements for mercury and the hydride-forming elements are shown in Fig. 2. Generally speaking, the AFS radiation is usually detected using a photo multiplier tube (PMT).

For any analytical procedure, several aspects of the cycle need to be addressed and controlled. Fig. 3 shows the processes involved. Without doubt the most important is the sampling itself so that a fully representative sample is taken which has not been compromised in any way or form.

For the determination of mercury and the hydride-forming elements, there are two fundamental parts of the measurement cycle. These are first the chemical process of generating the analyte in a vapor form and second the quantification of the analyte using a specific AFS instrument.

A schematic diagram of a continuous-flow vapor generator is shown in Fig. 4. The reductant, blank, and sample solutions are delivered by variable-speed, multichannel peristaltic pumps. An electronically controlled switching

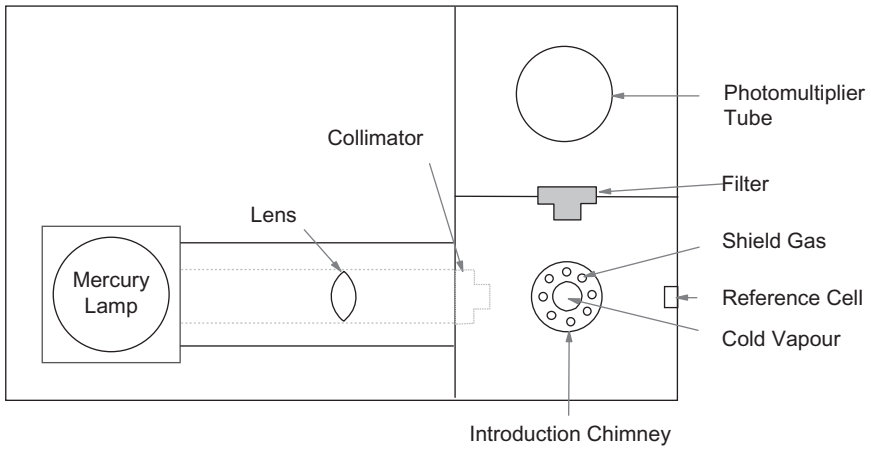

Fig. 2—Schematic diagram illustrating the optical configuration of an AFS system for mercury analysis. Taken from Ref [19].

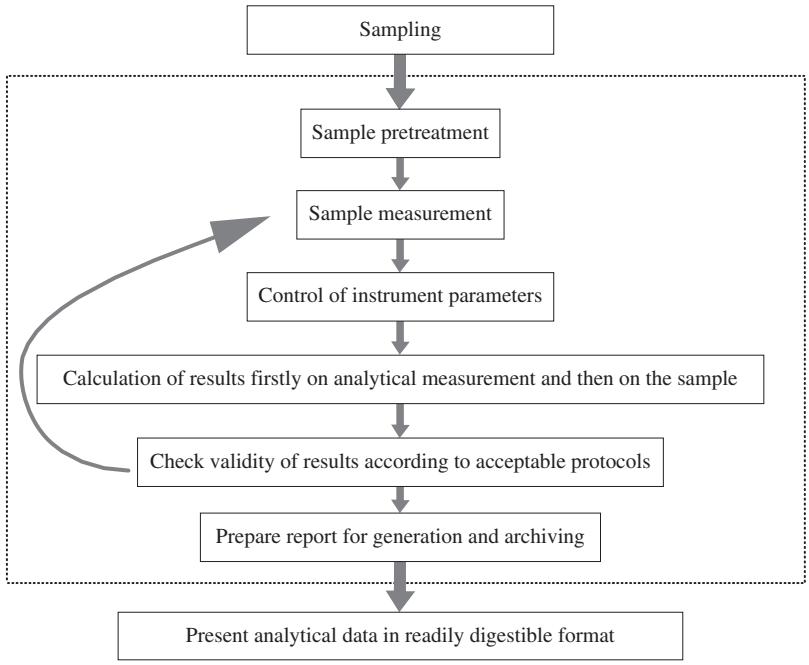

Fig. 3—The steps involved in analysis. Note: The steps enclosed within the dashed lines are normally under the control of the analyst. Those outside the dashed lines are not.

valve alternates between blank and sample solutions, and two of the liquid streams (reductant and sample or reductant and blank) are butt-mixed in the sample valve, where the reaction starts to occur. The streams and all gaseous products are continuously and rapidly pumped into a glass gas-liquid separator, from which the gaseous products are carried, by argon gas, through a dryer system, finally reaching the AFS detector.

The design of the AFS detector for mercury analysis is relatively simple owing to the absence of a thermally energized atomizer [20]. Generally, a UV mercury vapor lamp is used as excitation source and the fluorescence light is detected by a PMT, which is positioned perpendicular to the excitation source. In addition Fig. 4 illustrates the optical configuration of an AFS system [21].

A glass chimney is used to introduce mercury vapor into the optical path. The chimney is shielded with a high flow rate of argon; this retains the mercury in an acceptable flow path and acts as a gas cell to retain the mercury for measurement. A 253.7-nm interference filter is situated between the introduction chimney and the PMT to keep stray light away from the latter.

Because the system is used to determine total inorganic mercury (Hg^{2+}), the first requirement for performing the analysis is to liberate all mercury compounds from the sample matrices and convert all organic forms of mercury to Hg^{2+} by various digestion/oxidation procedures.

For natural water sample analysis, the previously employed hot oxidizing method using permanganate-peroxodisulfate has been found unsuitable for low-level mercury determination because of the high blanks found in these

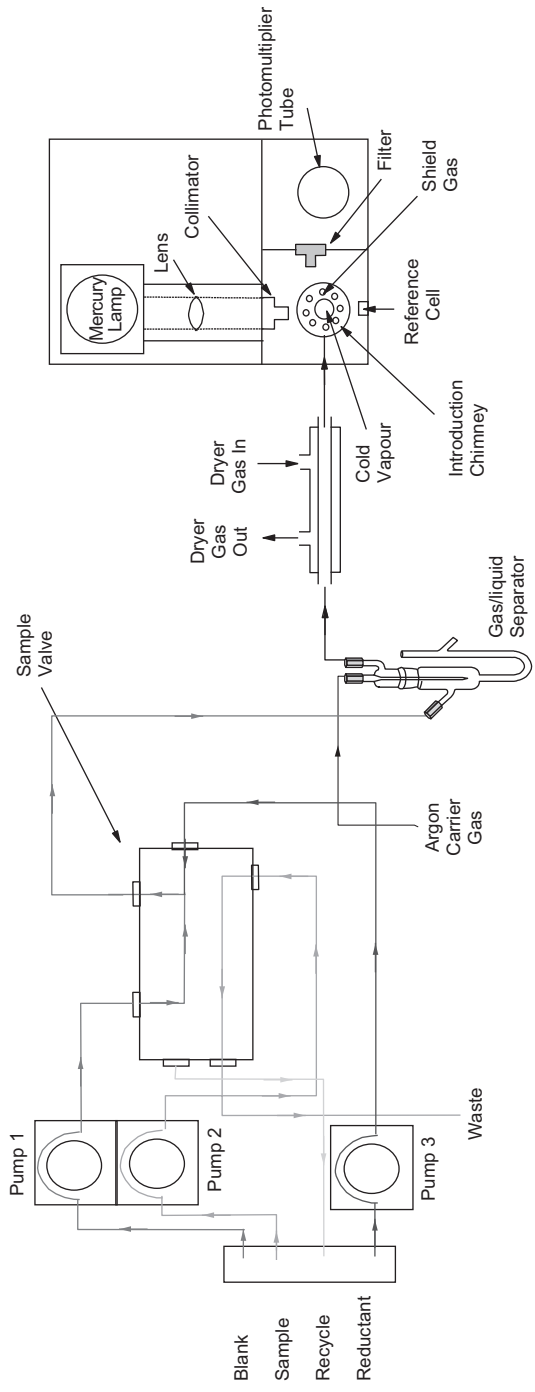

Fig. 4—Schematic diagram of the continuous flow vapor/hydride generator and illustrating the optical configuration of an AFS system for mercury analysis.

reagents [21]. Bromine monochloride has been found to be an excellent oxidant and preservative for total mercury in water samples [22], working faster and more efficiently on many organomercurials [21,22]. Hydroxylamine hydrochloride is added to destroy the excess bromine before analysis with cold vapor (CV)-AFS. This method has often been used for converting organic mercury to Hg^{2+} [23–28]. Once all forms of mercury have been converted to Hg^{2+}, the latter is reduced to elemental mercury (Hg^0) using either acidified or alkaline stannous chloride:

$$Hg^{2+} + Sn^{2+} \rightarrow Hg^0 + Sn^{4+} \quad (1)$$

The mercury vapor produced is carried by argon gas to the AFS instrument for detection.

Many environmentally important elements such as arsenic, selenium, bismuth, antimony, tellurium, germanium, tin, lead, and mercury can form volatile and covalent hydrides with "nascent" hydrogen. Hydride generation (HG) is a preferred technique when hydride-forming elements are to be analyzed by atomic spectrometry. The advantage of volatilization as a gaseous hydride clearly lies in the separation and enrichment of the analyte element and thus in a reduction or even complete elimination of interferences. Also, because the transfer of the vapor to the detector is extremely efficient, the detection levels (DLs) are consequently extremely low. The added advantage from this is should any interference be present at this stage further dilution is often possible to avoid these interferences.

Tsujii and Kuga in 1974 [29] were the first to describe HG coupled to nondispersive AFS. They reported a DL of 2 ng for arsenic analysis. Thompson in 1975 [30] was the first to apply a dispersive AFS system for determining arsenic, selenium, antimony, and tellurium after HG DLs using this system ranged from 0.06 to 0.1 μg L^{-1}.

Although various metal-acid reactions (e.g., Zn-HCI) have been used as a means of producing hydride, $NaBH_4$ is preferred as the reductant because the technique is easy to automate, since only solutions are involved, so that a high sample throughput can be achieved. Such a system is currently commercially available [31]. The design of this system is similar to that of the cold-vapor generation system used in CV-AFS for mercury analysis.

The schematic layout of the automated instrument to determine the hydride-forming elements is shown in Fig. 5. The optical configuration is similar in concept to that used for mercury analysis but makes use of a unique multireflectance filter to select the wavelengths of interest onto the photomultiplier (PMT) detector. This effectively provides a summation of the fluorescence lines for each element. The analyte that is measured is determined primarily by changing the excitation source, i.e., the boosted hollow cathode lamps. Commercially available lamps exist for all of the major elements required.

Once the hydride has been formed and driven out of the solution, it can be directly delivered by an inert gas such as argon to the atomizer where it is excited by a fluorescence light source and measured by a detector such as solar blind PMT.

As with any other technique, HG-AFS suffers from interferences. Welz [32] gave an extensive discussion about various interferences encountered in HG. However the sensitivity of the technique is such that it allows dilution of the

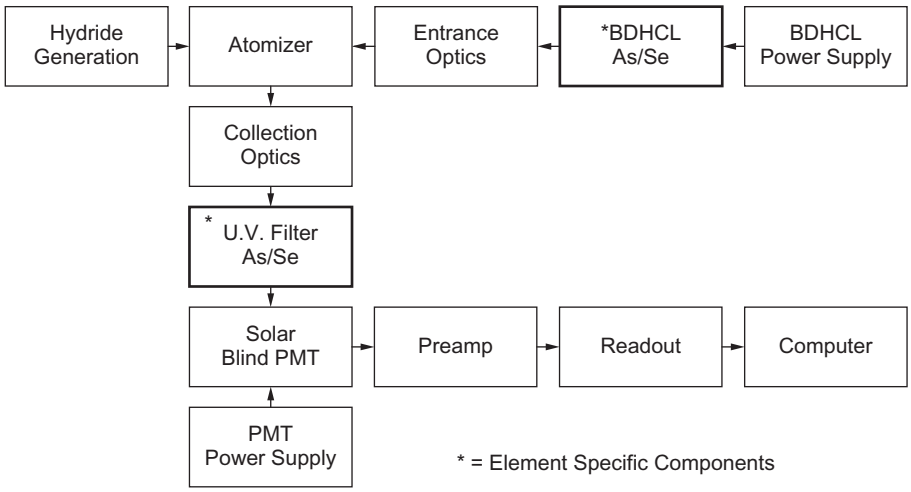

Fig. 5—Block diagram for an atomic fluorescence detector.

sample so that the interferences are reduced significantly. Spectral interference is not a problem for HG-AFS because the analyte element passes into the atomizer as gaseous hydride, and concomitants normally remain in the reaction vessel.

Several of the cited references refer to instrumentation that has been built in research departments–others have coupled commercially available AFS instruments to commercial chromatographic systems. To the author's knowledge, AFS instruments for analyzing mercury and some other elements are currently being manufactured by these companies: P S Analytical Ltd., Orpington, Kent, UK; Brooks Rand Inc., Seattle, WA; Tekran Inc., Ontario, Canada; Beijing Titan Instrument Co., Beijing; Rayleigh Analytical Instrument Corporation, East West Analytical Instruments, Beijing, and Beijing Kechuang Haiguang Instrument Co Ltd., all Chinese companies.

DETERMINATION OF MERCURY IN PETROCHEMICALS

In the petrochemical industry, the hydrocarbons present range from gaseous streams through to fully liquid streams, and it has been highlighted before that mercury can be present in all of these fractions. The techniques for determining the levels of mercury present and the strategies for its removal will be influenced by the form of these fractions. In addition, the safety requirements of any production site will also determine the construction of any process instrumentation. Determining mercury in these fractions requires unique approaches, particularly with respect to the need to provide a fully representative sample for the measurement stage.

Determination of Mercury in Natural Gas

Mercury-associated problems begin at each gas producing well. The investment required and the remote nature of well sites prohibit the installation of in situ mercury removal systems. As a result, mercury is introduced into the well-bore and gathering systems simply by the gas production. Mercury can also be

introduced accidentally by pressure testing equipment incorporating mercury type bellows.

As mercury accumulates in the pipelines, its concentration in the natural gas is reduced because of chemisorption onto the steel pipe walls. Leeper [6] suggests the following reactions for the reduction of mercury levels in a pipeline:

$$\begin{aligned} H_2S + Fe_2O_3 &\rightarrow 2FeO + S + H_2O \\ Hg + S &\rightarrow HgS \end{aligned} \tag{2}$$

Trace amounts of H_2S catalyze the reaction of mercury with the steel pipe. The mercurous sulfide precipitates and is adsorbed onto the pipe wall. Grotewold et al. [33] reported that for one 68-mile pipeline, the mercury concentration decreased from 50 to 20 μg m^{-3} along the length of the pipe. Pipe wall smoothness and adhesive forces influenced this reduction. Similar reductions are also experienced in pipes and vessels at the refineries and processing plants.

Other factors influence mercury distribution in flowing streams. Mercury can condense into the liquid phase of hydrocarbons and gas treating chemicals because of its higher solubility in higher molecular weight streams. In most gas processing installations there is a separation or dehydration stage. Grotewold et al. [33] reported that some 50–60 % of the inlet mercury accumulates at the bottom of the glycol absorber and that 15–20 % is separated in the scrubbers, leaving 20–35 % to enter the plant and pass down into the stream processing equipment or transportation pipelines or both.

Mercury has been found to be responsible for many cases of selective hydrogenation catalyst deactivation. Palladium-based catalysts are commonly used for the selective hydrogenation of actetylenic species in the steam cracking of C_2 to C_4 cuts.

Low levels of mercury can be present in a wide range of boiling points in a steam cracker feed condensate. During the cracking process the mercury is concentrated into the lighter fractions of the cracker effluent. For example, one particular European petrochemical manufacturer using a North African condensate had the cycle length of the C_3 hydrogenation catalyst shortened from the expected lifetime of 1,000 days down to just 30 days. The mercury content of the cracker feed was found to be less than 60 μg kg^{-1}, which can cause sintering of the palladium catalyst. The deactivation of the catalyst along with its shorter lifetime was also accompanied by the subsequent contamination of the catalyst regeneration gas [34].

Mercury is known to be the cause of corrosion problems with aluminum-based heat exchangers, rotors, and condensers at natural gas refinery plants. Nelson reported that in 1994 at least seven heat exchangers in service were operating with mercury-induced leaks [35]. Heat exchanger replacement is a costly operation because of the capital investment of the exchanger itself and the plant downtime incurred for its replacement. Two types of mercury-induced corrosion are known: mercury-induced stress cracking and mercury-catalyzed oxidation of aluminum by water.

Aluminum is the predominant choice for cryogenic service owing to its brazeability, excellent mechanical properties at low temperatures, and superior heat transfer characteristics. Brazed aluminum heat exchangers are known to be composed of a magnesium-rich phase at the metal grain boundaries. The

presence of this phase at the grain boundaries is due to its precipitation during welding. When liquid mercury is brought into contact with this anodic phase, dissolution occurs by the following reaction:

$$4Hg + Al_3Mg_2 \rightarrow 2MgHg_2 + 3Al \quad (3)$$

The dissolution of the grain boundary is rapidly accelerated if any stress is applied to the attacked region. Stress cracking occurs by the propagation of a crack from the point of mercury attack on the magnesium-rich phase through the connecting grain boundaries. Laboratory testing can consistently produce liquid metal embrittlement in aluminum 5083 welds with as little as 47 mg of mercury [36]. Fig. 6 shows a photograph of a typical weld crack caused by liquid mercury embrittlement; this is the most common type of mercury corrosion and does not require the presence of water.

The oxidation of aluminum by water is a highly exothermic process. However, this reaction does not normally proceed because of the formation of a protective layer of aluminum oxide on the external surface of aluminum. Small fissures in this protective layer render the clean metal surface susceptible to local oxidation by water. When metallic mercury is present on the clean metal surface, aluminum diffuses from the mercury aluminum interface into the mercury droplets and is rapidly converted to Al_2O_3 on the outer surface of the droplets. By this mechanism, metallic mercury bores holes into the aluminum surface, leaving "whiskers" of grey Al_2O_3.

$$2AlHg + 6H_2O \rightarrow 2Al(OH)_3 + 3H_2 + 2Hg \quad (4)$$

Operating conditions conducive to corrosion of cryogenic aluminum heat exchangers include derimming and shutdown. Derimming is a heat cycle process on the exchangers that removes "frost" (ice, hydrates, and solid carbon dioxide) buildup from exchanger internals. To melt the frost, the exchanger is normally taken off line and hot dry gas passed through the unit. The hot gas melts the frost and purges out moisture and impurities. Derimming is periodically necessary to improve exchanger efficiencies due to frost accumulation. Shutdown occurs when no gas is passed through the system, heat exchange can no longer take place, and the exchanger is warmed to ambient temperatures.

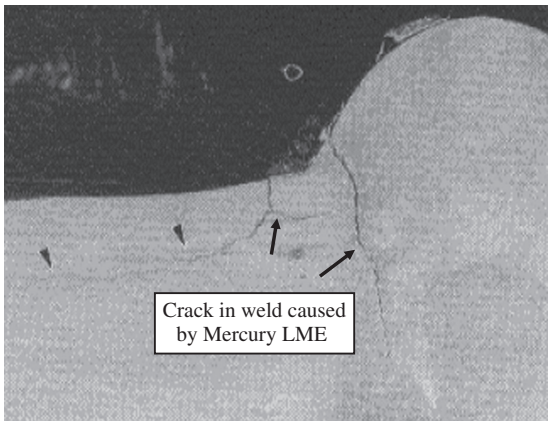

Fig. 6—Photograph of a typical weld crack caused by liquid mercury embrittlement.

The metal corrosion rate can be reduced if the temperature is maintained below the melting point of mercury, i.e., −39°C [37].

Derimming and shutdown frequency should be kept as low as possible to minimize the potential for a corrosive environment. Liquid water can be present during both of these operations. When the thaw gas is passed through the exchanger or when operations are resumed, gas containing trace amounts of mercury are allowed into contact with the aluminum in an aqueous environment so that mercury-induced stress cracking can take place.

Mercury Sampling Techniques for Natural Gas

Before the introduction of specific mercury measurement systems for natural gas, mercury was conventionally determined in one of three ways:

1. The gas sample is collected in a sample bomb for later analysis.
2. The gas can be pressure regulated to pass into a trapping solution.
3. The gas stream can be pressure regulated to pass directly over a sample collection trap.

In each case the sampling point should be representative of the gas being analyzed; this should therefore consider Joules-Thompson effects of adiabatic gas expansion and temperature inversion.

A typical pressure-temperature phase envelope for a dry natural gas sample is shown in Fig. 7. Phase diagrams are frequently used to predict the temperature required to keep the natural gas above the dew point and prevent hydrocarbon condensation. It can be seen that on decreasing the pressure from approximately 100 bar to 1 bar, the associated adiabatic temperature drop leaves the gas −30°C. This is below the dew point of the heavier hydrocarbon cuts, resulting in condensation from the gaseous to the liquid phase.

As the pressure is decreased, heavy hydrocarbon cuts are released from the vapor phases and condense as a liquid. Heavy hydrocarbons condensing on the collection medium have been shown to reduce the collection efficiency, thereby giving low results [12].

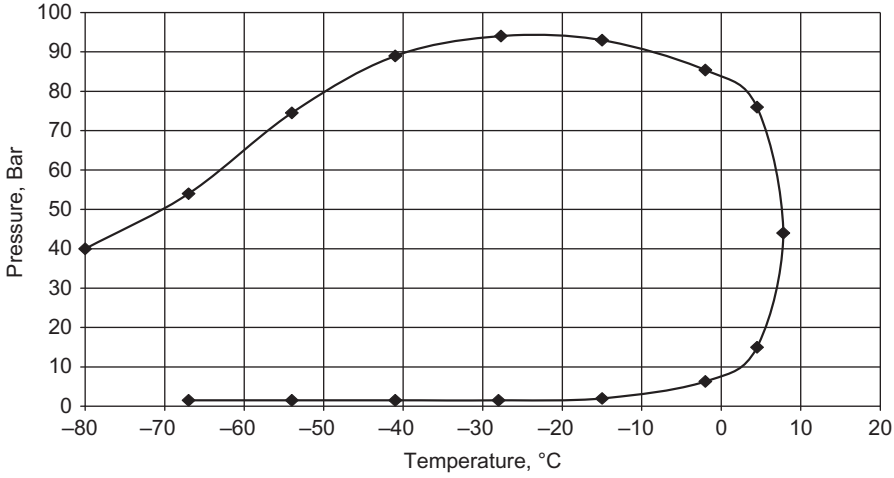

Fig. 7—Phase envelope diagram for a typical export North Sea natural gas sample.

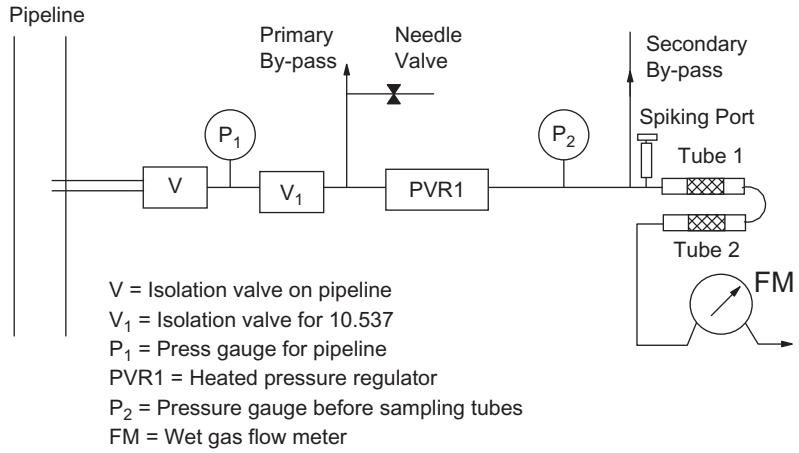

Fig. 8—Schematic diagram of a sampling system for the determination of mercury in natural gas.

To obtain a representative sample gas from a high-pressure gas stream, the use of heated regulators and heated sample transfer lines is necessary during the pressure letdown stage. In this way the sample gas at ambient pressures will have the same composition as that at the higher operating pressure. Losses of mercury by surface adsorption on stainless steel components can greatly affect results. To overcome these effects, it was found that a high flow rate primary bypass for the sample was required.

Given the above-mentioned sampling difficulties, the author developed an offline sampling device to ensure that a representative sample is collected. This is shown schematically in Fig. 8. The unit has been designed to operate in hazardous areas with appropriate components. This enables the samples to be collected at the pipeline and therefore minimizes any contamination or losses often found when high-pressure polytetrafluoroethylene (PTFE) lined cylinders have been used.

TABLE 1—Conditions for Offline Sampling Apparatus

Apparatus	PSA 10.537
Pressure Reduction (P2)	15 psi
Primary Bypass Flow Rate	> 30 L min^{-1}
Secondary Bypass Flow Rate	1.5 L min^{-1}
Sample Flow Rate	> 0.5 L min^{-1}
Vent Pressure	Atmospheric
Temperature of PVR1	150°C
Temperature of Sampling Tubes	140°C

TABLE 2—Collection Efficiency of Mercury Compounds on Gold Trap

Flow Rate (L min^{-1})	Hg^0	$HgCl_2$	$(CH_3)_2Hg$	CH_3HgCl	$(C_2H_5)_2Hg$	C_2H_5HgCl
1.0	99.8 ± 0.3	99.3 ± 0.4		99.9 ± 0.4	99.7 ± 0.4	98.8 ± 0.6
2.5	101.0 ± 0.6	99.7 ± 0.6	99.7 ± 0.5	99.1 ± 0.6	100.3 ± 0.6	99.1 ± 0.7
5.0	99.9 ± 0.5	99.8 ± 0.4	99.5 ± 0.4	100.7 ± 0.8	99.9 ± 0.4	99.9 ± 0.3

The conditions of operations are outlined in Table 1. To overcome condensation of hydrocarbons on the sampling tube, the adsorbent is maintained at 140°C, which is well above the dew point of the hydrocarbon gas. The trapping efficiency of the Amasil™ tube was studied by Dumarey et al. [38] for a wide range of mercury compounds, and in all cases excellent trapping efficiency was obtained. These results are summarized in Table 2.

The sample collection tube can be used at elevated temperatures of up to 200°C without breakthrough. This enables reliable collection of mercury from wet natural gas streams. Table 2 shows the collection efficiency of mercury compounds using Amasil. Table 3 summarizes the collection efficiency of elemental mercury at elevated temperatures. Excellent recoveries were obtained even up to 210°C.

Mercury Analyzer

The instrumentation operates on the principle of dual amalgamation coupled to atomic fluorescence spectrometry. A schematic diagram illustrating the automated thermal desorption arrangement is shown in Fig. 9. Before sampling, the sampling tubes are cleaned to give a reproducible blank.

The clean sample tubes are then taken to the sampling point and inserted into the sample tube furnace. The natural gas is then passed over the tube until a sufficient volume of gas has passed over the tube for reliable quantification. The detection limit for the instrumentation is 0.1 pg, which equates to 1 ng/m^3 for a 10 L sample volume. The upper working range is 300 $\mu g/m^3$. The wide linear dynamic range of the Sir Galahad allows relatively small sample volumes to be collected thus minimizing the time required for sampling. Typical results from a European gas plant showing the concentration of mercury in export natural gas are shown in Table 4. The reproducibility was typically better than 4 % relative standard deviation (RSD). The system has been used on various gas refineries around the world and has become invaluable when monitoring the efficiency of mercury removal units [39]. Fig. 10 shows an example of a gas plant in Europe with an average concentration of 516 $\mu g/m^3$ for the inlet gas. The gas plant uses a commercial mercury removal unit based on activated carbon impregnated with sulfur. The concentrations were reduced dramatically after the first removal tower, and after a second removal system the average concentration was found to be less than 8 ng/m^3, which is considered to be a sufficiently low concentration to operate the aluminum heat exchanger without damage.

Determination of Total Mercury in Liquid Hydrocarbons

Before the introduction of the technology described here, the determination of total mercury in condensate was based on treatments and digestion with

TABLE 3—Collection Efficiencies at Elevated Temperature for Elemental Mercury Vapor

Temperature (°C)	Percent Recovery (%)
30	97 ± 2
50	98 ± 3
80	100 ± 4
100	99 ± 3
120	100 ± 2
150	105 ± 3
160	103 ± 2
180	101 ± 2
200	98 ± 4
210	101 ± 3

oxidizing solutions [12,13,40,41] or high temperature reaction with air or oxygen before determination by a spectrometric detector [13,42]. These methods of treatment require large amounts of reagents and procedures that are often complicated and time consuming, increasing the risk of analytical errors and deteriorating detection limits through high and variable blank levels [12,13].

Unlike the gas condensate samples, the determination of total mercury in natural gas itself can be carried out accurately to very low detection limits by collecting the species on special gold impregnated silica traps. The mercury species adsorbed on the gold trap can be released by heating to high temperatures (about 900°C), and these are then swept through into a commercially available atomic fluorescence detector by argon gas [43,44]. However, trapping by this method has some restrictions. In the presence of heavier hydrocarbons

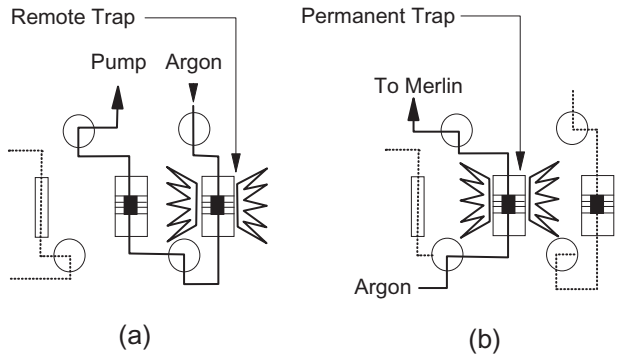

Fig. 9—Analysis cycle.

TABLE 4—Determination of Mercury in Export Natural Gas

Sample Reference	Gas Volume (L)	Tube No.	ng Hg/Tube	ng Hg/Tube Blank Corrected	ng Hg/Sample	μg Hg/m^3	Mean μg/m^3
Export Gas (V4500)	1.53 (T = 19°C)	1 2	41.88 2.897	41.38 2.293	43.673	28.54	27.89 ± 1.12
Export Gas (V4500)	1.53 (T = 19°C)	1 2	42.59 2.056	42.04 1.644	43.684	28.55	RSD = 4 % (n = 3)
Export Gas (V4500)	1.53 (T = 19°C)	1 2	38.79 2.738	38.43 2.255	40.685	26.59	
Export Gas (V4100)	1.52 (T = 22°C)	1 2	45.2 2.182	44.83	46.135	30.35	29.77 ± 0.71
Export Gas (V4100)	1.51 (T = 23°C)	1 2	42.63 2.103	42.29 1.465	43.755	28.98	RSD = 2.4 % (n = 3)
Export Gas (V4100)	1.5 (T = 25°C)	1 2	44.98 1.438	44.108 0.873	44.981	29.99	

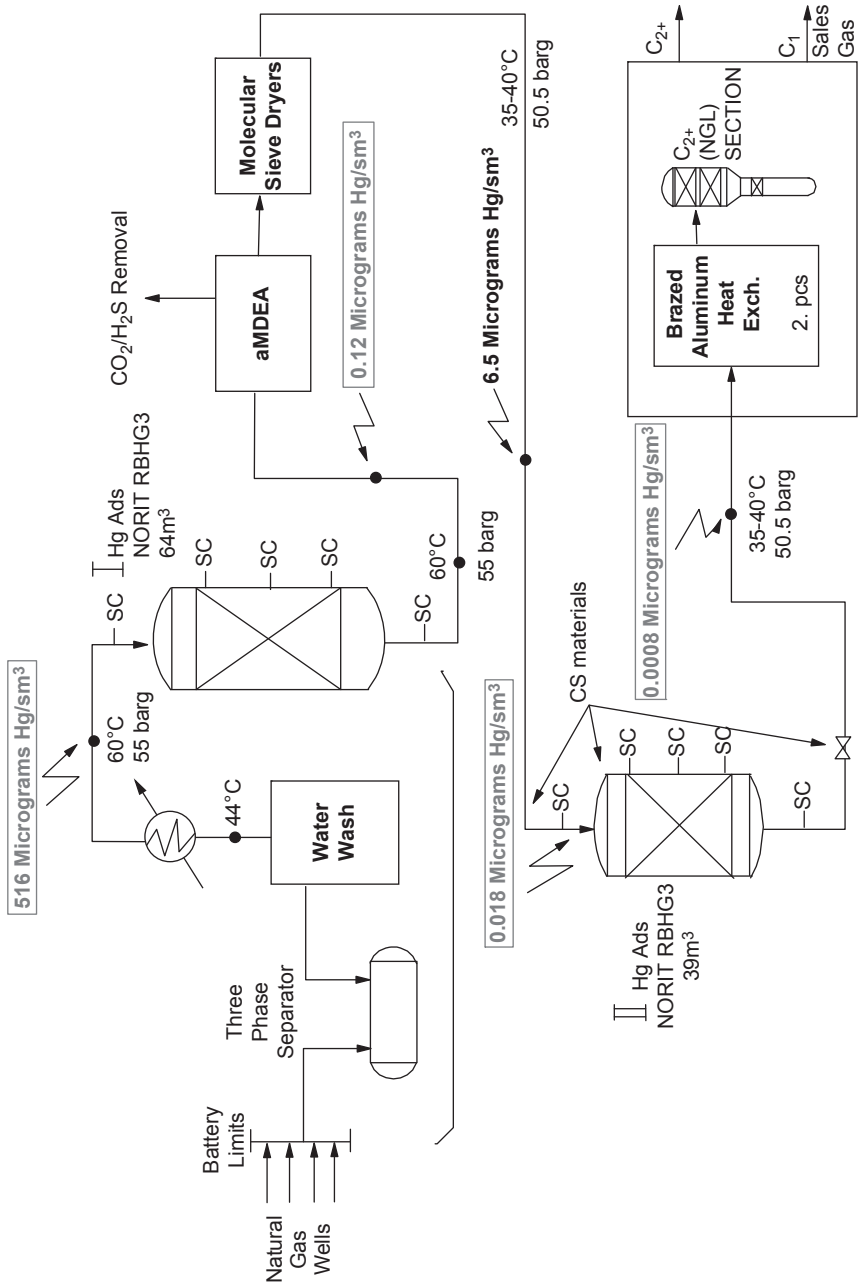

Fig. 10—Schematic of European gas plant showing mercury concentrations.

and wet conditions, the collection efficiency of the adsorbent may be affected. It was reported that the adsorption efficiencies could be sustained quantitatively by keeping the trap (Au/Pt) at 80°C to prevent condensation on the amalgamating surface. It was reported, for example, that elemental mercury was collected with 100 % efficiency. However, only 50 % dimethylmercury was recovered from the gas matrix [12]. This could give rise to errors when the mercury is present in different forms.

In this work the author sought to utilize the excellent sensitivity of AFS for determining mercury while addressing the matrix interference and species-dependent recovery problems highlighted previously. Figs. 11a and 11b show the schematic arrangement that was designed to quantitatively determine all forms of mercury in liquid condensates.

An accurately measured volume of sample (0.25 mL) was injected using a gas-tight syringe (Dynatech Precision, Baton Rouge, Louisiana) into a specially constructed vaporization chamber held at 400°C. Normally 5–10 minutes were required to vaporize the sample completely. The vapor generated was continuously swept by argon gas at between 300 and 400 mL min^{-1} through to a heated trap maintained at 200°C. The sample matrix (paraffins, aromatics, and naphthanes) was consequently carried in its vapor phases away from the trap and directed to a waste collector.

The mercury adsorbed on the trap was then released as elemental mercury by heating to 900°C and swept through to a second tube, which was subsequently analyzed by dual-amalgamation AFS that was described earlier. Schematic diagrams of the sequence of events for vaporization and collection are shown in Figs. 11a and 11b, respectively. The instrumental conditions are outlined in Table 5.

Calibration was based against elemental mercury for all species. The calibrations relied on the knowledge that at a fixed temperature, the saturated vapor pressure of mercury is known and a fixed volume of vapor will contain a known quantity of mercury. This volume was injected and adsorbed on the Amasil trap and then revaporized into the detector where the peak response was measured. Once the values of temperature and volume are known, the absolute quantity of mercury adsorbed on the trap can be calculated [45].

Elemental mercury can be used to calibrate the system for all species of mercury that can be present in gas condensate.

The stability of mercury adsorbed on the Amasil trap was evaluated by carrying out calibrations at room temperature and 200°C. The results, shown in Fig. 12, indicate that at 200°C the mercury calibration is both stable and quantitative.

Recovery experiments based on the standard additions technique, together with condensate sample analyses (various condensate fractions, oils, etc.) showed that the procedure was fit for the purpose. The performance of the trap in holding the mercury species (bleed-off effects) at 200°C was investigated. The sample (0.25 mL) containing 20 ng mL^{-1} of a mercury species was vaporized and swept through the trap using an argon gas flow (350 mL min^{-1}) using various collections times from 5 minutes to 1 hour. The results showed that no significant bleeding occurred up to 30 minutes (96–103 %) recovery and that the trap was capable of holding the mercury species at 200°C. It was observed that the traps did not suffer from memory effects, and the lifetime of a trap was also improved because of the higher trapping temperatures employed (200°C).

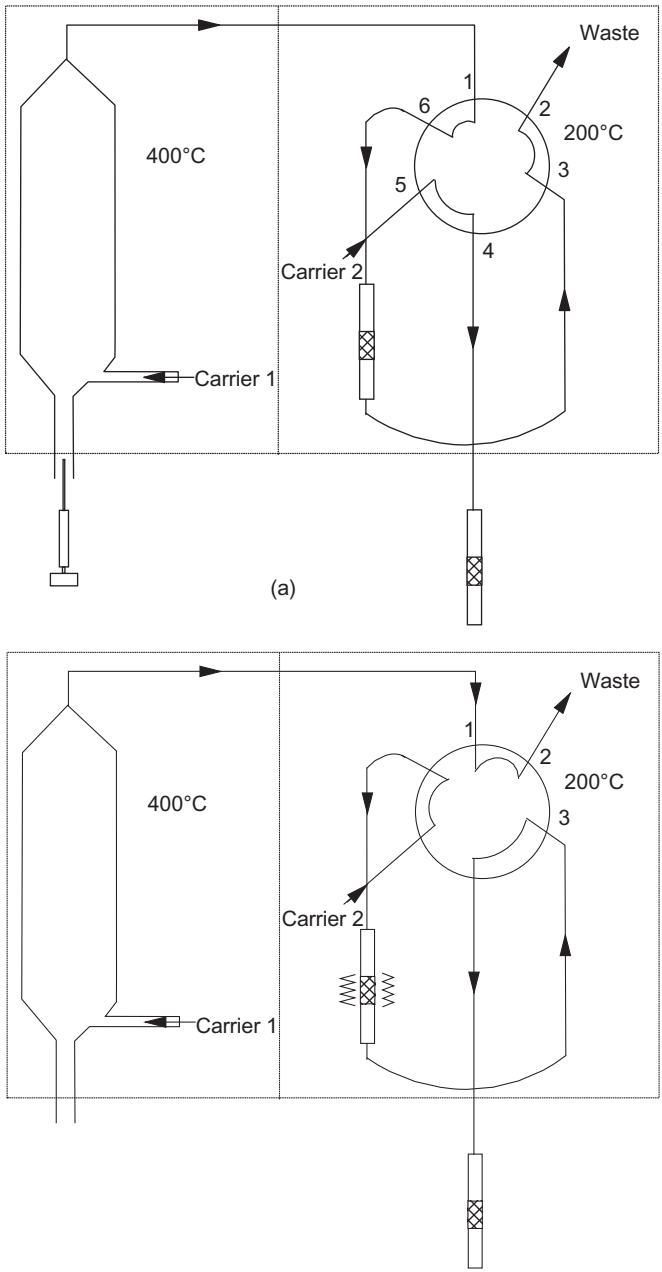

Fig. 11—(a) Sample injection and collection of mercury; (b) Thermal desorption cycle.

Recovery Performance of DMM and DPM Added to Toluene

The total mercury content of a toluene sample (control) was determined. The sample was vaporized at 400°C and the vapor was trapped at 200°C before desorption for mercury determination by the AFS detector. The analyses were

TABLE 5—Operating Conditions for Vaporization of Hydrocarbons

Condition	Value
Vaporization chamber temperature	400°C
Vaporization time	5–10 min
Argon carrier flow rate for vaporization	300–400 mL min^{-1}
Argon flow rate for detector	400 mL min^{-1}
Detector sheath gas flow rate	400 mL min^{-1}
Flushing time	30 s
Vaporization time	15 s
Vaporization temperature	900°C
Cooling period	2 min

conducted by injecting different sample volumes via the septum into the vaporization chamber. The mercury content in the toluene blank was found to be 2.0 ± 0.3, 2.4 ± 0.2, and 3.4 ± 0.4 ng mL^{-1} for volumes of 0.1, 0.25, and 0.5 mL, respectively (not corrected for the mercury contribution from the sweep gas). Dimethylmercury (DMM) and diphenylmercury (DPM) (50 ng mL^{-1} as mercury), when spiked into toluene and when different volumes were injected, indicated that the recovery was reduced by about 20 % if the sample injected was increased from 0.25 to 0.5 mL.

A volume of 0.25 mL was chosen for three reasons:

1. Representative sampling improved precision.
2. For the species, 85–90 % recovery was obtained.
3. The sensitivity of the system could be matched without saturating the gold trap sites with matrix during adsorption (competitive exclusion).

This recovery effect, which was dependent on the sample volume injected, was removed when a double-sized gold trap was employed. Up to 1.0 mL of sample gave the same recovery for the species as that of a 0.25 mL injection. These results are shown in Fig. 13. It is important to note that the increase in

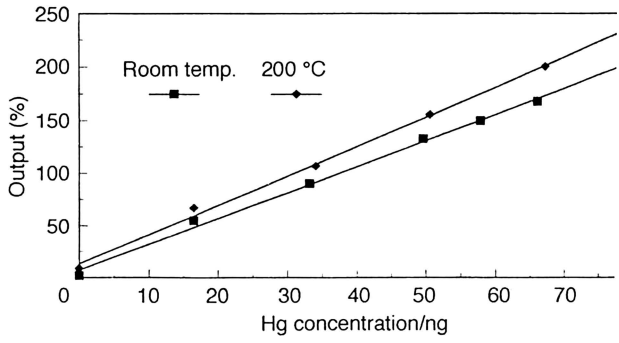

Fig. 12—Stability of calibration curve with temperature.

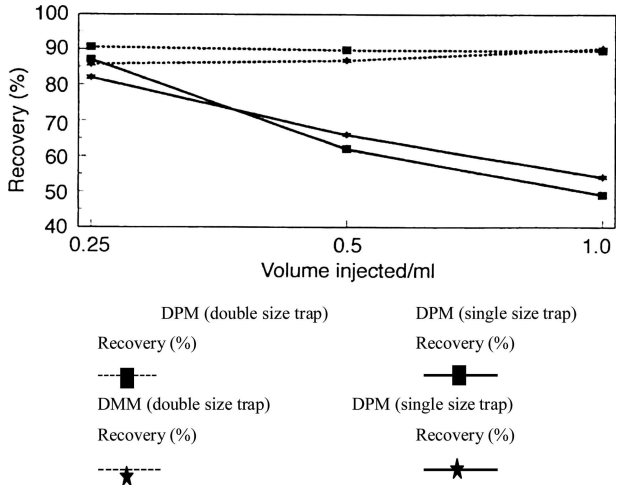

Fig. 13—Comparison of recovery performance between single- and double-sized traps for different sample volumes injected.

sample volume requires a longer vaporization period; hence a longer trapping time is needed. A correction for the mercury present in the argon carrier gas must therefore be made alongside any solvent blank contribution.

Recoveries for Mercury Species Added to Condensate Sample

The recovery of mercury species spiked into "real" gas condensate samples was evaluated. Two commercial gas condensate samples labeled GC1 and GC2, light gas condensates from different sites, were used. The final boiling points were in the range of 250–270°C. As with the toluene sample, the vaporization temperature used was 400°C, which was sufficient to vaporize the sample completely within 5 minutes.

Seven species of mercury—DMM, DEM, methylmercurychloride (MMC), ethylmercury (EMC), DPM, phenylmercurychloride (PMC), and mercurychloride (MC)—were spiked individually at difference concentrations, 10, 30, and 50 ng mL^{-1} (as mercury) into real gas condensates. For each experiment the total mercury content of the condensate samples was determined to be used for correction in the recovery experiments.

The results for different concentrations of mercury species spiked into condensates are given in Table 6. Considering the nature of the condensates, which are a very complex mixture of volatile hydrocarbons, the recoveries are mainly >80 %, with many above 90 %. For each given species the linearity of recovery data in the concentration range covered was better than $r^2 = 0.99$. The total mercury recoveries for a mixture of the seven species are also given in Table 6. These recoveries were in the range 88–97 %.

Precision of the Experimental Procedure

To determine the precision of the experimental procedure, the total mercury content in toluene, a commercial condensate (GC3), and a condensate (GC3) with three representative mercury compounds added at the 10 ng mL^{-1} mercury level, i.e., EMC acting as an organohalide mercury species, DEM as an

TABLE 6—Summary of recovery performance

Mercury Species Added	Recovery ± *s* (%)		
	10 ng mL^{-1}	20 ng mL^{-1}	30 ng mL^{-1}
DPM	74 ± 12	74 ± 2	77 ± 0
DMM	111 ± 13	119 ± 14	105 ± 9
MC(1)	80 ± 18	98 ± 13	89 ± 8
MC (2)	123 ± 8	98 ± 17	98 ± 3
EMC (1)	90 ± 19	86 ± 2	—
EMC (2)	108 ± 15	129 ± 2	119 ± 5
EMC (3)	92 ± 5	81 ± 5	77 ± 5
MMC	102 ± 4	92 ± 5	92 ± 8
PMC	77 ± 13	92 ± 6	99 ± 5
DEM	113 ± 8	92 ± 6	99 ± 5
Equal Mixture	90 ± 5[a]	88 ± 2[a]	97 ± 1[a]

[a] Total recovery where concentration stated is for each component.

organomercury species, and mercury(II) chloride as an inorganic mercury species, were analyzed 10 times for each species.

The mercury content for the toluene (0.25 mL injected) was 6.4 ± 0.2 ng mL^{-1}. For the condensate GC3 alone, the mercury value was 7.45 ± 0.34 ng mL^{-1}. The relative standard deviations (RSDs) for the analyses were 3.7 and 4.8 %, respectively. For the condensate GC3 spiked with 10 ng mL^{-1}(as mercury) of the three species, the total mercury content was determined as 17.55 ± 0.35 ng mL^{-1} (EMC), 17.28 ± 0.62 ng mL^{-1} (DEM), and 18.04 ± 0.86 ng ml^{-1} (MC), with RSDs between 2 and 5 %. It is of note that the recoveries for these spiking experiments with condensate were 101, 98, and 106 %, respectively (RSD between 4 and 7 %).

Conostan Mercury Standard

For the determination of mercury in oil and similar petroleum products, a suitable mercury standard, which allowed the use of standard addition techniques, was required. Conostan mercury standard, which is commercially available, is an alkylaryl dithiocarbamate mercury compound (Hg-S bonded) dissolved in white base (paraffin) oil. This standard was prepared at different dilutions in the parts per billion range and consistently gave between 103 ± 5 % recovery (n = 10).

Detection Limits

The detection limits that can be obtained with the proposed method depend to some extent on the complexity of the condensate sample, i.e., the volatility of both the condensate and the mercury species in the sample, together with the effect of any matrix sample condensing on the trap. The absolute detection

limits for the method (based on three times the standard deviation and a 0.25 mL volume sample injection) were 180 pg for toluene and 270 pg for GC3 condensate. For three different mercury species added to the GC3 condensate, the absolute detection limits were 270 pg for DEM, 450 pg for MC, and 630 pg for EMC. When based on the system alone, without sample introduction but monitoring the carrier gas (argon), the absolute limit of detection was reduced to 11 pg (n = 6).

TOTAL MERCURY MEASUREMENTS OF COMMERCIAL CONDENSATE

Five types of natural gas condensate, obtained from several sources, were analyzed for total mercury. The results indicate that the concentration of the mercury is independent of location and type of condensate. The total mercury concentrations of the condensate samples GC1–5 together with the precisions are given in Table 7. The RSDs for the analyses are in the range 4–7% for a 0.25 mL manual sample injection.

TABLE 7—Total Mercury Content of Commercial Condensate Samples

Sample	Test No.	Concentration (ng mL^{-1})	Mean ± s/(ng mL^{-1})	RSD (%)
GC1	1	23.3	22.3 ± 1.4	6
	2	22.5		
	3	21.9		
	4	21.5		
	5	19.9		
	6	21.3		
	7	21.7		
	8	23.8		
	9	22.6		
	10	24.7		
GC2	1	49.5	49.7 ± 2.6	5
	2	53.2		
	3	51.0		
	4	46.7		
	5	46.0		
	6	48.3		
	7	47.0		

(*Continued*)

TABLE 7—Total Mercury Content of Commercial Condensate Samples (Continued)

Sample	Test No.	Concentration (ng mL^{-1})	Mean ± s/(ng mL^{-1})	RSD (%)
	8	50.1		
	9	52.0		
	10	52.8		
GC3	1	7.5	7.5 ± 0.3	4
	2	7.6		
	3	8.0		
	4	7.6		
	5	7.2		
	6	7.2		
	7	6.8		
	8	7.6		
	9	7.2		
	10	7.7		
GC4	1	13.8	12.8 ± 0.9	7
	2	14.0		
	3	13.2		
	4	11.9		
	5	12.0		
	6	12.1		
GC5	1	42.4	43.3 ± 1.7	4
	2	45.2		
	3	45.6		
	4	42.4		
	5	42.8		
	6	43.6		
	7	40.8		

Speciation of Mercury in Liquid Hydrocarbons

Mercury may be present in natural gas condensate in its metallic form or as organometallic compounds or both with boiling points comparable to that of the range of condensates [10,46]. The elemental mercury content in liquid

hydrocarbons or gas condensate may be in the range of about 10 % or less of the total mercury in the samples because of the high volatility and the low solubility of elemental mercury [24].

Other species such as organomercury halide and inorganic salts (polar compounds) may also be present but are generally considered to be at a lower concentration in the nonpolar condensate matrix. The presence of these polar species is likely to be associated with the moisture or free water in the sample or with impurities such as particulate matter (which are able to adsorb mercury species).

In general, the majority of mercury speciation papers are focused on aqueous-based and related environmental samples rather than the complex and hydrophobic, liquid hydrocarbon sample type. Many coupled chromatographic-atomic spectrometric methods have been applied to the detection and determination of organomercurial compounds. For separation of the species, chromatographic techniques are most commonly used, including gas chromatography [47–54], high performance liquid chromatography [47,55–57], and ion chromatography [58]. For detection of mercury, the detection systems used are electron capture detector (ECD) [48–53], microwave induced plasma-emission spectrometry (MIP-AES), AAS, or AFS. The analytical technique most commonly used in earlier studies for the determination of organomercury compounds in environmental samples was gas chromatography using electron capture detection (GC-ECD). Speciation techniques have involved derivatization by butylation [59,60], aqueous phase ethylation [51,52,61], or hydridization [6], prior to use of a chromatographic separation technique coupled with a suitable mercury detector, e.g., GC-MS, GC-ICP-MS, GC-MIP-AES, HPLC-CV-AAS, and HPLC-CV-AFS. These procedures can be time consuming and can lead to contamination of analytes and losses during the procedure, and the derivatized products may not necessarily reflect the actual concentration of the various organic mercury species native to the samples.

To date, a complete and rapid technique for identifying and quantifying all the mercury species content in natural gas condensate is not well established. Few in-depth investigations have been carried out for speciation of mercury in liquid hydrocarbons and gas condensates, and most are targeted at single or a few species of interest [47,58,59]. A method for determination of mercury species in gas condensate by online coupled HPLC and CV-AAS has been reported [47]. Various organomercury species were first separated by reversed-phase HPLC using an aqueous-based gradient elution. Before the final measurement, the organic liquids and the matrix were destroyed by oxidation with $K_2CR_2O_7$. Mercury was detected by CV-AAS. However, when applied to a real natural gas condensate sample, only inorganic mercury (II) was detected and severe matrix interference was reported. Chemical rearrangements between the mercury species were also observed.

The determination of only the dimethylmercury species in natural gas condensate was reported [48] using an online amalgam trap or solid-phase micro-extraction with capillary GC-MIP-AES detection. This procedure eliminated background interference from carbon compounds passing through the plasma that occurred when a direct measurement approach was carried out. Monomethylmercury and inorganic mercury were stated to require derivatization (butylation) prior to the determination. More recent, mercury speciation in

natural gas condensate using GC-ICP-MS has been achieved, using a pretreated DB-1701 capillary column [54]. The condensate samples analyzed contained the dialkyl mercury species and little or no organomercury halide was detected.

In this work we have sought to develop a simple and rapid procedure for the accurate determination of all mercury species that may be present in natural gas condensate. This chapter describes their determination by using gas chromatography coupled via a pyrolysis unit with atomic fluorescence detection. The technique utilized the superior separation advantage of gas chromatography and the high sensitivity and element specific detection properties of atomic fluorescence for mercury speciation work. The utilization of a single gas, argon, to replace the dual type carrier gas [62], i.e., helium and argon, was studied. Direct injection without any pretreatment, derivatization, or extraction of the sample has been used. This was to avoid problems associated with the sample type and species having a relatively low boiling point (<250°C) and stability.

Instrumentation for Speciation of Mercury in Liquid

A schematic diagram of the capillary GC-AFS is shown in Fig. 14. The system has been used for a number of years, mainly for environmental applications, where organomercury compounds are extracted from the sample before injection [62].

Recently this instrument has been applied to the determination of organomercury in liquid hydrocarbons [63,64]. In this case no sample preparation was required. On column injection was used to introduce the sample onto a

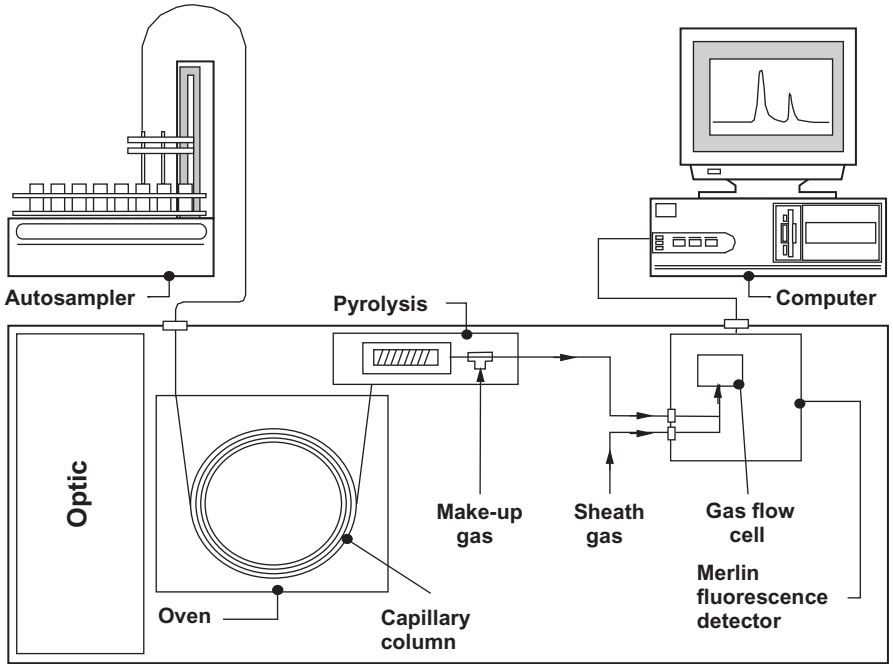

Fig. 14—Schematic diagram of a GC-AFS instrument.

TABLE 8—Typical Instrumental Conditions for the GC-AFS System	
Column	DB1
Column carrier flow rate (He)	8 mL/min
Make-up gas carrier flow rate (Ar)	100 mL/min
Sheath gas flow rate (Ar)	300 mL/min
Range	100 × 10
Injector (on-column) temperature	300°C
Injection volume	2 μL
Pyrolysis temperature	900°C
Mode	Ratio
Oven Program	
35°C	1 min
35–115°C	10°C
115°C	5 min
115–300°C	18°C/min
300°C	10 min

nonpolar DB1 megabore column. This separates the different organomercury compounds on the basis of boiling point. On exiting the column, the mercury species are pyrolized at 800°C to convert them to mercury vapor which is subsequently delivered to the AFS with the aid of an argon make-up gas. The instrumental conditions for the GC-AFS are summarized in Table 8.

One of the main advantages of AFS is that the linear range for mercury spans more than five orders of magnitude. The absolute detection limit was found to be 0.1 pg. Based on 1 μL injection volume, the method detection limit is about 0.1 ng/mL for liquid hydrocarbon samples. In principle, the programmable temperature vaporization device (PTV) should allow the injection of larger sample volumes and the method detection limit could be improved. The sensitivity is independent of the chemical species. One further advantage of the AFS is its excellent selectivity. Hydrocarbons do not respond to the detector or affect the measurement of mercury. At concentrations 10 times higher than the method detection limit, typical precision is about 8 % with manual injections. This can be improved to 5 % with the use of an autosampler.

A wide range of samples from different locations have been analyzed using the system described, and an example of condensate from Europe is shown in Fig. 15. Three species can be identified: dimethylmercury (DMM), methylethylmercury (MEM), and diethylmercury (DEM). Table 9 summarizes the results

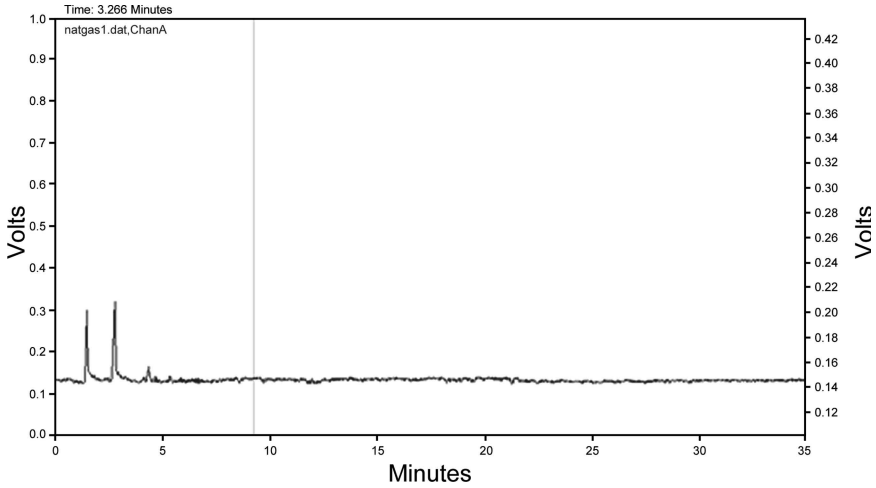

Fig. 15—Chromatogram for European condensate using the GC-AFS.

obtained for five replicate injections of 1 μL. Summation of the three compounds came to 11.3 ± 1.4 ng/mL, which correlates extremely well with the result obtained using measurements made using the preconcentration system described earlier [64].

A condensate from Indonesia was found to be less complicated, with only dimethylmercury present (Fig. 16) in the sample. Once again, this measurement correlated well with the results obtained from the total mercury levels (Table 9).

More recently, GC-AFS has been applied to the speciation of mercury in natural gas condensates at the picogram level [64]. The instrumentation is relatively simple and easy to operate. No pretreatment of the samples is required before mercury determination. Mass balance calculations show a good agreement between the total mercury content of samples analyzed using the vaporization technique [63] and the summation of all species eluted by GC-AFS.

TABLE 9—Results for Organomercury in Condensate Samples from Europe and Indonesia

Sample Reference	Compounds	Concentration (ng/mL)	Summation (ng/mL)	Total Mercury (ng/mL)
European Condensate	CH_3HgCH_3	4.2 ± 0.40		
	$CH_3CH_2HgCH_3$	5.6 ± 0.60	11.3 ± 1.4	11.5 ± 0.2
	$CH_3CH_2HgCH_2CH_3$	1.5 ± 0.40		
Indonesian Condensate	CH_3HgCH_3	3.53 ± 0.54	3.53 ± 0.54	3.884 ± 0.036

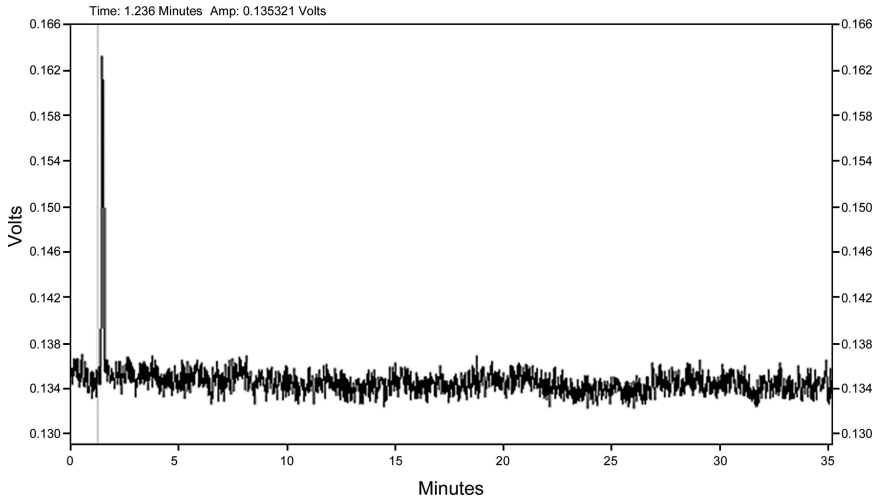

Fig. 16—Chromatograph for Indonesian condensate.

The major species observed in condensate samples were DMM, MEM, and DEM. The presence and proportion of mercury species are highly dependent on the source, the stage of production, the sampling technique used, and storage and age of the sample.

Online Determination of Mercury in Natural Gas

The levels of mercury in natural gas can be quite varied and problems caused by high levels can be quite catastrophic. A block diagram of a typical gas sampling system is shown in Fig. 17.

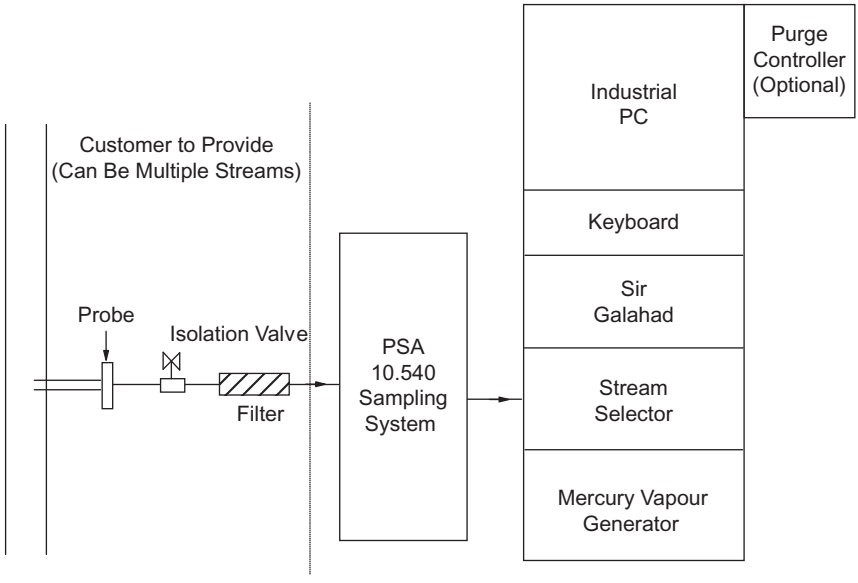

Fig. 17—Block diagram of a typical gas sampling system.

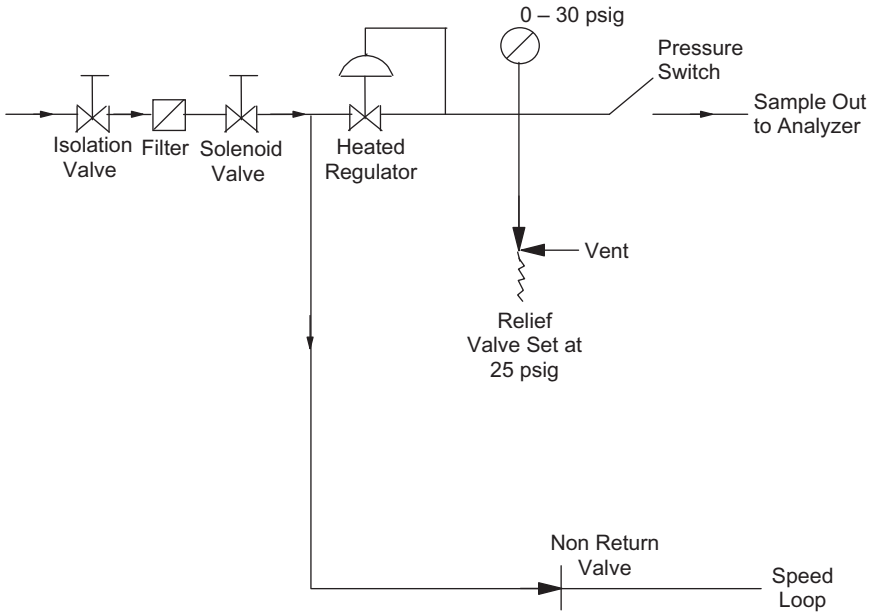

Fig. 18—Schematic diagram of a proven sampling system.

A major issue is to produce a reliable representative sample through to the analyzer itself. A schematic diagram of a proven sampling system is shown in Fig. 18. Basically the design uses a speed loop, which takes the sample from the stream under test and returns the excess sample back to the process stream further down the process line.

- Sample is delivered using speed loop.
- A normally closed high pressure solenoid valve is included in the speed loop to stop the sample flow under alarm conditions.
- Heated regulator reduces pressure of sample to 6 psig.
- Pressure switch and relief valve are used to prevent high pressure entering enclosure. Pressure switch activates solenoid in alarm conditions.
- All components are explosion proof.

Table 10 shows the principal requirements for such a system. It is important that this sampling system does not contribute any mercury to the stream, nor does it collect mercury, so the analyzer does not see mercury that is present in the stream.

The analyzer used to determine mercury is somewhat similar to that described previously for laboratory applications. The key components are shown in Fig. 19. A significant advantage provided by such a system is the addition of a mercury vapor generator that has been fundamentally traced by first principles and has been recognized both by the National Institute of Standards [65] and Technology and by the National Physical Laboratory [66] to provide reliable data. Furthermore, the Dumarey equation [38] has been validated by both ICP-MS and comparison to certified reference materials by a number of groups, including the author [67], such that measurement of the mercury levels

TABLE 10—Features of Online Software

- The online process control software provides a simple interface between the analyzer, the user, and control room.
- The software allows the user to define not only the sampling and calibration frequency but also actions to be performed under alarm conditions.
- The software connects to other systems either by 4-20mA, RS232, RS485, RS422, MODBUS, TCP/IP, or contact closure.
- The software is fully password protected, allowing you the ability to define who can do what.

can be relied on as accurate. These components are then based in a suitable explosion-proof cabinet that will require purging, with either air or nitrogen. The requirements for this cabinet will be set by its location in the plant and the industry where the facility is situated.

Typically the analytical procedure relies on an online dual amalgamation of the mercury levels followed by quantification using atomic fluorescence spectrometry. A typical sequence of events setting out the eight stages in the sequence is shown in Fig. 19. Care must be taken that no hydrocarbons are collected in the traps and that all forms of mercury are collected. The levels of mercury present in the sample will determine the measurement cycle time, and in general the sequence is to collect and flush out hydrocarbons, measure mercury levels, and then clean the trap. Basically the sequence carries out its own maintenance cycle, and after each measurement the traps are prepared for the next sample.

The process control software provided enables a range of interconnections to other process software and allows the user to set up simple protocols that are required for each particular site. Some details of the software are set out in Table 10.

A simple example of the installation is shown in Fig. 19. The sequence of operation is shown in the eight stages from sample collection through to measurement and trap cleaning before the next sequence. Measurements can be made both at the inlet and outlet stages, simply by managing the sample lines involved. Many of the systems that are installed worldwide are operating continuously with little if any additional maintenance required.

Online Determination of Mercury in Liquefied Natural Gas

These materials present a different range of challenges to the process chemists in order to obtain reliable data on which to make commercial decisions. The procedures described here have been implemented on operation sites successfully over a number of years.

Fig. 20 shows a schematic diagram of a multichannel analyzer to determine mercury in streams of liquefied natural gas. The analysis itself is similar to that used for natural gas, but the sampling system has been specifically developed to ensure reliable sampling and to prevent the addition or removal of mercury from the sample streams. The sampling system consists of a multichannel pressure reduction system to reduce the pressure of the various sample gases while heating them to prevent condensation of the heavier hydrocarbons and to minimize the losses of mercury on components. Depending on site regulations and conditions, the system may include a fast loop primary bypass that is either vented to flare or

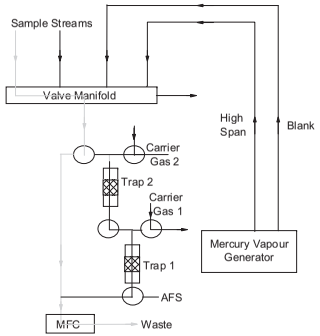

Stage 1- Pre-flush

The sample is passed over TRAP 2 & 1 in series. Both traps can be heated for the collection to prevent condensation of hydrocarbons.

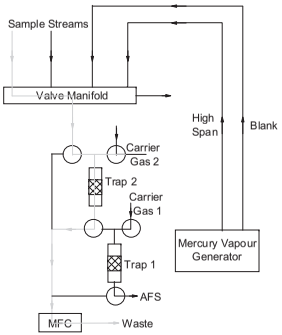

Stage 2- Sample collection

The sample is passed over TRAP 2 which is heated at an elevated temperature and the sample is collected

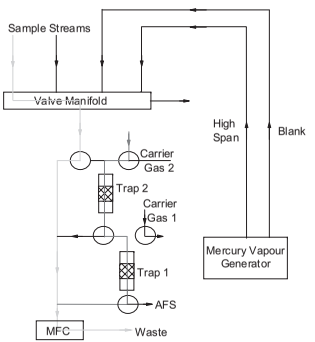

Stage 3- Pre-flush of TRAP 2

The sample stops passing over TRAP 2 and the system pre-flushes TRAP prior to heating

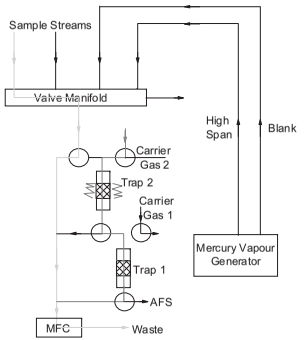

Stage 4- Desorb Trap 2

TRAP 2 is heated, driving off the Hg onto trap 1

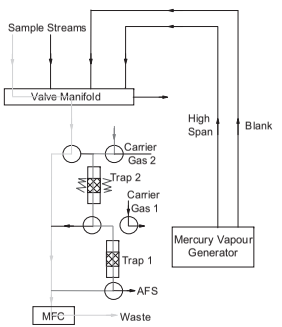

Stage 5- TRAP 2 is cooled

TRAP 2 is cooled ready for next sample

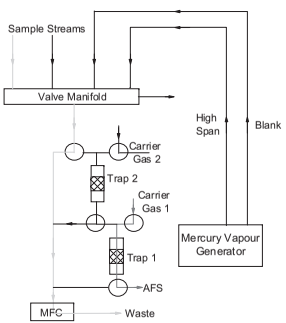

Stage 6- Pre-flush

TRAP 1 is pre-flushed prior to the heat cycle.

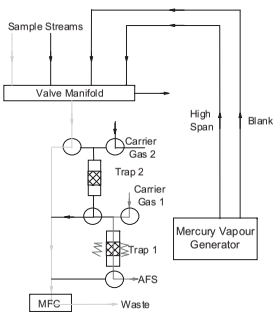

Stage 7- Desorb

TRAP 1 is heated to release Hg0 and this passes to the detector for analysis.

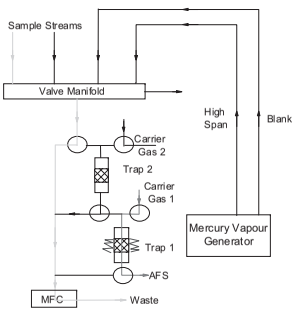

Stage 8- Cool

TRAP 1 is cooled ready for the next sample.

Fig. 19—Schematic representation of the sequence for natural gas measurements.

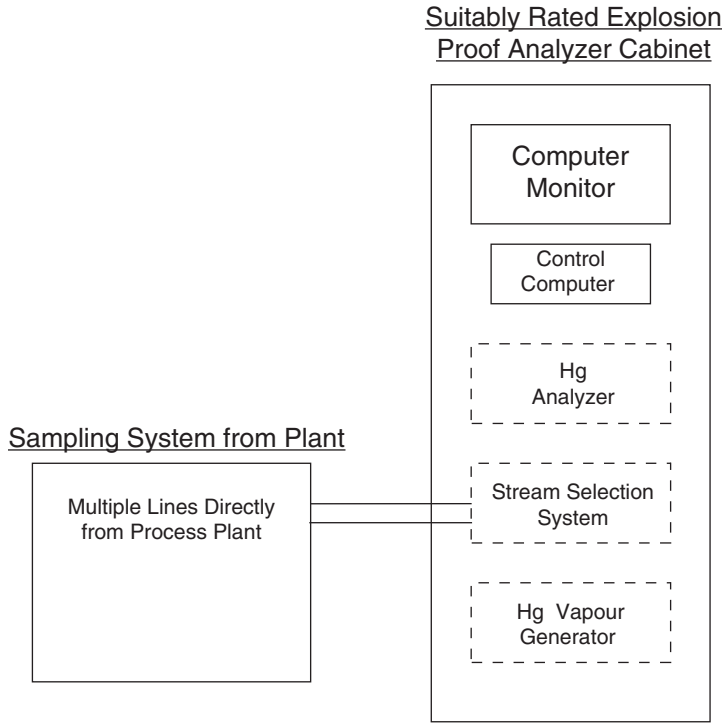

Fig. 20—Schematic diagram of online system to determine mercury in liquefied natural gas samples.

returned to the process stream. The system also incorporates a low-pressure secondary bypass that is vented to atmosphere or to a low-pressure flare.

A schematic diagram showing two sample streams is shown in Fig. 21. Within the sampling enclosure the various components are configured to enable safe and representative sampling. The heart of the system is the heated pressure regulator that both reduces the overall pressure to approximately 4 psig and heats the gas to 143°C, thereby preventing condensation of the hydrocarbon and avoiding losses of mercury from the sample streams.

As with the system described for natural gas streams, the availability of a certified calibration gas enables the user to provide a simple check on the performance of the sampling system by adding known amounts of mercury from time to time.

The analyzer performance follows similar lines to those set out for natural gas. Site and natural requirements determine the nature of safety requirements to avoid explosions in petrochemical environments.

Continuous Determination of Mercury in Liquid Hydrocarbons

A fully automated system has been developed and installed at a research establishment, providing valuable data for the process engineers developing specific catalytic reactor systems.

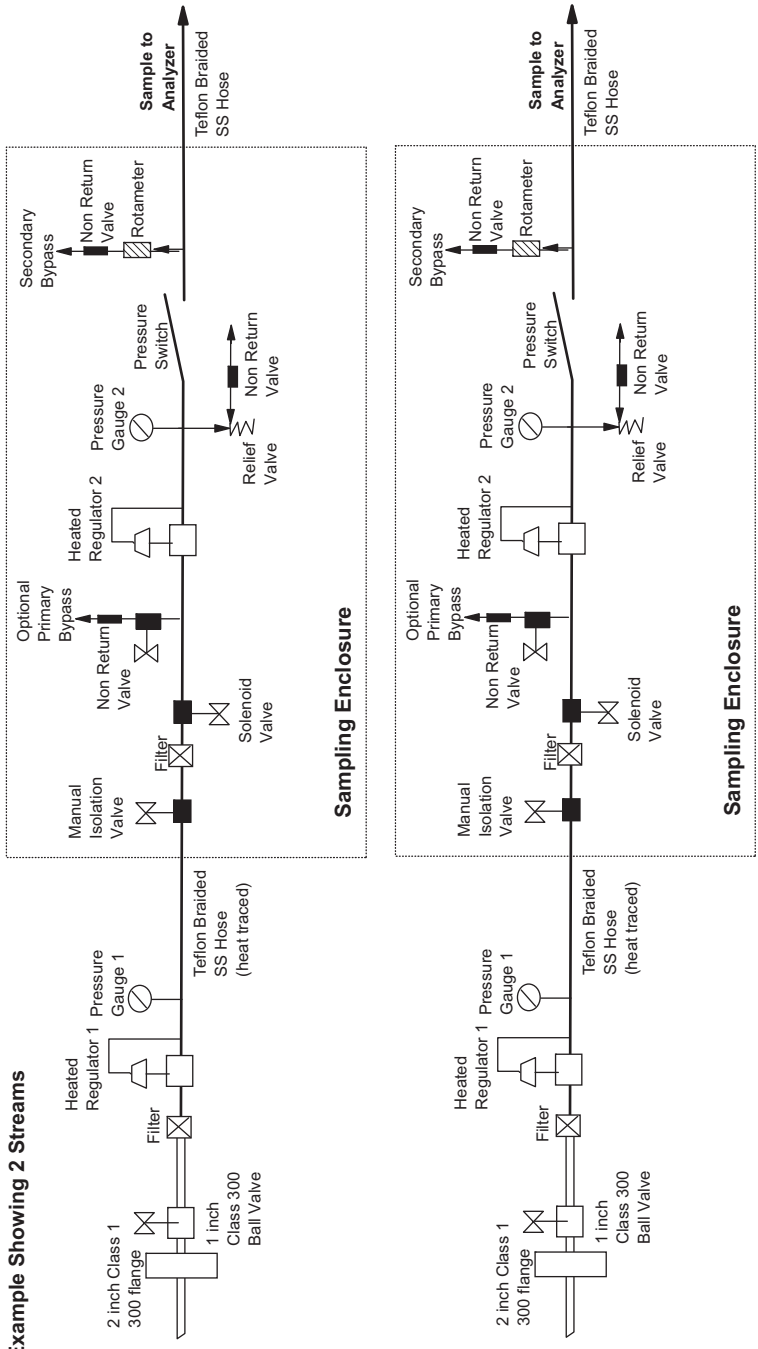

Fig. 21—Sampling system designed to provide representative samples of liquefied natural gas.

A simple and rapid procedure for the determination of total mercury in condensate has been developed despite the volatile and complex nature of natural gas condensate. Total mercury in liquid hydrocarbons, particularly condensate, can be determined using a procedure of vaporization and trapping of mercury species using an Amasil gold trap at an elevated temperature (200°C). The overall recoveries of mercury species spiked into real condensate were good. The recoveries of several species, i.e., DMM, DEM, DPM, MMC, EMC, PMC, and MC, and a mixture of them were almost 100 %. Other real gas condensates have also been analyzed for total mercury, and the results indicated the consistency of the procedure. The procedure offers rapid and consistent results without recourse to complicated methods such as digestion of volatile matrices or the use of chemical modifiers and reagents, which themselves may introduce contamination. Only small amounts of sample (0.25 mL) are required, and the simple instrumentation used was easy to set up and operate.

The only requirement for this direct injection method is that the hydrocarbon or condensate completely vaporizes at the trap temperature of 200°C. The typical carbon number for gas condensates, C_1–C_{15}, results in an organic liquid composition that easily meets the above requirement. For heavier samples, dilution to a desired concentration range with a suitable solvent is required to ensure complete vaporization of the sample, as demonstrated by the analysis of heavy gas oil.

The system is based on the preconcentration system described earlier; one of the main advantages of this approach is that relatively large sample volumes can be introduced without the risk of explosions. This can be achieved by multiple injections of fixed volume of sample to offer low detection limits with a wide dynamic range. Detection limits below 1 ppbw are thus achievable, with an upper linear range of 10,000 ppbw.

The sample outlet is continuously delivered at 1–5 mL/min to the auto injection system so that a representative sample is obtained. A sampling manifold system can be configured providing care is exercised to ensure no losses of mercury occur.

When triggered, the auto-injector will transfer the contents of the sample loop into a stream of argon or nitrogen flowing at approximately 100 mL/min. The injection volume will be between 100 to 250 μL, and the system will be configured so that multiple injections can be used to expand the linear range and maximize detection limits.

The system is configured so that it is possible to inject samples manually with a syringe. Standards, samples, and air saturated with elemental mercury can also be injected for quality control purposes or troubleshooting. The sample is vaporized in the presence of inert carrier gas at 400°C so that the sample is gasified and then delivered to a gold Amasil trap at elevated temperature. The mercury within the vaporized sample collects on the gold, offering preconcentration and matrix removal separation. One further advantage of this approach is that all species of mercury are collected, thus providing a total mercury measurement. After the collection period, the Amasil trap is heated to 800°C so that the mercury is released as elemental mercury. The desorbed mercury is then collected on a second Amasil trap located in the Sir Galahad mercury analyzer. The final stage of the measurement is to desorb the mercury from this trap into a carrier stream of argon or nitrogen so that it can be

delivered to a mercury-specific AFS. The combination of a two-stage amalgamation on gold with AFS offers a selective and sensitive approach to this application. The procedure forms the basis of the internationally accepted standards for the measurement of mercury in gaseous streams (ASTM 6350-98 [68] and ISO 6978-2 [69]). The typical cycle time is 10 minutes, although this can be optimized to provide the best performance. Calibration of the instrument is provided using manual injection of liquid hydrocarbons or saturated mercury vapor with known mercury content.

The development of a process analyzer to determine mercury in liquid hydrocarbons requires the development of a sampling strategy, and the system itself must be configured so that it fully meets the necessary safety standards for both the site and the location where it will be installed. Safety regulations will depend on the country or area where the facility is based, but it is likely that the equipment will need to be installed in an explosion-proof cabinet with either nitrogen or an air purge system. The author has experience developing such systems, but they are not described in detail in this chapter.

Fig. 23 shows a typical sampling manifold for liquid hydrocarbons. To meet plant safety criteria these systems must also be housed in appropriate explosion proof cabinetry. This is similar to that shown in Fig. 22 but has the addition of a multipoint valve, which is limited to the various process streams that are fed from the various stages of the process. As with all sampling systems, care must be exercised so that no mercury is either added to or extracted from the process: i.e., truly representative samples are presented to the mercury detector for measurement.

Further developments to transfer this technology from the laboratory to the process stream or a production plant require attention to the desired safety specification needs for the situation in an explosion-proof area.

Although many of the parameters are set by the safety requirements of the zonal definition, there are also further constraints or demands from the geographical location, and as a consequence because these requirements are subject to change, they are not described here.

Fully automated systems based on the concepts described have been successfully implemented on process plants. By generating continuous measurements, they overcame the need to take periodic group samples and provide continuous information on the operations of the plant.

Conclusions

The application of AFS to the measurement of mercury in particular and other elements such as arsenic has been described. The sensitivity of the technique makes it an ideal facilitator for these measurements. However, the analytical techniques are not the sole determinant of a reliable system, and the sampling and sample pretreatment illustrated in this chapter ensure that reliable data are provided, allowing the process operators to control the processes and avoid costly plant shutdowns.

Atomic fluorescence spectrometry was applied to a wide range of samples within the petrochemical industry. Specific sampling devices using appropriate components have enabled natural gas sampling on site. Sampling difficulties such as contamination and losses have been overcome by the use of elevated

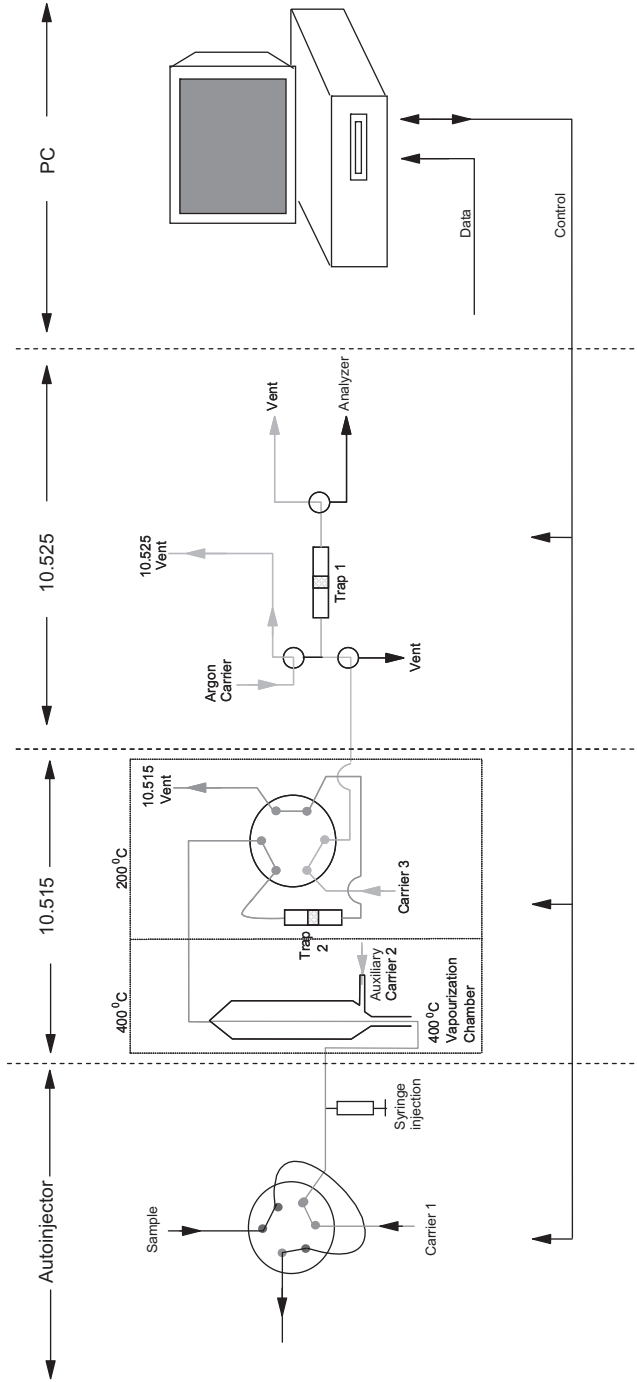

Fig. 22—Schematic diagram of a system for the continuous determination of mercury in liquid hydrocarbons.

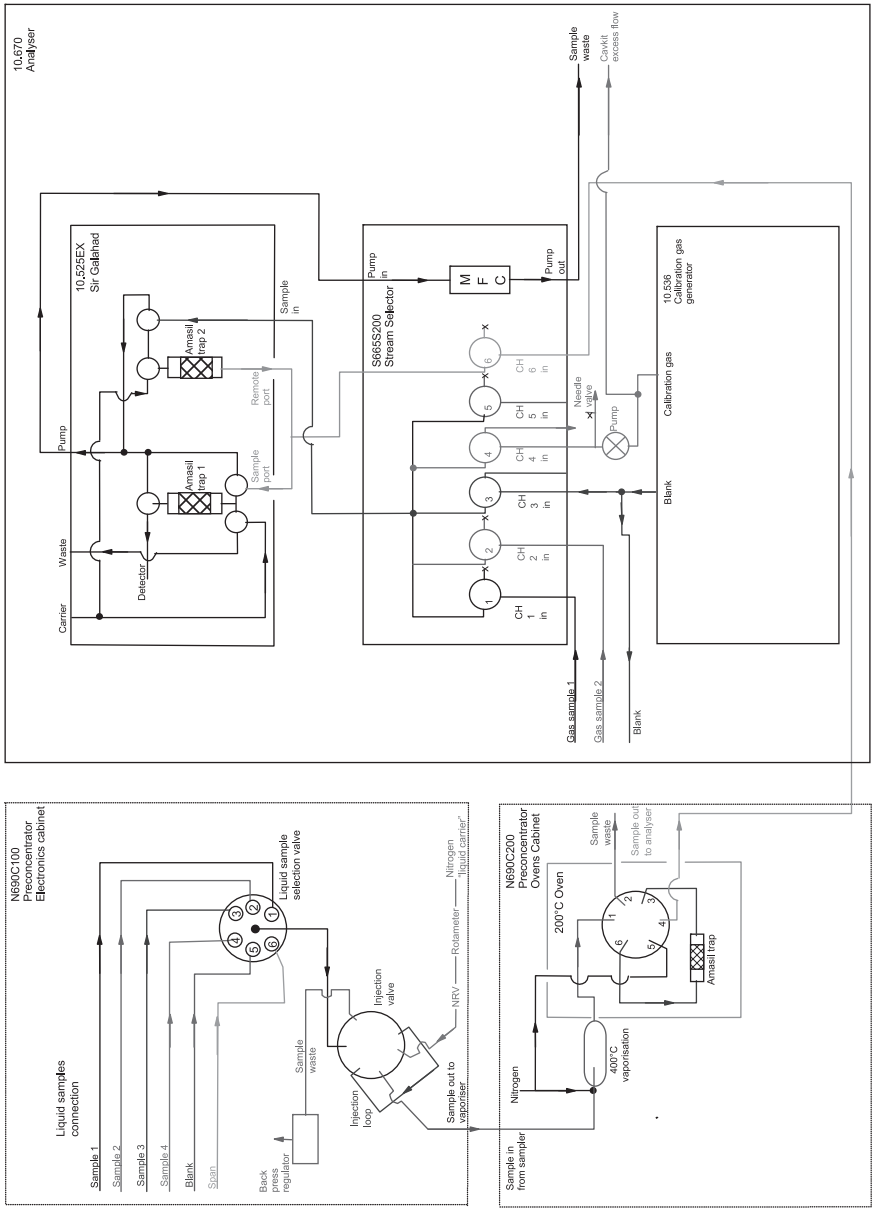

Fig. 23—Typical sampling manifold for liquid hydrocarbons.

temperatures and careful consideration to the materials of construction. Dual amalgamation using Amasil tubes has enabled high collection efficiencies for all species of mercury at elevated temperatures. This arrangement gave consistent results free from matrix interferences for total mercury measurements in natural gas, liquefied natural gas, and liquid condensates. However, with any technology, the application, scope, and performance are continuously evolving, and this article presents information that may be historical in some respect. Further current information is continuously updated on the P S Analytical website www.psanalytical.com.

ACKNOWLEDGMENTS

The author acknowledges Petronas, Malaysia, for the sponsorship of Azman Shafawi, who has successfully completed his PhD thesis on this topic. Zdravko Spiric of INA-Industrija Nafte, Croatia, is also acknowledged for his early work on mercury in natural gas. P S Analytical is also indebted to many of its clients, whose knowledge of their industry and specific sample types has been invaluable. P S Analytical also is indebted to our scientists, particularly Dr. Warren Corns, who have assisted greatly in the design, research, and development of technology to provide the solutions required and to provide fit-for-purpose instrumentation.

References

[1] Delgado-Morales, W., Mohan, M. S. and Zingaro, R. A., *Int. J. Env. Anal. Chem.,* 1994, Vol. 54, pp. 203–220.

[2] Delgado-Morales, W., Zingaro R. A. and Mohan, M. S., *Int. J. Env. Anal. Chem.,* 1994, Vol. 57, pp. 313–328.

[3] Irgolic, K. J., Spall, D., Puri, B. K., Ilger, D. and Zingaro R. A., *App. Organomet. Chem.,* Vol. 5, 1991, pp. 17–24.

[4] Bouyssiere, B., Baco, F., Savary, L., Garrand, H., Gallup, D. L. and Lobinski, R., *J. Anal. At. Spec.,* Vol. 16, 2001, pp. 1329–1332.

[5] Krupp, E. M., Johnson, C., Rechsteiner, C., Moir, M., Leong, D. and Feldmann, J., *Spectrochim. Acta Part B.,* Vol. 62, 2007, pp. 970–977.

[6] Bingham, M. D., *SPE Prod. Eng.*, May 1990, pp. 120–124.

[7] Haselden, G. G., "Challenges of LNG in the 1980's," *Mech. Eng.*, Vol. 103, 1981, pp. 46–53.

[8] Bodle, W. W., Attari, A. and Serauskas, R., "Considerations for Mercury in LNG Operations," *Institute of Gas Technology Sixth International Conference on Liquefied Natural Gas*, Kyoto, Japan, April 7–14, 1980.

[9] Leeper, J. E., *Energy Process Can.*, Vol. 46, 1981.

[10] Hennico, A., Barthel, Y. and Cosyns, J., "Mercury and Arsenic Removal in the Natural Gas, Refining and Petrochemical Industries," *Oil Gas European Magazine*, No. 2, 1991, pp. 36–38.

[11] Leeper, J. E., *Hydrocarbon Process.*, Vol. 59, 1980, pp. 237–240.

[12] Frech, W., Baxter, D. C., Dyvik, G. and Dybdahl, B., "On the Determination of Total Mercury in Natural Gases Using the Amalgamation Technique and Cold Vapour AAS," *J. Anal. At. Spectrom.*, Vol. 10, 1995, pp. 769–775.

[13] Frech, W., Baxter, D. C., Bakke, B., Snell, J. and Thomassen, Y., "Determination and Speciation of Mercury in Natural Gases and Gas Condensates," *Anal. Commun.,* Vol. 33, 1996, pp. 7–9.

[14] Snell, J., Frech, W. and Thomassen, Y., "Performance Improvements in the Determination of Mercury Species in Natural Gas Condensate Using an Online Amalgamation Trap or Solid-Phase Micro-Extraction with Capillary Gas Chromatography-Microwave-Induced Plasma Atomic Emission Spectrometry," *Analyst*, Vol. 121, 1996, pp. 1055–1060.

[15] Snell, J., Qian, J., Johansson, M., Smith, K. and Frech, W., "Stability and Reactions of Mercury Species in Organic Solution," *Analyst*, Vol. 123, 1998, pp. 905–909.

[16] Kirkbright, G. F., and Sargent, M., *Atomic Absorption and Fluorescence Spectroscopy*, Academic Press, London, 1974.

[17] Alkemade, C. Th. J. and Zeegers, P. J. Th., *Spectrochemical Methods of Analysis*, Wiley-Interscience, New York, 1971.

[18] Corns, W. T., Stockwell, P. B., Ebdon, L., and Hill, S. J., "Development of an Atomic Fluorescence Spectrometer for the Hydride-Forming Elements," *J. Anal. At. Spectrom.*, Vol. 8, 1993, pp. 71–77.

[19] PSA10.025 Millennium Merlin, *User Manual, Issue 3.2*, P S Analytical, Kent, UK, October 2008.

[20] Cai, Y., "Atomic Fluorescence in Environmental Analysis," *Encyclopaedia of Analytical Chemistry*, R. A. Meyers, Ed., John Wiley & Sons Ltd., New York, 2001, pp. 1–22.

[21] Olafsson, J., "A Report on the ICES Intercalibration of Mercury in Seawater for the Joint Monitoring Group of the Oslo and Paris Commissions," *Mar. Chem.*, Vol. 11, 1982, pp. 129–142.

[22] Szakacss, O., Lasztity, A. and Horvath, Zs., "Breakdown of Organic Mercury Compounds by Hydrochloric Acid-Permanganate or Bromine Monochloride Solution for the Determination of Mercury by Cold-Vapour Atomic Absorption Spectrometry," *Anal. Chim. Acta*, Vol. 121, 1980, pp. 219–224.

[23] Jones, R. D., Jacobson, M. E., Jaffe, R., West-Thomas, J., Arfstrom, C. and Alli, A., "Method Development and Sample Processing of Water, Soil and Tissue for the Analysis of Total and Organic Mercury by Cold Vapour Atomic Fluorescence Spectrometry," *Water Air Soil Pollut.*, Vol. 80, 1995, pp. 1285–1294.

[24] Hurley, J. P., Benoit, J. N., Babiarz, C. L., Shafer, M. M., Andren, A. W., Sullivan, J. R., Hammond, R. and Webb, D. A., "Influences of Watershed Characteristics on Mercury Levels in Wisconsin Rivers," *Environ. Sci. Technol.*, Vol. 29, 1995, pp. 1867–1875.

[25] Gagnon, C., Pelletier, A. and Mucci, A., "Behaviour of Anthropogenic Mercury in Coastal Marine Sediments," *Mar. Chem.*, Vol. 59, 1997, pp. 159–176.

[26] Jaffe, R., Cai, Y., West-Thomas, J., Morales, M. and Jones, R. D., "Occurrence of Methylmercury in Lake Valencia," *Bull. Environ. Contam. Toxic.*, Vol. 59, 1997, pp. 99–105.

[27] Mason, R. P. and Sullivan, K. A., "Mercury in Lake Michigan," *Environ. Sci. Technol.*, Vol. 31, 1997, pp. 942–947.

[28] Van Delft, W. and Vos, G., "Comparison of Digestion Procedures for the Determination of Mercury in Soils by Cold-Vapour Atomic Absorption Spectrometry," *Anal. Chim. Acta*, Vol. 209, 1988, pp. 147–156.

[29] Tsujii, K. and Kuga, K., *Anal. Chim. Acta*, Vol. 72, 1974, pp. 85–90.

[30] Thompson, K. C., *Analyst*, Vol. 100, 1975, pp. 307–310.

[31] P S Analytical. "PSA 10.055 Millenium Excalibur," http://www.psanalytical.com/products/millenniumexcalibur.html. Viewed on April 14, 2011.

[32] Welz, B., *Atomic Absorption Spectrometry*, 2nd edition, VCH, Weinheim, 1985.

[33] Grotewold, G., Fuhrberg, H. D. and Philipp, W., "Production and Processing of Nitrogen-Rich Natural Gases from Reservoirs in the NE Part of the Federal Republic of Germany," *Proceedings of the 10th World Petroleum Congress*, Bucharest, 1979, Vol. 4, pp. 47–54.

[34] Cameron, C., Benayoun, D., Dorbon, M., Michelot, S. and Robertson, M., "How Much and What Types of Mercury Are in Natural Gas and Associated Condensates: How Can Mercury be Eliminated?" *Teknik Kimia*, Bandung, October 24–25, 1995.

[35] Nelson, D. R., "Mercury Attack of Brazed Aluminium, Heat Exchangers in Cryogenic Gas Service," *73rd Annual Convention of the Gas Processors Association*, New Orleans, March 7–9, 1994, *Proceedings*, pp. 178–183.

[36] Lund, D. L., "Causes and Remedies for Mercury Exposure to Aluminium Cold-Boxes," *75th Annual GPA Convention*, Denver, Colorado, March 1–12, 1996.

[37] Sarrazin, P., Cameron, C. J. and Barthel, Y., "Processes Prevent Detrimental Effects from As and Hg in Feedstocks," *Oil Gas J.*, January 25, 1993, pp. 86–90.

[38] Dumarey, R., Dams, R. and Hoste, J., "Comparison of the Collection and Desorption Efficiency of Activated-Charcoal, Silver and Gold for the Determination of Vapour-Phase Atmospheric Hg," *Anal. Chem*., Vol. 57, 1985, pp. 2638–2643.

[39] Spiric, Z., "Mercury Removal from Natural Gas with Sulfur Impregnated Activated Carbon," *4th International Conference on Mercury as a Global Pollutant*, Hamburg, Germany, 1996.

[40] Schickling, C. and Broekaert, J. A. C., "Determination of Mercury Species in Gas Condensates by Online Coupled HPLC and Cold Vapour AAS," *Appl. Organomet. Chem*., Vol. 9, 1995, pp. 29–36.

[41] Hintelmann, H. and Wilken, R. D., "The Analysis of Organic Mercury Compounds Using LC with Online AFS Detection," *Appl. Organomet. Chem*., Vol. 7, 1993, pp. 173–180.

[42] Mercury in Naphtha, *UOP Method 938-95*, UOP, Des Plaines, IL, 1995.

[43] Stockwell, P. B. and Corns, W. T., *Hydrocarbon Asia*, October 1993, 36–41.

[44] Stockwell, P. B. and Corns, W. T., *Oil Gas Sci. Technol. Now*, 1994, Autumn, pp. 58–61.

[45] Weast, R. C., Ed., *CRC Handbook of Chemistry and Physics, 51st edition,* CRC Press, Cleveland, OH, 1971.

[46] Cameron, C. J., Didilion, B., Benayoun, D. and Dorbon, M., "Mercury: A Trace Contaminant in Natural Gas and Natural Gas Liquids," *Eurogas '96,* June 1996.

[47] Cai, Y., Jaffe, R., Alli, A. and Jones, R. D., "Determination of Organomercury Compounds in Aqueous Samples by Capillary Gas Chromatography AFS following Solid Phase Extraction," *Anal. Chim. Acta*, Vol. 334, 1996, pp. 251–259.

[48] Rubi, E., Lorenzo, R. A., Casais, C., Carro, A. M. and Cela, R., "Evaluation of Capillary Columns Used in the Routine Determination of Methylmercury in Biological and Environmental Samples," *J. Chromatogr*., Vol. 605, 1992, pp. 69–80.

[49] Bryan, G. W. and Langston, W. J., "Bioavailability, Accumulation and Effects of Heavy Metals in Sediments with Special Reference to UK Estuaries: A Review," *Environ. Pollut*., Vol. 76, 1972, pp. 89–131.

[50] Lansens, P., Casais, C., Meuleman, C. and Baeyens, W., "Evaluation of Gas-Chromatographic Columns for the Determination of Methylmercury in Aqueous Headspace Extracts from Biological Samples," *J. Chromatogr*., Vol. 586, 1991, pp. 329–340.

[51] Cappon, C. J. and Smith, J. C., "Gas-Chromatographic Determination of Inorganic Mercury and Organomercurials in Biological Materials." *Anal. Chem*., Vol. 49, 1977, pp. 365–369.

[52] Lee, Y. H., and Mowrer, J., "Determination of Methylmercury in Natural Waters at the Sub-nanograms per Liter Level by Capillary Gas-Chromatography after Adsorbent Pre-concentration," *Anal. Chim. Acta*, Vol. 221, 1989, pp. 259–268.

[53] Reilly, J. O., *J. Chromatogr*., Vol. 239, 1982, p. 437.

[54] Tao, H., Murakami, T., Tominaga, M. and Miyazaki, A., "Mercury Speciation in Natural Gas Condensate by Gas Chromatography-ICP-MS," *J. Anal. Atom. Spectrom*., Vol. 13, 1998, pp. 1085–1093.

[55] Emteborg, H., Sinemus, H. W., Radziuk, B., Baxter, D. C. and Frech, W., "Gas-Chromatography Coupled with Atomic Absorption Spectrometry: A Sensitive Instrumentation for Mercury Speciation," *Spectrochim. Acta, Part B*, Vol. 51, 1996, pp. 829–837.

[56] Munaf, E., Haraguchi, H. J., Ishii, D., Takeuchi, T. and Goto, M., "Speciation of Mercury Compounds in Waste Water by Microcolumn Liquid-Chromatography Using a Preconcentration Column with Cold Vapour-AAS," *Anal. Chim. Acta*, Vol. 235, 1990, pp. 399–404.

[57] Gracia, M. E., Gracia, R. P., Gracia, N. B. and Sanz-Mendel, A., *Talanta,* Vol. 41, 1994, pp. 1833–1839.

[58] Fujita, M. and Takabatake, E., "Continuous-Flow Reducing Vessel in Determination of Mercuric Compounds by Liquid-Chromatography Cold Vapour AAS," *Anal. Chem*., Vol. 55, 1983, pp. 454–457.

[59] Bulska, E., Baxter, D. C. and Frech, W., "Capillary Gas-Chromatography for Mercury Speciation," *Anal. Chim. Acta*, Vol. 249, 1991, pp. 545–554.

[60] Bulska, E., Emteborg, H., Baxter, D. C., Frech, W., Ellingsen, D. and Thomassen, Y., "Speciation of Mercury in Human Whole Blood by Capillary GC with a Complexometric Extraction and Butylation," *Analyst*, Vol. 117, 1992, pp. 657–663.

[61] Bloom, N. and Fitzgerald, W. F., "Determination of Volatile Mercury Species at the Picogram Level by Low Temperature GC with Cold Vapour AFS Detection," *Anal. Chim. Acta*, Vol. 208, 1988, pp. 151–161.

[62] Alli, A., Jaffe, R. and Jones, R., "Analysis of Organomercury Compounds in Sediments by Capillary GC with Atomic Fluorescence Detection," *J. of High Res. Chromatogr.*, Vol. 17, 1994, pp. 745–748.

[63] Shafawi, A., Foulkes, M. E., Ebdon, L., Corns, W. T. and Stockwell, P. B., "Determination of Total Mercury in Hydrocarbons and Natural Gas Condensate by Atomic Fluorescence Spectrometry," *Analyst*, Vol. 124, 1999, pp. 185–189.

[64] Shafawi, A., Foulkes, M., Ebdon, L., Corns, W. T. and Stockwell, P. B., "Preliminary Evaluation of Adsorbent-Based Mercury Removal Systems for Gas Condensate," *Anal. Chim. Acta.,* Vol. 415, 2000, pp. 21–32.

[65] National Institute of Standards, Gaithersburg, Maryland, 20899-1070, USA.

[66] National Physical Laboratory, Teddington, Middlesex, TW11 0LW, UK.

[67] Brown, A. S., Brown, R. J. C., Corns, W. T. and Stockwell, P. B., "Establishing SI Traceability for Measurements of Mercury Vapour," *Analyst*, Vol. 133, 2008, pp. 946–953.

[68] ASTM Standard D6350-98: Standard Test Method for Mercury Sampling and Analysis in Natural Gas by Atomic Fluorescence Spectroscopy, *Annual Book of ASTM Standards*, ASTM International, West Conshohocken, PA, 2003.

[69] BS EN ISO 6978-2: Natural Gas: Determination of Mercury: Sampling of Mercury by Amalgamation on Gold/Platinum Alloy, *British Standards*, BSI, 2005.

11

Applications of Mass Spectrometry in the Petroleum and Petrochemical Industries

Aaron Mendez[1] and Todd B. Colin[2]

MASS SPECTROMETRY

Mass spectrometry is approaching its first 100 years of being one of the most universal, versatile, and sensitive methods of analysis. It is the fastest-growing analytical technique of this decade, based on the great variety of detectors and their combination. It is an essential tool in the life sciences, where new high-resolution instrumentation, interfaces, and mass ranges have been reached. J. J. Thomson, almost a century ago, stated that this would be a technique that would resolve analytical problems with far more sensitivity and ease of use; this seems to be now an unarguable statement.

Basic Mass Spectrometry Instrumentation

A mass spectrometer is an analytical instrument that unequivocally identifies chemical species by exposing them to high ionizing energies, normally electrons at 70 eV, and recording and analyzing their characteristic fragmentation patterns. Frequently this analysis involves comparing mass spectra with standard libraries of several hundred thousand compounds. When there is a need to speciate complex volatile mixtures, coupling a mass spectrometer with a gas, liquid, or supercritical fluid chromatograph as a separating device makes it a powerful analytical tool with vast applications in all areas of science and technology.

A mass spectrometer operates under vacuum, normally in the 10^{-5} to 10^{-7} torr region. This is accomplished by a primary vacuum stage rotary pump and a secondary vacuum stage turbomolecular or diffusion pump. The primary vacuum stage, or fore vacuum, is performed by a rotary pump; this is the main cause of system contamination, so it is strongly advised to use an oil free pump or to have a trapping device to impede the oil from getting into the analyzer region. The schematic in Fig. 1 shows the system and its pressure regime.

The modern mass spectrometer is a versatile, highly repeatable, and multitask device capable of performing solid, liquid, and gaseous sample analysis in a timely manner with high sensitivity, precision, and no mass discrimination. It provides automatic scan/selective ion monitoring (SIM) fast scan and automatic operation. For special applications, diagnostics, and troubleshooting, it also has manual tuning and manual operation capabilities.

[1] *PAC Houston, Texas*
[2] *Colin Consulting Macedon, New York*

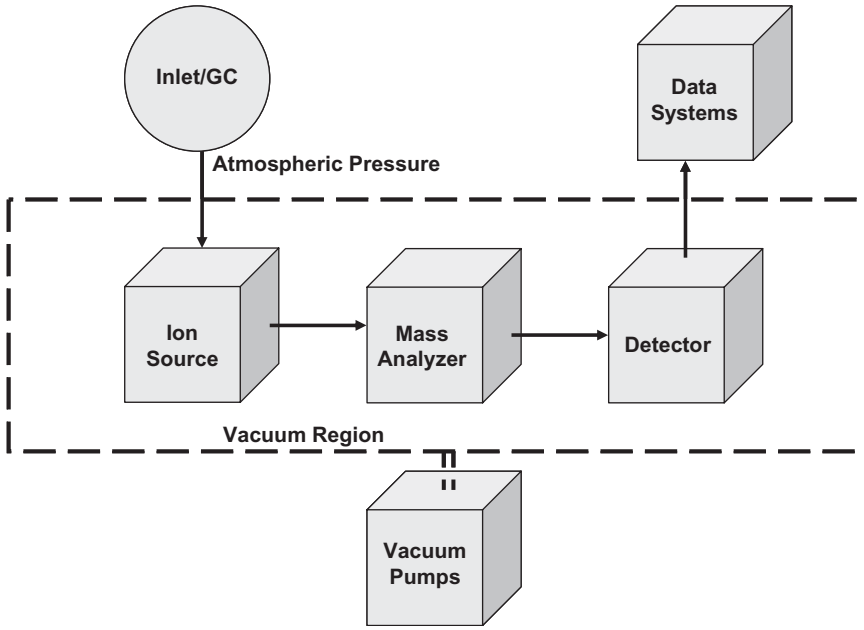

Fig. 1—Typical MS System Components.

Versatile means:

- Capable of using multiple scan functions
- Capable of using a single ionization source for electron impact (EI) and chemical ionization analysis
- Capable of using multiple inlet systems, i.e., interfaces to several separation chromatographs
- Wide range of multiramp source temperature programming
- Ease of interface with chromatographic detectors, dean switches, microfluidic splitters, etc.

Performing in a timely manner means:

- Fast scanning ranges
- Fast data processing
- Fast pumping efficiency and differential vacuum
- Fast acquisition rates
- Ease of operation:
  - Part exchange and maintenance: sources, filaments, gauges, and detectors
  - Independence of MS functions from GC inlet operation
  - Ample user friendly acquisition and data processing software
  - Built-in systems for checks and diagnostics
  - Amenable to most data processing and data management software

The way a sample is introduced into the ion source, the way it is ionized, and the type and number of mass analyzers constitute a vast variety of instrumentation, techniques, and applications.

When combined with a gas chromatograph, it uses a flow-through narrow tube known as the column, through which different chemical constituents of a sample pass in a gas stream (carrier gas, mobile phase) at different rates, depending on their various chemical and physical properties and their interaction with a specific column filling called the stationary phase. As the chemicals exit the end of the column at different retention times, they are detected, identified, and quantified electronically.

Low-Resolution Quantitative Methods

The petroleum industry played a very important role in the spread of mass spectrometry as a powerful tool to characterize petroleum gases and fuel distillates. The algorithms were based on the fact that group types of hydrocarbons under high-energy electrons produce characteristic fragments, enabling the expression of their content in terms of paraffin, naphthenes, and aromatic compounds.

With the use of low ionizing voltages and high mass resolving power, the production of ions is mainly due to ionized molecular species. In this case the algorithm is based on accurate mass processing to determine the best fit of empirical formulas and the degree of saturation or hydrogen deficiency.

Those standards, still in use today, were developed on single 180° magnetic sector mass spectrometers manufactured by the Consolidated Electrodynamic Corporation, specifically the CEC 101, 102, and 21–103 models.

Analysis of oil samples by mass spectrometry has been taking place for almost six decades. This application in fact is considered to be the first analytical application rapidly growing into other industries such as environmental, agriculture, forensic, medicine, and fundamental scientific research. Mass spectrometry is based on the ionization of neutral molecules with different sources of energy. The most common ionization technique is the use of high energy electron beams conventionally set at 70 eV. Ionization of molecules occurs mainly in the gas phase through thermodynamic processes that cause the molecules to lose valence electrons. When this process takes place, molecules yield a particular pattern of molecular and fragment ions characteristic to the molecules of interest. The high energy electron-impact ionization (EI) mass spectra are highly reproducible when keeping experimental conditions constant. This phenomenon was first applied in a petroleum laboratory by O. L. Roberts at the Atlantic Refining Company in October 1942, as reported by S. S. Kurtz [1]. Several researchers also applied the technique to analyze light hydrocarbon samples and low boiling organic compounds. However the first standard procedure on gasoline and naphtha fractions was introduced by Brown [2], providing a quantitative report by grouping the constituents of complex mixtures in families or compound types by summation and normalization of characteristic ions.

ASTM Committee D02 has currently under its jurisdiction the following group type quantitative methods:

D2650, Standard Test Method for Chemical Composition of Gases by Mass Spectrometry. This method covers the determination of gases including hydrogen, hydrocarbons with up to six carbon atoms, carbon monoxide, carbon dioxide, C1–C2 mercaptans, hydrogen sulfide, nitrogen, oxygen, and argon. [3] Concentration limit is 0.1 mole %.

D2789, Standard Test Method for Hydrocarbon Types in Low Olefinic Gasoline by Mass Spectrometry [3]. This method is applicable to gasoline having an olefinic content not higher than 3 %v and a final boiling point of less than 210°C. Although still in use, these methods developed in magnetic sector instruments are not favored because of the development of gas chromatographic multidimensional and dehydroepiandrosterone (DHA) applications considered to be more versatile and simpler to use.

D2445, Standard Test Method for Hydrocarbon Types in Middle Distillates by Mass Spectrometry [2]. This method determines the hydrocarbon types in virgin middle distillates with a final boiling point of 343°C. Because this is a low-resolution method, the sample has to be separated into aromatic and saturates fraction before analysis. The method reports 11 hydrocarbon types, including total paraffins, mono-, di-, and tricycloparaffins, alkylbenzenes, indanes and tetralins, and di- and tricyclicaromatics.

D2786, Standard Test Method for Hydrocarbon Type Analysis of Gas-Oil Saturates Fractions by High Ionizing Voltage Mass Spectrometry [3]. This method is applicable to hydrocarbon saturates with average carbon numbers of up to C32. It reports the distribution of seven saturates, hydrocarbon types, paraffins, C1–C6 ring naphthenes, and residual monoaromatics.

D3239, Standard Test Method for Aromatic Types Analysis of Gas-Oil Aromatic Fractions by High Ionizing Voltage Mass Spectrometry [4]. This method reports 18 aromatic hydrocarbon types and three aromatic thiophenes in petroleum fractions boiling within the range of 205° to 540°C. The sample should not contain more than 1 %w sulfur and must be nonolefinic.

The various methods reported, covering the whole distillation range, are generally accurate within ± 5 % relative standard deviation. They are based on the grouping of the characteristic molecular and fragment ions presented in Table 1. Because the masses of molecular ions and their corresponding fragment ions are identical for olefins and naphthenes of the same carbon number, the olefinic content in the sample should not exceed the maximum concentration recommended by the particular method being used.

This procedure works well on total samples only for gasoline range hydrocarbons. For high boiling fractions, the possibility of having mass overlap among different compound types becomes greater, which would require preparative liquid chromatographic separation of saturate and aromatic hydrocarbons before mass analysis. For example, paraffins overlap with alkyl naphthalenes above C_9 and with dibenzothiophenes above C_{13}. Naphthenes overlap with biphenyls above 154 Da. Dinaphthenes overlap with fluorenes and dibenzanthracenes above 278 Da. Tricycloparaffins overlap with phenanthrenes and naphthobenzothiophenes above mass 178. From the ions shown in Table 1, a series of inverse sensitivity matrices are constructed for quantitative analysis after corrections for isotopic contribution in the mass spectra. Based on this methodology, various ASTM standard methods of analysis were developed: D2650 for gases, D2789 for gasolines, D2425 for kerosines, D2786 for gas oil saturates, and D3239 for gas-oil aromatics [3,4].

Procedures in a similar approach for the different boiling point ranges are published by the oil industry [5–8]. O'Neal [5] set the basis of calculating the hydrocarbon type distribution for middle distillates up to C_{40}. In this approach, an all glass heated inlet system (AGHIS) was used for the first time to ensure

TABLE 1—Molecular and Fragment Ion Masses of Various Hydrocarbon Types	
Alkanes	43 = 43 + 57 + 71 + 85 + 99 + ...
Noncondensed cycloalkanes	55 = 55 + 69 + 83 + 97 + 98 + 111 + 112 + ...
Condensed dicycloalkanes	67 = 67 + 81 + 95 + 96 + 109 + 110 + 123 + 124 + ...
Condensed tricycloalkanes	93 = 93 + 107 + 121 + 135 + 149 + ... + 94 + 108 + 122 + 136 + 150 + 164 + ...
Alkyl benzenes	77 = 77 + 91 + 105 + 119 + 133 + ...
Indanes – Tetralins	104 = 104 + 117 + 118 + 131 + 132 + 145 + ...
Dinaphthenebenzenes	157 = 157 + 158 + 171 + 172 + 185 + 186 + ...
Alkyl naphthalenes	127 = 127 + 128 + 141 + 142 + 155 + 156 + 169 + ...
Fluorenes	165 = 166 + 180 + 194 + ... + 165 + 179 + 193 + ...
Acenaphthenes, Dibenzofurans	153 = 154 + 168 + 182 + ... + 167 + 181 + 195 + ...
Phenanthrenes	177 = 178 + 192 + 206 + ... + 177 + 191 + 205 + ...
Naphthenephenanthrenes	217 = 217 + 218 + 231 + 232 + 245 + 246 + ...
Chrysenes	241 = 241 + 255 + 269 + ... + 242 + 256 + 268 + ...
Biphenyls	153 = 154 + 168 + 182 + ... + 153 + 167 + 181 + ...
Dibenzanthracenes	277 = 278 + 292 + 306 + ... + 277 + 291 + 305 + ...
Benzothiophenes	133 = 133 + 147 + 161 + ... + 134 + 148 + 162 + ...
Naphthobenzothiophenes	247 = 248 + 262 + 276 + ... + 247 + 261 + 275 + ...
Dibenzothiophenes	183 = 184 + 198 + 212 + ... + 183 + 197 + 211 + ...

constant vapor pressure for reproducible results. Efforts were on the identification of sulfur compounds, especially for the thiophenic types, and condensed aromatics. At the same time, the expansion of the number of naphthenic condensed rings in the calculations and the increase of boiling range extend the methods to lubricating oil fractions.

The applications of mass spectrometry to other than virgin hydrocarbon samples came immediately. Gordon et al. [9] applied low ionizing voltage EIMS instead of the conventional 70 eV electron impact–mass spectrometry (EI-MS) and ultraviolet spectrophotometry to cracked gas oils to resolve ambiguities in the determination of aromatic compounds. At 10 to 20 eV ionizing energy, only aromatic molecular ions are produced with practically no fragmentation. In this circumstance, information based on fragment ions is no longer available. Because spectra were recorded at low resolution, the measured mass values correspond to nominal masses. As a result, the concept of Z-series to represent

hydrogen deficiency of the compound series was developed. The report is given according to the general formula:

$$C_nH_{2n+z} \quad (1)$$

Pioneering work on the molecular characterization of catalytic stocks was performed at low-resolution, low- and high-voltage mass spectrometry [10,11]. The combination of mass spectrometry (MS) with other techniques such as nuclear magnetic resonance (NMR), ultraviolet (UV), and infrared (IR) was established as a basic approach to gain information on the composition of very complex hydrocarbon mixtures of different natures.

Efforts continued on expanding the application of mass spectrometry toward higher boiling ranges. Special attention was paid to sulfur and nitrogen compounds. Lumpkin [8] and Hood and O'Neal [12] presented a method for middle distillates based on ASTM D2425. In their works, matrices were constructed for lineal paraffins and up to six naphthene condensed rings. Similarly, Snyder et al. [13] developed a method for the direct analysis of heavy reformates and hydrodealkylated products boiling in the kerosine range. These authors reported nine compound types: alkanes, noncondensed and condensed cycloalkanes, alkyl benzenes, indanes, tetralins and alkyl naphthalenes, aromatic hydrocarbons of the −14 and −16 Z series, and benzothiophenes. One very interesting feature of the Snyder et al. method is that even at the low mass resolution and the high ionizing voltage, it did not require the prior separation of the saturates and aromatic fractions.

Following the expansion of mass spectrometry, the convenience of avoiding preparative liquid chromatographic separations was rapidly recognized. This is particularly meaningful because it reduces the time of analysis and avoids sources of errors. Chromatographic separations lower the reproducibility and repeatability of final results due to solvent stripping, especially in the low boiling range, i.e., diesels, jet fuels, and kerosines. Gallegos et al. [14] applied high-resolution MS to analyze whole samples without chromatographic separation, which is discussed later in this chapter. Robinson [15] developed a low-resolution procedure applicable to a wide boiling range, 200–1100°F. A baseline technique artificially separates the aromatics from saturates and contributes side chain substitution of aromatics to the saturate signal. The procedure determines 4 saturate and 12 aromatic hydrocarbons types, including 3 sulfur compound types as reported in ASTM D3239.

The vast majority of contributions to group type analysis by mass spectrometry was developed in the magnetic mass spectrometers of the Consolidated Electrodynamics CEC 2100 series. With the advent of new instrumentation, discrepancies in the correlation of the Robinson procedure with the ASTM methods started to appear. Piemonti and Hazos [16] introduced a modified Robinson procedure to overcome this deficiency. The baseline separation was corrected using a Kratos MS-25Q mass spectrometer that allowed reasonable correlations with the standard ASTM procedures to be obtained.

This concern was brought up by Ashe [17], who pointed out on the scarce demand of expensive double-focusing sector instruments for routine refinery operations. As a replacement for the conventional magnetic sector instruments, he attached a quadrupole mass filter to a conventional AGHIS. After some experimental considerations derived from the different philosophy in the construction

of bench-top quadrupole mass analyzers, it was possible to reach very reproducible results and a good correlation with historical data from sector instruments.

Several authors have developed alternative procedures that require no lengthy preparative liquid chromatographic separations for gas chromatography (GC)/MS instrumentation [18,19]. Whether the inverse matrices and sensitivity factors obtained earlier for sector instruments are still applicable remains unanswered. The task of developing new coefficients and sensitivity factors for new instrumentation is not realistic. There are various reasons for this: a great variety of manufacturers and configurations and the lack of sources for research-grade pure hydrocarbons that were once available during the years of the atmospheric pressure ionization (API) projects and prepared by Carnegie Mellon University, Pennsylvania, make the task simply adamantly complex.

High-Resolution Mass Spectrometry

Mass spectrometry has been an important analytical tool for analyzing petroleum products since 1942. The spread of the technique is mainly due to its success in providing detailed information on the composition of very complex mixtures that fall beyond the instrumental resolution capabilities of capillary gas chromatographic columns, giving qualitative and quantitative information of the hydrocarbon group types present. It requires only a very small amount of sample and little or no preparation steps. However, there are some disadvantages such as the complexity of the spectra, the difficulty associated with isomer identification, and the requirement of vaporization of samples that limit its application to samples with high boiling points and poor thermal stability. The loss of sensitivity due to the narrowing of resolution slits in order to achieve the ultimate mass resolution also limits its range of quantitation.

The application of mass spectrometry in the petroleum industry started with the analysis of gas and low boiling liquid samples. Significant breakthroughs in its evolution include the introduction of heated inlet systems for the analysis of liquid and volatile solid compounds (AGHIS), temperature programmable inlets, low voltage EI techniques, high resolution instrumentation capable of measuring accurate masses and separating multiplets of the same nominal mass, and computerized data acquisition and handling systems. However, the compositional analysis of hydrocarbons and aromatics compounds containing one or more atoms of sulfur, nitrogen, and oxygen in distillates has become very important in refining of crude oils and in the storage and use of refined products. Moreover, sulfur- and nitrogen-containing species may poison catalysts and contribute to environmental pollution. Generally they must be removed before refining catalytic processes.

Detailed hydrocarbon analysis remains a problem because above naphthas and gasoline the resolving capabilities of a chromatographic column are very limited. The amount of coeluting compounds makes the characterization rather challenging.

The use of high-resolution mass spectrometry eliminates most of the interferences between saturate and aromatic hydrocarbons and, further, removes some of the multiplets of sulfur compounds with isobaric hydrocarbons. Resolving power (RP) is of vital importance for high-resolution mass spectrometric methods that determine elemental composition in terms of homologic series of compounds. Molecular ions containing one or more less-abundant

isotopes of its constituent elements (e.g., ^{13}C, ^{34}S) can contribute significantly to complicate the mass spectra of samples of interest. In addition, low-voltage electron ionization can produce non-negligible quantities of fragment ions. Different combinations of atoms can be nearly the same mass, e.g., $^{12}C_3$ vs. $^{32}SH_4$, ^{13}C vs. CH, CH_2 vs. ^{14}N, and CH_4 vs. O. Thus the presence of these overlapping ions can complicate the identification and quantification of various compound types present in a given sample, such as aromatic and polar crude oil fractions boiling up to 1050°F. Consequently, resolution of isobaric ions in these distillates requires mass resolution considerably in excess of 10,000. The RP needed for the separation of the most common doublets found in hydrocarbon samples is illustrated in Table 2.

RP is defined in terms of the overlap (or valley) between two peaks. Thus for two peaks of equal height, masses m1 and m2, when there is overlap between the two peaks to a stated percentage of either peak height (10 % is recommended), the RP is defined as m1/(m1 – m2). The percentage overlap (or valley) concerned must always be stated.

In high-resolution mass spectrometric methods, composition is determined in terms of the amount of homologs of various hydrocarbon and heteroatom-containing compound types. When the samples become more complex, the grouping in hydrocarbon types is not straightforward, and therefore results are expressed in terms of hydrogen deficiency Z-series. For high-resolution mass spectrometers, precise standardization of operating conditions is even more important for quantitative measurements than for low-resolution mass spectrometers. Generally, the higher the resolution, the weaker the signal and the longer the data acquisition time needed. Special mass standards that do not interfere with sample ions, mostly chlorinated hydrocarbon petroleum fractions, are employed for mass calibration. The chlorinated compounds are preferred because of their higher sensitivities at the low ionization voltage compared to those of the fluorinated standards common in regular EI-MS.

A technique was developed by McMurray et al. [20] to obtain high-resolution mass spectra from fast magnetic scans of gas chromatographic effluents.

The use of low- and high-resolution mass spectrometry for quantitative analysis based on group type calculation of saturates and aromatic fractions has been reported [21,22]. Table 3 lists a number of series that can be identified in one high-resolution mass scan. As indicated in this table, it is possible to obtain 27 different hydrocarbon series, and a number of single sulfur-, oxygen-containing series. So in one high-resolution scan, it is possible to determine more than 200 series and to have quantitative measurement of not only the Z-series but also carbon number in the series. In this case, the range can be expanded to gas-oil fractions boiling up to 1,200°F and eventually be applicable to crudes oils, coal liquids, shale oils, and refinery streams. These methods would be facilitated by the separation of the hydrocarbon mixture into saturate and aromatic fractions. This fact affects the efficiency of the technique in terms of turn-around times.

Gallegos et al. [23] reported the first multicomponent group-type analysis using high-resolution mass spectrometry to analyze high boiling petroleum fractions without silica gel separation. Their method made it possible to get quantitative data for seven saturate hydrocarbon compound classes from zero to six naphthene rings, nine aromatics compound classes, and three aromatic sulfur

TABLE 2—Resolution Required for Mass Doublets in Petroleum and Synthetic Samples

Doublet	ΔMass, u	Required Mass Resolution @ m/z 400
H_{16}/O	0.1303	3,100
O_2H_{16}/C_4	0.1150	3,500
H_{12}/C	0.0939	4,300
C_2H_8/S	0.0905	4,400
C_2H_8/O_2	0.0728	5,500
N_2H_8/C_3	0.0687	5,800
OH_8/C	0.0575	7,000
CH_4O/S	0.0541	7,400
N_2H_4/O_2	0.0476	8,400
O_2H_8/CN_2	0.0463	8,600
CH_4/O	0.0364	11,000
C_2H_4/N_2	0.0252	15,900
O_2H_4/C_3	0.0211	19,000
O_2/S	0.0178	22,500
$N_2H/^{13}CO$	0.0157	25,500
C_4/O_3	0.0153	26,100
CH_2/N	0.0126	31,700
N_2/CO	0.0112	35,700
H_4O_3/C_2N_2	0.0099	40,400
$^{13}CH/N$	0.0081	49,400
SH_4/C_3	0.0034	117,600

compound types covering the range of 500° to 950°F. However, this method does not account for all of the sulfur compounds that are present. Nevertheless, the agreement was very good when the weight % sulfur by mass spectrometry was compared with that determined by X-ray fluorescence.

Joly [24] used a 30 × 30 matrix at 10.00 mass resolution to obtain quantitative data for 3 saturate compound classes, 13 aromatics, and 14 sulfur compound classes.

Bouquet and Brumett [25] and later Fafet at al. [26] introduced very important modifications in the inlet system that enables the determination of 33 group

TABLE 3—Common Compound Types in Petroleum

Class	Compound Types Range in General Formulas	Number of Types
Hydrocarbons	C_nH_{2n} to C_nH_{2n-52}	27
Sulfur Compounds	$C_nH_{2n+2}S$ to $C_nH_{2n-42}S$	23
	$C_nH_{2n-12}S_2$ to $C_nH_{2n-30}S_2$	11
Sulfur-Oxygen Compounds	$C_nH_{2n-10}SO$ to $C_nH_{2n-30}SO$	11
	$C_nH_{2n-10}SO_2$ to $C_nH_{2n-18}SO_2$	5
	$C_nH_{2n-10}SO_3$ to $C_nH_{2n-20}SO_3$	6
Nitrogen Compounds	$C_nH_{2n-3}N$ to $C_nH_{2n-51}N$	25
	$C_nH_{2n-12}N_2$ to $C_nH_{2n-26}N_2$	8
	$C_nH_{2n-5}N_3$ to $C_nH_{2n-11}N_3$	4
Oxygen Compounds	$C_nH_{2n-2}O$ to $C_nH_{2n-50}O$	25
	$C_nH_{2n-6}O_2$ to $C_nH_{2n-46}O_2$	19
	$C_nH_{2n-6}O_3$ to $C_nH_{2n-32}O_3$	14
	$C_nH_{2n-10}O_4$ to $C_nH_{2n-20}O_4$	7
Nitrogen-Oxygen Compounds	$C_nH_{2n-7}NO$ to $C_nH_{2n-41}NO$	18 203

types without any sample separation of samples weighing up to 1,000 Da. They used high ionizing voltage but recorded the mass spectra at a resolution of 10,000 RP. They reported 4 saturates groups, from $Z = +2$ to $Z = -6$; 14 aromatics from $Z = -6$ to $Z = -30$, and 17 sulfur thiophenic compounds ranging from $Z = -26S$ to $Z = -32S_2$.

Early applications of high-resolution FT-ICR-MS measurements for hydrocarbon characterization were described by Hsu and coworkers [27]. They demonstrated the potential use of FT-ICR-MS in the analysis of complex hydrocarbon mixtures with resolving power beyond sector instruments. The high stability of accurate mass measurement even under different ion source conditions eliminated the need of mass reference standards. However, ultrahigh-resolution mass measurement was limited to rather narrow mass ranges to avoid space-charge effects. Nevertheless, these narrow mass ranges can be acquired and reconstructed into a wide mass range spectrum. For the determination of compound type distribution, it required the development of software capable of linking high-resolution quantification results of all individual mass segments.

Marshall et al. [28] published a report in which FT-ICR/MS was used to provide the best available mass resolution and mass accuracy for molecular ion type analysis of aromatic neutral fraction of gas oils. Their results resolved most common doublets found in hydrocarbon samples, such as C_3/SH_4, $^{13}C/CH$, and

$^{13}CH_3S/C_4$. Additional application of this technique was reported for the compositional analysis of processed and unprocessed diesel fuels [29]. By comparing the relative abundances of mass-resolved sulfur-containing species before and after hydrotreating, they found complete removal of the sulfur-containing species except for dimethyl-dibenzothiophene and higher alkyl-substituted dibenzothiophenes.

It is possible now to separate a significant number of compounds with a difference in mass of 0.0034 in species of, for instance, those with a nominal mass of 274 daltons ($C_{19}H_{14}S$, $C_{16}H_{18}S_2$, $C_{20}H_{18}O$, $C_{21}H_{22}$, $C_{18}H_{26}S$, $C_{20}H_{34}$).

Acidic and basic species have been also fully characterized by high-resolution negative and positive ionelectrospray ionization followed by FT-ICR/MS [30]. A vast spectrum of polar species could be identified based on the accurate mass data that corresponded to polycyclic monoaromatic carboxylic acids, SxOy mono- and polyaromatic species, and complex pyrrolic and phenolic species.

Gas Chromatography-Mass Spectrometry

Instrumentation in mass spectrometry has changed dramatically, partly because of the need to reduce investment costs and partly because of the need to spread its application and simplify the analytical process. Conventionally, mass spectrometry required highly qualified and experienced personnel to perform the analysis.

With the advent of GC-MS, its application to the oil industry and particularly for group type analysis was encouraged by the ability of the gas chromatograph to calibrate and quantify the separated peaks followed by the unambiguous mass spectrometric identification based on the fragmentation pattern library search [31]. The distribution of aromatics by carbon numbers and boiling points can be enhanced by carrying out low-voltage EI experiments [32]. With the miniaturization and automation of GC-MS systems and the reduction of prices, this instrumentation became highly disseminated in the scientific and industrial communities. The application of GC-MS in the hydrocarbon analysis passed through an explosive period very much similar to mass spectrometry in the 1950s [33–35].

Dzidic et al. [34] and Wadsworth and Villalanti [35] used a Townsend discharge source and nitric oxide (NO) as a chemical reagent to ionize hydrocarbon mixtures. The way NO^+ reacts with the different hydrocarbon types allows the performance of PNA (paraffins, naphthenes, and aromatics) analysis and sulfur compounds. In this reaction, aliphatic hydrocarbons will give only $(M–1)^+$ ions whereas aromatic hydrocarbons react to produce exclusively M^+ ions, which reflects the possibility to analyze total samples avoiding the preparative liquid chromatography separation step. The method also determines the distribution of hydrocarbons according to carbon number and hydrogen deficiency Z-series and can be applied to the whole distillation range up to VGO of approximately 1,000°F.

Combining gas chromatography with mass spectrometry also enables the PIONA (n-paraffins, iso-paraffins, naphthenes, and aromatics) analysis of gasolines to be performed in a very systematic way [36]. The procedure takes advantage of the resolving power of the chromatograph and the ability of the mass spectrometer to detect eluting compounds at very low levels and to identify them unambiguously. The special software by means of pure compound response factors allows for the resolution of overlapping compounds.

Several ionization modes have been used apart from electron impact at 70 eV. We have already described low-voltage eV and NO chemical ionization. Malhotra et al. [37] used field ionization (FI), which is a "soft" ionization technique, especially amenable to volatile compounds, yielding mainly molecular ions with little or no fragmentation. Using a special ion source design known as a volcano source on a HP 5971A mass selective detector, it was possible to produce a PNA and benzothiophenes report on several fuel samples such as gasolines, jet fuels, and an Arabian sweet crude oil. The gas chromatograph in this case provided the separation for the mass overlapping compounds (see Table 1). The quantification was performed in a very straightforward way: peak integration normalized by applying compound-specific sensitivity factors.

As was noted by several authors, there is a need for a GC-MS system with a universal soft ionization mode [17]. This point was expanded by Schoemakers et al. [38], who also presented an interesting comparison of two-dimensional GC and GC-MS. In search of this ideal soft ionization technique, important conclusions are made on the still-unreachable potential of the technique. Lately, FI-TOF (time-of-flight) mass spectrometers combined with gas and liquid chromatography have become commercially available [39]. A very useful feature of this type of instrumentation is that TOF allows for the determination of accurate mass at low resolution. Normally high resolving power is reached on sector instruments at the expense of sensitivity. Therefore, keeping the full sensitivity of the technique and the tremendous separation capabilities of chromatography in general will certainly increase enormously the possibility of measuring low concentrations and determining compound type distribution of hydrocarbons.

A very novel application of GC-MS that expands the use of the technique well beyond the separation capabilities of a chromatographic column has been reported by several authors [40–44]. Applying spectral deconvolution techniques [32], the relative concentration of four saturate and four aromatic compound types were reported on hydroconversion products of deasphalted vacuum residue by avoiding the need for separation. Ashe [41] and Roussis [42,43] patented and developed methods to predict physical and chemical properties of crude oils by means of simulated distillation mass spectrometry. The crude oil distillation profiles are converted to both weight and volume true boiling point curves, allowing the characterization of fractions of interest without the need for obtaining the physical cuts.

Mendez et al. [44] similarly obtained the boiling point profile of light crude oil samples and applied an algorithm [16] based on C. J. Robinson's approach [15] to get a quantitative report for both the total distillable fraction of the crude oil and the lubricant fractions of interest. Good correlations were obtained when the fractions of interest calculated from the whole crude total ion chromatogram (TIC) were compared with several lube-oil basestocks. Table 4 shows a quantitative group type report of three different lubricant base stocks, and Table 5 represent the same fractions taken out from the whole crude chromatogram, applying the algorithm in the same intervals for every one of the fractions. Fig. 2 represents a typical paraffinic whole crude oil chromatogram using a high temperature metallic capillary GC column. In this figure, the carbon number and boiling point are calibrated against retention time.

TABLE 4—Hydrocarbon Type Analysis of Lube-Oil Basestocks

	SPO[a]	LMO[b]	MMO[c]
Total Saturates, %w	**75.3**	**69.5**	**53.6**
Paraffins	39.7	27.2	17.4
Monocycloparaffins	13.1	14.2	13.4
Dicycloparaffins	7.2	12.6	10.3
Tricycloparaffins+	15.4	15.4	12.6
Total Aromatics, %w	**24.7**	**30.5**	**46.4**
Monoaromatics	10.5	12.9	21.0
Benzenes	3.3	4.0	7.0
Naphthenebenzenes	3.4	4.0	6.5
Dinaphthenebenzenes	3.7	4.9	7.4
Diaromatics	***5.2***	**3.5**	**6.9**
Naphthalenes	0.0	0.0	0.0
Acenaphthenes, Dibenzofurans	2.5	0.8	2.0
Fluorenes	2.7	2.7	4.9
Triaromatics	**1.9**	**2.2**	**3.0**
Phenanthrenes	1.1	1.0	1.6
Naphthenophenanthrenes	0.9	1.2	1.4
Tetraaromatics	**2.1**	**4.3**	**3.4**
Pyrenes	1.6	2.7	1.8
Chrysenes	0.5	1.6	1.6
Pentaaromatics	0.6	0.5	1.3
Perylenes	0.6	0.4	1.1
Dibenzanthracenes	0.0	0.1	0.2
Thiophenes	**4.2**	**6.8**	**6.8**
Benzothiophenes	2.1	2.3	2.4
Dibenzothiophenes	2.1	2.9	3.2
Naphthobenzothiophenes	0.0	1.6	1.2
Unidentified Aromatics	**0.0**	**0.3**	**4.1**
Class II	0.0	0.0	1.1

(*Continued*)

TABLE 4—Hydrocarbon Type Analysis of Lube-Oil Basestocks (Continued)			
	SPO[a]	LMO[b]	MMO[c]
Class III	0.0	0.0	0.4
Class IV	0.0	0.3	2.2
Class V	0.0	0.0	0.0
Class VI	0.0	0.0	0.1
Class VII	0.0	0.0	0.3

[a] Spindle oil
[b] Light machine oil
[c] Medium machine oil

TABLE 5—Hydrocarbon Type Analysis from Whole Crude			
	SPO[a] Time interval 21–33 min	LMO[b] Time interval 24–42 min	MMO[c] Time interval 28–54 min
Total Saturates, %w	**76.0**	**69.2**	**54.2**
Paraffins	42.7	33.5	20.2
Monocycloparaffins	14.3	13.8	12.2
Dicycloparaffins	10.4	10.9	9.4
Tricycloparaffins +	8.6	11.0	12.3
Total Aromatics, %w	**24.0**	**30.8**	**45.8**
Monoaromatics	10.8	11.9	20.7
Benzenes	3.8	3.8	7.1
Naphthenebenzenes	3.2	3.7	6.3
Dinaphthenebenzenes	3.9	4.4	7.2
Diaromatics	**4.0**	**5.4**	**7.6**
Naphthalenes	0.0	0.0	0.0
Acenaphthenes, Dibenzofurans	1.4	1.9	1.8
Fluorenes	2.6	3.5	5.7
Triaromatics	**2.7**	**3.8**	**1.7**
Phenanthrenes	2.0	2.4	1.2
Naphthenophenanthrenes	0.7	1.4	0.6

TABLE 5—Hydrocarbon Type Analysis from Whole Crude (Continued)

	SPO[a] Time interval 21–33 min	LMO[b] Time interval 24–42 min	MMO[c] Time interval 28–54 min
Tetraaromatics	**1.7**	**3.1**	**4.7**
Pyrenes	1.4	2.2	2.7
Chrysenes	0.3	1.0	1.9
Pentaaromatics	**0.0**	**0.3**	**0.8**
Perylenes	0.0	0.2	0.5
Dibenzanthracenes	0.0	0.1	0.3
Thiophenes	**4.7**	**6.2**	**7.3**
Benzothiophenes	2.4	2.5	2.6
Dibenzothiophenes	2.1	3.2	3.6
Naphthobenzothiophenes	0.2	0.5	1.1
Unidentified Aromatics	**0.0**	**0.1**	**3.1**
Class II	0.0	0.1	0.3
Class III	0.0	0.0	0.3
Class IV	0.0	0.0	2.3
Class V	0.0	0.0	0.0
Class VI	0.0	0.0	0.0
Class VII	0.0	0.0	0.1

[a] Spindle oil
[b] Light machine oil
[c] Medium machine oil

The boiling points and carbon numbers were measured by injecting on the same instrumental conditions a standard normal paraffin mixture. All of these contributions not only expand the use of a GC-MS system but provide for a method to rapidly screen a crude oil to asses the quality and yield of distillable fractions of interest.

The use of a GC-MS to produce a quantitative analysis based on group types of hydrocarbons proved that a modern GC-MS system can be used in place of the old conventional magnetic mass spectrometers that served to develop the ASTM methods.

This approach was further developed [45] to include an FID detector and a microfluidic splitter to split in a more controlled way the effluents to both detectors. Fig. 3 illustrates the system. The main reason to use this arrangement

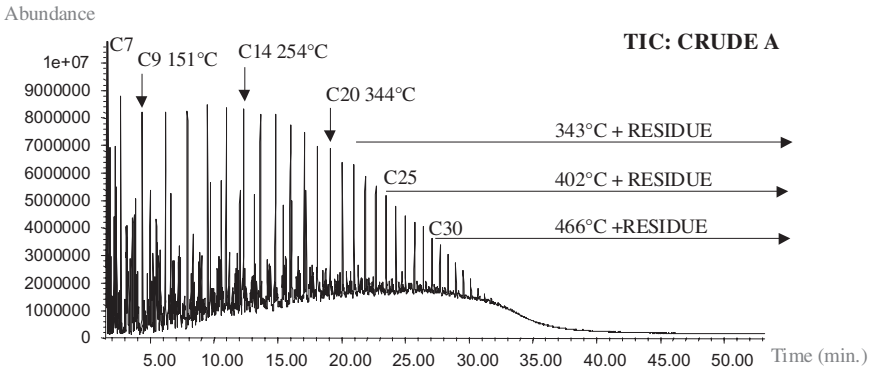

Fig. 2—Fingerprint representation of whole crude oil.

is to use the FID signal to perform the SimDist calculations complying with the ASTM standard methods D7213 and D7169. The MS signal was used to produce the group type quantitative reports such as those in Tables 4 and 5.

It was found that there was no noticeable discrimination of the signal below 16 minutes in either of the two detectors, as can be seen in Fig. 4 for a crude oil sample dissolved in CS_2 as per the ASTM D7169 SimDist method.

This approach was correlated with HPLC-ELSD analysis with the results presented in Table 6.

The ability to combine the physical properties of hydrocarbons with mass spectrometry allows the use of T50, which is the temperature value at 50 % recovery, as the average molecular weight. This is an important parameter for

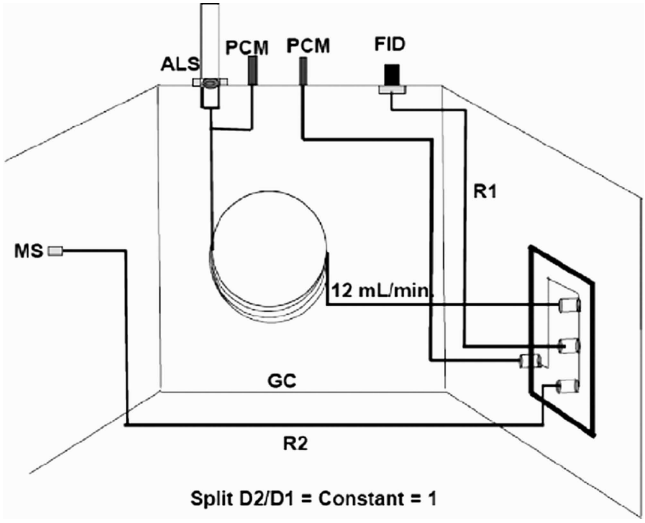

Fig. 3—Schematic diagram of the GC/MS/FID configuration.

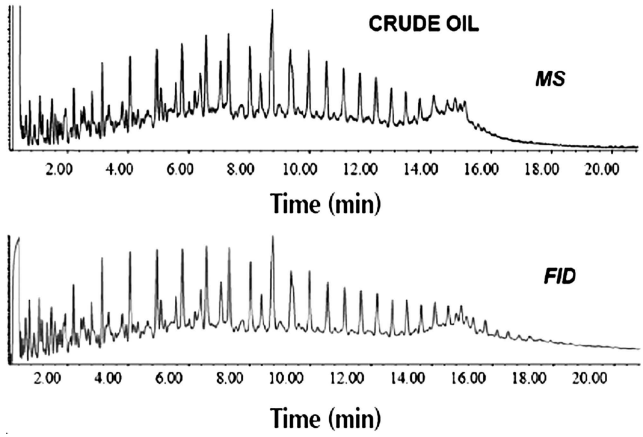

Fig. 4—FID and MS signal for a 2 % crude oil in CS_2.

the mass spectrometry algorithm conventionally obtained by vapor pressure osmometry (VPO). The algorithm is set to determine from the boiling point calibration curve the molecular weight for the corresponding inverse matrix calculations.

Table 7 shows the correlation between both determinations and its effects on the group type analysis values. This assumption speeds up the analysis because the lengthy procedure of using VPO can be avoided.

Similar correlations can be established to other group types with similar low impact on the results. Table 8 also shows the small effect on the total diaromatic content of the same set of samples.

Further validation of this approach as an alternative feasible replacement of the old CEC 21–103 instrumentations is reported in Table 9, where this method is compared to the conventional ASTM D2445 for middle distillates [46].

Several authors have used the concept that hydrocarbons elute from a chromatographic column in the order of their boiling points [43,46,47] with

TABLE 6—Correlation to LC-ELSD

	GC-SimDist-MS (%w)		HPLC (%w)		
	Saturates	Aromatics	Saturates	Aromatics	Diff.
Sample 1	62.73	37.27	62.3	37.7	0.43
Sample 2	69.48	30.52	70.0	30.0	−0.52
Sample 3	71.4	28.6	66.1	33.9	5.3
Sample 4	56.99	43.01	53.5	46.5	3.49
Sample 5	60.43	39.57	60.8	39.2	−0.37
Sample 6	44.2	55.8	48.4	51.6	−4.2

TABLE 7—Effect of Molecular Weight on the Total Saturates by Group Type Analysis Mass Spectrometry

Average Molecular Weight					Total Saturates (%V)				
VPO	SimDist	Average	DIFF	%RSD	(1)	(2)	Average	DIFF	%RSD
187	175	181	12	6.63	84.20	84.6	84.4	−0.4	−0.47
218	219	218.5	−1	−0.46	78.40	78.4	78.4	0	0.00
214	236	225	−22	−9.78	52.40	50.8	51.6	1.6	3.10
215	235	225	−20	−8.89	58.70	57.3	58	1.4	2.41
207	231	219	−24	−10.96	61.80	60.3	61.05	1.5	2.46
212	233	222.5	−21	−9.44	61.50	60.2	60.85	1.3	2.14
367	394	380.5	−27	−7.10	44.70	42.9	43.8	1.8	4.11
388	410	399	−22	−5.51	49.10	47.8	48.45	1.3	2.68
422	406	414	16	3.86	44.80	45.7	45.25	−0.9	−1.99
398	403	400.5	−5	−1.25	47.70	47.4	47.55	0.3	0.63
364	376	370	−12	−3.24	42.20	41.4	41.8	0.8	1.91
354	379	366.5	−25	−6.82	43.60	41.9	42.75	1.7	3.98
361	378	369.5	−17	−4.60	46.00	44.8	45.4	1.2	2.64
372	381	376.5	−9	−2.39	49.80	49.3	49.55	0.5	1.01
384	396	390	−12	−3.08	54.30	53.7	54	0.6	1.11
320	357	338.5	−37	−10.93	53.10	50.8	51.95	2.3	4.43

411	381	396	30	7.58	51.40	53	52.2	−1.6	−3.07	
408	400	404	8	1.98	38.50	39	38.75	−0.5	−1.29	
416	425	420.5	−9	−2.14	40.70	40.2	40.45	0.5	1.24	
369	365	367	4	1.09	63.60	63.8	63.7	−0.2	−0.31	
350	374	362	−24	−6.63	55.00	53.5	54.25	1.5	2.76	
388	386	387	2	0.52	47.50	47.6	47.55	−0.1	−0.21	
185	184	184.5	1	0.54	85.60	85.6	85.6	0	0.00	
217	220	218.5	−3	−1.37	77.20	77.1	77.15	0.1	0.13	
254	254	254	0	0.00	70.10	70.1	70.1	0	0.00	
280	293	286.5	−13	−4.54	47.20	46.2	46.7	1	2.14	
346	333	339.5	13	3.83	35.30	36.3	35.8	−1	−2.79	
321	336	328.5	−15	−4.57	38.00	36.8	37.4	1.2	3.21	
357	362	359.5	−5	−1.39	46.70	46.6	46.65	0.1	0.21	

TABLE 8—Effect of Average Molecular Weight Determination on the Total Diaromatics

Total Diaromatics (%V)				
(1)	(2)	Average	DIFF	%RSD
4.10	4	4.05	0.1	2.47
6.90	6.9	6.9	0	0.00
12.50	12.9	12.7	−0.4	−3.15
9.10	9.4	9.25	−0.3	−3.24
3.70	3.8	3.75	−0.1	−2.67
5.20	5.4	5.3	−0.2	−3.77
11.90	12.3	12.1	−0.4	−3.31
10.00	10.3	10.15	−0.3	−2.96
11.30	11.1	11.2	0.2	1.79
10.50	10.6	10.55	−0.1	−0.95
12.50	12.6	12.55	−0.1	−0.80
12.70	13.1	12.9	−0.4	−3.10
11.60	11.8	11.7	−0.2	−1.71
10.70	10.8	10.75	−0.1	−0.93
9.60	9.7	9.65	−0.1	−1.04
11.10	11.7	11.4	−0.6	−5.26
8.60	8.3	8.45	0.3	3.55
12.40	12.3	12.35	0.1	0.81
10.40	10.5	10.45	−0.1	−0.96
7.40	7.3	7.35	0.1	1.36
8.20	8.4	8.3	−0.2	−2.41
8.20	8.2	8.2	0	0.00
3.80	3.8	3.8	0	0.00
5.40	5.5	5.45	−0.1	−1.83
8.20	8.2	8.2	0	0.00
11.30	11.5	11.4	−0.2	−1.75
13.40	13.2	13.3	0.2	1.50
14.40	14.7	14.55	−0.3	−2.06
10.00	10.8	10.4	−0.8	−7.69

TABLE 9—Correlation of GC/MS/FID to ASTM D2445

		Sample ID:	Diesel Straight			Middle Aromatics			LCO I			LCO II		
		Mol. Weight VPO (SimDist)	M.W. = 224 (206)			M.W. = 224 (249)			M.W. = 224 (226)			M.W. = 224 (209)		
		% vol.	MS	GC/MS	S.D.	MS	GC/MS	S.D.	MS	GC/MS	S.D.	MS	GC/MS	S.D.
Saturates	Paraffins	Paraffins	28.80	24.50	3.04	0	0	0	35.50	36.16	0.47	22.40	18.69	2.62
	Monocycloparaffins	Monocycloparaffins	10.40	13.43	2.14	0	0	0	15.20	21.34	4.34	9.40	6.46	2.08
	Dicycloparaffins	Dicycloparaffins	11.40	13.95	1.80	0	0.88	0.62	14.50	18.95	3.15	28.90	30.1	0.85
	Tricycloparaffins+	Tricycloparaffins	**10.40**	**9.30**	**0.78**	**0**	**0.03**	**0.02**	**12.30**	**0.95**	**8.03**	**20.50**	**25.85**	**3.78**
		Tetracycloparaffins												
		Pentacycloparaffins												
		Hexacycloparaffins												
	Total Saturates		61.00	61.18	0.13	0	0.91	0.64	77.5	77.4	0.07	81.20	81.10	0.07
Aromatics	Monoaromatics	Benzenes	9.20	9.15	0.04	48.30	46.84	1.03	6.50	10.25	2.65	7.10	5.93	0.83
		Naphtenebenzenes	10.20	9.73	0.33	34.90	30.00	3.46	7.40	7.48	0.06	9.90	10.73	0.59
		Dinaphthenebenzenes	4.30	4.32	0.01	7.80	13.62	4.12	3.20	2.17	0.73	1.10	1.43	0.23
		Total Monoaromatics	23.70	23.20	0.35	91.00	90.46	0.38	17.10	19.90	1.98	18.10	18.09	0.01
	Diaromatics	Naphthalenes	4.60	5.17	0.40	2.00	2.96	0.68	2.40	1.70	0.49	0.50	0.53	0.02
		Acenaphthenes, Dibenzofurans	3.20	2.87	0.23	3.70	3.96	0.18	1.30	0.43	0.62	0.10	0	0.07
		Fluorenes	2.20	2.69	0.35	0.50	0.49	0.01	0.70	0.48	0.16	0	0.02	0.01
		Total Diaromatics	10.00	10.73	0.52	6.20	7.41	0.86	4.40	2.61	1.27	0.60	0.55	0.04
	Triaromatics	Phenanthrenes	1.20	1.13	0.05				0.40	0.03	0.26	0	0.18	0.13
		Naphtheno-phenanthrenes												
		Total Triaromatics	1.20	1.13	0.05				0.40	0.03	0.26	0	0.18	0.13

(*Continued*)

TABLE 9—Correlation of GC/MS/FID to ASTM D2445 (Continued)

		Sample ID:	Diesel Straight			Middle Aromatics			LCO I			LCO II		
		Mol. Weight VPO (SimDist)	M.W. = 224 (206)			M.W. = 224 (249)			M.W. = 224 (226)			M.W. = 224 (209)		
		% vol.	MS	GC/MS	S.D.	MS	GC/MS	S.D.	MS	GC/MS	S.D.	MS	GC/MS	S.D.
Aromatics	Tetraaromatics	Pyrenes				0.1	0.20	0.07						
		Chrysenes	0.10	0.08	0.01				0	0.01	0.01	0	0.04	0.03
		Total Tetraaromatics	0.10	0.08	0.01	0.10	0.20	0.07	0	0.01	0.01	0	0.04	0.03
	Pentaaromatics	Perylenes												
		Dibenzanthracenes												
		Total Petaaromatics												
	Thiophenoaromatics	Dibenzothiophenes	1.20	1.42	0.16	0	0	0						
		Naphthobenzo-thiophenes				0	0	0						
		Total Thiophenoaromatics	4.20	4.03	0.12	3.00	1.01	1.41	0.7	0.04	0.47	0.20	0	0.14
	Unidentified aromatics	Class II												
		Class III										0	0.04	0.03
		Class IV												
		Class V												
		Class VI												
		Class VII												
		Total Aromatics	39.20	39.17	0.02	100.3	99.08	0.86	22.60	22.59	0.01	18.90	18.90	0.00
TOTAL			100.20	100.35	0.11	100.3	99.99	0.22	100.1	99.99	0.08	100.10	100	0.07

mass spectrometry. Thus calibrating the retention time axis with a suitable mixture of n-paraffin chemical compositions based on characteristic fragmentation mass algorithms provides reports by boiling fractions of interest, even by carbon numbers.

The differences reside basically in the algorithm structure and in the number of detectors and their instrumental configurations. The method described in detail above combined the use of two detectors, FID and MS, by means of a microfluidic splitter to simultaneously obtain identical signal profiles of the sample.

This approach provides a very effective way of studying changes in chemical composition during catalytic conversion processes, especially hydrotreating, to produce better quality fuels.

Hydrotreating heavy vacuum gas oil (HVGO) to obtain more valuable distillates requires a simple, fast, and reliable method for process and quality control [48]. By simultaneously combining GC-simulated distillation with mass spectral data, it is possible to monitor compositional changes during catalytic conversion processes. Of particular interest is the reduction in sulfur and polyaromatic content. Table 10 reflects those changes.

From Table 10 it can be observed how the average molecular weight decreased to 408 daltons from 436 daltons; at the same time the monoaromatics increased from 21.96 %V to 33.06 %V and the total sulfur compounds decreased to 1.34 %V from an initial content of 8.99 %V. The amount of information gathered in one single analysis is very important to accurately follow refining processes in general.

TABLE 10—Changes in Composition of Hydrocarbon Feedstock during Hydrotreating

Sample ID: HVGO Chg & (Product)		
Average Molecular Weight: 436 & (408)		
	% Volume	**% Weight**
Saturates	**47.12 (49.66)**	**44.16 (47.62)**
Paraffins	12.47 (12.00)	11.14 (10.90)
Monocycloparaffins	12.60 (12.16)	11.54 (11.32)
Dicycloparaffins	12.07 (13.90)	11.58 (13.58)
Tricycloparaffins+	9.98 (11.60)	9.90 (11.84)
Aromatics	**52.88 (50.34)**	**55.84 (52.38)**
Monoaromatics	21.96 (33.06)	21.31 (32.68)
Benzenes	8.54 (12.24)	8.01 (11.67)
Naphthenebenzenes	6.71 (10.93)	6.65 (11.03)
Dinaphthenebenzenes	6.71 (9.89)	6.65 (9.98)

(*Continued*)

TABLE 10—Changes in Composition of Hydrocarbon Feedstock during Hydrotreating (Continued)		
Sample ID: HVGO Chg & (Product)		
Average Molecular Weight: 436 & (408)		
	% Volume	**% Weight**
Diaromatics	10.39 (6.98)	10.82 (7.39)
Naphthalenes	1.97 (1.26)	2.00 (1.30)
Acenaphthenes, Dibenzofurans	3.70 (2.65)	3.84 (2.79)
Fluorenes	4.72 (3.07)	4.99 (3.30)
Triaromatics	5.51 (3.48)	6.03 (3.90)
Phenanthrenes	2.92 (2.07)	3.12 (2.28)
Naphthenophenanthrenes	2.59 (1.40)	2.91 (1.62)
Tetraaromatics	3.77 (1.60)	4.36 (1.91)
Pyrenes	2.60 (0.94)	2.98 (1.11)
Chrysenes	1.16 (0.66)	1.37 (0.80)
Pentaaromatics	0.65 (0.41)	0.84 (0.56)
Perylenes	0.64 (0.41)	0.82 (0.56)
Dibenzanthracenes	0.02 (0.00)	0.02 (0.00)
Thiopheno Aromatics	8.99 (2.85)	10.40 (3.41)
Benzothiophenes	5.03 (1.34)	5.55 (1.51)
Dibenzothiophenes	3.02 (1.36)	3.67 (1.69)
Naphthobenzothiophenes	0.93 (0.16)	1.18 (0.20)
Unidentified Aromatics	1.62 (1.89)	2.08 (2.54)
Class II	0.00 (0.00)	0.00 (0.01)
Class III	0.02 (0.06)	0.02 (0.09)
Class IV	1.60 (1.82)	2.06 (2.44)
Class V	0.00 (0.00)	0.00 (0.00)
Class VI	0.00 (0.00)	0.00 (0.00)
Class VII	0.00 (0.00)	0.00 (0.00)

GC-MS has also been used as a powerful two-dimensional separation approach tool*** leading to compound class separation that offers many advantages over multidimensional chromatography in the sense that GC-MS can be combined with low fragmentation ionization methods to produce

accurate parent ion masses that would allow compound class separation and therefore better characterization of complex mixtures.

ASTM Sub-Committee D02.04 on Hydrocarbon Analysis is pursuing a major spread of this technique. At present it has standard method D5769 [4], which covers the determination of benzene, toluene, and total aromatics in finished gasolines by GC-MS. The method includes oxygenated blends and is applicable in the range of 0.1 to 4 %V for benzene, 1 to 13 %V for toluene, and a total aromatic content from 10 to 42 %V.

The detailed characterization of complex hydrocarbon mixtures that intervene in conversion or upgrading processes or both is a basic step to modeling the kinetics of such refining processes. Above naphthas, it is quite common to observe lumps of unresolved isobaric and coeluting compounds, especially iso-paraffins and cycloalkanes. Many procedures to improve the chemical resolution of analytical techniques have been published [49,50]. Ha et al. [51] used GC-MS (FIMS) input data to make molecular representation of fuels and computer-assisted establishment of thermodynamically stable molecules that correlate with other physical properties.

Instrumental improvements are still necessary to this technique. Because of the many advantages regarding speed of analysis and instrumental space sample volume needed for analysis, simulated distillation can be the reference method for obtaining distillation yields and other quality parameters. New and better columns in terms of thermal stability are required for better results. The technique needs to be expanded to higher boiling ranges for conversion of barrel bottoms; it also needs to be adapted to ultrafast GC conditions for higher throughputs.

PROCESS MASS SPECTROMETRY

Process mass spectrometry (PMS) is a powerful tool for process understanding and control. It allows a view into the chemical composition of a process in real time, providing both qualitative and quantitative measurements. Like so many other process measurement technologies, compromises need to be made to make the laboratory technique robust enough for routine process use. Understanding the limitations and strengths of PMS is essential to successful implementation and years of reliable process measurement and control. This section describes some of the essential issues in selecting and implementing PMS for the petroleum and petrochemical industries.

Mass Spectrometry Principles

The heart of mass spectrometry is based on the principle that moving charged particles can be deflected by a magnetic or electric field. This dispersion of particles may be compared to the way a light spectrum is broken down into its component colors by a prism. Fig. 5 shows the paths taken by light and heavy particles traveling through a magnetic field and the basic components of a mass spectrometer. If all the particles are moving at the same velocity, the heavier particles will be deflected less and the lighter particles will be deflected more. This gradient of particle mass can be detected to produce a spectrum of particle masses, which is known as a mass spectrum.

Typically, the analytes of interest are not charged particles in their natural states. Therefore, it is necessary to generate a charge on the molecule in order for it to be detected in a mass spectrometer. This is accomplished by the ion

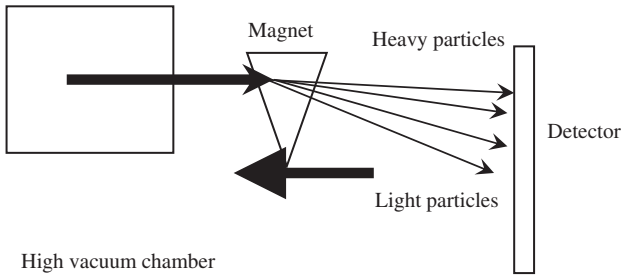

Fig. 5—Deflection of particles in a magnetic field.

source, as shown in Fig. 6. Most process mass spectrometers use electron impact ionization to generate ions. Electron impact ionization uses high-energy electrons to blast electrons and molecular fragments off the analyte molecules so that they become positively charged. The electrons typically have 70 electron volts of energy or more to achieve consistent ionization of most materials. A filament made of tungsten or iridium coated with thoria is used to generate the electrons. The sample is introduced into the electron beam where collisions between the electrons and the molecules generate ions. The ionization can be as simple as knocking an electron off the parent molecule to generate a molecular ion, or the collision can have more dire effects. There are three primary methods of ionization. Molecular ions are formed by the removal of one electron from the sample molecule to generate a positive charge. Fragment ions are formed by breaking a molecular bond, freeing an electron, and forming a positive charge on one of the fragments. The third method of ionization involves removing two electrons from the sample molecule to form a doubly charged ion. In a mass spectrometer these ions appear at one-half their actual

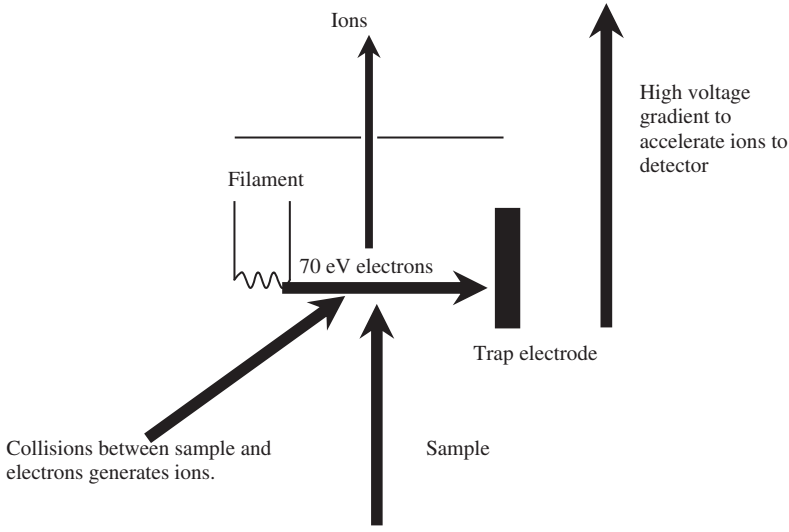

Fig. 6—Example of electron impact ion source.

mass. Isotopes of atoms in the sample can be ionized in all three methods, resulting in additional peaks in the mass spectrum. Therefore, fragmentation due to the impact of electrons leads to a complex mass spectrum of the molecule that is characteristic of its chemical composition. It is the fragmentation of analyte molecules that allows structural identification to be achieved. A complete discussion of ionization techniques is beyond the scope of this chapter, but many books on mass spectrometry cover the topic in detail [52,53].

Once the ions have been generated in the ion source, it is necessary to move them down the flight tube, through the magnetic field, and into the detector. A high voltage, called the ion energy, is used to accelerate the ions out of the source and to the detector. The ion energy used varies from instrument to instrument, but typically, a magnetic sector instrument will operate with ion energy of about 1 kV. The ions then travel from the source through the magnetic field to the detector. The most common types of detectors used in PMS instrumentation are a Faraday cup, a channeltron, and a microchannel plate. Theses detectors are described next.

A Faraday cup, shown in Fig. 7, is a metal cup that is placed in the path of the ion beam. It is attached to an electrometer, which measures the ion-beam current. The power supply of the electrometer provides electrons, which annihilate the positive ions that collide with the surface of the bucket. The resulting current is proportional to the number of ions impacting the cup. It is important to suppress secondary electrons, which will give a false reading. This can be accomplished by coating the inside of the cup and by placing a suppressor plate in front of the detector. This type of detector is usually used for analytes of higher concentrations ranging from about 10 ppm to 100 %.

A channeltron, shown schematically in Fig. 8, is a horn-shaped, continuous dynode structure that is coated on the inside with an electron emissive material. An ion striking the channeltron creates secondary electrons that have an avalanche effect to create more secondary electrons and finally a current pulse measured by an electrometer. These detectors are more sensitive than Faraday detectors and are not usually used for measurements of concentrations greater than 100 ppm.

The microchannel plate shown in Fig. 9 consists of an array of glass capillaries (10–25 micron inner diameter) that are coated on the inside with an

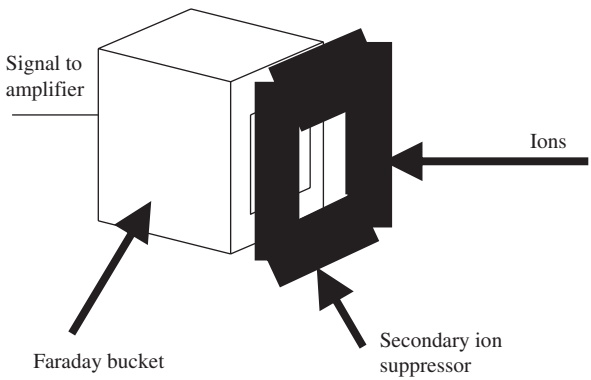

Fig. 7—Schematic diagram of a Faraday cup.

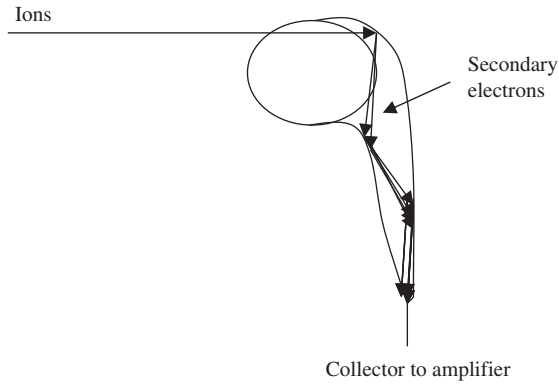

Fig. 8—Schematic diagram of a channeltron.

electron-emissive material. The capillaries are biased at a high voltage and, as in the channeltron, an ion that strikes the inside wall of one of the capillaries creates an avalanche of secondary electrons. This cascading effect creates a gain of 10^3 to 10^4 and produces a current pulse at the output. This detector is also used for low concentrations and is susceptible to damage by exposure to high concentrations while voltage is applied.

The vacuum system is an often-overlooked, but critical component of a mass spectrometer. Consider a beam of ions travelling through a chamber. At atmospheric pressure, the ions are scattered by gas molecules within the chamber. The distance an ion travels without being deflected is termed the mean free path of the molecule. The mean free path is inversely proportional to the density of gas molecules in the chamber, which translates to the absolute pressure (vacuum) in the chamber. This principle dictates that the lower the pressure (higher vacuum) the longer the mean free path. A simple method to illustrate how low the pressure needs to be is to use a constant called the IP value. The IP value is the product of the mean free path I and the pressure P. For any given gas, the IP value is a constant. Typical IP values for common

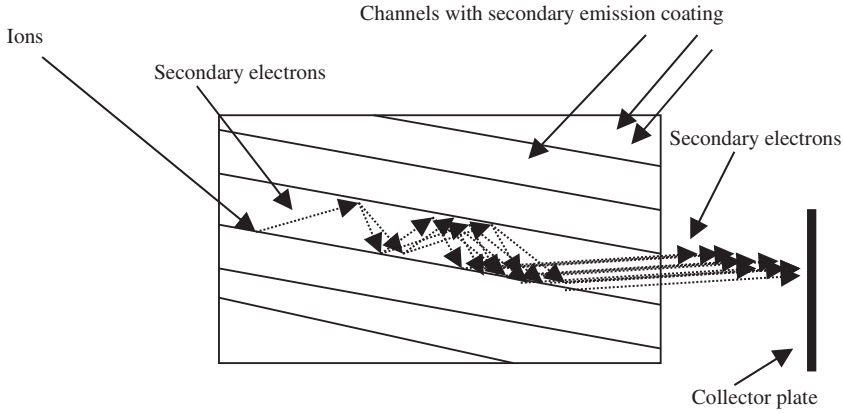

Fig. 9—Schematic diagram of a microchannel plate.

gases are approximately 6.0e-5 m/mbar. Therefore, at a pressure of 1 mbar, the mean free path is approximately 6e-5 m. A typical flight path from the ion source to the detector in a mass spectrometer can range from approximately 0.25 to 1 m. At a pressure of 1 mbar, the ion beam from the ion source will be scattered before reaching the detector, and therefore the instrument will not function. However at a pressure of 1e-5 mbar, the mean free path is approximately 6 m. At these low pressures (high vacuum), the majority of ions are not scattered and the ion beam can reach the detector, allowing the instrument to function.

Vacuum systems used in process mass spectrometers usually consist of a rotary pump and a turbo molecular pump. A typical pumping system is shown in Fig. 10. The rotary pump is used to reduce the pressure to 10^{-3} mbar, and the turbo molecular pump can then remove gas to achieve a pressure of 10^{-5}–10^{-9} mbar. There are two basic ways that the sample is introduced into a process mass spectrometer. First, a piece of capillary can be sized to allow just enough gas into the source to maintain the pressure at the desired level. This is shown as Option A in Fig. 10. Second, a bypass inlet can be used. The bypass inlet is shown as Option B in Fig. 10. This type of inlet reduces sample lag times by quickly transporting the sample to a molecular leak, then allowing part of the sample to flow into the mass spectrometer, while the bulk of the sample is pumped away to vent. This type of inlet is not effective if sample volume is severely limited.

Types of Spectrometers

Quadrupole mass spectrometers consist of four parallel rods arranged with the rods on the corners of a square. Two opposite rods have an applied potential of [U + Vcos (ωt)], and the other two opposite rods have a potential of –[U + Vcos (ωt)]. U is a dc bias voltage and Vcos (ωt) is an ac voltage. The applied voltages affect the trajectory of ions traveling down the flight path centered

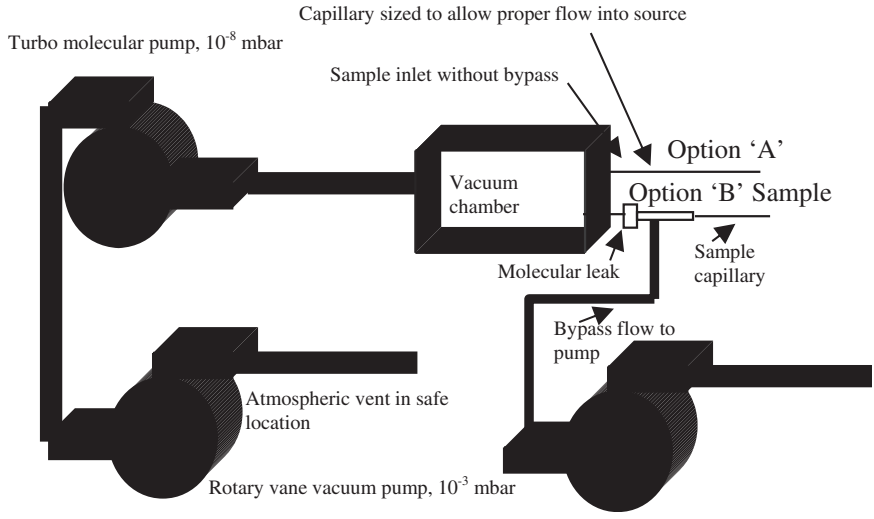

Fig. 10—Typical process mass spectrometer pumping system.

between the four rods. For any given dc and ac voltages, only ions of the mass-to-charge ratio, which travels through the center of the rods, reach the detector. All other ions are deflected away from the detector. A mass spectrum is obtained in one of two ways, either holding the frequency constant while varying the dc voltage or holding the dc voltage constant and varying the frequency of the ac component. The quadrupole mass spectrometer is shown schematically in Fig. 11.

Magnetic-sector mass spectrometers use a magnetic field to focus the trajectories of ions of interest to the detector. The ions are accelerated from the ion source to a kinetic energy of $0.5\ mv^2 = eV$, where m is the mass of the ion, v is its velocity, e is the charge of the ion, and V is the ion energy voltage. The ions enter the flight tube between the poles of a magnet, where they are deflected by the magnetic field H. Only ions of mass-to-charge ratio that have equal centrifugal and centripetal forces pass through the flight tube and impinge on the detector. Where $m/e = H^2r^2/2V$, r is the radius of curvature of the ion path. A typical magnetic sector mass spectrometer is shown in Fig. 12.

Ion trap mass spectrometers use electrodes to trap ions in a small volume. The mass analyzer consists of a ring electrode separating two hemispherical electrodes. A mass spectrum is obtained by varying the electrode voltages to eject the ions from the trap one at a time. This type of mass spectrometer is compact in size, has the ability to concentrate the sample to increase the signal-to-noise ratio, and improves detection limits. This is due to the ability to collect ions in the ion trap, effectively accumulating the sample.

TOF mass spectrometers use the difference in transit time through a drift region to separate ions of different masses. They operate in a pulsed mode, which requires that the ions be introduced into the spectrometer in bursts. The ions are accelerated by an electric field into a free-drift region. Because all the ions have the same kinetic energy, the lighter ions have a greater velocity than the heavy ions, separating them in space and time. The spectrum is then collected by detecting the time at which a given ion reaches the detector. The TOF mass spectrometer is shown schematically in Fig. 13.

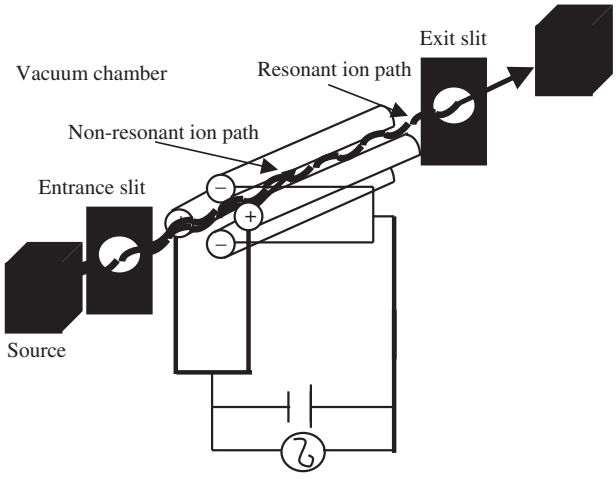

Fig. 11—Quadrupole mass spectrometer schematic.

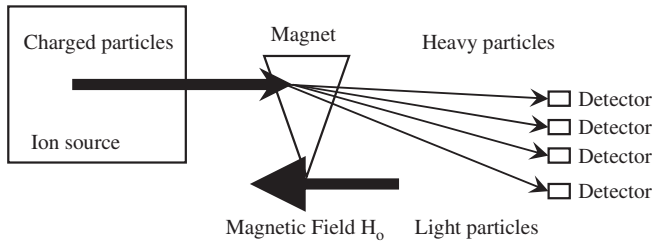

Fig. 12—High vacuum chamber.

Time-of-flight mass spectrometers are becoming very popular because of the advances in electronics. Measurements of the ion transit time to the detector are more accurate, and also the scanning function is linear, allowing the accurate interpolation of the mass measurement between two known reference peaks at high sensitivity. This fact is greatly enhanced by reflecting the ions back down the flight tube to effectively double the flight tube length.

Instrumentation and Operational Requirements

The two most common types of process mass spectrometers are the magnetic sector and the quadrupole. There are two types of magnetic sector instruments, scanning and fixed collector. Scanning systems scan either the magnetic field or the ion energy to sweep the desired mass fragment past the detector. Systems that scan the magnetic field are inherently more stable than those that scan the ion energy because changing electric fields in the ion source will reduce the ion source stability. Fixed collector systems have the advantage that they are very fast, but they suffer from a lack of ability to match the detectors, reducing the precision of the measurements. It is generally accepted that the magnetic sector will perform better in dirty sample streams because it employs higher ion energy, which is less susceptible to interference from contamination than quadrupole instruments. The magnetic sector source will still require cleaning in those environments; however, the maintenance frequency will be much lower than for a quadrupole, making the magnetic sector performance better than the quadrupole counterpart in most applications. Quadrupole process mass spectrometers tend to scan a little faster and have a higher mass range, but suffer from lower precision

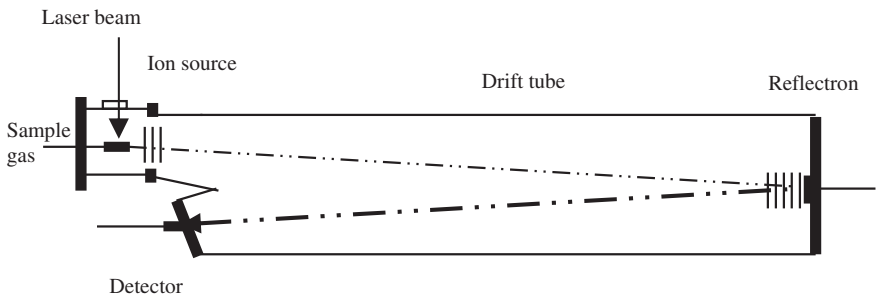

Fig. 13—Time-of-flight mass spectrometer.

than their magnetic sector counterparts. As is always the case with analytical equipment, a balance must be struck to meet the needs of any given application. The wide range of capabilities of commercial spectrometers allows the application engineer to find an instrument well suited to the application.

Process mass spectrometers can be a very reliable method of obtaining analytical information, but as with any piece of equipment, proper installation and maintenance are key to long-term performance. It is always a good idea to install the specific piece of equipment according to the manufacturer's recommendations; however, two additional tips have proven to be useful in creating low-maintenance installations. First, heat is the enemy of the mass spectrometer. The instrument uses large amounts of electric power, a substantial amount of which is converted into heat. The sensitive electronics employed to detect and process signals are sensitive to temperature changes and high temperatures. It is critical that the analyzer be kept cool. A good rule of thumb is that if you feel warm, so does the analyzer. Keep the instrument's internal temperature as close to 60°F (15°C) as possible. Second, clean power is critical to obtain low noise signals. High-quality power conditioning is not expensive compared to the cost of poor performance of the analyzer. Both the instrument and computer power supplies should be filtered.

Process mass spectrometers, which are to be mounted in production environments, must be suitable for the electrical classification of the area. The use of purge systems and explosion-proof vacuum pumps is often required. These systems should be designed and installed to meet the local electrical code requirements for the area in which the analyzer is to be installed.

Sampling Techniques

Process mass spectrometers are by nature extractive sampling devices. It is necessary to pull the sample from the sample point in the process to the instrument. When the sampling system is designed, careful attention must be paid to the distance the line is run. Typically, it is best to keep sample lines as short as possible; however, it is possible to pull sample from as much as 330 meters away from the instrument. In any case, the pumping system, sample line diameters, and sample line lengths must be carefully tuned to prevent excessive pressure drops at the inlet of the mass spectrometer. The sensitivity of the instrument will be determined in part by the sample pressure at the inlet of the spectrometer. Process mass spectrometers require a typical sample flow of 0.1–1 l/min at atmospheric pressure, which should be verified by rotameter. The required sample pressure depends on the pressure required to provide a given flow through the sample conditioning system and also the pressure drop, which is a function of the length and internal diameter of the pipe connecting the sample to the instrument, but is typically less than 100 mbar above atmosphere. The pressure drop due to the connecting pipework is given by the approximate equation $C = 0.006D^4P/L$, where C is the flow rate in l/min, D is the internal diameter of the pipe in millimetres, P is the differential pressure along the pipe in millibars, and L is the length of pipe in metres; as an example, if D = 3 mm and L = 10 m, then P is 4 mbar with a flow rate of 0.2 l/min. To summarize, the total sample pressure required is given by:

$$\text{Sample Pressure} = (150C + 170CL/D^4)\text{mbar}$$

where C is the flow rate in l/min, L is the length of sampling pipe in metres, and D its internal diameter in millimetres; e.g. where C = 0.2 l/min, L = 10 m, and D = 3 mm, then the sample pressure needs to be 34 mbar.

To protect the analyzer against blockage by liquids and dust, the use of a two-filter system comprising first a 1 micron glass filter (e.g. Swagelok FC™ series) followed by a membrane filter (Genie Membrane™ filter model 101 high flow, A+ Corp) is recommended. All of the sample system components must be compatible with the sample to prevent corrosion of the sampling system and loss of sample integrity.

Process mass spectrometers do very well with vapor samples; however, it is much more difficult to sample from a liquid stream. Liquid measurements on the mass spectrometer are actually vapor measurements as far as the instrument is concerned. The analytes are extracted from the liquid matrix and vaporized into a gaseous carrier stream before injection into the inlet of the mass spectrometer. There are three common methods to achieve this: flash vaporizers, spargers, and membrane inlets. Flash vaporizers, which are similar to gas chromatograph injectors, can be used; however, they will also form aerosols from solids dissolved in the liquid, which can cause plugging of the mass spectrometer inlet. Spargers are devices that bubble the carrier gas through the sample liquid directly, saturating the bubbles with the volatile vapors in the liquid. The partition of vapor in the bubble obeys Raoult's law such that the vapor concentration of any analyte is proportional to the concentration in the liquid matrix. Spargers are temperature sensitive, which requires the sample temperature to be carefully controlled to minimize errors. A membrane inlet consists of a flow of the liquid medium adjacent to a flow of an inert carrier gas, separated by a membrane, which allows vapors to pass but not liquids. Some membranes have selectivity to either analyte size or chemical property, allowing a selective analysis to be made. Fig. 14 shows a schematic of a membrane sampling system. The sample flows against a membrane at a rate high enough that the concentration of analyte in contact with the membrane never becomes depleted. The inert carrier gas flowing on the other side of the membrane picks up the gas emerging from the membrane. The carrier gas flow rate should be low enough that the concentration approaches saturation but never reaches it. The carrier gas must be inert to the analytes in the sample stream. Argon, helium, and nitrogen are good choices for carrier gases. Membrane systems are very temperature sensitive, and it is important to keep both the sample and the membrane at a constant temperature. If liquid sampling is to be done, the extraction method of choice is the membrane inlet.

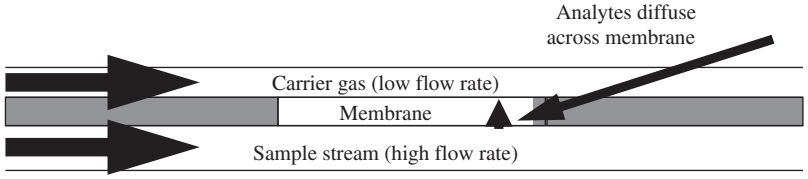

Fig. 14—Schematic of a membrane sampling system.

Advantages and Disadvantages of PMS

The main advantages of process mass spectrometry are threefold. First, the analysis is inherently fast. Most analysis takes only seconds to perform. Second, this high-speed analysis lends itself nicely to multistream analysis, which lowers the cost per sample point. Third, the process mass spectrometer has a wide dynamic range. It is possible to analyze for materials in the range of low part-per-billion to percent concentration. All these benefits combine to provide a very productive analytical system.

The drawback to process mass spectrometry is that the capabilities are very application dependent. The actual precision and accuracy that can be achieved depend on the degree of overlap of the analyte mass spectra. Some materials undergo chemical reactions in the ion source, which reduces precision and long-term stability. The equipment is also very expensive, making it harder to build a business case for purchase unless a large number of sample streams can be served. Process mass spectrometry can be extremely effective as an analytical tool to monitor process events, provided the application is carefully selected.

Quantitative Analysis

Quantitative analysis on process mass spectrometers is usually accomplished using a multivariate approach. Techniques such as principal component analysis, multiple linear regression, partial least squares regression, and matrix inversion are appropriate methods for quantification.

In general, the process mass spectrometer can be very precise, and accurate. A good estimate is to expect precision and accuracy to be better than 5 % of value. If the application permits, better precision and accuracy may be obtained. Nitrogen in air (78 %), for example, can be measured to a precision of 0.01 % 1 sigma relative standard deviation.

Calibration Requirements

The instrument needs to be calibrated for each gas component's response, including the fragmentation pattern and relative sensitivity. Backgrounds also need to be measured to account for residual gas and air leaks in the vacuum system. Recalibration (or realignment) of the mass scale may also be required to insure the measurement is done at the top dead center of each mass peak.

In a typical case, for a complete calibration, a minimum number N of calibration gases is required, where N is calculated as shown in Eq 2:

$$N = M + 2 \tag{2}$$

M is the total number of components having fragmentation patterns that are used in the analysis. The two additional gases are the background gas (typically helium) and the calibration blend mixture, which should approximate the process composition being measured.

Typically, binary blends are used to calibrate the fragmentation pattern of each component of interest. These calibration gases should use >99.9 % purity for gas preparation; however, binary mixture composition is required only to within 5 % tolerance. The binary blends are followed by a calibration blend that contains all the compounds of interest in a composition which reflects the real process. Calibration blend gases should be gravimetric mixes certified to better than 1 % relative. Helium is generally used as the background gas to

measure the residual signals at each mass peak. The background gas should use 99.995 % purity gas. Normal calibration cylinder sizes used are "A" size (218 cf). Cylinder pressures should be the maximum obtainable up to 2500 psig, consistent with being noncondensing. Double-stage regulators with 0–30 psig (or similar) output stages should be used in conjunction with the calibration gas cylinders to set the output pressure to the mass spectrometer calibration panel to approximately 15 psig.

Typically, a process mass spectrometer can be calibrated on a monthly schedule, using a set of calibration gases that match the application in question. The frequency will vary depending on the required precision and accuracy of the analysis.

Once a calibration method has been established, it is critical that the method be validated to determine the precision, accuracy, and cross talk between analytes. Consider a method with the analytes nitrogen, oxygen, argon, carbon dioxide, methanol, ethanol, and isopropanol. Once the analyzer is calibrated, a cross-talk check should be performed. This check serves two purposes: it checks that each analyte responds correctly and that the other analytes do not respond to other compounds in the matrix. This is accomplished by introducing binary standards containing each analyte and the balance gas. The response is then recorded in the form shown in Table 11. The table is a matrix where the analyte concentration is on the diagonal, and the cross-talk values are on the other positions. If the calibration were perfect, the error of the analyte concentrations on the diagonal would be zero and the cross-talk values would be zero. To exemplify the use of this matrix for fit quality, divide the matrix by the column of standard concentrations. This will yield a matrix of one on the diagonal with zero everywhere else for a perfect calibration. The degree of tolerable cross talk or calibration error needs to be assessed against the specifications for the actual measurement. If the cross talk is acceptable, the next validation check is to test the method on a standard mixture that is representative of the process sample. In the current example, the mixture could contain 100 ppm each of methanol, ethanol and isopropanol in air. The error in the concentrations should be noted. If these errors are acceptable, a low concentration standard near the required detection limit should be run to ensure that the method has sufficient sensitivity. In this example, a mixture of 10 ppm each of methanol, ethanol, and isopropanol would suffice. Again, the errors should be recorded and compared to the required specification for detection limit. Assuming there are no problems with the method, the final test is a stability test. This test is a two-part test. The first part is a short-term stability test.

TABLE 11—Verification of Cross Talk

	Gas Standard		
	Ethanol	**Methanol**	**Isopropanol**
Ethanol	100	0	0
Methanol	0	100	0
Isopropanol	0	0	100
Standard Concentration	100	100	100

The 100-ppm mixture used previously should be run for a period of 1–3 hours. The data should be averaged, and the standard deviation calculated. This provides information of the precision of the measurement. The easiest way to express precision is to use the 1-sigma standard deviation. The second part of the test is to run the mixture every day for a month and control chart the data. The data should be in control within the required precision specifications, and the average should correspond to the actual concentration of the gas. An example control chart for methanol is shown in Fig. 15.

The upper and lower control limits are calculated from the data using the rules for statistical process control. There are a number of texts on the subject, but Kaoru Ishikawa has an excellent text [54]. During the month shown in Fig. 15, the average concentration of methanol was 100.5 ppm. The concentration varied between 100.0 and 101.0, which is plus or minus 0.5 ppm. The standard deviation at 1 sigma was 0.2 ppm. It is advisable to continue the control charting for the lifetime of the analyzer to track instrument performance, and indicate when recalibration is required. Many analyzers can be configured to do this check automatically.

Precision is usually the most important parameter used to asses process instrument performance. Precision is often defined as the 1-sigma standard deviation over a defined period of time while measuring a standard gas sample. The standard deviation is defined as shown in Eq 3.

$$\sigma_{n-1} = \left[\sum (x_i - x_m)^2/(n-1)\right]^{1/2} \tag{3}$$

where: n refers to the number of measurements to which the statistical determination is to be applied, x_i refers to the individual measurements, and x_m is the mean value = $\{x_1 + x_2 + x_3 + ... x_n\}/n$.

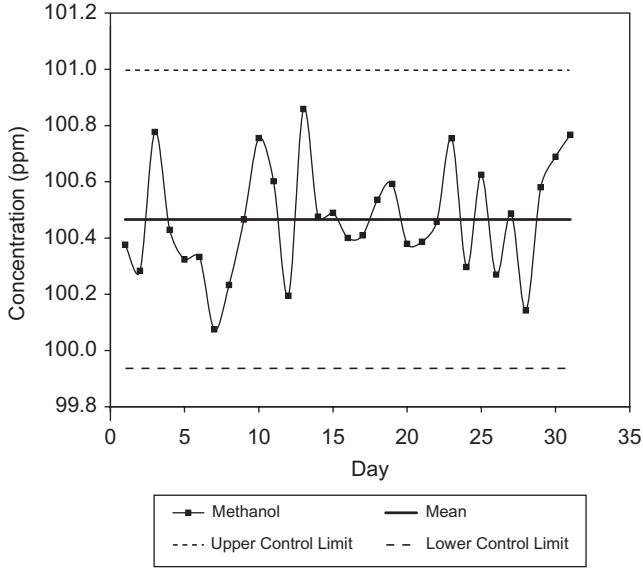

Fig. 15—Control chart for long-term stability of methanol.

To provide robustness against minor pressure fluctuations in the mass spectrometer, the analysis is on a normalized basis; i.e., the individual reported component concentrations are adjusted so that their sum equals 100 %.

One of the major drawbacks of multivariate calibration techniques is that they are sensitive to changes in the sample matrix, which can lead to undesired results. New components in the sample stream can cause interferences that can go undetected. This can manifest itself as an increase in cross talk or as the degradation of the accuracy of a particular analyte. It is therefore critical that the sample matrix be checked periodically for new components or radical changes in the existing components that may require an alteration to the calibration method [55].

On-Line Methods Currently in Use

GENERAL AREAS OF APPLICATION

Process mass spectrometry is often employed to make measurements in coke production, ethylene cracking, ethylene oxide production, polyethylene production, and fuel gas production. In these applications, the speed, wide dynamic range, and stability of the mass spectrometer are exploited to provide process measurement and control in real time. Many applications are suitable for process mass spectrometry, but the financial benefits are greatest when the fast analysis can be exploited to sample a large number of streams. It is possible to sample from 64 streams or more on a single analyzer. Some mass-spectral analyses take only a few seconds to make, allowing for a complete analysis of all streams in under 5 minutes. Under these conditions, the cost per sample point can be substantially reduced.

Volatile organic compounds (VOCs) lend themselves well to analysis by mass spectrometry. In many cases, large numbers of VOCs can be analyzed simultaneously to provide fast, accurate analysis of stack effluent or ambient air.

COKE OVEN GAS ANALYSIS

Coke Production Process Overview

The cokemaking process involves carbonization of coal at high temperatures (1,100°C) in an oxygen-deficient atmosphere in order to concentrate the carbon. The cokemaking operation involves the following steps: Before carbonization, the selected coals from specific mines are blended, pulverized, and oiled for proper bulk density control. The blended coal is charged into a number of slot type ovens, wherein each oven shares a common heating flue with the adjacent oven. Coal is carbonized in a reducing atmosphere and the off-gas is collected and sent to the by-product plant where various by-products are recovered. Hence, this process is called by-product cokemaking.

The coal-to-coke transformation takes place as follows: The heat is transferred from the heated brick walls into the coal charge. From about 375°C to 475°C, the coal decomposes to form plastic layers near each wall. At about 475°C to 600°C, there is a marked evolution of tar and aromatic hydrocarbon compounds, followed by resolidification of the plastic mass into semicoke. At 600°C to 1,100°C, the coke stabilization phase begins. This is characterized by contraction of coke mass, structural development of coke, and final hydrogen evolution. During the plastic stage, the plastic layers move from each wall toward the center of the oven, trapping the liberated gas and creating gas pressure buildup, which is transferred to the heating wall. Once the plastic layers have met at the center of the oven, the entire mass has been carbonized. The incandescent coke mass is then pushed from the oven and is wet or dry quenched.

On-line analysis

In a coke oven plant, a raw gas of high calorific value is produced as a by-product from the pyrolysis of coal. After purification, coke oven gas is used as fuel by other processes. Purification processes are necessary to remove problematic (naphthalene blockages) and environmentally harmful (H_2S, NH_3, benzene) components. On-line monitoring of H_2S and O_2 is often well established on coke oven plants. However, measurement of NH_3, naphthalene, and benzene is typically performed by wet chemical methods on a daily spot sample basis. Therefore, by using process mass spectrometry, it is possible to extend the range of components in purified coke oven gas being subjected to on-line monitoring and perform this on a single instrument. It has been found that on-line monitoring allows optimization of the scrubber plants [56,57].

Performance Specification

The typical coke oven gas analysis performance for a process mass spectrometer is shown in Table 12 along analysis precision.

The standard deviation is a measure of the reproducibility as observed over 24 hours assuming constant concentrations and is demonstrated using calibration gas 1 and 2, as shown in Table 13. Two gas cylinders are required because of the incompatibility of NH_3 with CO_2, HCN, and H_2S.

TABLE 12—Analytical Performance of Process Mass Spectrometer for Coke Oven Gas

	Sample Gas % Molar Concentration	Standard Deviation Mol %
H_2	62–64	0.08
CH_4	22–25	0.05
NH_3	0.013–1.3	0.001
H_2O	2.2–2.5	0.01
HCN	0.071–0.12	0.02
CO	5–6	0.05
N_2	1.5–2.7	0.05
C_2H_4	1.85	0.01
C_2H_6	0.85	0.01
O_2	0.1–0.15	0.002
H_2S	0.23–0.49	0.001
C_3H_6	0.1	0.001
CO_2	1–1.5	0.005
C_6H_6/ C_7H_8/ C_8H_{10}	0.17–0.86	0.001
$C_{10}H_8$	0.0007–0.025	0.0002

TABLE 13—Calibration Blends Used to Validate Performance

	Mix 1 % Molar Concentration	Mix 1 Precision % Absolute	Mix 2 % Molar Concentration	Mix 2 Precision % Absolute
H_2	64	0.08	64	
CH_4	24.9	0.05	23.6	
NH_3	0.1	0.001		
H_2O				
HCN			0.1	0.02
CO	6	0.05	6	
N_2	2	0.05	2	
C_2H_4	1.85	0.01	1.85	
C_2H_6	0.85	0.01	0.85	
O_2	0.1	0.002	0.1	
H_2S			0.1	0.001
C_3H_6	0.1	0.001	0.1	
CO_2			1.3	0.005
C_6H_6/ C_7H_8/ C_8H_{10}	0.1	0.001		
$C_{10}H_8$	0.002	0.0002		

The analysis time including stream switching used to meet the above precision is typically 30 seconds per stream. The typical calibration interval for this analysis is 1 month.

Calibration Gas Requirements

The calibration gases used to calibrate the mass spectrometer are shown in Table 14. Calibration gas 11 is prepared by bubbling N_2 through a sinter into saturated NaCl solution at a known temperature to provide an H_2O calibration gas. There should be two additional supplies of N_2 (>99.9 % purity)—one at 0.1 l/min to purge the sample conditioning system and the other to purge the rotary pump oil box at 0.1 l/min. This is to reduce the effect of H_2S and H_2O on the rotary pump oil.

Recommended Analysis Set-Up: Reference Information

The fragmentation pattern used for the coke oven gas analysis is shown in Table 15. The relative sensitivity is the sensitivity of the largest peak for a given gas relative to the largest peak for nitrogen. This analysis included the separation of nitrogen and CO. As can be seen by the fragmentation patterns, there is heavy overlap between the species. Since CO has a peak at m/z 28, it would have the same doubly charged ions as nitrogen and thus would contribute to

TABLE 14—Typical Calibration Gas Requirements

Component	Expected Level	Cal Gas 1	Cal Gas 2	Cal Gas 3	Cal Gas 4	Cal Gas 5	Cal Gas 6	Cal Gas 7	Cal Gas 8	Cal Gas 9	Cal Gas 10	Cal Gas 11	Cal Gas 12
H_2	62–64	64	64										
CH_4	22–25	24.9	23.6	100									
NH_3	0.013–1.3	0.1											
H_2O	2.2–2.5											2.0	
HCN		0.1											
CO	5–6	6	6		100								
N_2	1.5–2.7	2	2			100			99.9			98.0	
C_2H_4	1.85	1.85	1.85				10						
C_2H_6	0.85	0.85	0.85					10					
O_2	0.1–0.15	0.1	0.1										
H_2S	0.23–0.49		0.1						0.1				
C_3H_6	0.1	0.1	0.1							10			
CO_2	1–1.5		1.3								100		
C_6H_6	0.17–0.86	0.08											
C_7H_8		0.01											
C_8H_{10}		0.01											
$C_{10}H_8$	0.0007–0.025	0.002											
He							90	90		90			100

TABLE 15—Fragmentation Pattern Used for Analysis of Coke Oven Gas

	H_2	CH_4	NH_3	H_2O	HCN	CO	N_2	C_2H_4	C_2H_6	O_2	H_2S	C_3H_6	CO_2	C_6H_6	C_7H_8	C_8H_{10}	Naphthalene
Relative sensitivity	0.5	0.7	0.7	0.7	1	1.1	1	2.4	1.1	0.8	1.7	1.4	1.2	3.6	3.6	3.6	4
2	100																
12		1				1		0.37	0.1			0.2	2				
14		9				0.7	4	1.95	2			0.7					
15		100							3								
17		1	100	21													
18				100													
26					17			47	15			4					
27					100			55	23			22					
28						100	100	100	100				5				
30						0.2			31								
32										100	28						
34										0.4	100						
41												100					
42												75					
44													100				
78														100			
92															100		
106																100	
128																	100

mass 14. If the electron energy, or the energy use to remove electrons from the sample molecules, is reduced from 70 eV to 45 eV, then the doubly charged ions are reduced to an insignificant level, and the analysis provides much better results.

Sample Conditioning

In addition to the standard sample conditioning typically required, a temperature of 80 – 100°C is required to prevent condensation problems.

ETHYLENE CRACKER EFFLUENT GAS ANALYSIS

Ethylene Cracker Production Process Overview

Ethylene is produced in the petrochemical industry by steam cracking. In this process, gaseous or light liquid hydrocarbons are heated to 750°C−950°C, inducing numerous free radical reactions followed by immediate quenching to freeze the reactions. This process converts large hydrocarbons into smaller ones and introduces unsaturation. Ethylene is separated from the resulting complex mixture by repeated compression and distillation. In a related process used in oil refineries, high molecular weight hydrocarbons are cracked over zeolite catalysts. Heavier feedstocks such as naphtha and gas oils require at least two "quench towers" downstream of the cracking furnaces to recirculate pyrolysis-derived gasoline and process water. When cracking a mixture of ethane and propane, only one water quench tower is required.

The production process generally follows the steps in Fig. 16. Hydrogen sulfide and carbon dioxide are removed during acid gas removal. The entire cold cracked gas stream goes to the demethanizer tower. Complete recovery of all the methane is critical to the economical operation of an ethylene plant. The product ethylene is taken from the overhead of the tower and the ethane coming from the bottom of the splitter is recycled to the furnaces to be cracked again [58].

On-Line Analysis

Ethylene is produced in an ethylene cracking furnace; annual world production is about 150 billion pounds (50 billion pounds in the United States). A typical plant produces 1 billion pounds annually. Ethylene is used for making plastics (polyethylene, PVC, etc.), ethylene glycol, and many other materials. Its value is about $0.20 per pound, so a typical plant produces $200 million (p.a.) and a 1 % increase in yield, due to improved process control, for example, is worth $2 million (p.a.). In an ethylene cracker, hydrocarbon feed is pyrolized in the presence of steam at 800°C in tubular furnace with a residence time of about 0.5 seconds and at a pressure of about 2 bar. The product stream is called furnace effluent and is quenched by a heat exchanger. Various components (particularly ethylene) are separated out by further processes. Gas feed is typically ethane or propane or mixtures of these two components, or butane, another fuel gas. Liquid feed typically uses C10 and heavier hydrocarbons and can contain components up to C40. Efficient cracker operation relies on accurate determination of C1–C4 components in the effluent stream, particularly the ethylene concentration and, for a liquid feed ethylene furnace, the ratio of propylene to methane. Inefficient operation gives reduced yields and increased coking of the furnace pyrolysis tubes, resulting in increased plant down time for decoking. The typical sample point for an ethylene cracking furnace is shown in Fig. 17.

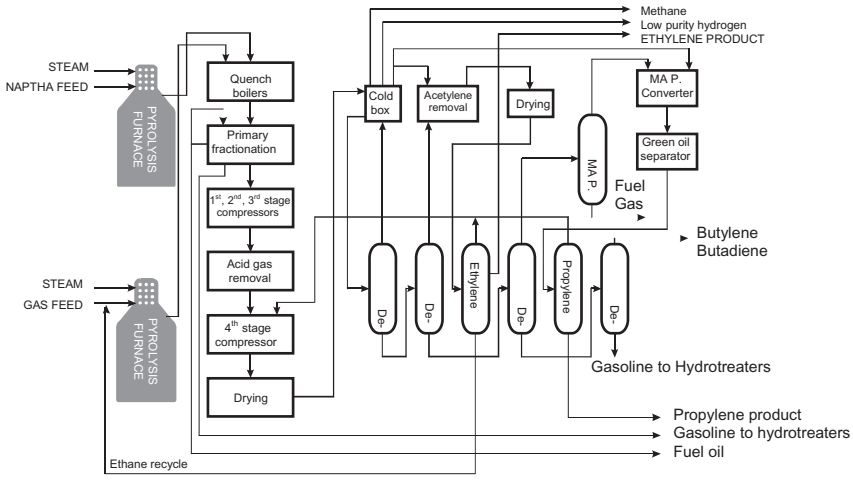

Fig. 16—Schematic view of ethylene cracking process.

Analytical Specification

The typical ethylene furnace effluent gas analysis performance for a process mass spectrometer is shown in Tables 16 and 17 along analysis precision. Table 16 describes the liquid feedstock case, and 17 describes the gas feedstock case.

The standard deviation is a measure of the reproducibility as observed over 24 hours assuming constant concentrations and is demonstrated using calibration gas 1 as shown in Table 18.

The analysis time including stream switching used to meet the above precision is typically 30 seconds per stream. The typical calibration interval for this analysis is 1 month.

Calibration Gas Requirements

The calibration gases used to calibrate the mass spectrometer are shown in Table 18.

Recommended Analysis Set-Up: Reference Information

The fragmentation pattern used for the ethylene cracking gas analysis is shown in Table 19. The relative sensitivity is the sensitivity of the largest peak for a given gas relative to the largest peak for nitrogen. It is essential to operate at a low source pressure in order to preserve filament life and source stability. There has been some correlation between more frequent maintenance and higher concentrations of 1,3 butadiene in the furnace effluence. The mass spectrometers appear to perform more reliably when the 1,3 butadiene concentration is less than 1.3 mol %.

Sample Conditioning

In addition to the standard sample conditioning typically required, a temperature of 80°C to 100°C is required to prevent condensation problems. If possible, the C_9 and heavier hydrocarbons, fuel oil components, etc., should be trapped out of the sample stream by a suitable device, e.g., a refluxing sample

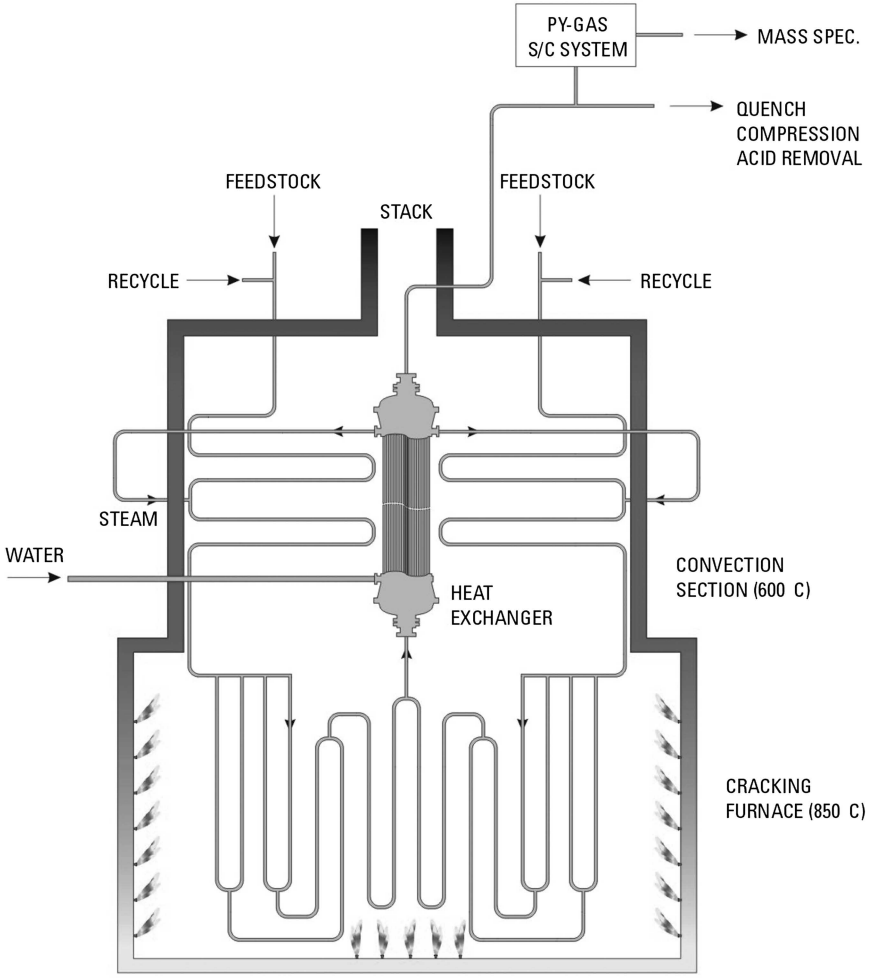

Fig. 17—Ethylene cracking furnace sample point.

conditioner like the Thermo Fisher Scientific Py-Gas Sampler™, without affecting the relative concentrations of the components of interest.

ETHYLENE OXIDE PRODUCTION OFF-GAS ANALYSIS

Ethylene Oxide Production Process Overview

Ethylene oxide is produced by reacting ethylene and oxygen over a silver catalyst. To achieve partial oxidation of ethylene, rather than complete oxidation to carbon dioxide and water, as an undesirable competing reaction, organic chloride is added (normally ethyl chloride, but formerly ethylene dichloride was commonly used). The addition of low ppm levels of organic chloride suppresses the oxidation reactions and because it suppresses carbon dioxide formation more than ethylene oxide formation, this enhances the process efficiency. Typically the reactor conditions are 250°C and 30 bar pressure. Methane is added to the process to

TABLE 16—Liquid Feed Furnace Effluent		
	Typical Level (Mole %)	**Standard Deviation (Mole %)**
Hydrogen	13.4	0.02
Methane	28.6	0.03
Ethylene	27.5	0.03
Ethane	4.8	0.02
Propylene	12.7	0.02
Propane	0.3	0.01
1,3-butadiene	2.9	0.01
Isobutene	3.6	0.01
Isobutane	0.3	0.01

prevent the explosive reaction between ethylene oxide and oxygen. The reactor outlet gas is treated with water to remove the ethylene oxide product as ethylene glycol, the main use for which is antifreeze. The remaining gas is then treated to remove carbon dioxide in an absorber and then recycled in the ethylene oxide process, because it still contains a high level of ethylene feed for further conversion.

TABLE 17—Gas Feed Furnace Effluent		
	Typical Level (Mole %)	**Standard Deviation (Mole %)**
Hydrogen	35.3	0.03
Methane	31.3	0.03
Ethylene	17.4	0.02
Ethane	11.8	0.02
Propylene	2.6	0.01
Propane	1.0	0.01
1,3-butadiene	0.3	0.01
Isobutene	0.2	0.01
Isobutane	$<$0.1	0.01

TABLE 18—% Molar Composition of Required Calibration Gases

Component	MW	Formula	Cal Gas 1	Cal Gas 2	Cal Gas 3	Cal Gas 4	Cal Gas 5	Cal Gas 6	Cal Gas 7	Cal Gas 8	Cal Gas 9	Cal Gas 10	Cal Gas 11	Cal Gas 12	Cal Gas 13	Cal Gas 14	Cal Gas 15	Cal Gas 16
Helium	4	He		100	90	90	90	90	90	90	90	90	90	90	99.5	99.5	99.5	99.5
Hydrogen	2	H_2	21															
Methane	16	CH_4	27															
Acetylene	26	C_2H_2			10													
Ethylene	28	C_2H_4	25			10												
Ethane	30	C_2H_6	10				10											
Methyl acetylene	40	C_3H_4						10										
Propylene	42	C_3H_6	7						10									
Propane	44	C_3H_8	3							10								
1,3 butadiene	54	C_4H_6	3								10							
Isobutene	56	C_4H_8	3									10						
N-butane	58	C_4H_{10}	0.5										10					
Isobutane	58	C_4H_{10}	0.5											10				
Isoprene	68	C_5H_8													0.5			
1-pentene	70	C_5H_{10}														0.5		
Isopentane	72	C_5H_{12}															0.5	
N-pentane	72	C_5H_{12}																0.5

TABLE 19—Example Values of Relative Sensitivities and Fragmentation

Gas	Rel Sen	2	16	26	27	29	30	39	40	41	42	43	44	54	56	57	58	66	67	68	70	72	78	81	84	86
Hydrogen	1.00	100																								
Methane	1.71		100																							
Acetylene	2.17			100	2.3																					
Ethylene	1.08			88.9	100	4.1																				
Ethane	0.75			52.1	81.6	75.7	100																			
Methyl acetylene	3.20			1.0	0.43	0.9		76.9	100	3.5	0.15															
Propylene	1.93			4.9	23.2	0.1		53.5	27.2	100	74.2	2.5	0.21													
Propane	2.22			4.2	25.5	100	2.0	12.4	2.2	12.0	6.4	28.8	38.8													
1_3-Butadiene	1.70			12.8	40.2	1.1		75.1	2.5					100												
Isobutene	2.32			3.1	12.6	9.7	0.44	31.1	8.03	100	3.6	0.18		3.2	60.2	2.7										
Isobutane	3.42			1.0	15.8	4.5	0.11	10.4	1.98	28.4	38	100	3.48	0.1	0.9	3.7	5.0									
n-butane	3.00			2.9	21.7	34.5	1.0	17.3	1.5	22.2	12.4	100	3.5	0.2	0.8	3.0	17.8									
1_3-Cyclo pentadiene	4.00			8.5	10.3			32.2	26.9		3.3		1		3.6	5.4		100	7.6	1.3						
Isoprene	2.03			2.37	21.5	2.4		38.6	30.7	26.1	16.8	0.8							100	94.1						
1-Pentene	3.29			1.66	15.2	18.9	0.4	21.4	6.5	36	100	4.12		1.1	2.68			0.14	1.2	0.1	42.6					
Iso pentane	2.71			1.31	20.7	32.1	0.78	13.4	2.72	50.6	94.3	100			21.2	63.5	2.8					14.4				
n-Pentane	4.19			1.07	17.8	16.8	0.4	9.4	2.09	31.3	62.9	100	3.4	0.12	2.6	15.1	0.68		0.05		0.13	18.0				
Benzene	6.41			0.76	0.8				0.1													0.2	100			
1_4-Hexadiene	2.81			2.0	16.9	9.0	0.1	30.6	6.6	40.8	5.8	0.86	0.1	20.3	1.8	0.3		3.2	100	5.6		0.2	1.6	15.7		
1-Hexene	2.20			1.5	33	28.9	0.5	28.1	6.0	78.8	75.5	58.2	2	5.8	100	6.4		0.1	1.8	0.4	1.6			0.2	49.4	
n-Hexane	3.27			0.9	18	18.7	0.94	18.3	2.2	68.9	34.8	69.5	2.2	0.5	47.9	100	4.4		0.2		0.8				0.3	30.3

Fig. 18 shows a simplified sketch of a typical ethylene oxide plant process, indicating as an example five possible streams for measurement using process mass spectrometry.

On-line Analysis: Analytical Specification

The performance specifications for the analysis of ethylene oxide are shown in Table 20. The standard deviation is a measure of the reproducibility as observed over 24 hours assuming constant concentrations and is demonstrated using calibration gas 1 as shown in Table 21.

The analysis time including stream switching used to meet the above precision is typically 20 seconds per stream. The typical calibration interval for this analysis is 1 month.

Calibration Gas Requirements

The calibration gases used to calibrate the mass spectrometer are shown in Table 21. Calibration cylinder 8 needs to be supplied only if analysis of organic chlorides is required. Calibration cylinders 1 and 8 must be free of impurities with molecular weight >= 50 (< 1 ppm total), if analysis of organic chlorides is required.

Recommended Analysis Set-Up

The fragmentation pattern used for the ethylene oxide gas analysis is shown in Table 22. The relative sensitivity is the sensitivity of the largest peak for a given gas relative to the largest peak for nitrogen. The organic chlorides need to be measured on the SEM detector. If ethylene dichloride is used as the organic chloride, this should be measured at mass 98.

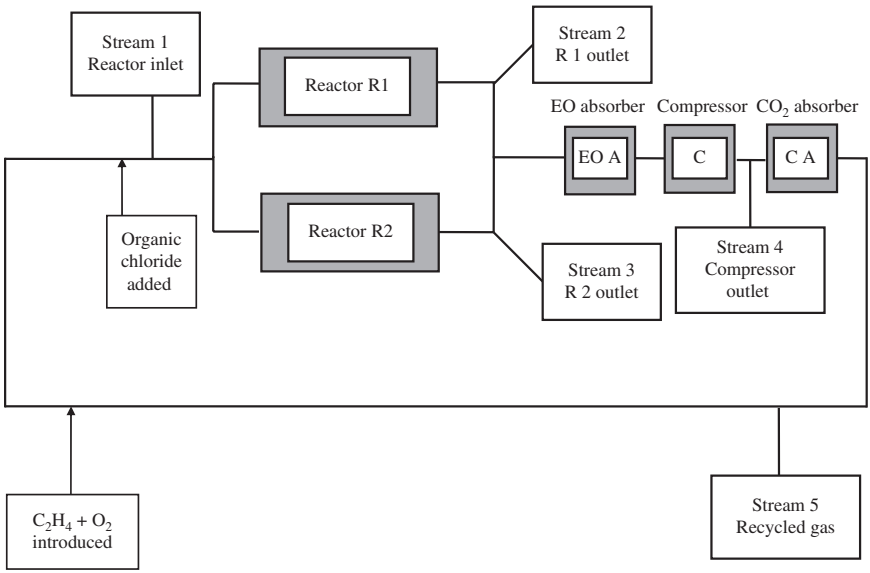

Fig. 18—Schematic of typical ethylene process and off-gas sampling points.

TABLE 20—Performance Specifications for Ethylene Oxide

Measurement	Concentration Range	Standard Deviation
mol % N_2	0–100	0.03 mol % or 0.1 % relative, whichever is greater
mol % O_2	0–10	0.005 mol % or 0.1 % relative, whichever is greater
mol % Ar	0–20	0.005 mol % or 0.1 % relative, whichever is greater
mol % CO_2	0–10	0.01 mol % or 0.1 % relative, whichever is greater
mol % CH_4	0–70	0.03 mol % or 0.1 % relative, whichever is greater
mol % C_2H_4	0–40	0.03 mol % or 0.1 % relative, whichever is greater
mol % C_2H_6	0–5	0.005 mol %
mol % EO	0–4	0.005 mol %
ppm methyl chloride	0–10	0.2
ppm vinyl chloride	0–10	0.2
ppm ethyl chloride	0–10	0.2
ppm allyl chloride	0–10	0.2

There are a number of potential problems with measurements of the chloride components in ethylene oxide process gas. First, ethylene glycol is generated in the reactor outlet stream by reaction between ethylene oxide and water, and this gives rise to a peak at mass 62, where vinyl chloride is measured. Since ethylene glycol is relatively involatile (it boils at 200°C), it is slow to build up in the mass spectrometer and also slow to be removed. The effect can only be minimized by operating the sampling system and inlet system and ion source at high temperatures (80°C−100°C for the inlet system, 140°C−180°C for the ion source) and elimination of cold spots (minimum temperature at any point between process take-off point and analyzer is 80°C). Second, ethylene oxide process streams in an electron impact ion source generate ion molecule reaction products, which give rise to background peaks at masses where the chloride peaks are measured, namely at masses 50 (methyl chloride), 62 (vinyl chloride), and 63.8 (ethyl chloride). These effects are reduced by operating at lower pressures (less than 5×10^{-6} mbar).

If water needs to be analyzed, this has to be calibrated manually because calibration cylinders for water are not readily available. Water can be calibrated

TABLE 21—Calibration Gas Cylinder Requirements

Calibration Cylinder	1	2	3	4	5	6	7	(8*)
mol % CH_4	40							40
mol % N_2	12.5	95						12.5
mol % C_2H_4	25		25					25
mol % C_2H_6	1			5				1
mol % O_2	5	5						5
mol % Ar	10							10
mol % EO	1.5				1.5			1.5
mol % CO_2	5					100		5
mol % He			75	95	98.5		100	
ppm methyl chloride								3
ppm vinyl chloride								3
ppm ethyl chloride								3
ppm allyl chloride								3

by inspection of the process data as follows. The sensitivity for water can be manually adjusted so that the increase in water between reactor inlet stream and reactor outlet stream is the same as the increase in carbon dioxide, as shown in Eq 4.

$$\begin{aligned} &H_2O\ [\text{reactor outlet stream}] - H_2O\ [\text{reactor inlet stream}] \\ &\quad = \text{Carbon Dioxide [reactor outlet stream]} \\ &\qquad - \text{Carbon Dioxide [reactor inlet stream]} \end{aligned} \tag{4}$$

This is because water is produced by the competing reaction in Eq 5.

$$C_2H_4 + 3O_2 \rightarrow 2CO_2 + 2H_2O \tag{5}$$

The main reaction is shown in Eq 6.

$$C_2H_4 + 1/2O_2 \rightarrow C_2H_4O \tag{6}$$

The relative sensitivity for water can be recalculated as shown in Eq 7.

$$\begin{aligned} \text{New Water sensitivity} = &\ \text{Old water sensitivity} \\ &\times (H_2O\ [\text{reactor outlet stream}] \\ &- H_2O\ [\text{reactor inlet stream}]) \\ &/(CO_2\ [\text{reactor outlet stream}] \\ &- CO_2\ [\text{reactor inlet stream}]) \end{aligned} \tag{7}$$

The new sensitivity is then edited into the instrument's calibration.

TABLE 22—Fragmentation Pattern Used for Analysis of Ethylene Oxide Off-Gas

	CH_4	N_2	C_2H_4	C_2H_6	O_2	Ar	EO	CO_2	Methyl Chloride	Vinyl Chloride	Ethyl Chloride	Allyl Chloride
Relative sensitivity	0.7	1.0	1.0	1.1	0.8	1.4	0.5	1.2	1000	1000	500	350
16	100				5.4			5.8				
24.5												
26			52.4	18.9			4.0					
28		100	100	100			6.6	5.7				
30				28.6			2.3					
32					100							
40						100						
43							25.2	0.02				
44							100	100				
50									100			
62										100		
63.8										33	100	
76												100

The carbon balance between the reactor inlet and outlet streams can be verified by determining the following in Eq 8 using the concentration data from the process mass spectrometer.

$$\frac{100 \times \{CH_4 + CO_2 + 2 \times (C_2H_4 + C_2H_6 + EO)\}_{outlet} \times Ar_{inlet}}{\{CH_4 + CO_2 + 2 \times (C_2H_4 + C_2H_6 + EO)\}_{inlet} \times Ar_{outlet}} \quad (8)$$

Ar_{inlet} refers to the argon concentration on the reactor inlet stream, and Ar_{outlet} refers to the argon concentration on the reactor outlet stream. The carbon balance is expected to be within the range 99 % – 101 %; this serves as a check on the integrity of the sampling conditioning and gas analysis system.

Sample Conditioning

In addition to the standard sample conditioning typically required, a temperature of 80° to 100°C is required to prevent condensation problems.

POLYETHYLENE PRODUCTION GAS ANALYSIS

Polyethylene Production Process Overview

Today, several different processes can be employed to convert ethylene to polyethylene, but a common method used in industry is to polymerize ethylene by means of a fluidized reactor bed. A fluidized reactor bed consists of metallic catalyst particles that are "fluidized" by the flow of ethylene gas; that is, catalyst particles are suspended in the ethylene fluid as ethylene gas is pumped from the bottom of the reactor bed to the top. Typical metallic catalyst for ethylene polymerization can be $Ti(OR)_aX_b$ or MgX_n, where X = Cl, Br, or I, a = 0 or 1, b = 2 or 4, a + b = 3 or 4, and R is an aliphatic or aromatic hydrocarbon containing 1 to 14 carbons.

Before ethylene is sent to the fluidized bed, it must first be compressed and heated. Pressures in the range of 100–300 PSI and a temperature of 100°C are necessary for the reaction to proceed at a reasonable rate. In addition, a catalyst stream is also pumped with the ethylene stream into the reactor as catalyst is consumed in the reactor. In effect, the catalyst is not actually consumed, it is simply incorporated with the polyethylene product as polyethylene molecules remain stuck to the catalyst particle from which they were produced.

The conversion of ethylene is low for a single pass through the reactor, and it is necessary to recycle the unreacted ethylene. Unreacted ethylene gas is removed off the top of the reactor, where it is expanded and decompressed to separate the catalyst and low molecular weight polymer from the gas. After purification, ethylene gas is then recompressed and recycled back into the reactor. Granular polyethylene is gradually removed as the polymer settles at the bottom of the reactor and is removed as flakes of polymer every 30 seconds and then dried in a flasher. It is this gas evolved in the flasher that is of interest because its composition is identical to the composition in the polymerization reactor. The main interest is in the levels of hydrogen, ethylene, 1-butene, and 1-hexene. Typically, a residence time of 3 to 5 hours results in a 97 % conversion of ethylene.

Performance Specification

The performance specifications for the analysis of polyethylene are shown in Table 23. The standard deviation is a measure of the reproducibility as observed over 24 hours assuming constant concentrations and is demonstrated using calibration gas 1 as shown in Table 24.

TABLE 23—Performance Specifications for Polyethylene Production

	Cal Mix 1 Molar Concentration	Cal Mix 1 Typical Precision Absolute
Hydrogen	1	0.01
Nitrogen	3	0.05
Ethylene	7	0.05
Ethane	1	0.01
1-butene	0.75	0.01
Isobutane	Balance	0.05
N-butane	0.2	0.05
1-hexene	0.7	0.005
Hexane	0.5	0.005

The analysis time including stream switching used to meet the above precision is typically 8 seconds per stream. The typical calibration interval for this analysis is 2 weeks.

Calibration Gas Requirements

For high-density polyethylene process gas analysis, the calibration gases shown in Table 24 are required. Care has to be taken with calibration gases 5, 6, and 7 to prevent condensing C4 compounds at the 100 % level, e.g., with temperature

TABLE 24—% Molar Composition of Calibration Cylinders

	1	2	3	4	5	6	7	8	9	10
Hydrogen	1									
Nitrogen	3	100								
Ethylene	7		100							
Ethane	1			100						
1-butene	0.75				100					
Isobutane	Bal					100				
N-butane	0.2						100			
1-hexene	0.75							1		
Hexane	0.5								1	
Helium								99	99	100

and pressure regulation. These problems can be avoided by using cylinders containing 10 % in balance helium.

Recommended Analysis Set-Up

The fragmentation pattern used for the polyethylene gas analysis is shown in Table 25. The relative sensitivity is the sensitivity of the largest peak for a given gas relative to the largest peak for nitrogen. It is essential to operate at a low source pressure in order to preserve filament life and source stability.

Sample Conditioning

In addition to the standard sample conditioning typically required, a temperature of 80°C−100°C is required to prevent condensation problems.

FUEL GAS PRODUCTION GAS ANALYSIS

Process Overview

Normally furnaces are operated at constant temperature. To achieve this, a gas-fire furnace would ideally burn a gas of constant composition, delivered at a constant rate and using a constant intake of air at the correct rate for complete combustion. However, in practice, the gas supply is of varying composition, especially in an iron and steel works where fuel gases from a variety of processes are used. Thus, maintaining a constant temperature requires varying the rate of the gas supply. In addition the rate of supply of air also needs to be varied, because there will be energy wastage if either too little air or too much air is used. Additionally, excess air present can cause surface defects on metal surfaces due to oxidation. For example, in an iron and steel works, the following gases are used as fuel gases either singly or in mixtures:

Coke oven gas (typical calorific value 4000 kcal/m^3, stoichiometric air requirement 4)
Natural gas (typical calorific value 9000 kcal/m^3, stoichiometric air requirement 10)

Analyzing the composition of the fuel gas allows the precise heating properties to be predicted. This enables a "feed-forward" method of control (rather than "feed-back"). The calorific value is calculated from the analyzed composition according to the sum of the pure component calorific values weighted on a mole fraction basis [59], as in Eq 9:

$$\begin{aligned}\text{Calorific Value of Mixture} = {} & [\text{Calorific Value of Pure Component}_1 \\ & \times \text{Mole Fraction of Component}_1 \\ & + [\text{Calorific Value of Pure Component}_2 \\ & \times \text{Mole Fraction of Component}_2] \\ & + [\text{Calorific Value of Pure Component}_3 \\ & \times \text{Mole Fraction of Component}_3] + \text{etc.} \quad (9)\end{aligned}$$

However, in practice, the fuel gas will flow through a restriction such as an orifice or valve, and the actual flow is inversely proportional to the square root of the density of the gas, so the property known as the Wobbe index is more useful than the calorific value. The Wobbe index is defined as follows in Eq 10:

$$\text{Wobbe index} = \text{Calorific Value}/\sqrt{\text{Specific Gravity}} \quad (10)$$

TABLE 25—Recommended Cracking Patterns for Polyethylene Gas Analysis										
	H_2	N_2	Ethylene	Ethane	O_2	1-butene	Isobutane	N-butane	1-hexene	Hexane
Rel sens	0.5	1	1.2	1.8	0.8	0.5	2.4	3.0	1.3	1.5
Mass										
2	100						0.1			
26			52.9	20.6		15.1	1.4	4.3	3.4	4.3
28		100	100	100		54.2	1.8	30	0	34
30				27		0.5	0.1	0.8		1.2
32					100					
43							100	100	61	100
56						100	0.5	0.9	100	69
58							4.4	17.8		6
84									43.3	
86										33.2

The Wobbe index indicates the effective heating value of the fuel gas.

The specific gravity is equal to the density divided by the density of the reference gas (normally air).

The density is calculated according to Eq 11:

$$\begin{aligned}\text{Density of Mixture} &= [\text{Density of Pure Component}_1 \times \text{Mole Fraction of Component}_1] \\ &+ [\text{Density of Pure Component}_2 \times \text{Mole Fraction of Component}_2] \\ &+ [\text{Density of Pure Component}_3 \times \text{Mole Fraction of Component}_3] \\ &+ \text{etc.}\end{aligned} \tag{11}$$

To predict the required ratio of air/fuel required for complete combustion, the property known as stoichiometric air requirement is calculated as shown in Eq 12:

$$\begin{aligned}\text{Stoichiometric Air Requirement} &= [\text{Stoichiometric Air Requirement of Pure Component}_1 \\ &\times \text{Mole Fraction of Component}_1] \\ &+ [\text{Stoichiometric Air Requirement of Pure Component}_2 \\ &\times \text{Mole Fraction of Component}_2] \\ &+ [\text{Stoichiometric Air Requirement of Pure Component}_3 \\ &\times \text{Mole Fraction of Component}_3] + \text{etc.}\end{aligned} \tag{12}$$

Again, because the actual flow of fuel gas flow through a restriction such as an orifice or valve is inversely proportional to the square root of the density of the gas, the property known as the CARI (combustion air requirement index) is more useful than the stoichiometric air requirement. The CARI is defined as follows in Eq 13:

$$\text{CARI} = \text{Stoichiometric Air Requirement} / \sqrt{\text{Specific Gravity}} \tag{13}$$

The ideal analyzer is capable of fast on-line determination of Wobbe index and CARI, to enable feed-forward control. Process mass spectrometry is establishing itself as the preferred technique for these measurements [60].

Fuel Gas Analysis Performance Specification

Process mass spectrometry is particularly well-suited to the measurement of fuel gas because the analysis is comprehensive, accurate, and fast. The analysis of all the components present in fuel gas, which typically contains many components (e.g., H_2, CH_4, CO, N_2, O_2, C_2H_4, Ar, C_3H_6, CO_2, C_3H_8, C_4H_{10}, C_6H6), is completed in less than 30 seconds, with a precision of typically better than 0.1 % relative or 0.01 mol % absolute.

Example compositions and derived fuel properties of blast furnace gas (BFG), coke oven gas (COG), LD converter gas (LDG), and natural gas (NG) are shown in Table 26 together with typical mass spectrometer precision of analysis.

The following fuel properties can be derived by the mass spectrometer:

- Lower heating value (lower calorific value)
- Higher heating value (higher calorific value)
- Density
- Specific gravity

TABLE 26—Gas Properties and Mass Spectrometer Specifications for Fuel Gas Sources										
BFG	**Gas properties: contribution per %**				**Analysis time including flushing time = 15 seconds**					
	Lower Heating Value kcal/Nm^3	Upper Heating Value kcal/Nm^3	Density kg/Nm^3	Air Requirement m^3/m^3	Composition mol %	Precision of Analysis by MS mol %	Contribution to Lower Heating Value kcal/Nm^3	Contribution to Upper Heating Value kcal/Nm^3	Contribution to Density kg/Nm^3	Contribution to Air Requirement
H_2	25.8	30.49	0.0009	0.0238	3.2	0.01	82.56	97.57	0.0029	0.0763
H_2O	0	0	0.0083	0		0.01				
CO	30.23	30.23	0.0125	0.0239	22	0.05	665	665	0.2751	0.5249
N_2	0	0	0.0125	0	54.1	0.05	0	0	0.6765	0
O_2	0	0	0.0143	0		0.001				
Ar	0	0	0.0178	0		0.001				
CO_2	0	0	0.0198	0	20.7	0.02	0	0	0.4092	0
TOTAL					100		747.56	762.57	1.3637	0.6012
LDG	**Gas properties: contribution per %**				**Analysis time including flushing time = 15 seconds**					
H_2	25.8	30.49	0.0009	0.0238	2	0.005	51.6	60.98	0.0018	0.0477
H_2O	0	0	0.0083	0		0.01				
CO	30.23	30.23	0.0125	0.0239	64.2	0.05	1940.59	1940.59	0.8029	1.5318
N_2	0	0	0.0125	0	15.9	0.05	0	0	0.1988	0
O_2	0	0	0.0143	0	0.1	0.001	0	0	0.0014	0
Ar	0	0	0.0178	0		0.001				

(*Continued*)

TABLE 26—Gas Properties and Mass Spectrometer Specifications for Fuel Gas Sources (Continued)										
LDG	**Gas properties: contribution per %**				**Analysis time including flushing time = 15 seconds**					
CO_2	0	0	0.0198	0	17.8	0.02	0	0	0.3519	0
TOTAL					100		1992.19	2001.57	1.3568	1.5795
COG	**Gas properties: contribution per %**				**Analysis time including flushing time = 25 seconds**					
H_2	25.8	30.49	0.0009	0.0238	57	0.05	1470.68	1737.93	0.0512	1.3583
CH_4	85.84	95.25	0.0072	0.0956	25	0.02	2145.93	2381.28	0.1794	2.3898
NH_3	35.89	45.46	0.0077	0.01	0.016	0.002	0.57	0.73	0.0001	0.0002
H_2O	0	0	0.0083	0		0.01				
HCN	69.38	71.77	0.0121	0.1075	0.08	0.01	5.55	5.74	0.001	0.0086
CO	30.23	30.23	0.0125	0.0239	5	0.05	151.14	151.14	0.0625	0.1193
N_2	0	0	0.0125	0	7	0.05	0	0	0.0875	0
C_2H_4	142.2	151.66	0.0126	0.1441	1.5	0.01	213.3	227.49	0.0189	0.2161
C_2H_6	153.96	168.19	0.0136	0.1686	0.7	0.01	107.77	117.73	0.0095	0.118
O_2	0	0	0.0143	0	0.1	0.002	0	0	0.0014	0
H_2S	55.9	60.65	0.0154	0.0723	0.013	0.001	0.73	0.79	0.0002	0.0009
Ar	0	0	0.0178	0		0.002	0	0	0	0
C_3H_6	209.58	223.95	0.0191	0.2187	0.3	0.001	62.87	67.19	0.0057	0.0656
C_3H_8	222.92	242.12	0.0201	0.2436		0.001				
CO_2	0	0	0.0198	0	1.8	0.005	0	0	0.0356	0

C_6H_6	372.4	387.92	0.0384	0.3937	0.1	0.001	37.24	38.79	0.0038	0.0394
C_7H_8	401.91	421.05	0.0411	0.4724	0.02	0.001	8.04	8.42	0.0008	0.0094
C_8H_{10}	466.51	490.43	0.0474	0.5512	0.02	0.001	9.33	9.81	0.0009	0.011
$C_{10}H_8$	540.67	557.42	0.0572	0.6299	0.005	0.0005	2.7	2.79	0.0003	0.0031
TOTAL					100		4215.86	4749.82	0.459	4.3398
NG	**Gas properties: contribution per %**				**Analysis time including flushing time = 15 seconds**					
CH_4	85.84	95.25	0.0072	0.0956	96.3	0.02	8266.13	9172.67	0.6909	9.2053
H_2O	0	0	0.0083	0		0.01				
N_2	0	0	0.0125	0	0.4	0.01	0	0	0.005	0
C_2H_6	153.96	168.19	0.0136	0.1686	2.59	0.01	398.75	435.61	0.0351	0.4367
C_3H_8	222.92	242.12	0.0201	0.2436	0.49	0.01	109.23	118.64	0.0098	0.1194
$I\text{-}C_4H_{10}$	295.61	320.08	0.027	0.3231	0.1	0.005	29.56	32.01	0.0027	0.0323
$N\text{-}C_4H_{10}$	296.67	321.14	0.027	0.3231	0.19	0.005	56.37	61.02	0.0051	0.0614
TOTAL					100		8860.05	9819.95	0.7486	9.855

- Lower Wobbe index (lower calorific value/(specific gravity))$^{0.5}$
- Higher Wobbe index (lower calorific value/(specific gravity))$^{0.5}$
- Air requirement
- CARI (air requirement/(specific gravity))$^{0.5}$

The precision of these measurements is normally better than 0.1 % relative.

The analysis times are shown in Table 26. If the four sample streams, BFG, COG, LDG, and LNG, are analyzed sequentially, the cycle time to measure all four sample streams is 70 seconds. Data are communicated to the plant host computer as they are measured, by one or more of a number of available methods, e.g. 4–20 mA or 0–10V analogue outputs, Modbus, Profibus, or OPC.

Typical calibration interval is 1 month and normally takes place automatically. The instrument requires minimal maintenance. Typical maintenance required is 1 day per year, so the instrument "up-time" is approximately 99.7 %.

References

[1] Kurtz, S. S., "The Developments of Hydrocarbon Analysis," *Preparation Symposium*, August 27–September 1, 1972, American Chemical Society, Division of Petroleum Chemistry, New York, NY.

[2] Brown, R. A., *Anal. Chem.,* Vol. 23, 1951, pp. 430–437.

[3] ASTM, *Annual Book of Standards,* Vol. 5.01, ASTM International, West Conshohocken, PA, 2004.

[4] ASTM, *Annual Book of Standards,* Vol. 5.02, ASTM International, West Conshohocken, PA, 2004.

[5] O' Neal, M. J. and Wier, T. P., *Anal. Chem.,* Vol. 23, 1951, pp. 830–843.

[6] Lumpkin, H. E. and Johnson, B. H., *Anal. Chem.,* Vol. 26, 1954, pp. 1719–1722.

[7] Hastings, S. H., Johnson, B. H. and Lumpkin, H. E., *Anal. Chem.,* Vol. 28, 1956, pp. 1243–1247.

[8] Lumpkin, H. E., *Anal. Chem.,* Vol. 28, 1956, pp. 1946–1948.

[9] Gordon, R. J., Moore, R. and Mueller, C. E., *Anal. Chem.,* Vol. 30, 1958, pp. 1221–1224.

[10] Bartz, K. W., Aczel, T., Lumpkin, H. E. and Stehling, F. C., *Anal. Chem.,* Vol. 34, 1962, pp. 1814–1820.

[11] Aczel, T., Bartz, K. W., Lumpkin, H. E. and Stehling, F. C., *Anal. Chem.,* Vol. 34, 1962, pp. 1821–1828.

[12] Hood, A. and O'Neal, M. J., *Advances in Mass Spectrometry,* AMSPA, Waldron, 1959.

[13] Snyder, L. R., Howard, H. E. and Ferguson, H. C., *Anal. Chem.,* Vol. 35, 1963, pp. 1676–1679.

[14] Gallegos, E. J., Green, J. W., Lindeman, L. P., LeTourneau, R. L. and Teeter, R. M., *Anal. Chem.,* Vol. 29, 1967, pp. 1833–1838.

[15] Robinson, C. J., *Anal. Chem.,* Vol. 43, 1971, pp. 1425–1434.

[16] Piemonti, C. and Hazos, M., "Aromatic and Saturate Analysis by Low Resolution Mass Spectrometry," American Chemical Society, Division of Petroleum Chemistry Symposium, Preprints, Washington D.C., August 23–28, 1992, Vol. 37, pp. 1521–1532.

[17] Ashe, T. R. and Colgrove, S. G., *Energy Fuels,* Vol. 5, 1991, pp. 356–360.

[18] Fafet, A., Bonnard, J. and Prigent, A., *Oil Gas Sci. Technol. Rev. IFP,* Vol. 54(4), 1999, pp. 453–462.

[19] Roussis, S. G., Fedora, J. W., Fitzgerald, W. P., Cameron, A. S. and Prouls, R., Chapter 12, "Advanced Molecular Characterization by Mass Spectrometry: Applications

for Petroluem and Petrochemicals," *Analytical Advances for Hydrocarbon Research,* C. S. Hsu, Ed., Kluwer Academic/Plenum Publishers, New York, 2003, pp. 285–312.
[20] McMurray, W. J., Green, B. N. and Lipsky, S. R., *Anal. Chem.,* Vol. 38, 1966, pp. 1194–1204.
[21] Aczel, T. and Lumpkin, H. E., "Detailed Characterization of Gas Oil by High and Low Resolution Mass Spectrometry," *Symposium on Advances in Analysis of Petroleum and Its Products,* August 27 –September 1, 1972, American Chemical Society, New York, NY.
[22] Chasey, K. L. and Aczel, T., *Energy Fuels,* Vol. 5, 1991, pp. 386–394.
[23] Gallegos, E. J., Green, J. W., Lideman, L. P., LeTourneau, R. L. and Teeter, R. M., *Anal. Chem.,* Vol. 39, 1967, pp. 1833–1838.
[24] Joly, D., "Analyse directe des coupes pétrolierés lourdes par spectrométrie do masse," *Proceedings of the International Symposium on Characteristics of Heavy Oils Petroleum Residues,* Technip, Paris, 1984, pp. 416–420.
[25] Bouquet, M. and Brumment, J., *Fuel Sci. Technol. Intl.,* 1990, Vol. 8, No. 9, 961–986.
[26] Fafet, A., Bonnard, J. and Prigent, F., *Oil Gas Sci. Technol. Rev. IFP,* Vol. 54, 1999, pp. 453–462.
[27] Hsu, C. S., Liang, Z. and Campana, J. E., *Anal. Chem.,* Vol. 66, 1994, pp. 850–855.
[28] Guan, S., Marshall, A. G. and Scheppele, S. E., *Anal. Chem.,* Vol. 68, 1996, pp. 46–71.
[29] Rodgers, R. P., White, F. M., Hendrickson, C. L., Marshall, A. G. and Andersen, K. V., *Anal Chem.,* Vol. 70, 1998, pp. 4743–4750.
[30] Stanford, L. A., Kim, S., Rodgers, R. P. and Marshall A. G., *Energy Fuels,* Vol. 20 (4), 2006, pp. 1664–1673.
[31] Hsu, C. S. and Drinkwater, D., *Chromatogr. Sci. Ser.,* Vol. 86, 2001, pp. 55–94.
[32] Kuras, M. and Hala, S., *J. Chromatogr.,* Vol. 51, 1970, pp. 45–57.
[33] Aczel, T. and Hsu, C. S., *Int. J. Mass Spectrom. Ion Processes,* Vol. 92, 1989, pp. 1–7.
[34] Dzidic, I., Petersen, H. A., Wadsworth, P. A. and Hart, H. V., *Anal. Chem.,* Vol. 64, 1992, pp. 2227–2232.
[35] Wadsworth, P. A. and Villalanti, D. C., *Hydrocarb. Proc.,* Vol. 71, 1992, pp. 109–112.
[36] Teng, S. T., Ragsdale, J. and Urdal, K., "SI-PIONA on the INCOS™ XL. A Novel GC-MS Approach to Gasoline Analysis," Application Report No. 225 Finnigan MAT, ThermoScientific, Waltham, MA.
[37] Malhotra, R., Coggiola, M. A., Young, S. E. and Sprindt, C. A., "GC-FIMS Analysis of Transportation Fuels," Symposium, *Advanced Testing for Fuel Quality and Performance,* Division of Petroleum Chemistry, 212th American Chemical Society National Meeting, Orlando, Florida, August 25–29, 1996.
[38] Schoemakers, P. J., Oomen, J. L. L. M., Blomberg, J., Genuit, W. and Van Velzen, G., *J. Chromatogr. A,* Vol. 892, 2000, pp. 29–46.
[39] Bateman, R., Bordoli, R., Gilbert, A. and Hoyes, J., "An Investigation into the Accuracy of Mass Measurement on a Q-TOF Mass Spectrometer," *Adv. Mass Spectrom.,* Vol. 14, 1998, pp. 1–10.
[40] Bacaud, R. and Rouleau, L., "Coupled Simulated Distillation-Mass Spectrometry for the Evaluation of Hydroconverted Petroleum Residues," *J. Chromatogr. A,* Vol. 750, 1996, pp. 97–104.
[41] Ashe, T. R., Roussis, S. G., Fedora, J. W., Felsky, G. and Fitzgerald, P., "Method for Predicting Chemical or Physical Properties of Crude Oils," U.S. Patent No. 5,699,269, December 16, 1997.
[42] Roussis, S. G., Fedora, J. W. and Fitzgerald, W. P., "Direct Method for Determination of True Boiling Point Distillation Profiles of Crude Oils by Gas Chromatography/Mass Spectrometry," U.S. Patent No. 5,808,180, September 15, 1998.
[43] Roussis, S. G. and Fitzgerald, W. P., "Gas Chromatographic Simulated Distillation-Mass Spectrometry for the Determination of the Boiling Point Distribution of Crude Oils," *Anal. Chem.,* Vol. 72, 2000, pp. 1400–1409.

[44] Mendez, A. and Bruzual, J., Chapter 4, "Molecular Characterization of Petroleum and Its Fractions by Mass Spectrometry," *Analytical Advances for Hydrocarbon Research,* C. S. Hsu, Ed., Kluwer Academic/Plenum Publishers, New York, 2003, pp. 73–94.

[45] Mendez, A., Meneghini, R. and Lubkowitz, J., *J. Chromatogr. Sci.,* Vol. 45, August 2007, pp. 683–689.

[46] Mendez, A., Meneghini, R., Bonini, A. and Lubkowitz, J., "Group Type Analysis of Middle Distillates Samples by Simulated Distillation GC/MS," *Gulf Coast Conference,* Galveston, TX, October 2007.

[47] Bacaud, R. and Rouleau, L., "Coupled Simulated Distillation-Mass Spectrometry for the Evaluation of Hydroconverted Petroleum Residues," *J. Chromatogr.,* Vol. 750, no. 1–2, 1996, pp. 97–104.

[48] Mendez, A., Meneghini, R. and Lubkowitz J. A., "GC/MS Serving to Screen Changes in Chemical Composition and Yields of Hydrocarbon Fractions Undergoing Conversion and Upgrading Refining Processes," *Pittsburgh Conference,* Chicago IL, February 25–March 2, 2007.

[49] Androulakis, I. P., Weisel, M. D., Hsu, C. S., Green, L. A. and Farrel, J. T., *Energy Fuels*, Vol. 19, 2005, pp. 111–119.

[50] Wang, F. C., Qian, K. and Green, L. A., *Anal. Chem.,* Vol. 77 (9), 2005, pp. 2777–2785.

[51] Ha, Z., Ring Z. and Liu S., *Energy Fuels,* Vol. 19 (6), 2005, pp. 2378–2393.

[52] Watson, J. T., *Introduction to Mass Spectrometry*, 2nd edition, Raven Press Books Ltd., New York, NY, 1985.

[53] McLafferty, F. W., *Interpretation of Mass Spectra*, 3rd edition, University Science Books, Mill Valley, CA, 1980.

[54] Ishikawa, K., "Guide to Quality Control," *Quality Resources*, White Plains, NY, 1991.

[56] Kandler, W., Sparlinek, W. and Wright, R., "Online-Messungen in Kokereigas zur Steuerung der Gaswäsche," *Proceedings of Conference 'Kokereifachtagung des Vereines Deutscher Kokereifachleute'*, Essen, May 7, 1998.

[57] Wright, R. G., "On-line Analysis of Complex Gas Mixtures by Mass Spectrometry," *J. Process Anal. Chem.,* Vol. IV, 1998, pp. 71–78.

[59] ISO 6976:1995 Natural gas – Calculation of calorific values, density, relative density and Wobbe index from composition. International Organization for Standardization, Geneva, Switzerland, 1995.

[60] Wright, R., "Mass Spectrometry: Gas Analysis," in P. J. Worsfold, A. Townshend and C. Poole, Eds., *Encyclopedia of Analytical Science,* 2nd edition, Vol. 5, Elsevier, New York, 2004, pp. 493–501.

12

Wavelength Dispersive X-ray Spectrometry

Bruno A. R. Vrebos[1] and Timothy L. Glose[2]

INTRODUCTION

The wavelength range of interest in X-ray fluorescence (XRF) spectrometry is roughly the range between 0.04 and 2 nm. This allows the analysis of the elements from fluorine upward to the transuranics, either on their K or L characteristic lines. Using special precautions and dedicated multilayers (see section on "Diffraction and the Analyzing Crystal"), the range can be enlarged to 11 nm, including the characteristic lines of beryllium. Energy and wavelength are related according to the following equation:

$$E = \frac{hc}{\lambda} \tag{1}$$

where E is the photon energy; h is Planck's constant ($6.626\ 10^{-34}$ J s, or $4.135\ 10^{-15}$ eV s); c is the speed of light in vacuum (3×10^8 m/s); and λ is wavelength. By substituting these values in Eq 1, and expressing photon energy in kiloelectronvolts and wavelength in nanometres, the following is obtained:

$$E = \frac{1.24}{\lambda} \tag{2}$$

or

$$\lambda = \frac{1.24}{E} \tag{3}$$

Most commercially available wavelength-dispersive X-ray (WD-XRF) spectrometers have a more limited wavelength range starting at about 0.04 nm (this corresponds to barium Kα). This is due to limited high voltage on the X-ray tube. Note that this does not affect their elemental range; as for the elements with atomic number Z higher than 56 (i.e. barium and higher), the L-lines can be used for analysis.

Attenuation of X-rays

Three different processes govern the interactions between electromagnetic radiation and matter in the energy range of X-rays: coherent scattering, incoherent scattering, and the photoelectric effect. The probability that a photon and an atom interact is given by the atomic cross section for the interaction considered. The total atomic cross section or attenuation coefficient μ is thus

[1] *PANalytical B.V., Almelo, the Netherlands*
[2] *PANalytical Inc. Westborough, MA*

composed of the cross sections for the photoelectric effect (τ), the coherent scattering (σ_{coh}), and the incoherent scattering (σ_{incoh}):

$$\mu = \tau + \sigma_{coh} + \sigma_{incoh} \tag{4}$$

The unit for these atomic cross sections is the barns/atom, which is equal to 10^{-24} cm^2. The conversion from barns/atom to the (in X-ray analysis) more common units of centimeters squared per gram is done by multiplying with Avogadro's number and dividing by the atomic weight of the element concerned. The attenuation of X-ray photons (of a given energy) by matter is proportional to the intensity of the incident photon beam and the mass per unit area. This mass per unit area can be calculated from the density ρ and the thickness t. For a layer of infinitesimal thickness dt, the mass per unit area is given by ρdt. The reduction in intensity dI can thus be described by

$$dI = -\mu I \rho dt \tag{5}$$

where μ is the mass attenuation coefficient. The minus sign is to indicate that the intensity I decreases as dt increases. Beer's law of absorption is obtained after integration of Eq 5

$$I(t) = I_0 \exp(-\mu\rho t) \tag{6}$$

where I_0 is the intensity of the incident beam, and $I(t)$ is the remaining intensity after traveling a distance t through the material. Mass attenuation coefficients μ are specific for each element and exhibit a strong energy dependence. Tables and algorithms to calculate mass attenuation coefficients can be found in the literature [1–5]. An overview has been published by Hubbell [6]. The attenuation coefficient for a compound material $\mu(E)$ at a given energy E can be calculated as the weighted sum of the elemental attenuation coefficients $\mu_j(E)$:

$$\mu(E) = \sum_{j=1}^{n} C_j \mu_j(E) \tag{7}$$

where C_j is the mass fraction of element j, and n is the number of elements.

Origin of Characteristic Radiation

The photoelectric effect is by far the largest contributor to the total attenuation of X-rays. In the photoelectric process, the energy of the incident photon is completely absorbed by an electron in an inner shell of an atom. The electron is ejected from its shell and the photon is annihilated. The ejected electron is called a photoelectron. The kinetic energy (E_{kin}) of the electron can be calculated from

$$E_{kin} = E_{photon} - E_{shell} \tag{8}$$

where E_{photon} is the energy of the incident photon and E_{shell} is the binding energy of the electron. Quite clearly, the energy of the incident photon must be larger than the binding energy of the electron for the photoelectric effect to be feasible. After the ejection of the photoelectron, the atom (rather ion) is in a highly excited state. The relaxation of the ionised atom is done by filling the vacancy with an electron from a shell with a lower binding energy. This, in turn, creates another vacancy, which can be relaxed by an electron from another

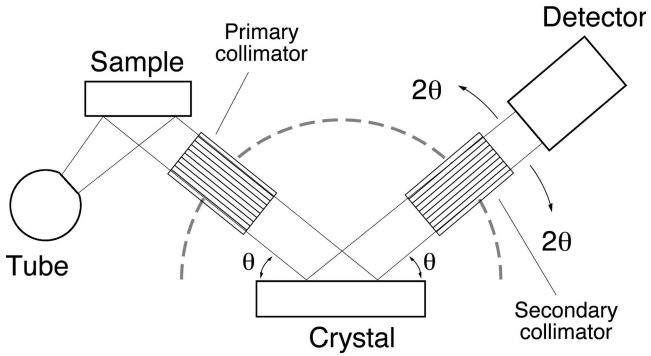

Fig. 1—WDS spectrometer.

shell (or the conduction band), and so on. The energy difference between the two shells involved in this process can be given off as a characteristic X-ray photon. Not all vacancies, however, involve the emission of an X-ray photon. The probability that the electron transition to a primary vacancy in a given shell involves X-ray emission is given by the fluorescence yield ω. The fluorescence yield depends on the shell involved and on the element; tabulated values can, for example, be found in the work by Bambynek et al. [7]. The energy E_{photon} of the emitted X-ray photon can be calculated directly from the energy difference between the atomic energy levels involved in the emission

$$E_{photon} = E_{initial} - E_{final} \tag{9}$$

The atomic energy levels are unique (characteristic) to the element; thus the energy difference is also a characteristic. Therefore, the resulting X-ray photon is called a characteristic photon. The energy of the characteristic photons is varying in a systematic way with the atomic number Z of the elements, a fact that can be represented using Moseley's law [8]:

$$E_{photon} = k(Z - s)^2 \tag{10}$$

where k is a constant for a given series (as defined by the shell with the initial vacancy) and s is the screening constant. A complete tabulation of the energies of characteristic radiation can for instance be found in the work by Bearden [9].

MAIN COMPONENTS OF A WD-XRF SPECTROMETER

The two basic designs of X-ray spectrometers are illustrated in Fig. 1.

The main difference between an energy dispersive (ED-XRF) and a WD-XRF spectrometer is the presence of the *analyzing crystal* in the latter. This analyzing crystal is typically a single crystal of a naturally occurring compound[3] (this is why this type of spectrometers is sometimes called a crystal spectrometer). These devices are fairly large; their dimensions are typically measured in centimeters (2 to 3 cm wide and 5 to 8 cm long, depending on the design of the instrument used). The purpose of this crystal is to diffract

[3] For the analysis of longer wavelengths (in excess of about 1 nm) artificial structures are used.

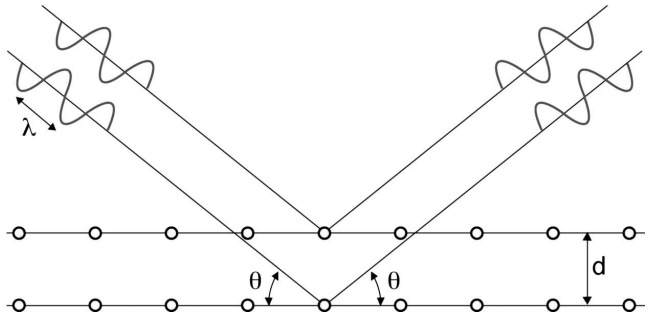

Fig. 2—Bragg.

photons of a selected, predetermined wavelength into the detector while suppressing photons with other wavelengths. This phenomenon of diffraction is most easily explained in terms of the wavelength of the X-ray photons, rather than in terms of their energy. Hence, this type of XRF spectrometer is denominated *wavelength dispersive*, although exactly the same electromagnetic radiation is analyzed as on their energy dispersive siblings.

Diffraction and the Analyzing Crystal

Fig. 2 illustrates the process of diffraction. The necessary condition for constructive interference can be described by Bragg's law:

$$n\lambda = 2d \sin\theta \tag{11}$$

where n is the order of reflection, λ is the wavelength of the photons considered, d is the spacing of the crystallographic planes, and θ is the angle of incidence (and reflection) with respect to the crystal's plane. In the vast majority of applications, the first order ($n = 1$) is used. For diffraction of photons with wavelength λ to occur, the angle θ must be selected such that the product of $2d \sin\theta$ must equal λ. In *X-ray diffraction*, the incident wavelength λ is fixed; the angles θ at which diffraction occurs are measured and the values of $2d$, corresponding to these diffraction peaks, are calculated. The set of $2d$ values is then used to identify the compound. In *qualitative WD-XRF analysis*, the $2d$ spacing is fixed (the analyzing crystal is selected), the angles θ at which diffraction occurs are measured, and the values of the wavelengths λ are calculated. From the wavelengths of the characteristic lines, the constituent elements in the specimen can be determined. In *quantitative WD-XRF analysis*, the wavelength λ of the desired characteristic line is obtained from tables, the crystal is selected, hence the $2d$ spacing is known and the angle θ at which diffraction occurs is then calculated. From the intensities of the wavelengths of the characteristic lines, the concentrations of the constituent elements in the specimen can be determined.

The $2d$ spacing of the crystallographic planes puts limits to the wavelength range that can be analyzed using a particular crystal. The longest wavelength that can be diffracted is theoretically equal to $2d$. Further limitations on the wavelength range are imposed by the geometry. At very low angles (e.g., $\theta < 7°$), parts of the secondary beam are directly entering the detector (i.e., without being diffracted). At very high angles, the detector system and the sample/primary collimator collide. In practice, the range of θ is limited to a maximum

TABLE 1—List of Common Analyzing Crystals

Crystal	Name	Reflection Plane	2*d* Spacing (nm)	Element Range
LiF(420)	Lithium fluoride	(420)	0.1802	Ni–U
LiF(220)	Lithium fluoride	(220)	0.2848	V–U
LiF(200)	Lithium fluoride	(200)	0.4028	K–U
Ge	Germanium	(111)	0.6532	P, S, Cl
PE or PET	Pentaerythritol	(002)	0.8742	Cl–Al
TlAP	Thallium acid phthalate	(1010)	2.575	Mg–O
	Layered synthetic microstructure		3–12	Mg–Be

of about 75 to 80° by mechanical limitations. To cover the wavelength range of interest, WD-XRF spectrometers come equipped with a variety of crystals, the most common of which are listed in Table 1. A more complete list of analyzing crystals can be found in the literature, for instance, in [10].

All of the crystals listed in Table 1, except the layered synthetic microstructures (LSM), are naturally occurring substances. Lithium fluoride is a face centered cubic crystal, belonging to the space group $Fm\bar{3}m$, and thus reflections on (100), (110), and (210) lattice planes are extinguished [11]. On the other hand, strong reflections exist on (200), (220), and (420) planes. The 2*d* spacing listed in Table 1 corresponds to the interplanar distances of the (200), (220), and (420) planes respectively. Pentaerythritol (PE) is an organic crystal (formula $C(CH_2OH)_4$); LSMs are man-made structures consisting of a repeating sequence of two layers of different electron-density (defined as the number of electrons per unit volume). The most common LSMs are structures consisting either of alternating layers of silicon and molybdenum or of silicon alternated with tungsten. The periodicity of the layers is about 5 nm, allowing analysis of the K-lines of the elements in the range of magnesium to oxygen. Other LSMs are specifically designed to yield high reflectivity in a very limited wavelength range, covering as little as one element, but providing superior reflectivity to the general purpose ones. There are other crystals available to the spectroscopist, but these are for specific applications and are not considered here. Also, in the past, crystals such as ADP, or ammonium dihydrogen phosphate ($NH_4H_2PO_4$), with a 2*d* spacing of 1.064 nm have been used for the determination of magnesium. These crystals can still be found in older X-ray spectrometers but have been succeeded by LSMs, which offer a much higher reflectivity.

Crystals are selected on the basis of their stability, high reflectivity, and dispersion. Dispersion can be calculated by differentiation of Bragg's law (Eq 11):

$$\frac{d\theta}{d\lambda} = \frac{n}{2d\cos\theta} \tag{12}$$

This equation allows the calculation of the angular separation between two slightly different wavelengths. A larger value for the dispersion indicates a

larger angular separation, and thus a smaller overlap. Decreasing the $2d$ spacing is an obvious way to improve on angular dispersion; the $2d$ spacing is, however, determined by the crystal used. For most of the wavelength range, at least two crystals are available: the one with the smaller spacing offers the better angular separation, but typically at a loss of intensity. An alternative is to use a higher order of reflection (increasing n). This is a method that has gradually lost importance over the years, as the associated significant intensity loss can be more than a factor of 3 for each successive order. Germanium and PE crystals can both be used for the determination of phosphorus, sulfur, and chlorine (see Table 1). A germanium crystal provides better angular resolution than PE for phosphorus, sulfur, and chlorine at a very high reflectivity, so a germanium crystal is in many cases to be preferred over PE for the determination of those elements.

The $2d$ spacing of the crystal is dependent on the temperature. The crystal with a particularly large thermal expansion coefficient compared to the other analyzing crystals is PE. At the Bragg angle for aluminum Kα, a temperature change of 1°C will cause the angle to change by 0.05° 2θ. The effect on the measured intensity is significant–unless the angle is adjusted to the maximum intensity prior to every single measurement. To avoid this waste of time, the temperature of the WD-XRF spectrometers is carefully kept constant, to within at least 0.1°C and generally much better.

Collimators

The diffraction process, as illustrated in Fig. 2, requires the photons to be incident on the analyzing crystal at a well defined angle θ. In order to achieve this (i.e., restrict the divergence of the incident beam) parallel plate *collimators* are used. Such a collimator consists of a stack of thin plates (typically 100 μm in thickness) arranged parallel to each other at a fixed distance. The divergence of the collimator and, consequently, the divergence of the beam incident on the crystal are determined by the interplanar distance and the length of the plates. The optimal degree of divergence is determined by the rocking width of the analyzing crystal. Using a collimator with a divergence wider than the rocking curve will result in a suboptimal peak to background ratio. Using too fine a collimator, on the other hand, will result in a sizeable reduction of sensitivity. In practice, the divergence of collimators varies from about 0.05° to 4°. Assuming a length of about 10 to 12 cm, the above divergences correspond to interplanar spacings of 100 μm to a few millimetres. The collimators with a smaller divergence are used in combination with crystal such as LiF(200) and LiF(220). The coarser collimators are used with the synthetic multilayered structures, for which the rocking width is rather large.

Goniometer

Most wavelength dispersive instruments use a goniometer to adjust the angle θ at will. The analysing crystal is at the center of rotation. The detector is fitted to the goniometer arm. This arm rotates in such a way that the detector is kept directed toward the diffracted beam. When the crystal makes an angle θ with the beam emanating from the sample, the detector arm is rotated to an angle of 2θ with respect to the secondary beam.

The angular range of the goniometers is typically from a few degrees to 150° 2θ. At higher angles, the detector and the sample collide. The angular accuracy of modern goniometers is often better than 0.001°, while the *reproducibility* is 10 to 50 times better. The reproducibility of a goniometer is the capability to return to the same angle each time for each measurement. Each individual wavelength of interest requires a specific setting of the angles θ and 2θ which can be calculated for a given crystal from Eq 11. Also, the choice of the crystal depends on the wavelength analyzed. Most goniometers are equipped with a crystal mill that can be fitted with several different analyzing crystals (typically 3 to 10). Depending on the requirement, one of these crystals can be moved into the plane of diffraction. All wavelengths are thus measured one after the other, sequentially in time. By slowly rotating the crystal and collecting the intensity as a function of angle of rotation, qualitative analysis can be performed.

Detectors

GENERAL

By far the two most commonly used detectors in WD-XRF are the gas flow detector and the scintillation detector. Because the X-ray beam is diffracted, the spectrum of the X-ray beam at the entrance window of the detector is much simpler than the spectrum as emitted by the sample. According to Bragg's law, for a given crystal (hence, given $2d$ spacing) and for a given angle θ, the only photons that diffract have wavelength λ (higher order reflections are ignored for now). That is the ideal situation, in which the only function of the detector and the counting electronics is reduced to simple *counting*, without any need for *energy discrimination*. However, a few phenomena complicate the situation—these are higher order lines, escape peaks, pulse shrinkage, and crystal fluorescence.

Higher order reflections ($n > 1$) occur when photons with a wavelength λ_2 (half the desired wavelength λ_1) are diffracted by the crystal. The diffraction of λ_1 is a first order diffraction ($n = 1$), and the diffraction of λ_2 is a second order diffraction with $n = 2$. The product $n\lambda$ in both cases is the same and is determined by Bragg's law:

$$n\lambda = 1 \times \lambda_1 = 2 \times \lambda_2 = 2d \sin\theta \tag{13}$$

where the factor 1 and the multiplication signs are explicitly added for clarity. For photons of wavelengths λ_1 and λ_2 to be diffracted both at the same angular setting θ, it is therefore required that λ_2 is half of λ_1. The detector system must be able to distinguish between photons with these two different wavelengths.[4] In other words: some form of energy discrimination is still required. However, because the wavelength differences are quite significant (given that λ_2 is half λ_1), this energy discrimination does not require high-resolution detectors. In energy terms, photons that are diffracted in second order have twice the energy of the photons diffracted in first order.

[4] In principle, reflections of higher order than 2 are possible, corresponding to $n = 3, 4, 5....$ The reflectivity of each successive higher order decreases by about a factor of 3 to 5, so, in practice, only second order reflections need to be considered.

Escape peaks are caused by the fact that the underlying mechanism for detection requires the photon to interact with the atoms in the active body of the detector. Where X-ray photons interact with matter, photoelectric absorption is possible. This, in turn, can lead to the emission of characteristic radiation. If these photons are reabsorbed within the detector (as the majority are), no problem arises. However, a fraction of these photons can *escape* the detector body. The remaining energy is then less than the energy corresponding to the incident photon. This results in a peak of lesser amplitude in the counting electronics. The energy difference (not the wavelength difference) between the escape peak and parent peak is equal to the energy of the characteristic photon that escaped. This energy difference is determined by the materials used in the construction of the detector's active body. The escape peak of a photon diffracted in the second order might have nearly the same energy as that of photons diffracted in first order.

Pulse shrinkage is caused by the fact that at very high counting rates the individual electric pulses, corresponding to individual photons, are no longer completely resolved. The processing of each pulse requires a finite time (100 to 200 ns) for the baseline to be completely restored.

In wavelength dispersive spectrometry, the analyzing crystal is, obviously, in the beam of characteristic photons. Although we would like these photons to be either diffracted (if they are of the correct wavelength) or totally ignored (if they are not of the correct wavelength), any X-ray photon can interact with matter in several different ways. It is important to realize that the analyzing crystals are no different from, for example, the specimen: the constituent atoms of the crystal can be excited (provided the incident beam has photons of short enough wavelength), just like the atoms in the sample. This results in emission of Auger electrons or characteristic radiation or both. Scattering of photons on the analyzing crystal is another possible interaction. Part of the radiation generated either by scattering or photoelectric absorption will find its way to the detector. Scattered radiation will manifest itself in the detector as a continuous background, and the characteristic radiation will show up as peaks. LiF crystals and PE have no noticeable crystal fluorescence because the energies corresponding to the characteristic radiation of their constituent elements are too low compared to the energy range that these crystals are used for. Germanium and TlAP crystals have pronounced and measurable crystal fluorescence due to the emission of the germanium K- and L-lines and the thallium M-lines, respectively. Whether or not a particular LSM exhibits crystal fluorescence depends entirely on the elemental composition of the layers.

The detectors and their associated electronics generate a pulse for each photon detected, the amplitude of which is directly proportional to the energy. Photons of a given wavelength do not generate pulses of the same, constant amplitude. There is considerable spread in the amplitude: the pulses have a Gaussian distribution about a mean height, which is proportional to the energy of the X-ray photons. *Pulse height selection* is an electronic method whereby only those pulses with amplitudes between given values are counted. Using pulse height selection, pulses originating because of higher order reflections or

crystal fluorescence can be eliminated. All modern instruments offer pulse height selection.

FLOW COUNTER (GAS PROPORTIONAL DETECTOR)

Gas-filled detectors for X-ray spectrometry consist of a volume filled with a gas mixture, the main component of which is a noble gas such as argon or krypton, and a wire running through the center. A photon can remove an outer (valence) electron of one of the inert gas atoms. For an argon-filled detector:

$$Ar \xrightarrow{h\nu} Ar^{+} + e^{-} \tag{14}$$

The energy required for the ionization, e_i, depends on the element; for argon, about 26 eV is required to create an ion-electron pair. The total number of such primary ionizations, n_p, caused per incident photon with energy E can then be calculated using

$$n_p = \frac{E}{e_i} \tag{15}$$

The wire is kept at a voltage of about 1 to 2 kV, and the cylindrical housing is kept at earth potential. Under the influence of the electric field, the electrons are accelerated toward the anode wire. The positive ions, on the other hand, will migrate toward the housing. The strength of the electric field in the immediate vicinity of the wire is such that the electrons get sufficient kinetic energy between collisions to cause additional ionizations. This creates an avalanche effect: the electrons created in these ionizations can ionize other atoms. The result of this avalanche effect is that for each individual electron originally created by the incident photon many more are finally collected at the anode wire. This is called the *gas amplification factor* and is typically about 10^4 to 10^5.

The ionizations generate not only free electrons but also positive ions. These are much heavier than the free electrons and drift toward the housing at a much slower speed. If this cloud is still around (i.e., has not reached the housing) when a subsequent photon is absorbed, it partially shields the electric field as seen by the electrons. The pulse corresponding to this photon will thus be registered as having a lower energy. This is one of the main factors contributing to pulse shrinkage. Only when the ion cloud has disappeared completely are the photons counted at the correct energy again.

The detectors are provided with an entrance window. This window should absorb as few of the incoming photons as possible–any photons absorbed into the window are lost from the counting circuit, thus reducing the sensitivity. A popular material exhibiting good mechanical properties, air-tightness, and low X-ray absorption is beryllium. Beryllium windows on detectors are typically between 300 μm and 13 μm thick, depending on the dimensions of the window, the wavelength of the photons of interest, and the pressure of the detector gas. The transmission efficiency of the windows depends on the thickness and the wavelength of the photons considered. For sulfur Kα photons, the transmission efficiency is about 90 % (13 μm) and 80 % (25 μm), respectively; but that reduces to 60 % and 40 %, respectively for aluminum Kα photons. At these thicknesses, the dimensions of the windows are limited because the window

must be able to withstand the pressure difference between the vacuum of the spectrometer chamber and the detector. For the detection of lower energy radiation, beryllium becomes less and less suitable (because of its absorption). Larger windows with lower attenuation for long wavelengths can be made from stretched polymers such as polyethylene or polyester. At thicknesses of 2 μm, the transmission is 90 % for aluminum Kα, and (obviously) higher for shorter wavelengths. These windows are no longer self-supported: they require a mechanical support to withstand the pressure. This support is most commonly provided by a small parallel plate collimator. Both the beryllium and the polymer windows need to be coated with a conductive material at the interior of the detector to provide for a homogeneous electric field. The detectors with beryllium windows can be sealed, in the sense that they are filled with the counting gas by the manufacturer and then hermetically sealed. The useful lifetime of such sealed detectors can exceed several years. On the other hand, polymer windows at the thicknesses mentioned have pinholes. This will cause the counting gas to gradually leak away. Such detectors would have only a very short lifetime before the counting gas leaked away or became so contaminated as to render the detector useless. To compensate for the leaks, a constant flow of counting gas is used, the excess of which is vented away out of the spectrometer chamber; such detectors are therefore called flow counters (or gas flow detectors). These are the preferred detectors for the detection of X-rays with very long wavelengths in wavelength dispersive spectrometers. The counting efficiency of the gas-filled detectors is determined by the absorption in the entrance window and the capture efficiency (absorption of the incident radiation) of the counting gas for the wavelengths of interest. The capture efficiency depends on the path length available within the detector, the composition of the counting gas, and its pressure. Because of considerations of cost, the gas most commonly used in gas flow detectors is argon. For sealed detectors, helium, krypton, and xenon can also be used,[5] depending on the wavelength range of interest. The pressure in sealed detectors for short wavelengths can be several bars. In wavelength dispersive spectrometers, gas flow detectors are not used for wavelengths shorter than about 0.15 nm. Sealed detectors can be used (depending on dimensions, nature of the gas, and pressure) down to wavelengths of 0.03 nm. For such short wavelengths, the absorption by a 50 μm (or even 100 μm) beryllium window is negligible, providing a window strong enough to withstand pressures of several bars.

In some instruments, a sealed gas detector is mounted immediately behind the gas flow detector. The gas flow detector is used for the longer wavelengths and the sealed detector (which is then usually filled with an inert gas such as xenon) is used for the shorter wavelengths. This setup is useful for the wavelength range where the counting efficiency of the gas flow detector is diminishing (but still considerable, say 40 to 60 %). The rest of the photons (those that are not absorbed in the gas flow detector) are then detected by the sealed gas detector. The total signal then comprises the sum of the intensities recorded in both detectors.

[5] Counting gases are mixtures of an inert gas (between 80 % and 98 % by volume) and a "quench" gas such as methane. The discussion about the function of the quench gas is beyond the scope of this chapter.

SCINTILLATION DETECTOR

For the detection of wavelengths shorter than those practical with a gas detector, WD-XRF instruments are generally fitted with a scintillation detector. The operation of the scintillation detector is based on two distinct stages. In the first stage, the incoming photon is absorbed by a *scintillating crystal*. In WD-XRF instruments, the scintillating crystal consists of a sodium iodide (NaI) crystal, doped with thallium. The excitation potential for such crystals is about 3 eV, and leads to the emission of photons with wavelengths of about 410 nm. The counting efficiency of the scintillation detector is largely determined by the thickness of the NaI crystal. A 3 mm thick crystal has counting efficiencies in excess of 99 % for wavelengths of 0.04 nm. The material and the thickness of the scintillating crystal must be such that the incident photons are absorbed with a high efficiency; yet, at the same time, it must be transparent to the re-emitted photons so that they can reach the photomultiplier. The scintillating crystal is coupled closely to a photomultiplier. A photomultiplier consists of a photocathode and a series of dynodes. The material of the photocathode is selected to have a high sensitivity to radiation in the 400 nm range. Upon impact, these photons create free electrons, which are then accelerated toward a series of dynodes. At each dynode, more electrons are generated. If ten dynodes are used, the total amplification provided is about a factor of 10^6. The hygroscopic nature of the NaI crystal forces it to be mounted in a sealed container with a beryllium entrance window. The scintillation detector exhibits many of the same artifacts as the gas-filled detectors, for example, pulse shrinkage at high count rates.

X-ray Tubes

Vacuum X-ray tubes are the preferred method to generate intense X-ray beams. The first X-ray tube with a hot cathode was made by Coolidge [12] in early 1913, and the principles of operation are still the same. The main components of the X-ray tube are the filament and the anode. The filament is the source of electrons, which are directed toward the anode under the influence of a strong electric field. Most of the energy of the electrons is converted into heat; a tiny fraction (about 10^{-3}), however, is converted into X-rays. The gradual slowing down (and changing directions) of the electrons in the anode generates Bremsstrahlung, which is a continuous spectrum. The shape of the continuum can be described by Kramer's law [13]:

$$dI_\lambda = KiZ\left(\frac{\lambda}{\lambda_{\min}} - 1\right)\frac{1}{\lambda^2}d\lambda \tag{16}$$

where dI_λ is the intensity in the wavelength interval $d\lambda$, K is a proportionality constant, i is the current through the tube, Z is the atomic number of the anode element, and λ_{min} is the minimum wavelength. The minimum wavelength λ_{min} corresponds to the event whereby the total energy of the electron is converted into an X-ray photon in a single collision. It is the shortest possible wavelength that can be generated, as the energy of the photon is identical to the energy of the incident electron; it can be calculated from

$$\lambda_{\min} = \frac{1.24}{V} \tag{17}$$

where V (in kilovolts) is the voltage applied to the tube. Eq 17 is very similar to Eq 3. From Eqs 16 and 17 it follows that the intensity of the continuum is

directly proportional to both the current through the tube and the atomic number of the anode element. Increasing the potential difference between the filament (cathode) and the anode will also increase the intensity–but in a nonlinear fashion–as well as alter the shape of the continuum due to the minimum wavelength decreasing as the voltage increases. Since most of the energy of the electrons is converted into heat, the thermal properties of the anode element are very important. Because of the large influx of heat, the melting point of the anode must be high, and it must have excellent thermal conductivity to allow adequate cooling.

X-ray tubes come in a wide variation of size and power ratings. Power ratings of up to about 5 kW can be obtained with stationary anodes. Such high-power X-ray tubes are expensive, but can last for years if properly operated. For even higher ratings (up to 12 kW or so), *rotating anode tubes* can be used. In rotating anode tubes, the anode consists of a large block of material that is rapidly spinning around its axis. This ensures that each fraction of the anode is exposed only briefly to the electrons while it is continuously cooled. Rotating anode tubes find no application in WDXRF instrumentation, mainly due to their high cost.

QUANTITATIVE ANALYSIS AND MATRIX EFFECTS

Quantitative analysis involves the conversion from measured intensities to the concentration of the analyte in the specimen. The most straightforward case is when the intensity of an analyte's characteristic radiation is determined only by the number of atoms present; the analysis can then be done by employing linear calibration graphs. This applies when analyzing dilute specimens (such as metallic elements in oils). In the more general case, the intensity of the radiation of the analyte is dependent not only on the analyte's concentration, but (admittedly to a lesser degree) also on the nature and the concentration of all other constituents in the specimen. The effects of these other constituents on the intensity of the analyte are called *matrix effects*. The root cause of the origin of matrix effects is the fact that, in X-ray fluorescence analysis, the samples are typically analyzed without dilution at all (alloys and liquids), or with a minimal dilution. Powder samples can be measured directly or after briquetting with (or without) binder. Alternatively, powders can be fused into a glassy disk with a relatively low dilution, such as 1 in 6. In such "condensed" samples, all the other elements (matrix elements) present in the specimen interfere with the emitted intensity of the analyte element, and some form of *matrix correction* is thus required.[6]

Two types of matrix effects can be distinguished: absorption and enhancement. The most general relationship for quantitative XRF analysis is

$$C = KIM \tag{18}$$

where C is the analyte concentration, I is the intensity of the characteristic radiation of the analyte, and M represents the matrix effect. The factor K is the slope of the calibration line.

[6] Strictly speaking, in XRF analysis, matrix effects also occur in diluted specimens–but they can be considered constant if the concentration of the analyte is low and if the composition of the matrix is constant.

Absorption

Absorption is the larger of the two matrix effects. It is always present; it is merely its *magnitude* that makes it more or less noticeable and dictates whether correction for it is required. In general, the relationship between intensity, analyte concentration, and absorption can be represented by

$$C = KI\mu_s^* \tag{19}$$

where C, I, and K have been defined earlier; μ_s^* describes the matrix effect and is a function involving absorption of both the incident (exciting) and characteristic radiation. When monochromatic incident radiation is used, μ_s^* can simply be calculated explicitly based on the composition of the specimen. In the more general case of excitation by a polychromatic X-ray beam (such as from an X-ray tube), the calculation involves a summation over the wavelengths of the incident beam (amounting to a numerical integration over the incident spectrum). The value of μ_s^* is determined by the contribution of *all* elements in the sample. Eq 19 is identical to Eq 18 in cases where absorption is the dominant matrix effect. If the total absorption effect μ_s^* is constant (or essentially the same) for all samples, the effect can be ignored, and a simple, straight-line calibration can be used. This is the case for all samples where only the concentrations of a few elements vary in a relatively small range, while the biggest fraction of the constituent elements making up the specimen is essentially constant. The varying concentrations of the analyte elements cause only a small variation of μ_s^* in those cases. Absorption effects typically *reduce* the intensity of the analyte's radiation, compared to the case where they are absent.

Enhancement

Enhancement is a more complicated matrix effect. It requires that a fraction of the photons in the incident beam are absorbed by an element j, which subsequently emits characteristic radiation of its own. If this characteristic radiation of element j can be absorbed by atoms of the analyte i, it causes additional fluorescence of the analyte element. This effect is also referred to as secondary fluorescence. Enhancement thus causes an *increase* of the intensity of the analyte, which is no longer determined by just the concentration of the analyte, but also by the concentration of the matrix element j. A necessary condition for this effect to occur is that the characteristic radiation of element j is sufficiently energetic to cause primary fluorescence of the analyte's atoms. This enhancement effect is particularly strong for the transition elements (atomic numbers Z between 20 and 32) where the K-line radiation of the elements with atomic number Z + 2 is very efficient in exciting atoms of elements with atomic number Z. On the other hand, the characteristic radiation of the element with atomic number Z + 2 is severely absorbed by the element with atomic number Z causing large absorption effects. Higher order enhancement, whereby the radiation of a third element causes fluorescence of a second element, which, in turn, excites the analyte, is also possible, but its contribution is generally negligible–it has been shown that it accounts for 2 to 3 % at most in favorable cases [14]. Enhancement effects are relative small–that stems from the fact that the intensity of characteristic radiation is proportional (not necessarily directly)

to the concentration. The enhancement effect is thus proportional to the product of the concentrations of the elements concerned. Nevertheless, it can boost the intensity by up to 20 % in some cases.

CORRECTION FOR MATRIX EFFECTS

Many different methods have been developed over the years to correct for matrix effects. A generally applicable classification of these methods is difficult to give. Only the main methods will be described in the following sections; ASTM E1361 [15] lists several other methods.

Fundamental Parameter Method

One of the most interesting features of XRF is that the processes involved lend themselves easily to a formal mathematical treatment. The derivation of the equation is beyond the scope of this chapter, and the interested reader is referred to the textbooks on XRF analysis or to the papers by Shiraiwa and Fujino [16] or Criss and Birks [17]. Suffice it to say that the derivation for the analysis of bulk samples[7] involves straightforward integration and a combination of fundamental constants such as mass attenuation coefficients and fluorescent yields. The resulting equation is referred to as the *fundamental parameter* equation. The choice of the word *parameter* is incorrect as the values are tabulated constants (albeit of limited accuracy), but they are not adjustable parameters. The fundamental parameter equation allows the calculation of the intensity of the characteristic radiation of an analyte as a function of the composition of the sample, the properties of the incident radiation, and some geometric details of the spectrometer. It is, unfortunately, not possible to derive an explicit equation for the calculation of the composition of a specimen as a function of the measured intensities. However, the composition of unknown specimens can be obtained by applying the fundamental parameter equation in an iterative way. The fundamental parameter method has been applied since the 1960s. Its use was originally limited to special cases due to the large amount of computing time required; that is, however, no longer an obstacle. The fundamental parameter method is often called a first principles method; this is the terminology used in ASTM E1631 [15].

Compton Correction

Compton, or incoherent, scatter is the process whereby the photon interacts with an outer electron of an atom. In the process, some of the photon's energy is transferred to the electron as kinetic energy. The energy (and thus the wavelength) is thus changed, as well as the direction of propagation. The competing scattering process is the Rayleigh, or coherent, scattering. In Rayleigh scattering, the photon is absorbed by an electron (electromagnetic radiation can cause charged particles to vibrate); and the vibrating electron emits a photon of the same wavelength (a vibrating electrical charge emits electromagnetic radiation).

[7] For samples of less than infinite thickness, the equations become more complicated but they can still be calculated explicitly.

After Rayleigh scattering, only the direction of propagation of the photon appears to be modified, not its energy or wavelength.

Using the conservation of energy and the conservation of momentum, the following relationship can be arrived at expressing the wavelength difference between Compton (incoherently) and Rayleigh (coherently) scattered peaks:

$$\lambda_C - \lambda_R = 0.0243(1 - \cos\varphi) \tag{20}$$

where λ_C is the wavelength of the Compton scattered peak and λ_R is the wavelength of the Rayleigh scattered peak. The wavelength difference in Eq 20 is called the Compton shift. The scattering angle φ is the angle between the direction of propagation of the incident photon and that of the scattered photon; φ is equal to the sum of the spectrometer incident and take-off angles. The Compton peaks appear on the high-angle side (lower energy, longer wavelength) of the Rayleigh peaks. Compton peaks are always broader than peaks due to either characteristic lines in the specimen or Rayleigh-scattered tube lines. The main reason for this broadening is the Doppler effect–the direction of movement of the electron with respect to the photon causes a slight difference in momentum, which affects the wavelength of the scattered photon in a given direction. The Compton correction method requires a measurement of the intensity of the Compton (incoherently) scattered primary (incident) radiation.

The intensity of the Compton scattered peak is wavelength-dependent: the intensity increases with decreasing wavelength of the scattered photon. The Compton scattered peak of the characteristic lines of a chromium anode X-ray tube (wavelength of the chromium Kα at about 0.23 nm) is less intense than if a molybdenum anode tube would be used (wavelength of the molybdenum Kα at about 0.071 nm). The intensity is also strongly dependent upon the mass attenuation coefficient of the specimen: the intensity increases with decreasing mass attenuation coefficient. More precisely, it can be shown that the intensity of the scattered radiation, I_C, is inversely proportional to the mass attenuation coefficient $\mu_s^*$of the specimen:

$$I_C = \frac{1}{\mu_s^*} \tag{21}$$

This latter property makes it an ideal method to correct for matrix effects when absorption is the dominant effect. Combining Eq 21 with Eq 19

$$C = KI\mu_s^* \tag{19}$$

yields

$$C = K\frac{I}{I_C} \tag{22}$$

Although the Compton correction has originally been derived as a purely empirical approach, it can be shown that its basis is a solid approach to a special case of the fundamental parameter method, correcting only for absorption, i.e., ignoring enhancement. This is based on the property that mass attenuation coefficients for a given element but at different wavelengths are proportional to each other; provided there are no absorption edges between the wavelengths considered. Eq 21 breaks down when there are significant absorption edges

between the wavelengths of the Compton scattered radiation and that of the analyte.

The method of Compton correction has found widespread application for the analysis of trace elements in specimens of geological origin such as soils and ores. Most of the trace elements of interest in those situations are elements with atomic number above 26 (iron); their characteristic radiation is subject mainly to absorption. There is some enhancement due to the characteristic radiation of trace elements with higher atomic number to the intensity of trace elements with lower atomic numbers, but this contribution can be neglected due to the low levels of concentration involved.

The intensity of the Compton scattered radiation is also referred to as an *internal standard method*, because the method consists of ratioing the intensity of the analyte to another intensity (from a "component" already present in the specimen, without having to make additions) that is assumed to be subjected to the matrix effects in a strictly proportional manner.

Test Method B of ASTM D5059 [18] for the determination of lead in gasoline uses Compton as a correction method. Also, ASTM C1456 [19] for the determination of uranium or gadolinium allows for the Compton method as a matrix correction method.

Influence Coefficient Algorithms

The most popular methods to correct for matrix effects are still methods based on the use of the *influence coefficients*. Influence coefficient algorithms use a single coefficient to express the total effect of one element on the intensity of another. Influence coefficient algorithms are as old as the application of the XRF technique to quantitative analysis; and many different approaches have been proposed. The early models lacked any solid theoretical basis and were entirely empirical: the numerical value of the coefficients was purely calculated from measurements. More recently, the most modern algorithms all have the same basic equation; all of them have a theoretical basis. The main difference between them is only in the way that the values of the coefficients are calculated.

THE LACHANCE-TRAILL ALGORITHM

The basic equation for influence coefficient algorithms is:

$$C_i = K_i I_i \left[1 + \sum_{\substack{j=1 \\ j \neq e}}^{n} \alpha_{ij} C_j \right] \tag{23}$$

where C_i and C_j are the concentrations of the analyte i and the interfering element j, respectively (expressed as weight fraction), and α_{ij} is the influence coefficient, expressing the influence of interfering element j on the analyte i. This equation was pioneered by Lachance and Traill [20] in 1966. The summation in the equation has n–1 terms; one of the constituent elements, e, has been eliminated. Indeed, because the sum of the concentrations of all elements (whether they are measured or not) in a specimen always totals 1, one element

can be eliminated. Lachance and Traill eliminate the analyte from Eq 23 (e always equals i), based on the fact that

$$C_i = 1 - \sum_{\substack{j=1 \\ j \neq i}}^{n} C_j$$

Because the eliminated element in the Lachance-Traill algorithm is always the analyte itself, the more common formulation is

$$C_i = K_i I_i \left[1 + \sum_{\substack{j=1 \\ j \neq i}}^{n} \alpha_{ij} C_j \right]$$

Upon comparing Eq 18 with Eq 23, it becomes clear that

$$M_i = \left[1 + \sum_{\substack{j=1 \\ j \neq e}}^{n} \alpha_{ij} C_j \right] \tag{24}$$

i.e., the matrix correction term is represented by the square brackets of the influence coefficient algorithm. Eq 24 is important, because it explicitly describes how the matrix effect can be calculated using influence coefficients. The majority of more elaborate algorithms are using the same format as Eq 24, and are basically providing methods that allow one to calculate the value of the influence coefficients α_{ij} as a function of specimen composition.

Lachance and Traill indicated that the value of the coefficients should be calculated from theory, but they only gave a simple and limited method, ignoring enhancement and the polychromaticity of the incident beam. Therefore, in many cases, the coefficients were determined using multiple regression methods. Many early variations on influence coefficient algorithms were based on regression techniques to calculate the value of the coefficients. This was mainly done for two reasons: either the theory behind the influence coefficient algorithm was not well developed, or the computing facilities to calculate them from theory were lacking. ASTM D6443 [21] allows the use of coefficients determined from either multiple regression or theory.

THE RASBERRY-HEINRICH ALGORITHM

One such algorithm is the one proposed by Rasberry and Heinrich [22]:

$$C_i = K_i I_i \left[1 + \sum_{\substack{j=1, \\ j \neq i}}^{n} A_{ij} C_j + \sum_{\substack{k=1, \\ k \neq i}}^{n} \frac{B_{ik}}{1 + C_i} C_k \right] \tag{25}$$

where A_{ij} is a constant used when the significant effect of element j on i is absorption; in such cases the values of the corresponding B_{ik} coefficients are zero and where B_{ik} is a constant used when the predominant effect of element k on i is enhancement, then the values of the corresponding A_{ij} coefficients are

zero. In cases where there is no significant enhancement, all B_{ik} are zero and Eq 25 reduces to the Lachance-Traill equation. The values of A_{ij} and B_{ik} need to be obtained from regression analysis. The algorithm has been derived explicitly for the analysis of iron, nickel, and chromium in steel. In that particular matrix, both enhancement and absorption effects are strong. One particular property of the Rasberry-Heinrich algorithm is the denominator of the second term. The concentrations are expressed in weight fraction; hence, even with a constant value of B_{ik}, the quotient $\frac{B_{ik}}{1+C_i}$ varies with analyte concentration: at low analyte concentrations ($C_i \approx 0.0$), the value is half that compared to when the analyte concentration is very high ($C_i \approx 1.0$). This behavior of the influence coefficient is not generally valid–it does, however, apply to iron-nickel-chromium alloys. For this reason, the Rasberry-Heinrich algorithm is not generally applicable. This was highlighted by Tertian [23].

THE DE JONGH ALGORITHM

One of the first descriptions of an influence coefficient algorithm based on theory was given by de Jongh [24]. His derivation also included the method to calculate the influence coefficients in all cases (polychromatic exciting beam, primary and secondary fluorescence). Furthermore, rather than eliminating the analyte, a different element for each equation, de Jongh eliminated the same element from all equations. He recommends eliminating the major element, such as iron in steels or silicon dioxide (SiO_2) in soils, or nonmeasurable elements such as the loss on ignition when analyzing fused beads. The influence coefficients, calculated with the method of de Jongh, are calculated around a *reference composition*. This reference composition is sometimes called the average composition in the sense that the reference composition is more or less in the center of the range of the concentrations of the analytes in unknown specimens. The influence coefficients are then considered constants. In reality, however, the value of the influence coefficients for a given analytical context varies with composition in a gradual fashion. This limits the applicability of both the Lachance-Traill and the de Jongh algorithms to analyses in a somewhat limited range around the reference composition. The extent of the range is difficult to determine, but it still covers more than 10 % in alloys, where the matrix effects are most severe. When dealing with diluted specimens, the range is unlimited. This applies already to specimens with low dilution, such as fused beads with a 1 to 6 dilution where the range of the constituent compounds is limited between 0 % to just over 16 % (due to the dilution); furthermore, in fused beads, the compounds are mostly oxides, reducing the actual variation of the concentration of the analyte elements even further. The de Jongh algorithm is the first of the influence coefficient algorithms, explicitly based on theory. ASTM D6443 [21] (determination of several trace elements in lubricating oils and additives) and ASTM D6376 [25] (trace elements in petroleum coke) allow for the use of such theoretically calculated influence coefficients.

It is also important because de Jongh was the first one to realize that any one element could be eliminated from the general equation, not necessarily the analyte, as is done with the Lachance-Traill and the Rasberry-Heinrich algorithms. This fact became important when he applied the algorithm to fused

beads with significant loss of ignition (LOI). When making fused beads, the sample and the flux are heated to high temperatures above 900°C if using lithium tetraborate or lithium metaborate fluxes (for more information regarding specimen preparation by fusion methods, the reader is referred to the textbooks by Bennet and Oliver [26] and to D. K. Smith et al. [27]). At those temperatures, materials lose much of their volatile constituents, such as absorbed water and carbon dioxide (from carbonates). The ability to eliminate the LOI from the equation is a large advantage in those circumstances.

THE LACHANCE (COLA) ALGORITHM

Lachance [28] proposed a method to calculate the value of the influence coefficients as a function of the composition of the specimen. The coefficient α_{ij} in Eqs 23 and 24 is now calculated from

$$\alpha_{ij} = \alpha_{ij1} + \frac{\alpha_{ij2} C_m}{1 + \alpha_{ij3}(1 - C_m)} \tag{26}$$

C_m is the total concentration of the matrix elements; i.e.,

$$C_m = 1 - C_i \tag{27}$$

The values for the factors α_{ij1}, α_{ij2}, and α_{ij3} are calculated from fundamental parameters. Note that there is a different C_m for each analyte. The values for the influence coefficients α_{ij} calculated using Eq 26 are very accurate for binary specimens. For binary systems, consisting of only two components, C_m is simply equal to C_j; that is, however, no longer the case for multielement systems, and the use of C_m becomes mandatory to maintain accuracy [29]. For use in multicomponent specimens, *cross-product coefficients* α_{ijk} are included, which leads to:

$$C_i = K_i I_i \left[1 + \sum_{j \neq i}^{n} \left(\alpha_{ij1} + \frac{\alpha_{ij2} C_m}{1 + \alpha_{ij3}(1 - C_m)} \right) C_j + \sum_{j \neq i}^{n} \sum_{\substack{k \neq i \\ k > j}}^{n} \alpha_{ijk} C_j C_k \right] \tag{28}$$

The origin of cross-product coefficients has been discussed by Tertian [30] and, more recently, by Vrebos and Willis [29]. The value of the coefficients α_{ijk} is also calculated from fundamental parameters. All of the coefficients are calculated for given measurement conditions (tube anode, tube voltage, spectrometer geometry, and so on) before the calibration is performed. Eq 28 is valid over the complete concentration range from 0 to 100 % by weight. The calculation of the composition of the unknown specimens involves solving a set of equations such as Eq 28 for each analyte. This is done by an iterative process, which is a fast and relatively simple calculation. Because of the general applicability of the algorithm, it has also been called the COLA algorithm, for COmprehensive LAchance algorithm.

A simple program that calculates the values of the coefficients has been published by Pella et al. [31]. It must be noted, however, that the computer code in [31] is rudimentary and should be replaced by more elaborate programs. A noted deficiency of the program as proposed in [31] is the fact that it takes several shortcuts to save computation time. The characteristic lines,

e.g., contributing to enhancement, are limited so a single line of the enhancing element, and that is the line for analysis of that particular element. Such shortcuts are nowadays no longer needed, and it is easy to verify if the implementation of the algorithm is still applying those: the following method can be used:

1. Calculate the coefficients for silicon in an iron-silicon binary; use the Kα line for both elements (make sure that the voltage on the X-ray tube is 8 kV or higher).
2. Calculate the coefficients again for the same measurement conditions, except for the analytical line of iron, in which case the Lα line is now selected, instead of the Kα.
3. Compare the values of the coefficients for silicon–these should be identical in both cases, because the matrix effects on silicon are the same. The elements present (silicon and iron) and the measuring and excitation conditions for silicon are the same, so the matrix effect on silicon is the same in both cases. With the original implementation, the program would recognize only the enhancement of iron Kα in the first case (where the Kα is the characteristic line used for analysis); whereas in the second case, the enhancement of silicon by the iron Kα and Kβ lines would not be considered, as the only line of iron considered is the Lα.

The above is a simple test that allows one to verify the absence of known shortcuts. There is no reason for these–and similar–shortcuts to exist in current-day computer programs.

A comparison of the accuracy of several common influence coefficients methods can be found in reference [32], for example.

Internal Standard

The internal standard method, or more accurately, the *added internal standard method*, is simple and elegant in design. It works as follows: an element s (other than the analyte i) is added to all specimens in a constant proportion. The element s is not present in the specimens, so its concentration is the same for all specimens–and so would be the measured intensity of its radiation. Any variation in its intensity (other than the variation due to the counting statistical error) is due to the presence of matrix effects. The idea is to choose the internal standard element s so that it is subject to the same matrix effects as the analyte element considered. Both the intensities of the analyte and the added element change thus in the same direction–they increase or they decrease proportional to one another depending on the matrix effect. The following equations apply for the analyte i:

$$C_i = K_i I_i M_i \tag{18}$$

and, for the internal standard s:

$$C_s = K_s I_s M_s \tag{29}$$

In the latter equation, C_s is a constant. Taking the ratio of Eqs 18 and 29, and solving for the only unknown, C_i, yields

$$C_i = \frac{K_i M_i C_s}{K_s M_s} \frac{I_i}{I_s} \tag{30}$$

It is important to note that the terms of the first fraction in Eq 30 are either all constants (K_i, K_s and C_s) or are proportional to one another (M_i/M_s). Eq 30 can thus be reduced to

$$C_i = K_i^* \frac{I_i}{I_s} \tag{31}$$

where all of these constants are collected in K_i^*.

It is clear that the main application of the added internal standard method is in the analysis of relatively few analytes in liquids. The main challenge in the method is the selection of the element to serve as the internal standard. This element must not be present in the specimens (or at most at very low levels, so as not to interfere with the analysis); the characteristic radiation used must be subject to the same matrix effects as the analyte's; and its emission spectrum should not cause interference. In particular, care must be taken to ensure that the analyte element and the internal standard are both subject (or both are not subject) to enhancement by a matrix element. Similarly, matrix elements that strongly absorb the analyte should also strongly absorb the internal standard element. The absorption properties change abruptly when crossing *absorption edges*; hence, this aspect of the requirement is often formulated as "avoid the presence of absorption edges between the wavelengths of the analyte(s) and of the internal standard element."

The requirement that the characteristic radiation of both the analyte and the internal standard is subject to the same matrix effects can most easily be satisfied when the samples are organic matrices. These matrices do not fluoresce, which simplifies finding a suitable internal standard. In this case, a simple guideline is often the best: choose an element that is not present in the samples, and that has an emission line close to that of the analyte (wavelength-wise). The characteristic lines do not have to be the same or even from the same series; the method also works when the analytical line is a Kα and the line of the internal standard is, for example, a Lβ. It must be noted that the internal standard element does not have to be a pure element–stable compounds that are soluble in the solvent are often used. The solvent is in many cases the same as the base material of the specimens and the calibration standards. If more than one internal standard element is to be used, it is recommended that both elements/compounds are added in a single internal standard solution, to minimize errors.

ASTM C1456 [19] prescribes yttrium or strontium as internal standard elements for uranium and samarium for gadolinium, while ASTM D4927 [33] recommends the use of tin or titanium for the determination of barium and calcium, the use of zirconium for phosphorus, and nickel for zinc. In both standard test methods, the compounds to be used to make up the internal standard are listed.

The method of the internal standard can be very accurate, and compensates for both absorption and enhancement; but it is also labor intensive.

Discussion

The wide choice of matrix correction methods available to the analyst may seem overwhelming to the novice. Many of the methods proposed in the past are variations on the same theme; others have been superseded by more modern methods, with a sounder theoretical basis. This applies especially to some of the influence coefficient algorithms.

The mathematically based matrix correction methods such as the fundamental parameter method and the theoretical influence coefficient algorithms require that, in the course of the analysis, the complete composition of the sample is known. This applies even if the analyst is interested in only a few analytes. This requirement of total sample composition is due to the very basis of these methods: they calculate the value of the matrix correction term M_i from all components. As all of the constituent components influence the analyte through absorption, and, less frequently, through enhancement, complete knowledge of the specimen is thus required. This requirement can be relaxed somewhat–elements present at trace levels might be omitted. In general, the total of the known components should be as close to 100 % w/w as possible; in practice, totals of 95 % (and higher, but not exceeding 105 %) are acceptable. The same requirement obviously applies to the standard samples used in the calibration.

The methods using an internal standard or Compton correction do not calculate the matrix correction term explicitly. Rather, they work on the basis that by ratioing the intensity of the analyte by the intensity of another signal that is subject to the same (or similar) matrix effects, adequate compensation of matrix effects is achieved. For such *compensation methods*, the requirement of total sample composition does not apply. Such methods are therefore ideally suited for the analysis of a few analytes at low and trace levels in a variable matrix. Note that the Compton correction method does not correct for enhancement. If the matrix contains one (or more elements) that enhance (cause secondary fluorescence of) the analyte significantly, the accuracy of the results will be disappointing unless the concentration of that interfering matrix element is constant from one sample to the next. Similarly, disappointing results will be obtained with the internal standard method if the matrix contains an element that enhances the analyte, but not the internal standard element. In this case, the assumption that the internal standard element and the analyte are subject to the same matrix effect is no longer satisfied. The observations made here obviously also apply to the standard samples used.

There is no unique or best way to perform accurate matrix correction–for many routine applications, the choice of matrix correction method used is often rather a personal preference than the result of an exhaustive study. Fundamental parameter methods and methods using theoretically calculated influence coefficients are capable of yielding results of similar precision; they are well suited for "complete" analysis–analysis whereby the complete sample is analyzed (except perhaps a few trace elements). On the other hand, the Compton correction method and the method of the internal standard are often excellent choices when only a few analytes are determined and when the matrix may vary from one sample to the next.

CALIBRATION

Calibration is relatively straightforward: measure some standard materials containing the analytes and covering the range of interest. Depending on the situation, perform the matrix correction and determine the slope and the intercept of the calibration curve. Recall Eq 18:

$$C_i = K_i I_i M_i \tag{18}$$

For standard samples, the concentrations C_i are known. This enables one to calculate the value of the matrix effect M_i for each analyte of interest using, e.g., Eqs 24, 25, or 28. The intensity I_i is obtained from measurement. This leaves only the value of the factor K_i to be determined. If the internal standard method is used, Eq 31 applies.

In a more general format, Eq 18 is written as

$$C_i = B_i + K_i I_i M_i \tag{32}$$

where B_i is the intercept of the calibration line and all other symbols have been defined before. The factor B_i is essentially the concentration equivalent of remaining background intensity and K_i is the reciprocal of the sensitivity of the spectrometer expressed in concentration units over intensity unit. Typically, several standard samples are used and the values of the coefficients B_i and K_i are determined from regression analysis.

In general, corrections for background are required when the intensity of the background under the peak is of comparable magnitude to the peak itself, or when the background intensity is varying between standards (or between standards and samples). In that case, the background intensity cannot be considered a constant as is assumed in Eq 32. The value of K_i can be determined from several standards using regression methods.

In some cases one of the characteristic lines of one element in the sample has a wavelength very close to the wavelength of the analytical line considered. This effect is called spectral overlap or spectral interference. This yields a contribution to the measured intensity that is not due to the analyte, but rather to the interfering element. If this contribution is sufficient, it must be corrected for. Details of the operation of these corrections are not given here.

CONCLUSION

The excellent stability provided by modern instrumentation and the ability to maintain a calibration over extended periods of time, with only minimal effort spent on monitoring drift and correction for it, are part of the attraction of the technique. It is furthermore well suited to automation. This makes it an ideal tool for routine analysis. The relatively high initial investment can be amortized over a large number of samples, which, coupled with a high up-time and low cost of sample preparation, makes it a cost-effective analytical method.

List of ASTM methods using wavelength dispersive XRF	
D2622	Sulfur in petroleum products
D4927	Elemental analysis of lubricant and additive components – Ba, Ca, P, S, and Zn by WD-XRF spectroscopy
D5059	Lead in gasoline by WD-XRF
D6376	Trace elements in petroleum coke by WD-XRF
D6443	Ca, Cl, Cu, Mg, P, S, and Zn in unused lubricating oils and additives by WD-XRF spectrometry (mathematical correction)
D7343	Optimization, sample handling, calibration, and validation of XRF spectrometry methods for elemental analysis of petroleum products and lubricants

Suggestions for Further Reading

Handbook of X-ray Spectrometry – Methods and Techniques, R. E. van Grieken and A. A. Markowicz, Eds., Marcel Dekker, New York, 1993.

Atomic Spectroscopy in Elemental Analysis, M. Cullen, Ed., Blackwell Publishing Ltd, Oxford, UK, 2004.

References

[1] McMaster, W. H., Delgrande, N. K., Mallet, J. H. and Hubbell, J. H., *Compilation of X-Ray Cross Sections*, UCRL 50174, Sec. II, Rev. 1, University of California, 1969.

[2] Heinrich, K. F. J., *The Electron Microprobe*, T. D. McKinley, K. F. J. Heinrich, and D. B. Wittry, eds., Wiley, New York, 1966, p. 296.

[3] Leroux, J. and Thinh, T. P., *Revised Tables of Mass Attenuation Coefficients*, Corporation Scientifique Claisse, Quebec, Canada, 1977.

[4] Veigele, W. J., *Handbook of Spectroscopy*, J. W. Robinson, ed., Vol. 1, CRC Press, Cleveland, OH, 1974, p. 28.

[5] de Boer, D. K. G., "Fundamental Parameters for X-ray Fluorescence Analysis," *Spectrochim. Acta*, Vol. 44B, 1989, p. 1171.

[6] Hubbell, J. H., "Compilations of Photon Cross-Sections: Some Historical Remarks and Current Status," *X-ray Spectrom.*, Vol. 28, 1999, p. 215.

[7] Bambynek, W., Crasemann, B., Fink, R. W., Freund, H. U., Mark, H., Swift, C. D., Price, R. E. and Venugopala Rao, P., "X-ray Fluorescence Yields, Auger, and Coster-Kronig Transition Probabilities," *Rev. Mod. Phys.*, Vol. 44, 1972, p. 716.

[8] Moseley, H. G. J., "The High Frequency Spectra of the Elements," *Philos. Mag.*, Vol. 26, 1913, p. 1024.

[9] Bearden, J. A., "X-ray Wavelengths," *Rev. Mod. Phys.*, Vol. 39, 1967, p. 78.

[10] Willis, J. P. and Duncan, A. R., *Understanding X-ray Spectrometry, Vol. 1, Basic Concepts and Instrumentation*, PANalytical, Almelo, the Netherlands, 2008.

[11] Birkholz, M., Fewster, P. F. and Genzel, C., *Thin Film Analysis by X-ray Scattering*, Wiley-VCH, Weinheim, Germany, 2006.

[12] Coolidge, W. D., "A Powerful Röntgen Ray Tube with a Pure Electron Discharge," *Phys. Rev.*, Vol. 2, 1913, p. 409.

[13] Kramers, H. A., "On the Theory of X-ray Absorption and of the Continuous X-ray Spectrum," *Philos. Mag.*, Vol. 46, 1923, p. 836.

[14] Shiraiwa, T. and Fujino, N., "Theoretical Correction Procedures for X-ray Fluorescence Analysis," *X-ray Spectrom.*, Vol. 3, 1974, p. 64.

[15] ASTM E1361, Standard Guide for Correction of Interelement Effects in X-ray Spectrometric Analysis, ASTM International, West Conshohocken, PA,

[16] Shiraiwa, T. and Fujino, N., "Theoretical Correction for Coexistent Elements in Fluorescent X-ray Analysis of Alloy Steel," *Adv. X-ray Anal.*, Vol. 11, 1968, p. 63.

[17] Criss, J. W. and Birks, L. S., "Calculation Methods for Fluorescent X-ray Spectrometry: Empirical Coefficients versus Fundamental Parameters," *Anal. Chem.*, Vol. 40, 1968, p. 1080.

[18] ASTM D5059, Standard Test Methods for Lead in Gasoline by X-ray Spectroscopy, ASTM International, West Conshohocken, PA,

[19] ASTM C1456, Standard Test Method for the Determination of Uranium or Gadolinium, or Both, in Gadolinium Oxide-Uranium Oxide Pellets or by X-ray Fluorescence (XRF), ASTM International, West Conshohocken, PA,

[20] Lachance, G. R. and Traill, R. J., "A Practical Solution to the Matrix Problem in X-ray Analysis, Part 1: The Method," *Canad. Spectrosc.*, Vol. 11, 1966, p. 43.

[21] ASTM D6443, Standard Test Method for Determination of Calcium, Chlorine, Copper, Magnesium, Phosphorus, Sulfur, and Zinc in Unused Lubricating Oils and

Additives by Wavelength Dispersive X-ray Fluorescence Spectrometry (Mathematical Correction Procedure), ASTM International, West Conshohocken, PA,

[22] Rasberry, S. D. and Heinrich, K. F. J., "Calibration for Interelement Effects in X-ray Fluorescence Analysis," *Analytical Chem.*, Vol. 46, 1974, p. 81.

[23] Tertian, R., "Mathematical Matrix Correction Procedures for X-ray Fluorescence Analysis, A Critical Survey," *X-ray Spectrom.*, Vol. 15, 1986, p. 188.

[24] de Jongh, W. K., "X-ray Fluorescence Analysis Applying Theoretical Matrix Corrections: Stainless Steel" *X-ray Spectrom*., Vol. 2, 1973, p. 151.

[25] ASTM D6376, Standard Test Method for Determination of Trace Metals in Petroleum Coke by Wavelength Dispersive X-ray Fluorescence Spectroscopy, ASTM International, West Conshohocken, PA,

[26] Bennet, H. and Oliver, G. J., *XRF Analysis of Ceramics, Minerals and Allied Materials*, John Wiley & Sons, Inc., New York, 1992.

[27] Buhrke, V. E., Jenkins, R. and Smith, D. K., *A Practical Guide for the Preparation of Specimens for X-ray Fluorescence and X-ray Diffraction Analysis*, John Wiley & Sons, Inc., New York, 1998.

[28] Lachance, G. R., "The Role of Alpha Coefficients in X-ray Spectrometry," paper presented at *International Conference on Industrial Inorganic Elemental Analysis*, Metz, France, June 1980, Philips Science and Industry Division, Eindhoven, the Netherlands.

[29] Vrebos, B. A. R. and Willis, J. P., "Use of *Cm* and Cross Product Coefficients in Influence Coefficient Algorithms for Quantitative XRF Analysis," *X-ray Spectrom*., Vol. 34, 2005, p. 73.

[30] Tertian, R. and Vié Le Sage, R., "Crossed Influence Coefficients for Accurate X-ray Fluorescence Analysis of Multicomponent Systems," *X-ray Spectrom*., Vol. 6, 1977, p. 123.

[31] Tao, G. Y., Pella, P. A. and Rousseau, R. M., *NBSGSC—A Fortran Program for Quantitative X-ray Fluorescence Analysis*, NBS Technical Note 1213, National Institute of Standards and Technology, U.S. Dept. of Commerce, U.S. Govt. Printing Office, Washington, DC, 1985.

[32] Vrebos, B. and Helsen, J., "Evaluation of Correction Algorithms with Theoretically Calculated Influence Coefficients in Wavelength Dispersive XRF," *X-ray Spectrom*., Vol. 15, 1986, pp. 167–171.

[33] ASTM D4927, Standard Test Methods for Elemental Analysis of Lubricant and Additive Components–Barium, Calcium, Phosphorus, Sulfur, and Zinc by Wavelength-Dispersive X-ray Fluorescence Spectroscopy, ASTM International, West Conshohocken, PA,

13

Energy Dispersive X-ray Fluorescence and Its Applications in the Field of Petroleum Products and Lubricants

C. A. Petiot[1] and M. C. Pohl[2]

INTRODUCTION

Henry Moseley was perhaps the father of the X-ray fluorescence (XRF) technique. He was the first to build an X-ray tube that could be used to bombard samples with high-energy electrons. In 1925, Coster and Nishina [1] began using the X-rays coming from the bombardment of an electrode to excite an actual sample. Glocker and Schreiber [2] attempted to use the infant technique for quantitative analysis in 1928. Poor quality detector tubes made this nearly impossible until the late 1940s. The first commercially available instruments were offered in the 1950s. In 1970, the lithium drifted silicon detector was developed and it is still in use today!

X-RAY FLUORESCENCE PRINCIPLES

X-ray fluorescence spectrometry is an elemental analysis technique with broad application in science and industry. This technique is based on the principle that individual atoms can be excited and they will then emit X-rays of a characteristic energy. If the number and energy of such X-ray photons are determined, the element of interest can be identified and quantitated. Modern instruments can analyze solid, liquid, or thin-film samples for the determination of elements from the mass percentage level all the way down to the milligrams per kilogram level. The analysis is typically rapid with minimal sample preparation.

Elemental identification (qualitative analysis) can be performed because of the characteristic X-ray energy emanating from the inner electronic shells of the atoms. These energies are constant and unique for each element. To understand this phenomenon, the method of X-ray generation must first be examined. When a high-energy electron beam is made to impinge on a material, one of the results is the emission of a broad range of energetic photons with a continuum of energy. This radiation, called Bremsstrahlung or "braking radiation," is a result of the deceleration of the electrons inside the material being bombarded. An example of the Bremsstrahlung continuum for a tungsten target is illustrated in Fig. 1 [3]. This loss of energy is commonly referred to as inelastic scattering. It is represented by a single electron losing its energy to multiple atoms along its trajectory in the target.

Another possible result of the interaction of the beam with the sample is the ejection of electrons from the inner shells of the target material as can be seen

[1] *Oxford Instruments, Bucks, England*
[2] *Horiba Instruments, Inc., Irvine, CA*

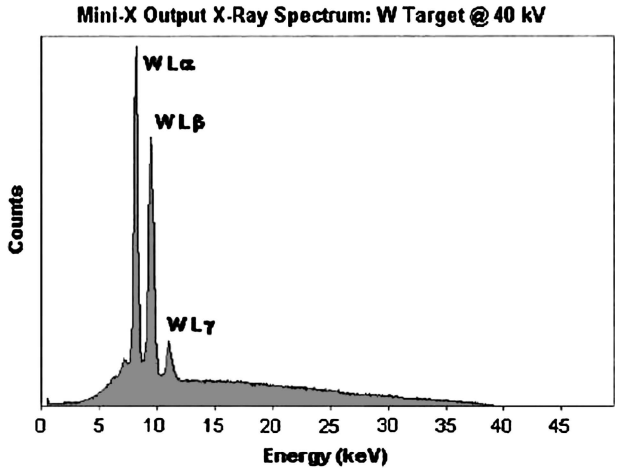

Fig. 1—Intensity output from a W anode X-ray tube.

in Fig. 2. These electrons leave with a kinetic energy (E−Q), which is the energy of the electron beam minus the binding energy of the electron in the atom. The departing electron leaves a hole in the electronic structure of the target atom. Very quickly, the remaining electrons in the target element rearrange with an electron from a higher energy level, filling the hole. The decay of this electron produces energy in the form of an X-ray, whose energy is determined by the initial and final state of the electron. The detection of this X-ray photon energy allows the determination of the element from which it originated [4, 5]. By also measuring the rate of production of these photons, the actual quantity of an element may be determined.

Since any of a number of inner shell electrons can be ejected and a variety of electrons can decay to the inner shell, X-rays of a variety of energies will be produced. The main X-ray designations come from the orbital where the ejected electron originated. These would be K, L, and M, with K being the highest energy because this electron originated the closest to the nucleus. The next part of the designation, e.g., α, β, γ, comes from the energy level where the collapsing electron originated. Since there are sublevels within each energy level, i.e., 3s, 3p, or 3d electrons, a numerical subscript is required. The sublevel designation originates from the strength of the radiation produced. The strongest line is designated as 1 and so forth through the weaker lines. For example, molybdenum Kα1 transition yields a photon of wavelength 0.071 nm [4]. It is important to note that only high-resolution instruments could resolve Kα1 from Kα2. So in many cases only Kα lines would be referenced [6]. As is shown in Fig. 3, once the excitation energy of the incident electron beam exceeds the molybdenum K transition energies, these lines begin to appear in the spectrum.

Unfortunately, when the X-rays strike the material of interest, other phenomena besides absorption and electron ejection, followed by X-ray photon emission, take place. The incident X-rays may also simply be transmitted through the target or may be scattered by the target. When the exciting X-ray is scattered with no change in energy, it is called Rayleigh scattering. When an

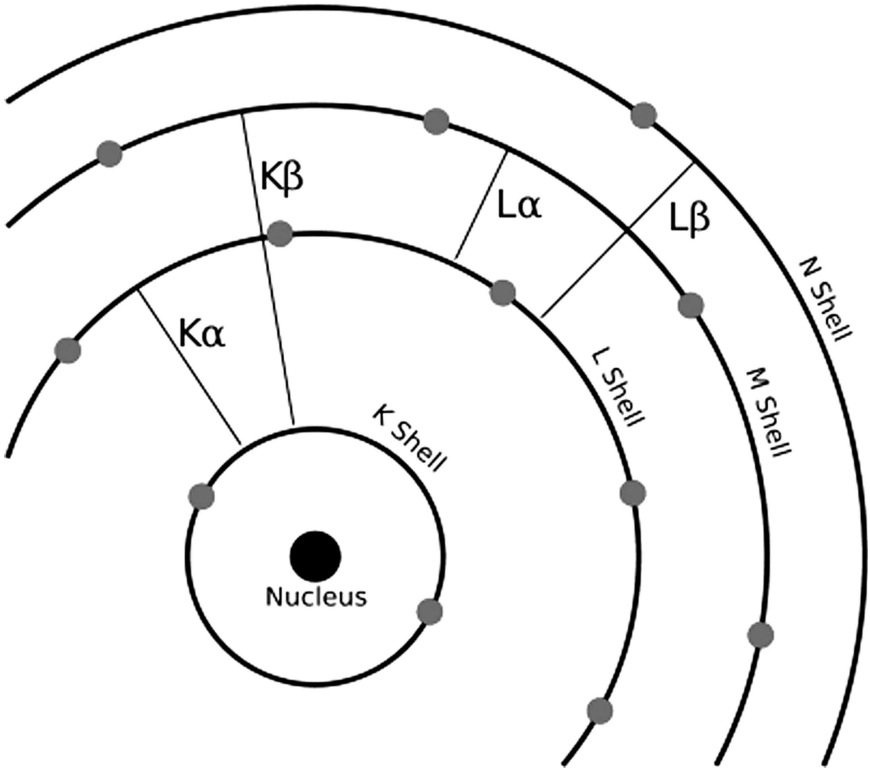

Fig. 2—Electronic transitions in a calcium atom. Note: when electrons are jumping down, one of the electrons in the lower orbital is missing!

amount of energy is lost, the phenomenon is inelastic scattering. The dominant inelastic scattering is typical Compton scattering. All of these extraneous X-rays contribute to high levels of background radiation, which is known to complicate the experiment greatly [5].

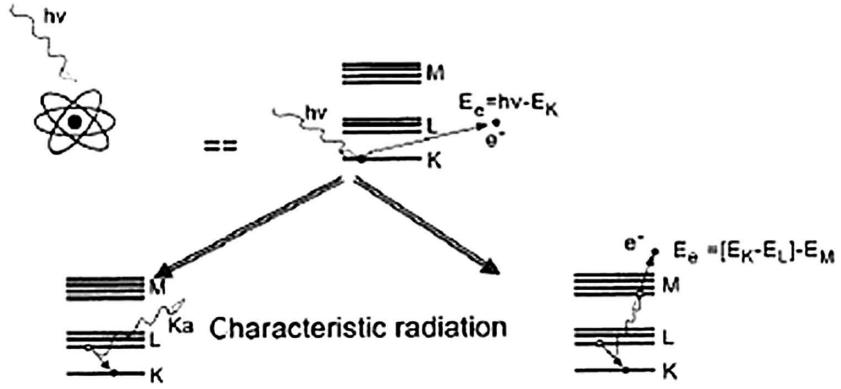

Fig. 3—XRF process.

One of the real strengths of this technique is that it is not sensitive to the chemical environment of the element of interest. Since the chemistry is taking place with the valence electrons of the element, the effect on the inner shell electrons is negligible. The result is that the X-ray photon produced from the inner electrons is insensitive to the external chemical environment. The one exception is the case of low atomic number (Z) elements with comparatively few electrons. The lack of chemical shift in the fluorescent X-rays allows elements to be determined, whether they are present in elemental or compound form [6].

Most of the XRF instruments in use today fall into one of two general categories: energy-dispersive X-ray fluorescence (EDXRF) and wavelength-dispersive X-ray florescence (WDXRF). These two broad categories include a wide variety of instrument configurations. These encompass various combinations of X-ray sources, X-ray source and detector optics, and the detectors themselves. This chapter discusses the most common EDXRF instruments in use, with particular attention being paid to those featuring the more advanced or specialized components.

COMPONENTS OF A TYPICAL ENERGY-DISPERSIVE X-RAY FLUORESCENCE SPECTROMETER

All XRF spectrometers include two essential components: an X-ray source and a detection system (collecting and processing secondary X-rays coming from the sample). Filters can be added on the X-ray source side and on the detection side to optimize the performance of the analysis head (Fig. 4).

X-ray sources generate the primary X-rays that irradiate the sample and excite the atoms within the samples to emit characteristic X-ray spectral lines. X-ray sources can be:

- Radioisotope sources such as ^{55}Fe, ^{109}Cd, or ^{241}Am
- X-ray tubes.

Radioisotope sources contain a specified amount of a radioisotope, which is encapsulated to prevent its dispersion into the environment. Sources are also shielded so they emit radiations only in a particular direction. Radioisotope sources used for XRF normally emit X-rays of a particular energy. Because of disposal and half-life considerations, they are now rarely used in EDXRF spectrometers and have been replaced by X-ray tubes.

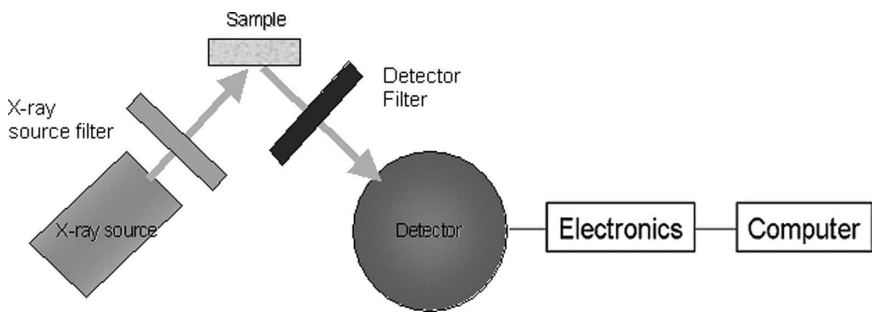

Fig. 4—Basic components of EDXRF system.

In X-ray tubes, a large current is passed through a filament, usually a tungsten wire, heating it until it emits thermal electrons. These electrons are accelerated to the target of the tube (anode) when a potential difference is applied between the filament (cathode) and the anode. The target is either a thin disk metal (typically palladium, rhodium, titanium, or silver), or a coating of the target metal on a copper block. The target material emits primary X-rays in all directions (Bremsstrahlung radiation as well as X-ray lines characteristic of the anode material), and some escape through the X-ray tube window. The tube window is usually made of beryllium and is transparent to X-rays. The energy of the X-rays emitted depends on the anode material and the voltage applied to the anode, so excitation conditions can be customized to excite specific elements in the sample. Fig. 5 shows a schematic of a side-window X-ray tube.

There is no one-size-fits-all approach to the source selection in an EDXRF instrument. The power applied to the tube may be set at various levels. It can range from a fraction of a watt for an EDXRF instrument to tens of kilowatts for a WDXRF instrument. In the case of very high-powered tubes, cooling must be provided to dissipate the heat generated. The anode material must be chosen carefully to ensure that the proper excitation energy is available to irradiate the sample. Typical anode materials include aluminum, chromium, tungsten, palladium, rhodium, gold, or silver. For the proper excitation of light elements, a high-intensity beam of low energy, i.e., 1 to 10 keV, must be available. Heavy elements, on the other hand, require much higher energy radiation (30 to 50 keV) [6,7]. A key consideration in tube selection is the fact that the detector is required to detect a weak sample X-ray signal in the presence of an intense X-ray source beam.

A primary beam filter, placed between the X-ray source and the sample, is often used to favor good excitation and low background for a particular region of the energy spectrum, therefore improving sensitivity for the elements in this region of the spectrum. EDXRF spectrometers can include several primary beam filters of different material and different thicknesses to optimize performance for various regions of the spectrum. This type of system is illustrated in Fig. 6, where E_m represents the maximum energy for exciting the element of interest by the unfiltered beam.

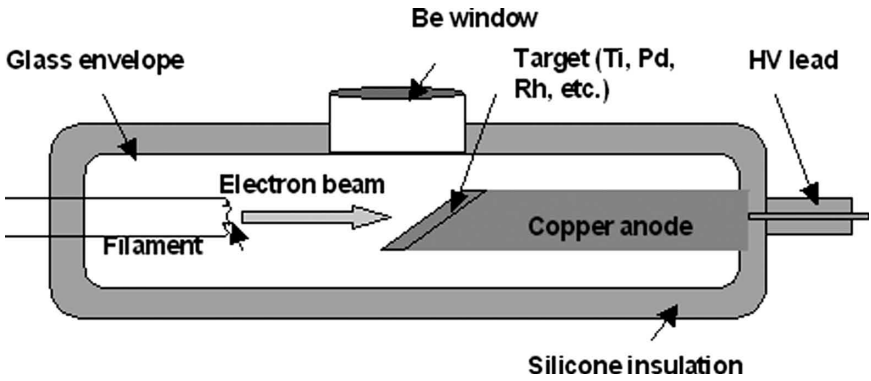

Fig. 5—Schematic of a side-window X-ray tube. Note: Another possible source of high-intensity, coherent, monochromatic X-ray beam is the use of synchrotron radiation. Time and cost considerations limit synchrotron experiments to very critical scientific experiments.

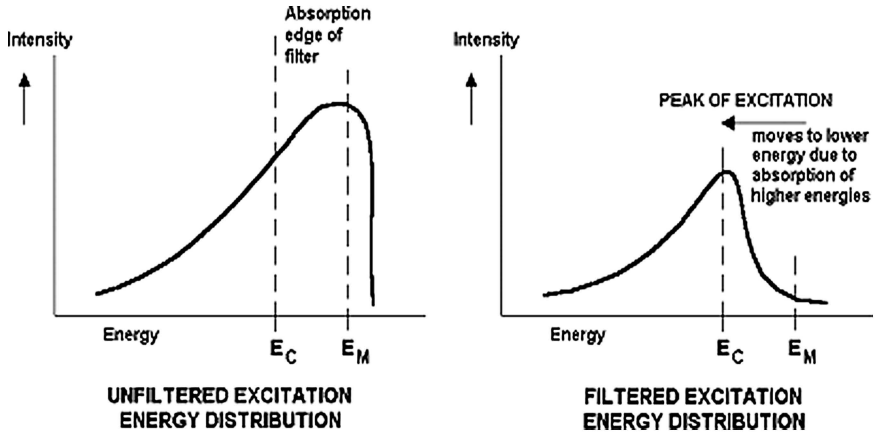

Fig. 6—Typical example of selective excitation using primary beam filtration.

Detector filters, also called secondary beam filters, can be placed between the sample and the detector. They can improve the instruments' effective resolution, sensitivity, and limit of detection, in particular with gas-filled proportional counters. The transmission (or absorption) of the secondary filter depends on the absorption edge of its constituent material. Fig. 7 illustrates how it works, with a niobium filter being used to absorb the characteristic K lines of chlorine, while letting the sulfur K lines pass.

Detector systems used in EDXRF are of two main types:

- Sealed, gas-filled proportional counters
- Semiconductor detectors.

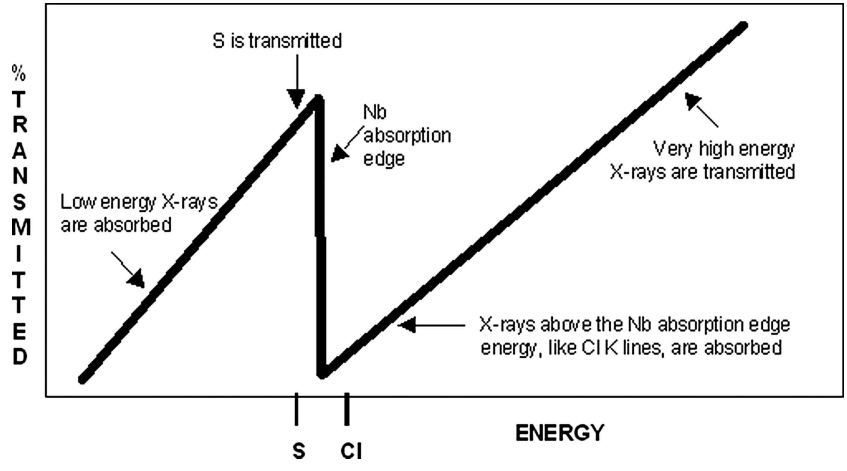

Fig. 7—Transmission of sulfur (S) and chlorine (Cl) X-rays through a niobium (Nb) secondary beam filter.

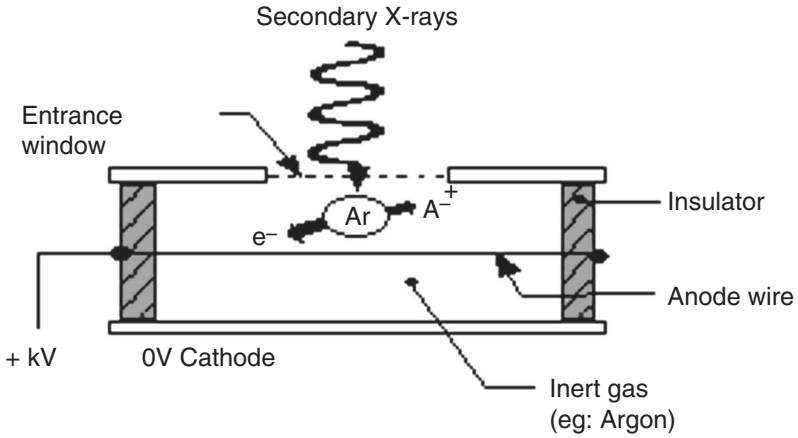

Fig. 8—Schematic of an argon (Ar) filled proportional counter.

In gas-filled detectors, X-rays coming from the sample (secondary X-rays) enter the detector via a window, and strike atoms of a "noble" gas (e.g., argon, neon, and xenon) contained in a volume that is subjected to a strong symmetrical electric field. Electrons generated in the ionization process are accelerated toward a central wire (anode), creating more ionizations in their path. The negative electrical pulses on the anode are picked up and amplified by electronics. This output is then subjected to pulse-height analysis, where pulse height is proportional to X-ray photon energy. Spectral resolution of gas-filled detectors is normally around 800 to 1,000 eV, and detector filters are often used to eliminate overlapping elements in the spectrum. Another gas, called quench gas, is also present in the detector to enable the ionized noble gas atoms to return to a stable state, preventing them from striking the cathode and generating more electrons.

In semiconductor detectors, radiation is measured by means of the number of charge carriers set free in the detector, which is arranged between two electrodes. Ionizing radiation produces free electrons and holes. The number of electron-hole pairs is proportional to the incident photon energy. As a result, a number of electrons are transferred from the valence band to the conduction band, and an equal number of holes are created in the valence band. Under the influence of an electric field, electrons and holes travel to the electrodes, where they result in a pulse that can be measured in an outer circuit (feedback capacitor, charge sensitive preamplifier, main amplifier). The holes travel into the opposite direction and can also be measured. As the amount of energy required to create an electron-hole pair is known, and is independent of the energy of the incident radiation, measuring the number of electron-hole pairs allows the energy of the incident radiation to be found [8].

The energy required for production of electron-hole pairs is very low compared to the energy required for production of paired ions in a gas-filled detector. Consequently, in semiconductor detectors the statistical variation of the pulse height is smaller and the energy resolution is higher. As the electrons travel fast, the time resolution is also very good, and is dependent on rise time [8]. Compared with gaseous ionization detectors, the density of a semiconductor

detector is very high, and charged particles of high energy can give off their energy in a semiconductor of relatively small dimensions.

EDXRF spectrometers can include various types of semiconductor detectors, such as PIN diodes and silicon drift detectors. PIN diode detectors are widely used. They are small, require only Peltier (thermoelectric) cooling, and offer adequate resolution and sensitivity for many EDXRF applications. PIN diodes have three detector regions: an intrinsic layer (I) is sandwiched between a positive (P) and a negative layer (N). A bias is applied across the detector to create a depletion layer. This is where the ionizations due to incoming X-rays occur. There again, the pulse of charge is proportional to the incident energy.

Silicon-drift detectors (SDDs) provide high resolution (typically < 150 eV at manganese Kα), high count rate, and excellent signal to noise ratio. They normally operate at room temperature and require only moderate cooling (no liquid nitrogen cooling). The detector consists of a volume of fully depleted silicon in which a strong component parallel to the surface of the electric field "drifts" signal electrons towards a small sized collecting anode (see Fig. 9). The drift field is generated by a number of increasingly reverse biased field rings. The radiation entrance side is a nonstructured p+-junction, or back contact, giving a homogeneous sensitivity over the whole detector area. The fully depleted volume of the detector is sensitive to the absorption of X-rays. SDDs also have low capacitance, which means that more events (signal electrons) can be collected and processed, hence the high count rate.

For all pulse processing systems, there is some probability that two pulses might accidentally arrive at exactly the same time. A pileup rejecter is incorporated into the system. The final clean-up pulse is converted to a digital signal and processed by the multichannel analyzer (MCA) [5].

This is the point where the computing power is used. In the MCA, dead time caused by high counting rates must be corrected. Sophisticated, proprietary algorithms then smooth peaks in the energy spectra. Algorithms correct for high background noise caused by Compton scattering and other effects [9]. Algorithms analyze various peaks in the spectra and correct for matrix effects

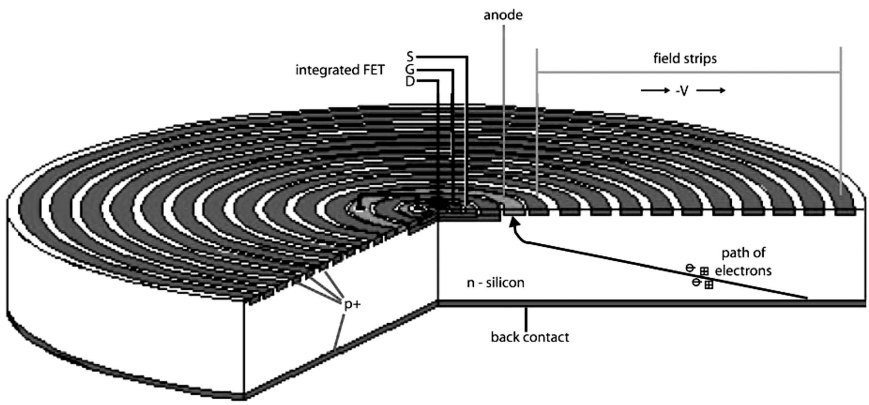

Fig. 9—Schematic of the cross section of a silicon drift detector.

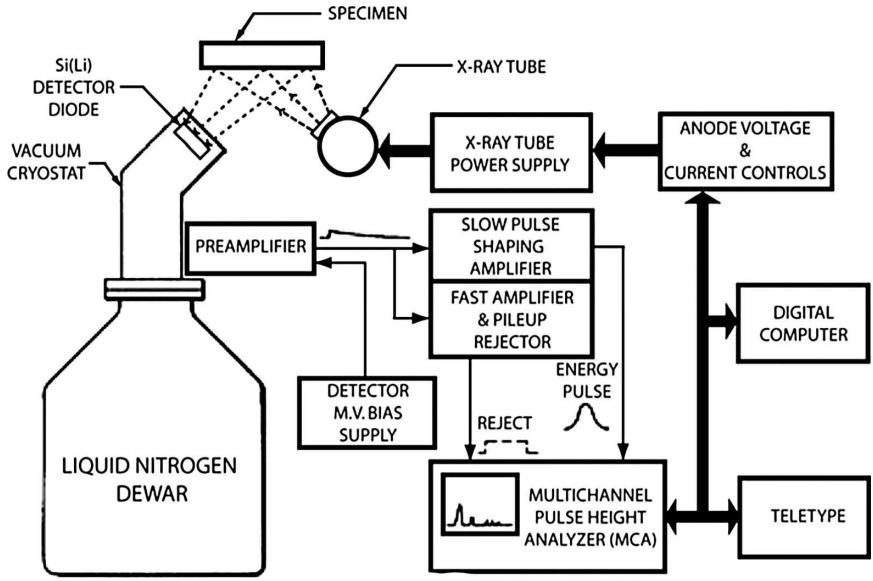

Fig. 10—Typical EDXRF system.

and the effects from other interfering elements. All of these "black box" calculations produce a result that is proportional to the concentration of the element of interest in the sample. Calibrations of the instrument with standards of known concentrations of the elements of interest permit the quantitation of the elements of interest.

ADVANCED EDXRF SYSTEMS

In the past decade, environmental and health and safety concerns have seen the emergence of new analytical requirements for the determination of very low levels of elements in various types of samples (e.g., sulfur in petroleum products, toxic metals in soil and in toys). EDXRF instrumentation has continued to evolve and improve to rise to these new challenges, both on the excitation side and on the detection side.

Polarized EDXRF uses polarization to enhance signal-to-noise ratio by removing the continuous background from the X-ray tube. A major cause of background is the scatter of source radiation by the sample into the detector. This scatter adds to the background due to the detector itself. X-ray polarization requires precise alignment of X-ray optic elements, where tube, scatterer, sample, and detector must be arranged in an XYZ geometry (also called Cartesian geometry). The scattering (or diffracting) crystal is placed between the X-ray source and the sample to reflect and polarize the excitation radiation. This reduces the intensity of the primary X-ray beam dramatically, and a high-power X-ray tube is required to regain sensitivity. The Cartesian geometry, illustrated in Fig. 11, reduces the scattered radiation, thus reducing the background.

This type of instrumentation now achieves sub-ppm limit of detection for low atomic number elements such as sulfur in a petroleum matrix.

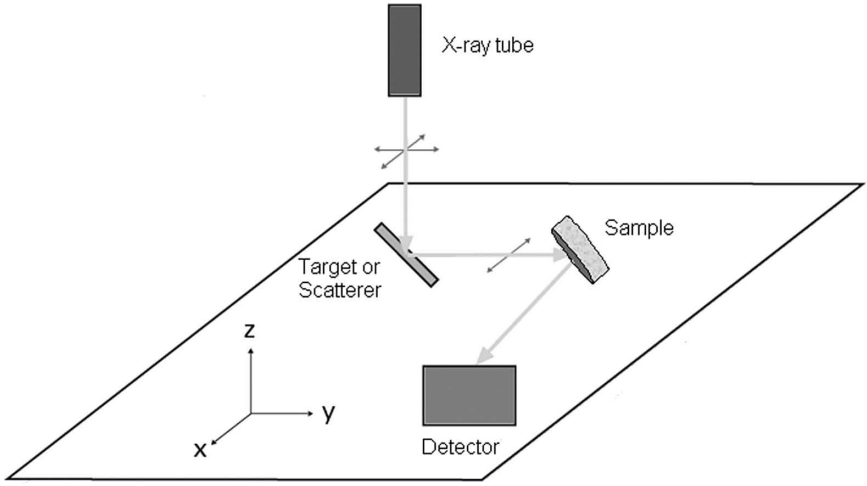

Fig. 11—Components of an EDXRF spectrometer using polarization (Cartesian geometry).

Secondary targets can also be used to increase signal-to-noise ratio by reducing background, and are an alternative to primary beam filters. The primary X-rays, consisting of characteristics X-ray lines from the anode and Bremsstrahlung continuum radiation, excite the secondary target material (e.g., molybdenum), which in turns emit X-rays that are characteristic of the target material. The characteristic radiation of the target material is nearly monochromatic and produces a low background. This radiation is nonpolarized, as the primary X-rays from the tube scatter on the target and into the detector. By placing secondary targets in a Cartesian geometry, the scatter from the tube is also reduced.

Secondary targets yield lower background but require much more primary excitation, therefore they demand the use of a higher power X-ray tube as compared to what is needed for direct excitation. A typical configuration of the use of a secondary target is illustrated in Fig. 12. Also, like primary beam filters, it is sometimes necessary to use more than one secondary target to get best performance across the energy spectrum.

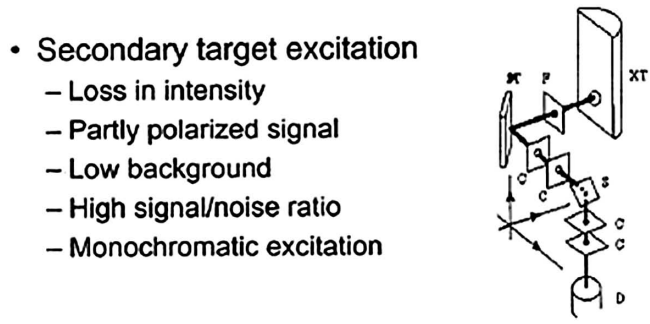

Fig. 12—Schematic of a secondary target XRF system.

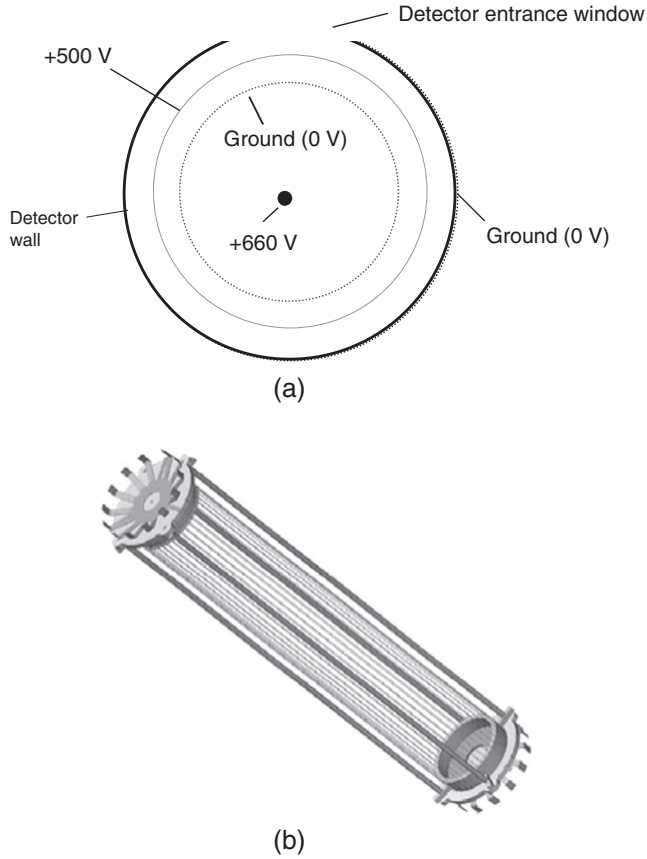

Fig. 13—Schematics of internal structure of the low-background proportional counter.

Secondary targets are generally used for the determination of very low levels (sub to low mg/kg) of medium to high atomic number elements (typically from iron).

For ultra-low sulfur determination, another method uses a specially designed proportional counter that dramatically reduces the background compared to that of a conventional gas-filled proportional counter. A schematic of such a system is shown in Fig. 13. Simple X-ray calculations show that most of the background in the low energy spectrum is most probably an artifact produced in the detector. Some of the ionizations generated close to the detector wall are not collected onto the central anode. This incomplete charge collection causes a low energy tail in the spectrum, raising the background level under the sulfur peak. Because this event arises in a specific volume of the detector, it is possible to detect and reject it. The low background proportional counter (US Patent 6967329; European Patent 1 326094) is based on a normal proportional counter with its central anode, but it also comprises extra sets of electrodes that effectively split the detector's outer and inner volumes. The electronic

counting circuits reject all signals from the outer volume, and the complete charges, detected in the inner volume, are processed to give a true background signal. This "false background" rejection gives lower spectral background and a lower limit of detection for sulfur (< 1 mg/kg), while the whole system retains all the advantages of a low-power benchtop EDXRF spectrometer.

Because of its versatility, speed, and ease of use, EDXRF spectrometry is an ideal analytical technique for determining elemental composition of a wide variety of materials. Some additional information on these topics is contained in Refs [11–17].

APPLICATIONS OF EDXRF AND ASTM TEST METHODS

Benchtop EDXRF spectrometers have been used for many years in the petroleum and lubricants industries, usually as quality or process control tools, but also in the product certification process.

The international EDXRF community has worked alongside ASTM Committee D02 to develop standard test methods meeting as much as possible the following criteria:

- Safety (apparatus, reagents)
- Ease of use (sample preparation, apparatus, results interpretation)
- Cost-effectiveness
- Reliability of results (accuracy and precision)
- Fitness for purpose.

The current ASTM methods under D02 jurisdiction are described in this section:

- D4294: Sulfur in petroleum and petroleum products by EDXRF spectrometry
- D6445: Sulfur in gasoline by EDXRF spectrometry
- D6481: Phosphorus, sulfur, calcium, and zinc in lubricating oils by EDXRF spectrometry
- D7212: Low sulfur in automotive fuels by EDXRF spectrometry using a low-background proportional counter
- D7220: Sulfur in automotive fuels by polarization XRF spectrometry.

All EDXRF test methods above follow the same simple principle, and rely on calibrations to establish the relationship between the X-ray signal for the elements of interest and their concentrations. The analysis procedure consists of pouring the liquid petroleum sample into a sample cup fitted with X-ray film, and placing the cup in the X-ray spectrometer for analysis. There an X-ray beam irradiates the sample. The intensity of the elements of interest's characteristic X-ray lines emitted by the sample are measured, and the corresponding concentrations are calculated from the calibration equation. Other regions of the spectrum are often measured to correct for background and matrix variations.

The D4294 test method is applicable for total sulfur determination in petroleum products that are single phase, and either liquid at ambient temperature, liquefiable with moderate heat, or soluble in hydrocarbon solvents. Such materials include diesel fuel, jet fuel, kerosine, other distillates, naphtha, residual oil, lubricating base oil, hydraulic oil, crude oil, unleaded gasoline, gasohol, biodiesel, and similar petroleum products. For samples with high oxygen content (> 3 % m/m), sample dilution or matrix matching must be performed to obtain accurate results. The scope of the method is 16 mg/kg to 4.6 % m/m. Samples

containing a higher sulfur concentration can be diluted to bring the sulfur concentration of the diluted material within the scope of this test method. A fundamental assumption of this test method is that the standards and the sample matrices are well matched, or that the matrix differences are accounted for. Matrix mismatch can be caused by carbon/hydrogen ratio differences between samples and standards, or by the presence of other heteroatoms.

Two to three different calibration ranges are usually used to span the method's concentration range. This method's WDXRF counterpart is D2622.

The D6445 test method applies to the determination of total sulfur in unleaded gasoline and gasoline-oxygenate blends in the sulfur range of 48 to 1000 mg/kg sulfur. Only one calibration range is required to span the range covered by this method. The matrix effects in this method are similar to those mentioned in the D4294 test method.

The D6481 test method covers the determination of additive elements—phosphorus, sulfur, calcium, and zinc—in unused lubricating oils. In that sense, this EDXRF method is a counterpart of its WDXRF method D4927 (this also includes barium). This method uses interelement correction factors calculated from empirical calibration data. The method is not suitable for measuring magnesium or copper at the concentrations generally present in the lubricating oils, and it excludes lubricating oils that contain chlorine or barium as additive elements.

The D7212 test method determines total sulfur content in automotive fuels in the concentration range 7 to 50 mg/kg. The apparatus for this method combines a titanium-target tube and primary filtration to generate nearly monochromatic primary radiation of 4.51 keV, and a low-background proportional counter as an X-ray detector to reduce background at the sulfur energy. This improves peak-to-background ratio for sulfur. One group of calibration standards is required to span the concentration range from 0 to 150 mg/kg sulfur. The most likely interference is chlorine found in biodiesel derived from recycled waste vegetable oil, and it is corrected for when present. The presence of water or oxygenates may also alter the sensitivity for sulfur.

The D7220 test method measures total sulfur content in automotive fuels in the range 6 to 50 mg/kg. A fundamental assumption of this test method is that the standard and sample matrices are well matched. Matrix mismatch can be caused by carbon/hydrogen ratio differences between the samples and the standards, or by the presence of other heteroatoms. In this method the sample is placed in a polarized X-ray beam and the peak area of sulfur Kα line at 2.307 keV is measured. The background spectrum, measured with a sulfur-free white oil or other matrix matching blank sample, is adapted to the measured spectrum using adjustment regions following the instrument manufacturer's instructions and then subtracted from the measured spectrum.

The precision of these EDXRF test methods is compared in Table 1.

ASTM PROFICIENCY TESTING

For the past 10 years, ASTM Committee D02 on Petroleum Products and Lubricants has conducted a large program on proficiency testing of various petroleum products and lubricants among nearly 2,500 worldwide oil industry laboratories [10,11]. EDXRF methods are used in some of these programs,

TABLE 1—Precision of EDXRF Test Methods

Test Method	Element	Range	Repeatability	Reproducibility
D4294	S	16 mg/kg to 4.6 % m/m	$0.4347X^{0.6446}$ % m/m	$1.9182X^{0.6446}$ % m/m
D6445	S	48 to 1000 mg/kg	$12.30(X+10)^{0.1}$ mg/kg	$36.26(X+10)^{0.1}$ mg/kg
D6481	P	0.02 to 0.3 % m/m	0.0060 mass %	0.0199 % m/m
	S	0.05 to 1.0 % m/m	$0.01648(X+0.0141)^{0.8}$ % m/m	$0.1024(X+0.0141)^{0.8}$ % m/m
	Ca	0.02 to 1.0 % m/m	$0.008795(X+0.0120)^{0.5}$ % m/m	$0.1492(X+0.0120)^{0.5}$ % m/m
	Zn	0.01 to 0.3 % m/m	$0.003274X^{0.25}$ % m/m	$0.02165X^{0.25}$ % m/m
D7212	S	7 to 50 mg/kg	$1.6196X^{0.1}$ mg/kg	$3.7668X^{0.1}$ mg/kg
D7220	S	6 to 50 mg/kg	$1.0348X^{0.25}$ mg/kg	$2.0591X^{0.25}$ mg/kg

Note: X is the mean content for the element of interest.

particularly for the determination of sulfur. For the evaluation of alternate test methods, it is an obvious benefit of these programs that several laboratories use alternative methods for the analysis of the same analyte. Some of the data obtained through this program are summarized in Tables 2 through 4. These data are excerpted from the ASTM statistical reports produced after each cross-check is completed. In all the tables, the data are expressed as robust mean ± robust standard deviation (number of valid data points).

Table 2 compares the results for calcium, phosphorus, and zinc in three sets of lubricating oils analyzed by six different techniques: AAS (D4628), WDXRF with mathematical corrections and internal standards (D4927 A and B, respectively), two ICP-AES methods (D4951 and D5185), and the EDXRF method D6481. Results by all methods are comparable to each other within the reproducibility of these quite diverse technical methods.

Table 3 compares the results for sulfur determination in a number of petroleum products such as motor gasoline, diesel fuel #6, diesel fuel # 2, jet turbine fuel, lubricating base oil, crude oil, and reformulated gasoline by alternative techniques. The three methods compared here are D2622 WDXRF, D5453 UV-fluorescence, and D4294 EDXRF methods. All three methods are widely used in the industry. Some data are also provided for results using D7039 (MWDXRF) method.

Generally, results by all methods are equivalent to each other within the reproducibility of the individual methods. A large number of laboratories use EDXRF method D4294 compared with other methods, because of its ease of use, cost-effectiveness, and fast turnaround. However, in several cases its precision

TABLE 2—Results Comparison for Lubricating Oil Analysis by Various Spectroscopic Methods

ASTM Sample	Test Method	Calcium, % m/m	Phosphorus, % m/m	Zinc, % m/m
LU 0605	D4628 AAS	0.2042 ± 0.0111 (19)	...	0.0874 ± 0.0071 (19)
	D4927 A WDXRF	0.2136 ± 0.0113 (11)	0.0773 ± 0.0038 (8)	0.0878 ± 0.0014 (11)
	D4927 B WDXRF	0.2153 ± 0.0084 (19)	0.0796 ± 0.003 (18)	0.0888 ± 0.0028 (19)
	D4951 ICP-AES	0.2088 ± 0.0082 (78)	0.0776 ± 0.0038 (77)	0.0887 ± 0.0029 (82)
	D5185 ICP-AES	0.2060 ± 0.0135 (73)	0.0761 ± 0.0051 (68)	0.0867 ± 0.0064 (72)
	D6481 EDXRF	0.2167 ± 0.0093 (8)	0.0773 ± 0.0072 (6)	0.0917 ± 0.0082 (9)
LU 0705	D4628 AAS	0.2010 ± 0.0045 (10)	...	0.0809 ± 0.0050 (12)
	D4927 A WDXRF	0.2068 ± 0.0124 (10)	0.0758 ± 0.0062 (9)	0.0847 ± 0.0034 (10)
	D4927 B WDXRF	0.2091 ± 0.0110 (16)	0.0769 ± 0.0033 (14)	0.0840 ± 0.0031 (16)
	D4951 ICP-AES	0.2004 ± 0.0069 (74)	0.0749 ± 0.0028 (72)	0.0835 ± 0.0041 (74)
	D5185 ICP-AES	0.1994 ± 0.0089 (66)	0.0740 ± 0.0029 (65)	0.0819 ± 0.0040 (67)
	D6481 EDXRF	0.2000 ± 0.0104 (12)	0.0750 ± 0.0039 (9)	0.0750 ± 0.0039 (9)
LU 0801	D4628 AAS	0.2128 ± 0.0130 (9)	...	0.0912 ± 0.0087 (9)
	D4927 A WDXRF	0.2222 ± 0.0313 (6)	...	...
	D4927 B WDXRF	0.2197 ± 0.0077 (17)	0.0806 ± 0.0045 (16)	0.0890 ± 0.0036 (16)
	D4951 ICP-AES	0.2061 ± 0.0110 (67)	0.0760 ± 0.0039 (64)	0.0858 ± 0.0051 (66)
	D5185 ICP-AES	0.2048 ± 0.0129 (63)	0.0744 ± 0.0054 (67)	0.08398 ± 0.0052 (65)
	D6481 EDXRF	0.1981 ± 0.0092 (9)	0.0761 ± 0.0084 (6)	0.0861 ± 0.0037 (10)

TABLE 3—Results Comparison for Sulfur Determination by XRF Methods

ASTM Sample	Concentration Unit	D2622 (WDXRF)	D4294 (EDXRF)	D5453 (UVF)	D7039 (MWDXRF)
Motor gasoline 0712	mg/kg	55.5 ± 5.2 (37)	66.7 ± 23.3 (22)	52.4 ± 4.2 (53)	55.50 ± 2.59 (7)
Fuel #6 06801	% m/m	1.099 ± 0.051 (20)	1.108 ± 0.027 (143)	. . .	. . .
Diesel fuel #2 0710	mg/kg	606.5 ± 16.3 (80)	630 ± 33 (170)	597.0 ± 44.7(69)	590.6 ± 27.1 (19)
Jet fuel 0703	mg/kg	133.8 ± 7.3 (55)	144 ± 21 (120)	130.3 ± 8.9 (64)	. . .
Base oil 0712	% m/m	0.5333 ± 0.0185 (13)	0.5418 ± 0.0205 (17)	. . .	. . .
Crude oil 0711	% m/m	0.1978 ± 0.0072(18)	0.202 ± 0.010 (73)	. . .	. . .
Reformulated gasoline 0711	mg/kg	329.8 ± 19.8 (36)	335 ± 27 (20)	308.5 ±22.6 (58)	311.2 ± 13.6 (21)

seems less desirable than those of other established methods, particularly when the sulfur concentration is in the mg/kg range rather than in the % m/m level.

Table 4 contains the 2007 ASTM crosscheck results for sulfur determination in ultra low sulfur diesel (ULSD) samples. The samples ranged between 5 to 10 mg/kg sulfur. The test methods used here are those allowed by the U.S. Environmental Protection Agency (EPA) for certifying diesels leaving the refinery, terminals, or blending plants. The originally mandated test methods–D2622 WDXRF, D3120 microcoulometry, D5453 UV-fluorescence, and D6920 electrochemistry–were replaced with any performance-based method that can be shown to produce acceptable results under the accuracy and precision criteria set by the U.S. EPA. The ULSD crosscheck program has taken place every year since 2004, with a sample being measured each month. There is therefore a very large amount of data available to compare the different methods used for this important analysis. Although the EDXRF methods are not yet widely used for these very low levels of sulfur determination (only a small number of laboratories reported EDXRF results), examples are given that show that the techniques used in D7212 and D7220 are capable of measuring sulfur at such levels.

The column "EDXRF Methods" in Table 4 shows individual laboratories' average result, or robust mean ± robust standard deviation (number of valid data points) when available. Sometimes the individual values are quite different from each other. As more laboratories become familiar with these newer EDXRF methods and participate in the future crosscheck programs, it is very likely that this deviation will not be noticeable when enough data points are available to carry out a full statistical analysis.

TABLE 4—Results for Sulfur Determination in ULSD Samples by Various Spectroscopic Methods (All results are in mg/kg)

ASTM ULSD Sample #	D2622 (WDXRF)	D5453 (UV-FL)	D7039 (MWDXRF)	EDXRF Methods
701	9.08 ± 0.92 (86)	8.95 ± 0.57 (210)	8.69 ± 0.57 (65)	D7212: 6.75 D7220: 8.50; 10.95
702	5.73 ± 0.87 (88)	5.49 ± 0.48 (206)	5.54 ± 0.49 (63)	D7212: 6.50 D7220: 5.30; 5.45
703	5.44 ± 0.95 (95)	5.04 ± 0.51 (229)	5.18 ± 0.41 (70)	D7212: 5.80; 4.70 D7220: 4.40
704	8.81 ± 0.82 (96)	8.88 ± 0.54 (227)	8.71 ± 0.54 (75)	D7212: 8.20; 7.80 D7220: 7.30; 8.45
705	5.07 ± 0.84 (89)	4.63 ± 0.44 (225)	4.88 ± 0.54 (60)	D7220: 5.10; 4.90; 2.35
706	5.37 ± 0.86 (94)	4.94 ± 0.48 (242)	5.02 ± 0.42 (74)	D7212: 4.70 ± 0.93 (7) D7220: 4.70; 3.35
707	8.71 ± 0.88 (86)	8.89 ± 0.68 (234)	8.72 ± 0.67 (68)	D7212: 8.20; 7.50; 5.10 D7220: 8.55; 8.60
708	4.90 ± 0.88 (90)	4.62 ± 0.46 (242)	4.85 ± 0.45 (86)	D7212: 5.10; 3.90; 4.10
709	5.46 ± 0.87 (82)	5.94 ± 0.51 (240)	5.38 ± 0.42 (80)	D7212: 4.45; 5.10 D7220: 5.60; 4.80
710	8.63 ± 0.80 (78)	8.78 ±0.61 (231)	8.80 ± 0.62 (76)	D7212: 9.90; 9.20; 9.50 D7220: 9.40; 8.40
711	4.94 ± 1.02 (76)	4.55 ± 0.44 (220)	4.88 ± 0.46 (80)	D7212: 4.20; 5.15; 6.25; 5.80 D7220: 5.30
712	5.66 ± 1.04 (74)	6.03 ± 0.53 (212)	5.45 ± 0.44 (76)	D7212: 5.35; 5.55; 2.00 D7220: 3.30; 6.10

Overall, the results obtained by EDXRF methods are in good agreement with those obtained using other techniques. Thus, EDXRF is a very useful, simple, robust, cost-effective, and fast-turnaround technique compared with other techniques and instrumentation.

CONCLUSION

EDXRF spectrometry is a reliable, fast, versatile, and easy-to-use analytical technique. EDXRF spectrometers include two main components, the X-ray source and the detector. They can be selected depending on the performance and the range of applications to be covered by the spectrometer. Other components can also be used to optimize spectral resolution and sensitivity (peak to background ratio).

The EDXRF technique has been used in laboratories around the world for many years, and its good performance agreement with other, more costly, labor-intensive techniques has enabled the development and use of many ASTM standard test methods, particularly in the petroleum industry.

References

[1] Coster, D. and Nishina, J., "On the Quantitative Chemical Analysis by Means of X-ray Spectrum," *Chem. News*, Vol. 1, No. 30, 1925, pp. 149–152.

[2] Glocker, R. and Schreiber, H., "Quantitative Rontgenspektralanalyse mit Kalterregung des Spectrums," *Ann. Physic*, Vol. 85, 1928, p. 1089.

[3] Amptek Inc., Amptek Technical Brochure on the Mini-X X-ray Tube Design, Bedford, MA, 2009.

[4] Jenkins, R., *X-ray Fluorescence Spectrometry*, John Wiley & Sons, Inc., New York, 1988.

[5] Anzelmo, J. A. and Lindsay, J. R., "X-ray Fluorescence Spectrometric Analysis of Geological Materials Part 1: Principles and Instrumentation," *J. Chem. Educ.*, August, Vol. 64, No. 8, 1987, pp. A18–A185.

[6] Skoog, D. A., Holler, F. J. and Nieman, T. A., *Principles of Instrumental Analysis*, 5th ed., Thomson Learning, Inc., Belmont, CA, 1998.

[7] Jenkins, R., Gould, R. W. and Gedcke, D., *Quantitative X-ray Spectrometry*, 2nd ed., Marcel Dekker, Inc., New York, 1995.

[8] Knoll, G. F., *Radiation Detection and Measurement*, 3rd ed., Wiley, Ann Arbor, MI, 1999.

[9] Metz, V., Hoffman, P., Weinbruch, S. and Ortner, H. M., "A Comparison of X-ray Fluorescence Spectrometric (XRF) Techniques for the Determination of Metal Traces, Especially in Plastics," *Microchim. Acta*, Vol. 117, 1994, pp. 95–108.

[10] Nadkarni, R. A. and Bover, W. J., "Bias Management and Continuous Improvements through Committee D02's Proficiency Testing," *ASTM Standardization News,* Vol. 32, No. 6, 2004, pp. 36–39.

[11] Nadkarni, R. A., "Determination of Trace Amounts of Sulfur in Petroleum Products and Lubricants: A Critical Review of Test Performance," *Amer. Lab.,* Vol. 32, No. 22, 2000, pp. 16–25.

[12] Beckhoff, B., Kanngießer, B., Langhoff, N., Wedell, R. and Wolff, H., *Handbook of Practical X-ray Fluorescence Analysis*, Springer, Berlin, 2006.

[13] Bertin, E. P., *Principles and Practice of X-ray Spectrometric Analysis*, Kluwer Academic/Plenum Publishers, New York, 1970.

[14] Buhrke, V. E., Jenkins, R. and Smith, D. K., *A Practical Guide for the Preparation of Specimens for XRF and XRD Analysis*, Wiley, New York, 1998.

[15] Jenkins, R., *X-ray Fluorescence Spectrometry*, Wiley, Chickester, UK, 2000.

[16] Jenkins, R. and De Vries, J. L., *Practical X-ray Spectrometry*, Macmillan, London, UK, 1970.

[17] Jenkins, R., R. W., Gould, R. W. and Gedcke, D., *Quantitative X-ray Spectrometry*, Marcel Dekker, New York, 1995.

[18] Van Grieken, R. E. and Markowicz, A. A., *Handbook of X-ray Spectrometry*, 2nd ed., Vol. 29, Marcel Dekker Inc., New York, 2002.

14

Low-Power Monochromatic Wavelength-Dispersive X-ray Fluorescence–Principle and Applications in Petroleum Products

Z. W. Chen and Fuzhong Wei[1]

INTRODUCTION

X-ray fluorescence (XRF) using polychromatic X-rays is a powerful elemental analysis tool for petroleum products. XRF with an energy dispersive spectrometer (EDS) provides rapid multielement analysis in oil, lubricants, and raw materials. Energy dispersive XRF (EDXRF) systems can be compact and robust. Several ASTM methods are based on EDXRF techniques, including D4294, D6445, D6481, and D7212. However, the limitations of an EDXRF system include 1) susceptibility to elemental interference due to relatively poor energy resolution, and 2) low limit of detection (LOD) in the range of 5 to 10 ppm for sulfur, chlorine, and phosphorus in low atomic number matrix, which is not adequate for trace-level analysis. Another option, wavelength-dispersive XRF (WDXRF), provides superior energy resolution and lower LOD. A high-power WDXRF system has an LOD of about 0.5 ppm for sulfur, chlorine, and other elements. Several ASTM methods are well established for petroleum applications, including D2622, D6334, and D6376. The disadvantage of a WDXRF system is that it typically requires a high-power X-ray tube in a sophisticated system involving precision alignment and scanning. It is also bulky and not suitable for field testing.

Recently, a new XRF method, monochromatic WDXRF (MWDXRF), was developed for low-level sulfur and chlorine analysis based on doubly curved crystal (DCC) optics and a low-power X-ray tube [1]. Unprecedented LODs for sulfur and chlorine were achieved using a compact MWDXRF benchtop analyzer. In this chapter, the principle and applications of MWDXRF are reviewed.

PRINCIPLE OF FOCUSED BEAM MWDXRF SYSTEM

The basic configuration of a compact XRF/WDS unit with a single channel based on DCCs is shown in Fig. 1. It consists of an X-ray tube, a point-focusing excitation DCC, a sample mount, a focusing collection DCC, and an X-ray detector. The X-ray tube has power of 10 to 75 W, and its spot size is in the range of several hundreds of micrometres. In this system, the first-point focusing DCC captures a narrow bandwidth of X-rays from the source, typically a characteristic line of the X-ray tube, and focuses an intense monochromatic beam in a small spot on the sample. The monochromatic primary beam excites elements of interest in the sample, and secondary characteristic fluorescence X-rays are emitted from the

[1] *XOS, East Greenbush, New York*

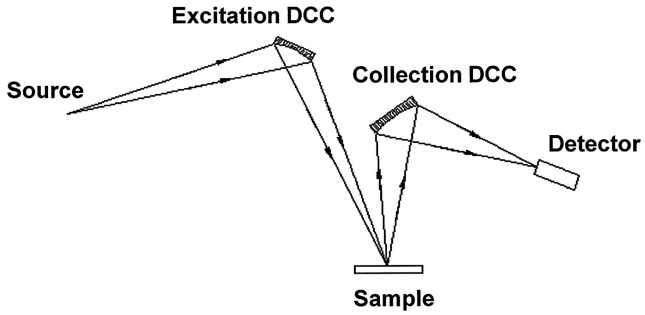

Fig. 1—The basic configuration of the monochromatic wavelength dispersive XRF.

excitation volume. The second DCC, the collection crystal, collects characteristic X-rays for an element and focuses them on the detector. The collection DCC has an energy resolution of 2 to 20 eV, and it detects only one element in the sample. For multiple-element detection, multiple collection DCCs can be used. The X-ray detector can be a proportional counter or a solid-state detector.

This XRF/WDS analyzer provides several advantages. The first is that the signal/background (S/B) is improved because of monochromatic excitation by the characteristic line from the source. The primary beam is highly monochromatic, and the Bremsstrahlung photons with energies less than fluorescence peaks can reach the detector only through scattering, therefore improving the S/B ratio drastically compared to polychromatic excitation. Certain high-energy photons from the Bremsstrahlung are due to high-order reflection of the DCC, but their intensity is typically three orders weaker than the characteristic line intensity. The second advantage is that the focusing ability of the collection crystal also allows the use of a small-entrance aperture of the X-ray counter for further reduction of background. The third advantage is that there are no moving parts in the system. This is important for robustness and reliability. Finally, monochromatic excitation also provides another important advantage over polychromatic excitation: simplified quantification and matrix effect correction. With a single wavelength for the primary beam, the fluorescence intensity of an element in a sample can be related to its concentration by a very simple equation using fundamental parameters. This eliminates the need for a sophisticated software package and makes the measurement results accurate and reliable.

DCC OPTICS FOR MWDXRF

DCC optics are key for the low-power MWDXRF technique. Doubly curved crystal optics have been proposed to focus and monochromatize X-rays since 1950 [2,3,4,5]. Widespread use and practical applications of DCC optics for monochromatic beam applications were impeded, however, by the difficulty of fabricating DCC optics. An important development was reported in 1997 [6] and 1998 [7]. In these reports, an intense micro copper $K_{\alpha 1}$ beam was obtained using a Johann-type doubly curved mica crystal for monochromatic microfocus XRF applications. The high-intensity beam of the mica DCC was based on a novel crystal-bending technology. This technology has been further developed [8,9]. It can provide elastic bending of crystals into various complex shapes with precise profile control.

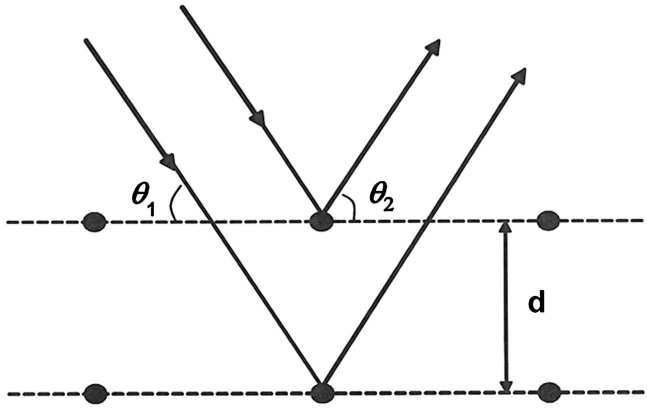

Fig. 2—Bragg diffraction.

Crystal Optics for X-rays

Crystal optics reflect X-rays based on Bragg diffraction. As shown in Fig. 2, a set of atomic planes with a spacing of d in a single crystal reflect X-rays when the following two conditions are satisfied:

$$\theta_1 = \theta_2 = \theta_b \tag{1}$$

$$2d \sin\theta = n\lambda \tag{2}$$

where θ_1 and θ_2 are the incident angle and reflection angle with respect to the crystal planes, λ is the wavelength of the refracted X-rays, and n is an integer. The first condition arises from the fact that the scattering X-rays from the atoms in a diffracting plane have to be in phase. The second condition is the well-known Bragg's law, which was derived from the fact that the scattering X-rays from different atomic planes also have to be in phase. Bragg conditions impose a strong constraint on crystal optics. Only X-rays with incident angles very close to the Bragg angle can be reflected significantly. For a perfect crystal, the acceptance angular width for a given wavelength can be derived by the X-ray diffraction dynamical theory. This angular width, called rocking curve width, is typically narrow. For instance, the intrinsic rocking curve width for germanium(111) at 5.4 keV photons is about 0.01°.

Because of the constant incident angle imposed by the Bragg condition for a given wavelength, common crystal optics for divergent X-rays are based on Rowland circle principles, which rely on the property of a circle that an arc segment subtends a constant angle for any given point on the circle. The two major focusing geometries are Johansson and Johann geometry for two–dimensional focusing of X-rays as shown in Fig. 3. In Johann geometry, crystal planes are bent to a radius of 2R, where R is radius of the Rowland circle. For the Johann geometry, there is a geometrical aberration due to the crystal surface profile deviated from the Rowland circle. This angular deviation at a given point on the crystal surface can be calculated from [4]

$$\Delta\theta \approx \left(\frac{x}{2R}\right)^2 \cot\theta_B \tag{3}$$

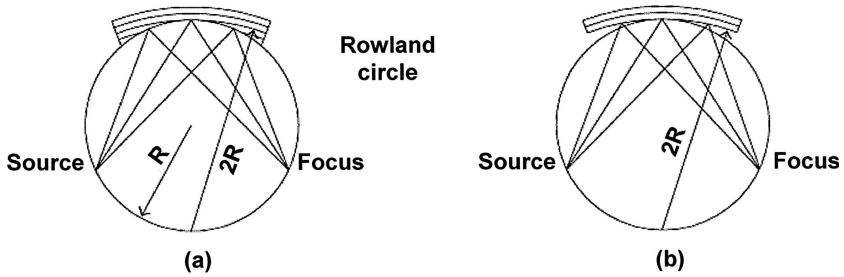

Fig. 3—(a) Johansson geometry; (b) Johann geometry.

where x is the X coordinate of crystal surface and θ_B is the Bragg angle. The X axis is defined as the direction of the source relative to the focus (see Fig. 4). In Johansson geometry, crystal planes are bent to a radius of 2R with the surface ground to radius of R. There is no geometrical deviation for the Johansson geometry, and so a larger collection solid angle can be achieved. But the fabrication is relatively difficult because of the grinding process.

Point-Focusing DCC Optics

Three-dimensional, point-to-point focusing geometries are obtained by rotating the Johansson or Johann geometry around the source-focus line.

The geometry of a Johann-type DCC is shown in Fig. 3. In this geometry, the diffracting planes of the crystal are parallel to the crystal surface. The crystal surface has a toroidal shape and has the Johann geometry in the focal circle plane. It is axially symmetric along the line going through Source and Focus. The crystal surface has a radius of curvature of 2R in the plane of the focal circle and a radius of curvature of $2Rsin^2\theta_B$ in the mid-plane perpendicular to the Source–Focus segment, where R is the radius of the focal circle and θ_B is the Bragg angle. X-rays diverging from a point Source, and striking the crystal surface with incident angles within the acceptance rocking curve width of the crystal, will be reflected efficiently to the Focus. A simulated image of the beam profile is shown in Fig. 4.

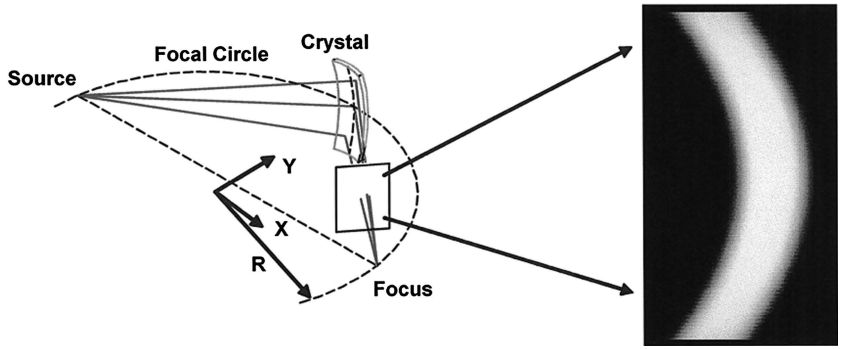

Fig. 4—Geometry of Johann point-focusing crystal.

The Johansson-type DCC crystal is free of geometrical aberration and theoretically provides a larger solid collection angle than the Johann type. But the Johansson DCC is very difficult to achieve in practice. Efforts were made in the past to fabricate a Johansson-type DCC, but the efficiency was too low for practical application [10]. A segmented Johansson DCC is used to approximate this geometry [11]. The segmented DCC consists of multisegments of thin crystals. Each crystal is curved in a toroidal shape with Johann-type geometry. The optic reflection plane has an angle of γ to the surface, as shown in Fig. 5. The value of γ increases as it moves away from the top of the focal circle to form a step-function approximation of the Johansson geometry. The approximated Johansson DCC provides a flux gain of 2 to 5 compared to a Johann DCC.

Logarithmic Spiral DCC

The geometry of a logarithmic spiral has long been of interest [12] because it has the property that the incident angle relative to the curve is constant at any point on the curve for rays diverging from a source at the origin of the spiral. Fig. 6a shows a logarithmic spiral. The equation of a logarithmic spiral in polar coordinates (Fig. 6a) about the point source S is given by:

$$r = r_o \exp(a\varphi) \tag{4}$$

where r_o and a are constants and a is related to the incident angle θ by:

$$\tan\theta = \frac{rd\varphi}{dr} = \frac{1}{a} \tag{5}$$

Because of the constant incident angle, high collection efficiency for a crystal optic can be achieved if a crystal is bent to a logarithmic spiral shape.

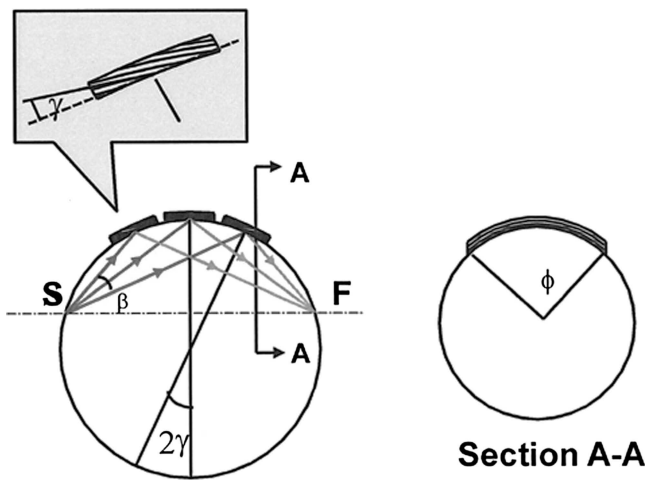

Fig. 5—Geometry of point-to-point approximated Johansson DCC with three multiple segment crystals, each with a different value of a crystal plane inclined angle AND the angle between the crystal plane and the surface. The inclined angles for the three crystals from left to right are $-\gamma$, 0, γ, respectively.

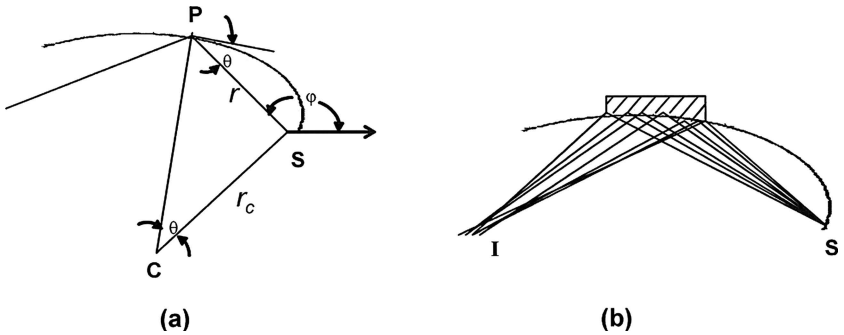

Fig. 6—(a) Geometry of a logarithmic spiral curve. S is the origin and C is the center of curvature for point P on the curve. (b) Caustic of a logarithmic spiral with a point source at the origin.

In addition, when a point X-ray source is placed at the spiral origin S, the reflected rays diffracted by a finite-size crystal with logarithmic spiral shape converge to a caustic, as shown in Fig. 6b. The advantage of the logarithmic spiral over the Johansson geometry is that the diffracting planes can be parallel to the crystal surface, and thus fabrication is easier. Larger collection efficiency is achieved if a so-called revolving logarithmic spiral, or log-spiral DCC, is used. This geometry is obtained by rotating the logarithmic spiral around a line joining the source and image points. The obvious disadvantage of the logarithmic spiral is that high collection efficiency can be obtained only for one Bragg angle with a given spiral. Therefore, the logarithmic spiral is particularly useful for a single-element detection.

Characteristic of DCC Optics in an MWDXRF System

An MWDXRF system consists of two sets of DCC optics: excitation optics and collection optics. The approximated Johansson geometry would be used for the excitation optics and logarithmic spiral geometry would be used for the collection optics.

CHARACTERISTIC OF EXCITATION OPTICS

For excitation of sulfur and chlorine atoms, chromium Kα X-rays have been selected. The chromium Kα line has good efficiency for the excitation. Based on consideration of the optimum design parameters and results, an approximated Johansson germanium(111) DCC optic will be used for focusing the chromium Kα X-rays. The design parameters and performance of this DCC optic are listed in Table 1.

Characterization of the excitation optic would be done in an X-ray optical enclosure that has numerous motorized stages, an X-ray camera, a chromium X-ray tube, and a silicon drift detector. The motion and data acquisition is PC controlled. The characterization includes flux, focal distances, and spot size measurements for the excitation optic. The flux of the excitation DCC reaches as high as 5×10^9 photons/s, and the spot size is about 300 μm.

TABLE 1—The Design Parameters and Performance of the Excitation Optic

Crystal Plane	Focusing Energy	Source-Optic Distance	Solid Angle	Flux with 50 W Source	Focal Spot Size
Ge(111)	5.4 keV	117 mm	0.05 sr	5×10^9 photons/s	300 μm

CHARACTERISTIC OF LOG-SPIRAL COLLECTION OPTICS

The design parameters and performance of the collection optics are shown in Table 2.

A standard process for fabrication of log-spiral DCC optics has been established. Characterizations of the collection optics are carried out by using a secondary sulfur or chlorine fluorescence source. The fluorescence source will be generated by using a focused X-ray beam on a target. A focusing X-ray beam, or an X-beam, is produced by integration of a focusing X-ray optic with an X-ray tube. The size of the fluorescence source can be controlled by placing the target in or out of the focal plane of the X-ray beam. The collection efficiency and effective solid angle of the DCC collection optic are measured for various source sizes; also, the energy resolution of the collection optic is measured. Fig. 7 shows the rocking curve of a sulfur collection optic, and the resolution of 6 eV was achieved.

MWDXRF SYSTEM FOR SULFUR OR CHLORINE

System Integration

Fig. 8 shows a schematic diagram of an analyzer. The analyzer chamber, called an analyzer engine, consists a low-power X-ray tube, two doubly curved crystal optics, and a proportional counter detector. The engine is evacuated to minimize the absorption of sulfur or chlorine X-rays in air. A thin polyimide window is used on the engine to allow the sample to be analyzed in air. A power supply system provides various DC supplies for the X-ray tube and the detector. A programmable logic control (PLC) is used for system control and data acquisition. The PLC, engine, power supply, and other electronics are enclosed in a cabinet. A small oil-free vacuum pump is used to evacuate the engine chamber; it is enclosed in the cabinet as well.

In operation, sulfur or chlorine X-rays from the sample are collected by the collection crystal optic in the chamber and directed to the proportional counter. A pulse-type signal is formed by the incoming sulfur or chlorine X-rays, and

TABLE 2—The Design Parameters and Performance of the Collection Optic

Geometry Type	Focusing Energy	Crystal Plane	Optic-Sample Distance	Reflection Efficiency	Solid Angle
Log spiral	2.307 or 2.622 keV	Ge(111)	108 mm	5 %	0.5 sr

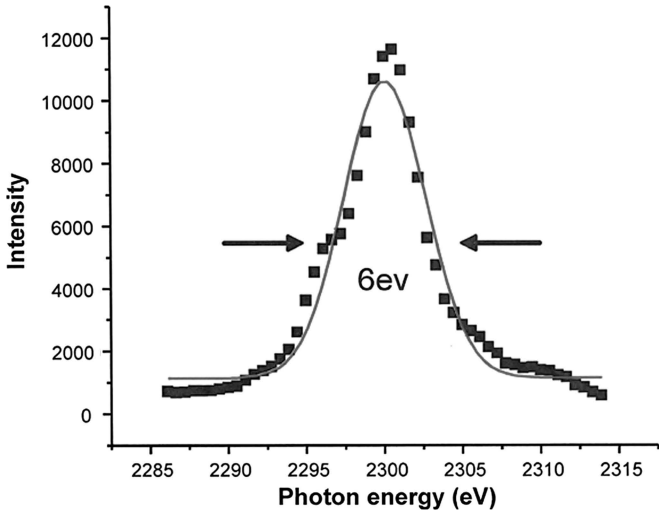

Fig. 7—The energy resolution of collection optics for sulfur.

the signal is amplified and analyzed by a single-channel analyzer (SCA). A counter on the PLC registers the digital output pulses from the SCA, and the number of sulfur or chlorine X-ray photons is obtained. The relationship between the sulfur or chlorine concentration in the sample and the total counts of the counter for a given measurement time is found to be linear for low sulfur content. The slope and the intercept of the linear relationship are determined by a calibration curve that is obtained by using three to six sulfur- or chlorine-based standards with sulfur or chlorine concentration bracketing the range of interest (typically

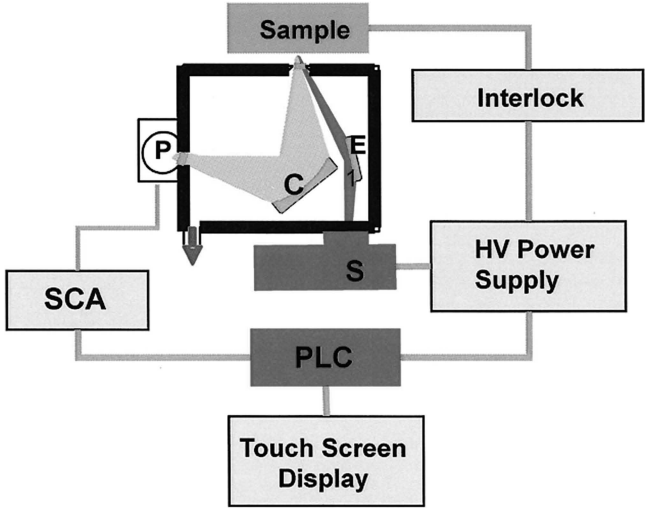

Fig. 8—Schematic diagram of an analyzer: X-ray source S, excitation optic E, collection optic C, and proportional counter P.

TABLE 3—Sulfur and Chlorine Intensities with Corresponding Concentration Standards

Concentration of Sulfur, ppm	Measured Counts, 300 s	Concentration of Chlorine, ppm	Measured Counts, 300 s
0	229	0	213
5	1,500	10	2,941
10	2,898	25	6,973
20	5,554	100	27,448
100	26,487	250	68,061
300	79,867	500	135,678

0 to 500 ppm). The sulfur or chlorine concentration in the sample is determined from the counting rate using the slope and the intercept.

Calibration and Linearity

The analyzers would be calibrated using commercial, gravimetrically based, diesel standards. The measured sulfur and chlorine fluorescent X-ray intensities, in counts, for each standard are listed in Table 3.

The linear regression function can be written as $Y = A + B \times X$, where Y is the X-ray counts obtained in 300 s, X is the concentration, A is the calibration intercept, and B is the slope of the calibration curve. To minimize the error of intercept, a weighted regression is necessary. Errors from counting statistics are used as a weighed factor in the linear regression. The weighted regression output includes the intercept, the slope, and the linear correlation coefficient R (Table 4). The calibration line with the data points is shown in Fig. 9.

Sensitivity, Background, and LOD

From the calibration curves in Fig. 9, the sensitivity and background level could be calculated: the slope of the calibration curve represents the counts of 300 s per unit concentration. For sulfur, the sensitivity R_s is $265/300 = 0.8833$ counts per second per ppm (cps/ppm), and the background counting rate R_b is $183/300 = 0.61$ cps. For chlorine, R_s is $271/300 = 0.9033$ cps/ppm and R_b is $254/300 = 0.85$ cps.

TABLE 4—The Linear Regression Results for Sulfur and Chlorine Measurements

Calibration Set	Intercept A, Counts	Slope B, Counts/ppm	Linear Correlation Coefficient, R
Sulfur	183 +/− 23	265 +/− 0.4	0.9999
Chlorine	254 +/−15	271 +/− 0.2	1.0000

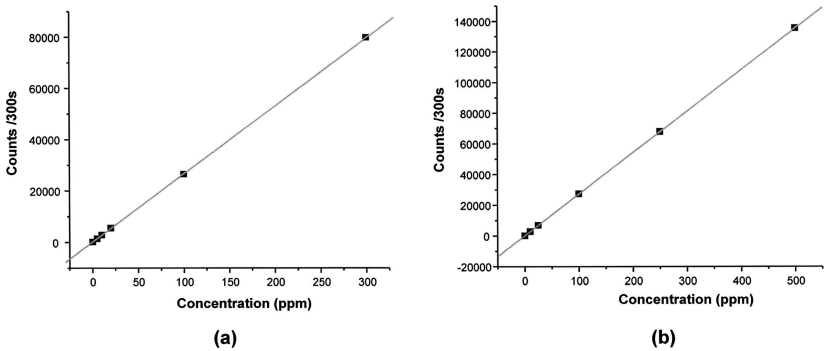

Fig. 9—The calibration curves for analyzers: (a) sulfur, (b) chlorine.

The minimum LOD of an analyzer can be determined either by measuring the standard deviation of the background or by using the formula:

$$LOD = \frac{3\sqrt{B}}{S} \times C = \frac{3 \times \sqrt{R_b \times T}}{R_s \times T} \tag{6}$$

where B is the background counts, S is the signal counts for the standard with the concentration of C, and T is the measurement time in seconds.

Based on the calibration curves and the formula, the LODs for sulfur and chlorine analyzers with a collection time of 300 s were calculated, and the results are shown in Table 5.

The LODs can be verified experimentally by measuring the variation of a sample with an S level close to a blank. An *iso*-octane sample with sulfur concentration 0.3 ppm was prepared gravimetrically and was tested in the latest analyzer. The testing time is 600 s for each measurement. The test results are shown in Fig. 10. The standard deviation of 20 measurements for 20 specimens was found to be 0.031 ppm. This results in an LOD of 0.09 ppm for 600 s testing time.

MATRIX EFFECT AND INTERFERENCE

Matrix Effect

The absorption of both the excitation beam and the characteristic sulfur and chlorine X-rays of the sample is matrix dependent. That means the differences between the elemental composition of test samples and the calibration standards can result in biased sulfur or chlorine determinations. The only important elements contributing to the biased determinations are hydrogen, carbon, and oxygen. In general, the matrix effect is minor and there is no need for correction. However, if a test sample has high oxygen content or very different

TABLE 5—The Limit of Detection of Sulfur and Chlorine Analyzers

Analyzer	Sensitivity (cps/ppm)	Background (cps)	LOD (ppm)
Sulfur	0.8833	0.605	0.15
Chlorine	0.9033	0.847	0.18

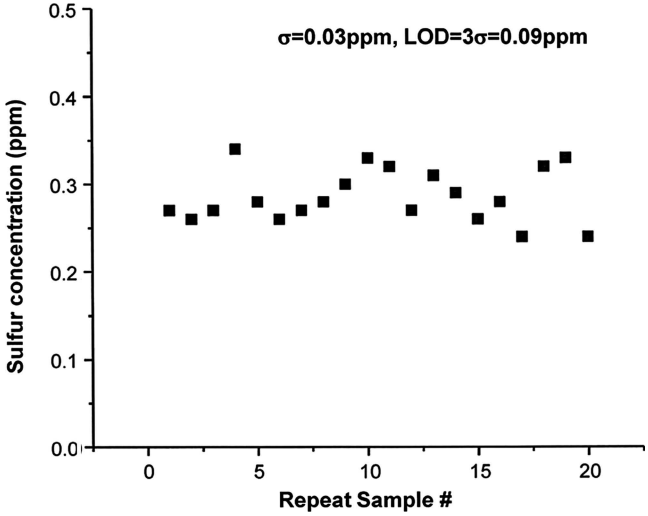

Fig. 10—Twenty repeat measurements at a sub-ppm S level that shows an LOD of 0.09 ppm.

hydrogen-to-carbon ratio compared to the calibrants, matrix correction will be necessary. The monochromatic excitation makes the matrix correction simple if the major composition of the matrix is known. The primary fluorescence intensity for an element in the matrix can be simply found from the first principle for monochromatic excitation [13]:

$$I_i(E_i) = \frac{\eta(E_i)}{G_0} \frac{Q_i(E_i) I(E_o)}{(\mu(E_o) + G\mu(E_i))} W_i \tag{7}$$

where $\eta(E)$ is detector efficiency, $Q(E_i)$ is the fundamental parameter for element i, $I(E)$ is the excitation beam intensity, W_i is the concentration of the element by weight, $\mu(E)$ is the average mass absorption coefficient at energy E for the matrix, and G_o and G are geometrical factors related to the beam and sample configuration. The term $\mu_M = [\mu(E_o) + G\mu(E_i)]$ is the only parameter related to the matrix.

For petroleum applications, the sample matrix consists of carbon, hydrogen, and oxygen. A matrix-correction factor (C) is used to account for differences in the matrix between a test sample and the calibration standards according to the following equation:

$$C = [{}^{\lambda 0}\mu_{test} + {}^{\lambda S}\mu_{test} G] / [{}^{\lambda 0}\mu_{cal} + {}^{\lambda S}\mu_{cal} G] \tag{8}$$

where:

${}^{\lambda 0}\mu = {}^{\lambda 0}\mu_C X_C + {}^{\lambda 0}\mu_O X_O + {}^{\lambda 0}\mu_H X_H$

${}^{\lambda S}\mu = 198.3 X_C + 468.3 X_O + 0.58 X_H$

G = a constant determined by the angle between the sample surface and the incident and emitted beams. For the analyzer, the design value is 0.87.

${}^{\lambda 0}\mu$ = average, mass absorption coefficient (cm^2/g) for the incident-beam wavelength ($\lambda 0$),

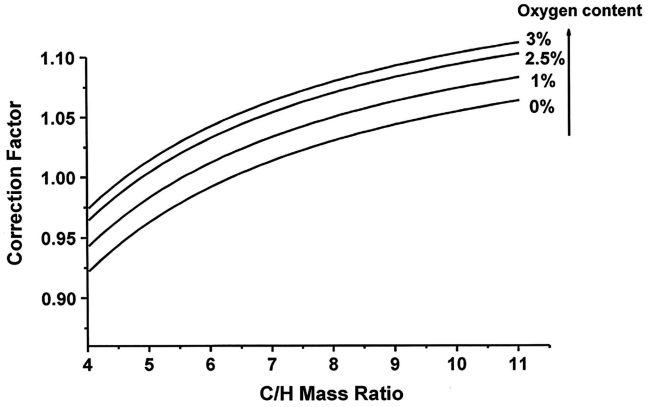

Fig. 11—Matrix correction factor relative to a diesel matrix.

${}^{\lambda S}\mu$ = average, mass absorption coefficient (cm^2/g) for sulfur radiation at $\lambda = 0.5373$nm,
${}^{\lambda 0}\mu_C$ = mass absorption coefficient (cm^2/g) of carbon for $\lambda 0$ (=14.8 for Cr Kα excitation),
${}^{\lambda 0}\mu_O$ = mass absorption coefficient (cm^2/g) of oxygen for $\lambda 0$ (=37.7 for Cr Kα excitation),
${}^{\lambda 0}\mu_H$ = mass absorption coefficient (cm^2/g) of hydrogen for $\lambda 0$ (=0.34 for Cr Kα excitation),
X_C = mass fraction of carbon in calibrant or sample of interest,
X_O = mass fraction of oxygen in calibrant or sample of interest, and
X_H = mass fraction of hydrogen in calibrant or sample of interest.

The subscript "cal" refers to the calibration standards and the subscript "test" refers to test sample.

The correction factor C is calculated and plotted as a function of the carbon/hydrogen mass ratio in Fig. 11. The calculated results are based on a diesel matrix with a carbon/hydrogen mass ratio of 6.7. For diesel and gasoline, the variation of carbon/hydrogen mass is small and matrix effect can be negligible. For a sample with significant oxygen content, a matrix correction is necessary.

To investigate the matrix effect for a sample with high oxygen content, a set of ethanol standards and a set of water standards with known sulfur concentration were used for testing in an MWDXRF analyzer. A set of diesel standards was also tested, and the results are plotted in Fig. 12. The sensitivities for the three matrixes were determined from the linear fits of the curves. The measured sensitivities and the matrix correction factor relative to the diesel matrix are listed in Table 6. The calculated matrix correction factors from Eq 5 for water and ethanol are also listed for comparison. The measured matrix effect agrees well with the theoretical calculation. Therefore, Eq 8 is very useful for matrix correction for practical applications.

Interferences

As shown in Fig. 7, the spectral resolution of the MWDXRF method is very high. Common interference of phosphorus, chlorine, and argon in the EDXRF method is no longer an issue for the MWDXRF method. There are still,

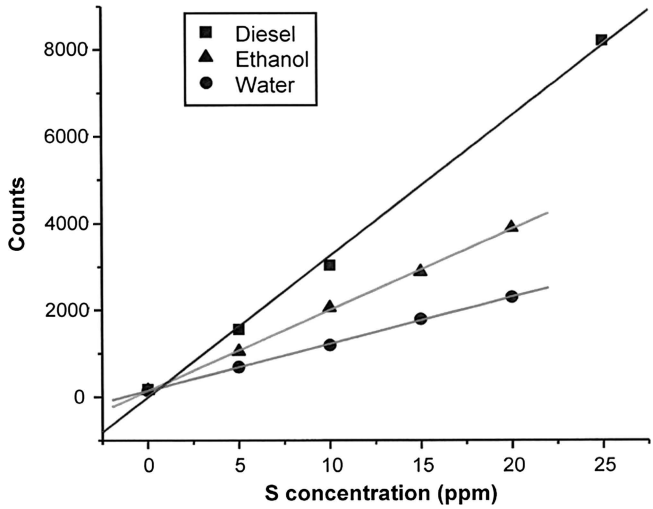

Fig. 12—Calibration curves for diesel, ethanol, and water illustrate the sensitivity difference due the matrix effect.

however, several possible uncommon interferences. Some impurities may have interference with the measurements because those X-ray photons with energy very close to sulfur K_α radiation (K_α: 2.307 keV) will be partly collected. For the sulfur analyzer, three major elements might have such an effect: molybdenum (L_α: 2.293 keV), lead (M_α: 2.346 keV), and zircon (L_γ: 2.302keV). To estimate the interference effect of these elements, sulfur-free water standards with known concentrations of these elements were tested for interference. Table 7 lists the counts and sulfur reading of 1,000 ppm samples. The sulfur reading is based on the water calibration curve. Molybdenum has the most severe interference. The bias of sulfur measurement due to the presence of molybdenum in a sample can be very significant. But the presence of molybdenum in fuel is rare, and this interference is not an issue in general. The interference effect of lead is small because of the larger energy gap between the lead M_α line and the sulfur K_α line. Although the zircon L_γ line is very close to the sulfur line, the Zr L_γ line is a weak line in the L shell and its intensity is low. In general, both interferences of lead and zircon can be negligible unless there is very high content of lead and zircon in the testing sample.

TABLE 6—Comparison of Matrix-Correction Factor between Experiment and Theory

Matrix	Sensitivity	Measured C	Theoretical C
Diesel	0.933	. . .	. . .
Ethanol	0.614	1.52	1.56
Water	0.359	2.6	2.55

TABLE 7—The Interference of Molybdenum, Lead, and Zircon in Sulfur Measurements

Sample	Water	1,000 ppm Mo in Water	1,000 ppm Pb in Water	1,000 ppm Zr in Water
Counts /300 s	214	4731	342	737
Sulfur reading (ppm)	0	105	3.8	5.2
Percentage	0	10.5 %	0.38 %	0.52 %

Site Precision and Accuracy

Numerous data were collected during quality control for analyzer production at the factory. For each analyzer, after the establishment of the calibration using a set of commercial standards, various samples were measured to determine the site precision. Table 8 shows the measurement results for 20 sulfur analyzers. The measurement time is 300 s.

From the table, the repeatability was determined to be 1.2 ppm for 10 ppm diesel sample and 4.4 ppm for 300 ppm diesel sample.

A standard reference material (SRN) 2723a from NIST is used to check the accuracy of the analyzer. This standard has a certified sulfur value of 11.0 mg/kg $\pm$ 1.1 mg/kg in diesel fuel oil. Table 9 lists the results for ten analyzers. All the measurements are within the error bar of the SRM 2723a.

Reproducibility, Repeatability, and Cross-Check Comparison

The method based on MWDXRF has been accepted and recognized as a standard method (D7039) by ASTM. Several round-robin studies were conducted, and the repeatability and reproducibility of D7039 were determined. Repeatability and reproducibility for ultra-low sulfur diesel are [14] $0.0626x + 0.1584$ ppm and $0.017x + 0.7131$ ppm, respectively, where x is the concentration of the sulfur in ppm.

An ultra-low sulfur diesel (ULSD) interlaboratory cross-check program has been launched since 2003. More than 40 laboratories with MWDXRF analyzers based on D7039 have participated in this program. In this cross-check program, a ULSD diesel sample was mailed to each participating laboratory. The test results were collected from all laboratories and the data were statistically analyzed. From these cross-check data, the D7039 MWDXRF method can be compared with the high-power wavelength dispersive XRF method (D2622) and UV fluorescence method (D5453). Table 10 lists the latest results for ten ULSD samples, and Fig. 13 and Fig. 14 show the comparison of reproducibility and repeatability among D2622, D5453, and D7039. D7039 shows better precision than D2622 in both repeatability and reproducibility. D5453 has the best repeatability among all the three testing methods. D7039 has the best reproducibility among all the test methods.

CONCLUSION

A low-power monochromatic wavelength-dispersive XRF method using doubly curved crystal optics was successfully developed. The MWDXRF method uses at

TABLE 8—Repeat Measurements for Sulfur Analyzers with Diesel Standards

Analyzer ID No.	10 ppm Standard			300 ppm Standard		
	First measurement (ppm)	Second measurement (ppm)	Δ (ppm)	First measurement (ppm)	Second measurement (ppm)	Δ (ppm)
1	10.3	10.1	−0.2	302.1	303.4	1.3
2	10.6	11.2	0.6	298.8	298.8	0
3	9.9	9.7	−0.2	301	300.1	−0.9
4	10.1	10.2	0.1	301.6	303.1	1.5
5	10.1	10.5	0.4	300.2	303.6	3.4
6	9.8	10.4	0.6	303.5	303.8	0.3
7	9.6	10.3	0.7	299.2	300	0.8
8	9.6	10.1	0.5	301	303.3	2.3
9	9.6	9.8	0.2	302.6	305.2	2.6
10	10.1	10	−0.1	301.8	303.6	1.8
11	9.9	10.3	0.4	303.1	304	0.9
12	9.8	9.5	−0.3	298.4	298.7	0.3
13	9.3	10.1	0.8	303.8	300.7	−3.1
14	10.1	10.2	0.1	298.3	299.7	1.4
15	9.8	9.6	−0.2	299.9	301.7	1.8
16	10.7	10.3	−0.4	298.8	302	3.2
17	10.6	9.8	−0.8	300.7	303.2	2.5
18	10.3	10.1	−0.2	301	299.3	−1.7
19	10.3	10	−0.3	304.4	305	0.6
20	10.6	10.1	−0.5	300.7	300.6	−0.1
Standard deviation			0.45			1.62

TABLE 9—Accuracy Check for Sulfur Analyzers with NIST SRM 2723a (11.0 ± 1.1 ppm)

Analyzer No.	1	2	3	4	5	6	7	8	9	10
Results (ppm)	10.3	11.4	11.0	10.7	11.3	10.7	11.0	10.8	11.0	10.4

TABLE 10—The Results of Cross Check for the Current Major ASTM Methods

	D2622				D5453				D7039			
Sample ID	Robust Mean	Robust Std Dev	R	r	Robust Mean	Robust Std Dev	R	r	Robust Mean	Robust Std Dev	R	r
ULSD0801	10.99	1.14	3.18	1.25	10.93	0.76	2.11	0.23	11.03	0.63	1.76	0.62
ULSD0802	5.13	0.72	2.01	0.56	4.63	0.47	1.31	0.20	4.94	0.47	1.31	0.41
ULSD0803	8.93	1.06	2.96	0.41	8.87	0.69	1.92	0.20	8.83	0.51	1.42	0.62
ULSD0804	10.58	1.35	3.76	0.84	10.91	0.79	2.19	0.31	11.13	0.75	2.09	0.82
ULSD0805	8.54	1.00	2.79	0.82	8.93	0.66	1.83	0.22	8.78	0.59	1.64	0.64
ULSD0806	5.06	1.20	3.34	0.70	5.31	0.49	1.36	0.20	5.56	0.44	1.23	0.39
ULSD0807	10.44	1.62	4.51	0.84	10.93	0.76	2.11	0.27	10.99	0.47	1.31	0.82
ULSD0808	5.24	0.94	2.62	0.66	5.28	0.47	1.31	0.18	5.53	0.41	1.14	0.53
ULSD0809	7.80	0.79	2.20	0.60	7.66	0.54	1.50	0.20	7.76	0.53	1.48	0.39
ULSD0810	10.90	0.92	2.56	0.53	10.86	0.70	1.94	0.31	11.09	0.57	1.59	0.59

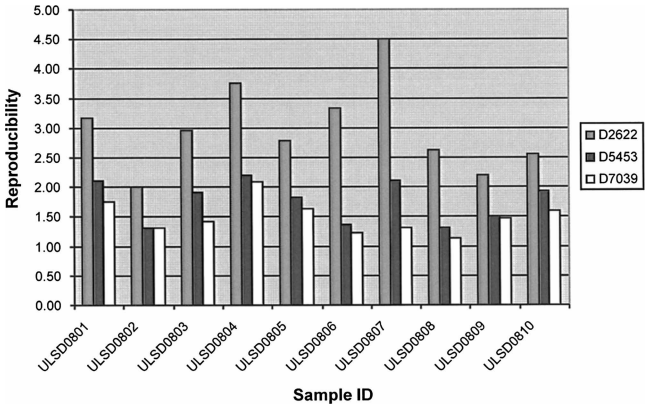

Fig. 13—The comparison of the reproducibility of ASTM methods D2622, D2543, and D7039.

least two doubly curved crystal optics, one for monochromatic focusing and one for fluorescence collection. Doubly curved crystal optics enable high sulfur/nitrogen ratio, small spot, low power, and compact design. Unprecedented low detection limits for sulfur and chlorine analysis in petroleum products were achieved.

Based on round-robin studies and the interlaboratory cross-check study, the low-power MWDXRF method showed the best precision for ULSD analysis among XRF methods. It also showed the best reproducibility between laboratories among the current sulfur analysis methods. Its high precision, simplicity, and compactness result in the MWDXRF analyzer becoming a powerful tool for petroleum applications.

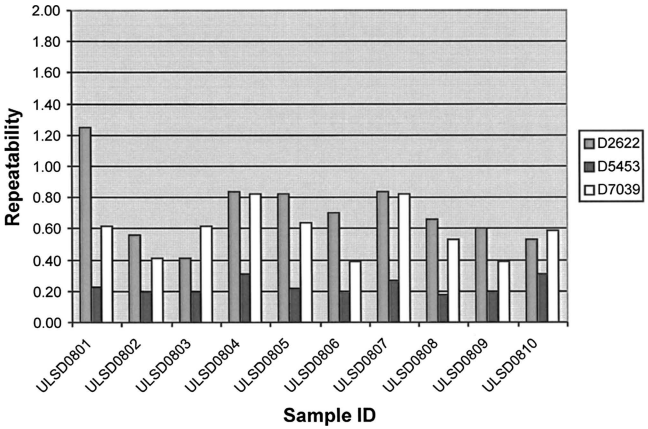

Fig. 14—The comparison of the repeatability of ASTM methods D2622, D2543, and D7039.

References

[1] Chen, Z. W., Wei, F., Radley, I. and Beumer, B., "Low-Level Sulfur in Fuel Determination Using Monochromatic WD XRF – ASTM D7039," *J. ASTM Intl.*, Vol. 2, No. 8, 2005, Paper ID JAI12971.

[2] Berreman, D. W., Dumond, J. W. M. and Marmier, P. E., "New Point-Focusing Monochromator," *Rev. Sci. Instruments*, Vol. 25, 1954, pp. 1219–1220.

[3] Wittry, D. B. and Golijanin, D. M., "Alignment and Characterization of Doubly-Curved X-ray Diffractors," *Microbeam Analysis*, R. H. Geiss, Ed., San Francisco Press, 1987, pp. 51–55.

[4] Wittry, D. B. and Sun, S., "X-ray Optics of Doubly Curved Diffractors," *J. Appl. Phys.*, Vol. 67, 1990, pp. 1633–1638.

[5] Wittry, D. B. and Sun, S., "Properties of Curved X-ray Diffractors with Stepped Surfaces," *J. Appl. Phys.*, Vol. 69, 1991, pp. 3886–3892.

[6] Chen, Z. W. and Wittry, D. W., "Microprobe X-ray Fluorescence with the Use of Point-focusing Diffractor," *Appl. Phys. Lett.*, Vol. 71 (13), 1997, p. 1884.

[7] Chen, Z. W. and Wittry, D. W., "Microanalysis by Monochromatic Microprobe X-ray Fluorescence – Physical Basis, Properties and Future Prospects," *J. Appl. Phys.*, Vol. 84 (2), 1998, p. 1064.

[8] Chen, Z. W., "Recent Development of Doubly-curved Crystal Focusing Optics and their Applications for Micro XRF," *Proc. SPIE*, Vol. 3767, 1999, p. 114.

[9] Chen, Z. and Gibson, W. M., "Doubly Curved Crystal (DCC) X-ray Optics and Applications," *Powder Diffraction*, Vol. 17, 2002, pp. 99–103.

[10] Wittry, D. B. and Golijanin, D. M., "Larger Aperture Point-focusing Diffractor for X-rays," *Appl. Phys. Lett.*, Vol. 52 (17), 1988, p. 1831.

[11] Chen, Z. W., "An Optical Device for Directing X-rays Having a Plurality of Optical Crystals," U.S. Patent 7,035,374, 2007.

[12] Huizing, A., Zegers, C., Heijmans, T. J. A. and Van Tol, M. W., "X-ray Spectrometer Having a Doubly Curved Crystal," U.S. Patent 4949367, 1990.

[13] Jankins, R., Gould, R. W. and Gedcke, D., *Quantitative X-ray Spectrometry*, 2nd ed., Marcel Dekker, New York, 1995.

[14] Mason, R. L. and Buckingham, J. P., *EPA 2005 Sulfur in Diesel Fuel Round Robin Test Plan and Data Analysis*, 2005, http://www.epa.gov/diesel/documents/rr-finalreport.pdf.

15

Neutron Activation and Gamma Ray Spectrometry Applied to the Analysis of Petroleum Products

R. A. Kishore Nadkarni[1]

INTRODUCTION

After World War II, with its advent of nuclear energy, one of the peaceful uses of nuclear energy was the development of neutron activation analysis (NAA) as an accurate tool for characterizations of elements in a variety of matrices. NAA is a technique based on irradiation in a nuclear reactor or other irradiation source and measuring resultant radioactivity of specific isotopes; it is a very accurate and precise technique. A large body of data exists on the applications of this technique to crude oil and petroleum products. At one time, several universities in the United States, such as the University of Kentucky, University of California at San Diego, University of California at Irvine, Purdue University, University of Missouri, Georgia Tech, Texas A&M University, Cornell University, University of Oregon, University of Maryland, and Washington State University, had active programs in NAA of fossil fuels and other matrices. Because of the difficulty of access to a nuclear reactor and associated radiation hazards, however, it has found only limited use in petrochemical or oil company laboratories. But one does not need one's own nuclear reactor for NAA because several commercial companies provide such services at a reasonable price. The universities mentioned also provide irradiation services to interested parties.

When neutrons collide with stable isotopes of most elements, they produce radioactive nuclides that, as they decay, emit characteristic beta and gamma rays which can be used for qualitative and quantitative determination of these elements. For most elements in NAA, thermal neutrons are used as the bombarding particles because most elements have high thermal neutron cross sections, and very powerful fluxes of thermal neutrons are available in the nuclear reactors. Usually, the pool type reactors operating at power levels of 10 to 1,000 kW range produce thermal and fast neutron fluxes in the range of 10^{11} to 10^{13} n/cm^2-s.

Once the sample has been irradiated, the next step is the measurement of characteristic beta or gamma rays emitted by the nuclei of interest. Usually for gamma ray measurements, multichannel gamma ray analyzer or spectrometer (MCA) is used. The spectrometer consists of a lead-shielded NaI(Tl), Ge(Li), or hyperpure germanium detector scintillation counter, and a multichannel pulse height analyzer that discriminates between gamma ray energies, usually displayed on a screen or plotted on a chart. When the activated nuclei emit only beta rays or the gamma rays emitted are too close to those of

[1] *Millennium Analytics, Inc. East Brunswick, NJ*

other isotopes, radiochemical separations based on precipitation, ion exchange, or solvent extraction have to be employed to isolate the element of interest before its radioactivity can be measured.

Since the petroleum products contain essentially a carbon-hydrogen-oxygen matrix that does not get activated during thermal neutron irradiation, there is very little background interference. There could, however, be interference from other trace element nuclei present in the sample. Generally, these isotopic interferences are well known, and suitable alternate interference-free gamma rays can be used for quantitative analysis. Each radionuclide is characterized by its half-life and the type of energy emitted during its decay to a stable state. Gamma rays are high-energy photons, and their penetration power is much greater than alpha or beta rays emitted by the radionuclides. The half-life of a radionuclide is the time required for half of its radioactivity to decay. For example, radionuclide sodium^{24} has a half-life of approximately 15 h. Thus, in 15 h, half of the sodium nuclei will disintegrate and release their energy in the form of gamma radiations of 1.369 and 2.754 MeV. This decay process continues in this fashion so that every 15 h half of the remaining portion of the isotope will decay. After about 10 half-lives, only 0.1 % of the radioactive nuclei remain.

NAA methods are comparable in precision and accuracy to X-ray fluorescence or atomic spectroscopic methods for most elements, particularly when the analytical matrix is a "clean" one such as gasoline. Particularly in national research laboratories and universities, NAA was widely used for the determination of trace elements in petroleum products. The use of this technique, however, has been limited in the oil industry laboratories because of the need to have access to a nuclear reactor for most sensitive determinations. See reviews by Nadkarni [1] and Filby [2] for a detailed discussion and literature citations of applications of NAA methods for the analysis of fossil fuels. Also, see the bibliography of U.S. literature on NAA from 1936 to 1977 compiled by Nadkarni [3].

Although several versions of NAA are available, the largest body of work in the application of NAA to fossil fuels concerns using reactor thermal neutron irradiation followed by direct instrumental gamma ray counting or appropriate radiochemical separations followed again by gamma ray counting. Gamma ray measurements were achieved at one time with NaI(Tl) detectors, which did not have good discrimination power between gamma rays. High-resolution Ge(Li) or hyperpure germanium detectors made instrumental NAA a reliable, multielement analytical tool. The pulses received by the counter are converted into electric signals that are amplified before being resolved by a pulse height analyzer, which discriminates in the increasing order of pulse heights. Thus, the gamma radiation is resolved according to their energies. Instrumental neutron activation analysis (INAA) is a nondestructive method that can measure about 40 elements in fossil fuels.

NAA has the advantages of being a very sensitive method with detection limits of 10^{-3} to 10^{-7} μg/g, characteristic of the element being detected, and interferences from other elements in the matrix being minimized by judicious choice of measurement time and measured gamma ray energy. On the other hand, NAA requires a nuclear reactor for most irradiations, not always an easy task. In many matrices, the radionuclides produced may have a very short or a very

long half-life, making it difficult to make measurements in a reasonable time for sample analysis turnaround, and many nuclides may produce overlapping or close-proximity gamma ray peaks, making it difficult to distinguish between them or calculate their presence accurately.

In practice, about 100 mg of a sample in sealed quartz vials along with elemental standards are irradiated for varying periods of time in a nuclear reactor in a thermal neutron flux of 1×10^{12} n/cm^2/s. During irradiation, the stable isotopes of elements are excited to radioactive isotopes, which emit characteristic gamma rays during their decay. Post-irradiation, these gamma rays are counted on a high resolution Ge(Li) or hyperpurity germanium detectors coupled to a multichannel detector for varying periods of time. Since different isotopes have different half-lives, judicious selection of measurement time enables one to measure a number of elements over a period of few weeks. The elements with shorter half-life isotopes are measured soon after the irradiation, and those with longer half-life isotopes are measured at a later date after the short half-life isotopes have decayed to an insignificant level. A typical plan for sequential irradiation and measurement is given in Table 1.

RADIOCHEMICAL NAA

Despite the high-resolution capability of modern gamma ray detectors, several trace elements cannot be easily determined by INAA because of their low concentration levels in the sample, their poor activation parameters, or interferences from matrix elements. In such cases, radiochemical separations are employed to isolate the radionuclides of interest from other high-intensity gamma ray emitters or matrix. These separations may involve solvent extractions, ion exchange, gravimetric precipitations, and so on. After the radioactive species are separated by these procedures, they are counted on a Ge(Li) detector with a pulse height analyzer to make quantitative determinations. A known amount of inactive element in the same chemical form is added to the

TABLE 1—Sequential Thermal INAA Scheme

Irradiation Time	Decay Time	Elements Measured
2 min	2–4 min	Al, Cu, S, V, Ti
	10 min	Ca, Mg
	26 min	Cl, I
	30–60 min	Ba, Cu, Mn, Na, Ni
8–24 h	2 days	Cu, K, Na
	3–4 days	As, Br
	7 days	Ca, Sb
	15 days	Ba, Cr
	25 days	Co, Fe, Ni, Sb, Se, Sr, Zn

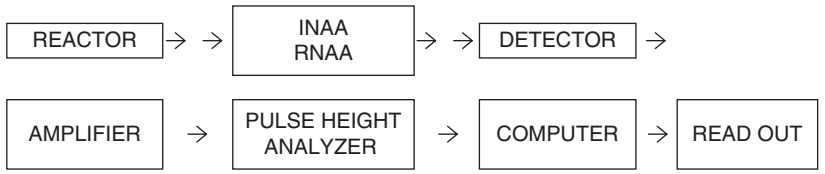

Fig. 1—Schematic diagram of neutron activation analysis.

irradiated sample as a carrier for that isotope of the element. Necessary chemical separations are carried out to isolate a pure chemical compound of that isotope, and the yield of recovery is determined. By comparing the gamma ray intensity of the compound separated from the sample with that of a standard taken through the same process allows one to calculate the determination of the element in the original sample. Whether the isolated compound is radiochemically pure or not can be ascertained by looking at the gamma ray spectrum of the separated product to check if it contains any gamma ray peaks not associated with the isotope of interest.

A brief schematic diagram of the NAA sequence of events is given in Fig. 1. A fast NAA (FNAA) schematic is shown in Fig. 2. Typical gamma ray spectra from irradiating a sample of Libyan crude oil and measuring after a 2-day and a 10-day decay, respectively, are shown in Figs. 3 and 4. Short-lived nuclei are seen in Fig. 3, and longer-lived nuclei are seen in Fig. 4. Thus, by taking advantage of time discrimination, a large number of isotopes produced can be quantitated [21].

Some of the elements of interest in fossil fuels that are amenable to INAA or radiochemical neutron activation analysis (RNAA) are listed in Table 2. This, however, does not mean that all the nuclides can be determined in all matrices. That will depend on a function of their concentration level and other elements present that may also emit gamma rays in close proximity to the species of interest.

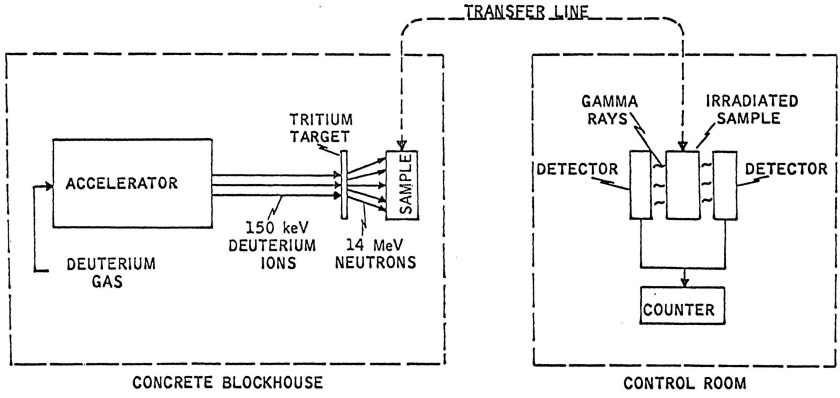

Fig. 2—Schematic diagram of fast neutron activation analysis.

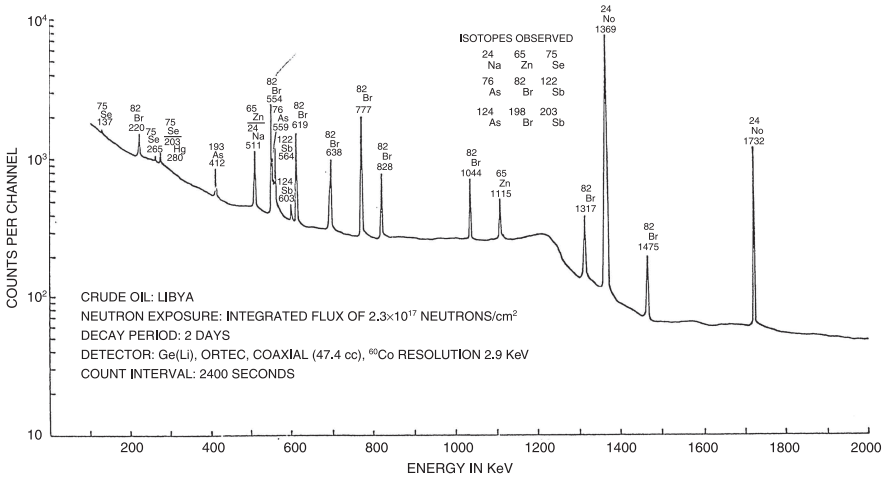

Fig. 3—Gamma ray spectrum of irradiated crude oil after 2 days of decay.

FAST NEUTRON ACTIVATION ANALYSIS

As opposed to thermal neutrons of slow speed, fast neutrons of energy in the range of 1 MeV to many megaelectronvolts react by (n, p) reaction with the nuclei rather than (n, g) reaction of thermal neutrons. For example, the oxygen[16] isotope will convert to the nitrogen[16] isotope with a half-life of 7.35 s

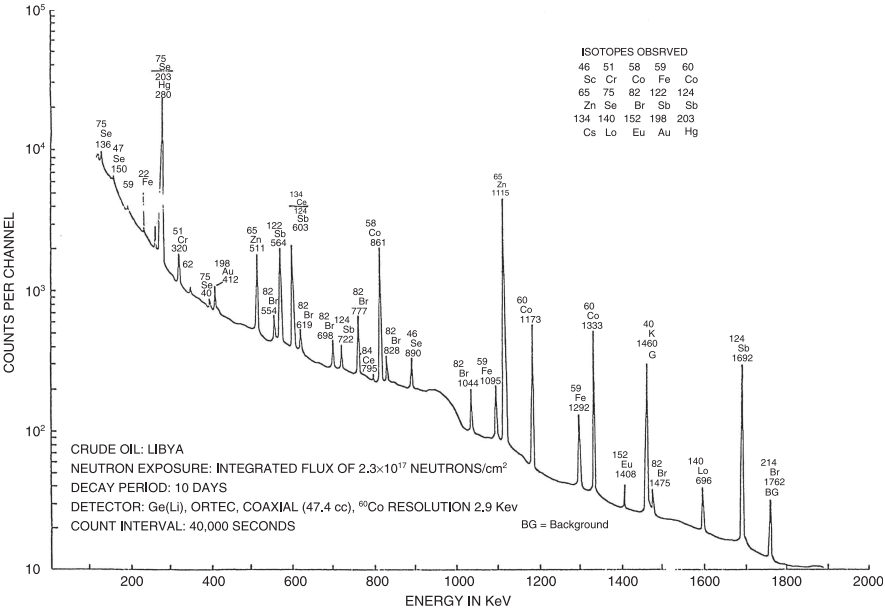

Fig. 4—Gamma ray spectrum of irradiated crude oil after 10 days of decay.

TABLE 2—Nuclear Properties of Some Radioelements for Analysis of Petroleum Products[a]

Radioisotope	Half-Life	Thermal Neutron Cross Section, barns[b]	Gamma Ray Energies, MeV	Detection Limits,[c] μg
Al^{28}	2.31 min	0.235	1.780	0.01
As^{76}	26.4 h	4.5	0.559; 0.657; 1.22	0.005
Ba^{139}	85 min	0.5		0.1
Br^{80}	17.6 min	8.5	0.511; 0.61	0.005
Br^{82}	35.3 h	3	0.554; 0.619; 0.777	
Cl^{38}	37.3 min	0.4	1.60; 2.17	0.1
Co^{60}	5.26 y	19	1.173; 1.332	0.5
Cr^{51}	27.8 d	17	0.320	1
Cu^{64}	12.8 h	4.5	0.511; 13.4	0.001
Fe^{59}	45.6 d	1.1	0.143; 0.192; 1.095	200
Hg^{197}	25 h	3100		0.002
K^{42}	12.4 h	1.2	0.31; 1.524	0.05
Mg^{27}	9.5 min	0.19	0.84	0.5
Mn^{56}	2.58 h	13.3	0.847; 1.811; 2.11	0.00005
Mo^{99}	67 h	0.45		0.1
Na^{24}	14.96 h	0.53	1.369; 2.754	0.005
Ni^{65}	2.56 h	1.5	0.368; 1.115; 1.481	0.5
Ti^{51}	5.8 min	. . .	0.32	0.004
V^{52}	3.8 min	4.5	1.44	0.002
Zn^{65}	245 d	0.46	0.511; 1.115	0.1

[a] Excerpted from Guinn [4] and Pinta [5].
[b] Thermal neutron cross sections are given in "barns," equivalent to 10^{-24} cm^2.
[c] Sensitivities calculated based on irradiation of 1 h or less in a thermal neutron flux of 1.8×10^{12}.

by (n, p) reaction. As a matter of fact, determination of oxygen in various matrices is one of the principal applications of 14 MeV FNAA.

Fast neutrons are produced using 100 to 200 keV Cockcroft-Walton deuteron accelerators or 2 to 3 MeV Van de Graaff electron accelerators. Some of the unique applications of fast NAA are analyses that cannot be accomplished easily by reactor thermal NAA; these are listed in Table 3. Oxygen, nitrogen, chlorine, sulfur, magnesium, fluorine, and silicon, among others, are quite important in the characterization of fossil fuels. Although there may

TABLE 3—Fast NAA of Selected Elements in Petroleum Products (Excerpted from Pinta [Ref 5])

Element	Aluminum	Oxygen	Chlorine	Magnesium	Nitrogen	Sulfur	Silicon
Reaction	$Al^{27}(n, \alpha)Na^{24}$	$O^{16}(n, p)N^{16}$	$Cl^{35}(n, \alpha)P^{32}$	$Mg^{24}(n, p)Na^{24}$	$N^{14}(n, 2n)N^{13}$	$S^{32}(n, p)P^{32}$	$Si^{28}(n, p)Al^{28}$
Cross section, mbarns	116	49	0.19	0.19	5.67	0.30	0.22
Half Life	15 h	7.4 s	14.2 d	15 h	10 min	14.3 d	2.3 min
Gamma Rays, MeV		6.13; 6.9; 7.12	...		0.511	...	1.78
Detection Limit, μg	6×10^{-3}	9×10^{-3}	9×10^{-3}	4×10^{-3}	7×10^{-2}	4×10^{-3}	4×10^{-3}

not be a large number of publications in the area of petroleum products, Ehmann et al. have demonstrated the capability of applying this technique to a number of matrices such as meteorites, lunar rocks, and coal [6–9]. It was found that gamma ray self-absorption was serious when using rock standards for analyzing coal liquids. A set of high-boiling organic liquid standards gave more accurate oxygen results when used in conjunction with the coal liquids [10].

Oxygen

Of particular interest is the determination of oxygen by FNAA. The only nuclear interference in this analysis is from fluorine and boron, neither of which is very likely to be present in a petroleum product. Thus, the determination of oxygen by FNAA is a rare example of an analytical technique that is virtually interference free and uses a short half-life, thus permitting a very rapid analysis. In practice, about a gram of the sample is packed into an oxygen-free polyethylene "rabbit." The sealed sample rabbit and a rabbit containing an oxygen standard are transferred by a fast, pneumatic system to the generator where they are irradiated for 15 to 20 s in the neutron flux of about 10^8 n/cm^2/s and then transferred back by the pneumatic system to a NaI(Tl) scintillation detector and counted for about 30 s. Thus, an analysis takes only about a minute.

Nitrogen

Similar to oxygen, nitrogen is also easily determined by FNAA using the reaction ^{14}N(n, 2n)^{13}N with a product half-life of 10 min and counted at 0.511 MeV positron emission. In practice, the samples are packed in polyethylene rabbits under helium, irradiated for about 10 min, allowed to decay for about 10 min to permit the radioactivity caused by oxygen, silicon, and aluminum to decay, and are then counted for 5 to 10 min. Ehmann calculated that approximate possible error in coal analysis due to interfering nuclear reactions is about 1 %, almost all of it from the ^{39}K(n, 2n)^{38}K reaction [7,9]. For coal liquids, Ehmann found that a set of organic liquids as standards gave more accurate nitrogen results. The liquid standards minimize the problem of uniform irradiation and counting geometries, and self-absorption differences related to varying matrix densities. The liquid standards were selected based on their high boiling points, well-defined stoichiometry, high-purity nonhygroscopic nature, and simple carbon-hydrogen-nitrogen elemental composition [11]. Not unexpectedly, in almost all cases Ehmann found the FNAA nitrogen results to be higher than the values obtained by using the Kjeldahl method [7]. The latter method is known to be biased low because of its inability to convert certain nitrogen compounds to ammonium form, while the FNAA method accounts for all species of nitrogen.

Silicon

FNAA can determine silicon in fossil fuels using the reaction ^{28}Si (n, p)^{28}Al with the daughter half-life of 2.3 min and a 1.78 MeV gamma ray emission. The only possible interfering nuclear reactions are ^{31}P (n, alpha)^{28}Al and ^{56}Fe(n, p)^{56}Mn.

In crude oils, silicon is usually present in low concentrations of low parts-per-million to parts-per-billion levels, but iron can be fairly high in heavy crude oils and present as corrosion-derived materials in products. Given the small amounts of phosphorus or iron present in oils, however, this is not a significant interference.

^{252}CALIFORNIUM AS A NEUTRON SOURCE

Californium 252 isotope decays by spontaneous fission with neutron emission with an energy of 2.3 MeV and a half-life of 2.73 years. This isotope can be used as a source of thermal neutrons for neutron activation analysis. Only limited use of it has been made in the petroleum field.

Sulfur in oil has been determined by neutron capture gamma ray spectrometry using a 0.24 μg ^{252}Cf source. This is probably the weakest neutron source used for capture gamma ray analysis. A 0.5 m % sulfur detection limit was achieved. A stronger source such as 5 μg ^{252}Cf will permit shorter analysis time and better sensitivity and precision [12]. An on-stream vanadium analyzer using ^{252}Cf is described by Orange and Larson [13].

Some examples of NAA in the area of petroleum products are listed in Table 4. Of interest are the trace element data used for oil spill identification [14,15]. Nearly 300 trace element patterns were accumulated, by means of which it could be ascertained whether two samples were from the same or different oil sources [16].

SUBSTOICHIOMETRIC RNAA

A number of papers have been published using the technique of substoichiometric neutron activation analysis. The technique developed by Jaromir Ruzicka [17,18] is based on reacting the elements of interest after nuclear irradiation with a suitable organic reagent that forms a complex with the element and is then extracted and separated from the matrix and other elements present in the sample. The reagent added is a less than chemically equivalent amount for completing the main reaction. This also prevents other cations in the solution from competing with the reagent solution and allows only the cation with strongest affinity with the reagent to interact. Obviously a reagent specific for the element of interest is key to selectivity. The isolated extract or the precipitate containing only the compounds of the radioactive element of interest is then counted on a beta or a NaI(Tl) detector and pulse height analyzer.

The procedure is simple and requires no extraordinary instrumentation, thus making it possible for use in underdeveloped countries. A review of available substoichiometric NAA methods was prepared by Nadkarni [19].

Given in Table 4 are several examples of applications of NAA in the petrochemical field. Also, in Table 5 analyses of petroleum products for trace elements using NAA are listed.

In summary, although the applications in the oil industry are limited mainly because of the difficulty of access to a nuclear reactor, neutron activation analysis remains a powerful, sensitive, and interference-free analytical technique, with wide-ranging applications in other fields.

TABLE 4—Examples of NAA Applied to the Analysis of Petroleum Products[a]

Elements	Matrix	Comments	References
Na, S, Cl, K, Ca, V, Mn, Cu, Ga, Br	Petroleum	Nondestructive analysis	20, 22
S	Petroleum products	Fast neutrons used	21, 23
V	Mineral oils	Nondestructive analysis	24, 28
Sr, As, Cr, Se, Fe	Petroleum	. . .	25, 29
29 trace elements	Crude oils	. . .	27, 31
Trace elements	Crude and fuel oils	Nondestructive analysis	26, 32
. . .	Tar sands	. . .	15, 20, 21
. . .	Petroleum and crude oils	. . .	20, 33
Na, V	Fuel oils	14 MeV FNAA	. . .
V	Oils	Cf ^{252}source	31, 35
S	Oils	Cf ^{252}source	36
V	Crude oils	On-line with Cf^{252} source	16, 34
. . .	Petroleum	. . .	37
. . .	Petroleum	Review	38
As and 5 other trace elements	Crude oils	. . .	35, 39
Cl	Petroleum products	. . .	40
Trace elements	High purity lubricants	. . .	41
10 trace elements	Petroleum	. . .	42
13 trace elements	Petroleum	. . .	43
Trace elements	Crude oils	Spill source identification	44
Trace elements	Crude oils	Spill source identification	36, 45
Trace elements	Crude oils	Spill source identification with charged particle activation	37, 46
Cd	Petroleum	Ion exchange	47
Trace elements	Petroleum components	. . .	48
S	Oils	Capture gamma ray analysis	49
Mercury	Petroleum	. . .	50

(*) Excerpted in part from Pinta [5] and Nadkarni [1].

TABLE 5—INAA of Fossil Fuels		
Element, mg/kg	**Libyan Crude Oil, mg/kg [20]**	**Shale Oil, mg/kg [51]**
Arsenic	0.34 ± 0.005	5.0
Bromine	0.65 ± 0.02	0.079
Calcium	21.3 ± 2.3	
Chlorine	2.35 ± 0.04	
Cobalt	0.094 ± 0.008	0.37
Chromium	1.94 ± 0.09 ppb	0.04
Iron	3.66 ± 0.09	30
Potassium	3.35 ± 0.16	
Manganese	1.45 ± 0.05	
Sodium	5.93 ± 0.06	19.4
Nickel	105 ± 6	
Antimony	0.038 ± 0.001	0.008
Scandium	0.32 ± 0.04	
Selenium	0.22 ± 0.007	0.86
Uranium	3.70 ± 0.82 ppb	0.005
Vanadium	46.8 ± 0.22	
Zinc	12.9 ± 0.85	2.70

References

[1] Nadkarni, R. A., "Nuclear Activation Methods for the Characterization of Fossil Fuels," *J. Radioanal. Nucl. Chem.,* Vol. 84, 1984, pp. 67–87.

[2] Filby, R. H. and Shah, K. R., in "Nuclear Methods in Environmental Research," Vol. 1, 1971, p. 86.

[3] Nadkarni, R. A., "The Radioanalytical Bibliography of USA 1936–1977," *J. Radioanal. Chem*., Vol. 66, 1981, p. 25–225.

[4] Guinn, V. P. and Lukens, Jr., H. R., in *Trace Analysis: Physical Methods*, G. H. Morrison, Ed., John Wiley and Sons, New York, 1965.

[5] Pinta, M., *Modern Methods for Trace Element Analysis*, Ann Arbor Science, Ann Arbor, MI, 1978.

[6] Khalil, S. R., Koppenaal, D. W. and Ehmann, W. D., *Anal. Letters,* Vol. 13, 1980, p. 1063.

[7] Khalil, S. R., Koppenaal, D. W. and Ehmann, W. D., *J. Radioanal. Chem.,* Vol. 57, 1980, p. 195.

[8] James, W. D., Ehmann, W. D., Hamrin, C. E. and Chyi, L. L., *J. Radioanal. Chem.,* Vol. 32, 1976, p. 195.

[9] Chyi, L. L., James, W. D., Ehmann, W. D., Sun, G. H. and Hamrin, C. E., *Proc. Sci. Ind. Appl. Small Accelerators,* Vol. 4, 1976, p. 281.
[10] Ehmann, W. D., Koppenaal, D. W. and Khalil, S. R., in *Atomic and Nuclear Methods in Fossil Energy Research*, Plenum Press, New York, 1982.
[11] Ehmann, W. D., Khalil, S. R. and Koppenaal, D. W., *J. Radioanal. Chem.,* Vol. 59, 1980, p. 407.
[12] Jacobs, F. S. and Filby, R. H., in *Atomic and Nuclear Methods in Fossil Energy Research*, Plenum Press, New York, 1982.
[13] Orange, J. M. and Larson, J. G., *Anal. Instrum.,* Vol. 13, 1975, p. 87.
[14] Filby, R. H. and Shah, K. R., in *Nucl. Methods Environ. Res.,* Vol. 1, 1971, p. 86.
[15] Lukens, H. R., Bryan, N. A. and Schlesinger, H. L., Gulf-RT-A-10684, 1971.
[16] Lukens, H. R., Gulf-RT-A-10973, 1972.
[17] Ruzicka, J. and Stary, J., *Talanta,* Vol. 10, 1963, p. 287; and Vol. 11, 1964, p. 697.
[18] Ruzicka, J. and Stary, J., *Substoichiometry in Radiochemical Analysis*, Pergamon Press, Oxford, U.K., 1968.
[19] Nadkarni, R. A., "Substoichiometry in Neutron Activation Analysis," *J. Radioanal. Chem.,* Vol. 20, 1974, pp. 139–158.
[20] Shah, K. R., Filby, R. H. and Haller, W. A., *J. Radioanal. Chem.,* Vol. 6, 1970, p. 413.
[21] Filby, R. H. and Jacobs, F. S., *Anal. Chem.,* Vol. 55, 1983, p. 74.
[22] Jervis, R. E., Ho, K. L. R. and Tiefenbach, B., *J. Radioanal. Chem.,* Vol. 71, 1982, p. 225.
[23] Block, C. and Dams, R., *J. Radioanal. Chem.,* Vol. 46, 1978, p. 137.
[24] Meier, H., Zeitler, G. and Menge, P., *J. Radioanal. Chem.,* Vol. 38, 1977, p. 267.
[25] Pouraghabagher, A. R. and Profio, A. E., *Anal. Chem.,* Vol. 46, 1974, p. 1223.
[26] Guinn, V. P., Lukens, H. R. and Steele, E. L., "The Role of Small Accelerators and Nuclear Reactors in Neutron Activation Analysis of Petroleum," *Proc. Amer. Petrol. Inst.,* Vol. 44-III, 1964, p. 234.
[27] Al-Shahristani, H. and Al-Atyia, M. J., *J. Radioanal. Chem.,* Vol. 14, 1973, p. 401.
[28] Meyer, G. A., *Anal. Chem.,* Vol. 59, 1987, p. 1345A.
[29] Persiani, C. and Shelby, W. D., *Environ. Sci. Technol.,* Vol. 7, 1973, p. 125.
[30] Colombo, U. P., Sironi, G., Fasolo, G. B. and Malvaro, R., *Anal. Chem.,* Vol. 36, 1964, p. 802.
[31] Yule, H. P., *Nucl. Applic.,* Vol. 3, 1967, p. 637.
[32] Flaherty, J. P. and Eldrige, H. B., *Appl. Spectrometry,* Vol. 24, 1970, p. 534.
[33] Filby, R. H., et al., Eds., *Atomic and Nuclear Methods in Fossil Energy Research*, Plenum Press, New York, 1982.
[34] Beunafama, H. D., in *Atomic and Nuclear Methods in Fossil Energy Research*, R. H. Filby et al., Eds., Plenum Press, New York, 1982, p. 29.
[35] Filby, R. H. and Shah, K. R., in *Role of Trace Elements in Petroleum*, T. F. Yen, Ed., Ann Arbor Science Publishers, Ann Arbor, MI, 1975, pp. 89.
[36] Ndiokwere, C. L., *Radiochem. Radioanal. Lett.,* Vol. 59, 1983, p. 201.
[37] Block, C. and Dams, R., *J. Radioanal. Chem.,* Vol. 46, 1978, p. 137.
[38] Guinn, V. P., "Activation Analysis in the Petroleum and Chemical Industry," in *Activation Analysis: Principles and Applications*, J. M. A. Lenihan and S. J. Thomson, Eds., Academic Press, New York, 1965, p. 129.
[39] Veal, D. J., "Nondestructive Activation Analysis of Crude Oils for Arsenic to One ppb and the Simultaneous Determination of Five Other Trace Elements," *Anal. Chem.,* Vol. 38, 1966, p. 1080.
[40] Braier, H. A. and Mott, W. E., "Activation Analysis for Chlorine in Petroleum Products and Related Materials," *Nucl. Appl.,* Vol. 2, 1966, p. 44.
[41] Jester, W. A. and Klaus, E. E., "Activation Analysis of High Purity Lubricants for Trace Elements," *Nucl. Appl.*, Vol. 3, 1967, p. 375.

[42] Shah, K. R., Filby, R. H. and Haller, W. A., "Determination of Trace Elements in Petroleum by Neutron Activation Analysis. I. Determination of Na, S, Cl, K, Ca, V, Mn, Cu, Ga, and Br," *J. Radioanal. Chem.,* Vol. 6, 1970, p. 185.

[43] Shah, K. R., Filby, R. H. and Haller, W. A., "Determination of Trace Elements in Petroleum by Neutron Activation Analysis. II. Determination of Sc, Cr, Fe, Co, Ni, Zn, As, Sc, Sb, Eu, Au, Hg, and U," *J. Radioanal. Chem.,* Vol. 6, 1970, p. 413.

[44] Lukens, H. R., Bryan, D. E. and Hiatt, M. A., "Oil Slick Identification Certainties with the Method of Neutron Activation Analysis," in *Nuclear Methods in Environmental Research*, University of Missouri, Columbia, MO, 1971, p. 62.

[45] Filby, R. H. and Shah, K. R., "Mode of Occurrence of Trace Elements in Petroleum and Relationship to Oil-Spill Identification Methods," in *Nuclear Methods in Environmental Research*, University of Missouri, Columbia, MO, 1971, p. 86.

[46] Mandler, J. W., Reed, J. H. and Moler, R. B., "Oil Slick Identification Utilizing Charged Particle Activation Techniques," in *Nuclear Methods in Environmental Research*, University of Missouri, Columbia, MO, 1971, p. 111.

[47] Filby, R. H. and Shah, K. R., "Determination of Cadmium in Petroleum by Neutron Activation Analysis," *Symp. Role of Trace Metals in Petroleum*, Chicago, IL, 1973, p. 615.

[48] Filby, R. H., "Trace Element Distribution in Petroleum Components," *Symp. Role of Trace Elements in Petroleum*, Chicago, IL, 1973, p. 630.

[49] Profio A. E. and Pouraghabagher, A. R., "Capture Gamma Ray Analysis of Sulfur in Oil," *Trans. Amer. Nucl. Soc.,* Vol. 21, 1975, p. 109.

[50] Larson, J. O. and Tandeski, E. V., "Analysis of Petroleum for Trace Metals: Loss of Mercury from Polyethylene Samples Vials in Neutron Activation Analysis," *Anal. Chem.,* Vol. 47, 1975, p. 1475.

[51] Fruchter, J. S., Laul, J. C., Petersen, M. R., Ryan, P. W. and Turner, M. E., *Amer. Chem. Soc. Advances in Chemistry Series,* Vol. 170, 1978, p. 255.

16

A Review of Applications of NMR Spectroscopy in the Petroleum Industry

John C. Edwards[1]

NUCLEAR MAGNETIC RESONANCE (NMR) SPECTROSCOPY HAS been applied to petroleum chemistry since the first days of its commercial existence. Petroleum companies such as Texaco and Marathon were among the first to use ^{1}H NMR to provide detailed information on the hydrocarbon chemistry of raw petroleum and its various products. The literature associated with almost 60 years of applications is large and cannot be accommodated in a single book chapter. However, there have been numerous reviews of petroleum NMR applications as well as a number of excellent articles and book chapters that cover the literature up to the early 1990s [1–6]. Since then, there have been no definitive books or review chapters published, though the use of NMR throughout the petroleum chemistry research arena has been widespread. In this chapter we concentrate on the applications that have been developed over the past two decades and how NMR technology has developed to encompass the entire scope of petroleum chemistry from down-hole exploration tools to online refinery process analysis.

NMR continues to be an exceedingly useful tool to study the proton and carbon chemistry of many petroleum-derived products and raw materials. We discuss liquid and solid-state NMR applications and also the application of NMR to raw materials previously not considered as petroleum. In this period of alternative energy awareness, it is important to include many alternative energy applications such as coal-to-liquids, gas-to-liquids, biofuels, and biomass conversion. The synthetic fuel products produced by these processes will become increasingly the focus of research and analysis, and NMR offers a unique perspective on the chemistry of these products. Rather than go into a detailed description of NMR spectroscopy theory, a brief description of current NMR technology is provided along with an overview of how the various technology platforms are being used to supply detailed physical and chemical information on a broad range of petroleum-related materials.

NMR SPECTROSCOPY

NMR is a radiofrequency spectroscopy that is based on the electromagnetic manipulation of nuclear spins. As a fall-out from the development of radar technology in World War II, scientists used radio frequency (RF) spectrometers and permanent magnet systems to confirm the presence of nuclear magnetic moments and in doing so produced a spectroscopy that has become one of the principal tools for hydrocarbon chemical analysis. Though many nuclei in the periodic table are NMR active, the petroleum analysis field is dominated by the application to ^{1}H and

[1] *Process NMR Associates, LLC, Danbury, Connecticut*

^{13}C nuclei. Other nuclei of interest to petroleum chemists, particularly in the catalytic research area, are ^{2}H, ^{29}Si, ^{27}Al, ^{31}P, ^{11}B, ^{23}Na, and ^{15}N.

The physical basis of the NMR technique is the interaction of nuclear magnetic moment of certain nuclei with applied magnetic fields. The nuclear magnetism arises from the fact that the nucleus contains an odd number of nucleons (protons and neutrons). When these nuclei are placed in a strong magnetic field, provided by a superconducting solenoid magnet or a permanent magnet, each nuclear spin aligns with the applied field and precesses around it with a unique frequency, called the Larmor frequency, directly proportional to the applied field. If the precessing spins are irradiated at a resonance frequency corresponding to their particular precession frequency (radiofrequency energy range: 100 kHz to 900 MHz, depending on the magnetic field strength), there is a resonant adsorption of the applied radiofrequency energy. This energy adsorption, at the Larmor frequency, causes the magnetic moments of the nucleus under observation to move out of alignment with the applied external magnetic field, and when the radiofrequency pulse is turned off, the spins are restored to equilibrium alignment.

The rates at which this realignment with the applied magnetic field occurs are referred to as relaxation times [7]. The rate at which the spins align along the magnetic field axis is referred to as spin-lattice relaxation time (T_1), and the rate at which spin coherence is lost in the perpendicular plane of the laboratory magnetic field is referred to as the spin-spin relaxation time (T_2). The values of these relaxation times contain inherent information about the interactions of the nuclear spins with their physical and chemical environment. Differences in T_1 and T_2 are indicative of molecular structure, chemistry, and intermolecular interactions. Relative differences in the absolute value and the distribution of T_1 or T_2 values can be used to great advantage when observing NMR-active nuclei in molecules present in a complex mixture such as petroleum-related materials. Of note are the T_1 and T_2 differences observed between hydrocarbons and water due to the higher diffusion rates of water. Also of interest are the shorter proton T_2 times found in asphaltenes and heavy residue samples due to the high molecular weight and paramagnetic content with metals such as vanadium being present.

The precession of the spins as they realign with the applied magnetic field generates a voltage in the NMR probe coil within which the sample is situated. The ^{1}H and ^{13}C nuclei in different chemical environments on a petroleum-derived molecule have different electronic environments that affect the precession frequency of the nucleus, which leads to a dispersion of signals that yield chemical information about the nuclei producing that signal. These electronically induced signal dispersions are called chemical shifts, and they allow analysts to observe and quantify various chemical functionalities and determine absolute molecular structure. The voltage generated in the coil contains a dispersion of frequencies related to the chemical makeup of the sample. This voltage is collected by the NMR spectrometer through an analog-to-digital converter and stored as the raw data of the NMR analysis. This stored signal is called the free induction decay (FID). In low field (time domain) TD-NMR, the FID is typically the final result of the experiment. In high-field, high-resolution NMR, the Fourier transformation of the FID yields a frequency spectrum that contains resonance peaks corresponding to protons or carbons in different

TABLE 1—^{1}H Chemical Shift Ranges for Various Proton Types Present in Petroleum

Description	Start (ppm)	End (ppm)
Triaromatic CH	9	8
Diaromatic CH	8	7.25
Monoaromatic CH	7.25	6.4
Total Aromatic H	9	6.4
Olefinic CH/CH_2	6.4	4.5
CH_2 Alpha to 2 Aromatics	4.5	3.4
Alpha-CH	3.4	2.8
Alpha-CH_2	2.8	2.4
Alpha-CH_3	2.4	2
Beta Paraffinic CH/CH_2 and Naphthenic CH/CH_2	2	1.28
Epsilon CH_2 (Long Chain)	1.28	1.24
Paraffinic CH_2 and Beta CH_3	1.24	1
CH_3 (Gamma)	0.95	0.5
Total Aliphatic H	4.5	0.5

chemical environments. The areas under the peaks are quantitative to the amount of ^{1}H or ^{13}C present as that chemical type. Integration of the peaks and subsequent manipulations and calculations yield quantitative proton and carbon type analyses as well as average molecule representations.

Further description of the NMR phenomenon and the experimental developments in multinuclear and multidimensional NMR is beyond the scope of this review but can be found in the extensive NMR literature [8–11]. Tables 1 and 2 show the basic chemical shifts observed for ^{1}H and ^{13}C NMR nuclei, respectively.

NMR TECHNOLOGY BACKGROUND

It is important to briefly describe the NMR technologies that are currently available for the analyst to study petroleum chemistry and production processes. Contrary to conventional perception, NMR technology is robust, is relatively easy to execute, and can be relatively inexpensive to implement. Although NMR manufacturers and users have always driven the technology to higher and higher magnetic field strengths requiring superconducting magnet technologies, for much of petroleum chemistry, extra-high magnetic field strengths are overkill because of the complex mixture nature of petroleum samples, which means the spectra consist of many hundreds, if not thousands, of unresolved peaks. Critical and complete information can be obtained for lower magnetic field instruments operating at or below 400 MHz. In fact, for solid-state ^{13}C, NMR operating at frequencies at or below 200 MHz has particular advantages

TABLE 2—^{13}C Chemical Shift Ranges for Carbon Types Present in Petroleum

Description	Start (ppm)	End (ppm)
Carbonyl	215	190
Carboxyl	190	160
Phenolic Carbon	160	150
CH_2/CH Substituted Aromatic Carbon	150	138
Naphthene Substituted Aromatic Carbon	138	135
Methyl Substituted Aromatic Carbon	135	133
Internal Aromatic Carbon	133	129.5
Internal + Protonated Aromatic Carbon	129.5	124
Protonated Aromatic Carbon	124	120
Heteroaromatic Carbon	120	90
Methine Carbon	60	37
Methylene Carbon	37	22.5
Alpha Methyl Carbon	22.5	20
Methyl Carbon	20	0.5

that are described later. Developments in permanent magnet technology, spectrometer design, and materials have also enabled the development of compact NMR systems that can be used for online process control or for mobile NMR analysis. Several types of NMR instrumentation are used in petroleum chemistry studies, and each is described briefly in the coming sections along with applications that are performed with each type.

LOW-RESOLUTION NMR, ALSO KNOWN AS TIME-DOMAIN NMR

Low-resolution NMR instruments are the smallest, lowest cost implementation of NMR technology and are serviced by several commercial companies such as Bruker, Oxford Instruments, Magritek, and Process NMR Associates. They are based on small permanent magnet systems that produce relatively inhomogeneous fields at strengths of 0.04–1.47 T (corresponding to ^{1}H resonance frequencies of 2–60 MHz). Depending on the manufacturer and the applications desired, the instrumentation costs between $25,000 and $60,000. The magnetic field produced by these small magnet systems is inhomogeneous, and only very basic NMR data can be obtained related to total hydrogen content or relaxation times of protons in the sample. Relaxation times, T_1 and T_2, are time constants that can be determined from multipulse NMR experiments that are related to molecular mobility, viscosity, and paramagnetic nuclear interactions. The relaxation times can also be used to determine water content in oil or oil content in water. Obviously, these parameters are of interest to petroleum chemists

Fig. 1—Typical TD-NMR Bench-top Spectrometer operating at 20 MHz, comprises a digital spectrometer (left), which is USB connected to a small computer. The 10-mm magnet system (right) weighs 8.5 kg and is 16 by 16 by 16 cm in dimension.

because these relaxation times can be attributed to chemical and physical properties of petroleum materials, such as molecular size, asphaltene content, wax content, vanadium content of heavy ends, hydrogen content of all streams undergoing further processing, and water content of crude oils. Fig. 1 shows a typical bench-top TD-NMR system. Typical NMR data produced by such a system are shown in Fig. 2. Instruments of this type have been used extensively in down-hole tools operated by oil exploration and production companies. Excellent overviews of time-domain (TD) NMR technology used for down-hole analysis have been published by these companies [12–13], and the patent literature is filled with new instrument designs and applications. Over the past decade, developments in multipulse sequences and mathematical algorithms (such as one- and two-dimensional Laplace inversions) have allowed distributions of relaxation times to be determined as well as the correlation between T_1 and T_2, or T_2 and diffusion coefficients [14–15]. These new developments have opened up new avenues of research to discern chemical and physical differences between petroleum samples.

HIGH-RESOLUTION NMR AT LOW MAGNETIC FIELDS: PROCESS NMR INSTRUMENTATION

High-resolution NMR was developed in the 1990s and is based on arrays of NdFeB permanent magnets that allow for the production of an intermediate magnetic field strength (1.47 T), high basic field homogeneity, and tight magnet temperature control. Mechanical and electrical shim systems allow high-resolution NMR data to be obtained at a resolution of about 0.025 ppm and a ^1H resonance frequency of 60 MHz. Currently there is only one manufacturer of this type of NMR instrumentation. The magnet itself is fully shielded (has no external fringe field), is stable, and is field mountable in chemical plants and refineries. Laboratory versions of the instrument cost about $80,000; field-mountable systems cost $200,000 to $450,000, depending on the application and the number of streams to be analyzed and their sample handling requirements. Online process

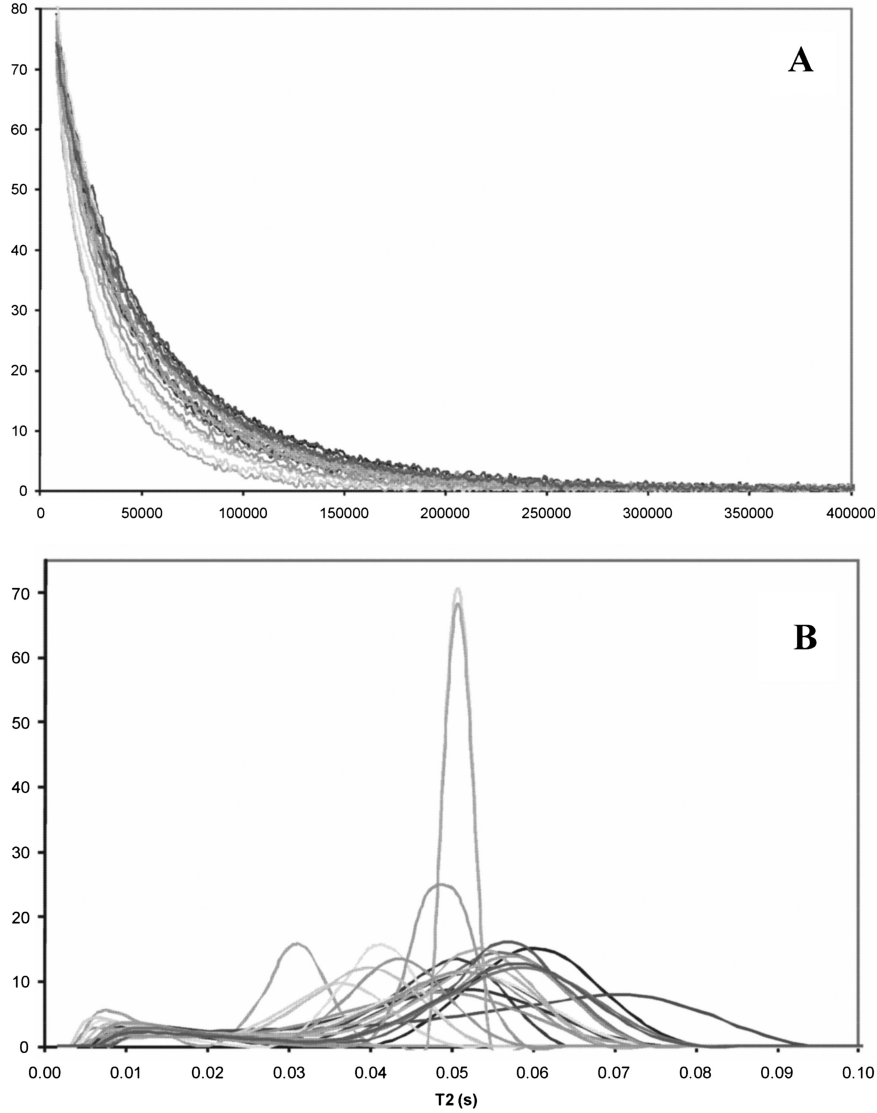

Fig. 2—(A) T_2 relaxation curves from CPMG (Carr-Purcell-Meiboom-Gill) experiments on a 20 MHz TD-NMR instrument, and (B) calculated T_2 distributions obtained from inverse Laplace transformation, for fluid catalytic cracker (FCC) feeds showing differences in heavy/light component concentrations as well as viscosity and paramagnetic content.

control applications involve correlation of ^{1}H NMR spectral variability with chemical and physical properties of interest to engineers for continuous quality assessment or feed-forward and feed-back process control and optimization of refining processes. Laboratory configurations of the instrument are available for at-line analysis and laboratory-based application development. A Qualion 60 MHz NMR system is shown in Fig. 3. This spectrometer is available in a laboratory

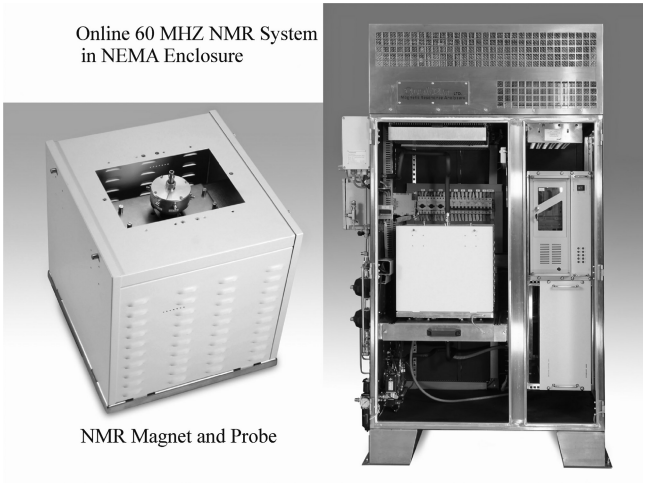

Fig. 3—60 MHz high–resolution process NMR spectrometer.

configuration and as a fully certified online instrument housed in an explosion-proof housing.

Typical ^{1}H NMR spectra of finished gasoline product obtained on such an instrument are shown in Fig. 4 with a description of the proton chemistry observed. At the present time approximately 25 process NMR systems are online at various refineries around the world.

HIGH-FIELD (>200 MHz) NMR INSTRUMENTATION FOR LIQUID AND SOLID-STATE NMR ANALYSIS

The NMR instrumentation used to derive detailed multinuclear hydrocarbon information is based on superconducting magnet technologies that allow

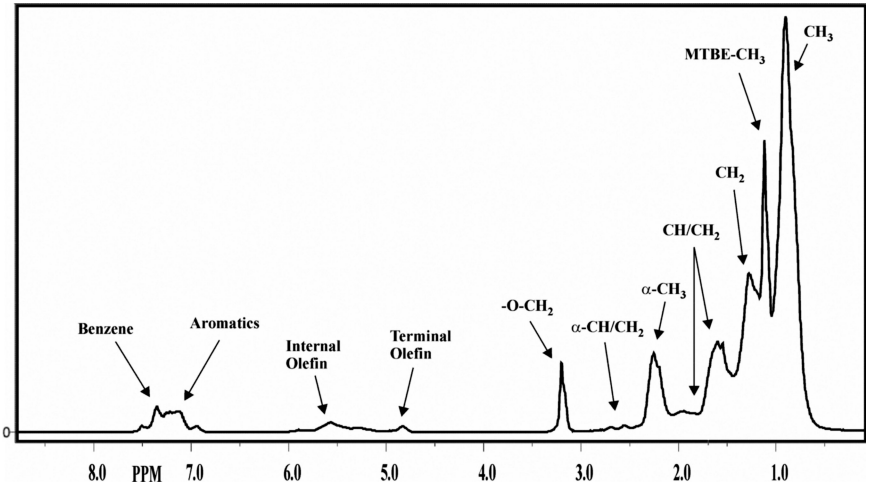

Fig. 4—60 MHz ^{1}H NMR of a finished gasoline obtained on a process NMR unit.

high-resolution NMR to be obtained at resonance frequencies of 200–1000 MHz for ^{1}H, and 50–250 MHz for ^{13}C. The cryogenically cooled magnet solenoids are immersed in liquid helium (fill frequency of 3 months to 1 year) and further insulated by a jacket of liquid nitrogen (fill frequency 10–14 days). As the magnetic field strength increases, the instrument price rises from $200,000 to as much as $4,000,000. With increasing magnetic field strength the experimental sensitivity increases, meaning that experiments take less time and the spectral resolution improves, yielding higher resolving power between different types of ^{1}H or ^{13}C chemistry. However, in the author's experience, instrumentation with field strengths of 7–11.7 T (^{1}H resonance frequencies of 300–500 MHz) is adequate for most liquid-state petroleum applications as the higher resolving power at very high fields does not provide any extra discernment of detailed chemistry. In the case of solid-state NMR experiments (typically performing ^{13}C NMR analysis on carbonaceous materials), field strengths of 2.35–4.7 T (^{1}H resonance frequency of 100–200 MHz) are optimal for quantitative and qualitative experiments because they allow slower magic angle spinning (MAS) speeds to be used while avoiding overlap of aromatic carbon spinning sidebands with aliphatic carbons. Solid-state NMR instrumentation is essentially laboratory based, and very few implementations of the technology have been applied anywhere outside the typical research center laboratory environment. As a comparison of the higher resolution of ^{1}H NMR experiments performed on superconducting NMR systems with the 60 MHz NMR systems, several spectra of a diesel fuel are shown from the two spectrometers in Fig. 5. More peaks are resolved at

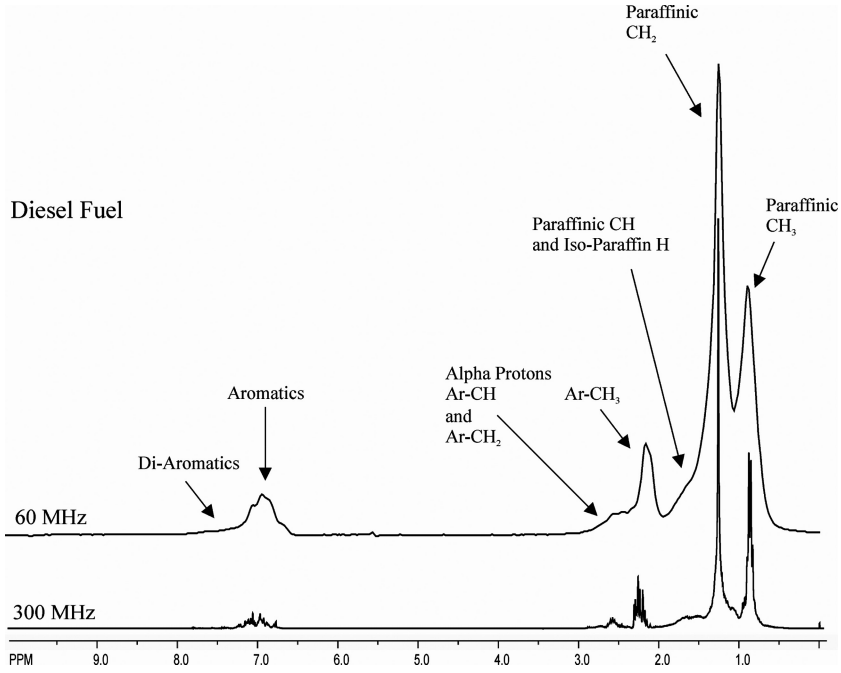

Fig. 5—^{1}H NMR of diesel fuel at different resonance frequencies: 60 MHz process NMR and 300 MHz superconducting NMR. Observed proton chemistry is indicated on the spectrum.

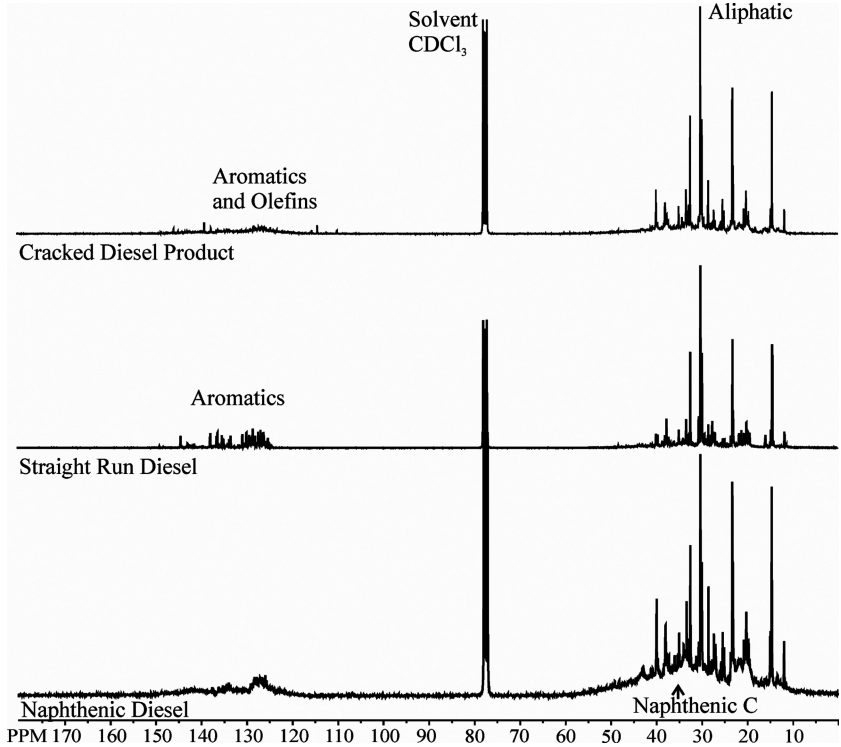

Fig. 6—Quantitative ^{13}C NMR on three diesel fuels from different refinery processes. Cracked diesel shows the presence of olefinic carbon, straight run diesel shows a narrow distribution of aromatics, and naphthenic diesel shows a typical "hump" in the aliphatic carbon region. This hump can be quantified to calculate the fraction of naphthenic and paraffinic carbons.

300 MHz, but the overall chemistry can be seen to be the same. Examples of the corresponding ^{13}C NMR spectra of different diesel fuels are shown in Fig. 6.

As described in previous reviews, high resolution/high field NMR instrumentation also brings the entire range of NMR experiments to bear on petroleum chemistry. Multidimensional NMR experiments such as correlation spectroscopy (COSY) and heteronuclear correlation (HETCOR) can yield important information about ^{1}H–^{1}H and ^{1}H–^{13}C connectivity on petroleum molecules. This can be a very important tool to allow analysis and quantification of difficult-to-observe chemical functionality in NMR spectra of complex mixtures when NMR signals are highly overlapped. As an example, identifying conjugated di-olefins is made possible by ^{1}H–^{1}H COSY experiments where the olefin chemical shift range can be used to show the presence of protons that are adjacent to each other on conjugated olefin double bonds [16]. An example of a COSY result obtained on a coker naphtha is shown in Fig. 7.

Another useful ^{1}H–^{13}C NMR technique known as distortionless enhancement by polarization transfer (DEPT) allows discernment between methyl (CH_3), methylene (CH_2), methane (CH), and quaternary carbons. This technique is a vital component in the analysis of hydrocarbon branching, as well as providing

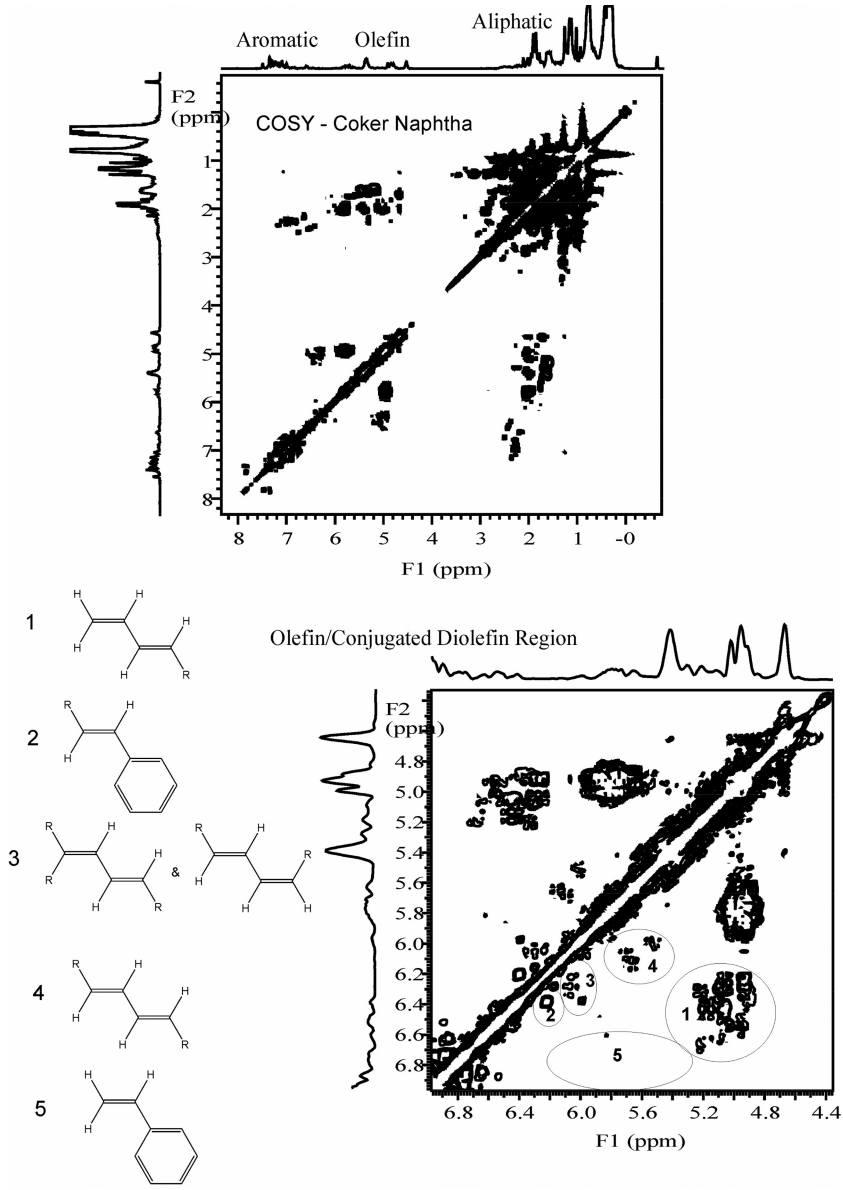

Fig. 7—^{1}H–^{1}H COSY (correlation spectroscopy) of a coker naphtha stream. Correlation of olefinic protons with adjacent olefin and aromatic protons yields a distribution of conjugated diolefins that can then be quantified in the one-dimensional NMR spectrum.

data crucial to the calculation of aromatic ring system sizes and average molecule descriptions. An example of a DEPT NMR result is shown in Fig. 8. Comparison of the signal intensity observed in the aromatic CH region of both the DEPT and quantitative ^{13}C spectra of heavy petroleum materials, compared to the signal intensity of methylenes in a known weight of a standard material

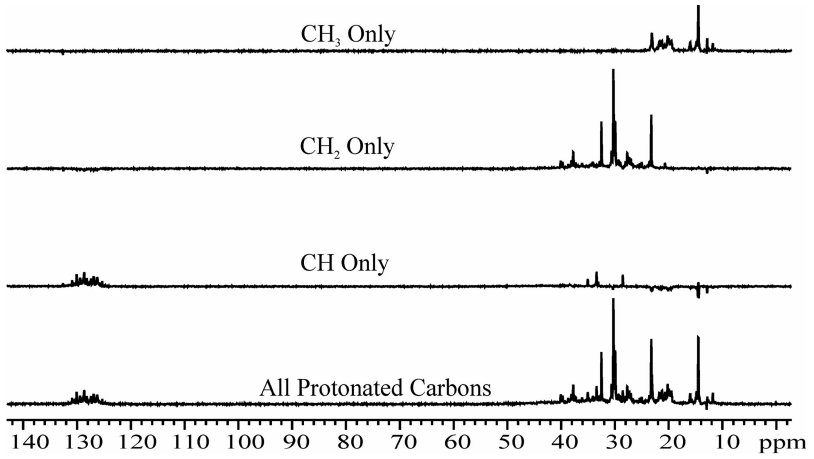

Fig. 8—^{1}H–^{13}C DEPT NMR of a diesel fuel showing the calculated subspectra for CH_3, CH_2, and CH carbons; quaternary carbons are not observed. Comparison of DEPT results with the quantitative ^{13}C single pulse excitation spectrum allows quaternary carbons to be identified and quantified.

(such as 1500 molecular weight polyethyleneglycol [PEG-1500]), can allow the mole fraction of bridgehead aromatic carbons to be calculated. This then facilitates the further calculation of average aromatic ring size and many average molecule parameters. In conjunction with carbon type analysis, these average molecule parameters describe the petroleum product in such a way that differences due to chemical and physical property variation as well as refinery processing can be observed and understood.

Solid-state ^{1}H and ^{13}C NMR is widely used to study heavy petroleum solids such as asphaltenes, coal, shale, bitumen, engine deposits, soots, biomass, refinery coke, refinery residues and tars, catalyst cokes, gums, lignites, humics, and soils. Fig. 9 shows a few example spectra obtained by solid-state ^{13}C NMR

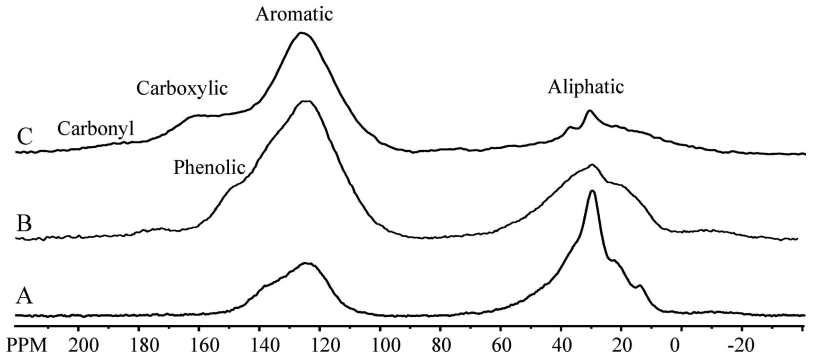

Fig. 9—Solid-state ^{13}C cross polarization spectra obtained with magic angle spinning and high power inverse-gated decoupling: A) petroleum-precipitated asphaltene, B) Illinois No. 6 coal, and C) gasoline engine combustion chamber deposit.

with cross-polarization. Carbon type analysis as well as average molecule parameters can be derived from integration or deconvolution of these spectra. Of particular interest is the carbon aromaticity and phenolic and carboxylic content, as well as the average aromatic cluster size. These techniques involve higher powered RF pulses and specialized NMR probes. In solid samples the molecules are not tumbling rapidly as they do in the liquid state. This means that internuclear spin-spin interactions (dipolar couplings) and orientation dependent interactions between static electronic environments and the magnetic field (chemical shift anisotropy) cause severe broadening of the NMR peaks, leading to peaks that are several kilohertz wide and from which little detailed chemical information can be obtained. The higher power levels are required to adequately excite the broad spectral range of NMR signals and to adequately decouple ^{1}H from ^{13}C in the gated acquisition of ^{13}C FIDs. The probes are designed to allow high power operation and to rapidly spin the solid samples at a "magic angle" orientation about the applied magnetic field. In the case of ^{1}H and ^{13}C NMR experiments, the mathematical derivations of the dipole-dipole coupling and chemical shift anisotropy contain a sample orientation related multiplication factor of $(3Cos^{2}\theta–1)$. When the sample is oriented at $54^{o}44'$ with respect to the applied magnetic field, and spun rapidly (3–50 kHz), the broadening interactions are averaged away and high-resolution isotropic resonances are obtained. An artifact of the solid-state MAS experiment is that in the case of larger chemical shift anisotropy carbons (such as aromatic or carboxylic carbons), spinning sidebands are observed in the spectrum at multiples of the spinning frequency. Along with the isotropic resonances, these sideband peaks must be quantified as part of the signal intensity from these carbon types. Application of this technique to ^{13}C has been very successful over the years, though ^{1}H is still challenging because of the extremely strong dipole-dipole interaction that cannot be removed by slower MAS speeds and homonuclear decoupling schemes. The MAS probes employ high tolerance ceramics and air drive/bearing systems that spin cylindrical ceramic rotors containing the sample. These rotors can be 1.5–14 mm in diameter and be spun at rates of 40–50 kHz and 2–3 kHz, respectively.

APPLICATIONS: LOW-FIELD NMR

The first and most obvious application of low-field NMR (2-30 MHz) to petroleum characterization was the early development in the 1950s of a continuous wave NMR analyzer that observes an absorbtive NMR signal by sweeping through a range of radio frequencies, typically centered on 20 MHz. The strength of the NMR absorption could be calibrated using standard materials (such as pure toluene or dodecane) to yield an absolute weight % hydrogen content value. ASTM methods were developed using this technology–D3701 [17] for the hydrogen content analysis of aviation turbine fuels, and D4808 [18] for the hydrogen content analysis of light and middle distillates, gas oils, and residua. However, the NMR technology and methodology used in the development of these methods are now obsolete as low-field bench-top instrumentation has moved from frequency sweeping where single frequencies are sequentially irradiated to pulsed radio frequency technology where a broadband range of radio frequencies are simultaneously excited. In the 1990s an effort was undertaken to develop an ASTM method based on current pulsed NMR technology to replace the previous

obsolete methods. The product of that development was ASTM D7171 (Standard Test Method for Hydrogen Content of Middle Distillate Petroleum Products by Low-Resolution Pulsed Nuclear Magnetic Resonance Spectroscopy) [19]. This method yields the same information as the previous methods and allows the use of modern spectrometers [20]. Variations of the method using deuterated solvents have also been developed to allow analysis of sample limited quantities of petroleum materials or particularly heavy petroleum products that are difficult to handle and introduce into the spectrometer for analysis. These test methods involve the NMR signal intensity measurement of known weights of a series of standards (pure petroleum components such as dodecane, which is 15.386 wt % hydrogen) compared to the signal intensity of a known weight of the unknown petroleum sample. Direct comparison of the intensity after adjustment for sample weight yields the weight % hydrogen of the sample. The use of TD-NMR in a refinery has been limited predominantly to hydrogen content analysis alone, and the technology is confined to the laboratory and has yet to migrate to online application.

By far the most prevalent use of NMR in the exploration industry is in well logging, where NMR incorporated into down-hole tools yields quantitative information on the presence of water and oil mixtures as well as the viscosity of the formation liquids and the porosity of the formation [12–15]. Discernment of water from hydrocarbon is relatively straightforward because the diffusion coefficient of water is considerably greater than that of hydrocarbons, which leads to considerable differences in relaxation behavior. These applications developed from strong research efforts into a combination of rugged instrument design for high pressure and temperature operation, unilateral magnet designs, and the development of one- and two-dimensional Laplace inversion algorithms applied to multipulse NMR experimental data. Numerous articles have been published on the subject, and it is currently an active area of development. By a combination of T_1, T_2, diffusion, and hydrogen index measurements, in combination with the density, temperature, and pressure of the fluids, it is possible to identify the fluid type, formation porosity and permeability, water saturation level, oil viscosity, and gas content. These analyses are performed on dead crudes (degassed) and live crudes (pressurized samples containing gas). Much emphasis is placed on the discrimination of different distributions of T_1 and T_2 relaxation times as well as the interdependence of the relaxation profiles with each other by means of two-dimensional T_1-T_2, T_2-diffusion, and T_1-diffusion. It is an obvious extension of this approach that three-dimensional T_2-T_1-D relaxometry is plausible to find added dimensions of variability in NMR-derived data. The distributions and relaxation phenomena allow the separation and quantification of overlapping fluid signals such as those arising from heavy oil hydrocarbons and capillary-bound and clay-bound water. T_2 measurements are obtained from CPMG (Carr-Purcell-Meiboom-Gill) echo experiments. T_1 measurement is obtained from inversion recovery or 90-tau-90 experiments, and diffusion coefficients are derived from a series of echo experiments with pulsed field gradients applied during the echo-delay (PGSE, pulsed gradient solid echo). Two-dimensional correlations of these relaxation and diffusion parameters are obtained by T_1 or T_2 encoding before the observation experiment is performed [21–28]. Fig. 10 shows how a CPMG combined with PFG can generate 2D T_2-D rate data that yield information on porosity and heavy oil molecular weight distributions.

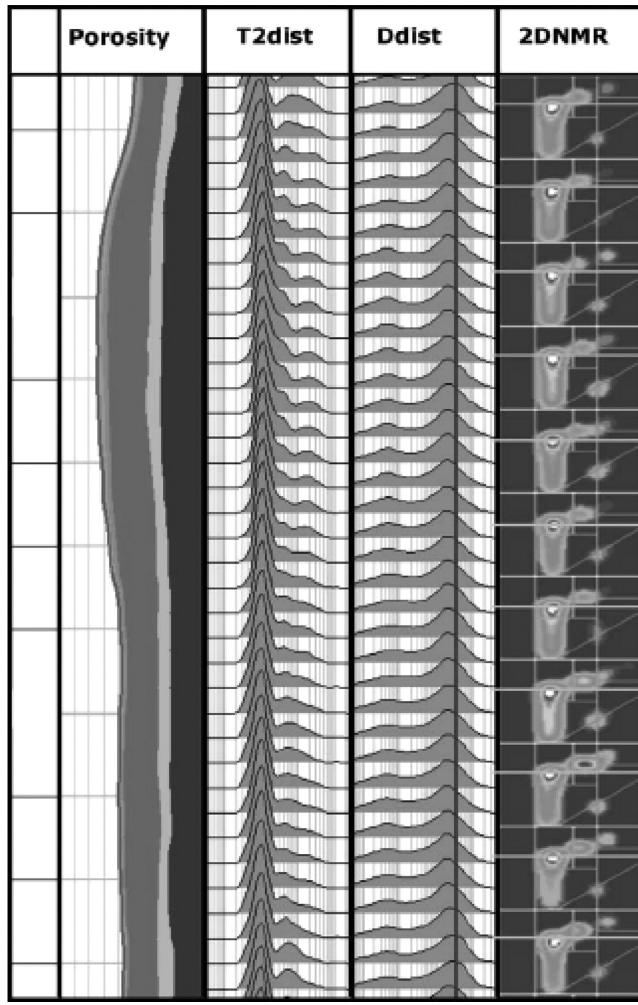

Fig. 10—2D NMR log obtained from the field. Shows T_2-D plot as well as the projections of the T_2 (Track 2) and D (Track 3) distributions. Track 1 shows the volume ratio of different fluid components. (Reprinted with permission from Ref [22]; © 2007 Elsevier.)

Another area of development for low-field NMR is the application to bitumen exploration and processing, particularly in the tar sand fields of Alberta [29]. The TD-NMR tools developed for well logging have been applied successfully to the estimation of bitumen content in cores taken in the field, and to the viscosity of bitumen, which is vital for successful recovery and processing operations [30]. Oil sands require multiple stages of processing before they are finally refined. Water-in-oil stability can prove to be a difficult processing issue because that processing must produce a complete separation of bitumen, water, and solids (such as clay) before refining. TD-NMR is well suited to the study of water-in-bitumen emulsions and the effect of processing conditions and addition of

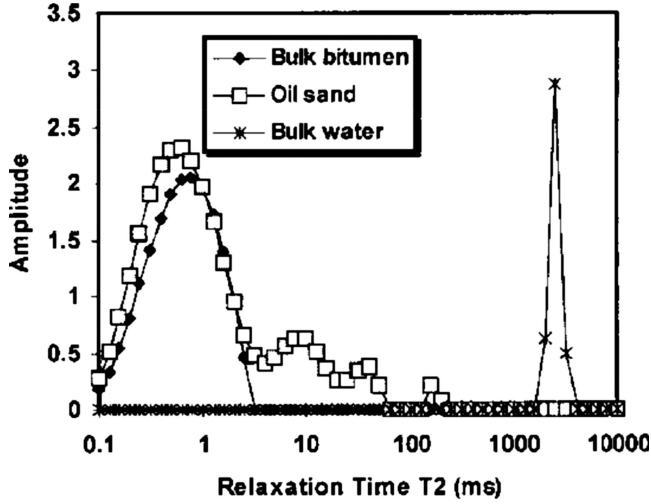

Fig. 11—T_2 distribution for an Alberta oil sand compared to the distribution from bulk water and bulk bitumen. (Reprinted with permission from Ref [29]; © 2005 Wiley.)

demulsifiers and naphtha on phase stability and drop-size distributions present in these mixtures. Asphaltene precipitation and flocculation as well as their rate dependence on asphaltene concentrations can be observed. NMR can also provide the relative quantities of solvent and water in bitumen froths and bitumen-solvent mixtures [31–32]. Fig. 11 shows an example of a T_2 distribution obtained on an Alberta tar sand compared to the T_2 distributions of bulk water and bitumen. Bulk water has a long T_2 of about 2 s, while the viscosity and paramagnetic content of bulk bitumen lead to a distribution of short T_2 relaxation times of 0.1–3 ms. In a tar sand sample, water is trapped in the pores of the sand and thus is interacting with the pore structures, which leads to shortened T_2 times compared to bulk water. From the plot shown here it is possible to determine the relative intensities of the water and bitumen components. Fig. 12 shows a plot of NMR-calculated water content versus the actual Dean Stark water measurement on the samples. The effect of processing conditions on the viscosity of the bitumen products is another vital parameter. Finally, the processing of process water will be an obvious extension of the application of TD-NMR technology to bitumen processing. NMR analysis of the hydrocarbon content of waste water and the characterization of tailings is an area that is being explored [33].

The effect of temperature on bitumen softening is of interest to civil engineers who wish to determine the role of bitumen chemistry on the mechanical properties and durability of asphalt layers on road construction [34]. NMR-based melting curves can be used to determine the correct bitumen to use in road construction in areas with different freeze-thaw and winter-summer temperature variations.

Australian coal researchers have developed a methodology to determine the hydrogen, carbon, and moisture content of coal. This approach involves the characterization of each coal as a signal intensity surface obtained by performing a 30-step T_1 encoding (the t1 dimension) of a pulse sequence that consists

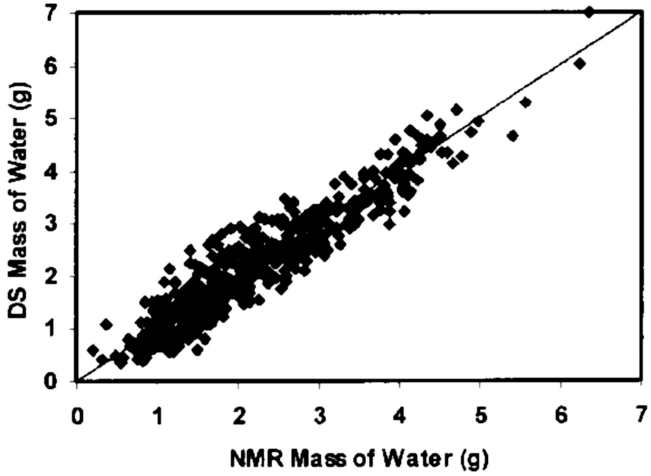

Fig. 12—NMR-predicted water content from T2 distributions obtained by CPMG and Laplace inversion versus Dean Stark water content of Alberta oil sand ores. (Reprinted with permission from Ref [29]; © 2005 Wiley.)

of an FID + 4 spin echoes (the t2 dimension). The resulting three-dimensional signal intensity surfaces were fit as a combination of five relaxation decays of exponential and Gaussian character. The relative contents of five identified proton components correlated to two types of water (interacting with clays and organic phase), as well as three types of organic protons (a rigid organic phase [80 % of protons], mobile aliphatic phase organics, and a high aromatic organic phase). The T_2 value of the rigid organic phase is affected greatly by chemical and physical changes caused by coalification, making this parameter a good indicator of coal rank [35]. From this quantification it was possible to determine the water, hydrogen, and carbon content of the coals. Taking the NMR analysis a step further, they introduced a temperature-dependent aspect to the experiment by obtaining the NMR parameters at a series of temperatures. Fig. 13 shows a plot of typical signal surface obtained from the experimental measurement as well as a plot of the relationship between the five components and the amplitude surface for each of the 275 coal samples analyzed.

The five calculated NMR parameters obtained at different temperatures were then utilized as a "coal NMR spectrum" (not a spectrum in the traditional sense), and a partial least squares regression was used to establish a correlation between the NMR relaxation "spectrum" and traditional coal parameters. Good correlations were obtained for wt % moisture, wt % volatile matter, wt % hydrogen, wt % carbon, wt % oxygen, gross specific energy, petrographic composition (vitrinite and intertinite vol %), and reflectance [36]. These analyses will be directly applicable to other carbonaceous solids such as kerogen, shale, coke, and various deposits.

Online process control using TD-NMR real-time analysis of refinery streams is currently not in practice but will soon be a reality thanks to the reduction in cost of basic NMR instrumentation capable of performing these measurements. Several companies are developing NMR platforms that can perform real-time

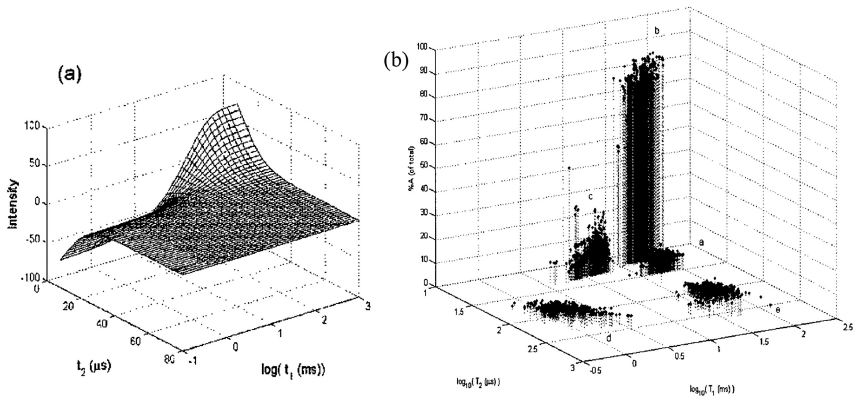

Fig. 13—Coal TD-NMR analysis: (a) signal amplitude surface obtained by inversion recovery encoding of an FID + 4 echoes sequence, and (b) the five NMR relaxation components for 275 coal samples that can be obtained from fitting the signal surfaces from each coal. (Reprinted with permission from Ref [35]; © 2001 Elsevier.)

hydrogen analysis and T_2-T_1-diffusion distribution analysis for analysis of heavy oils, bitumen, crude oils, and heavy refinery streams [37]. Use of such systems has been ongoing in the petrochemical industry where TD-NMR has been used for polyolefin analysis since the late 1980s [38–40].

APPLICATIONS: HIGH-RESOLUTION, LOW-FIELD NMR

High-resolution NMR performed at frequencies of 30–60 MHz have been carried out in NMR studies of petroleum starting in the early 1950s. However, as NMR superconducting magnet technology emerged in the 1960s (200 MHz systems), then improved to 300 + MHz during the 1970s and 1980s, the number of studies at 60 MHz decreased as continuous wave 60 MHz instruments such as the Varian EM-360 or JEOL FX-60 were replaced. In the early 1990s, a new permanent magnet/electrical shimming technology was developed that yielded small (60 kg), high homogeneity, inherently shielded, stable NMR magnet systems ideal for online process NMR and laboratory-based application development. In 1995, a 53 MHz NMR analyzer was placed on a fuel gas stream from a Texaco refinery's cogeneration unit in Los Angeles [41]. The analyzer measured Btu, specific gravity, methane content, hydrogen content, olefinic hydrogen, and hydrocarbon content; the NMR compared favorably with the GC analysis used before the NMR installation. Unlike the GC, the process NMR did not require component speciation to determine Btu and specific gravity. Rather, the Btu was calculated directly from the C–H bond types observed in the ^{1}H NMR spectrum. The following year, a process NMR system was installed on a Stratco Alkylation unit at the same refinery. The NMR response of the acid/hydrocarbon emulsion was used to calculate sulfuric acid strength (wt %). This was done by correlation of the varying acid peak position (relative to the stationary chemical shift values for covalent CH protons on the acid soluble oils and hydrocarbons in the emulsion) with titrated acid strength values [42]. A further development allowed ^{1}H NMR analysis of the spent acid to provide acid strength, acid soluble oil content, and water content. Fig. 14

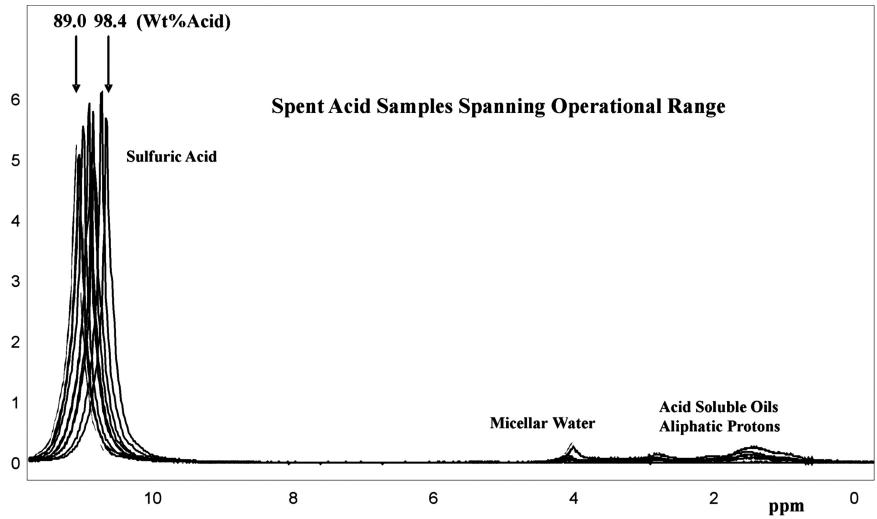

Fig. 14—Online ^{1}H NMR analysis of the spent acid present in a settler of a refinery alkylation unit.

shows the ^{1}H NMR spectra obtained on spent acid in the third settler of a train of refinery alkylation units. Acid strength is a vital number for control as low acid strength leads to runaway polymerization of the butane leading to process shutdown and major clean-up operations.

Since 1994, on-line process NMR applications have involved partial least-squares (PLS) regression modeling, where the entire (or partial) NMR spectral variability is regressed against chemical and physical parameter values obtained from primary testing methods (typically ASTM test methods). An early version of the process NMR equipment operating at 42 MHz was used to correlate ^{1}H NMR response to MTBE (methyl tertiary butyl ether) content in gasoline [43]. Meanwhile, Texaco researchers developed a number of PLS regression correlations for a wide range of gasolines between ^{1}H NMR and a number of chemical and physical properties such as ASTM research octane (ASTM D2699), motor octane (ASTM D2700), distillation values (ASTM D86 - T5, T10, T50, T90, T95), benzene content (ASTM D3606), aromatic content (ASTM D1319 and D5769), olefin content (by supercritical fluid chromatography [SFC] and ASTM D1319), oxygenate content (MTBE or ethanol by ASTM D5599), and density (ASTM D4052) [44]. An Australian refinery is currently using NMR to certify gasoline entering the gasoline pool [45].

A UK refinery is using full-spectrum PLS analysis of ^{1}H NMR spectra to control a reformer unit where the NMR predicts ASTM research octane (ASTM D2699), motor octane (ASTM D2700), benzene content (ASTM D3606), and aromatic content (ASTM D5769). Fig. 15 shows an example of stacked 60 MHz ^{1}H NMR data obtained on reformate samples with different research octane numbers. The ^{1}H spectra have been converted into 140 by 0.1 ppm integral bins; this is a process whereby the entire spectrum from 12 to -2 ppm is integrated every 0.1 ppm. This is a resolution reduction that improves the signal to noise

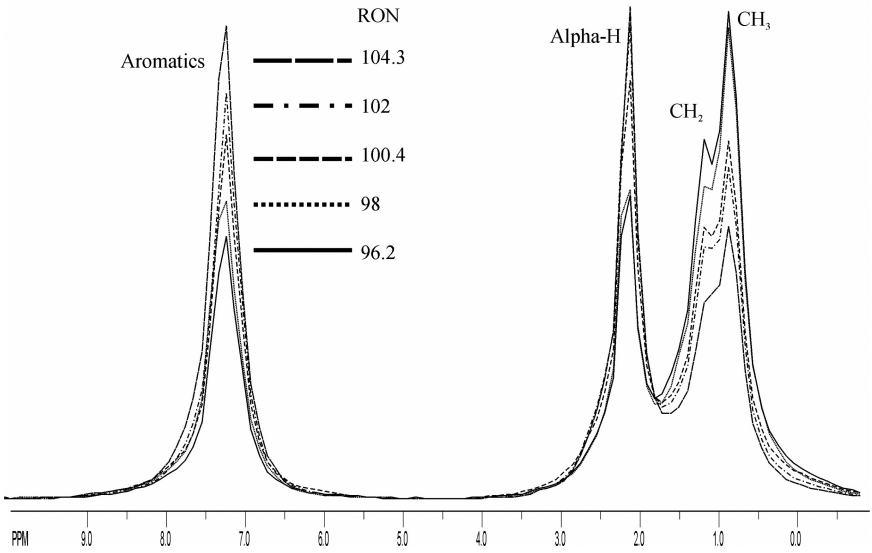

Fig. 15—^{1}H NMR spectra of reformates with different research octane numbers.

ratio of the data and allows various normalizations to be performed to avoid issues with density changes and presence of contaminants in the analysis streams.

Perhaps the most challenging PLS regression analysis has been between ^{1}H spectral variability and GC-PINA (gas chromatography - paraffins, isoparaffins, naphthenes, aromatics) analysis with speciation of each hydrocarbon type into C_4 through C_{10} carbon number distribution. This analysis was applied to naphtha analysis and was used for feed-forward control of ethylene and propylene cracking units [46–47]. Another application included the analysis of an NMR to monitor and control a cracker used to process both naphtha condensates and diesel range material [48]. Fig. 16 shows typical spectral response of naphthas at 60 MHz as well as an example of real-time PINA data used for control.

Another challenging application is the NMR crude oil assay, which involves regression analysis of ^{1}H NMR against true boiling point and density data on crude oils. Crude oil blending applications have been studied, as has feed-forward control of refinery crude units. In one application, a Caribbean refinery performed a complete optimization project on a crude unit, monitoring the true boiling point of the crude feed as well as the distillation (ASTM D86), freeze point (ASTM D2386), and flash point (ASTM D93) of the kerosine product, and the distillation (ASTM D86) values of the naphtha product [49]. Other applications have been installed online for crude unit product analysis. The streams analyzed by chemometric predictions vary depending on the control strategy and the economics of the refinery. Some installations analyze naphtha, kerosine, diesel, and gas oils. Others concentrate heavily on crude unit diesel as well as hydrotreated diesel streams or cracked cycle oils that are routed to the same analyzer [50–51]. In the analysis of diesel, the ^{1}H NMR can predict the cold flow properties, distillation points (ASTM D86 or D2887, Simulated Distillation), density,

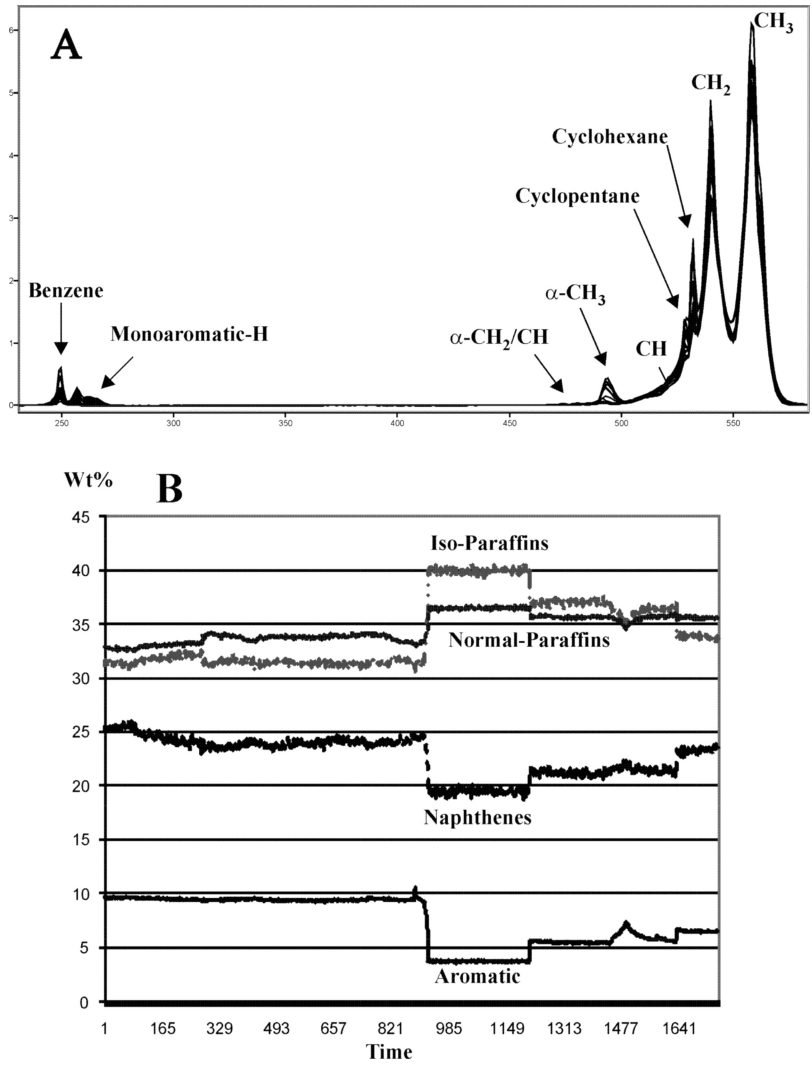

Figure 16—Process ^{1}H NMR PLS prediction of naphtha PINA analysis: (A) typical NMR spectral variation, and (B) 4 days of online predictions showing chemical component variation.

aromatics content, olefin content, and cetane index (or cetane number) of the diesel stream. In a further application of the technology, the customer is receiving carbon number distributions obtained from simulated distillation data to better predict the cut points of the diesel product in order to avoid inclusion of dibenzothiophene in the diesel product, ensuring the diesel meets ultralow sulfur specifications.

A European refiner has applied online NMR analysis to a base oil manufacturing process [52]. ^{13}C NMR-based NMR parameters (aromatic carbon content % [Fa], naphthenic carbon content % [Fn], and paraffinic carbon content % [Fp])

were regressed against the online ^{1}H NMR spectra to obtain an excellent correlation allowing ^{13}C NMR parameters to be predicted by ^{1}H NMR analysis. The refractive index, simulated distillation, density, and viscosity index were predicted for the vacuum gas oil feedstream, the intermediate raffinate, and the final base oil product. Online application of these three ^{13}C NMR parameters and the other physical property measurements has also been ongoing at several online NMR installations on FCC feed streams. Online ^{1}H NMR analysis of light cycle oils and cracked spirits is also found at the above-mentioned FCC installations.

APPLICATIONS: HIGH-RESOLUTION, HIGH-FIELD NMR LIQUID-STATE ANALYSIS

In the more familiar arena of high-resolution NMR in which commercial spectrometers operating at 200–600 MHz are used to observe ^{1}H and ^{13}C NMR, the approach to the chemical information present in an NMR spectrum varies widely, depending on the researcher. There are several approaches that can yield useful information which informs the researcher about sample-to-sample variability of the petroleum material under observation, or informs one of the changes that have occurred to chemical and macromolecular properties during petroleum processing. ^{1}H NMR parameters are derived predominantly by liquid-state NMR because of the paucity of data that has emerged from solid-state ^{1}H NMR experiments still plagued by poor resolution. ^{13}C NMR parameters are obtained for liquid-state NMR experiments and solid-state MAS experiments. Quantitative conditions can be obtained in ^{1}H NMR studies by using appropriate relaxation delays between the accumulating pulses. For liquid-state ^{13}C NMR experiments, it is important that relaxation agents such as chromium (III) acetylacetanoate be used in the deuterated solvents (usually $CDCl_3$ or a $CDCl_3$-CS_2 combination) in which the petroleum samples are dissolved. The relaxation agents reduce the ^{13}C relaxation rates from paramagnetic interactions, and thereby shorten the required relaxation delays between pulses, allowing rapid signal accumulation and timely experimental results. Inverse gated decoupling is also a requirement to avoid nuclear overhauser effects (NOE) that cause carbons with different protons to be enhanced to different degrees, rendering the data nonquantitative from one carbon type to another throughout the entire sample chemistry. This decoupling simply means that the ^{1}H decoupling is only applied during the FID acquisition.

One approach is to determine the ^{1}H and ^{13}C NMR molecular parameters directly from the spectrum. Typical ^{1}H and ^{13}C derived chemistry parameters are given in Table 3 and Table 4. Another approach is to calculate average structural parameters that describe the "average" chemistry of the sample as an idealized single molecule. Typical average structural parameters for liquid- and solid-state NMR studies are shown in Table 5. The basis for these tables are the exhaustive data tables presented in the book by Boduszynski and Altgelt [53–54]. The derivation and use of these parameters as descriptors of the true chemistry of the sample is open to much interpretation and has lead to academic disputes on the calculation methodologies and the meaning and usage of the NMR derived parameters [55–56]. NMR analysis does not yield the distribution and skewness of the ^{1}H or ^{13}C chemistry distributions around the calculated average. NMR cannot determine the true molecular speciation or the distribution of the entire petroleum mixture.

TABLE 3—Proton Types Obtained from ^{1}H NMR Analysis
Sample
Total Aromatic-H %
Total Aliphatic-H %
Total Olefinic-H % - can be further broken down into internal and terminal olefin
Alpa-H % - ^{1}H on carbons alpha to aromatic rings - can be broken into CH_3 and CH_2/CH
Epsilon-CH_2 % - Methylenes distanced from chain terminals and branches
Beta - CH/CH_2 % - Paraffinic CH_2 and CH other than alpha and epsilon
Total Aliphatic CH/CH_2 %
Gamma - Methyl CH_3
Alpha-CH_3 %. Alpha-CH_2 %. Alpha-CH %. CH_2 Alpha to 2 Aromatic Rings %
Monoaromatic-H %. Diaromatic-H%. Triaromatic+-H %
Aliphatic CH_3 to CH_2/CH Ratio
Mono/PNA Aromatic Ratio

The average molecule description is always limited by the many assumptions that are made in the calculations. For example, in many experiments one has to assume that all aliphatic carbons are in groups that are attached to aromatic rings. This has to be done because NMR cannot discern between free paraffin molecules and alkyl carbons on substituted aromatic molecules. The NMR spectrum informs the researcher that there are alpha protons (CH, CH_2, and CH_3 groups attached to aromatic rings); it does not inform you of the breakdown of the molecular distribution that would link the signals in the aliphatic region to those particular pendant groups. As such, it is recommended that researchers follow changes in chemistry observed directly from the spectrum. Average molecule parameters can be used as an alternative method to follow gross chemistry trends with processing changes, and should not be used to represent the true changes to ^{1}H or ^{13}C chemistry.

Another approach is the reduction of ^{1}H NMR spectral data into NMR molecular parameters followed by regression analyses that derive predictive equations for the calculation of physical and chemical parameters of interest for the petroleum product being analyzed. Cookson and Smith published a series of papers on composition-property correlations for diesel and kerosine fuel based on a general equation derived from a combination of HPLC data and standard ^{13}C molecular parameters [57–59]:

$$P = a_1[n] + a_2[BC] + a_3[Ar] \quad (1)$$

where P is the fuel property value, and [n], [BC], and [Ar] are the weight fractions of *n*-alkanes, branched plus cyclic saturates, and aromatics, respectively. These values are obtained from HPLC data processed with response factors estimated from ^{13}C NMR results on the same sample [60]. The coefficients a_1, a_2, and a_3 are

TABLE 4—Carbon Fraction Parameters Obtained from Quantitative ^{13}C NMR

NMR Carbon Fraction	Description
Fa^{CO}	Fraction of carbonyl (%) sp2 - aldehydes and ketones
Fa^{COO}	Fraction of carboxyl (%) sp2 - acids, esters, amides
Fa^{P}	Fraction of phenolic carbon (ar-C-OH) (%) sp2
Fa^{S}	Fraction of substituted aromatic carbon (%) sp2
$Fa^{B} + Fa^{H}$	Fraction of combined bridgehead and protonated aromatic carbon (%) sp2
Fa^{N}	Fraction of non-protonated aromatic carbon (%) sp2
Fa^{C}	Fraction of sp2 carbon present as carbonyl and carboxyl (%) sp2
Fa'	Fraction of aromatic carbon (%) sp2
Fa	Fraction of sp2 carbon (aromatics and carboxyl/carbonyl) (%) sp2
Fal	Fraction of sp3 (aliphatic) carbon sp2
Fa^{B}	Fraction of bridgehead aromatic carbon sp2
Fa^{H}	Fraction of protonated aromatic carbon sp2
Fal^{O}	Fraction of ether carbon (sp3 carbon adjacent to O)
Fal-amine	Fraction of amine carbon (sp3 carbon adjacent to N)
Fal-CH/CH_2	Fraction of CH and CH2 in naphthenics and paraffins (sp3)
Fal-Arom-CH_3	Fraction of CH3 attached to aromatics (sp3)
Fal-Aliphatic-CH_3	Fraction of CH3 attached to paraffins or naphthenes (sp3)

determined from multiple linear regression analysis. It was also found that a four-parameter model containing separate coefficients for monoaromatic and diaromatic content marginally improved the property predictions.

In a further development, studies were published for composition-property relations based solely on ^{13}C NMR data that fit the following type of equation [61]:

$$P = a_1 C_n + a_2 C_{ar} + c \quad (2)$$

where C_n is the % *n*-alkyl carbon, and C_{ar} is the % aromatic carbon. Jet fuel properties predicted included smoke point, aromatic content, hydrogen content, heat of combustion, freeze point, and inverse specific gravity. For diesel, the predicted properties were pour point, cloud point, hydrogen content, aniline point, diesel index, cetane index, and inverse specific gravity. Fig. 17 shows examples of calculated versus actual quality properties for jet and diesel fuels derived from ^{13}C analysis alone utilizing Eq 2. The property predictions were further improved by developing models for jet and diesel fuels with variable boiling ranges [62]. In these analyses Eq 2 was used in conjunction with GC-simulated distillation

TABLE 5—Typical Structural Parameters for Average Molecule Descriptions[a]

Symbols	Definition - Determination of Calculation
M_W	Average Molecular Weight (by LD-MS)
C_{ar}	Total Aromatic Carbons (by ^{13}C NMR)
C_{al}	Total Aliphatic Carbons (by ^{13}C NMR)
C_{us}	Unsubstituted Aromatic Carbons (by ^{1}H NMR)
C_s	Alkyl-Substituted Aromatic Carbons Except CH_3 (by ^{13}C NMR)
C_{CH3}	Methyl-Substituted Aromatic Carbons (by ^{13}C NMR)
C_{sub}	Alkyl-Substituted Aromatic Carbons ($C_{sub} = C_s + C_{CH3}$)
C_p	Peripheral Aromatic Carbons ($C_p = C_{us} + C_{sub}$)
C_h	Carbons Attached to Heteroatoms (by ^{13}C NMR)
C_{int}	Internal Quaternary Aromatic Carbons ($C_{int} = 6 + C_{ar} - 2C_p$)
C_{ext}	External Quaternary Aromatic Carbons ($C_{ext} = C_{ar} - (C_p + C_h + C_{int})$)
F_a	Aromaticity ($f_a = C_{ar} / (C_{ar} + C_{al})$)
R_a	Aromatic Ring Number ($R_a = ((C_{ar} - C_p)/2) + 1$
n	Average Length of Alkyl Side Chains ($n = C_{al}/C_{sub}$)
CI	Condensation Index ($CI = (C_{int} + C_{ext})/C_{ar}$)

[a]Reprinted with Permission from Ref [94]; © 2000 American Chemical Society.

data to provide an equation that accommodates the effects of variations in boiling range:

$$P = a_1 C_n + a_2 C_{ar} + \sum b_i T_i + k \quad (3)$$

where T_i represents a series of temperatures at which a specific weight % of the fuel has boiled, and coefficients a_1, a_2, b_i, and k are determined by multiple linear regression. Table 6 shows the coefficients obtained for property prediction of jet and diesel fuels.

In another series of papers spread over the past decade, researchers at Indian Oil Corporation have used a ^{1}H NMR methodology whereby intensity data from chemical shift regions correlating to different hydrogen types are regressed against property parameters obtained from primary testing methods. As an example, the various hydrocarbon types (total aromatics, olefins, and oxygenates) in motor gasoline were obtained by NMR correlated to gas chromatography (GC: ASTM D5580 and D4815) and fluorescent indicator absorption (FIA: ASTM D1319) test methods [63]. It is advantageous when working with refinery engineers that NMR results be converted to gas chromatography values given in wt % or vol %. ^{1}H and ^{13}C NMR values for aromatics yield numbers that are much different than an engineer

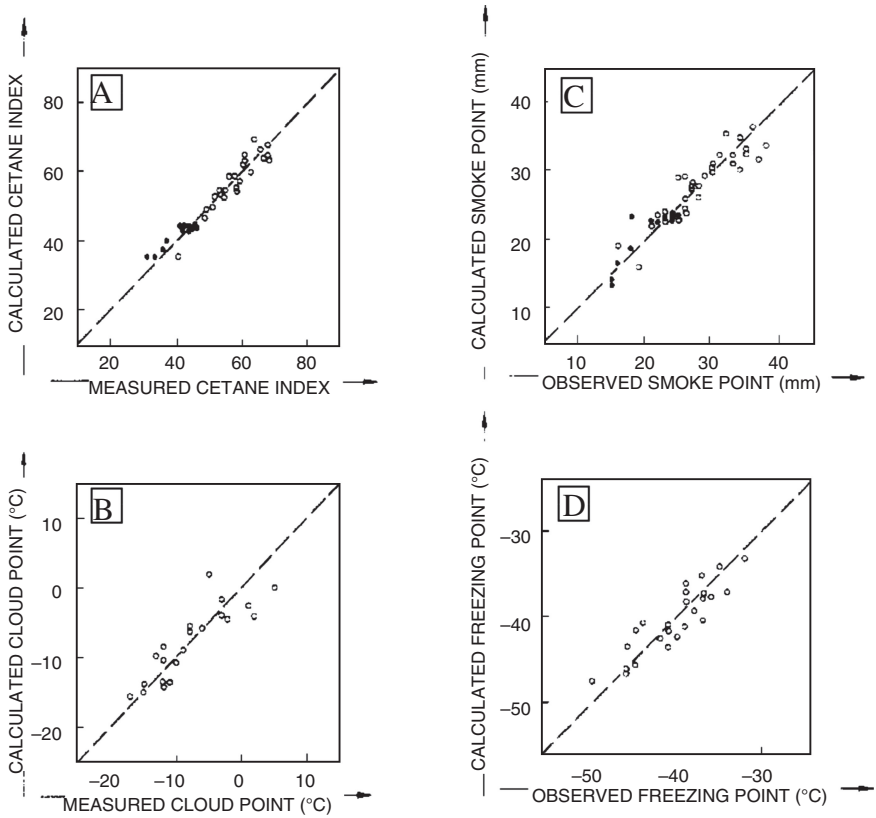

Fig. 17—Plots of measured versus calculated values of (A) cetane index, (B) cloud point of diesel fuels, and the (C) smoke point, (D) freezing point of jet fuels (○ = petroleum • = synfuel) based on Eq 2. (Reprinted with permission from Ref [61]; © 1990 American Chemical Society.)

would expect when he deals with GC values for control and property evaluation. Also the fact that NMR yields hydrocarbon types in terms of nuclear percentages rather than by molecular type means that there is a disconnect between what NMR defines as aromatic and what is defined as aromatic by GC.

As an example of the disparity between GC and NMR analysis or aromatics, dodecylbenzene is considered 100 % aromatic by GC, while to NMR it is 21.7 % aromatic (5H on aromatic ring/23H on aliphatic chain). By obtaining GC or FIA data and then correlating ^{1}H NMR spectral variability to those values, the ^{1}H NMR can yield GC values in wt % for the hydrocarbon types of interest. To do this directly from the observed ^{1}H NMR chemical types, the Indian Oil Company researchers integrated the spectrum into eight distinct regions yielding relative intensity data on aromatics (region A, 6.5–8.0 ppm), olefins (region U, 4.5–6.2 ppm), oxygenates (region O, 3.0–3.5 ppm), alpha-CH_2/CH (region B, 2.45–3.0 ppm), alpha-CH_3 (region C, 2.05–2.45 ppm), CH/CH2 in naphthenes, normal and isoparaffins (region E, 1.4–2.05 ppm), CH_2 in long alkyl chains (region G, 1.05–1.4 ppm), and methyls (region H, 0.5–1.05 ppm). The calculation of chemical and physical properties is

TABLE 6—Statistical Data for Composition-Property Relations based on Eq 3 for Variable Boiling Range Fuels[a,b]

Property	a_1	a_2	b_1	b_2	k	r.m.s.p.e	adi R^2
Jet Fuels							
Smoke Point (mm)	29.3	−74.7	−0.065	−0.045	43.4	1.6	0.94
Aromatics Content (vol%)	−4.8	121.0	0.072	0.015	−11.9	2.1	0.94
Hydrogen Content (wt%)	2.35	−4.89	−0.006	−0.006	16.2	0.13	0.94
Density (g cm^{-3})	−0.137	0.0386	0.0005	0.0004	0.6577	0.008	0.91
Freezing Point (°C)	81.1	53.6	0.255	0.338	−206.2	2.5	0.93
Diesel Fuels							
Cloud Point (^{0}C)	33.2	−12.3	0.154	0.422	−189.4	2.8	0.92
Pour Point (°C)	29.3	−24.5	0.192	0.389	−186.4	3.7	0.87
Aniline Point (°C)	55.6	−67.7	0.078	0.073	18.7	3.0	0.94
Hydrogen Content (wt%)	2.41	−5.62	−0.003	−0.002	14.48	0.13	0.95
Density (g cm^{-3})	−0.157	0.0655	0.0003	0.0001	0.7652	0.008	0.92
Cetane Index (AP)	52.0	−71.4	0.094	0.066	3.7	2.2	0.96
Cetane Index (BP)	55.1	−25.1	0.002	0.046	22.8	2.5	0.95
Cetane Number	49.1	−32.4	0.061	0.025	24.3	2.2	0.95

[a]Model: $P = a_1 C_n + a_2 C_{ar} + b_1 T_{10} + b_2 T_{90} + k$.
[b]Reprinted with permission from Ref[62]; © 1995 Elsevier.

performed on a carbon basis. This means that the ^{1}H NMR data must be converted to represent the relative number of carbons in each carbon type (T_C) as well as the relative molecular weights of each carbon type group (T_W). An estimation of the substituted aromatic carbon (Ar_s) (and in some cases the bridgehead aromatic carbons [Ar_b]) must be derived from the alpha-proton (2.05–3.0 ppm) and aromatic proton (7.4–9.0 ppm) regions of the spectrum. The proton intensity data are reduced to carbon type values by dividing each integral value by the number of protons attached to each carbon type (see Eq 4). The group molecular weights are obtained by multiplying the calculated carbon number values by the molecular weight of the group (12 for C, 13 for CH, 14 for CH_2, and 15 for CH_3), as follows:

$$T_C = A/1 + 1.12U + B/2 + C/3 + E/2 + F/1 + G/2 + H/3 + Ar_q + O/2 \quad (4)$$

where Ar_q = substituted aromatic carbon, calculated indirectly through alpha-H = (B/2 + C/3).

Substituting for Ar_q and multiplying by the molecular weight of each carbon type, T_W is obtained:

$$T_W = 13(A + F) + 14B + 10C + 7(E + G) + 5H + 14.36U + 7O \quad (5)$$

Now that we have the total group molecular weight, we can calculate the wt % of the individual components. For example, to calculate total aromatics (A_W), the group molecular weight is calculated as:

$$\begin{aligned} A_W &= 13(A/1) + 14n(B/2) + 15(C/3) + 12(B/2) + 12(C/3) \\ &= 13A + 7nB + 9C + 6B \end{aligned} \quad (6)$$

$$\text{Total Aromatic Content (Wt\%)} = 100 \times A_W/T_W \quad (7)$$

Fig. 18 shows the correlations between NMR-calculated total aromatics in gasolines and the wt % values obtained on the same samples by FIA and GC separation methods.

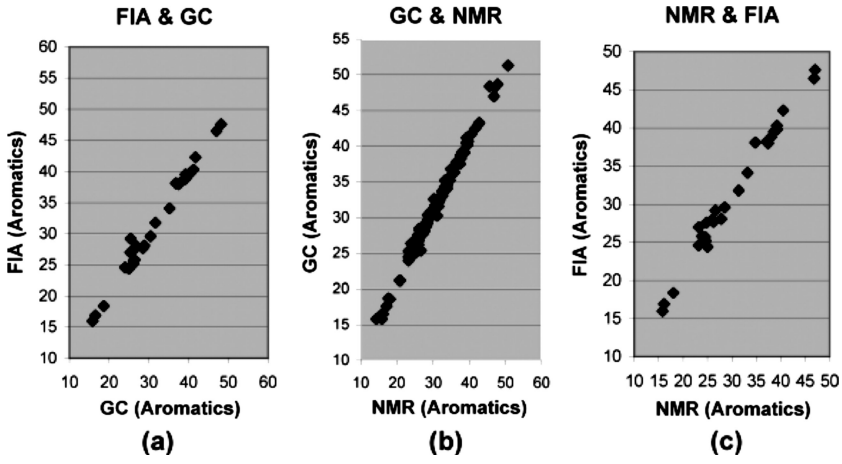

Fig. 18—Plots of the correlation between GC and FIA analysis methods and the calculated value of total aromatics from Eq 8; units are wt%. (Reprinted with permission from Ref [63]; © 2008 American Chemical Society.)

For gasoline range material, various predictive equations based on this approach have been developed for PONA [64,65,67], benzene and total aromatics [66,67], oxygenates [67–69], and octane number [70]. Total aromatic content was estimated for aviation turbine fuels by ^{1}H NMR [71]. A number of papers were published on this approach to the estimation of properties of middle distillates and diesel fuels to yield the following parameter estimations:

- Total aromatics and the mono- and di-plus aromatics distribution by ^{1}H and multidimensional NMR [72]
- Bromine number (ASTM D-1159) by ^{1}H and ^{13}C NMR [73]
- Total aromatics by ^{1}H NMR; comparison with mass spectrometry [74].

The technique was extended to vacuum gas oil (VGO) fractions [75], as well as feedstocks to both FCC (fluid catalytic cracker) and RFCC (residual fluid catalytic cracker) [76], in which total aromatic content by open column chromatography (ASTM D2549) was calculated according to the previous methodology. Other important process control information was also derived from the ^{1}H and ^{13}C NMR with respect to alkyl chain lengths, aromatic substitution patterns, and degree of substitution, allowing estimates to be calculated for the product profile, yield pattern, and expected coking tendency of the feed.

In a modified approach, the Indian research group has applied multiple linear regression (MLR) to develop predictive equations based on 18 integrals representing specific proton types in the ^{1}H NMR spectrum. The integrals were stored as a "modified spectrum," and "spectrum" was regressed against various chemical and physical properties for diesel samples. The regression analyses produced regression statistical correlations with $R^2 > 0.99$ [77]. Fig. 19 shows the correlations obtained between NMR-calculated values and a number of chemical and physical property laboratory test methods. The equations that the calculations are based on are shown in Table 7.

A similar approach, employing PLS regression, was taken by another group that obtained 12 integral values from the ^{1}H NMR spectra of Colombian crude oils. These were regressed against crude properties to yield a true boiling point prediction of the product fractions (yield of naphtha, jet A, diesel, gas oil, and residue), sulfur content, nitrogen content, waxes, micro-Conradson residue (MCR), asphaltene content (nC_7 insolubles), nickel, and vanadium [78]. A full spectrum approach was taken by Edwards and Kim, where integrated spectra (integral binned every 0.1 ppm from 12 to −2 ppm), and "spectra" created from hydrogen and carbon molecular and structural parameters calculated from both ^{1}H and ^{13}C data, for both diesel and VGO samples, were correlated to diesel and vacuum gas oil parameters with PLS regression [79]. In this study, PLS regression models were developed that allowed 34 detailed ^{13}C NMR parameters to be calculated from ^{1}H NMR spectra, thus drastically reducing the time involved in obtaining detailed carbon type analysis.

In other applications of multivariate analysis and neural networks to NMR analysis of gasoline, a ^{1}H NMR method was developed to identify gasoline adulterated by solvents by both principal components analysis (PCA) and hierarchical cluster analysis (HCA) [80], and a method was demonstrated for obtaining octane numbers from ^{13}C NMR spectra and neural networks [81]. Correlation of ^{1}H NMR structural parameters to the concentration of hydrocarbon groups (paraffinic + naphthenic % and aromatic %) of heavy oils such as tail oil, catalytic slurry oil, catalytic heavy tar, and waxy oil, can be developed directly from

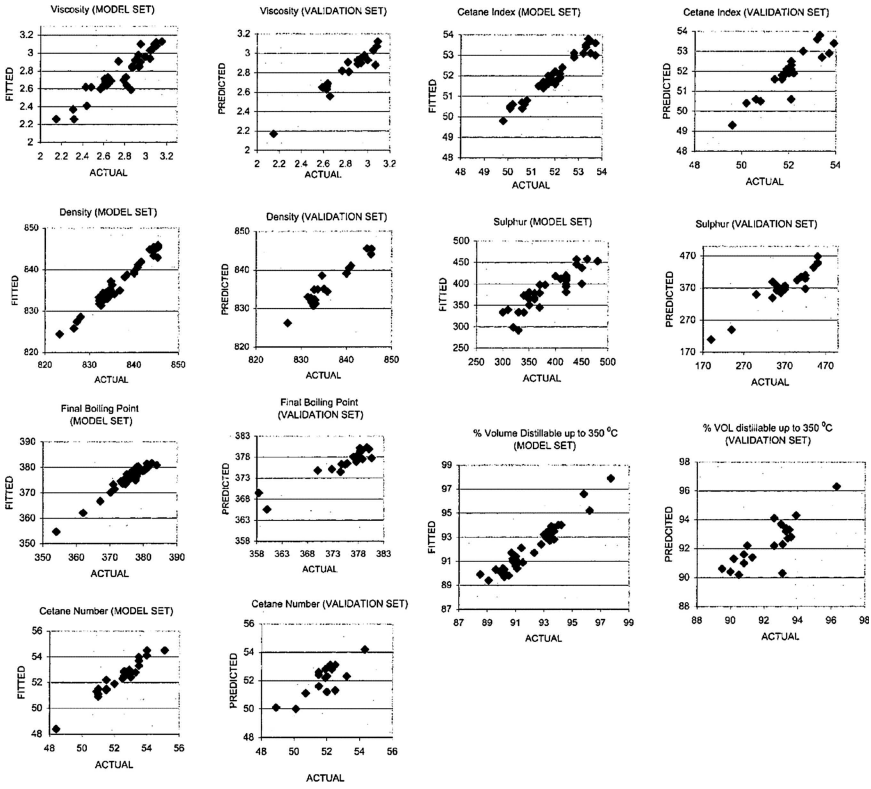

Fig. 19—Correlation between NMR-calculated chemical and physical properties of diesel and the laboratory experimental value for a validation set of samples. (Reprinted with permission from Ref [77]; © 2001 American Chemical Society.)

the NMR spectrum by fitting the relative proton types (%H) versus chromatographic data in order to determine aromatic, naphthenic, and paraffin hydrocarbon contents [82].

Many examples can be found of molecular and structural parameters derived from both ^{1}H and ^{13}C NMR applied to the study of processing changes in heavy oils, bitumen, and heavy refinery streams. Many of these papers contain similar approaches with regard to molecular representations and molecular and structural parameter calculation from the ^{1}H and ^{13}C data. However, on close examination, many papers use different chemical shift ranges, assume conflicting or different chemistry in the ranges chosen, miss some chemistry types entirely, and utilize different calculation approaches. Some researchers fully describe the calculation process they have used, and others do not reveal how the calculations are performed at all. With the growing importance of these NMR-derived parameters in heavy petroleum processing, a consistency of approach, a standard method development process, and even a final "master spreadsheet" for the calculations should be considered, perhaps within the auspices of standard testing organizations such as American Society for Testing and Materials (ASTM), Institute of Petroleum (IP), or American Petroleum

TABLE 7—Property Correlation Equations Calculated by MLR from 18 ^{1}H NMR Integral Regions[a]

Property	Model Equation	R^2	Std Error
Density	5.092(A + B) + 2.537(H + I) + 1.732(J) + 1.083(L) + 4.279(M) + 1.704(O) + 0.830(P) + 2.380(Q) + 0.426(R)	0.998	1.11
Viscosity	−0.097(D + E + F + G) − 0.438(H) + 0.333(I) − 0.0446(L) + 0.0073(P) + 0.091(Q) − 0.0245(R)	0.998	0.09
Cetane Number	−0.272(A + B + C + D) + 0.570(H + I) + 0.653(J) − 0.712(L) + 3.001(M) − 0.408(N) + 0.0886(P) + 0.152(R)	0.998	0.4
Cetane Index	−0.713(C + D) + 0.528(K) − 1.268(M) + 0.075(P) + 0.240(Q)	0.998	0.27
Sulfur	11.01(A + B + C + D + E + F + G) + 37.46(H + I) −43.8(J) − 9.959(L) −5.065(M) + 1.358(P) − 12.639(Q) + 2.864(R)	0.992	24
%Vol up to 350°C	0.72(A + B + C + D + E + F + G) + 1.052(J) − 0.916(K) + 0.437(L) −5.065(M) + 0.719(O) + 0.031(P) − 0.434(Q) + 0.215(R)	0.992	0.63
FBP	−3.249(C + D) − 2.903(E + F + G) + 3.661(K) + 7.828(M) + 0.453(P) + 1.771(Q) + 0.146(R)	0.998	1.46

[a]Reprinted with permission from Ref [77]; © 2001 American Chemical Society.

Institute (API). The advantage of NMR for many of these analyses is that it is a direct experimental technique that yields chemically rich information even on heavy petroleum streams that can be approached only with difficulty by chromatography or mass spectrometry to obtain reliable chemical information. The issue that hinders NMR from developing into a more widely applicable technique is the absence of official regulation of NMR methodology and experimental execution. In the petroleum industry especially, NMR operates outside the realms of standard test methods and standard operating procedures. This has become a weakness in the development and implementation of NMR technology to routine petroleum sample analysis. In high-resolution NMR analysis of petroleum products, the only standard test method is ASTM D5292-99 (Standard Test Method for Aromatic Carbon Contents of Hydrocarbon Oils by High Resolution Nuclear Magnetic Resonance Spectroscopy) [83]. This standard method represents the simplest ^{13}C NMR analysis–in the future, it too will face problems as there is a push toward synthetic crudes and fuels where olefin content will be high and aromaticity numbers will need to be developed that discern between aromatic and olefinic carbon the signals of which overlap heavily in the ^{13}C spectrum–this will require combined ^{1}H and ^{13}C as well as two-dimensional heteronuclear approaches that allow identification of olefinic carbons. This is routine methodology that needs to be developed and standardized

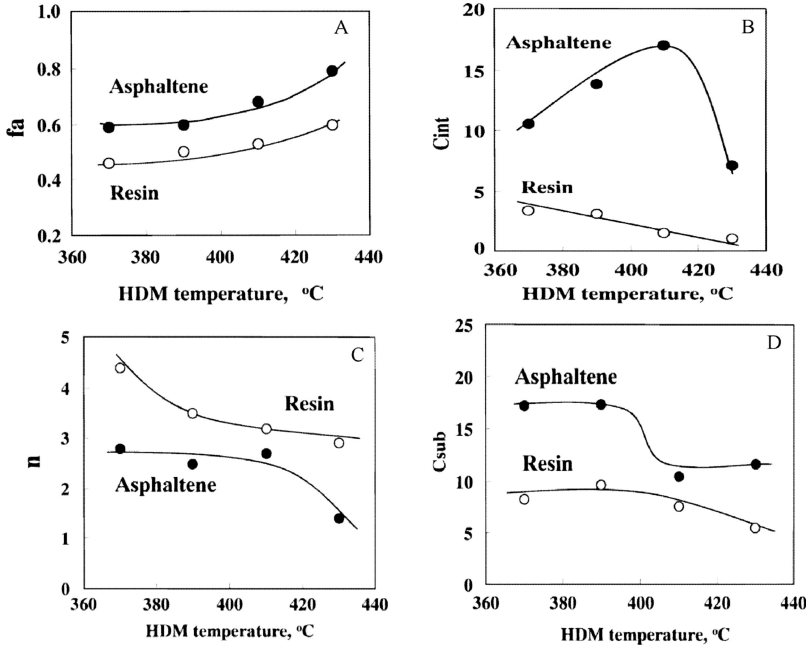

Fig. 20—Effect of temperature and HDM reactor conditions on asphaltene and resin average molecule structural parameters calculated from ^{1}H and ^{13}C NMR. (Reprinted with permission from Ref [94]; © 2000 American Chemical Society.)

so that it can be equally implemented by interested testing parties. The molecular and structural parameters described previously must be standardized so that they can be implemented with confidence in the areas of refinery control [84–86], bitumen processing [87–90], and asphaltene chemical analysis [91–99]. For these heavy petroleum fractions in particular there is a need to develop uniform methodologies to calculate the average aromatic ring sizes from which the remainder of the average molecule parameters are derived in ^{13}C NMR analysis. A number of combination methodologies using quantitative ^{13}C NMR and DEPT-45 experiments hold promise to allow consistent analysis of overlapping protonated and bridgehead aromatic carbons in the 110–129.5 ppm region of the spectrum. Many researchers have published results indicating that DEPT experiments can be used to obtain semiquantitative NMR parameters that can be consistently calculated [84,90,99–108]. Average molecule parameters derived from ^{13}C and ^{1}H NMR are used to monitor processing effects on aromatic ring size and the length of aliphatic substitutions. Fig. 20 shows typical data obtained from a series of hydrodemetallization (HDM) reactions at different temperatures. NMR was used to monitor average molecule parameters such as C_{int} (internal aromatic carbon, sometimes called bridgehead aromatic carbon), f_a (carbon aromaticity), C_{sub} (number of alkyl attachments per aromatic ring system, and n (alkyl side chain). Variation in these values can be attributed to changes from conversion of catacondensed to pericondensed aromatic ring systems or vice versa, reduction in ring sizes due to removal of

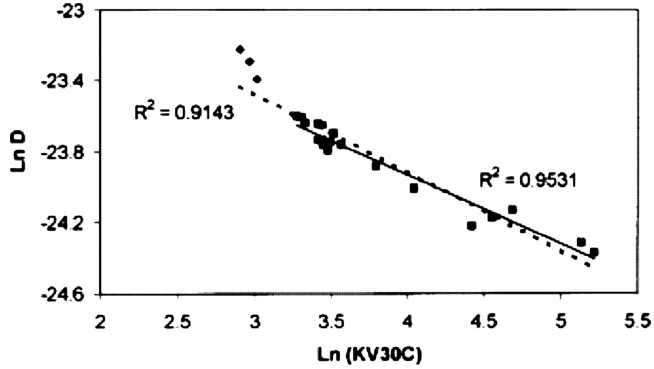

Fig. 21—Diffusion coefficients derived from ^{1}H PFG-NMR show excellent correlation with kinematic viscosity at 30°C. (Reprinted with permission from Ref [109]; © 2003 American Chemical Society.)

heteroatoms from the aromatic structures, and cracking of alkyl side chains leading to shorter attachments and fewer substitutions on the rings.

The same NMR approaches that are used to envision changes in aromatic and aliphatic chemistry in heavy oils and bitumens are used in the study of lubricant base oils. Some approaches are simplistic, such as the utilization of pulsed field gradients (PFG) in NMR echo and DOSY (diffusion ordered spectroscopy) experiments to discern between high and low molecular weight components in a base oil mixture via their self-diffusion coefficients. The experimental results can be related to the kinematic viscosity and pressure viscosity coefficients of the base oil at different operational temperatures [109–110]. PFG applied to a series of lubricant base stocks showed a good correlation with kinematic viscosity, as shown in Fig. 21. The effect of hydrotreating and dewaxing operations can be readily observed by either structural or molecular parameters from ^{1}H and ^{13}C NMR [111]. Oxidative stability test results performed on pure or additized base oils can also be related to NMR-derived parameters [112–113]. In all these studies important information is derived from ^{13}C-derived values of F_a, F_p, and F_n, average chain length, alkyl substitution, aromatic carbon distribution, isoparaffin content, and branching index. In studies of thermo-oxidative and physical property behavior, directional changes in the values of these NMR parameters yield informative chemical correlations that can be used to formulate lubricant mixtures and additized products, or to optimize the base oil manufacturing process. A few examples are as follows: 1) higher branching leads to lower oxidation stability, 2) increases in average alkyl chain length lead to increase viscosity, 3) branching index and naphthenic content increase while normal paraffin content and aromatic content decrease, increasing severity of the hydrogenation process, 4) aromatic carbon decrease and saturated carbon increase lead to an increase in viscosity index during hydrogenation, and 5) average chain length of paraffinic base oils decreases with hydrogenation while it increases in aromatic extracts [111]. Details of the ^{13}C NMR assignments for base oils produced by different manufacturing processes as well as those for hydrocracked base stocks can be found in articles by Sarpal et al. [114–115]. ^{13}C NMR is uniquely suited to analyze branching

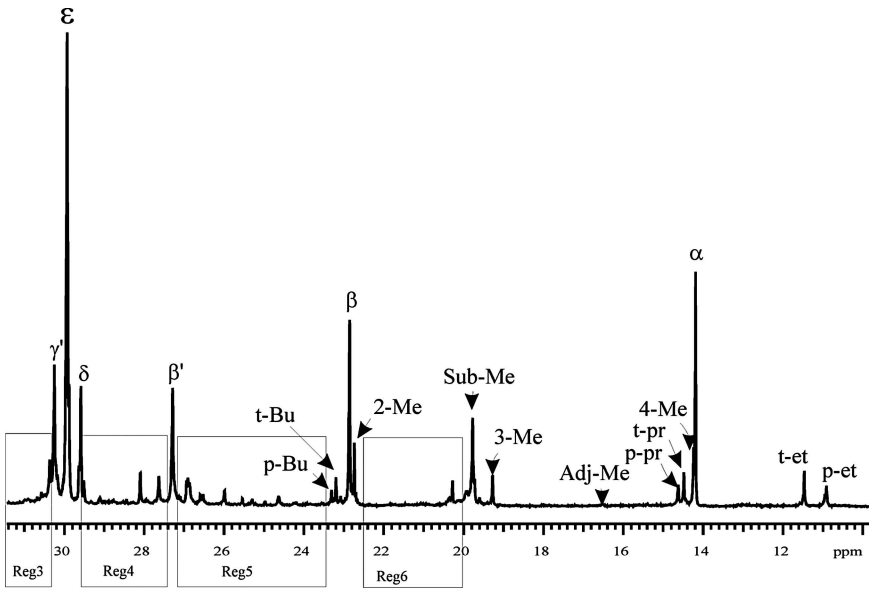

Fig. 22—Identification of peaks associated with various pendant and terminal methyl carbons in the aliphatic carbon region of the spectrum. Also identified are the α, β, γ, δ, ε resonances due to carbons in linear regions of a paraffin chain, as well as β′ and γ′ resonances that are methylenes two and three carbons away from a branch point.

structures of isoparaffins. Approaches to the analysis involve use of DEPT experiments to identify either CH carbons at branching points or CH_3 carbons whose chemical shift varies depending on the proximity of a molecule termination or a branching point. Fig. 22 shows the peaks in the aliphatic region of the ^{13}C NMR spectrum that are associated with CH_3 chemistry, and Table 8 shows the chemical shifts of various CH branching points.

Another area of interest is the application of ^{13}C NMR to Fischer-Tropsch base stocks. The fact that these waxes are almost entirely paraffinic makes assignment and quantification of most branching types straightforward. In particular, ExxonMobil [116], Chevron [117], and Mobil [118] have been very active in defining products by way of ^{13}C detailed branching calculations.

One of the concepts developed is the free carbon index (FCI), which is a measure of linear paraffin chain character, defined as the number of carbons more than four carbons removed from a terminal methyl group and more than three carbons removed from a branching point (ε carbons):

$$\text{FCI} = 100 \times (\varepsilon \text{ carbons})/\text{average carbon number},$$

where average carbon number is obtained from GC analysis (ASTM D2502). As an example of how NMR is being used to define the properties of a lube stock product range, we can take an excerpt from the example ExxonMobil patent that describes the product in terms of NMR branching character:

1. "... at least about 75 wt % iso-paraffins"
2. "FCI typically in the range of 4 to 12, preferably less than 10"

TABLE 8—Chemical Shift Assignments of Methine Carbons in Paraffinic Branches[a]

Group	Chemical Shift (ppm)	Corresponding Branching of Isoparaffins
CH-a	28.00–29.00	2-metyhl branching
CH-b	32.75–32.90	4-methyl branching
CH-c	32.90–33.15	8- or inner methyl branching
CH-d	33.15–33.25	7-methyl branching
CH-e	33.25–33.45	3-methyl branching
CH-f	33.45–33.60	7- or inner ethyl branching
CH-g	34.50–34.80	5-, 6-methyl, 4-, 5-, 6-ethyl branching
CH-h	39.00–39.50	3-ethyl branching

[a]Reprinted with permission from Ref [120]; © 2009 American Chemical Society.

3. "A further Criterion which differentiates these materials structurally from polyalphaolefins is the branch length ... at least 75 % of the branches, as determined by NMR, are methyls and the population of ethyl, propyl and butyls falls sharply with increasing molecular weight to the point where no more than 5 % are butyls. Typically the ratio of 'free carbons' to end methyl is in the range of 2.5 to 4.0"
4. "...basestocks have, on average, from 2.0 to 4.5 side chains per molecule."

This approach to defining and patenting products in terms of branching carbon distributions indicates that petroleum product manufacturers should be routinely performing ^{13}C NMR analysis on everything they produce to prove that their products are either different from their competitors or to establish the branching details in order to prove "prior art" when those products are patented by a competitor. This approach is not solely performed in the lubricant oil area of Fischer Tropsch products, it has also expanded into diesel fuel product descriptions by ^{13}C NMR branching values [119–120]. In the case of the ExxonMobil descriptions of diesel fuel analysis, the ^{13}C detailed branching values were regressed in order to yield predictive equations for cetane number, cold filter plugging point, cloud point, and pour point.

Another area of utility for NMR is in biofuels production, quality assessment, and blending operations. Reaction monitoring in biorefineries will be an area where the chemical specificity of NMR will be invaluable. At the moment, NMR is considered the primary method for analysis of esterification reactions used to produce fatty acid methyl esters (FAME) from vegetable oils [121–124]. Other techniques are used for real-time monitoring, but these techniques (NIR, FT-IR, Raman) are calibrated with ^{1}H NMR data. NMR will also play a role in the study of biodiesel stability during storage and the effect of air exposure on the unsaturated fatty acids present in the biodiesel [125]. Fig. 23 shows the ^{1}H

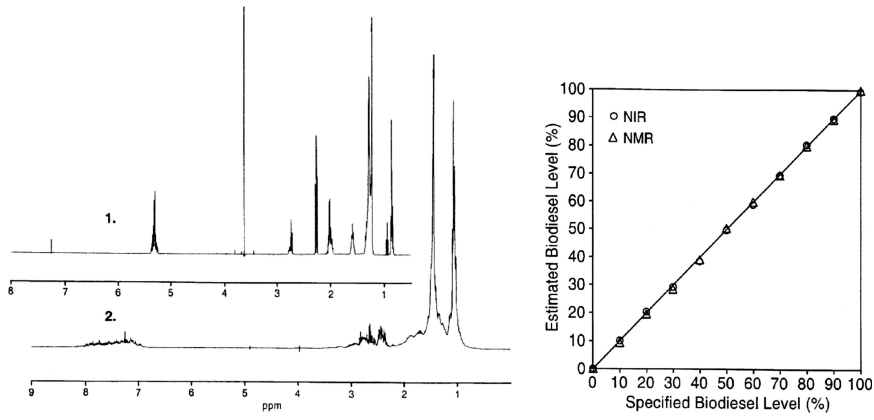

Fig. 23—^{1}H NMR spectra of FAME biodiesel from soybeans (1) and petroleum derived diesel (2) along with the plot of the NMR- and NIR-predicted biodiesel blend content versus actual blend concentration (vol%). (Reprinted with permission from Ref [124]; © 2001 AOCS Press.)

NMR spectra of FAME and conventional diesel as well as the excellent correlation between NMR-calculated FAME content on a series of calibrated blends.

NMR allows methods to be developed that monitor types of unsaturation and the relative concentrations as samples are exposed to different storage conditions with respect to temperature, presence of light and air, presence of metal, etc. In the United States, the commercialization of B20 (20 % biodiesel/80 % petroleum-derived diesel) has begun, and in Europe and Brazil B2 blends are being developed. ^{1}H NMR is an ideal method for monitoring the blend ratio during production and throughout the distribution network. PLS models were evaluated and found to produce adequate prediction capability [126]. NMR instrumentation at 60 MHz would be ideal for many biofuel applications and has sufficient resolution to allow real-time reaction monitoring and ready observation of biodiesel in diesel.

APPLICATIONS: HIGH-FIELD NMR SOLID-STATE ANALYSIS

Solid-state ^{13}C NMR is the predominant analysis performed in the characterization of petroleum macromolecules that are too large and insoluble to be analyzed in solvent solutions. ^{1}H NMR of carbonaceous solid materials does not yield reasonable results because of the large dipole-dipole interactions that require extremely high spinning speeds to average. For many years researchers attempted to use fast spinning and multipulse decoupling techniques, but in general the results are disappointing and very little useful information is obtained.

^{13}C NMR has been found to be very useful in the study of carbonaceous solids, and two approaches are typically taken experimentally—cross polarization (CP) and single pulse excitation (SPE), both performed with MAS. The SPE experiment is also known as Bloch decay (BD). Initially, most work was performed using CP-MAS because it has a number of time-saving advantages over SPE-MAS. The CP technique uses a polarization transfer experiment

whereby the magnetization is initially excited by a 90°pulse on the protons in the sample, and that magnetization is then transferred from the protons to the ^{13}C coupled to those protons during a thermal mixing period called a "contact time." After an optimized contact time, the mixing pulses are turned off and the ^{13}C NMR signal is collected while the protons are decoupled. This experiment has the advantage that a considerable sensitivity enhancement is gained and the experiment is performed on the T_1 time scale of the ^{1}H in the sample, which are considerably shorter than those of ^{13}C, allowing for faster acquisition of NMR spectra. The technique also has disadvantages in that quantitation is made difficult by the different rates at which the polarization from protons to carbons occurs in different chemical and motional environments. Molecular motion modulates the H-C dipole contact through which the polarization occurs, so that faster motion leads to less efficient transfer. Also, internuclear C-H distances also affect the rate of polarization transfer, and any carbon that is further than 7 A from a proton will not be observed at all. In carbonaceous materials with extended aromatic structures, this leads to nonobservation of a large amount of aromatic material. In general, this leads to SPE-MAS yielding higher aromaticity (fa) values than CP-MAS experiments. SPE-MAS also has issues with quantitation due to the long T_1 times associated with quaternary carbons and other carbon types found in petroleum. The main issue is the amount of time involved in acquisition of ^{13}C SPE-MAS experiments, which can be considerable. The instrumentation that one employs in performing these experiments also dictates which experiment the researcher will have to employ. Aromatic and carboxylic carbons have a considerably large chemical shift anisotropy (CSA), which leads to the fact that these carbon types yield an isotropic NMR peak that is surrounded by progressively smaller spinning sidebands because of the incomplete averaging of the CSA by magic angle spinning. These spinning sidebands are inherently part of the aromatic signal and must be integrated and accounted for in the various structural parameter calculations. The CSA scales with increasing NMR magnet strength. Thus, in the case of a 200 MHz NMR spectrometer the sample must be spun at 7 kHz in order for the first spinning sideband to be beyond the aliphatic region and thus able to be properly quantified. At 400 MHz, the MAS speed required for avoidance of MAS sideband overlap with aliphatic carbon signals is 14 kHz, and at 600 MHz it is 21 kHz. Interestingly, at 60 MHz, the MAS requirement is only 2.1 kHz, which means that lower magnetic field instrumentation at 60 MHz is ideal for ^{13}C CP-MAS experimentation. Lower sensitivity at 60 MHz (15 MHz for ^{13}C) field strength can be overcome by using larger sample rotors of 10–14 mm (which can easily spin at 2.1 kHz). This is an important issue because at spinning speeds above 7 kHz the C-H dipolar coupling through which the CP experiment works begins to be averaged by the MAS and thus the experiment becomes less quantitative when performed on a high-field NMR instrument. If lower MAS speeds are used, the overlap of sidebands with isotropic carbon peaks becomes a considerable quantitation problem. To avoid this issue, researchers perform only SPE-MAS experiments at higher fields where they have good sensitivity from the higher field magnet systems. However, because of the necessity to spin at 14–21 kHz, the sample rotors used are much smaller in diameter (4 mm) and some of the sensitivity gain is lost because of less sample being analyzed.

SPE-MAS does have the advantage that all carbon is potentially observed, and if long relaxation delays are used, the data yield results that are considered more representative than those obtained by CP-MAS.

The seminal paper describing the acquisition and calculation of average molecule and carbon type structural parameters was written by Solum, Pugmire, and Grant [127]. The experiments and processing/calculation methodology described have been used by many research groups as the basis for subsequent solid-state ^{13}C analysis of solid carbonaceous materials such as coal [127–138], kerogen [139–143], peat and lignites [144], refinery coke and residues [145–147], catalyst coke [148–149], bitumen and pitch [150–151], and soots and combustion deposits [152–157]. An excellent overview of the ^{13}C NMR methodology to determine the carbon skeletal structure of carbonaceous materials is presented by Solum et al. in a study of soot [152; see appendix therein]. A combination of three different experiments is required to obtain datasets from which structural parameters can be derived.

1. Variable contact time (VCT) CP-MAS experiment—a series of 20 contact times varied from 100 μs to 20 ms, the analysis of which allows the aromaticity of the sample to be determined independent of the contact time.
2. Dipolar-dephased CP-MAS, in which a series of timings for a delay and echo that are inserted after the mixing pulses are turned off and the decoupling is turned on. This experiment yields a decaying NMR signal that is fit to both Gaussian and Lorentzian decays (protonated and nonprotonated carbon signals, respectively) to yield a fraction of aromatic and aliphatic carbons that decay with a Gaussian behavior (parameter M_{0G}). As protonated carbons decay with Gaussian behavior, this allows the relative amount of protonated and nonprotonated aromatic (or aliphatic) carbons to be calculated.
3. A high signal-to-noise CP-MAS NMR obtained with a 2-ms contact time. This experiment is used to accurately determine the various integral intensity values for the different carbon types observed in the spectrum. Table 9 shows the ^{13}C chemical and structural average molecule parameters that can be calculated by a combination of the three experiments. Fig. 24 shows the plot of the mole fraction of bridgehead aromatics (X_b) versus C, where C is the number of carbons per aromatic cluster. X_b is obtained from the various integral intensity calculations. This parameter is the starting point for the average molecule structural parameter calculations. Using the plot of X_b versus C, the value of C is derived. Having reduced the carbon fraction parameters to a 100 carbon basis, it is then possible to calculate how many aromatic clusters there are per 100 carbons (Fa′/C). The rest of the calculated structural parameters are a logical progression from this value.

The utility of these solid-state ^{13}C parameters is clear for coal analysis, and the delineation between coal and petroleum chemistry is becoming less distinct with the advent of coal-derived synthetic fuels from coal-liquefaction and gasification–Fischer Tropsch processes. ^{13}C NMR is being used to predict coal liquefaction reactivity; Table 10 shows the correlations between coal carbon structure and liquefaction product yields of hydrocarbon gas, CO_x gas, water, oil, and residue.

TABLE 9—Solid-State ^{13}C NMR Parameters: Chemical Shift Ranges Utilized, Parameter Descriptions, and Calculations

Parameter	Shift Range (ppm)	Description	Calculation
F_a	90–240	Carbon Aromacity	
F'_a	90–165	Aromaticity - not including Carboxyl/Carbonyl	$F'_a = F_a - F_a^C$
F_a^C	165–240	Carboxylic and Carbonyl Carbon	
F_a^{CO}	185–240	Carbonyl - Ketone, Aldehyde	
F_a^{COO}	165–185	Carboxylic - Acid Ester, Amide	
F_a^P	150–165	Phenolic Aromatic Carbon	
F_a^S	135–150	Alkyl-Substituted Aromatic Carbons	
F_a^H	90–165	Protonated Aromatic Carbon	DD Aromatic - $F_a^H = F'_a M_{0G}$
F_a^N	90–165	Non-Protonated Aromatic Carbon	$F_a^N = F'_a - F_a^H$
F_a^B	90–165	Bridgehead Aromatic Carbon	$f_a^B = F_a^N - F_a^P - F_a^S$
F_{al}	0–50	Total Aliphatic Carbon	
F_{al}^O	50–90	Oxygenated Aliphatic Carbon	
F_{al}^H	22–50	Protonated Aliphatic Methylene and Methine	DD Aliphatic – $F_{al}^H = f_{al} M_{0G}$
F_{al}^*	0–22	Methyl Carbons	$F_{al}^* = F_{al} - F_{al}^H$
X_b		Mole fraction of Bridgehead Carbons	$X_b = F_a^B / F'_a$
C		Carbons per Aromatic Cluster	See Fig. 24 - C is calculated from Xb
$\sigma + l$		Average Number of Alkyl Attachments	$\sigma + l = (F_a^P + F_a^S)$ x C/F'_a
P_o		Fraction of Intact Bridges and Loops	$P_o = (F_a^P + F_a^S - F_{al}^*/(F_a^P + F_a^S)$
B.L.		Bridge and Loop Alkyl Attachments	B.L. $= P_0(\sigma + l)$
S.C.		Terminal Alkyl Side Chains	S.C. $= (\sigma + 1) -$ B.L.
Mw		Average Molecular Weight of a Cluster	$M_w = 12.01$ C / (F'_a x %C/100) %C from Elemental
M_T		Average Molecular Weight of Attachments	$M_T = (M_w - 13MQ_GC - 12(1\text{-}MQG)C)/(\sigma + 1)$

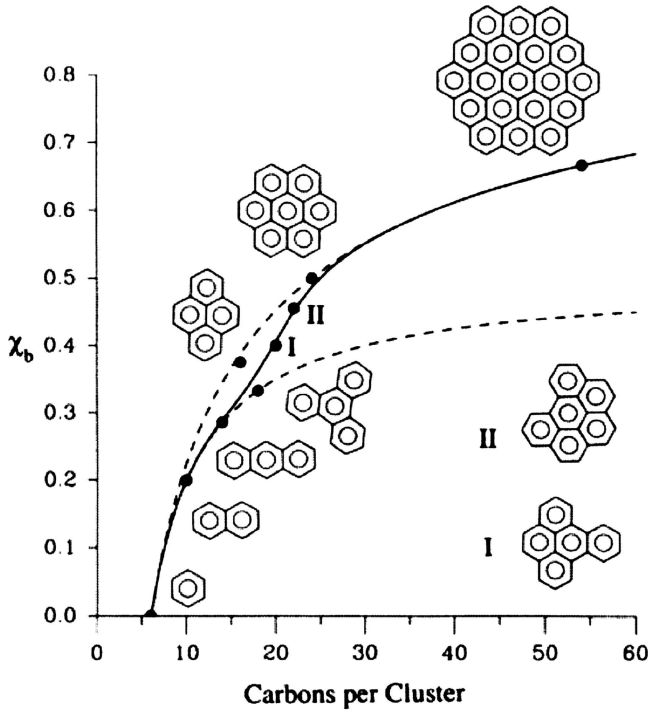

Fig. 24—Mole fraction of bridgehead aromatic carbon (X_b) versus the average number of carbons per aromatic cluster. Used in the calculation of average molecular structural parameters for carbonaceous materials by solid-state ^{13}C NMR. (Reprinted with permission from Ref [127]; © 1989 American Chemical Society.)

As alternate energy sources are investigated, the analysis of organic sedimentary solids other than coal is increasing. Type I, II, and III kerogens were studied directly by solid-state ^{13}C NMR, and the hydrogen-rich Type II and III kerogens were found to have increasing fa′, decreasing $f_a^S/(\sigma+1)$, decreasing

TABLE 10—^{13}C Carbon Types in Coal Used in Calculations to Correlate to Coal Liquefaction Yields[a]

Hydrocarbon gas (HC (wt%)) = $0.33(CH_2 + CH_3)\% + 6.15$	$25 < CH_2 + CH_3 < 45$
CO_x gas (O_{CO_x} (wt%)) = 1.43 (C=O + COOH)% − 1.45	$2 < C{=}O + COOH < 5.5$
Water (O_{H_2O}(wt%)) = 2.03 (Ar–O–OCH_3)% − 10.84	$6 < Ar{-}O{-}OCH_3 < 12$
Oil (wt%) = 0.86 CH_2% + 27.5	$20 < CH_2 < 35$
Residue (wt%) = 122.0fa − 49.2	$0.5 < fa < 0.7$

[a]Reprinted with permission from Ref [138]; © 2002 Elsevier.

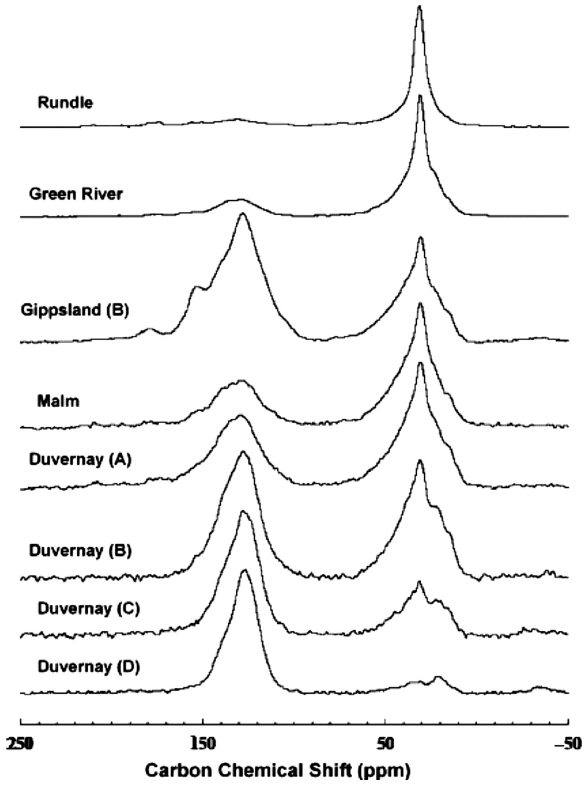

Fig. 25—Solid-state ^{13}C CP-MAS NMR spectra of a wide range of kerogens spanning a range of organic matter types and thermal maturation. (Reprinted with permission from Ref [139]; © 2007 American Chemical Society.)

attachment chain length, increasing values of C, and decreasing F_a^C, with increasing thermal maturity. Example ^{13}C spectra for a range of kerogen materials are shown in Fig. 25. The ^{13}C NMR structural parameters obtained on this broad kerogen dataset are shown in Table 11, demonstrating the large differences that are observable in the NMR-derived parameters.

CONCLUSION

NMR spectroscopy has provided detailed chemical information on the proton and carbon chemistry of petroleum materials for more than 60 years. NMR analysis will help researchers and engineers meet the future challenges involved in online process control, alternative energy exploration and production, and improved petroleum product quality. Developments in field programmable gate array electronics is currently leading to the development of cheaper and smaller NMR instrumentation platforms, which, combined with improved automated data processing and chemometric analysis software, will place NMR in the hands of many more researchers as an increasingly routine analyzer.

TABLE 11—Solid-State ^{13}C NMR Average Molecule Lattice Parameters for Kerogen and Lower Limit Estimate for Organic Oxygen $[F_a^C + 0.5(F_a^P + F_{al}^O) \times 100]$[a]

Sample	C	FAA	Cn′	$f_a^C+0.5(f_a^P+f_{al}^O)$ (×100)
Green River	16	0.40	10.3	7.0
Rundle	10	0.42	15.0	11.0
Duvernay (A)	12	0.43	4.5	12.0
Duvernay (B)	19	0.32	3.8	4.5
Duvernay (C)	19	0.30	3.4	6.0
Duvernay (D) ↓	20	0.24	1.1	4.5
Oxford Clay	13	0.40	12.5	11.2
Paradox	17	0.29	6.1	4.1
Malm	13	0.40	7.2	11.5
Draupne	17	0.36	7.6	5.8
Bakken	12	0.27	8.2	5.4
Monterey	12	0.26	15.0	7.5
Gippsland (A)	15	0.37	2.3	10.0
Gippsland (B)	14	0.31	3.1	5.5
Proprietary (A)	16	0.35	3.4	10.2
Proprietary (B)	19	0.26	1.6	3.6
Proprietary (C) ↓	18	0.15	1.8	1.2
Fruitland	14	0.32	3.8	7.9

[a]Reprinted with permission from Ref [139]; © 2007 American Chemical Society.
↓ = thermal maturity sequence, A = immature, B-C = oil window, D = post-mature

References

[1] Petrakis, L. and Allen, D., *NMR for Liquid Fossil Fuels*, Analytical Spectroscopy Library, Vol. 1, Elsevier, Amsterdam, 1987.

[2] Altgelt, K. H. and Boduszynski, M. H., *Composition and Analysis of Heavy Petroleum Fractions*, Chemical Industries Series, Vol. 54, Marcel Dekker, New York, 1993.

[3] Retcofsky, H. L. and Link, T. A., "High Resolution ^1H, ^2H, ^{13}C NMR in Coal Research," *Analytical Methods for Coal and Coal Products*, C. Karr, Ed., Vol. 2, Ch. 24, Academic Press, New York, 1978.

[4] Hirsch, E. and Altgelt, K. H., "Integrated Structural Analysis. A Method for the Determination of Average Structural Parameters of Petroleum Heavy Ends," *Anal. Chem*., Vol. 42(12), 1970, pp. 1330–1339.

[5] Cantor, D. M., "Nuclear Magnetic Resonance Spectrometric Determination of Average Molecular Structure Parameters for Coal-Derived Liquids," *Anal. Chem.*, Vol. 50(8), 1978, pp. 1185–1187.

[6] Cookson, D. J. and Smith, B. E., "One- and Two-Dimensional NMR Methods for Elucidating Structural Characteristics of Aromatic Fractions from Petroleum and Synthetic Fuels," *Energy Fuels*, Vol. 1, 1987, pp. 111–120.

[7] Murali, N. and Krishnan, V. V., "A Primer for Nuclear Magnetic Resonance in Liquids," *Concepts Magn. Reson., Part A*, Vol. 17A(1), 2003, pp. 86–116.

[8] Becker, E. D., *High Resolution NMR Theory and Chemical Applications*, Academic Press, San Diego, CA, 2000.

[9] Claridge, T. D. W., *High Resolution NMR Techniques in Organic Chemistry*, 2nd ed. Tetrahedron Organic Chemistry Series, Vol. 27, Elsevier, Amsterdam, 2009.

[10] Jacobsen, N. E., *NMR Spectroscopy Explained – Simplified Theory, Applications and Examples for Organic Chemistry and Structural Biology*, Wiley, Hoboken, NJ, 2007.

[11] Wershaw, R. L. and Mikita, M. A., Eds., *NMR of Humic Substances and Coal*, Lewis Publishers Inc., Chelsea, MI, 1987.

[12] Coates, G. R., Xiao, L. and Prammer, M. G., *NMR Logging Principles and Applications,* Halliburton Energy Services and Gulf Professional Publishing, Houston, 2001. Available at: http://www.halliburton.com/public/lp/contents/Books_and_Catalogs/web/Nmr_textbook/H02308.pdf. Accessed April 11, 2011.

[13] Allen, D., Flaum, C., Ramakrishnan, T. S., Bedford, J., Castelijns, K., Fairhurst, D., Gubelin, G., Heaton, N., Minh, C. C., Norville, M. A., Seim, M. R., Pritchard, T. and Ramamoorthy, R., "Trends in NMR Logging," *Oilfield Rev.*, Autumn 2000, pp. 2–19, Schlumberger, Ridgefield. Available at: http://www.slb.com/media/services/resources/oilfieldreview/ors00/aut00/p2_19.pdf. Accessed April 24, 2011.

[14] Sun, B. and Dunn, K. J., "Two-Dimensional Nuclear Magnetic Resonance Petrophysics," *Magn. Reson. Imaging*, Vol. 23, 2005, pp. 259–262.

[15] Sun, B. and Dunn, K. J., "A Global Inversion Method for Multi-Dimensional NMR Logging," *J. Magnet. Reson.*, Vol. 172, 2005, pp. 152–160.

[16] Altgelt, M. I. and Fitzpatrick, C. P., "Identification of Conjugated Diolefins in Fossil Fuel Liquids by ^{1}H NMR Two-Dimensional Correlated Spectroscopy," *Fuel*, Vol. 73, No. 2, 1994, pp. 223–228.

[17] ASTM Standard D3701-01: Standard Test Method for Hydrogen Content of Aviation Turbine Fuels by Low Resolution Nuclear Magnetic Resonance Spectrometry, *Annual Book of ASTM Standards*, ASTM International, West Conshohocken, PA, 2006.

[18] ASTM Standard D4808-01: Standard Test Method for Hydrogen Content of Light Distillates, Middle Distillates, Gas Oils, and Residua by Low Resolution Nuclear Magnetic Resonance Spectroscopy, *Annual Book of ASTM Standards*, ASTM International, West Conshohocken, PA, 2006.

[19] ASTM Standard D7171-05: Standard Test Method for Hydrogen Content of Middle Distillate Petroleum Products Low Resolution Pulsed Nuclear Magnetic Resonance Spectroscopy, *Annual Book of ASTM Standards*, ASTM International, West Conshohocken, PA.

[20] Kennedy, G. J., Kohout, F. C., Dabkowski, M. J. and Moy, E. A., "Improved Hydrogen Determination in Petroleum Streams Using a Bench Top Pulsed NMR Analyzer," *Energy Fuels*, Vol. 12, No. 4, 1998, pp. 812–817.

[21] Hirasaki, G. J., Lo, S. W. and Zhang, Y., "NMR Properties of Petroleum Reservoir Fluids," *Magn. Reson. Imaging*, Vol. 21, 2003, pp. 269–277.

[22] Sun, B., "In Situ Fluid Typing and Quantification with 1D and 2D NMR Logging," *Magn. Reson. Imaging*, Vol. 25, No. 4, 2007, pp. 521–524.

[23] Pena, A. A. and Hirasaki, G. J., "Enhanced Characterization of Oilfield Emulsions via NMR Diffusion and Transverse Relaxation Experiments," *Adv. Colloid Interface Sci.*, Vol. 105, 2003, pp. 103–150.

[24] Britton, M. M., Graham, R. G. and Packer, K. J., "Relationships Between Flow and NMR Relaxation of Fluids in Porous Materials," *Magn. Reson. Imaging*, Vol. 19, 2001, pp. 325–331.

[25] Watson, A. T., Hollenshead, J. T., Uh, J. and Chang, C. T. P., "NMR Determination of Porous Media Property Distributions," *Ann. Rep. NMR Spectrosc.*, Vol. 48, 2002, pp. 113–144.

[26] Lamanna, R., "On the Inversion of Multicomponent NMR Relaxation and Diffusion Decays in Heterogeneous Systems," *Concepts Magn. Reson. Part A*, Vol. 26A, No. 2, 2005, pp. 78–90.

[27] Song, Y. Q., "Resolution and Uncertainty of Laplace Inversion Spectrum," *Magn. Reson. Imaging*, Vol. 25, 2007, pp. 445–448.

[28] Aichele, C. P., Chapman, W. G., Rhyne, L. D., Subramani, H. J., Montesi, A., Creek, J. L. and House, W., "Nuclear Magnetic Resonance Analysis of Methane Hydrate Formation in Water-in-Oil Emulsions," *Energy Fuels*, Vol. 23(2), 2009, pp. 835–841.

[29] Kantzas, A., Bryan, J. L., Mai, A. and Hum, F. M., "Applications of Low Field NMR Techniques in the Characterization of Oil Sand Mining, Extraction, and Upgrading Processes," *Can. J. Chem. Eng.*, Vol. 83, 2005, pp. 145–150.

[30] Bryan, J., Kantzas, A. and Bellehumeur, C., "Oil-Viscosity Predictions from Low-Field NMR Measurements," *SPE Reserv. Eval. Eng.*, Vol. 8, No. 1, 2005, pp. 44–52 (SPE-89070-PA).

[31] Wen, Y. W. and Kantzas, A., "Monitoring Bitumen-Solvent Interactions with Low-Field Nuclear Magnetic Resonance and X-ray Computer-Assisted Tomography," *Energy Fuels*, Vol. 19, 2005, pp. 1319–1326.

[32] Jiang, T., Hirasaki, G., Miller, C., Moran, K. and Fleury, M., "Diluted Bitumen Water-in-Oil Emulsion Stability and Characterization by Nuclear Magnetic Resonance (NMR) Measurements," *Energy Fuels*, Vol. 21, 2007, pp. 1325–1336.

[33] Motta, C., Bryan, J. and Kantzas, A., "Characterization of Oil Sands Tailings Using Nuclear Magnetic Resonance (NMR) Technique," *10th International Mine Water Association Congress*, Karlovy Vary, Czech Republic, June 2008. Available at http://www.imwa.info/docs/imwa_2008/IMWA2008_056_Motta.pdf. Accessed April 11, 2010.

[34] Dolinsek, J., Jeglic, P., Apih, T., Lahajnar, G., Naglic, O. and Sever, A., "Temperature-Dependent Bitumen Softening Studied by NMR," *J. Phys. D: Appl. Phys.*, Vol. 33, 2000, pp. 1615–1624.

[35] Harmer, J., Callcott, T., Maeder, M. and Smith, B. E., "A Novel Approach for Coal Characterization by NMR Spectroscopy: Global Analysis of Proton T1 and T2 Relaxations," *Fuel*, Vol. 80, 2001, pp. 417–425.

[36] Harmer, J., Callcott, T., Maeder, M. and Smith, B. E., "A Rapid Coal Characterization by Low-Resolution NMR Spectroscopy and Partial Least-Squares Regression," *Fuel*, Vol. 80, 2001, pp. 1341–1349.

[37] Nordon, A., McGill, C. A. and Littlejohn, D., "Evaluation of Low-Field Nuclear Magnetic Resonance Spectrometry for At-Line Process Analysis," *Appl. Spectrosc.*, Vol. 56, No. 1, 2002, pp. 75–82.

[38] Todt, H., Guthausen, G., Burk, W., Schmalbein, D. and Kamlowski, A., "Time Domain NMR in Quality Control: Standard Applications in Food," *Modern Magnetic Resonance*, G. A. Webb, Ed., Springer, Dordrecht, 2008, pp. 1739–1743.

[39] Roy, A. K. and Marino, S. A., "NMR in Process Control," *Am. Lab.*, Vol. 31, No. 21, 1999, pp. 32–33.

[40] Sardashti, M., Gislason, J. J., Lai, X., Stewart, C. A. and O'Donnell, D. J., "Determination of Total Styrene in Styrene/Butadiene Block Copolymers by Process NMR and Chemometrics Modeling," *Appl. Spectrosc.*, Vol. 55, No. 4, 2001, pp. 467–471.

[41] Giammatteo, P. J., Edwards, J. C., Cohen, T. and Blakley, M. W., "Process Applications of NMR on Flowing Gaseous Streams. Part III. The Installation and Operation

of an On-Line NMR in a Refinery," *37th Experimental NMR Conference*, Pacific Grove, CA, March 17–22, 1996.

[42] Edwards, J. C. and Giammatteo, P. J., "On-line Acid Strength Measurement and Sulfuric Acid Alkylation Process Control Using Process NMR," *ISA Tech-Expo Technology Update*, Vol. 2, 1998, pp. 63–67.

[43] Skloss, T. W., Kim, A. J. and Haw, J. F., "High-Resolution NMR Process Analyzer for Oxygenates in Gasoline," *Anal. Chem.*, Vol. 66, 1994, pp. 536–542.

[44] Edwards, J. C., Giammatteo, P. J., Firmstone, G. P. and Cusatis, P. D., "Development of a Process NMR Gasoline Analysis System," *37th Experimental NMR Conference*, Pacific Grove, CA, March 17–22, 1996.

[45] Corrado, L., Roobottom, L. J. and Palmer, L. D., "Application of Magnetic Resonance Analysis (MRA) for the Production of Clean Fuels," *Chemeca 2005*, Brisbane, Australia, September 25, 2005.

[46] Edwards, J. C. and Giammatteo, P. J., "Detailed Hydrocarbon Analysis of Naphtha by On–Line NMR : Integration of Real-Time NMR Feed Analysis With Advanced Process Control and Optimization," *Eastern Analytical Symposium*, Somerset, NJ, November 18–21, 2002.

[47] Edwards, J. C., "Steam Cracker Performance Optimized by Process MRA," *Control*, July 2003. Available at: http://www.controlglobal.com/articles/2003/252.html. Accessed April 24, 2011.

[48] Barnard, P. A., Gerlovich, C. and Moore, R., "The Validation of an On-line Nuclear Magnetic Resonance Spectrometer for Analysis of Naphthas and Diesels," *ISA Analytical Division Meeting,* Calgary, Alberta, April 2003.

[49] Seshadri, R., Offerman, A., Cijntje, J., McFarlane, R. and Lough, V., "Optimization of a Refinery Crude Unit," *Petrol. Technol. Q.*, Winter, 2002, pp. 1–7.

[50] Giammatteo, P. J. and Edwards, J. C. "On-Line Analysis of Crude Feeds and Distillation Products: Utilization of On-Line NMR on a Refinery's Crude Distillation Unit," *Eastern Analytical Symposium*, Somerset, NJ, November 18–21, 2002.

[51] Giammatteo, P. J. and Edwards, J. C., "Counting Carbons for Tighter Control: Combining GC and NMR to Improve Distillate Manufacturing," *104th Gulf Coast Conference*, Galveston, TX, January 20–21, 2009.

[52] Guanziroli, S., Giardino, R., Farina, A., Lough, V. and Edwards, J. C., "Process MRA - Lube Plant Application," *ERTC Computing Conference*, Milan, Italy, June 23–25, 2003.

[53] Altgelt, K. H. and Boduszynski, M. H., "Structural Group Characterization of Heavy Petroleum Fractions," *Composition and Analysis of Heavy Petroleum Fractions*, Chemical Industries Series, Vol. 54, Chapter 5, pp. 159–201, Marcel Dekker, New York, 1993.

[54] Altgelt, K. H. and Boduszynski, M. H., "Structural Group Characterization by Advanced NMR Techniques," *Composition and Analysis of Heavy Petroleum Fractions*, Chemical Industries Series, Vol. 54, Chapter 8, pp. 309–363, Marcel Dekker, New York, 1993.

[55] Mullins, O. C., Martinez-Haya, B. and Marshall, A. G., "Contrasting Perspective on Asphaltene Molecular Weight. This Comment vs the Overview of A. A. Herod, K. D. Bartle, and R. Kandiyoti," *Energy Fuels*, Vol. 22, 2008, pp. 1765–1773.

[56] Herod, A. A., Bartle, K. D. and Kandiyoti, R., "Comment on a Paper by Mullins, Martinez-Haya, and Marshall 'Contrasting Perspective on Asphaltene Molecular Weight. This Comment vs the Overview of A. A. Herod, K. D. Bartle, and R. Kandiyoti,'" *Energy Fuels*, Vol. 22, 2008, pp. 4312–4317.

[57] Cookson, D. J., Lloyd, C. P. and Smith, B. E., "Investigation of the Chemical Basis of Kerosene (Jet Fuel) Specification Properties," *Energy Fuels*, Vol. 1, 1987, pp. 438–447.

[58] Cookson, D. J., Lloyd, C. P. and Smith, B. E., "Investigation of the Chemical Basis of Diesel Fuel Properties," *Energy Fuels*, Vol. 2, 1988, pp. 854–860.

[59] Cookson, D. J. and Smith, B. E., "Observed and Predicted Properties of Jet and Diesel Fuels Formulated from Coal Liquefaction and Fischer-Tropsch Feedstocks," *Energy Fuels*, Vol. 6, 1992, pp. 581–585.

[60] Cookson, D. J., Shaw, I. M. and Smith, B. E., "Determination of Hydrocarbon Compound Class Abundances in Kerosene and Diesel Fuels: Chromatographic and Nuclear Magnetic Resonance Methods," *Fuel*, Vol. 66, 1987, pp. 758–765.

[61] Cookson, D. J. and Smith, B. E., "Calculation of Jet and Diesel Fuel Properties Using ^{13}C NMR Spectroscopy," *Energy Fuels*, Vol. 4, 1990, pp. 152–156.

[62] Cookson, D. J., Iliopoulos, P. and Smith, B. E., "Composition-Property Relations for Jet and Diesel Fuels of Variable Boiling Range," *Fuel*, Vol. 74, No. 1, 1995, pp. 70–78.

[63] Bansal, V., Krishna, G. J., Singh, A. P., Gupta, A. K. and Sarpal, A. S., "Determination of Hydrocarbon Types and Oxygenates in Motor Gasoline: A Comparative Study of Different Analytical Techniques," *Energy Fuels*, Vol. 22, 2008, pp. 410–415.

[64] Kapur, G. S., Singh, A. P. and Sarpal, A. S. "Determination of Aromatics and Naphthenes in Straight Run Gasoline by ^{1}H NMR Spectroscopy. Part I," *Fuel*, Vol. 79, 2000, pp. 1023–1029.

[65] Sarpal, A. S., Kapur, G. S., Mukherjee, S. and Tiwari, A. K., "PONA Analyses of Cracked Gasoline by ^{1}H NMR Spectroscopy. Part II," *Fuel*, Vol. 80, 2001, pp. 521–528.

[66] Singh, A. P., Mukherji, S., Tewari, A. K., Kalsi, W. R. and Sarpal, A. S., "Determination of Benzene and Total Aromatics in Commercial Gasolines Using Packed Column GC and NMR Techniques," *Fuel*, Vol. 82, 2003, pp. 23–33.

[67] Burri, J., Crockett, R., Hany, R. and Rentsch, D., "Gasoline Composition Determined by ^{1}H NMR Spectroscopy," *Fuel*, Vol. 83, 2004, pp. 187–193.

[68] Meusinger, R., "Qualitative and Quantitative Determination of Oxygenates in Gasolines Using ^{1}H Nuclear Magnetic Resonance Spectroscopy," *Anal. Chim. Acta*, Vol. 391, 1999, pp. 277–288.

[69] Sarpal, A. S., Kapur, G. S., Mukherjee, S. and Jain, S. K., "Estimation of Oxygenates in Gasoline by ^{13}C NMR Spectroscopy," *Energy Fuels*, Vol. 11, 1997, pp. 662–667.

[70] Hiller, W. G., Abu-Dagga, F. and Al-Tahou, B., "Determination of Gasoline Octane Numbers by ^{1}H- and ^{13}C-NMR Spectroscopy," *J. für Praktische Chemie/Chemiker-Zeitung*, Vol. 334, No. 8, 1992, pp. 691–695.

[71] Mukherjee, S., Kapur, G. S., Chopra, A. and Sarpal, A. S., "^{1}H NMR Spectroscopic-Based Method for the Estimation of Total Aromatic Content of Aviation Turbine Fuels (ATF): Comparison with Liquid Chromatographic Methods," *Energy Fuels*, Vol. 18, 2004, pp. 30–36.

[72] Bansal, V., Kapur, G. S., Sarpal, A. S., Kagdiyal, V., Jain, S. K., Srivastava, S. P. and Bhatnagar, A. K., "Estimation of Total Aromatics and their Distribution as Mono and Global Di-Plus Aromatics in Diesel-Range Products by NMR Spectroscopy," *Energy Fuels*, Vol. 12, 1998, pp. 1223–1227.

[73] Bansal, V., Sarpal, A. S., Kapur, G. S. and Sharma, V. K., "Estimation of Bromine Number of Petroleum Distillates by NMR Spectroscopy," *Energy Fuels*, Vol. 14, 2000, pp. 1028–1031.

[74] Bansal, V., Vatsala, S., Kapur, G. S., Basu, B. and Sarpal, A. S., "Hydrocarbon-Type Analysis of Middle Distillates by Mass Spectrometry and NMR Spectroscopy Techniques–A Comparison," *Energy Fuels*, Vol. 18, 2004, pp. 1505–1511.

[75] Kapur, G. S., Chopra, A. and Sarpal, A. S., "Estimation of Total Aromatic Content of Vacuum Gas Oil (VGO) Fractions (370–560°C) by ^{1}H NMR Spectroscopy," *Energy Fuels*, Vol. 19, No. 3, 2005, pp. 1065–1071.

[76] Bansal, V., Krishna, G. J., Chopra, A. and Sarpal, A. S., "Detailed Hydrocarbon Characterization of RFCC Feed Stocks by NMR Spectroscopic Techniques," *Energy Fuels*, Vol. 21, No. 2, 2007, pp. 1024–1029.

[77] Kapur, G. S., Ecker, A. and Meusinger, R., "Establishing Quantitative Structure–Property Relationships (QSPR) of Diesel Samples by Proton-NMR & Multiple Linear Regression (MLR) Analysis," *Energy Fuels*, Vol. 15, 2001, pp. 943–948.

[78] Molina, D. V., Uribe, U. N. and Murgich, J., "Partial Least-Squares Correlation Between Refined Product Yields and Physicochemical Properties with the ^{1}H Nuclear Magnetic Resonance (NMR) Spectra of Colombian Crude Oils," *Energy Fuels*, Vol. 21, 2007, pp. 1674–1680.

[79] Edwards, J. C. and Kim, J., "RCC Feed-Stream Analysis by ^{1}H and ^{13}C NMR: Multivariate Prediction of Physical and Chemical Properties," *Preprint Papers, American Chemical Society, Division of Petroleum Chemistry*, Vol. 53, No. 2, 2008, pp. 54–57.

[80] Monteiro, M. R., Ambrozin, A. R. P., Lião, L. M., Boffo, E. F., Tavares, L. A., Ferreira, M. M. C. and Ferreira, A. G., "Study of Brazilian Gasoline Quality Using Hydrogen Nuclear Magnetic Resonance (^{1}H NMR) Spectroscopy and Chemometrics," *Energy Fuels*, Vol. 23, No. 1, 2009, pp. 272–279.

[81] Meusinger, R. and Moros, R., "Determination of Octane Numbers of Gasoline Compounds from their Chemical Structure by ^{13}C NMR Spectroscopy and Neural Networks," *Fuel*, Vol. 80, 2001, pp. 613–621.

[82] Yang, Y., Liu, B., Xi, H., Sun, X. and Zhang, T., "Study on Relationship Between the Concentration of Hydrocarbon Groups in Heavy Oils and their Structural Parameter from ^{1}H NMR Spectra," *Fuel*, Vol. 82, 2003, pp. 721–727.

[83] ASTM Standard D5292-99: Standard Test Method for Aromatic Carbon Contents of Hydrocarbon Oils by High Resolution Nuclear Magnetic Resonance Spectroscopy, *Annual Book of ASTM Standards*, ASTM International, West Conshohocken, PA, 2004.

[84] Behera, B., Ray, S. S. and Singh, I. D., "Structural Characterization of FCC Feeds from Indian Refineries by NMR Spectroscopy," *Fuel*, Vol. 87, 2008, pp. 2322–2333.

[85] Al-Zaid, K., Khan, Z. H., Hauser, A. and Al-Rabiah, H., "Composition of High Boiling Petroleum Distillates of Kuwait Crude Oils," *Fuel*, Vol. 77, No. 5, 1998, pp. 453–458.

[86] Ali, F., Khan, Z. H. and Ghaloum, N., "Structural Studies of Vacuum Gas Oil Distillate Fractions of Kuwaiti Crude Oil by Nuclear Magnetic Resonance," *Energy Fuels*, Vol. 18, 2004, pp. 1798–1805.

[87] Zhao, S., Sparks, B. D., Kotlyar, L. S. and Chung, K. H., "Correlation of Processability and Reactivity Data for Residua from Bitumen, Heavy Oils, and Conventional Crudes: Characterization of Fractions from Super-Critical Pentane Separation as a Guide to Process Selection," *Catal. Today*, Vol. 125, 2007, pp. 122–136.

[88] Zhao, S., Kotlyar, L. S., Woods, J. R., Sparks, B. D., Hardacre, K. and Chung, K. H., "Molecular Transformation of Athabasca Bitumen End-Cuts During Cooling and Hydrocracking," *Fuel*, Vol. 80, 2001, pp. 1155–1163.

[89] Desando, M. A. and Ripmeester, J. A., "Chemical Derivitization of Athabasca Oil Sand Asphaltene for Analysis of Hydroxyl and Carboxyl Groups via Nuclear Magnetic Resonance Spectroscopy," *Fuel*, Vol. 81, 2002, pp. 1305–1319.

[90] Christopher, J., Sarpal, A. S., Kapur, G. S., Krishna, A., Tyagi, B. R., Jain, M. C., Jain, S. K. and Bhatnagar, A. K., "Chemical Structure of Bitumen-Derived Asphaltenes by Nuclear Magnetic Resonance Spectroscopy and X-ray Diffractometry," *Fuel*, Vol. 75, 1996, pp. 999–1008.

[91] Calemma, V., Rausa, R., D'Antona, P. and Montanari, L., "Characterization of Asphaltenes Molecular Structure," *Energy Fuels*, Vol. 12, 1998, pp. 422–428.

[92] Artok, L., Su, Y., Hirose, Y., Hosokawa, M., Murata, S. and Nomura, M., "Structure and Reactivity of Petroleum-Derived Asphaltene," *Energy Fuels*, Vol. 13, 1999, pp. 287–296.

[93] Sheremata, J. M., Gray, M. R., Dettman, H. D. and McCaffrey, W. C., "Quantitative Molecular Representation and Sequential Optimization of Athabasca Asphaltenes," *Energy Fuels*, Vol. 18, No. 5, 2005, pp. 1377–1384.

[94] Seki, H. and Kumata, F., "Structural Change of Petroleum Asphaltenes and Resins by Hydrodemetallization," *Energy Fuels*, Vol. 14, 2000, pp. 980–985.

[95] Scotti, R. and Montanari, L. "Molecular Structure and Intermolecular Interaction of Asphaltenes by FT-IR, NMR, EPR," *Structures and Dynamics of Asphaltenes,* O. C. Mullins and E. Y. Sheu, Eds., Plenum Press, New York, Ch. III, 1998, p. 79.

[96] Bansal, V., Patel, M. B. and Sarpal, A. S., "Structural Aspects of Crude Oil Derived Asphaltenes by NMR and XRD and Spectroscopic Techniques," *Petrol. Sci. Technol.*, Vol. 22, 2004, pp. 1401–1426.

[97] Michon, L., Martin, D., Planche, J-P. and Hanquet, B., "Estimation of Average Molecule Parameters of Bitumens by ^{13}C Nuclear Magnetic Resonance Spectroscopy," *Fuel*, Vol. 76, 1997, pp. 9–15.

[98] Japanwala, S., Chung, K. H., Dettman, H. D. and Gray, M. R., "Quality of Distillates from Repeated Recycle of Residue," *Energy Fuels*, Vol. 16, 2002, pp. 477–485.

[99] Durand, E., Clemancey, M., Lancelin, J-M., Verstraete, J., Espinat, D. and Quoineaud, A-A., "Effect of Chemical Composition on Asphaltene Aggregation," *Energy Fuels*, Vol. 25, 2010, pp. 1051–1062.

[100] Netzel, D. A., "Quantitation of Carbon Types Using DEPT/QUAT NMR Pulse Sequences: Application to Fossil Fuel Derived Oils," *Anal. Chem.*, Vol. 59, 1987, pp. 1775–1779.

[101] Netzel, D. A. and Guffey, F. D., "NMR and GC/MS Investigation of the Saturate Fraction from the Cerro Negro Heavy Petroleum Crude," *Energy Fuels*, Vol. 3, 1989, pp. 455–460.

[102] Dereppe, J. M. and Moreux, C., "Measurement of CH_n Group Abundances in Fossil Fuel Materials Using DEPT ^{13}C NMR," *Fuel*, Vol. 64, 1985, pp. 1174–1176.

[103] Jiang, B., Xiao, N., Liu, H., Zhou, Z., Mao, X. and Liu, M., "Optimized Quantitative DEPT and Quantitative POMMIE Experiments for ^{13}C NMR," *Anal. Chem.*, Vol. 80, 2008, pp. 8293–8298.

[104] Montanari, L., Montani, E., Corno, C. and Fattori, S., "NMR Molecular Characterization of Lubricating Base Oils: Correlation with their Performance," *Appl. Magn. Reson.*, Vol. 14, 1998, pp. 345–356.

[105] Diaz, C. and Blanco, C. G., "NMR: A Powerful Tool in the Characterization of Coal Tar Pitch," *Energy Fuels*, Vol. 17, 2003, pp. 907–913.

[106] Morgan, T. J., George, A., Davis, D. B., Herod, A. A. and Kandiyoti, R., "Optimization of ^{1}H and ^{13}C NMR Methods for Structural Characterization of Acetone and Pyridine Soluble Fractions of a Coal Tar Pitch," *Energy Fuels*, Vol. 22, 2008, pp. 1824–1835.

[107] Masuda, K., Okuma, O., Nishizawa, T., Kanaji, M. and Matsumura, T., "High Temperature NMR Analysis of Aromatic Units in Asphaltenes and Preasphaltenes Derived from Victorian Brown Coal," *Fuel*, Vol. 75, 1996, pp. 295–299.

[108] Begon, V., Suelves, I., Islas, C. A., Millan, M., Dubau, C., Lazaro, M-J., Law, R. V., Herod, A. A., Dugwell, D. R. and Kandiyoti, R., "Comparison of Quaternary Aromatic Carbon Contents of a Coal, a Coal Extract, and its Hydrocracking Products by NMR Methods," *Energy Fuels*, Vol. 17, 2003, pp. 1616–1629.

[109] Sharma, B. K. and Stipanovic, A. J., "Pulsed Field Gradient NMR Spectroscopy: Applications in Determining the Pressure Viscosity Coefficient and Low Temperature Flow Properties of Lubricant Base Oils," *Ind. Eng. Chem. Res.*, Vol. 42, 2003, pp. 1522–1529.

[110] Kapur, G. S. and Berger, S., "Pulsed Field Gradient (PFG) NMR Spectroscopy: An Effective Tool for the Analysis of Mixtures of Lubricating Oil Components," *Tribotest J.*, Vol. 6, No. 4, 2000, pp. 323–336.

[111] Sharma, B. K., Adhvaryu, A., Perez, J. M. and Erhan, S. Z., "Effects of Hydroprocessing on Structure and Properties of Base Oils Using NMR," *Fuel Proc. Technol.*, Vol. 89, 2008, pp. 984–991.

[112] Adhvaryu, A., Perez, J. M. and Singh, I. D., "Application of Quantitative NMR Spectroscopy to Oxidation Kinetics of Base Oils Using a Pressurized Differential Scanning Calorimetry Technique," *Energy Fuels*, Vol. 13, No. 2, 1999, pp. 205–206.

[113] Adhvaryu, A., Pandey, D. C. and Singh, I. D., "NMR and DSC Studies of Base Oils," *Tribotest J.*, Vol. 5, No. 3, 1999, pp. 313–320.

[114] Sarpal, A. S., Kapur, G. S., Mukherjee, S. and Jain, S. K., "Characterization by ^{13}C NMR Spectroscopy of Base Oils Produced by Different Processes," *Fuel*, Vol. 76, No. 10, 1997, pp. 931–937.

[115] Sarpal, S. A., Kapur, G. S., Chopra, A., Jain, S. K., Srivastava, S. P. and Bhatnagar, A. K., "Hydrocarbon Characterization of Hydrocracked Base Stocks by One- and Two-Dimensional NMR Spectroscopy," *Fuel*, Vol. 75, No. 4, 1996, pp. 483–490.

[116] Murphy, J. W., Cody, I. A. and Silbernagel, B. G., "Lube Basestock with Excellent Low Temperature Properties and a Method for Making," U.S. Patent 6,676,827, 2004.

[117] Miller, S. J., O'Rear, D. J. and Rosenbaum, J., "Processes for Producing Lubricant Base Oils with Optimized Branching," U.S. Patent 7,018,525, 2006.

[118] Trewella, J. C., Forbus, T. R., Jiang, Z., Partridge, R. D. and Schramm, S. E., "Isoparaffinic Lube Basestock Compositions," U.S. Patent 6,090,989, 2000.

[119] Cook, B. R., Berlowitz, P. J., Silbernagel, B. G. and Sysyn, D. A., "Uses of ^{13}C NMR Spectroscopy to Produce Optimum Fischer-Tropsch Diesel Fuels and Blend Stocks," U.S. Patent 6,210,559, 2001.

[120] Kobayashi, M., Saitoh, M., Togawa, S. and Ishida, K., "Branching Structure of Diesel and Lubricant Base Oils Prepared by Isomerization/Hydrocracking of Fischer-Tropsch Waxes and α-Olefins," *Energy Fuels*, Vol. 23, No. 1, 2009, pp. 513–518.

[121] Satyarthi, J. K., Srinivas, D. and Ratnasamy, P., "Estimation of Free Fatty Acid Content in Oils, Fats, and Biodiesel by ^{1}H NMR Spectroscopy," *Energy Fuels*, Vol. 23, No. 4, 2009, pp. 2273–2277.

[122] Jin, F., Kawasaki, K., Kishida, H., Tohji, K., Moriya, T. and Enomoto, H., "NMR Spectroscopic Study on Methanolysis Reaction of Vegetable Oil," *Fuel*, Vol. 86, 2007, pp. 1201–1207.

[123] Mello, V. M., Oliveira, F. C. C., Fraga, W. G., do Nascimento, C. J. and Suarez, P. A. Z., "Determination of the Content of Fatty Acid Methyl Esters (FAME) in Biodiesel Samples Obtained by Esterification Using ^{1}H NMR Spectroscopy," *Magn. Reson. Chem.*, Vol. 46, No. 11, 2008, pp. 1051–1054.

[124] Knothe, G., "Determining the Blend Level of Mixtures of Biodiesel with Conventional Diesel Fuel by Fiber Optic NIR Spectroscopy and ^{1}H NMR Spectroscopy," *J. Am. Oil Chem. Soc.*, Vol. 78, 2001, pp. 1025–1028.

[125] Knothe, G., "Analysis of Oxidized Biodiesel by ^{1}H NMR and Effect of Contact Area with Air," *Eur. J. Lipid Sci. Technol.*, Vol. 108, 2006, pp. 493–500.

[126] Monteiro, M. R., Ambrozin, A. R. P., Santos, M. S., Boffo, E. F., Pereira-Filho, E. R., Lião, L. M. and Ferreira, A. G., "Evaluation of Biodiesel-Diesel Blends Quality using ^{1}H NMR and Chemometrics," *Talanta*, Vol. 78, 2009, pp. 660–664.

[127] Solum, M. S., Pugmire, R. J. and Grant, D. M., "^{13}C Solid-State NMR of Argonne Premium Coals," *Energy Fuels*, Vol. 3, 1989, pp. 187–193.

[128] Fletcher, T. H., Kerstein, A. R., Pugmire, R. J., Solum, M. S. and Grant, D. M., "Chemical Percolation Model for Devolatilization. 3. Direct Use of ^{13}C NMR Data to Predict Effects of Coal Type," *Energy Fuels*, Vol. 6, 1992, pp. 414–431.

[129] Hu, J. Z., Solum, M. S., Taylor, C. M. V., Pugmire, R. J. and Grant, D. M., "Structural Determination in Carbonaceous Solids Using Advanced Solid State NMR Techniques," *Energy Fuels*, Vol. 15, 2001, pp. 14–22.

[130] Fletcher, T. H., Bai, S., Pugmire, R. J., Solum, M. S., Wood, S. and Grant, D. M., "Chemical Structure Features of Pyridine Extracts and Residues of the Argonne Premium Coals Using Solid-State C-13 NMR Spectroscopy," *Energy Fuels*, Vol. 7, 1993, pp. 734–742.

[131] Maroto-Valer, M. M., Atkinson, C. J., Willmers, R. R. and Snape, C. E., "Characterization of Partially Carbonized Coals by Solid-State ^{13}C NMR and Optical Microscopy," *Energy Fuels*, Vol. 12, 1998, pp. 833–842.

[132] Kawashima, H. and Saito, I., "Interactions of Organic Liquids with Coals: Analysis by Solid-State ^{13}C Nuclear Magnetic Resonance," *Energy Fuels*, Vol. 18, 2004, pp. 1723–1731.

[133] Genetti, D., Fletcher, T. H. and Pugmire, R. J., "Development and Application of a Correlation of ^{13}C NMR Chemical Structural Analyses of Coal Based on Elemental Composition and Volatile Matter Content," *Energy Fuels*, Vol. 13, 1999, pp. 60–68.

[134] Suggate, R. P. and Dickinson, W. W., "Carbon NMR of Coals: The Effects of Coal Type and Rank," *Int. J. Coal Geol.*, Vol. 57, 2004, pp. 1–22.

[135] Maroto-Valer, M. M., Andresen, J. M. and Snape, C. E., "Verification of the Linear Relationship Between Carbon Aromaticities and H/C Ratios for Bituminous Coals," *Fuel*, Vol. 77, 1998, pp. 783–785.

[136] Bandara, T. S., Kannangara, G. S. K., Wilson, M. A., Boreham, C. J. and Fisher, K., "The Study of Australian Coal Maturity: Relationship Between Solid-State NMR Aromaticities and Organic Free-Radical Count," *Energy Fuels*, Vol. 19, 2005, pp. 954–959.

[137] Masuda, K., Olkuma, O., Nishizawa, T., Kanaji, M. and Matsumura, T., "High Temperature N.M.R. Analysis of Aromatic Units in Asphaltenes and Preasphaltenes Derived from Victorian Brown Coal," *Fuel*, Vol. 75, 1996, pp. 295–299.

[138] Yoshida, T., Sasaki, M., Ikeda, K., Mochizuki, M., Nogami, Y. and Inokuchi, K., "Prediction of Coal Liquifaction Reactivity by Solid-State ^{13}C NMR Spectral Data," *Fuel*, Vol. 81, 2002, pp. 1533–1539.

[139] Kelemen, S. R., Afeworki, M. L., Gobarty, M. L., Sansone, P. J., Kwiatek, P. J., Walters, C. C., Freund, H., Siskin, M., Bence, A. E., Curry, D. J., Solum, M., Pugmire, R. J., Vandenbroucke, M., Leblond, M. and Behar, F., "Direct Characterization of Kerogen by X-ray and Solid-State ^{13}C Nuclear Magnetic Resonance Methods," *Energy Fuels*, Vol. 21, 2007, pp. 1548–1561.

[140] Wei, Z., Gao, X., Zhang, D. and Da, J., "Assessment of Thermal Evolution of Kerogen Geopolymers with their Structural Parameters Measured by Solid-State ^{13}C NMR Spectroscopy," *Energy Fuels*, Vol. 19, 2005, pp. 240–250.

[141] Werner-Zwanziger, U., Lis, G., Mastalerz, M. and Schimmelmann, A., "Thermal Maturity of Type II Kerogen from the New Albany Shale Assessed by ^{13}C CP/MAS NMR," *Solid State Nucl. Mag. Reson.*, Vol. 27, 2005, pp. 140–148.

[142] Conte, P. and Berns, A. E., "Dynamics of Cross Polarization in Solid State Nuclear Magnetic Resonance Experiments of Amorphous and Heterogeneous Organic Substances," *Anal. Sci.*, Vol. 24, 2008, pp. 1183–1188.

[143] Freund, H., Walters, C. F., Kelemen, S. R., Siskin, M., Gorbarty, M. L., Curry, D. J. and Bence, A. E., "Predicting Oil and Gas Compositional Yields via Chemical Structure-Chemical Yield Modeling (CS-CYM): Part 1 – Concepts and Implementation," *Org. Geochem.*, Vol. 38, No. 2, 2007, pp. 288–305.

[144] Kelemen, S. R., Afeworki, M., Gorbarty, M. L. and Cohen, A. D., "Characterization of Organically Bound Oxygen Forms in Lignites, Peats, and Pyrolyzed Peats by X-ray Photoelectron Spectroscopy (XPS) and Solid-State ^{13}C NMR Methods," *Energy Fuels*, Vol. 16, 2002, pp. 1450–1462.

[145] Michel, D., Pruski, M. and Gerstein, B. C., "NMR of Petroleum Cokes, I: Relaxation Studies and Quantitative Analysis of Hydrogen by Magnetic Resonance," *Carbon*, 32, No. 1, 1994, pp. 31–40.

[146] Pruski, M., Michel, D. and Gerstein, B. C., "NMR of Petroleum Cokes, II: Studies by High Resolution Solid State NMR of ^{1}H and ^{13}C," *Carbon*, Vol. 32, No. 1, 1994, pp. 41–49.

[147] Siskin, M., Kelemen, S. R., Eppig, C. P., Brown, L. D. and Afeworki, M., "Asphaltene Molecular Structure and Chemical Influences on the Morphology of Coke Produced in Delayed Coking," *Energy Fuels*, Vol. 20, 2006, pp. 1227–1234.

[148] Snape, C. E., McGhee, B. J., Martin, S. C. and Andresen, J. M., "Structural Characterization of Catalytic Coke by Solid-State ^{13}C-NMR Spectroscopy," *Catal. Today*, Vol. 37, 1997, pp. 285–293.

[149] Hauser, A., Marafi, A., Stanislaus, A. and Al-Adwani, A., "Relation Between Feed Quality and Coke Formation in a Three-Stage Atmospheric Residue Desulfurization (ARDS) Process," *Energy Fuels*, Vol. 19, No. 2, 2005, pp. 544–553.

[150] Kersaw, J. R. and Black, K. J. T., "Structural Characterization of Coal-Tar and Petroleum Pitches," *Energy Fuels*, Vol. 7, 1993, pp. 420–425.

[151] Pugmire, R. J., Solum, M. S., Grant, D. M., Critchfield, S. and Fletcher, T. H., "Structural Evolution of Matched Tar-Char Pairs in Rapid Pyrolysis Experiments," *Fuel*, Vol. 70, 1991, pp. 414–423.

[152] Solum, M. S., Sarofim, A. F., Pugmire, R. J., Fletcher, T. H. and Zhang, H., "^{13}C NMR of Soot Produced from Model Compounds and a Coal," *Energy Fuels*, Vol. 15, 2001, pp. 961–971.

[153] Jiang, Y. J., Solum, M. S., Pugmire, R. J., Grant, D. M., Schobert, H. H. and Pappano, P. J., "A New Method for Measuring the Graphite Content of Anthracite Coals and Soots," *Energy Fuels*, Vol. 16, 2002, pp. 1296–1300.

[154] Winans, R. E., Tomczyk, N. A., Hunt, J. E., Solum, M. S., Pugmire, R. J., Jiang, Y. J. and Fletcher, T. H., "Model Compound Study of the Pathways for Aromatic Hydrocarbon Formation in Soot," *Energy Fuels*, Vol. 21, 2007, pp. 2584–2593.

[155] Yan, S., Jiang, Y-J., Marsh, N. D., Eddings, E. G., Sarofim, A. F. and Pugmire, R. J., "Study of the Evolution of Soot from Various Fuels," *Energy Fuels*, Vol. 19, 2005, pp. 1804–1811.

[156] Edwards, J. C. and Choate, P. J., "Average Molecular Structure of Gasoline Engine Combustion Chamber Deposits Obtained by Solid-State ^{13}C, ^{31}P and ^{1}H Nuclear Magnetic Resonance Spectroscopy," SAE Technical Paper Series, SAE Paper 932811, SAE International, Warrendale, PA, 1993.

[157] Owrang, F., Mattsson, H., Olsson, J. and Pedersen, J., "Investigation of Oxidation of a Mineral and a Synthetic Engine Oil," *Thermochim. Acta*, Vol. 413, 2004, pp. 241–248.

17

Infrared Spectroscopic Analysis of Petroleum, Petroleum Products, and Lubricants

James M. Brown[1]

INTRODUCTION

Infrared (IR) refers to electromagnetic radiation that is infra (below) the red end of the visible spectrum. The IR region covers wavelengths from approximately 0.78 to 1,000 μm, or frequencies from 12,800 to 10 cm^{-1}. IR spectroscopy is the study of the absorption of IR radiation by matter.

IR absorption occurs at frequencies that correspond to molecular vibrations and, in the case of the gas phase, molecular rotations. For a nonlinear molecule having N atoms, there will be 3N-6 molecular vibrations. These vibrations are associated with sets of quantum states, and the absorption of IR radiation induces a transition from the ground (lowest) quantum state to an excited quantum state. Although the vibrations are complex motions of all N atoms, in most instances, the principal contribution to the motion is due to an isolated portion of the molecule referred to as a functional group. The functional group vibration occurs at a characteristic frequency that is minimally perturbed by the rest of the molecule. Absorption at these characteristic frequencies allows the spectroscopist to infer the presence of the functional groups and, in many cases, what the functional group is attached to. For example, the carbonyl (C=O) group absorbs at ~1,700 cm^{-1}. As shown in Table 1, the exact frequency of the C=O absorption depends on the specific type of carbonyl functionality as well as its immediate environment.

Since most molecular functionalities contain multiple functional groups, specific structures can be inferred from combinations of IR absorptions. Thus, for example, absorption at 1,740 cm^{-1} might indicate aldehyde if it is accompanied by C-H bands in the 2,700 to 2,800 cm^{-1} range, or an ester if there is a C-O band in the 1,400 to 1,000 cm^{-1} range. A comprehensive list of functional group frequencies and their variation with molecular structure is given by Bellamy [1].

For mixtures, some caution must be applied in assigning structures based on functional group frequencies since the observed band positions are affected by intermolecular interactions (e.g., solvency, hydrogen bonding). Intermolecular interactions are illustrated in Table 2, which shows observed frequencies for the C=O absorptions of n-methyl pyrrolidone (NMP, a secondary amide) in various solvents and mixtures.

Not all molecular vibrations give rise to an IR absorption. To be IR active, a vibration must result in a change in the molecular dipole moment. Thus

[1] *ExxonMobil Research and Engineering Co., Annandale, NJ*

TABLE 1—Typical Functional Group Frequencies for Various Carbonyl Functionalities

Molecular Functionality	Specific Structure[a]	Functional Group	Frequency (cm^{-1})
Carboxylic acid	R–(C=O)–OH	C=O	1,710 (dimer) 1,760 (monomer)
		C=O	1,690 (dimer)
	Ar–(C=O)–OH	OH	3,000–2,500 (dimer)
			3,530 (monomer)
Ketone	R–(C=O)–R	C=O	1,715
	Ar–(C=O)–R	C=O	1,685
	Ar–(C=O)–AR	C=O	1,665
Aldehyde	R–(C=O)–H	C=O	1,735
	Ar–(C=O)–H	C=O	1,705
		(C=O)–H	2,900–2,700
Ester	R–(C=O)–OR	C=O	1,740
	Ar–(C=O)–OR	C=O	1,725
	R–(C=O)–OAr	C=O	1,770
		C–O	1,300–1,100

[a] R = aliphatic group, Ar = aromatic group

homonuclear diatomic molecules (hydrogen, oxygen, nitrogen) have no infrared spectrum, whereas heteronuclear diatomic molecules (carbon monoxide [CO], hydrochloric acid [HCl]) do. Note that it is not necessary for the molecule to have a permanent dipole moment to be infrared active. For example, the

TABLE 2—Example of Solvent and Hydrogen Bonding Effects on Carbonyl Band Positions

1% NMP in	Free NMP Peak (cm^{-1})	Hydrogen Bonded NMP Peak (cm^{-1})
Cyclohexane	1,712	...
50/50 cyclohexane/toluene	1,705	...
Toluene	1,698	...
100 N distillate	1,705	1,684
100 N raffinate	1,710	1,688
100 N extract	1,705	1,684

symmetric stretch of carbon dioxide (CO_2) in which both C=O bonds stretch and contract simultaneously is IR inactive since this motion does not change the molecular dipole. The asymmetric stretch, in which one C=O bond stretches while the other contracts is IR active since the asymmetric motion induces a dipole moment. For aromatics, the symmetric aromatic ring stretching vibration occurs near 1,600 cm^{-1}, but this vibration is absent in the spectrum of benzene since the symmetric ring stretch does not induce a dipole moment. For toluene, adding a methyl (CH_3) group to the ring removes the symmetry, and allows the ring stretch to induce a weak dipole moment change, and thereby cause a weak aromatic ring stretch absorption at 1,608 cm^{-1}. Addition of a hydroxyl (OH) group increases the ring dipole moment, and the ring stretch for phenol is appreciably more strongly absorbing.

TRANSMITTANCE AND ABSORBANCE

The transmittance, T, is defined (E131) as the ratio of radiant power transmitted by the sample to the radiant power incident on the sample. In practice, the power incident on the sample cannot be directly measured. Instead, separate measurements will be made of the power reaching the detector when the sample is present (I), and when the sample is absent or replaced with a suitable reference (I_0). The transmittance is the ratio $T = I/I_0$.

The absorbance, A, is defined (E131) as the negative of the logarithm to the base 10 of the transmittance, $A = -\log_{10}T$. For a homogeneous sample, Bouguer's or Lambert's law states that absorbance is directly proportional to the thickness of the sample in the optical path. Beer's law states that for a homogeneous sample containing an absorbing substance, the absorbance is directly proportional to the concentration of the absorbing species. The combination of these laws yields the equation $A = abc$, where a is the proportionality constant, referred to as the absorptivity, b is the pathlength the light travels through the sample, and c is the concentration. Infrared quantitative analysis is based on this Beer-Lambert equation.

NEAR-, MID-, AND FAR-INFRARED

The IR region is divided into three subregions, the far-infrared region covering approximately 400 to 10 cm^{-1} (25 to 1,000 μm), the mid-infrared region covering approximately 4,000 to 400 cm^{-1} (2.5 to 25 μm), and the near-infrared region covering approximately 12,800 to 4,000 cm^{-1} (0.78 to 2.5 μm). These subdivisions are somewhat arbitrary, and not universally applied in a consistent fashion.

If the absorption of IR radiation causes the excitation of a molecular vibration from its ground state to its first excited state, the resultant absorption band is referred to as a fundamental. For hydrocarbons, the fundamental vibration bands occur exclusively in the mid-infrared region, below 3,700 cm^{-1}. If absorption of IR causes excitation of a molecular vibration from its ground state to a higher excited state, the resultant absorption band is referred to as a vibrational overtone. The first overtone corresponds to excitation into the second excited state, the second overtone into the third excited state, and so on. Absorptions that simultaneously excite two different vibrational modes are referred to as combination bands. The strength of the IR absorption decreases

significantly as one moves from fundamentals to higher overtones and combination bands.

It is a common misconception that overtones and combination bands are associated exclusively with the near-infrared. Although it is true that all vibrational absorptions occurring in the near-infrared range are due to overtones and combination bands, the first overtones and combination bands of fundamentals falling below 2,000 cm^{-1} occur in the mid-infrared. For example, aromatic C-H out-of-plane bending vibrations occur between approximately 1,000 and 740 cm^{-1} and are very characteristic of aromatic substitution patterns. The overtones and combination bands for these same vibrations occur in the range from 2,000 to 1,500 cm^{-1}, and are equally characteristic of the ring hydrogen positions. Since the strength of the infrared absorption decreases significantly for higher level excitations, the higher level overtones and combinations of these low frequency fundamentals will typically not be observed in near-infrared spectra. For example, for an aliphatic ester with a C=O fundamental at 1,740 cm^{-1}, a much weaker overtone is observed near 3,480 cm^{-1}, but higher overtones are typically not observed. Thus absorptions occurring in the near-infrared region are almost exclusively associated with overtones and combinations of the C-H, O-H, and N-H stretching vibration fundamentals. The near-infrared spectrum of a hydrocarbon thus contains less structural information than the mid-infrared spectrum.

For measurements on hydrocarbons, the term near-infrared does not completely define what measurement is being conducted. The near-infrared could actually be subdivided into several subregions based on which overtones and combination bands are being measured (see Fig. 1). Absorptions in the "far"-near-infrared (~6,250 to 4,000 cm^{-1}) are typically measured using pathlengths of 0.25 to 0.5 mm. The stronger bands in the 4,500 to 4,000 cm^{-1} range include combinations of the methyl and methylene C-H stretching and bending vibrations. The bands in the 6,000 to 5,600 cm^{-1} range are overtones of the

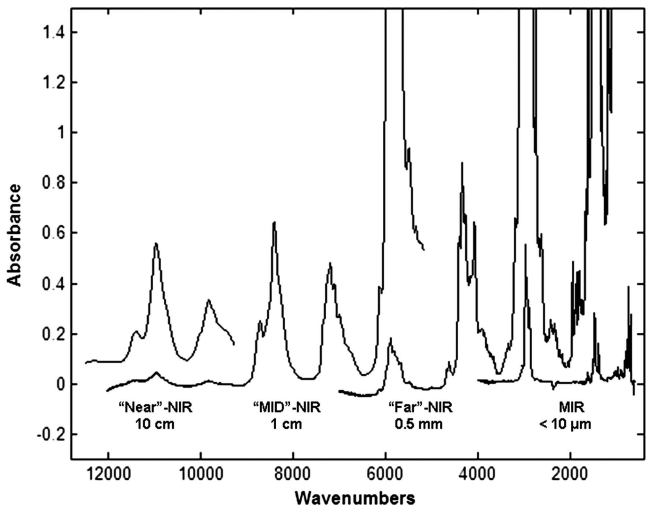

Fig. 1—Near-infrared spectral ranges.

C-H stretching vibrations. Absorptions in the "mid"-near-infrared range (~9,200 to 6,250 cm^{-1}) are typically measured with pathlengths of 1.0 cm. Absorptions in the "near"-near-infrared (12,800 to 9,200 cm^{-1}, sometimes called the far-visible) are typically measured with pathlengths on the order of 10 cm. The absorbances observed in all these regions are dominated by overtones and combinations of the aliphatic methylene (CH_2) and CH_3 stretching and bending vibrations. Absorptions due to overtones and combinations of aromatic C-H vibrations are typically much less intense. Measurements of visibly opaque samples such as crude oils can be obtained in the "far"-near-infrared region. However, due to interferences with electronic absorptions, measurements in the "mid"-near-infrared are limited to lightly colored samples, and measurements in the "near"-near-infrared to colorless samples.

In the gas phase, infrared absorption can excite molecular rotations. If only rotational states are excited, the absorption will occur in the far-infrared region. Although fundamentals for hydrocarbons tend to occur at higher energies, fundamental vibrations for molecules containing heavier atoms such as metals occur in the far-infrared.

INSTRUMENTATION

Most general-purpose infrared spectrophotometers fall into one of two categories: dispersive instruments and Fourier-transform instruments. For dispersive systems, the IR radiation is dispersed into individual wavelengths and detected sequentially. For Fourier-transform instruments, radiation is modulated by an interferometer and all wavelengths are detected simultaneously.

Although the first dispersive IR spectrophotometers used salt prisms to disperse the infrared radiation, current systems use reflective gratings. The basic configuration is shown in Fig. 2. For a grating with a groove density of n grooves/mm, the wavelength (in micrometres) reaching the detector is given by the grating equation

$$\lambda = \frac{2 * 10^3}{n} \sin\left(\frac{\alpha + \beta}{2}\right) \cos\left(\frac{\beta - \alpha}{2}\right) \quad (1)$$

The spectrum is measured by rotating the grating so as to sequentially scan the wavelengths. Double-beam versions of these instruments will include a means of alternately directing the light through a sample and reference beam

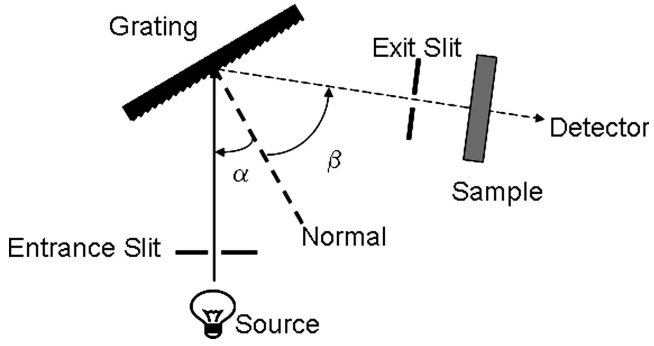

Fig. 2—Grating spectrophotometer.

path, and detecting the ratio (transmittance). For single-beam systems, separate reference (I_0) and sample (I) measurements are recorded and ratioed.

Fourier-transform (FT) instruments are based on interferometers. Fig. 3 shows a schematic of a variant on the conventional Michelson interferometer wherein the usual flat mirrors are replaced by corner cubes. Light from the source is incident on a beamsplitter, a semireflecting device used to create and then recombine spatially separate beams. For an ideal beamsplitter, half of the radiation incident at point (a) is reflected toward the fixed corner cube reflector, and half is transmitted toward the moving corner cube reflector. When the reflected beams recombine at point (b), interference will take place. For a monochromatic source with wavelength $\lambda = 1/\bar{\nu}$ and intensity $I(\bar{\nu})$, the modulation in the intensity of the light leaving the interferometer in the direction of the sample and detector is given by

$$I(\delta) = 0.5 * I(\bar{\nu}) \cos 2\pi\bar{\nu}\delta \tag{2}$$

δ, the retardation, is the difference in the optical path in the two arms of the interferometer. When δ is a multiple of the wavelength, λ, constructive interference occurs, and the maximum intensity is output toward the detector. When δ is $\lambda/2$ more than a multiple of the wavelength, destructive interference occurs and the minimum intensity is output toward the detector. Commercial FT-IR instruments include a helium-neon (HeNe) laser monochromatic source, and use the resultant cosine signal to monitor mirror position and trigger sampling.

For a polychromatic source, constructive interference can occur for all wavelengths only at $\delta = 0$. The modulation in the intensity exiting the interferometer is given by

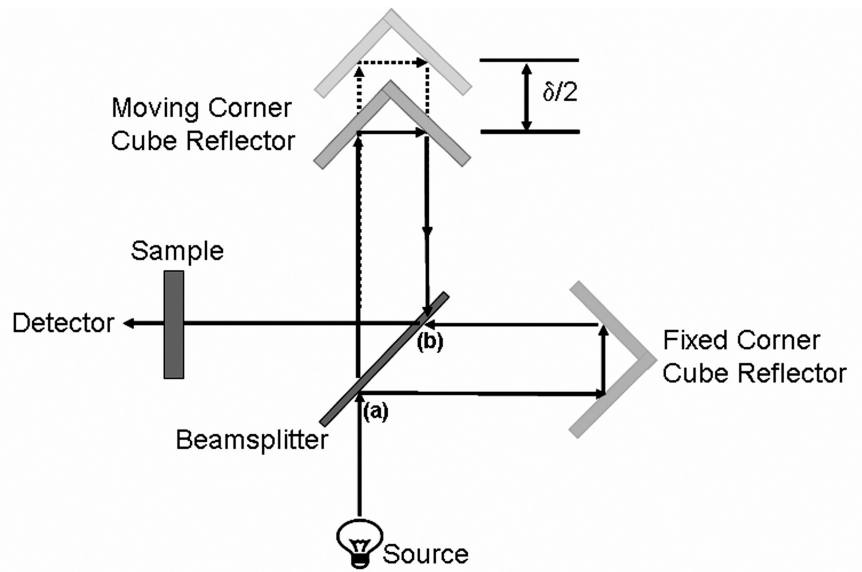

Fig. 3—Corner cube version of Michelson interferometer.

$$I(\delta) = \int_{-\infty}^{+\infty} S(\bar{\nu}) \cos 2\pi\bar{\nu}\delta d\bar{\nu} \tag{3}$$

This modulated signal is referred to as an interferogram. The single beam spectrum, $S(\bar{\nu})$, is obtained by taking the Fourier transform of the interferogram:

$$S(\bar{\nu}) = \int_{-\infty}^{+\infty} I(\delta) \cos 2\pi\bar{\nu} d\delta \tag{4}$$

As with dispersive measurements, separate measurements of a reference ($I_0 \rightarrow S_0$) and sample ($I \rightarrow S$) are taken and ratioed to produce a transmission spectrum. The FT-IR measurement process is shown schematically in Fig. 4.

Various interferometer designs are commercially available. The corner cube reflector version shown in Fig. 3 offers advantage over the more conventional flat mirror Michelson in that it is more resistant to optical errors introduced by mirror tilt because any ray entering the corner cube exits along a parallel path. Some interferometers move both mirrors. One commercial FT-IR system [2] achieves retardation by moving a wedged shaped salt plate into the beam. A more thorough discussion of FT-IR systems is given by Griffiths and de Haseth [3] and by Smith [4].

Filter-based IR spectrophotometers are employed in several D02 test methods. These spectrometers consist of a set of narrow bandwidth filters that are selected such that their center frequency corresponds to IR frequencies of interest. The filters serve essentially the same function as a grating, transmitting a narrow range of wavelengths to the sample and detector. The filters are placed sequentially between a broad band source and the IR detector to allow the spectrum to be "scanned." Because filter spectrometers typically collect only data at a limited number of wavelengths, they are typically used as dedicated quantitative analyzers for specific components and properties.

The types of spectrophotometers used in various D02 methods are summarized in Table 3.

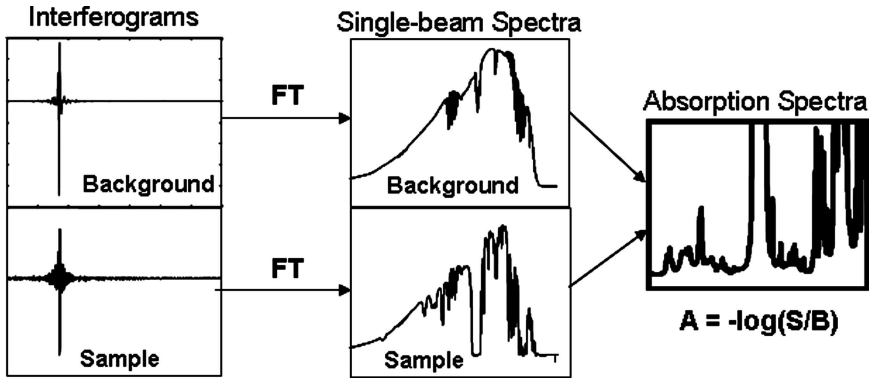

Fig. 4—FT-IR measurement process.

TABLE 3—Types of Spectrophotometers Used in Petroleum Methods and Practices					
Method	**Committee**		**Dispersive**	**FT-IR**	**Filter**
D3414	D19	Comparison of Waterborne Petroleum Oils by Infrared Spectroscopy	X	X	
D3921	D19	Method for Oil and Grease and Petroleum Hydrocarbons in Water	X	X	
D4053	D02	Method for Benzene in Motor and Aviation Gasoline by Infrared Spectroscopy	X	X	
D5845	D02	Method for Determination of MTBE, ETBE, TAME, DIPE, Methanol, Ethanol and tert-Butanol in Gasoline by Infrared Spectroscopy	X	X	X
D5986	D02	Method for Determination of Oxygenates, Benzene, Toluene, C_8–C_{12} Aromatics and Total Aromatics in Finished Gasoline by Gas Chromatography/Fourier Transform Infrared Spectroscopy		X	
D6277	D02	Method for Determination of Benzene in Spark-Ignition Engine Fuels Using Mid Infrared Spectroscopy		X	X
D7214	D02	Method for Determination of the Oxidation of Used Lubricants by FT-IR Using Peak Area Increase Calculation		X	
D7371	D02	Method for Determination of Biodiesel (Fatty Acid Methyl Esters) Content in Diesel Fuel Oil Using Mid Infrared Spectroscopy (FTIR-ATR-PLS Method)		X	
D7418	D02	Practice for Set-Up and Operation of Fourier Transform Infrared (FT-IR) Spectrometers for In-Service Oil Condition Monitoring		X	
E2412	E13	Practice for Condition Monitoring of Used Lubricants by Trend Analysis Using Fourier Transform Infrared (FT-IR) Spectrometry		X	

Infrared sources are hot, blackbody emitters. For mid-IR (MIR), Globars, Nernst glowers, and nichrome coils are used. These sources are electrically heated to 1,000°C to 1,500°C, and will appear "red hot." For near-IR (NIR), where higher temperature sources are required, a "white hot" tungsten filament bulb is used.

Infrared detectors are of two types: thermal detectors and quantum detectors. Thermal detectors sense a change in the operating temperature of the detecting material resulting from the absorption of the IR radiation. Many MIR instruments use a thermal deuterated triglycine sulfate (DTGS) detector because it can be operated at ambient conditions. Quantum detectors are semiconductors in which absorption of IR radiation will cause excitation of electrons to a higher energy state. MCT detectors used in the MIR are quantum detectors. MCTs have higher sensitivity and response than DTGS detectors, but they must be cooled with liquid nitrogen or a cryocooler. Lead sulfide (PbS), lead selenide (PbSe), and indium gallium arsenide (InGaAs) NIR detectors are all quantum detectors.

ASTM Committee E13 has published various standards that can be used to evaluate the performance of infrared instruments. These practices provide a basis for qualifying spectrophotometers for their intended use. The practices include:

- E275 Standard Practice for Describing and Measuring Performance of Ultraviolet, Visible, and Near-Infrared Spectrophotometers
- E387 Standard Test Method for Estimating Stray Radiant Power Ratio of Dispersive Spectrophotometers by the Opaque Filter Method
- E932 Standard Practice for Describing and Measuring Performance of Dispersive Infrared Spectrometers
- E1421 Standard Practice for Describing and Measuring Performance of Fourier Transform Mid-Infrared (FT-MIR) Spectrometers: Level Zero and Level One Tests
- E1866 Guide to Establishing Spectrophotometer Performance Tests
- E1944 Standard Practice for Describing and Measuring Performance of Fourier Transform Near-Infrared (FT-NIR) Spectrometers: Level Zero and Level One Tests

SAMPLING

IR sampling methods are summarized in E1252, and references therein. A summary of practical sampling techniques has been published by Coleman [5].

The simplest IR methods involve direct measurement of transmittance, the ratio of the radiant power transmitted by the sample relative to the radiant power incident on the sample (E131). For liquids and gases, the samples are contained in a cell, referred to as a transmission or absorption cell. The cell consists of two IR transparent windows separated by a space where the sample resides. Various cell window materials are used, depending on the spectral range that needs to be measured and the reactivity of the materials with the sample or the environment. Properties of IR window materials are summarized in E1252, Table 1. For gas samples, pathlengths up to 20 m are obtained using multipass transmission cells. Open-path (OP) gas measurements conducted using FT-IR (E1982) are used to monitor gases and vapors in air. OP/FT-IR is

used for environmental monitoring along perimeters of industrial facilities, hazardous waste sites, and landfills, and in response to spills or releases.

Transmission spectra of solid samples can be obtained using several methods. If a solid sample is soluble in a volatile solvent, it can be cast as a thin film on an IR transparent substrate. Although there is no such thing as a totally transparent IR solvent, many solvents have transmission windows through which solute absorptions can be measured (E1252, Table 2). Powdered solids may be dispersed in an alkali halide matrix and pressed into a pellet.

The use of the word reflection in discussing IR sample methods is somewhat of a misnomer. Although these spectral measurement may involve the reflection of the IR radiation, the intent is to measure absorbance, or at least a signal that can be transformed so as to be proportional to absorbance. Specular reflectance occurs at a surface when the angle of incidence equals the angle of reflection. For liquid or solid samples, the specular reflectance at the sample surface is governed by the complex refractive index. True specular reflectance spectra will typically contain derivative-shaped bands known as *reststrahlen*, which are due to large changes in the refractive index across absorption bands. Although it may be possible to extract an absorption spectrum via use of a Kramers-Kronig transform, such specular reflectance measurements are not used for petroleum analysis. The term specular reflectance is often misused to describe a measurement of a thin coating on a reflective surface. Such measurements are more properly described as double transmission because the IR beam passes through the sample twice, before and after reflection from the underlying reflective substrate.

Attenuated total reflectance (ATR) is used for mid-infrared sampling. ATR, which is sometimes referred to as internal reflection, is described in detail in E573. Typical ATR configurations are shown in Fig. 5. The IR beam passes into a ATR element, a crystal having a higher refractive index than the sample. At the interface, total internal reflection occurs. At each bounce, the IR beam penetrates a distance d_p into the sample that is in contact with the ATR element. The reflected intensity is attenuated by any sample absorbance.

The penetration depth, d_p, is a function of the angle of reflection and the ratio of the refractive indices of the sample and ATR element. The penetration depth is on the order of micrometres, allowing ATR to measure absorbances that are often too strong to measure via transmission. For example, the aliphatic C-H stretching vibrations occurring in the 3,000 to 2,800 cm^{-1} region can be directly measured using single-bounce ATR. For more weakly absorbing species, multiple-bounce ATR provides longer effective pathlengths and thus increased sensitivity.

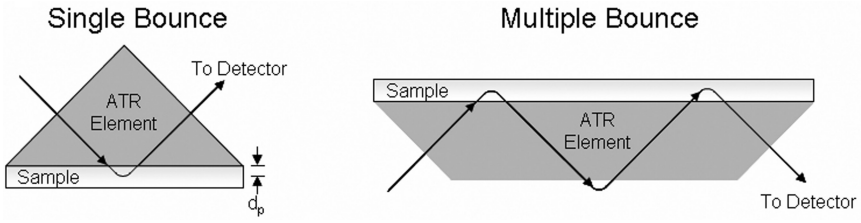

Fig. 5—ATR.

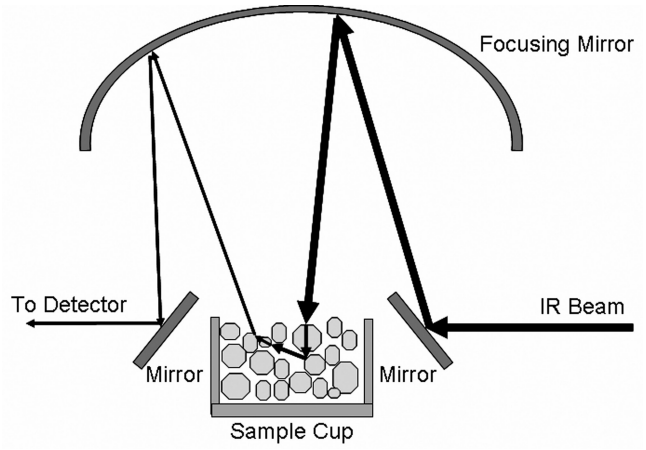

Fig. 6—Schematic of diffuse reflectance measurement.

Various ATR elements are commercially available. The useful range and properties of these materials are summarized in E573, Table 1. These elements have been adapted into a wide variety of commercial sampling accessories, including ATR flow cells and probes, which are often used in dedicated laboratory and process analyzers.

Diffuse reflectance is a common sampling technique for solids, particularly in the NIR. A simplified diffuse reflectance measurement is shown schematically in Fig. 6. The IR beam is focused onto a solid sample. Some of the IR radiation will be specularly reflected from the sample surface. However, much of the IR radiation will penetrate into the sample, passing through individual particles. Frequencies at which the sample absorbs will be attenuated. If the particle is optically thin, the IR radiation will pass out of the particle and be incident on a particle farther down in the sample. At the particle surface, reflection of the IR beam may occur. The beam may pass through and be reflected off multiple particles before exiting the sample. Because of the random orientation of the particles, the final direction of the beam is also random.

For FT-MIR, diffuse reflectance measurements are known by the acronym DRIFT. NIR reflectance measurements are done via diffuse reflectance. A reference (background) spectrum is obtained by scanning the spectrum of a nonabsorbing material, typically potassium bromide (KBr) or potassium chloride (KCl) for DRIFT and polytetrafluoroethylene (PTFE) or barium sulfate ($BaSO_4$) for NIR reflectance. For DRIFT, powdered samples may be run neat or dispersed in the nonabsorbing matrix. For NIR reflectance, samples are typically analyzed neat. The ratio of the spectrum of the sample to the spectrum of the nonabsorbing reference is called the reflectance spectrum, R.

Unlike transmission, the measured reflectance is not directly related to absorbance. Various transforms are applied to convert the measured reflectance into a function that is proportional to absorbance, and thus via Beer's law to concentration. The Kubelka Munk function, $KM = (1 - R)^2/2R$, is commonly

used to transform DRIFT spectra. For NIR reflectance, a $\log_{10}(1/R)$ transform is more often applied. Both of these transforms are approximations "designed to linearize the relationship between the measured reflectance, R, and the concentration of the absorbing species" (E1655).

IR spectrometers are often used as detectors on other analytical instruments, producing what is referred to as "hyphenated techniques" despite the fact that their acronyms use a slash instead of a hyphen. GC/IR is described in E1642, and is the basis of D02 Method D5986 for determining oxygenates, benzene, toluene, C8-C12 aromatics, and total aromatics in finished gasoline. Uses of IR detection in liquid chromatography (LC/IR) and in size exclusion chromatography (SEC/IR) are described in E2106, and use of IR detection in thermogravimetric analysis (TGA/IR) is described in E2105.

Many NIR spectrophotometers, particularly those used for on-line analysis, are equipped with silica-based fiber optics. The fibers allow the spectrophotometer to be located at a distance from the actual measurement point. For on-line analysis of petroleum liquids, the fibers will typically be coupled to a transmission cell/probe or to a transflectance probe (a double-pass transmission cell with a mirror at one end). Fiber optic reflectance probes are available for measuring solid samples, but to date, these are not often used in petroleum process analysis. MIR process instruments have conventionally used mirrors to direct the IR beam to flow transmission or ATR cells. Recently, MIR silver chloride (AgCl) fibers coupled to ATR probes have been introduced.

QUALITATIVE ANALYSIS

As discussed previously, IR absorption at characteristic functional group frequencies allows the spectroscopist to infer the presence of the functional groups and, in many cases, the molecular structure in the vicinity of the functional group. Fig. 7 demonstrates how IR can be used to identify specific structural groups in a petroleum sample.

The utility of IR for identifying individual molecules in petroleum samples is generally limited to light, narrow boiling fractions (narrow, low molecular weight distributions). IR can be used to identify and quantify xylene isomers in a mixed C8 stream. However, the spectrum of a 50:50 mole percent mixture of n-octane and n-dodecane will typically be indistinguishable from a spectrum of n-decane in most IR spectral ranges, and such homologs are essentially never distinguishable in petroleum samples.

The application of IR to the analysis of formulated lubricants and greases has been discussed by Coates and Setti [6]. Comparison to reference spectra allows oil additives to be identified, and the IR "fingerprint" of a formulated lubricant will often be sufficiently unique to allow IR to be used in oil identification.

IR can be used for identification of gas-phase molecules. In GC/IR, the identification of an eluent can be made by comparison to reference spectra collected under similar conditions. Such identifications are typically made using spectral search algorithms to compare the eluent spectra to spectra in a digital library. E2310 describes the use of spectral searching by curve-matching algorithms. Libraries of gas phase spectra are commercially available.

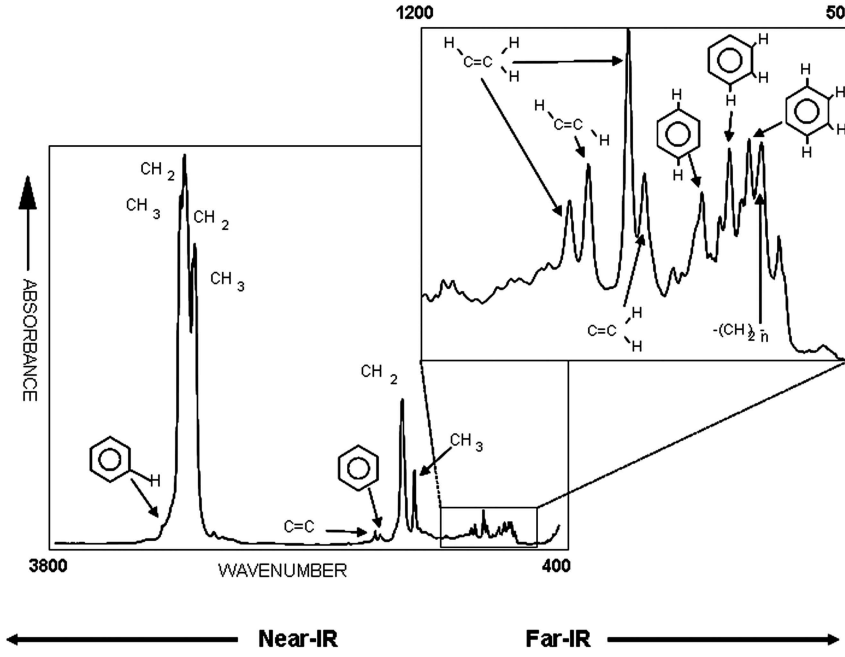

Fig. 7—FT-MIR Spectrum of Delayed Coker Mid-Distillate.

QUANTITATIVE ANALYSIS

All quantitative IR analysis is based on Beer's law (Beer's Lambert equation), $A = abc$. Quantitative analysis involves two steps: calibration ($a = A/bc$) and analysis ($c = A/ab$). Although the c in Beer's law refers to concentration, calibrations and analyses can be developed for any property that is (or nearly is) a linear function of concentrations.

Usually, IR quantitative analyses were conducted by measuring peak heights or peak areas and developing a calibration "curve" to relate these values to concentration. These conventional methods are described in E168. Method D4053 for measurement of benzene in gasoline employs peak height measurements.

Increasingly, IR quantitative analysis is done using multivariate methods, often referred to as chemometric methods. Multivariate models replace the calibration curve with a calibration model. Practice E1655 describes IR multivariate analysis done via multilinear regression (MLR), principal components regression (PCR), and partial least squares (PLS). Multivariate IR analyses use a matrix form of Beer's law, $\mathbf{y} = \mathbf{X}^t\mathbf{p}$, where $\mathbf{y}$ (the y-block) is a column vector of concentration or property values, $\mathbf{X}$ (the X-block) is a matrix whose columns are spectra, and $\mathbf{p}$ is a *prediction vector* that relates the spectra to the properties. Again, the quantitative analysis involves two steps: calibration wherein the $\mathbf{p}$ is estimated and analysis where $\mathbf{y}$ is estimated for an unknown based on the dot product of its measured spectrum and $\mathbf{p}$. Typically, during calibration, the number of data points (frequencies or wavelengths) per spectrum exceeds

the number of calibration samples, and $\mathbf{y} = \mathbf{X}^t\mathbf{p}$ cannot be solved directly for **p**. MLR, PCR, and PLS are three alternative means of estimating **p**. In MLR, individual IR data points (frequencies or wavelength) are selected so as to reduce the number of points to less than the number of calibration samples, thereby allowing for **p** to be estimated via matrix inversion. PCR involves extracting the major sources of variation in **X** (the principal components), and then regressing these against **y** to obtain the estimate of **p**. PLS differs in that the *latent variables* that are extracted attempt to explain the variance in both **X** and **y**. The mathematics of these methods are described in detail in E1655 and references therein.

MLR was more widely used in the 1980s when available computers were taxed by the size of **X**. Brown and Elliott [7] described the analysis of lubricant additives via the K-matrix method, which is a variant of MLR. Filter-based IR analyses typically use MLR-based methods.

PCR and PLS both seek to estimate the X-block data in terms of a small set of orthogonal basis vectors. PCR computes these basis vectors (principal components) so as to account for the maximum amount of the variation in the spectral data in the fewest number of vectors. PLS, on the other hand, seeks to maximize the covariance between the basis vectors and the y-block. There are numerous literature references as well as patents in which PCR and PLS are used to relate MIR or NIR spectra to component concentrations (benzene, toluene, xylenes, oxygenates, PIONA, saturates/olefins/aromatics), to physical properties (specific gravity, RVP) and to performance properties (RON, MON, cetane number). Various authors have argued the relative merits of these two methods. Wentzell and Montoto [8] reviewed many of these references as part of a simulation study which concluded that there was no substantial difference between PCR and PLS models. In fact, for many applications, both methods will produce nearly equivalent results. In this author's experience:

- When modeling major components or properties that depend on the entire sample composition, PLS and PCR will typically produce comparable calibrations.
- If the precision of the X-block (spectral data) is high, and the precision of the y-block (concentration/property data) is poor, there is little incentive to use PLS.
- If the absorption of the component of interest is a small fraction of the total spectral variance, then the use of the y-block in PLS may help isolate the signal, leading to a more precise model.
- The "best" model is the one that produces the most accurate and precise estimates when applied to an independent set of validation samples (e.g., samples that were not used in the calibration).
- If it is critical to detect extrapolation of the multivariate model, then PCR provides much more reliable outlier detection, particularly if multiple components/properties are to be calibrated based on the same X-block.

For many applications, being able to detect when an analysis represents an extrapolation of the multivariate model is critical. Samples that extrapolate the model are referred to as outliers. E1655 and D6122 describe two types of outliers. Mahalanobis distance or leverage outliers are samples that have the same components as the calibration samples, but at more extreme concentrations. Spectral residual outliers are samples which contain components that were not

present in the calibration. Spectral residuals cannot be computed for MLR models, and are often less meaningful for PLS models, so with respect to detecting new components, PCR models are more reliable.

The development of multivariate calibrations via E1655 will generally involve the collection of a relatively large set of samples that span the range of composition/process variation over which the analysis is to function. The set must be large enough to supply both calibration and validation samples. Composition/property data are measured by a *in-control* reference method, and spectra are collected using a *qualified* spectrometer. It is critical that the performance of both the spectrophotometer and the reference method be established at the time of calibration so as to provide a basis for evaluating future performance.

Because of the relatively large number of samples and analyses involved, the development of an IR calibration can be a time-consuming and fairly costly endeavor. It is often desirable to use a calibration on more than one spectrophotometer. However, differences in wavelength/frequency scale, resolution, and response linearity can cause inaccuracy and imprecision when a calibration developed on a reference (master) instrument is used for analyses on a target (slave) instrument. Such inaccuracies and imprecision are minimized through the use of instrument standardization or calibration transfer. Instrument standardization involves hardware or software adjustment of the target instrument such that the spectral data match data from the master instrument to within the precision required by the application. Calibration transfer involves collecting spectra of common samples on the reference and target instrument, and building a mathematical model that allows either the transformation of target spectra to look as if it had been collected on the reference instrument, or the transformation of the calibration to act as if it had been developed using the target instrument. As with the calibration itself, it is essential that the instrument standardization or calibration transfer methodology be validated for the intended application. Even if all analyses will be conducted on the reference instrument, it is essential to have a plan for instrument standardization or calibration transfer since maintenance can often turn the reference instrument into a target.

Multivariate IR analysis involves several different forms of validation:

- For new applications, it is necessary to demonstrate that it is feasible to develop a calibration model whose accuracy and precision meet or exceed the user's specifications. Model validation is discussed in E1655.
- For each application, instrument standardization or calibration transfer methodology must be validated to ensure that the accuracy and precision for the target instrument meet user specifications, and to ensure that the application is robust to instrument maintenance.
- After installation of the model on a target instrument, and after major maintenance, the initial performance of the application should be validated using the methodology described in D6122. Although D6122 deals principally with online IR analyzers, the general methodology is equally applicable to laboratory or at-line analyzers.
- During normal use, periodic validation should be conducted wherein the results of the IR analysis are compared to the in-control reference method.

D6122 describes how the D6299 QA tools are applied for this periodic validation.

A common application of the IR multivariate methods is in process analysis. IR measurements can be conducted in seconds to minutes, providing results at a rate adequate for process control. Where allowed by regulation and contract, IR analyzers can be used for product quality monitoring and certification.

Although PCR, PLS, and MLR are the most commonly used multivariate methods, they are not the only methods employed for IR multivariate analysis. Topological-based methods have been employed [9], as have neural networks [10]. The use of a multivariate mixture analysis for analyzing crude oils has also been described [11]. Committee E13 recently developed standard practice E2617 for validation of empirically derived multivariate calibrations to provide a more general framework for validation of models that are not based on PCR, PLS, or MLR.

CALIBRATION USING SURROGATE MIXTURES

Because of the large number of diverse sample types required to develop a multivariate IR calibration, it is difficult to develop standard methods that employ these techniques. It is impractical to store calibration and validation standards for long periods of time, and any set used in an interlaboratory exchange would not necessarily span the range needed by a particular refiner. Thus the methodology described in E1655 is most commonly used to develop lab/refinery specific calibrations.

For some applications, IR multivariate methods have been calibrated using surrogate mixtures, i.e., gravimetric mixtures of pure compounds or tightly specified process samples. The mixtures serve as surrogates for actual process samples, and represent compositions that are sufficiently reproducible to allow for calibration and validation of the method on different instruments in different laboratories. D5845 for the determination of oxygenates in gasoline, D6277 for the determination of benzene in spark-ignition engine fuels, and D7371 for the determination of fatty acid methyl esters (FAME) in biodiesel are all examples of IR multivariate calibrations based on surrogate mixtures.

Various vendors sell dedicated IR analyzers that are precalibrated to perform these tests. Whether a user is purchasing a precalibrated system or calibrating a general-purpose instrument to perform these tests, it is critical that the user qualify the instrument. The purpose of the qualification is to demonstrate that the instrument performance is adequate to produce results of similar precision to those reported in the method. The methodologies for establishing the qualification criteria and for applying them to qualify an instrument are described in E2056.

CONDITION MONITORING

Condition monitoring is defined as “a field of technical activity in which selected physical parameters associated with an operating machine are periodically or continuously sensed, measured and recorded for the interim purpose of reducing, analyzing, comparing and displaying the data and information so obtained and for the ultimate purpose of using interim results to support

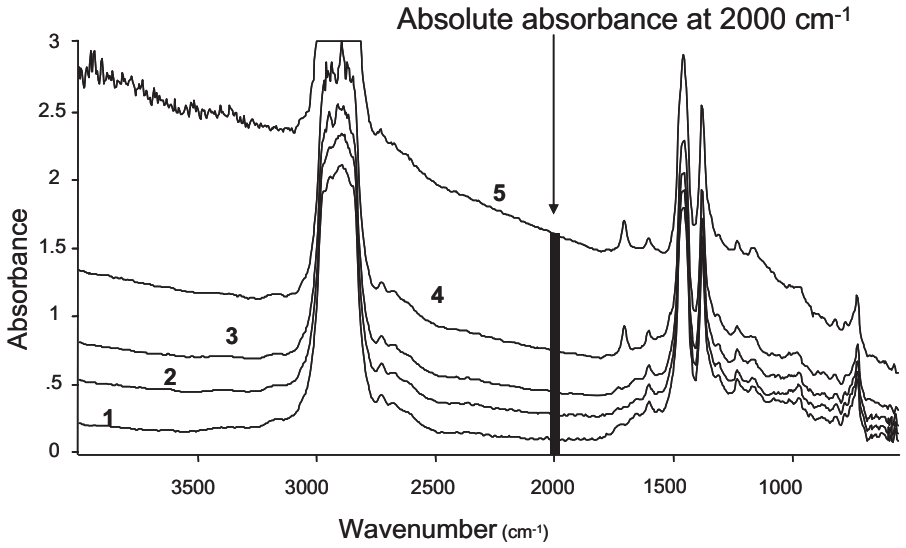

Fig. 8—FT-IR soot measurement.

decisions related to the operation and maintenance of the machine" [12]. FT-IR is widely used in condition monitoring to monitor additive depletion, contaminant buildup, and base stock degradation in lubricants, hydraulic fluids, and other machinery related fluids.

Practice E2412 describes two different approaches for using FT-IR in condition monitoring. Direct trending uses peak height or area measurements that are made directly on the as-measured spectrum of the in-service lubricant. For

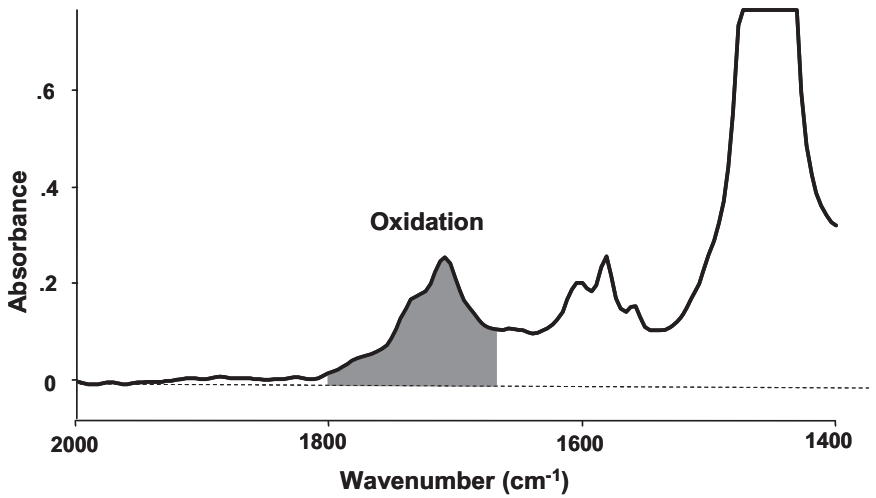

Fig. 9—Oxidation by direct trending.

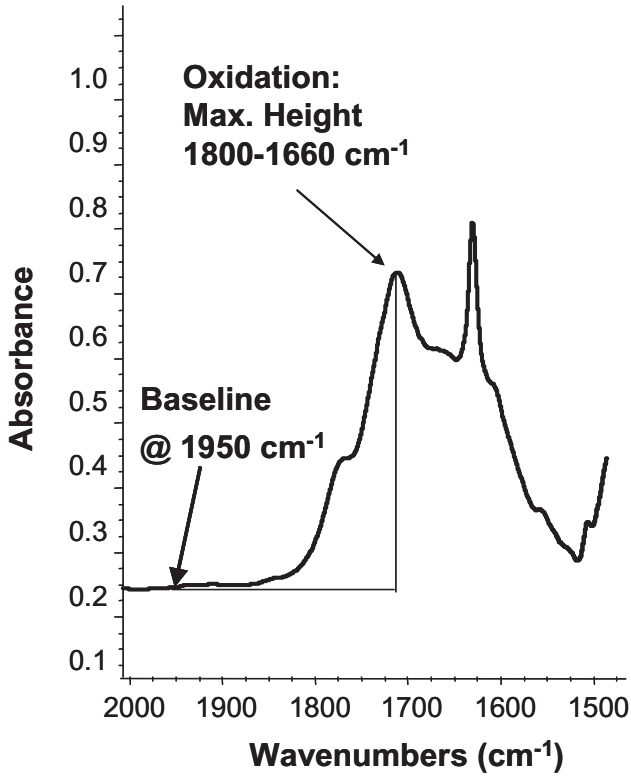

Fig. 10—Oxidation by spectral subtraction.

spectral subtraction, analyses are done on a difference spectrum generated by subtracting a spectrum of a reference lubricant (typically new oil) from the spectrum of the in-service lubricant. Both approaches have been applied to the measurement of water, soot, oxidation, nitration, anti-wear components, sulfation, and fuel dilution. Data generated from the FT-IR analysis are compared to historical data for the same lubricant/application to monitor changes in lubricant quality.

Figs. 8 through 12 show examples of FT-IR condition monitoring measurements. Fig. 8 demonstrates how the spectral baseline is affected by soot scattering as soot concentration increases (from 1 to 5). The soot level is monitored as the absorbance at 2,000 cm^{-1}. Note that since direct trending and spectral subtraction methodologies were developed separately, they do not always use the same spectral information for a particular monitoring parameter. For example, in direct trending, oxidation is measured as the integral of the absorbance in the 1,800 to 1,670 cm^{-1} range relative to a two-point baseline. The baseline is drawn between minima in the spectra occurring in the ranges from 2,200 to 1,900 cm^{-1} and from 650 to 550 cm^{-1} (Fig. 9). For spectral subtraction, oxidation is measured as the maximum peak height in the range from 1,800 to 1,660 cm^{-1} relative to a single-point, horizontal baseline corresponding

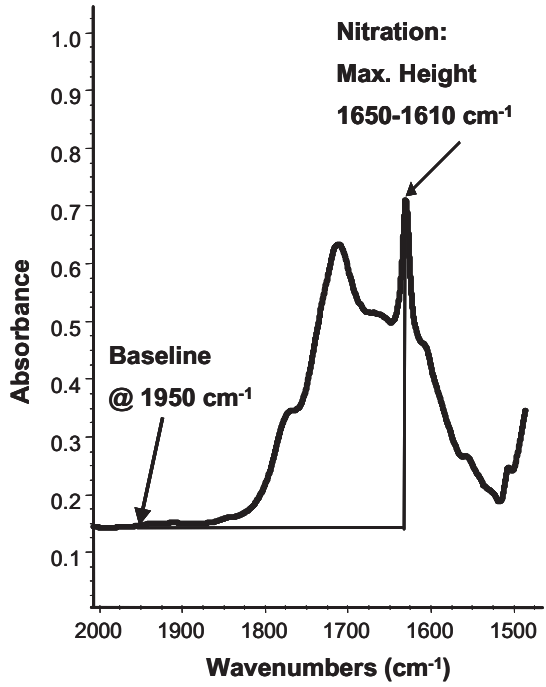

Fig. 11—Nitration by spectral subtraction.

to the absorbance at 1,950 cm^{-1} (Fig. 10). Figs. 11 and 12 show measurement of nitration by spectral subtraction and sulfate by-products by direct trending.

Although FT-IR condition monitoring is intended as a quick, inexpensive means of monitoring in-service lubricant quality, results must be interpreted in

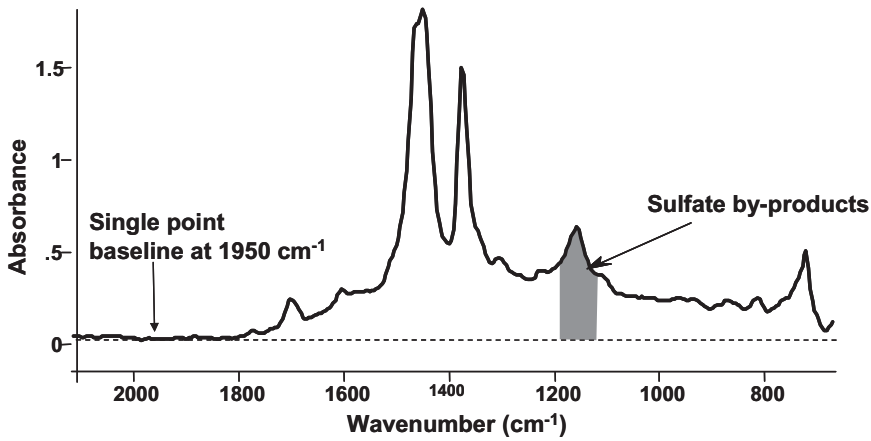

Fig. 12—Sulfate by-products.

terms of the type of lubricant and the application. Different oil formulations can have significantly different spectra, so results must always be trended relative to a fresh oil of the same formulation. In addition, results must be interpreted in terms of known application chemistry. For instance, an increase in absorbance at 1,630 cm^{-1} for some applications may indicate nitration, but for other applications it may be more likely due to water, or carboxylic acid salts formed by reaction of oxidation products with over-based additives. Results can be affected by changes in fuel chemistry as well. Peaks used for fuel dilution measurements are due to heavier aromatic fuel components, so the sensitivity of IR to fuel dilution is highly dependent on the fuel composition. With low-sulfur fuels, it is unlikely that sulfation measurements are really monitoring sulfate formation.

Condition monitoring is a large business, and many vendors make equipment to support this industry. Until recently, however, there has been little standardization of the measurements produced across the industry. The CS-96 FT-IR Task Group has been working to standardize FT-IR condition monitoring methods, and to this end has published D7418 on the set-up and operation of FT-IR spectrometers for in-service oil condition monitoring. This practice describes standard conditions that will be used as the basis for future standards on individual parameters (e.g., soot, oxidation, nitration). Figs. 8 through 12 are from methods currently under development by the CS-96 FT-IR Task Group.

References

[1] Bellamy, L. J., *The Infrared Spectra of Complex Molecules*, Chapman and Hall, London, 1975.

[2] Doyle, W. M., McIntosh, B. C. and Clarke, W. L., "Refractively Scanned Interferometers for Fourier Transform Infrared Spectrophotometry," *Appl. Spectrosc.*, Vol. 34, 1980, pp. 599–603.

[3] Griffiths, P. R. and De Haseth, J. A., *Fourier Transform Infrared Spectrometry (Chemical Analysis: A Series of Monographs on Analytical Chemistry and Its Applications)*, John Wiley & Sons, Hoboken, NJ, 2007.

[4] Smith, B. C., "*Fundamentals of Fourier Transform Infrared Spectroscopy,*" CRC Press, Boca Raton, FL, 1996.

[5] Coleman, P. B., *Practical Sampling Techniques for Infrared Analysis*, CRC Press, Boca Raton, FL, 1993.

[6] Coates, J. P. and Setti, L. C., *Oils, Lubricants, and Petroleum Products, Characterization by Infrared Spectroscopy*, Marcel Dekker, New York, 1985.

[7] Brown, J. M. and Elliott, J. J., "The Quantitative Analysis of Complex, Multicomponent Mixtures by FT-IR; The Analysis of Minerals and Interacting Organic Blends," in *Chemical, Biological and Industrial Applications of Infrared Spectroscopy*, J. R. Durig, Ed., John Wiley & Sons, New York, 1985, pp. 111–128.

[8] Wentzell, P. D. and Montoto, L. V., "Comparison of Principal Components Regression and Partial Least Squares Regression through Generic Simulation of Complex Mixtures," *Chem. Intel. Lab. Syst.*, Vol. 65, 2003, pp. 257–279.

[9] Jin, L. Pierna, J. A. F., Xu, Q., Wahl, F., de Noord, O. E., Saby, C. A. and Massar, D. L., "Delaunay Triangulation Method for Multivariate Calibration," *Anal. Chim. Acta,* Vol. 448, 2003, pp. 1–14.

[10] Falla, F. S., Larinci C., Le Roux G. A. C., Quina F. H., More L. F. L. and Nascimento, C. A. O., "Characterization of Crude Petroleum by NIR," *J. Petrol. Sci. Engin.*, Vol. 51, 2006, pp. 127–137.

[11] Brown, J. M., "Virtual Assay," *ACS Petroleum Div. Preprints*, ACS Meeting, San Francisco CA, September 10–14, 2006.

[12] ISO, "Terminology for the Field of Condition Monitoring and Diagnostics of Machines," ISO/TC 108 N 605, International Standards Organization, Geneva, 1992.

18

Ion Chromatography in the Analysis of Industrial Process Waters and Petroleum Products

Kirk Chassaniol[1]

INTRODUCTION

Several books [1–4] have been published on ion chromatography (IC). It is a branch of liquid chromatography, and has several unique characteristics to meet the needs of ion analysis. The eluents, or mobile phases, used are often acid, alkaline, or high in salt content. The high-pressure pump used should have an all nonmetallic flow path in order to reliably deliver these eluents without contaminating the column or detection methods used. The ion exchange columns provide the unique ion separation capabilities, while chemically suppressed conductivity detection is the primary detector used for IC. Other detectors such as ultraviolet/visible light absorbance and electrochemical detectors are also often used. Like all forms of liquid chromatography, an IC includes a pump, injection valve, separation column, and detector. Fig. 1 is a representation of a liquid chromatograph used to determine ions. The hardware used to perform IC is similar to that used for high-performance liquid chromatography (HPLC), although it is typically made of inert polymer that is resistant to corrosive acid and base solutions frequently used in IC. Some form of sample introduction device and a means of recording the output signal are also required.

Although there are a number of separation and detection schemes that can be used in IC, the most commonly used approach is the combination of an ion exchange separation with suppressed conductivity detection, i.e., the concept as first described by Small, Stevens, and Bauman [5]. In an ion exchange separation, ionic analytes are separated by virtue of their electrostatic attraction to a stationary phase that carries immobilized ion exchange sites. The ion exchange site carries a charge that is opposite to the charge on the analyte. For example, anions are separated using a column that carries positively charged ion exchange sites. The stronger an analyte interacts with the column, the longer the retention time. The relative affinity of the ion exchange site for ions is dependent on the charge, charge density, and hydrophobicity of the eluent and analyte ion. Analytes are identified by their retention time and quantitatively determined (primarily) by peak area.

COMPONENTS OF AN ION CHROMATOGRAPH

Eluent

The function of the eluent (mobile phase) is primarily to provide counterions for the ion exchange process. Secondary functions include providing a stable

[1] *Dionex Corporation, Bannockburn, Illinois*

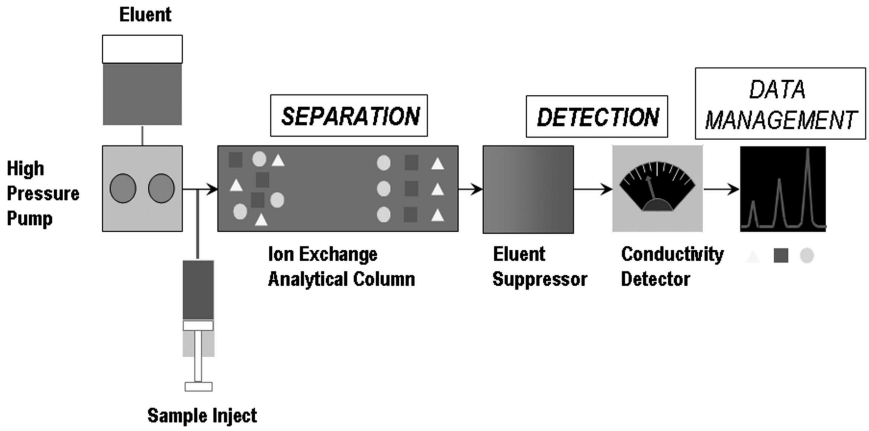

Fig. 1—Ion chromatography system.

environment for the sample ions and kinetic flow of the sample ions through separation and detection. The most common eluents used in ion chromatography are sodium or potassium hydroxide or sodium or potassium carbonate/bicarbonate for anion determinations. For cations, methanesulfonic acid, sulfuric acid, or nitric acid is most commonly used as the eluent.

Pump

The pump in the ion chromatograph delivers liquid eluent to the resin packed column with minimum pulsation at the flow and pressure range of the instrumentation and separation column. Because of the possibility of using strong acid and base eluents, the pump wet components and system tubing are constructed of polyetheretherketone (PEEK™).

Electrolytic Eluent Generation and Suppression

Since the introduction of eluent generation in 1998 [6], many customers have taken advantage of an instrument that "makes its own eluents." RFIC™ systems generate high-purity eluents automatically using only deionized water feeding the pump (Fig. 2). In addition to saving time and labor, this technology enhances separation flexibility and sensitivity through the use of gradients by eliminating one variable (eluent preparation) and source of possible contamination (eluent purification); the result is retention time stability and quieter baseline of the conductivity detector.

Injection

A fixed length of tubing of known internal diameter constitutes the sample loop. The sample loop can be filled either manually or with an autosampler. A high pressure 6-port or 10-port 2-way valve is switched in-line into the flowing eluent stream and the loop contents are carried on to the anion exchange guard and separator column.

Separation Column and Guard Column

The separation column provides stable support for stationary phase ions that act as active sites in the dynamic ion exchange process. Fig. 3 illustrates a

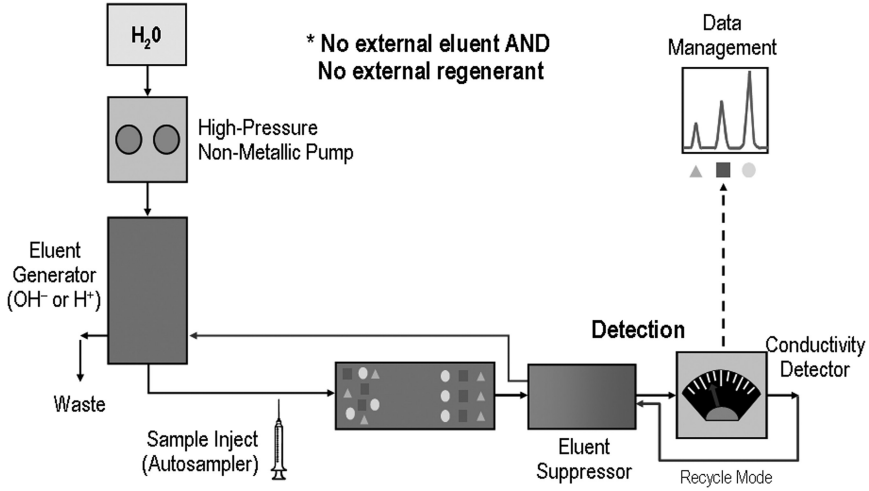

Fig. 2—Reagent-Free™ IC system.

typical anion exchange resin bead. The active sites compete with the counterions in the mobile phase for retention of analytes. The choice of column is the primary determinant of separation of important analytes, capacity to retain any given sample component, and analyte peak efficiency–minimal band broadening in the ion chromatographic separation process [1]. The sample ions are separated into discrete bands as they move through the column. Different ions migrate at different rates depending on their relative affinities for the resin. A shorter length guard column serves to protect the separation column and is packed with the same resin as the separation column or a neutral (nonfunctionalized) resin to remove possible hydrophobic contaminants resin.

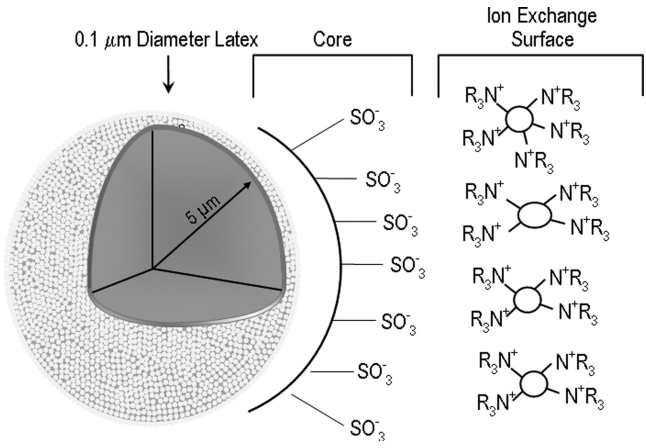

Fig. 3—Pellicular anion exchange bead (latex).

Conductivity Detector

A conductivity detector measures the electrical conductance of analyte ions as they pass through a conductivity cell. A conductivity detector is the primary method of detection used in IC. The detector produces a signal based on a chemical or physical property of an analyte. For optimal results, a detector must exhibit high sensitivity, low noise, and a wide linear range. It is ideal for small inorganic and organic ions.

Chemical suppression technology is the breakthrough in IC that has allowed it to become a preferred technique for ions. The suppressor is a post-column reactor specific to IC, which allows more sensitive conductivity detection. Conductivity detection is a universal (bulk property) detector for IC as all ions are conductive. Chemical suppression provides a significant improvement in signal-to-noise, making ion chromatography a truly practical tool.

Fig. 4 illustrates the effect of chemical suppression in a typical ion exchange separation of anions with conductivity detection. The effluent from the analytical column is monitored by conductivity as it passes immediately from the column; a chromatogram similar to that shown on the upper right would be obtained. This chromatogram has a very high background from the conductive eluent, a large counterion peak at the column void volume, and analyte peaks with low response.

In contrast, by passing the column effluent through a chemical suppressor, the chromatogram shown in the lower right corner is obtained. The chemical suppressor exchanges cations in the eluent for hydronium ions. The hydronium used in IC systems is supplied by electrolysis of recycled eluent or external water reservoir or dilute sulfuric acid. The hydronium ions then neutralize the

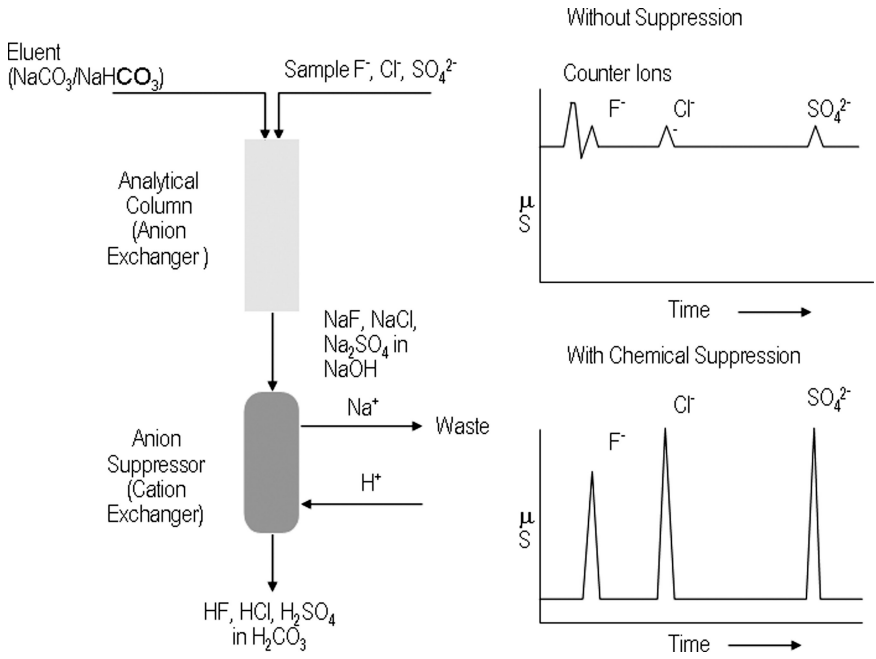

Fig. 4—The role of chemical suppression.

carbonate ions in the eluent, resulting in fluoride, chloride, and sulfate ions in carbonic acid, which is slightly dissociated, resulting in typical background detector signals of 15–30 μS cm^{-1}. Counterions of the analytes, which are cationic and thus elute in the void, are also removed. This accounts for the absence of the large system peak after suppression. A third advantage is that the anions are now paired with hydronium counterions, resulting in a much larger response for these ions because they enter the conductivity detector cell in a more conductive form. The detector response for a peak using conductivity detection is proportional to the sum of the equivalent conductivity of the anion and its associated cation. The equivalent conductivities for anions and cations are typically between 35 and 80 S cm^2 mol^{-1}. The hydronium ion, H_3O^+ (denoted as H^+ in Fig. 4), with 350 S cm^2 mol^{-1} and hydroxide ion (regenerants for cation separations) with 198 S cm^2 mol^{-1} are the only exceptions [7]. The use of suppression in IC results in as much as a 10-fold increase in detector response for anion methods [1].

Suppressor design and performance has expanded the range of IC methods from packed bed batch suppression to membrane-based continuous suppression. The first chemical suppressor was a batch suppressor, and although it delivered good signal to noise, it had to be frequently removed from the chromatographic separation stream for regeneration [5]. A micromembrane suppressor supplies continuous suppression due to a high suppression capacity permitting use of high capacity columns and gradient operation in ion chromatography.

Auto suppressors continuously make their own regenerants electrolytically with deionized water and eliminate the need to handle acids and bases. Fig. 5 illustrates the role suppression plays when hydroxide-based eluents are used

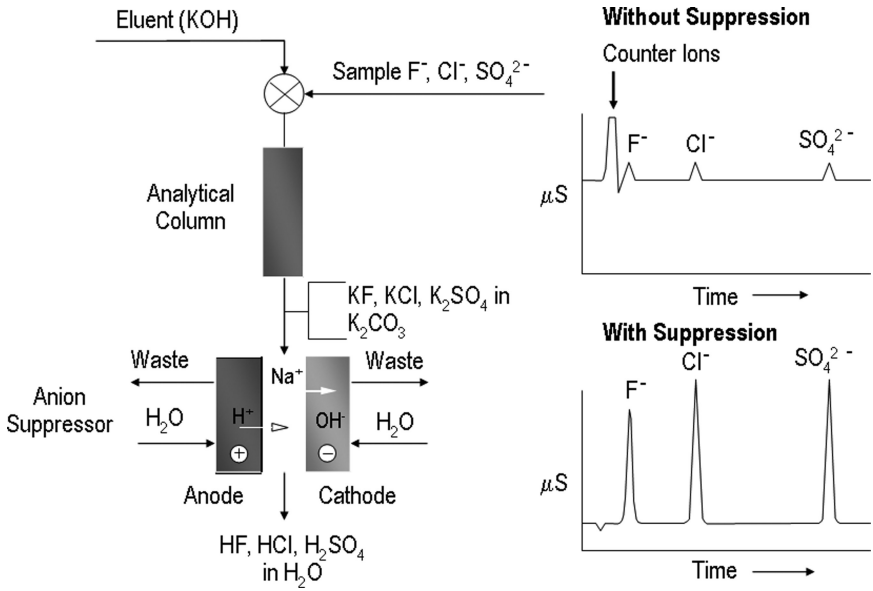

Fig. 5—The role of suppression (KOH eluent).

using AutoSuppression® and electrolytic eluent generation of potassium hydroxide. Note the suppressor product is water (as opposed to carbonic acid when carbonate-based eluents are suppressed), resulting in higher sensitivity due to less detector signal background, which is typically less than 2 μS cm^{-1} [8].

Eluents used for cation separations include methanesulfonic acid and sulfuric acid. These highly conductive eluents are suppressed using an anion exchange device or cation suppressor. Using this device, hydroxide anions are exchanged for either methanesulfonate or sulfate anions, thus reducing absolute background conductivity contribution of the eluent. Hydroxide ions are generated either through the electrolysis of water/recycled eluent or with dilute base [8].

Other Detectors for Ion Chromatography

AMPEROMETRIC DETECTION

Some inorganic and organic ion determinations are not well suited for conductivity detection. Amperometric detection is used to measure the current or charge resulting from oxidation or reduction of analyte molecules at the surface of a working electrode. For analytes that can be oxidized or reduced, detection is sensitive and highly selective because many potentially interfering species cannot be oxidized or reduced, and so are not detected. When a single potential is applied to the working electrode, the detection method is dc amperometry. Pulsed amperometry and integrated amperometry (PAD and IPAD, respectively) employ a repeating sequence of potentials [9].

Separation of carbohydrates by high pH anion exchange followed by IPAD detection is used to detect wood sugars, mannitol, fucose, arabinose, rhamnose, galactose, glucose, sucrose, xylose, mannose, fructose, and ribose (Fig. 6). IC here is employed for evaluating pulping and biomass conversion operations.

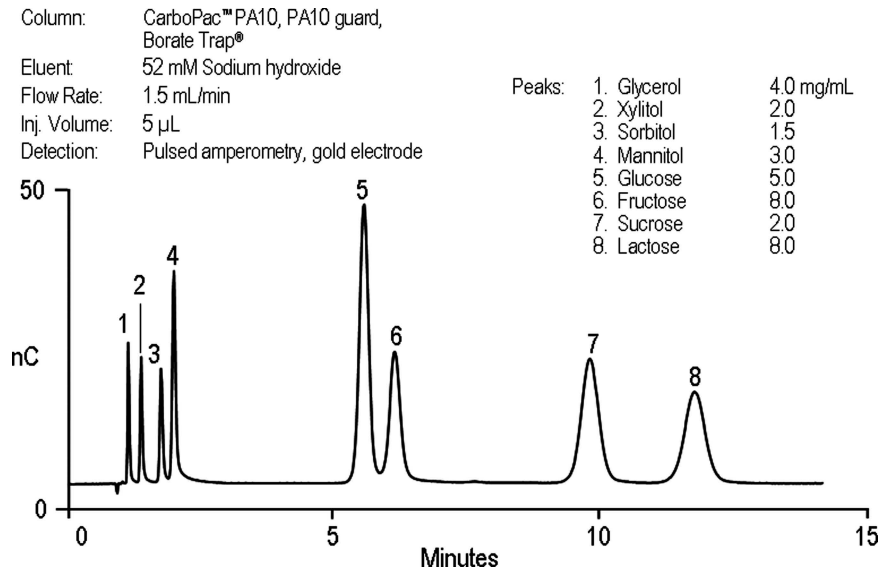

Fig. 6—Carbohydrate analysis by HPAE-PAD.

ULTRAVIOLET/VISIBLE LIGHT ABSORBANCE

Commonly used in HPLC, ultraviolet/visible light absorbance (UV/Vis) is also used in IC as a complement to conductivity detection for identifying and quantifying aromatic and heterocyclic molecules, transition metals, and certain inorganic ions. UV/Vis absorbance detection quantifies analytes by measuring the amount of light they absorb at a specific wavelength.

MASS SPECTROMETRY

Combining IC separations with mass spectrometry (MS) detection using standard IC conditions improves MS performance by removing high ionic strength eluents using a suppressor. IC with MS detection offers high specificity of analytes by avoiding coelution interferences and background interferences. It is also possible to quantitate target analytes and identify unknowns [12].

IC METHODS USED IN PETROLEUM INDUSTRY

Refining

IC has aided in improvement of refinery amine unit operation. Heat stable salts have been known to be a source of refining inefficiencies since the mid-1980s. "Sour" gases present in various quantities in natural gas and liquid petroleum are "scrubbed" before transport and further refining. The most effective scrubbing solutions consist of 20 % to 30 % alkanolamine. This class of base is recommended for the type of hydrocarbon and its associated acid gases, which consist of predominantly hydrogen sulfide and carbon dioxide. Natural gas or refinery gas streams are passed through the amine stripper, where hydrogen sulfide and carbon dioxide are retained. These gases are later removed by heat. Inorganic, organic anions, and even amino acids (formed from nitrogen-containing compounds) not removed are referred to as heat stable salts (HSS; see Table 1).

Buildup of HSSs in the amine scrubber reduces scrubbing efficiency and can cause corrosion and foaming problems. Refiners and gas processors have developed technology to remove heat stable salts and thereby improve amine quality. IC is the recommended tool for monitoring several points throughout the amine unit. Gradient IC is preferred for two reasons: (1) solvent-compatible column technology allows for full front-end resolution of organic acids such as acetate, formate, and glycolate; and (2) it will efficiently resolve and detect sulfur species from sulfite and sulfate to the strongly retained anions such as thiosufate and thiocyanate within a single chromatographic run (Fig. 7). Adding organic modifier to the potassium hydroxide eluent, 15 % methanol, improves peak shape and resolution.

Improvements in cation exchange technology enable amine unit operators to pinpoint amine leakage and direct treatment options. A high-capacity cation exchange column maximizes sodium to ammonium resolution, which allows measurement of trace amounts of ammonium and amines in the presence of percentage amounts of sodium (see Fig. 8). Maintenance problems in the unit are discovered when wastewater monitoring indicates ammonium and amine levels outside of the control range of the treatment units [12].

ASTM Method 6919 allows both suppressed and nonsuppressed conductivity detection. Figs. 9a and b show examples of cation separations with both forms of detection.

TABLE 1—Common Sources of the Anions of Heat Stable Salts	
Anion	**Source**
Chloride	Make-up water. Brine with inlet gas.
	Well treatment chemicals with inlet gas.
Nitrate, Nitrite	Make-up water. Corrosion inhibitors.
Sulfate, Sulfite, Thiosulfate	Sulfur species oxidation products.
	Component in gas.
Formate, Oxalate, Acetate	Acid in the feed gas. O_2 degradation.
	Thermal degradation.
Thiocyanate	Reaction product of H_2S and CN–.
Phosphate	Corrosion inhibitors. Phosphoric acid activated carbon. Cotton filters.
Fluoride	Well treatment chemicals with inlet gas.
Source: Ref [11]	

Ion chromatography has proven to be a useful technique for determining amines and their breakdown products (usually other smaller amines and ammonium). Alternate techniques using gas chromatography and HPLC require derivitization for separation and detection. Typically these samples are water based since amines are used extensively as organic bases for pH adjustment in aqueous process streams (e.g., boiler water) or product formulations (scale inhibitor). Ion chromatography with suppressed conductivity detection offers the convenience of analyzing water-based systems with excellent sensitivity and minimal effort (Fig. 10).

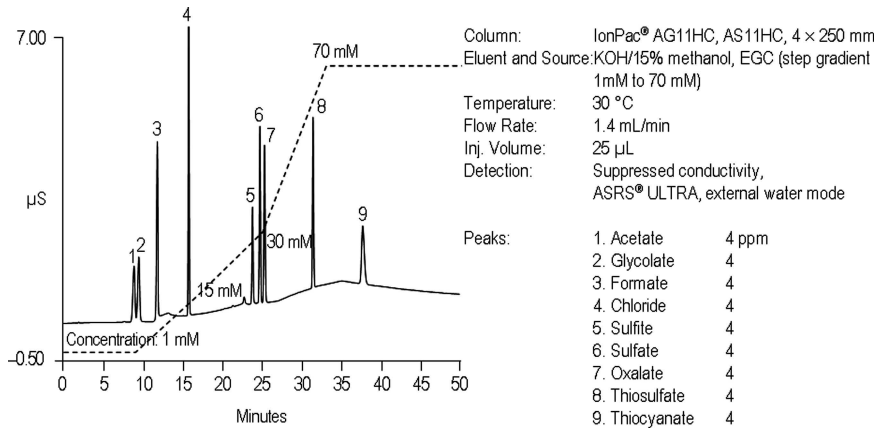

Fig. 7—Refinery heat-stable salt monitoring.

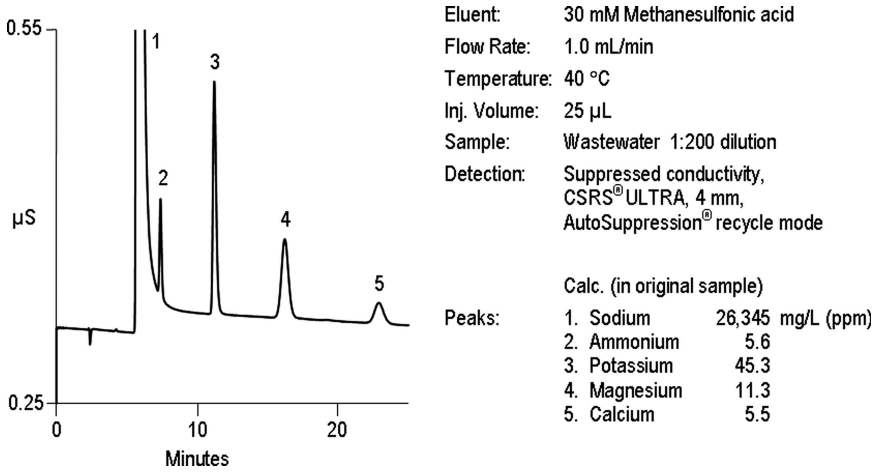

Fig. 8—Cation analysis of wastewater sample.

Efficient management of process streams in petrochemical production requires frequent monitoring for contamination prior to use or disposal. For example, natural gas liquids and liquid petroleum gas (LPG) streams are typically "washed" with dilute caustic (2–14 wt% sodium hydroxide) to remove residual organic sulfur compounds, such as mercaptans. As another example, alkanolamine solutions are used to remove acidic components (hydrogen sulfide, carbon dioxide) from these hydrocarbon streams. Caustic washing may also be employed to neutralize the acid alkylation process effluents to minimize corrosion of plant piping and mechanical components. Ion chromatography is an effective analytical tool for measuring cation contaminants such as alkali and alkaline earth metals, ammonium, and alkanolamines in spent caustic washes, akanolamine solutions, and other process streams such as wastewater, as shown in Fig. 11[13].

Exploration and Production

In the oil field, drilling fluid technology has spurred investment in more exploratory and production wells. Formation waters are analyzed for the presence of anions and cations, which may lead to scale, a problem when drilling for and transporting produced fluids. Of the potential scales that might form, the most expensive to deal with is the precipitation of barium sulfate. A common application is the prediction of scale in the oil well or surface pipes. Barium sulfate scale is resistant to most chemical removal techniques that have a reasonable cost. The best way to deal with this problem is to predict where it may occur and use precipitation inhibitors. The conventional turbidimetric analytical method for analyzing sulfate and barium (Fig. 12) is subject to large positive errors in many oil field related water samples. These errors lead to large, expensive, scale prevention projects that are often not needed. Ion chromatography is not subject to this error [14].

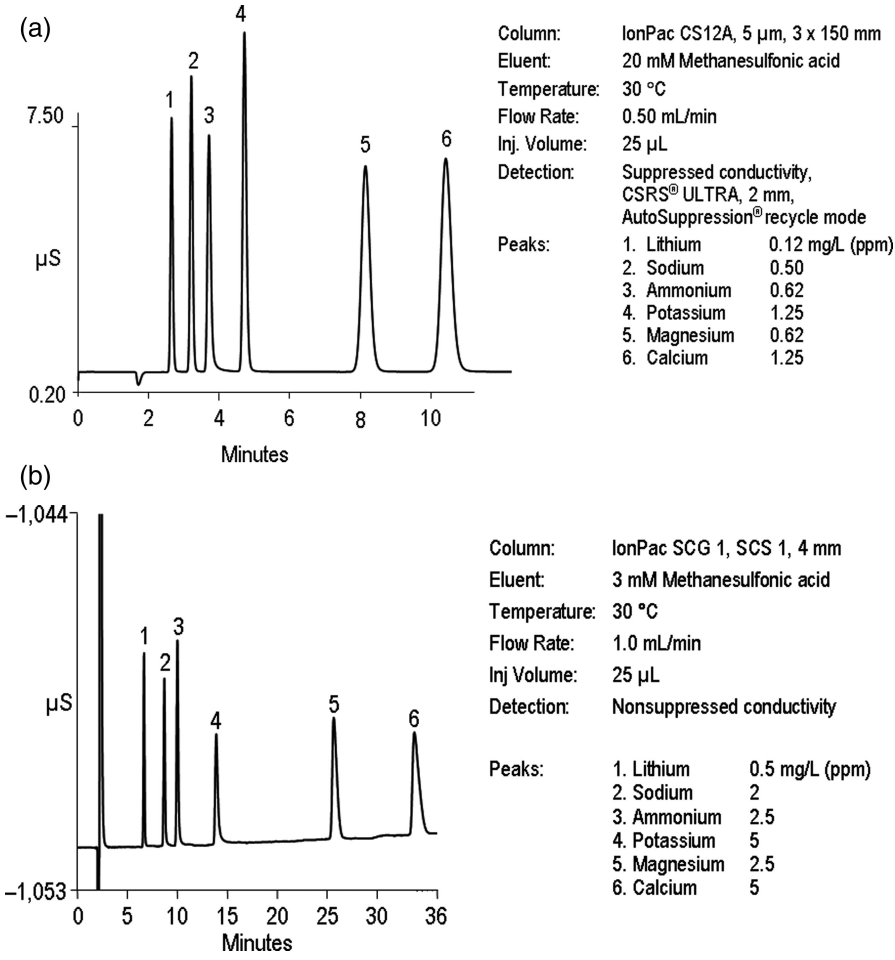

Fig. 9(a)—ASTM D6919 with suppressed conductivity detection; **(b)**—ASTM D1919 with non-suppressed conductivity detection.

Common Anions

Ion chromatography with suppressed conductivity detection is approved by the U.S. Environmental Protection Agency using method 300.0 for the determination of inorganic anions in drinking water, reagent water, and surface water. Many standards organizations (including International Standards Organization [ISO], American Society of Testing Materials [ASTM], and American Water Works Association [AWWA]) have validated IC methods for analyzing inorganic anions in drinking water. It is also approved for National Pollution Discharge Elimination System (NPDES) permit compliance monitoring (Fig. 13). Fluoride, chloride, nitrate, orthophosphate, and sulfate are quantified in a single run.

Nonaqueous samples have always been a challenge for IC methods. Various sample preparation techniques commonly used for this analysis include direct injection with or without dilution in water or evaporation according to ASTM D7319 (Fig. 14) or D7328.

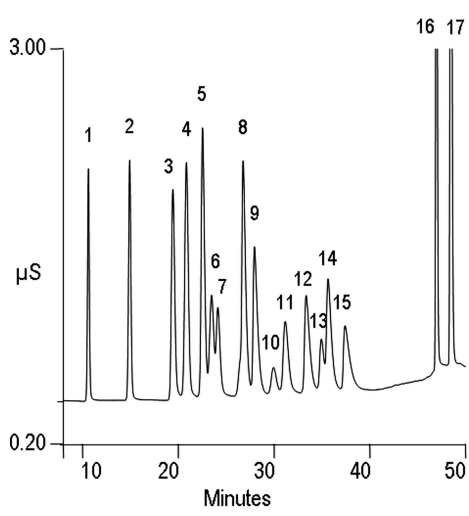

Column:	IonPac® CG16, CS16, 3 × 250 mm
Eluent:	MSA (EGC gradient)
Temperature:	60 °C
Flow Rate:	0.5 mL/min
Inj. Volume:	10 µL
Detection:	Suppressed conductivity, CSRS® ULTRA II, recycle mode

Peaks:

1. Lithium	0.5 ppm
2. Sodium	2
3. Ammonium	2.5
4. Monoethanolamine	1
5. Methylamine	0.5
6. Diethanolamine	1
7. Ethylamine	1.5
8. Potassium	5
9. Dimethylamine	1
10. Triethanolamine	1
11. Methyldiethanolamine	1
12. Dimethylethanolamine	1
13. Morpholine	5
14. 1-Methoxypropylamine	1
15. Dimethylamino-2-propanol	1
16. Magnesium	2.5
17. Calcium	5

Fig. 10—Separation of anticorrosion amines and cations.

Sample Preparation

The final two topics are two types of sample preparation used to analyze ionic contamination in nonaqueous matrices encountered in the petroleum and petrochemical industry.

MATRIX ELIMINATION

Matrix effects can include baseline disruptions and spurious peaks that interfere with the ions of interest. Evaporating the volatile organic matrix is a technique for off-line matrix elimination followed by reconstitution in water. A technique for direct injection of denatured ethanol or isopropanol for determining trace anions uses in-line matrix elimination for flushing away the matrix and subsequent analysis by IC (Fig. 15) [15].

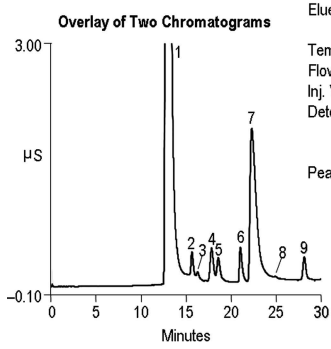

Column:	IonPac® CG16 and CS16, 3 x 250 mm
Eluent:	12 mM methanesulfonic acid for 6 min 12 to 55 mM from 6–25 min
Temperature:	30 °C
Flow Rate:	0.5 mL/min
Inj. Volume:	50 µL
Detection:	Suppressed conductivity, CSRS® ULTRA II, 2 mm Autosuppression, recycle mode

Peaks:

1. Sodium	50,332	ppm
2. Ammonium	55	
3. Unknown	—	
4. Unknown	—	
5. Unknown	—	
6. Potassium	174	
7. *n*-Methyldiethanolamine	5,247	
8. Magnesium	3	
9. Calcium	65	

Fig. 11—Cations and alkanolamines (MDEA) in spent caustic.

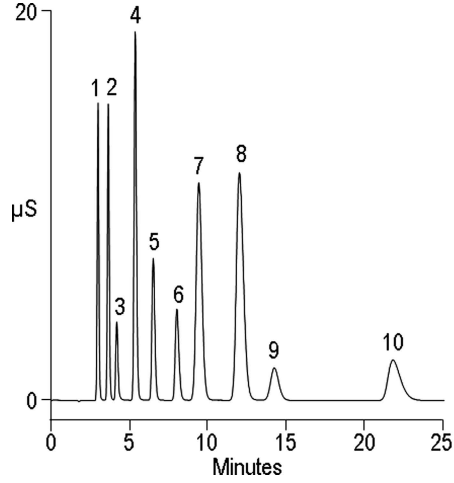

Column:	IonPac® CS12A, 4 mm
Eluent:	18 mN Methanesulfonic acid
Flow Rate:	1.0 mL/min
Inj. Volume:	25 μL
Detection:	Suppressed conductivity, CSRS® recycle mode

Peaks:		
	1. Lithium	1.0 mg/L (ppm)
	2. Sodium	4.0
	3. Ammonium	5.0
	4. Potassium	10.0
	5. Rubidium	10.0
	6. Cesium	10.0
	7. Magnesium	5.0
	8. Calcium	10.0
	9. Strontium	10.0
	10. Barium	10.0

Fig. 12—Separation of expanded alkali and alkaline earth metals and ammonium.

Anions (or cations) can be enriched from such a matrix using an additional pump and valve. The following steps illustrate how this mode of concentration/matrix elimination works.

1. The sample is first loaded into a large sample loop with the loading valve in the "Load" position.
2. The loading valve is then switched to the inject position and a pump, using ion-free water, pushes the sample through the concentrator column mounted on the concentration valve. The pump continues to pump water and flushes the matrix to waste (as shown in Fig. 16).

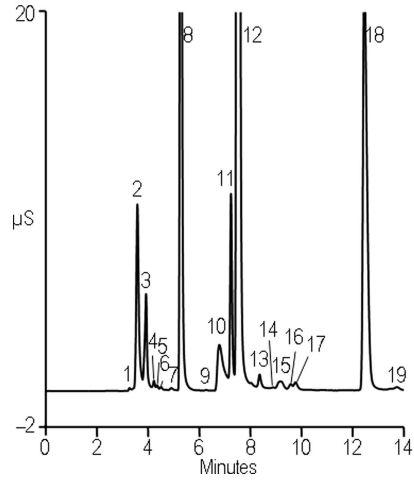

Column:	IonPac® AS18, 4 mm
Eluent:	Potassium hydroxide: 12–44 mM from 0–5 min and 44–52 mM from 8–10 min
Eluent Source:	EGC-KOH with CR-ATC
Temperature:	30 °C
Flow Rate:	1.0 mL/min
Inj. Volume:	100 μL
Detection:	Suppressed conductivity, ASRS® ULTRA, 4 mm, 150 mA, AutoSuppression® recycle mode
Sample Prep:	Wastewater sample diluted 100:1

Peaks:		
	1. Fluoride	11. Sulfite
	2. Acetate	12. Sulfate
	3. Formate	13. Bromide
	4. Unknown	14. Unknown
	5. Unknown	15. Nitrate
	6. Unknown	16. Unknown
	7. Unknown	17. Unknown
	8. Chloride	18. Thiosulfate
	9. Nitrite	19. Unknown
	10. Carbonate	

Fig. 13—Analysis of a chemical plant wastewater sample.

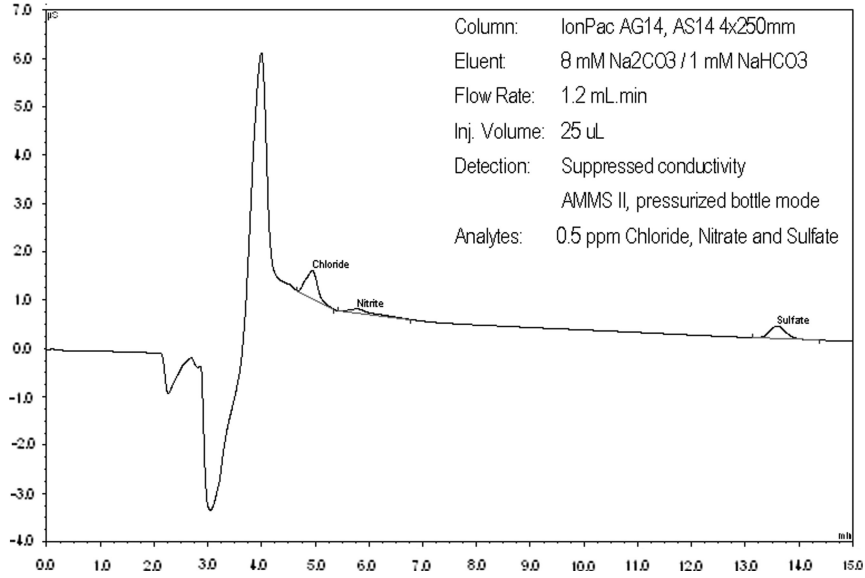

Fig. 14—Trace anions in denatured ethanol direct injection, ASTM D7319.

3. With the ions of interest loaded on the concentrator column, the "Concentration Valve" is switched to the inject position and the eluent displaces the ions onto the analytical column for chromatographic analysis

COMBUSTION ION CHROMATOGRAPHY

Oxidative combustion for sample preparation can be coupled with an IC system to analyze combustion products. A variety of analytical methods employing

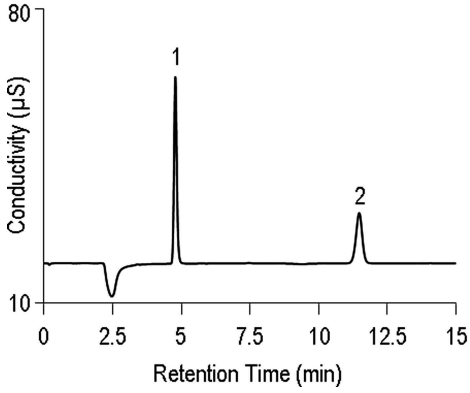

Column:	IonPac® AS22 + guard, 4 mm	
Eluent:	4.5 mM Sodium carbonate 1.4 mM Sodium bicarbonate	
Temperature:	30 ° C	
Flow Rate:	1.2 mL/min	
Inj. Volume:	200 µL	
Concentrator:	TAC-ULP1	
Detection:	ASRS® ULTRA II (recycle)	
Current:	31 mA	
Sample:	Ethanol with 5% gasoline spiked with aqueous standards	
		mg/L
Peaks:	1. Chloride	4.0
	2. Sulfate	4.0

Fig. 15—Determination of sulfate and chloride after in-line matrix elimination.

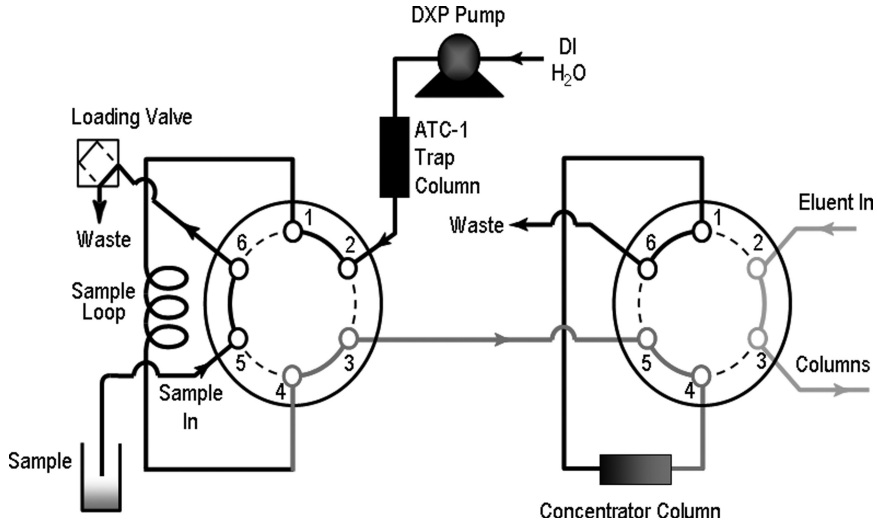

Fig. 16—Schematic of IC system for trace contaminant analysis concentrating the sample and eliminating the matrix.

oxygen bombs to decompose these sample types for analysis by IC have been developed and used for product quality and waste characterization (Fig. 17). These methods require manual sample loading and vessel rinse of the combustion products. The technique (oxidative bomb combustion) used in these steps significantly affects recoveries and sample throughput [16].

An automated method to analyze trace halogenated and sulfur compounds in plastics, polymers, rubber, coal, and petroleum liquids has been developed.

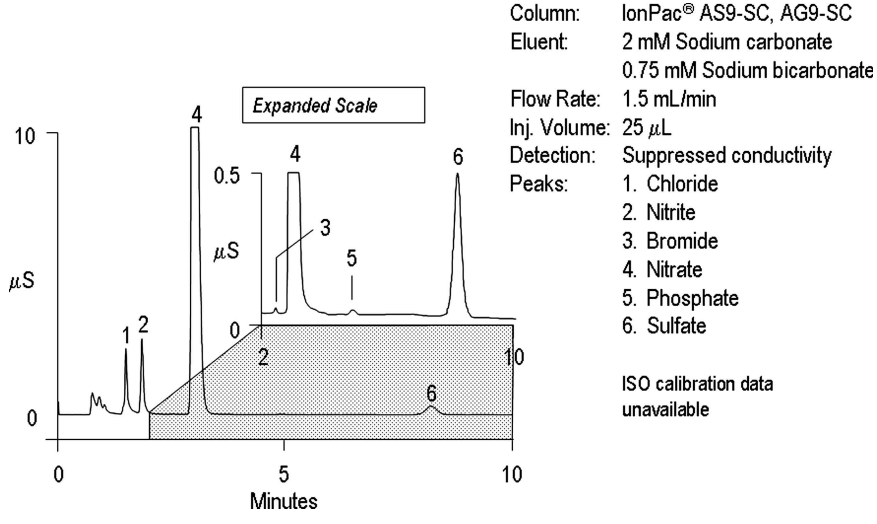

Fig. 17—Combustion IC of used motor oil.

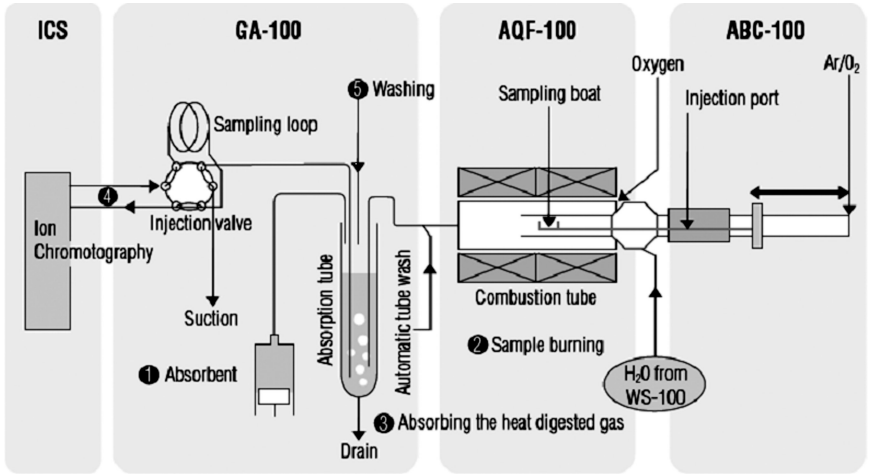

Fig. 18—Schematic of in-line combustion IC.

This analysis coupled with an IC system for analyzing the combustion products is used to identify and measure:

- Source of contaminants in production and manufacturing
- Additives for fire retardants and antioxidants (plastics, polymers, textiles)
- Environmental impact of use (coal), disposal, and recycling (plastics and solvents)
- Product specification and QC/QA.

A schematic of an in-line combustion system with IC is depicted in Fig. 18. The Combustion IC Prep Station consisted of an automatic boat controller for sample introduction, and a 1,000°C furnace equipped with quartz pyrolysis tube

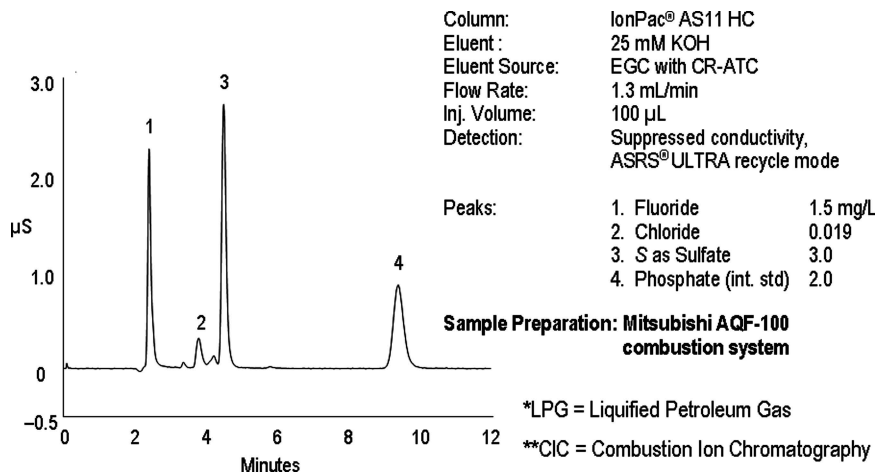

Fig. 19—Total halides and sulfur in liquified petroleum gas (LPG) by on-line combustion ion chromatography.

with inlets for sample boat, argon, oxygen, and water. The water provides a pyrohydrolytic environment (humidity) necessary for acceptable recoveries of halogens. The products of combustion are gaseous and are absorbed into a fixed volume (3 to 5 mL) of aqueous absorption solution consisting of water, hydrogen peroxide, and a phosphate anion internal standard [17].

Fig. 19 is a chromatogram of total halides and sulfur in an LPG sample. This analysis is used to monitor hydrogen fluoride alkylation unit effectiveness.

ASTM METHODS UTILIZING IC

Standard Designation	Title
D4327	Test Method for Anions in Water by Chemically Suppressed Ion Chromatography
D4856	Standard Test Method for Determination of Sulfuric Acid Mist in the Workplace Atmosphere (Ion Chromatographic)
D5085	Standard Test Method for Determination of Chloride, Nitrate, and Sulfate in Atmospheric Wet Deposition by Chemically Suppressed Ion Chromatography
D5257	Standard Test Method for Dissolved Hexavalent Chromium in Water by Ion Chromatography
D5542	Standard Test Methods for Trace Anions in High Purity Water by Ion Chromatography
D5794	Standard Guide for Determination of Anions in Cathodic Electrocoat Permeates by Ion Chromatography
D5827	Test Method for Analysis of Engine Coolant for Chloride and Other Anions by Ion Chromatography
D5896	Standard Test Method for Carbohydrate Distribution of Cellulosic Materials (Wood Sugars)
D6581	Standard Test Method for Bromate, Bromide, Chlorate, and Chlorite in Drinking Water by Chemically Suppressed ION Chromatography
D6832	Standard Test Method for the Determination of HEXAVALENT Chromium in Workplace Air by Ion Chromatography and Spectrophotometric Measurement Using 1,5-diphenylcarbazide
D6919	Standard Test Method for Determination of Dissolved Alkali and Alkaline Earth Cations and Ammonium in Water and Wastewater by Ion Chromatography
E1511	Standard Practice for Testing Conductivity Detectors Used in Liquid and ION Chromatography
E1787	Standard Test Method for Anions in Caustic Soda and Caustic Potash (Sodium Hydroxide and Potassium Hydroxide) by Ion Chromatography

(Continued)	
Standard Designation	**Title**
D7319-07	Standard Test Method for Determination of Total and Potential Sulfate and Inorganic Chloride in Fuel Ethanol by Direct Injection Suppressed Ion Chromatography
D7328-07	Standard Test Method for Determination of Total and Potential Inorganic Sulfate and Total Inorganic Chloride in Fuel Ethanol by Ion Chromatography Using Aqueous Sample Injection

References

[1] Weiss, J., *Ion Chromatography*, 3rd ed., Wiley-VCH, Weinheim, Germany, 1995.

[2] Small, H., *Ion Chromatography*, Plenum Press, New York, 1989.

[3] Haddad, P. R. and Jackson, P. E., *Ion Chromatography, Principles and Applications*, Elsevier Science B.V., Amsterdam, the Netherlands, 1990.

[4] Fritz, J. S. and Gjerde, D. T., *Ion Chromatography*, Wiley-VCH, Weinheim, Germany, 2000.

[5] Small, H., Stevens, T. S. and Bauman, W. C., "Novel Ion Exchange Chromatographic Method Using Conductometric Detection," *Anal. Chem*., Vol. 47, 1975, pp. 1808–1809.

[6] Small, H., Liu, Y. and Avdalovic, N., "Electrically Polarized Ion-Exchange Beds in Ion Chromatography: Eluent Generation and Recycling," *Anal. Chem.*, Vol. 70, 1998, pp. 3629–3635.

[7] Coury, L., "Conductance Measurements Part 1: Theory," *Curr. Separations*, Vol. 18, No. 3, 1999, pp. 91–96.

[8] *Anion/Cation Self Regeneration Suppressor 300 Manual*, Dionex Corporation, Sunnyvale, CA, 2008.

[9] "Analysis of Carbohydrates by High Performance Anion Exchange Chromatography with Pulsed Amperometric Detection (HPAE-PAD)," Dionex Technical Note 20, LPN 032857-04 5M 6/2000, Dionex Corporation, Sunnyvale, CA, 2000.

[10] Slingsby, S. and Pohl, J. "The Measurement of Haloacetic Acids in Drinking Water Using IC-MS/MS–Method Performance," Poster Reprint LPN 2117-01 9/08 Dionex Corporation, Sunnyvale, CA, 2008.

[11] Kadnar, R. and Rieder, J., "Determination of Anions in Amine Solutions for Sour Gas Treatment," *J. Chromatogr*., Vol. 706, 1995, pp. 339–343.

[12] Chassaniol, K., "Ion Chromatography Analysis: Improve Facility Operations with this Valuable Technique," *Hydrocarb. Proc*., Vol. 77, February 2003, pp. 135–137.

[13] Chassaniol, K., *A New Gradient Ion Chromatography (IC) Method for Inorganic Cations and Amines*, LC/GC North America, Iselin, NJ, 2003, p. 46.

[14] "Solutions for Increased Productivity, an Applications Guide for Chemical, Petrochemical, and Petroleum Producers," *Dionex Applications Guide*, Dionex Corporation, Sunnyvale, CA, June 1999.

[15] "Determination of Sulfate and Chloride in Ethanol Using Ion Chromatography," *Dionex Application Update 161*; LPN 1920-02 PDF 09/08; Dionex Corporation, Sunnyvale, CA, 2008.

[16] "Analytical Methods for Oxygen Bombs," *Parr Instrument Company Manual*, Monline, IL, 2004.

[17] Chassaniol, K. D. and Manahan, M., *Determination of Total Halides and Sulfur in Plastics/Polymers Using Ion Chromatography and In-line Sample Combustion*, LC/GC North America, Iselin, NJ, 2005, pp. 82–83.

19

Chromatography Applied to the Analyses of Petroleum Feedstocks and Products: A Brief Overview

Frank P. Di Sanzo[1]

INTRODUCTION

Chromatography is a widely accepted and important analytical tool in petroanalyses. The technique provides composition of volatile and nonvolatile organic and certain inorganic compounds that affect feedstock catalytic processing and product quality. Analyses range from percentages to trace ppm and ppb concentration levels. A large number of ASTM methods apply chromatographic techniques.

The forms of chromatography used by the petroleum industry include gas chromatography (GC), liquid chromatography (LC), supercritical fluid chromatography (SFC), and ion chromatography (IC). Other forms such as electrophoresis (CE) may be sporadically used. In many petroleum applications, chromatography is coupled with hyphenated techniques such as gas chromatography-mass spectrometry (GC-MS, SFC-GC-MS, LC-MS) and spectroscopic detectors such as atomic emission (AED) and inductively coupled plasma (ICP-MS), infrared (IR), flame photometric (FPD), and sulfur and nitrogen chemiluminescence (SCD and NCD) to enhance qualitatively the selectivity for the analytes and simplify their quantification.

The following sections give a brief overview of several chromatographic applications for the analyses of petroleum products with emphasis on current ASTM methodologies.

Gas Chromatography

Gas chromatography [1] uses a pressurized gas cylinder that contains the carrier gas such as helium, hydrogen, or nitrogen to carry the solutes of sufficient vapor pressure and stability through the separation column and to the detector (Fig. 1).

The separation column can be packed tubing or a wall coated open tubular (WCOT) capillary column. Packed columns are used mostly in gas analyses; most other applications use WCOT for their resolving power. Even certain gas analyses are carried out by WCOT employing specialty phases.

The most common detectors used in GC are the "universal" thermal conductivity detector (TCD) and flame ionization detector (FID). The TCD is used mostly to detect gases (such as hydrogen, oxygen, and nitrogen) and hydrocarbons such as in gas analyses or portable micro-GCs, and FID is used to detect volatile hydrocarbons ranging from methane to approximately C100–C120

[1] *ExxonMobil Research and Engineering Co., Annandale, New Jersey*

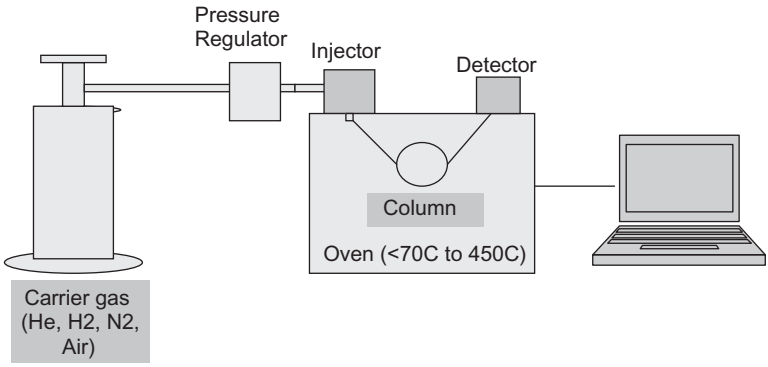

Fig. 1—Gas chromatographic (GC) system.

and organic compounds containing heteroatoms (such as sulfur, nitrogen, and oxygen). "Selective" detectors include SCD/NCD, AED, thermoionic nitrogen/phosphorous (NPD), electrolytic ("Hall") for halogens (fluorine, bromine, chlorine) and sulfur and nitrogen, electron capture (ECD), FPD, GC/OFID (oxygen specific), MS, and infrared (FTIR).

In GC, there are two types of separation mechanisms: gas adsorption and gas-liquid. Gas adsorption GC involves a packed or capillary column with an adsorbent used as the stationary phase. Common adsorbents are zeolite, silica gel, and alumina. This GC mechanism is mostly used to separate mixtures of gases.

Gas-liquid GC (GLC) is a more common type of analytical GC and consists of a "liquid" polymeric stationary phase coated on a particle (e.g., diatomaceous earth support) as in packed columns or coated or stabilized on the inner walls of the WCOT. GLC with WCOT is used for most separations involving nongaseous liquids. The solutes are separated as each has a different partitioning into the stationary phase as they migrate along the WCOT to the detector.

ASTM GC applications in the petroleum industry range from detailed composition analyses of gasoline range streams, to simulated distillation of fractions boiling up to 750°C, to gas analyses. Many of these GC methods are used in product certifications and regulatory compliance of products.

Liquid Chromatography

Liquid chromatography (LC) [2–3] plays a large role in petro-applications because of its many different unique mechanisms in solute-stationary phase interactions that lead to different separations which cannot be accomplished by GC. LC consists of a liquid pump, injector, column, and detector (Fig. 2). Isocratic separations use a single solvent to elute all of the solutes, and a gradient or solvent strength programming with two or more solvents can be used to elute more complex solute mixtures that exhibit a wider range of retention.

Users may choose LC for separations requiring bulk hydrocarbon group types, for obtaining larger quantities of separated fractions (preparative LC) for further solutes characterization by other techniques (IR, NMR, MS, etc.) and for quantification of nonvolatile or thermally unstable solutes such as additives. A number of ASTM methods have been approved for such applications.

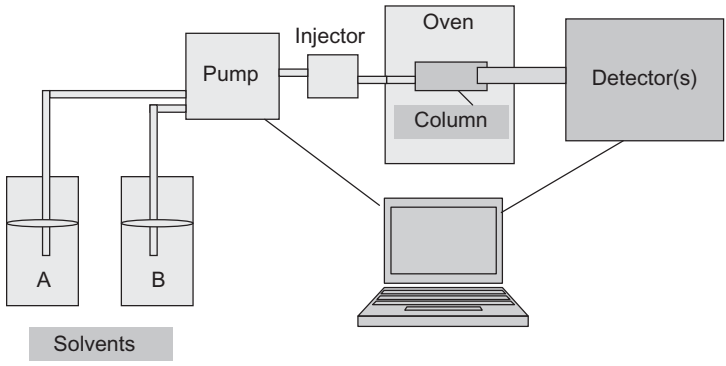

Fig. 2—Liquid chromatographic (LC) system.

Liquid chromatography can be classified by the type of separation mechanism (Fig. 3) such as normal phase (NP-LC), reverse phase (RP-LC), gel permeation chromatography(GPC) or size exclusion chromatography (SEC), and ionic exchange for charged solutes (IC/ion exchange). For petroleum separation, generally NP-LC is used to separate hydrocarbons into group types according to the polarity of the hydrocarbons using increasingly polar eluant solvents, for example, heptane to methanol. For example, total saturated hydrocarbons can be separated from total aromatics or aromatics according to aromatic ring number or both. The stationary phases in NP-LC can range from silica, alumina to chemically bonded cyano, amino groups. The bonded phases generally retain their activities from repetitive analysis, whereas adsorbent phases like silica gel and alumina can be deactivated by water and strongly retained solutes over time.

RP-LC is a powerful analytical tool that involves a hydrophobic, low-polarity stationary phase which is chemically bonded to an inert solid such as silica. Stationary phases commonly used in RP include C18 alkyl group bonded to a silica substrate. Other phases can include, for example, phenyl groups.

In RP, particular solutes such as additives or individual hydrocarbons within same group class can be separated according to the hydrophobic alkyl

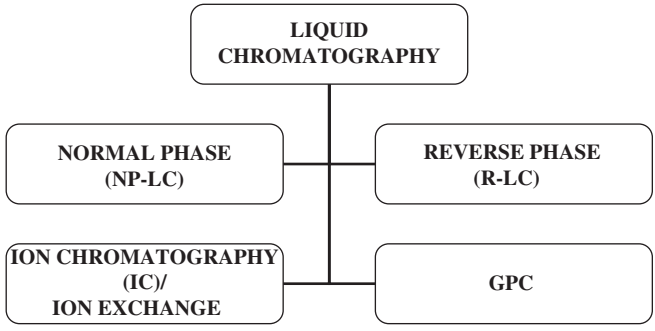

Fig. 3—Types of liquid chromatography (LC).

substitution on the solute by using a relatively polar solvent mixture such as water and methanol, acetonitrile, or tetrahydrofuran mixtures.

Ion exchange chromatography is used to isolate ionic solutes such as acid and bases or charged in-organic species. One form of such separation is the analytical-scale ion chromatography or IC [4] for separation of acids, bases, and ionic charged ions such as $Ca++$ and $NH4+$. Generally, there are two types of ion exchange: cation exchange in which the stationary phase carries a negative charge that is used to separate positively charged solutes, and anion exchange in which the stationary phase carries a positive charge that is used to separate negatively charged solutes. The ionic solutes will not elute from the column until a solution of varying pH or ionic strength is passed through it. Separation by this mechanism can be highly selective. Ion exchange chromatography using inexpensive resins containing high capacities can be used also for preparative scale to isolate, for example, acid/base species from crude oils.

GPC or SEC or gel filtration lacks an interaction between the stationary phase and solute. Instead, the liquid passes through a porous gel that separates the molecules by size. The pores are normally small and exclude the larger solute molecules than the molecular volumes of smaller molecules, which enter the pores. The latter mechanism causes the larger molecules to pass through the GPC column at a faster rate than the smaller ones. As a result, the larger molecules are detected first. GPC can be used to obtain molecular weight distributions of heavier petroleum fractions, the analyses of additives in various products matrices, and characterization of polymers such as polypropylene, etc.

Common detectors used in LC include the universal response refractive index (RI or RID), spectroscopic such as UV/VIS and fluorescence, LC-MS and ICP-MS, evaporative (mass) light scattering detection (ELSD), multi-angle light scattering, and electrochemical. Other detectors such as IR (either direct on-line reading or post column effluent trapping) and LC/NCD also have been used. Less reliable FID detectors have been developed over the years for liquid chromatography, but generally these have not been sufficiently rugged and are not readily available commercially. In the place of the LC-FID, the ELSD has been used where universal mass detection is needed for less volatile compounds. The main drawback of the ELSD is its relatively narrow linearity range, which requires extensive calibration and the variation in its relative response factors among the solutes when compared to the FID.

Supercritical Fluid Chromatography

SFC [5] uses a supercritical fluid as the mobile phase carrier (Fig. 4). Supercritical conditions are attained by varying the column oven and the pressure of the carrier fluid. The required pressure within the column is maintained by using a restrictor at the end of the column. Supercritical carbon dioxide mixed with or without a modifier is a popular carrier. SFC effective separations are somewhat between GC and LC. Both GC type of columns (bonded capillary WCOT) and LC type of packed columns are used depending on the separation desired. One advantage of SFC over LC for petroleum applications is that a rugged FID detector, similar to that applied in GC, can be used with carbon dioxide with no organic modifier for reasonable mass quantification of the hydrocarbons. Other common detectors used with SFC include UV/VIS, MS, and chemiluminescence detectors such as the SCD.

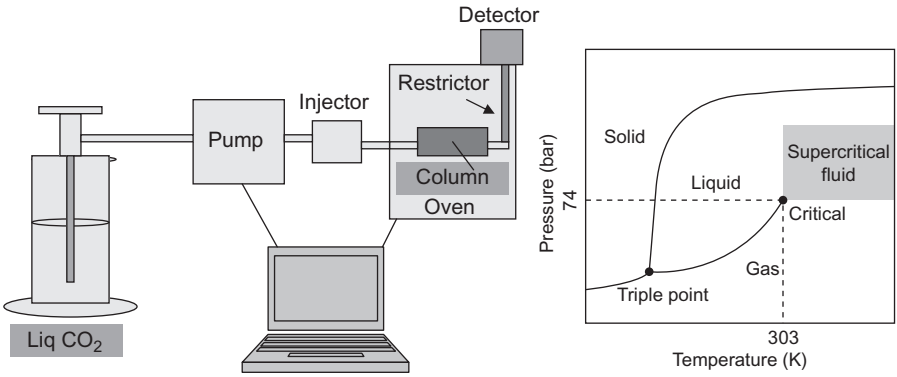

Fig. 4—Supercritical fluid chromatographic (SFC) system.

ANALYSES OF PETROLEUM FRACTIONS BY GAS CHROMATOGRAPHY

Detailed Hydrocarbon Analyses and Multidimensional PIONA

The analyses of petroleum fractions in the carbon number range of C_1–C_{12} are performed by GC/FID [6–10] and in some cases by GC/MS and GC/FTIR. The sample types include individual process stream feeds and final products such as blended gasolines, refinery product streams, and chemical feedstocks.

Streams derived directly from crude oil, such as virgin naphthas, contain a high concentration of naphthenes (cyclo-paraffins) and little or no olefins. Other streams may contain olefins. Streams containing high concentrations of naphthenes and olefins are more difficult to analyze. Generally, at $>C_7$ an overlap of compounds may occur, and such streams may require a more sophisticated separation scheme for accurate quantification of the hydrocarbon types. Fig. 5 shows some common process streams in this boiling point range.

Virgin naphthas may be upgraded further to reformate to enhance its octane. Generally virgin naphtha requires extensive desulfurization to <1 ppm before reforming it. Olefinic streams (e.g., fluid catalytic cracking [FCC], coker and steam cracked naphthas [SCN]) are derived from the conversion of higher boiling crude cuts. Other streams like alkylates are usually produced from a reaction of butenes and isobutane via acid (HF or H_2SO_4) alkylation, forming isooctanes (high octane components). Certain synthetic streams such as methanol to gasoline (MTG) and Fischer-Tropsch (FT) are derived from methanol or syngas conversion. Whereas MTG may be used directly as a gasoline product, FT products generally need further upgrading for fuel use. Ethanol up to >85 % has been used also as a fuel.

Many of the individual processed streams mentioned are blended to produce motor gasoline. Some of the streams contain a high concentration of sulfur and may require further hydroprocessing to reduce the sulfur concentration to the desired levels to meet fuel regulations. Oxygenated hydrocarbons such as ethanol may be blended into fuels.

The common analyses of naphthas using GC/FID are summarized in Table 1. Table 2 lists the designations for various detailed hydrocarbon analyses (DHA) and multidimensional PIONA analyses types that are obtainable depending on the naphtha.

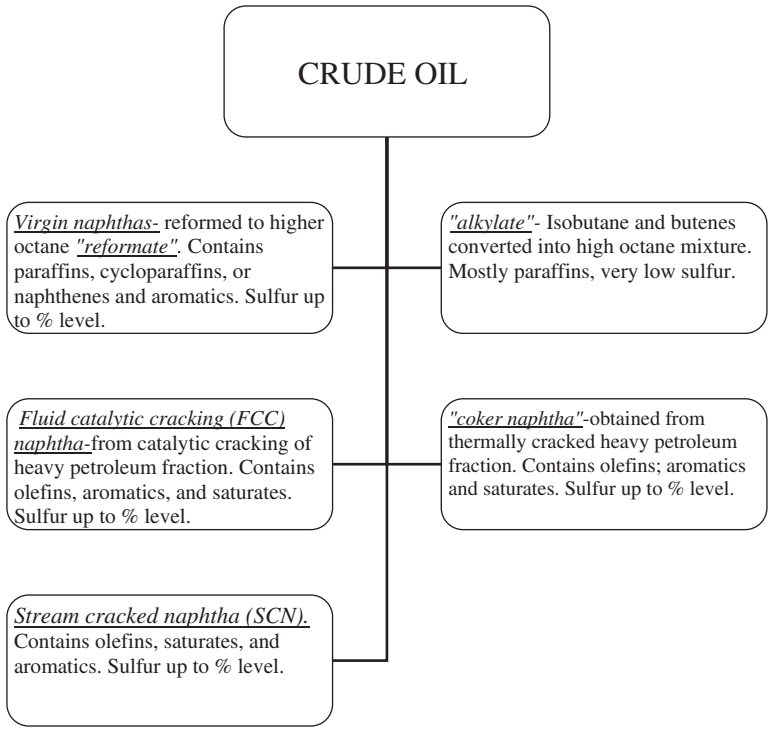

Fig. 5—Gasoline range common streams derived from crude oil processing.

Several test methods have been approved by ASTM using 50-m and 100-m capillary columns coated with dimethylsiloxane stationary phases for the DHA analysis (Table 3). Some users have also developed similar separations using 150-m WCOT at the expense of a longer analysis time to enhance further the separations of several key components.

ASTM methods include the PIONA multidimensional analyzer (Table 3) (hereafter referred to as the PIONA analyzer). The PIONA analyzer is an effective approach for the accurate and precise analyses of most gasoline range

TABLE 1—GC Methods for Analysis of Gasoline Range Streams

Single Capillary WCOT (DHA)	Multidimensional
• Detailed hydrocarbon analysis (DHA) of individual compounds/isomers • Relatively simple • 50–60, 100, 150-m methylsiloxane capillary column WCOT/FID • For highly naphthenic and olefinic streams accurate analysis limited to approximately C_1–C_8	• PIONA analyzer system • Carbon number distributions only • Complex GC system • Best overall analyses for all types of naphthas • Analyzes oxygenates (ethanol etc.) • Commercially available • Used for certification of blended gasolines in certain countries

TABLE 2—Modes of Analyses for DHA and PIONA Analyzer	
PIONA Analyzer	**Modes Designations**
PNA	Paraffins, Naphthenes, Aromatics
nPiPNA	n-Paraffins, Isoparaffins, Naphthenes, Aromatics
PONA	Paraffins, Olefins, Naphthenes, Aromatics
PIONA	Paraffins, Isoparaffins, Olefins, Naphthenes, Aromatics
nPiPONA	n-Paraffins, Isoparaffins, Olefins, Naphthenes, Aromatics
O-PONA	Oxygenates, Paraffins, Olefins, Naphthenes, Aromatics
DHA	
PIANO	Paraffins, Isoparaffins, Aromatics, Naphthenes, Olefins

streams up to 200°C. The analyzer provides only hydrocarbon carbon number distributions up to C_{12}. For a schematic and functionalities of such analyzer, see ASTM methods D6839 and D5443. The PIONA analyzer also can be

TABLE 3—ASTM DHA and PIONA Analyzer Test Methods	
ASTM Test Method	**Application**
D5134 Standard Test Method for Detailed Analysis of Petroleum Naphthas through n-Nonane by Capillary Gas Chromatography	DHA (50m); Virgin naphtha
D6733 Standard Test Method for Determination of Individual Components in Spark Ignition Engine Fuels by 50-Meter Capillary High Resolution Gas Chromatography	DHA (100m); Final Blended Gasolines
D6730 Standard Test Method for Determination of Individual Components in Spark Ignition Engine Fuels by 100-Metre Capillary (with Precolumn) High-Resolution Gas Chromatography	DHA(100m); Final Blended Gasolines
D6729 Standard Test Method for Determination of Individual Components in Spark Ignition Engine Fuels by 100 Meter Capillary High Resolution Gas Chromatography	DHA (100m); Final Blended Gasolines
D6839 Standard Test Method for Hydrocarbon Types, Oxygenated Compounds and Benzene in Spark Ignition Engine Fuels by Gas Chromatography	Multidimensional PIONA Analyzer. Final Blended Gasolines
D5443 Standard Test Method for Paraffin, Naphthene, and Aromatic Hydrocarbon Type Analysis in Petroleum Distillates Through 200°C by Multi-Dimensional Gas Chromatography	Multidimensional PIONA Analyzer; PNA content in Virgin Naphthas

TABLE 4—Limitations of DHA vs. PIONA Analyzer for Virgin Naphthas Containing Naphthenes

Hydrocarbon Types	DHA (mass %)	Multidimensional PIONA Analyzer (mass %)
Paraffins	52.2	44.1
Olefins	0.0	0.0
Naphthenes	23.8	40.1
Aromatics	21.2	15.8
Oxygenates	2.8	0.0

Note: DHA shows major inaccurate results for total paraffins, total naphthenes and total aromatics.

equipped with a prefractionator to allow analysis of the naphtha portion when mixed in samples with a higher final boiling point, such as crude oils.

DHA methods employ long capillary WCOT columns and can determine a large number of the individual hydrocarbons and isomers present; however, coelution of compounds may still exist and a complete accurate total group type PIONA analysis may not be possible. For samples containing a significant amount of olefins, interfering coelution with the olefins above C_7 is possible. Similarly, samples containing significant amounts of naphthenes (cyclic paraffins), as in virgin naphthas, may reflect significant errors in type grouping above *n*-octane. For such samples, the use of the PIONA analyzer is recommended for an overall accurate PIONA analysis. For detailed and accurate analyses of gasoline components, it may be possible to combine results from a DHA and PIONA analyzer. The DHA is used for detailed distribution of C_1–C_7 components; the PIONA analyzer will provide accurate carbon number distributions of the C_8–C_9+ components. Tables 4 and 5 demonstrate the shortcomings of the DHA analyses when compared to those obtained by the more accurate PIONA analyzer. In Table 4, the overall paraffin-naphthene-aromatic split is inaccurate because of the overlap of these compounds on the DHA WCOT. For this type of analysis, the PIONA analyzer is recommended. Table 5 demonstrates

TABLE 5—Limitations of DHA vs. PIONA Analyzer for Samples High in Olefin Content

Test Method	Light FCC Naphtha Cut (Total Olefins)	Medium FCC Naphtha Cut (Total Olefins)	Heavy FCC Naphtha Cut (Total Olefins)
DHA (100 meter) (mass %)	42.9	20.9	10.3
PIONA Analyzer (mass %)	50.2	37.9	30.0

Note: As the boiling point of the olefin-rich naphtha cuts increases, the deviation between DHA and PIONA analyzer increases. In this case the PIONA analyzer results are considered more accurate.

that as the boiling point of a naphtha rich in olefins (e.g., naphthas derived from FCC) increases, the results obtained by the DHA method deviate significantly from those obtained by the PIONA analyzer. In the latter case, the PIONA analyzer results are considered more accurate because of the selectivity enhancement inherent in the analyzer that uses a selective olefin trap to remove the olefins away from the other compound classes.

GC Methods for Final Blended Gasoline Analysis

Other methods for the analyses of gasolines are used or have been used in the regulation of gasoline parameters. Table 6 summarizes some of these methods. Mass spectrometric (GC/MS D5789) and spectroscopic (GC/FTIR D5986) test methods have been developed and used successfully, in addition to GC/FID methods. D5769 determines individual and total aromatics and has been used for regulatory analyses. The main drawback of the GC-MS method is that the total aromatic content is less accurate if samples contain significant amounts of C10+ aromatics because an average response factor is used for such compounds. The GC-FTIR method is an extremely stable system leading to long-term calibration stability versus other methods. D5986 can be used to determine oxygenates (ethanol, etc.), benzene, and other aromatics. The PIONA analyzer test method similar to D6839 has been used to certify blended gasolines because one analysis can simultaneously provide content of benzene, total aromatics, total olefins, and several blended oxygenates (e.g., ethanol).

Other multidimensional GC methods such as D5580 and D3606 are currently popular for determining benzene (D3606 and D5580) and total aromatics (D5580). Test methods D4815 and the more selective D5599 (GC/OFID) are used for determining individual and total oxygenates in gasoline.

Simulated Distillation Using Gas Chromatography

Another important use of GC is for simulated distillation (sometimes abbreviated as simdis or simdist). Simdis determines the boiling range distribution of

TABLE 6—Methods That Currently Provide Composition of Blended Gasolines

Method	Parameter Determined	Technique
ASTM D5580	Benzene, toluene, total aromatics	Multidimensional GC
ASTM D5769	Benzene, toluene and many other specified individual aromatics; total aromatics	GC/MS
ASTM D5986	Oxygenates, benzene, other specified individual aromatics, total aromatics	GC/FTIR
ASTM D3606	Benzene	Multidimensional GC
ASTM D4815	Specific oxygenates in gasolines	Multidimensional GC
ASTM D5599	Specific oxygenates in gasolines	GC/OFID
ASTM D5501	Ethanol content	GC/FID

petroleum fractions. Simdis analysis by GC is a rapid analytical tool that is widely used to replace conventional distillation methods for control of refining operations and product specification testing. The technique uses relatively small sample sizes instead of performing large-scale distillations as in D1160, D86, or D2892.

In simdis, samples are analyzed on a nonpolar chromatographic column, usually dimethylsiloxane, which separates the hydrocarbons approximately in order of their boiling points. Most applications for simdis use WCOT columns with increased temperature stability, particularly for high boiling samples.

The gas chromatograph is normally calibrated for boiling point versus retention times using a series of n-paraffins that are analyzed under the same conditions as the petroleum sample. Results are reported as a correlation between the boiling points and the percentages of the sample eluted from the column. ASTM D2887 and other ASTM simdis test methods give detailed descriptions on how to construct calibration curves and calculate final results. Generally the calculation procedure is performed by ASTM standardized software available through many simdis instrument vendors.

Because petroleum streams vary significantly in boiling point ranges, for example, crude oils, vacuum resides, and jet fuels, it has not been possible to use a single simdis method for all stream types. As a result, ASTM has developed a series of simdis methods for various applications that are optimized for the boiling point range of interest. These test methods are listed in Table 7 with their applicable boiling point ranges.

TABLE 7—Popular Simulated Distillation Methods

Test Method	Description	Applicable BP Range, °C
D2887	Standard Test Method for Boiling Range Distribution of Petroleum Fractions by Gas Chromatography	IBP to C
D6352	Standard Test Method for Boiling Range Distribution of Petroleum Distillates in Boiling Range from 174° to 700°C by Gas Chromatography	174 to 700°C
D7096	Standard Test Method for Determination of the Boiling Range Distribution of Gasoline by Wide-Bore Capillary Gas Chromatography	
D7169	Standard Test Method for Boiling Point Distribution of Samples with Residues Such as Crude Oils and Atmospheric and Vacuum Residues by High Temperature Gas Chromatography	IBP to 750°C+
D7213	Test Method for the Boiling Range Distribution of Petroleum Distillates in the Boiling Range from 100° to 615°C by Gas Chromatography	100° to 615°C
D7398	Standard Test Method for Boiling Range Distribution of Fatty Acid Methyl Esters (FAME) in the Boiling Range from 100° to 615°C by Gas Chromatography	100° to 615°C

Generally, the complexity and time required (analyzer maintenance, etc.) to obtain precise and accurate data increase with the final boiling point of the samples to be analyzed. Simdis of gasolines (e.g., D7096), for example, uses relatively "mild" GC conditions to perform the analyses, which results in relatively rugged analyses.

Samples with final boiling points >500°C require more sophisticated injection techniques such as cool injection into temperature programmable vaporizers and more thermally stable WCOT columns that can withstand GC temperatures up to 430°C to 450°C. These simdis methods, such as D7169 for whole crudes and residua, can be referred to as high temperature (HT). For HT simdis, shorter WCOTs with thinner phase thicknesses are used to elute the higher boiling compounds. For D7169, for example, columns of 5 m by 0.53 mm inner diameter and film thickness of 0.09 to 0.15 μm are used. Figs. 6 through 9 show calibration and chromatograms of high boiling stream samples obtained with such a WCOT column. The amount not eluted is estimated by the external standard technique and the total amount eluted (% recovery) is calculated for each sample. Samples that are totally eluted before end of column temperature programming should yield recoveries of 100 % (±2 % − 3 %). In addition, the column must produce a reproducible baseline close to a maximum operating temperature of approximately 430°C to allow a precise subtraction of the background bleed signal from the sample signal. Generally, the initial boiling point (IBP) area's accuracy is compromised by the elution of large amounts of solvent (usually 99.9 % of sample injected is solvent). Some laboratories circumvent the problem with the IBP by performing a separate analysis of the crude oil that determines the C_5–C_9 content using a

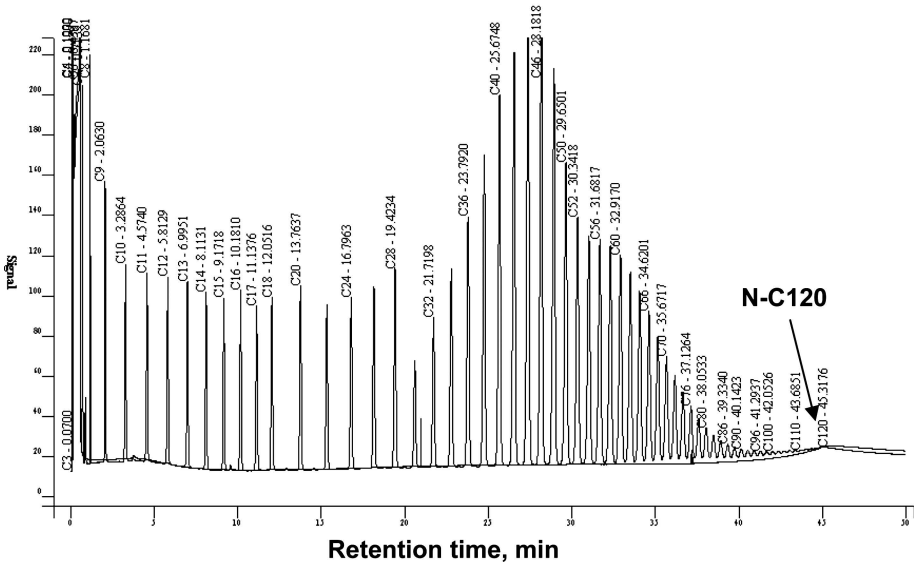

Fig. 6—Gas chromatogram of n-paraffin boiling point calibration mixture for a high-temperature simdis test method.

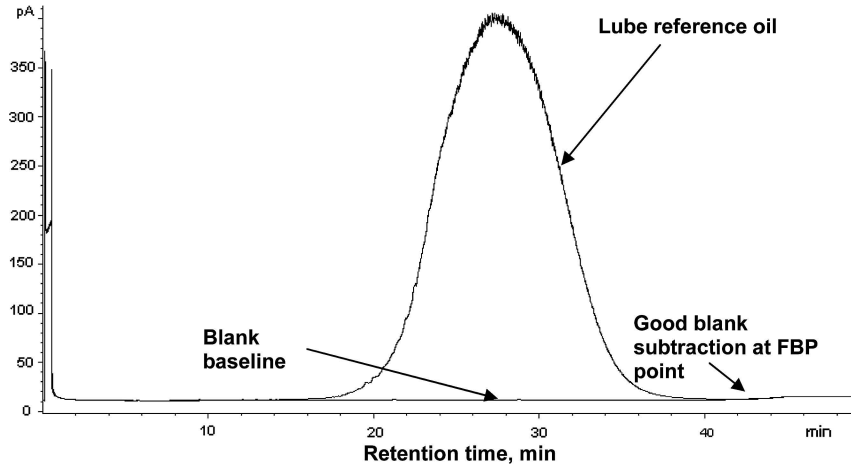

Fig. 7—Gas chromatogram of a lube base stock reference material for a high-temperature simdis test method.

prefractionator with a DHA analysis, which then is "merged" with the simdis analysis to correct the IBP region of simdis.

These HT simdis analyses require a "clean" chromatographic system from injection port inserts to the FID detection system for high precision and accuracy. Frequent replacement of consumables such as injection port inserts and WCOTs may be necessary, depending on the amount of residue left behind and not eluted. The residue amount left behind may increase baseline instability at higher oven temperatures and also creates adsorbent sites where part of subsequent samples is adsorbed, not recovered, leading to an overall analysis error.

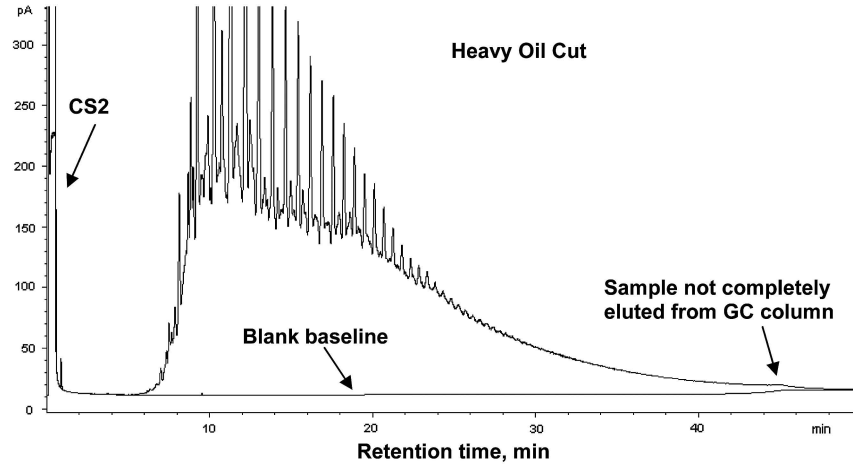

Fig. 8—Gas chromatogram of a crude oil cut obtained from a high-temperature simdis test method.

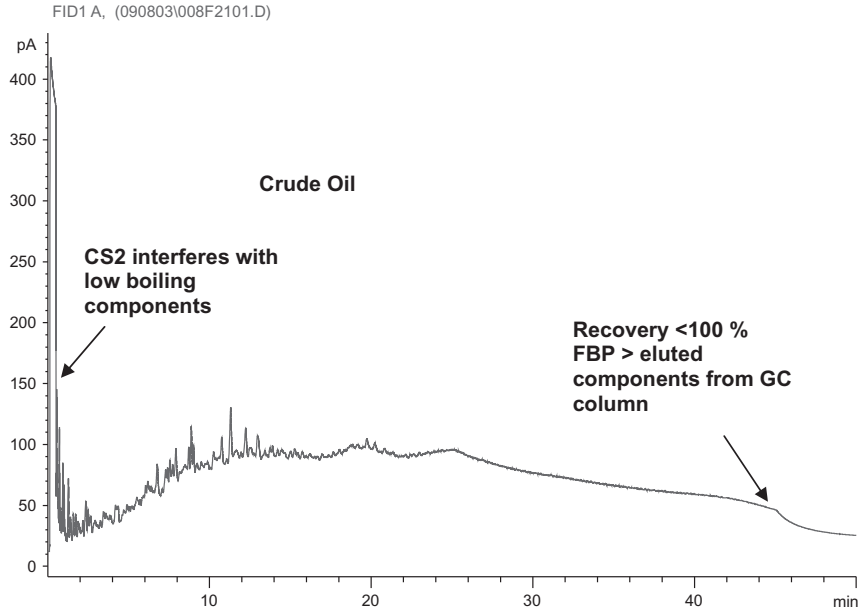

Fig. 9—Gas chromatogram of a full range crude oil obtained from a high-temperature simdis test method.

With ongoing developments in more stable WCOT and new column heating/cooling technologies, faster GC methods for simdis are being developed. Fig. 10 shows a simdis chromatogram using ultrafast (120 s/min) heating column technology, which results in an analysis cycle time (analysis plus cool down time) of <4 min. Some of these new technologies will most likely result in additional new ASTM methods in the future.

Current Developments in GC Analyses

Currently, GC continues to expand its breadth of applications in the characterization of complex hydrocarbon or nonhydrocarbon matrices or both by its hyphenation or coupling with other techniques. Two areas that are growing rapidly include GC-field ionization mass spectrometry (GC-FIMS) [11–12] and comprehensive two-dimensional gas chromatography (GC × GC) [13–21]. The coupling of GC to FIMS is interesting for the fact that a "soft" ionization approach is used to produce mostly molecular ions, which simplifies quantification of hydrocarbons because FI affords reduced molecular fragmentation and much higher molecular ion intensities compared with electron impact ionization, which has been used in several ASTM MS methods (D2425, D2789, D3239) in the past. This production of molecular ions renders assignment of peaks to compound types relatively straightforward, it allows one to perform quantitation based on the intensity of molecular ions only, and it obviates the need for complex matrix inversion routines as in current ASTM MS methods. FIMS (GC-FIMS) also in many cases creates the possibility of analyzing complex, multicomponent, hydrocarbon mixtures without prior LC separation. Although

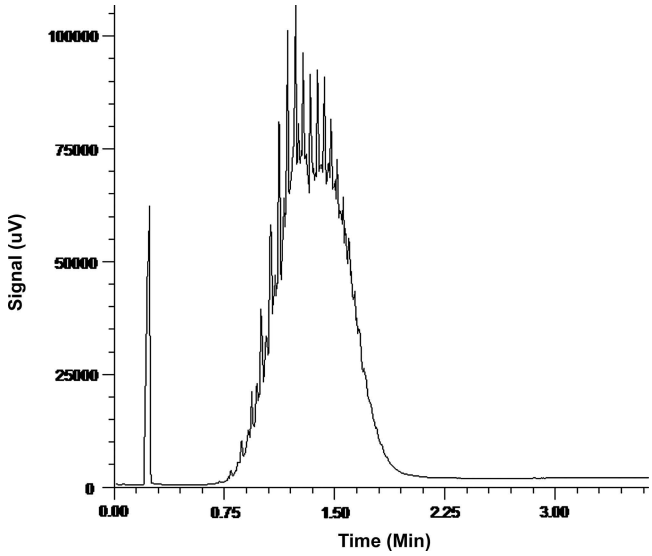

Fig. 10—Gas chromatogram of a crude oil cut using ultrafast (120°C/min) heating simdis procedure.

there are no current ASTM methods for hydrocarbon types based on GC-FIMS, this area is expected to continue to grow as instrument ruggedness and cost are improved.

Another area that has been growing rapidly is GC × GC. GC × GC is a multidimensional technique but, unlike the conventional classical two-dimensional "heart-cutting" GC approach, GC × GC subjects all of the analytes eluting from the first-dimension WCOT to a second-dimension WCOT separation using a fast temporal modulation. Similar to conventional GC-FID, GC × GC can be interfaced to selective detectors such as SCD [21], NCD, AED, and MS. An ASTM study group has been established to expand the use of the technique to petroanalyses.

SELECTIVE SPECTROSCOPIC/SPECTROMETRIC DETECTORS FOR PETROLEUM FRACTIONS

Selective detectors are extremely useful when targeting a given element or compound in a complex matrix that makes detection of a targeted compound difficult by other techniques. Selective spectroscopic detectors include SCDs and NCDs, FPDs for sulfur/phosphorous, AED, MS, ICP-MS for a multitude of elements (e.g., sulfur, nitrogen, oxygen, nickel, mercury, vanadium, and selenium), and FTIR. Some of these detectors are described here.

Sulfur Chemiluminescence Detector

The SCD combusts sulfur compounds using either a single- or a double-stage burner or furnace (Fig. 11) at high temperatures to form sulfur monoxide (SO). Subsequently, a chemiluminescence reaction of SO with ozone (O_3) yields

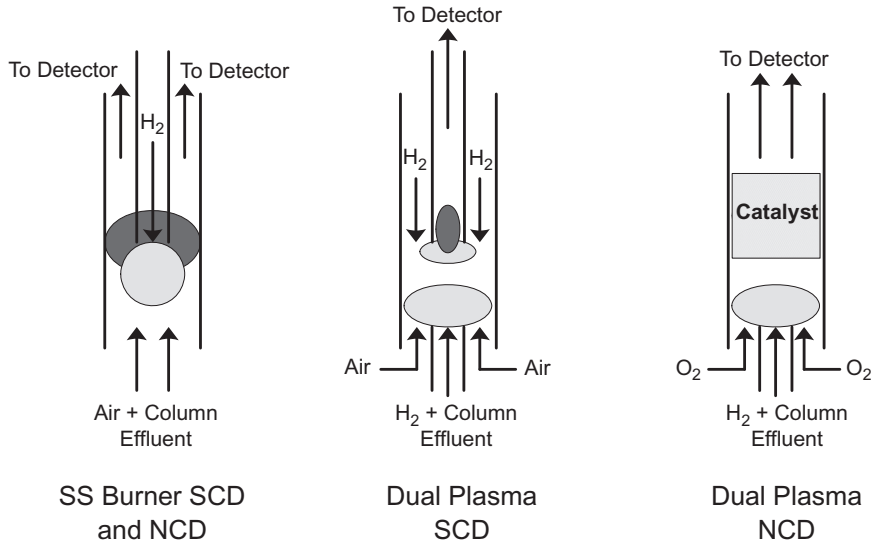

Fig. 11—SCD and NCD chemiluminescence single and double plasma burners.

an emission that is detected. The reaction mechanism is:

$$\text{S-compound} + O \rightarrow SO + \text{Other Products}$$

$$SO + O_3 \rightarrow SO_2 + O_2 + h\nu\ (300 - 400\ \text{nm})$$

The emitted light (hν) passes through an optical filter and is detected by a photomultiplier tube (PMT). The light emitted is directly proportional to the amount of sulfur in the sample. Fig. 12 gives a schematic of the GC-SCD system. The system consists of a GC for separation of the sulfur compounds, followed by furnace combustion and then detection. The effluent from the furnace enters a reaction chamber where the SO species is reacted with O_3 and detection by the PMT after passage though the optical filter, which isolates the wavelength of interest.

Some advantages of the SCD include:

1. Used with GC or SFC, for which other detectors are difficult to interface.
2. Very low detection limits, picogram level. In hydrocarbon streams, generally detection limits of approximately 50 ppb sulfur per compound can be attained under optimized conditions.
3. Little or no hydrocarbon quenching when compared to nonpulsed flame photometric detection systems.
4. Linear, equimolar response to sulfur compounds simplifies quantification of known and unknown solutes.
5. With a simple coupling adapter, can be used for simultaneous SCD and FID detection.

The SCD is used in several ASTM test methods (Table 8). The SCD has been used for the simulated distillation of sulfur species, and such methods are available on commercial instruments as turnkey package. In addition, the SCD has

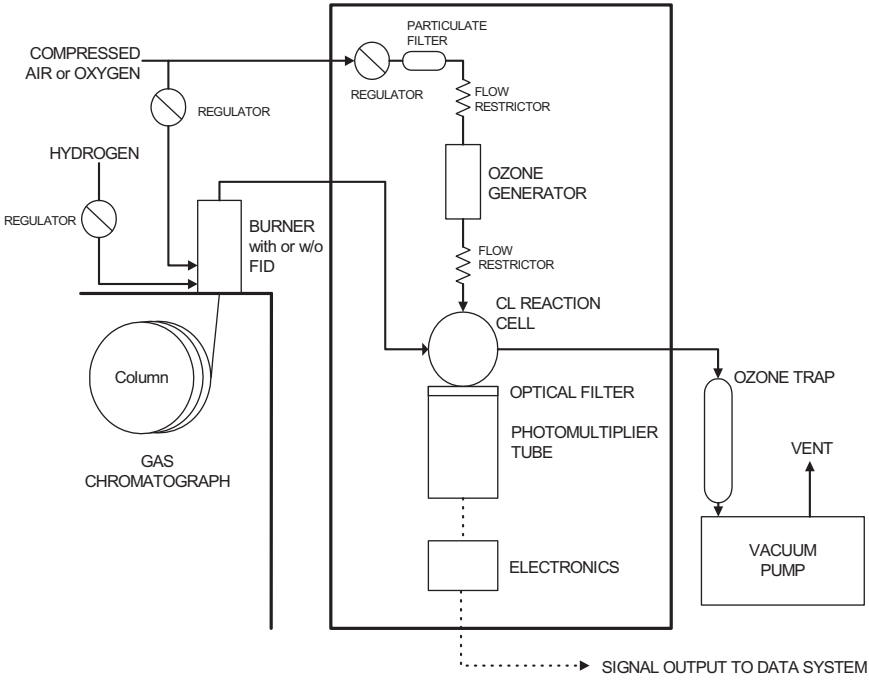

Fig. 12—Schematic of SCD and NCD chemiluminescence detectors for GC.

been used in comprehensive GC × GC [21] and conventional GC [22] for determination of sulfur compounds

Nitrogen Chemiluminescence Detector

The NCD is a nitrogen-specific detector that produces a linear and equimolar response to nitrogen compounds, similar to the SCD (Fig. 12). This is accomplished by using a single- or a two-stage burner (Fig. 11) to achieve high-temperature combustion of nitrogen-containing compounds to form nitric oxide (NO). Nitric oxide reacts with ozone to form electronically excited nitrogen dioxide. The excited nitrogen dioxide emits light in the red and infrared region of the spectrum (600–3200 nm). The light emitted is detected by a PMT and is

TABLE 8—ASTM GC Sulfur Speciation Methods	
D5504	Determination of Sulfur Compounds in Natural Gas and Gaseous Fuels by Gas Chromatography and Chemiluminescence
ASTM D5623	Sulfur Compounds in Light Petroleum Liquids by Gas Chromatography and Sulfur Selective Detection
ASTM D7011	Determination of Trace Thiophene in Refined Benzene by Gas Chromatography and Sulfur Selective Detection

directly proportional to the amount of nitrogen in the sample. Because of the specificity of the reaction, complex sample matrices can be analyzed with little or no interference.

$$\text{N-compound} + O \rightarrow NO + \text{Other Products}$$
$$NO + O_3 \rightarrow NO_2 + O_2 + h\nu\ (600 - 3200\ \text{nm})$$

In addition to detecting organic nitrogen compounds, the NCD responds to ammonia, hydrazine, hydrogen cyanide, and nitrous oxides (NOx).

The advantages of the NCD over other nitrogen detectors, such as the NPD, include equimolar response, higher selectivity over background hydrocarbons, lack of quenching due to matrix effects, and greater reliability.

The NCD, similar to the SCD, can be used as a single detector or coupled in series with an FID, allowing for a chromatographic signal to be acquired from both detectors simultaneously.

Currently there are no known ASTM methods in the petroleum area using the GC-NCD. However, the detector has been used extensively to determine many nitrogen compounds that are amenable to GC, such as carbazoles in diesels, additives used to enhance petroleum products, etc. Detection limits in the range of <1 ppm as nitrogen per compound have been attained readily in routine analysis.

Atomic Emission Detector

The advantage of the AED (Fig. 13) is its ability to simultaneously determine the atomic emissions of many of the elements (e.g., carbon, hydrogen, sulfur, nitrogen, oxygen, phosphorous, vanadium, nickel, mercury) in volatile and stable organic analytes that elute from a WCOT column. As the solutes elute, they are introduced into a helium microwave-powered plasma (or discharge) cavity where the solutes are decomposed and their comprising elemental atoms are excited by the energy of the plasma. The light emitted by the excited atoms is segregated into individual emission lines using a grating and detected by a photodiode array. The associated emissions signals for individual emission lines of interest are recorded and selective atomic chromatograms are

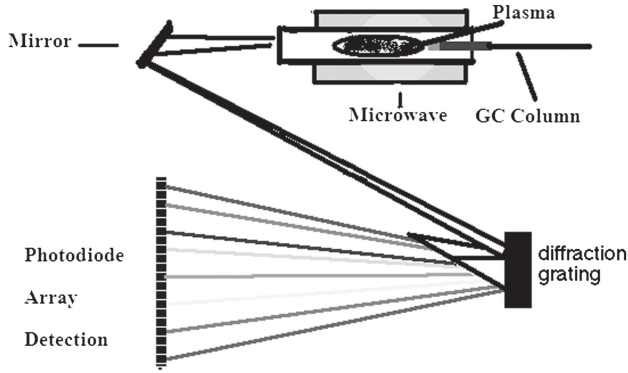

Fig. 13—Schematic of a helium microwave atomic emission detector (AED).

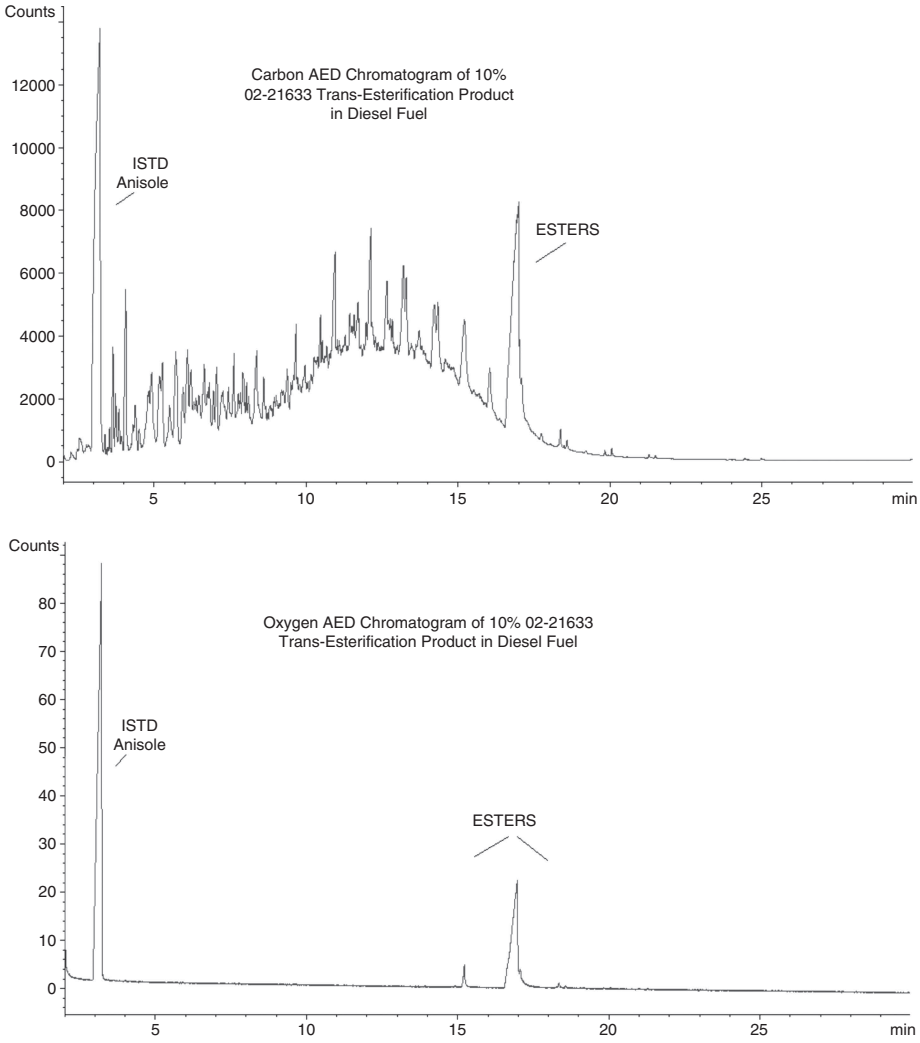

Fig. 14—(top) Gas chromatogram of carbon emission signal from AED for diesel sample spiked with biodiesel esters and (bottom) gas chromatogram of oxygen emission signal from AED for diesel sample (top) showing the selective detection of the esters.

produced for each element. Fig. 14 demonstrates the power of the AED in the selective detection of biodiesel components fatty acid methyl esters (FAME) blended into conventional diesel hydrocarbon matrix using the oxygen and carbon emission lines.

Flame Photometric Detector

The conventional FPD is a relatively rugged detector for determining sulfur and phosphorous species. Fig. 15 shows a schematic of the FPD. The signal from the emission of sulfur or phosphorous from combustion in the flame is

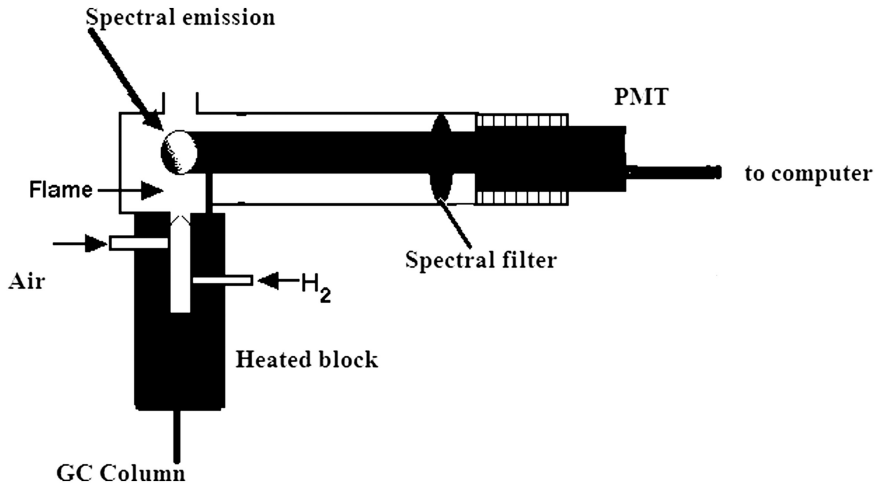

Fig. 15—Schematic of a conventional flame photometric detector (FPD).

segregated through an optical filter to increase selectivity. The emitted light is detected by a PMT. The FPD uses one of two available band pass filters to selectively detect compounds containing either sulfur or phosphorus. Compounds containing phosphorus are detectable with the 526-nm filter; sulfur-containing compounds are detected with a 394-nm filter. While not completely selective, the FPD is still approximately 100,000 times more sensitive to sulfurous and phosphorous compounds than it is to hydrocarbons. Compounds like H_2S or SO_2 can be detected to limits as low as approximately 200 ppb, and phosphorus compound detection limits reach a low of approximately 10 ppb.

Some advantages of the FPD include:

1. Relatively more rugged and simple to operate than current SCD.
2. Can be used for sulfur as well as for phosphorous containing organocompounds.

Some key disadvantages of the conventional FPD include:

1. Single FID type of FPD can result in some quenching of the sulfur signal when high amounts of hydrocarbons are coeluting with the sulfur compound being analyzed. In some simpler sample matrices cases, this can be avoided by selecting a proper GC stationary phase or chromatographic operating conditions that will resolve the sulfur compound of interest from very high concentrations of coeluting hydrocarbons. Some commercial FPDs were designed with a double FID combination (two flames stacked on top of each other), which minimized the quenching effect and also resulted in a more uniform response among many sulfur species found in petroleum streams. Double FID systems currently are less available commercially.
2. The response is nonlinear and proportional to the square of the sulfur concentration. Some electronics include a function to obtain the square root of the signal to linearize the response.

Recently, the FPD's applicability and popularity has expanded because a variation known as the pulsed-FPD (pFPD) [23] has been introduced commercially. The pFPD has several distinct advantages over the static FPD, for example:

1. Increased sensitivity (10–100 ×, depending on FPD)
2. Increased selectivity (10 × or more, depending on FPD)
3. Equimolar response for sulfur and phosphorus; response can be linearized
4. Detection of up to 28 different elements for unique applications.

ICP-MS Detection System

ICP-MS instrumentation (Fig. 16) provides lower detection limits than most other detection systems and allows multielement detection in a single analysis. In addition, the ICP-MS detection system for chromatography, unlike the AED, is unique because it can be interfaced to several types of chromatography (GC, LC, IC, CE) using a properly designed interface, thus allowing the multielement analysis of volatile, nonvolatile, and ionic solutes in various matrices. In addition, ICP-MS offers isotopic information of the elements of interest, which also allows the use of isotope dilution for quantification.

When used as a GC detector, ICP/MS argon plasma is more stable than the helium microwave-induced plasma in GC-AED, and solvent venting in GC-ICP-MS is not necessary. The GC-ICP-MS interface is a heated transfer line interfaced to the ICP-MS. The GC column extends through the flexible transfer line and terminates within the ICP torch injector tube, just upstream of the plasma, so that separated species are carried directly into the plasma by a heated gas flow. For LC or IC-ICP-MS, the interface uses a nebulizer in a spray chamber.

Some applications of ICP-MS detection include:

- Total sulfur and sulfur species in hydrocarbon fuels using GC/ICP/MS
- Mercury speciation.

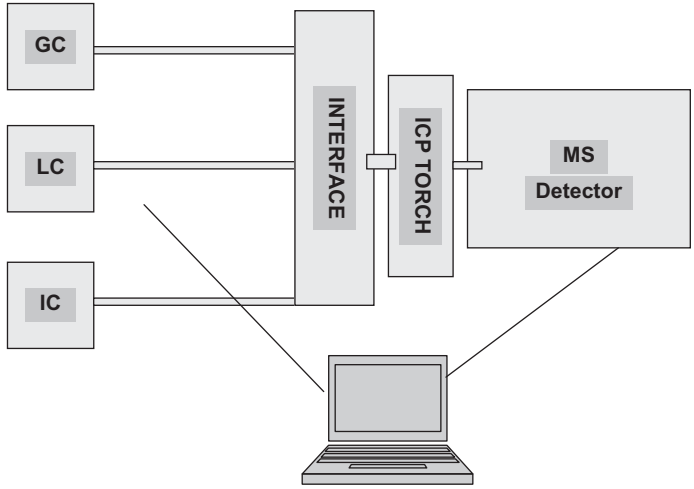

Fig. 16—Schematic of a multichromatography ICP-MS detection configuration system.

LC AND SFC APPLICATIONS

Several ASTM chromatographic methods (Tables 9–10) have been developed for the analysis of petroleum products using high performance liquid chromatography (HPLC) and SFC. In addition, many laboratories have developed a large number of LC methods to target specific products. This section gives a brief overview of the more common test methods used.

TABLE 9—Partial List of ASTM Liquid Chromatography Methods for Petroleum

Test Method	Title	Size or Scale
D1319	Standard Test Method for Hydrocarbon Types in Liquid Petroleum Products by Fluorescent Indicator Adsorption	Analytical; manual; visual read-out; slow
D2002	Test Method for Isolation of Representative Saturates Fraction from Low-Olefinic Petroleum Naphthas	Preparative
D2003	Test Method for Isolation of Representative Saturates Fraction from High-Olefinic Petroleum Naphthas	Preparative
D2007	Standard Test Method for Characteristic Groups in Rubber Extender and Processing Oils and Other Petroleum-Derived Oils by the Clay-Gel Absorption Chromatographic Method	Preparative
D2549	Standard Test Method for Separation of Representative Aromatics and Nonaromatics Fractions of High-Boiling Oils by Elution Chromatography	Preparative
D3712	Standard Test Method of Analysis of Oil-Soluble Petroleum Sulfonates by Liquid Chromatography	Analytical
D6379	Standard Test Method for Determination of Aromatic Hydrocarbon Types in Aviation Fuels and Petroleum Distillates - High Performance Liquid Chromatography Method with Refractive Index Detection	Analytical
D6591	Standard Test Method for Determination of Aromatic Hydrocarbon Types in Middle Distillates - High Performance Liquid Chromatography Method with Refractive Index Detection	Analytical
D7419	Determination of Total Aromatics and Total Saturates in Lube Basestocks by High Performance Liquid Chromatography (HPLC) with Refractive Index Detection	Semi-preparative in column usage but analytical scale in quantification

TABLE 10—ASTM Test Methods Based on SFC		
D7347	Standard Test Method for Determination of Olefin Content in Denatured Ethanol by Supercritical Fluid Chromatography	SFC; Analytical
D5186	Standard Test Method for Determination of Aromatic Content and Polynuclear Aromatic Content of Diesel Fuels and Aviation Turbine Fuels by Supercritical Fluid Chromatography	SFC; Analytical
D6550	Standard Test Method for Determination of Olefin Content of Gasolines by Supercritical-Fluid Chromatography	SFC; Analytical

High Performance Liquid Chromatography

LC (Fig. 3) is used very extensively in the petroleum industry for the separation of hydrocarbon types (by NP-LC), additives and contaminants in feedstocks and products (by NP-LC or R-LC), characterization of polymeric materials (by GPC), and analysis of ionic solutes (by IC).

NP-LC is used extensively for hydrocarbon type analyses such as separating petroleum feeds and products into saturates, aromatics (or ring distributions), and polar components. Generally, analytical-scale separations using on-the-fly detectors for quantification and preparative large-scale separations are employed.

In preparative separations, the isolated fractions are weighed gravimetrically and percent saturates, aromatics, and polars are reported. Isolated fractions may be submitted for additional analyses such as MS and NMR. The preparative-scale methods can be automated with autosamplers, the mobile phases can be regulated precisely by pumping systems, and detectors can be used to establish and monitor cut points for the fractions separated. The petroleum fractions isolated have an initial boiling point of approximately 250°C, mainly because the lighter boiling compounds are lost during the solvent removal step. Preparative methods generally tend to be slow and time consuming.

The most popular NP-LC substrates for separations include silica gel, alumina, Florisil, and clay (D2007) for separating hydrocarbons into saturates, aromatics, and polars. The use of silver loaded columns [24] allows excellent separation for difficult-to-separate hydrocarbon fractions such as basestocks, and particularly very high boiling lube basestocks known as "bright stocks."

D7419 is an example of an automated analytical-scale test method developed for the analyses of total aromatics in basestocks from 0.2 to approximately 40 mass %. This test method is more effective in the analyses of total aromatics <10 mass % as may be required in basestock specifications. The test method uses semipreparative-sized separation columns for increased loadability; however, quantification is performed exclusively by the calibration of the RID used as shown in Fig. 17. The spectroscopic UV/VIS detector is optional but useful in setting an optimum and critical backflush time for the aromatics. After the elution of the total saturates from the silica gel column(s), the total aromatics are backflushed as a single component peak. A cyano precolumn is used to protect the silica column from any polar compounds in the sample;

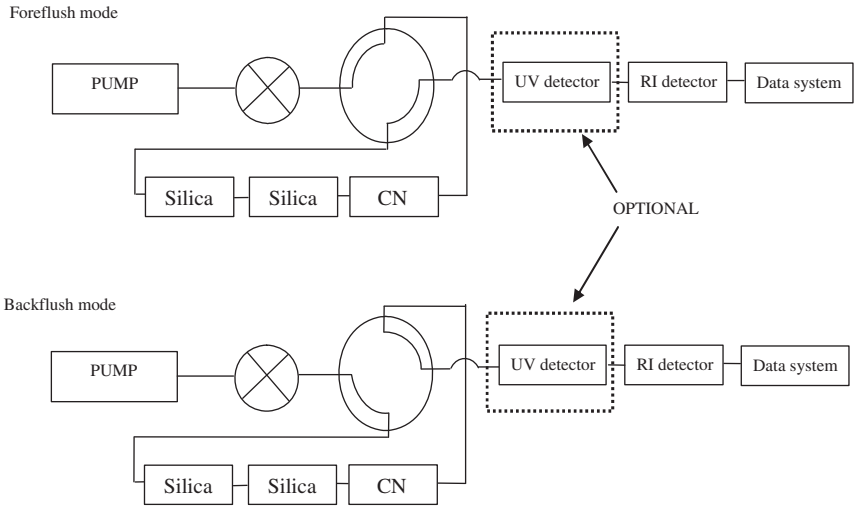

Fig. 17—Schematic of LC system for determination of total aromatics in basestocks (ASTM method D7419).

it also facilitates the backflush of the polars to be included in the total aromatics peak. Fig. 18 shows a chromatogram of the two components used to calibrate the method when analyzed in the "no backflush" mode to initially determine the required column resolution. Fig. 19 shows the calibration of the RID detector using two pure compounds to represent saturates and aromatics. This approach where applicable is much simpler and more precise than a manual procedure like D2007.

Analytical-scale quantitative instrumental HPLC methods have been used also for the analyses of total saturates, monoaromatics, diaromatics, and triaromatics in jet and diesel fuels. A RID is used for quantification. Using such an

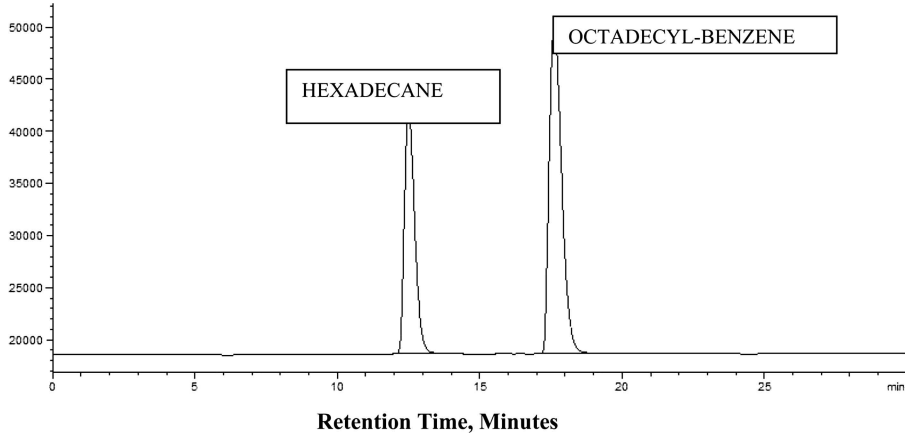

Fig. 18—Liquid chromatogram of calibration standard for ASTM D7419 showing the two components to verify column resolution (no backflush of the aromatic component).

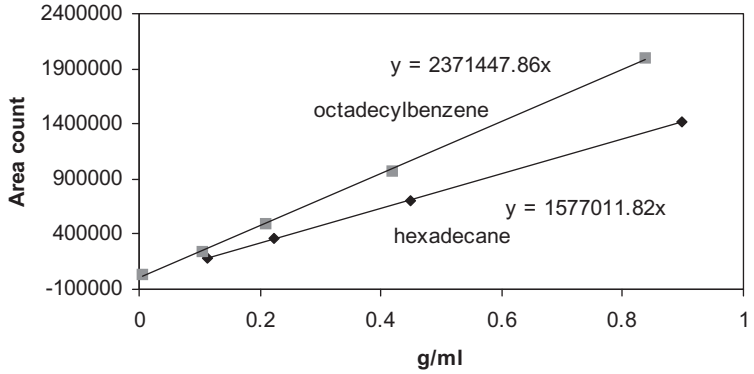

Fig. 19—Calibration curve for ASTM D7419.

approach, ASTM D6379 determines monoaromatic and diaromatic hydrocarbon contents in lighter streams, such as aviation kerosines and petroleum distillates boiling in the range from 50°C to 300°C. Similarly, ASTM D6591 is used for the determination of monoaromatic, diaromatic, and polyaromatic hydrocarbon contents in diesel fuels and petroleum distillates boiling in the range from 150°C to 400°C. A further extension of these methods is the European EN 12916, originally developed to account for the elution and quantification of biodiesel FAME and aromatic ring components in diesel fuels.

Non-ASTM test procedures for heavy oils (e.g., basestocks, residues) using the ELSD also have been used [25] and proven rugged. Because of the nature of the ELSD, which requires the removal of the solvent by a high flow of an inert gas such as nitrogen, most of the light petroleum compounds with an initial boiling point below 300°C are not detected.

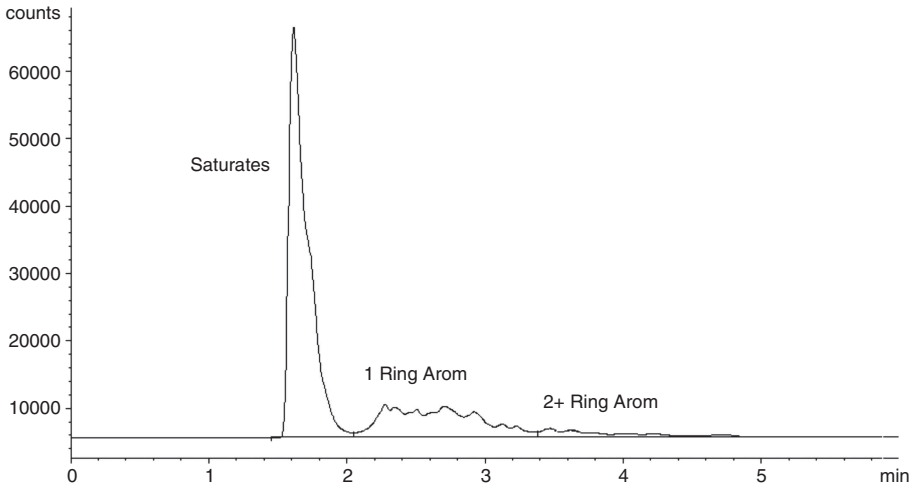

Fig. 20—SFC chromatogram of a diesel fuel.

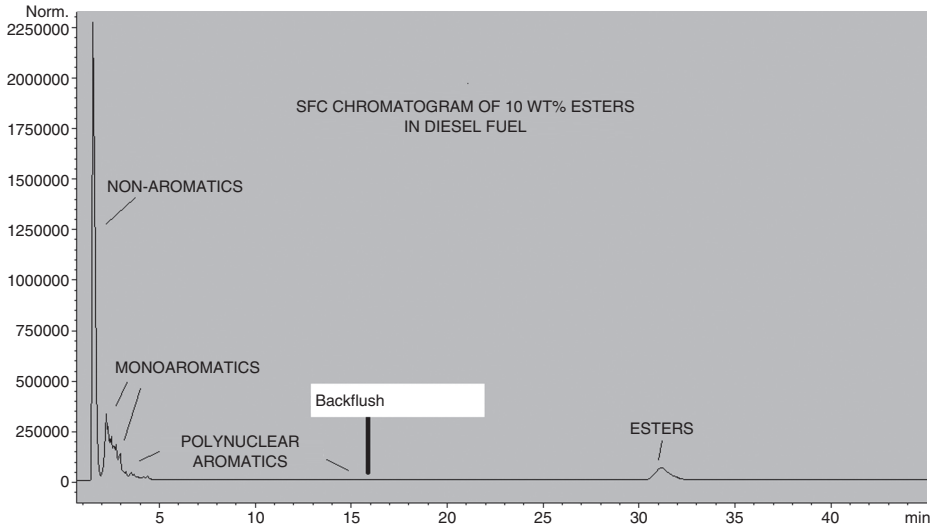

Fig. 21—SFC chromatogram of modified D5186 to include backflush elution of biodiesel esters.

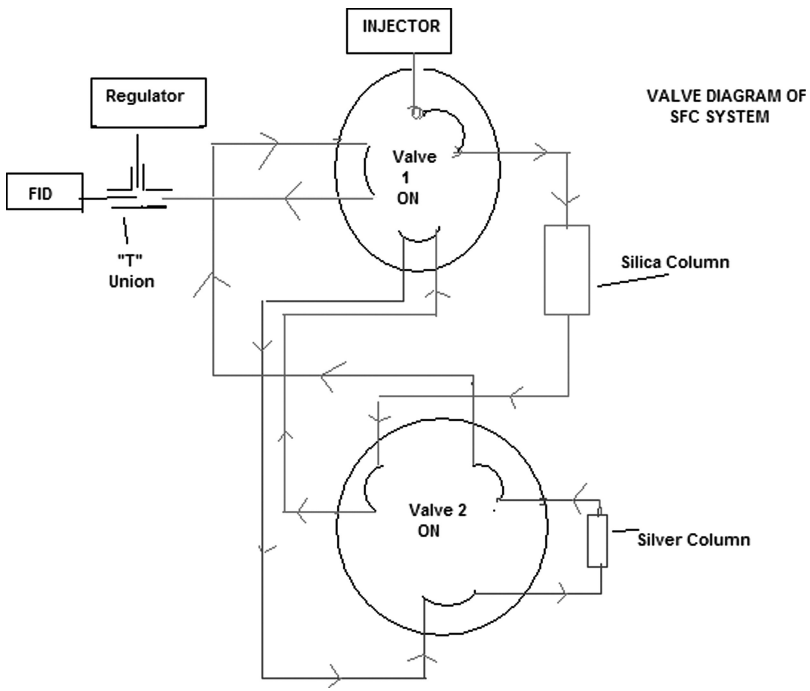

Fig. 22—Schematic of SFC valve configuration for D6550 for analysis of olefins in gasolines.

Supercritical Fluid Chromatography

SFC is used in the analyses of hydrocarbons [26–28], including interface to MS [28]. The main advantage of SFC with supercritical carbon dioxide as the mobile phase is that an FID can be used for quantification. With proper optimization, the response factor for most hydrocarbons is approximately unity, thus simplifying quantitative analysis. ASTM test method D5186 for diesel (Fig. 20) and D6550 for gasolines (Table 10) provide total saturates (paraffins and naphthenes) and total aromatics in jet and diesel fuels and olefins in gasolines.

D5186 configuration can be modified to incorporate a backflush valve for the analysis of biodiesel FAMEs [29]. Fig. 21 shows such an analysis. Note that the FAME components eluted as a single peak after backflushing the silica gel column after the elution of the higher ring aromatic hydrocarbons.

D6550 (Fig. 22) shows the configuration of D6550 using silica- and silver-impregnated columns to isolate the olefins in gasoline. The olefins are then backflushed to the FID for quantification

References

[1] Grob, R. L. and Barry, E. F., *Modern Practice of Gas Chromatography,* 4th ed., John Wiley and Sons, Hoboken, NJ, 2004.

[2] Snyder, L. R. and Kirkland, J. J., *Modern Practice of Liquid Chromatography*, 2nd ed., John Wiley and Sons, Hoboken, NJ, 1979.

[3] Meyer, V. R., *Practical High-Performance Liquid Chromatography*, 4th ed., Wiley-VCH Verlag, Weinheim, Germany, 2004.

[4] Smith, R. M., Hawthorne, S. B. and Lefler, J., *Supercritical Fluids in Chromatography and Extraction Principles and Applications of Supercritical Fluid Chromatography*, Elsevier Science, 1997.

[5] Fritz, J. and Gjerde, D., *Ion Chromatography*, 4th ed., Wiley-VCH Verlag, Weinheim, Germany, 2009.

[6] Di Sanzo, F. P. and Giarrocco, V. J. "Analysis of Pressurized Gasoline Range Liquid Hydrocarbon Samples by Capillary Column and PIONA Analyzer Gas Chromatography," *J. Chromatogr. Sci*., Vol. 28, 1988, pp. 258–266.

[7] Di Sanzo, F. P., Lane, J. L. and Yoder, R. E., "Application of State-of-the-art Multidimensional High Resolution Gas Chromatography for Individual Component Analysis of Gasoline Range Hydrocarbons," *J. Chromatogr. Sci*., Vol. 26, 1988, pp. 206–209.

[8] Di Sanzo, F. P., "Chromatographic Analyses of Fuels," *Analytical Advances for Hydrocarbon Research*, S. Hsu, Ed., Chapter 6, Kluwer Academic/Plenum Publishers, New York, 2003.

[9] Diehl, J. W. and Di Sanzo, F. P., "Determination of Aromatic Hydrocarbons in Gasolines by Flow Modulated Comprehensive Two-Dimensional Gas Chromatography," *J. Chromatogr. A*, Vol. 1080, 2005, pp. 157–165.

[10] Beens, J., Feuerheim, H. T., Frohling, J., Watt, J. and Schaatsbergen, G., "A Comparison of Ten Different Methods for the Analysis of Saturates, Olefins, Benzene, Total Aromatics, and Oxygenates in Finished Gasoline," *J. Chromatogr. Sci*., Vol. 14, 2003, pp. 564–569.

[11] Ha, H. Z., Ring, Z., and Liu, S. "Data Reconciliation Among PIONA, GC-FIMS, and Simdis Measurements for Petroleum Fractions," *Petro. Sci. Technol.,* Vol. 26, 2008, pp. 7–28.

[12] Briker, Y., Ring, Z., Iacchelli, A., McLean, N., Rahimi, P. M., Fairbridge, C., Malhotra, R., Coggiola, M. A. and Young, S. E., "Diesel Fuel Analysis by GC–FIMS: Aromatics, *n*-Paraffins, and Isoparaffins," *Energy Fuels*, Vol. 15, 2001, pp. 23–37.

[13] Blomberg, J., Schoenmakers, P. J., Beens, J. and Tijissen, R., "Comprehensive Two-Dimensional Chromatography (GC × GC) and Its Applicability to the Characterization of Complex Mixtures," *J. High Resol. Chrom*., Vol. 20, 1997, pp. 539–544.

[14] Philips, J. B. and Ledford, E. B., "Thermal Modulation: A Chemical Instrumentation Potential Value in Improving Portability," *Field Anal. Chem. Tech.*, Vol. 1, 1996, pp. 23–29.

[15] Blumberg, L. M., "Comprehensive Two-Dimensional Gas Chromatography: Metrics, Potentials, Limits," *J. Chromatogr. A*, Vol. 985(3), 2003, pp. 29–38.

[16] Hua, R. X., Ruan, C. H., Wang, J. H., Lu, X., Liu, J., Xiao, K., Hong, H. W. and Xu, G. W., "Research of Group Separation of Petroleum Fractions by Comprehensive Two-Dimensional Gas Chromatography," *Acta Chim. Sin.*, Vol. 60(12), 2002, pp. 2185–2191.

[17] Reinchenbach, S. E., Ni, M., Zhang, D. and Ledford, Jr., E. B., "Image Background Removal in Comprehensive Two-Dimensional Gas Chromatography," *J. Chromatogr. A*, Vol. 985, 2003, pp. 47–56.

[18] Shao, Y., Marriott, P., Shellie, R. and Hugel, H., "Solid-Phase Micro-extraction–Comprehensive Two-Dimensional Gas Chromatography of Ginger (*Zingiber officinale*) Volatiles," *Flav. Fragr. J.*, Vol. 18(1), 2003, pp. 2185–2191.

[19] Adahchour, M., Beens, J. and Brinkman, U. A. T., "Single-Jet, Single-Stage Cryogenic Modulator for Comprehensive Two-Dimensional Gas Chromatography (GC × GC)," *Analyst*, Vol. 128(3), 2003, pp. 213–216.

[20] Frysinger, G. S., Gaines, R. B., Xu, L. and Reddy, C. M., "Resolving the Unresolved Complex Mixture in Petroleum-Contaminated Sediments," *Environ. Sci. Technol.*, Vol. 37(8), 2003, pp. 1653–1662.

[21] Wang, F. C., Robbins, W. K., Di Sanzo, F. P. and McElroy, F. C., "Speciation of Sulfur-Containing Compounds in Diesel by Comprehensive Two-Dimensional Gas Chromatography," *J. Chromatogr. Sci.*, Vol. 41, 2003, pp. 519–523.

[22] Chawla, B. and Di Sanzo, F. P., "Determination of Sulfur Compounds in Light Petroleum Streams by High Resolution Gas Chromatography with Chemiluminescence Detection," *J. Chromatogr.*, Vol. 589(1-2), 1992, pp. 271–279.

[23] Chambers, L. and Duffy, M., "Determination of Total and Speciated Sulfur Content in Petroleum Samples Using a Pulsed Flame Photometric Detector," *J. Chromatogr. Sci*., Vol. 14, 2003, pp. 528–584.

[24] Di Sanzo, F. P., Herron, F. P., Chawla, B. and Holloway, D., "Determination of Total Aromatic Hydrocarbons in Lube Base Stocks by Liquid Chromatography with Novel Thermospray Flame Ionization Detection," *Anal. Chem.*, Vol. 65, 1993, pp. 3359–3362.

[25] Robbins, W. K., "Quantitative Measurement of Mass and Aromaticity Distributions for Heavy Distillates 1. Capabilities of the HPLC-2 System," *J. Chromatogr. Sci*., Vol. 36, 1998, pp. 457–466.

[26] Di Sanzo, F. P. and Yoder, R. E., "Determination of Aromatics in Jet and Diesel Fuels by Supercritical Fluid Chromatography with Flame Ionization Detection (SFC-FID): A Quantitative Study," *J. Chromatogr. Sci*., Vol. 29, 1991, pp. 4–7.

[27] Skaar, H., Norli, H. R., Lundanes, E. and Greibrokk, T., "Group Separation of Crude Oil by Supercritical Fluid Chromatography Using Packed Narrow Bore Columns, Column Switching and Backflushing," *J. Microcolumn Separations*, Vol. 2(5), 1990, pp. 222–228.

[28] Qian, K., Diehl, J. W., Dechert, G. J. and Di Sanzo, F. P., "The Coupling of Supercritical Fluid Chromatography and Field Ionization Time-of-Flight High-Resolution Mass Spectrometry of Petroleum Middle Distillates," *Eur. J. Mass Spectrom.*, Vol. 10, 2004, pp. 187–196.

[29] Diehl, J. W. and Di Sanzo, F. P., "Determination of Total Biodiesel Fatty Acid Methyl, Ethyl Esters and Hydrocarbon Types in Diesel Fuels by Supercritical Fluid Chromatography/Flame Ionization Detection," *J. Chromatogr. Sci*., Vol. 45(10), 2007, pp. 690–693.

Part 3: Analytical Applications

20

Spectroscopic Methods for the Determination of Sulfur in Petroleum Products

R. A. Kishore Nadkarni[1]

INTRODUCTION

Sulfur either in elemental form or as its organic and inorganic compounds is present in most petroleum products and lubricants in varying concentrations, from high levels in some crude oils and lubricant additives to trace amounts in certain processed petroleum products. Sulfur originates in crude oil from natural sources from its marine animal and vegetative origins deposited with sediment in coastal waters in prehistoric times. Over the millennia, sulfur, oxygen, nitrogen, and other volatile compounds evolved out of this primordial mixture due to the bacterial actions and thermal and environmental pressure leaving behind a mixture of hydrocarbons containing some of these elements, metals, and other compounds. In additives and lubricating oils, sulfur compounds are added as metal compounds acting as performance improvers [1].

A part of the crude assay of oil includes assay for sulfur. The presence of sulfur compounds in refined petroleum products is undesirable because they impart odor and can react with and corrode end-product containers. Acidic sulfur compounds may also corrode the metallic parts of internal combustion engines. The severity of such corrosion is dependent on the types of sulfur compounds present in the fuel used. Additionally, sulfur oxides formed during gasoline combustion can hinder the performance of catalytic converters in automobiles. In aviation gasoline, sulfur compounds have a deleterious effect on the antiknock efficiency of the alkyl lead compounds. Sulfur in diesel fuels causes wear due to the corrosive nature of the combustion products and increases the amount of deposits in the combustion chamber and on pistons. High boiling range fractions and residual fuels usually contain higher amounts of sulfur, which creates corrosion and pollution problems. The conversion of sulfur to sulfur trioxide during combustion and later reaction with water forms sulfuric acid, corroding the metal surfaces of equipment. In many petroleum processes, even low levels of sulfur in feedstocks may poison expensive catalysts [2].

Additionally, emission of sulfur oxides formed during combustion of fuel oils in commercial or domestic applications is one of the main causes of "acid rain," which affects vegetation and quality of life in general. Hence, industrial sulfur emissions are controlled by regulatory agencies in most countries of the world. In most of the industrially developed countries, sulfur levels in fuels have been steadily decreasing over the last decade toward essentially zero sulfur by 2010. Emissions from fuels used for automobiles, aviation, off-road

[1] *Millennium Analytics, Inc., East Brunswick, NJ*

TABLE 1—Typical Sulfur Content of Crude Oils from Some Giant Oil Fields [1]

Country	Sulfur, m%	Country	Sulfur, m%
Abu Dhabi	0.62–0.77	Nigeria	0.10–0.26
Algeria	0.02–0.31	Saudi Arabia	1.25–3.91
Canada	0.20–3.67	United States	
Colombia	0.25–1.11	Alaska (N. Slope)	1.07
Egypt	0.84–2.06	California	0.2–1.2
Indonesia	0.07–0.18	Louisiana	0.1–0.8
Iran	0.76–3.68	Oklahoma	0.2–1.8
Iraq	1.36–2.10	Texas	0.1–2.4
Kuwait	1.82–2.58	Wyoming	0.1–.44
Libya	0.13–1.04		

vehicles, marine vessels, power generation plants, and home heating products have been steadily reduced [3,4].

Sulfur is removed from the refinery streams by a hydrosulfurization process with high pressure and catalysts. This process also affects other diesel characteristics such as density, aromatics, cetane number, and cloud point. Some refractory sulfur compounds such as 4,6-dimethyl dibenzothiophene are not easily removed.

On the other hand, several metal sulfonates are intentionally added to fuel additives and lubricating oils to enhance their performance. These usually include sulfonates of barium, calcium, copper, magnesium, zinc, and molybdenum sulfide.

TEST METHODS FOR SULFUR DETERMINATION

Given this importance of sulfur in the petrochemical field, it can be readily imagined that a plethora of analytical methods are available for the determination of this element. Over the years, the focus has shifted from sulfur determination at percent levels to trace levels. The first analytical method issued by ASTM for sulfur in petroleum products was D129 in 1922. This was the fifteenth standard ever issued by ASTM Committee D02. More than 20 standards for sulfur determination have since been issued by ASTM, and several more are in development [5,6].

Some of these methods are used for higher levels of sulfur; more recent ones are used for much lower amounts of sulfur in fuels. The five most widely used methods in the industry for fuel analysis are D2622 (WD-XRF), D4294 (ED-XRF), D4927 (WD-XRF), D5453 (UV-Fl), and D7039 (MWD-XRF). Out of these, three XRF methods are described in detail in Chapters 11, 12, and 13 of this book, respectively. Highlights of each of these methods and their comparative capability and experience in Interlaboratory Studies (ILS) are

TABLE 2—Typical Sulfur Content of Diesel Fuels [2]

Diesel Fuel	Sulfur m%
Diesel fuel oil grade 1 D	0.50
2 D	0.50
4 D	2.0
Kerosine	0.12
Premium diesel	0.0015
Railroad diesel	0.05
Marine distillate diesel	0.05

discussed here. The precision of these methods is given in Table 8 later in this chapter. Although ICP-AES methods D4951 and D5185 are capable of determining sulfur, they are used more often for metal analysis rather than for sulfur. D4927 is also a WD-XRF method used for sulfur determination along with other additive elements in lubricants and lube additives.

Many of these ASTM methods have been reproduced in part or whole by other international standards writing bodies. Technically these methods should be equivalent although there may be small differences in verbiage and style. The alternative methods for sulfur determination are summarized in Table 5 [7].

D2622 – WD-XRF

The method uses a wavelength dispersive X-ray fluorescence spectrometer equipped for X-ray detection in the wavelength range from about 0.52 nm to about 0.55 nm. Usually, X-ray tubes with anodes made up of rhodium, chromium, or scandium are used, although other anodes can be used. Calibration standards made from mass dilution of certified di-n-butyl sulfide with sulfur-free white oil or other suitable base material are used. Alternative calibration

TABLE 3—Sulfur Levels in Lubricants [2]

Lubricant Product	Sulfur, m%
Automatic transmission fluids	0.1–0.3
Gear oils	1.5–2.0
Lubricating oils	0.3–0.7
Automotive lubricant additives	0.5–3.5

TABLE 4—ASTM Methods for Sulfur Determination in Petroleum Products

Wet Chemistry	Spectroscopic	Other
D129 Bomb Combustion	D2622 WD-XRF	D3120 Coulometric
D1266 Lamp Combustion	D4294 ED-XRF	D3246 Coulometric
D1552 Leco Combustion	D4927 WD-XRF	D4045 Hydrogeneolysis
D2784 Oxyhydro Combustion	D4951 ICP-AES	D5453 UV-Fluorescence
	D5185 ICP-AES	D6920 Electrochemical
	D6334 WD-XRF	
	D6443 WD-XRF	D6667 UV-Fluorescence
	D6445 ED-XRF	
	D7039 MWD-XRF	D7041 GC-FPD On-line
	D7212 ED-XRF	
	D7220 ED-XRF	

standards can also be made from mixing of certified reference materials or by mass serial dilution of polysulfide oils with sulfur-free white oil.

This method is applicable to liquid petroleum products such as diesel fuel, jet fuel, kerosine, other distillate oils, naphtha, residual oil, lubricating base oil, hydraulic oil, crude oil, unleaded gasoline, gasohol, and biodiesel. The range of this test method is between the PLOQ (Pooled Limit of Quantitation as defined in the ASTM standard practice D6259) of 3 mg/kg total sulfur and at least up to 4.6 m % total sulfur. Samples containing more than 4.6 m % sulfur can be diluted to bring the sulfur concentration of the diluted material within the scope of this method. The samples that are diluted can have higher errors than indicated by the precision of undiluted samples. Volatile samples (such as high vapor pressure gasolines or light hydrocarbons) may also not meet the precision stated in the method because of the selective loss of light materials during the analysis. A fundamental assumption of this test method is that the calibration standard and the sample matrices are well matched, or that the matrix differences are accounted for. Matrix mismatches can be caused by carbon/hydrogen ratio differences between samples and standards, or by the presence of other interfering heteroatoms or species. The values of the limits of quantitation and method precision for a specific laboratory's instrument depend on the instrument source power (low or high power), sample type, and the practice established by the laboratory to perform the method.

In this method, a sample is placed in the X-ray beam of the XRF instrument, and the peak intensity of the sulfur K alpha line at 0.5373 nm is measured. The background intensity measured at a recommended wavelength of 0.5190 nm (0.5437 nm for a rhodium target tube) is subtracted from the peak intensity. The resultant net counting rate is then compared to a previously prepared calibration curve or equation to obtain the concentration of sulfur.

TABLE 5—International Standards for the Determination of Sulfur[a]

Analysis	ASTM	IP	DIN	AFNOR	JIS	ISO
Bomb Method	D129	61	51–577	T60–109		
Lamp Method	D1266	107		M07–031		
HT Method	D1552			M07–025		
WD-XRF	D2622		51–400T6		K 2541	14596
Oxidative Microcoulometry	D3120			M07–022	K 2276	16591
Oxidative Microcoulometry	D3246	373		M07–052		
ED-XRF	D4294	336		M07–053		8754
WD-XRF	D4927	407	51–391T2			
UV–Fluorescence	D5453			M07–059		

[a]Excerpted from Ref [7]. IP: Institute of Petroleum, U.K.; DIN: Deutsche Institut fur Normung (Germany); AFNOR: Association Francaise de Normalisation (France); JIS: Japan Industrial Standards; ISO: International Organization for Standardization.

Although the equipment for this method tends to be more expensive than that required for alternative test methods, such as the ASTM D4294 ED-XRF method, this method provides a rapid and precise measurement of total sulfur in a variety of petroleum products with a minimum of sample preparation. A typical analysis time is 1 to 2 minutes per sample.

Interferences—When the element composition (excluding sulfur) of samples differs significantly from the standards, errors in the sulfur determination can result. Differences in the carbon/hydrogen ratio of samples and calibration standards introduce errors in the determination. Some other interferences and their concentration in m % tolerated include the following:

Phosphorus	0.3	Zinc	0.6	Barium	0.8	Lead	0.9
Calcium	1	Chlorine	3	Oxygen	2.8	FAME	25
Ethanol	8.6	Methanol	6				

One way of minimizing or eliminating such interferences is to dilute the sample with blank sulfur solvent to reduce the interferent concentration below the values given to mitigate the effect of interference.

Fuels containing large amounts of ethanol or methanol have a high oxygen content, leading to significant absorption of sulfur K alpha radiation and low sulfur results. Such fuels can, however, be analyzed using this test method provided either that correction factors are applied to the results (when calibrating with white oils) or that the calibration standards are prepared to match the matrix of the sample. In general, petroleum products with compositions that vary from white oils can be analyzed with standards made from base materials that are of the same or similar composition. Thus, a gasoline may be mimicked by mixing *iso*-octane and toluene in a ratio that approximates the expected aromatic content of the samples to be analyzed. Standards made from such simulated gasoline can produce results that are more accurate than the results obtained using white oil standards.

D4294 – ED-XRF

This test method determines sulfur using the energy dispersive X-ray fluorescence technique. It is applicable to hydrocarbon samples such as diesel, naphtha, kerosine, residuals, lubricating base oils, hydraulic oils, crude oils, unleaded gasolines, M-85 and M-100 gasohols, and other distillates. The applicable concentration range is 150 mg/kg to 5.0 m % of sulfur. In this method, a sample is placed in the beam emitted from X-ray source. The resultant excited characteristic X radiation is measured and the accumulated counts are compared with counts from previously prepared calibration standards that bracket the sample concentration range of interest to obtain the sulfur concentration. This is a rapid and precise method for sulfur determination by XRF. A typical analysis time is 2 to 4 minutes. The equipment is far less expensive than the WD-XRF instrumentation described previously. Compared to other test methods for sulfur determination, this test method has high throughput, minimal sample preparation, and good precision, and is capable of determining sulfur over a wide range of concentration.

Interferences—If this test method is applied to petroleum products with significantly different composition than the white oil calibration material, matrix interferences may occur. Also, spectral interferences may arise from samples containing water, lead alkyls, silicon, phosphorus, calcium, potassium, and halides if present in concentrations greater than one tenth of the measured concentration of sulfur or more than a few hundred milligrams per kilogram. Matrix effects may be caused by variations in concentrations of the elements present in the sample. These variations directly influence X-ray absorption and change the measured intensity of each element. Oxygenates in gasolines may have this effect. Both these types of interferences are compensated for in contemporary instruments with the use of built-in software. These interferences should be periodically checked and the software corrections offered by the instrument manufacturer should not be accepted at face value. Corrections should be verified for new formulations of products.

M-85 and M-100 fuels contain 85 and 100 % methanol, respectively, and hence, have a high oxygen content, resulting in absorption of sulfur K alpha radiation. Such fuels can, however, be analyzed by ED-XRF if the calibration standards are prepared to match the sample matrix. However, there may be loss of sensitivity and precision.

In general, petroleum products with compositions that vary from white oil calibrants used may be analyzed with standards made from base materials that are of the same or similar composition. Thus, a gasoline may be simulated by mixing *iso*-octane and toluene in a ratio that approximates the true aromatic content of the samples to be analyzed. Standards made from this simulated gasoline will produce results that are more accurate than the results obtained using white oil standards.

D4927 – WD-XRF

This test method is mainly meant for the determination of some specific elements (barium, calcium, phosphorus, sulfur, and zinc) in lubricating additives and oils. This method is more suitable than D2622 for sulfur determination in lubricating oils and additives, because D4927 implements interelement correction factors. The range for sulfur determination is 0.1 to 4.0 m %. Higher levels of sulfur can be determined by diluting the sample with appropriate sulfur-free solvent.

There are two test procedures in this method depending on whether internal standard correction or mathematical correction procedure is used. For sulfur determination, a lead internal standard is used in the first procedure.

Interferences—The additive elements present in lubricating oils affect the measured intensities from the elements of interest to a varying degree. In general, for the lubricating oils, the X-radiation emitted by the element of interest is absorbed by the other elements in the sample matrix. Also, the X-radiation emitted from one element can further excite another element. These effects are significant at concentrations varying from 0.03 m % due to the heavier elements to 1 m % for the lighter elements. The measured intensity for a given element can be mathematically corrected for the absorption of the emitted radiation by other elements present in the sample. Suitable internal standards can also compensate for X-ray interelement effects. If an element is present at significant concentrations and an interelement correction for that element is not employed, the results can be low due to absorption or high due to enhancement.

D4951 AND D5185 – ICP-AES

These two inductively coupled plasma-atomic emission spectrometric (ICP-AES) methods are very similar in operation and instrumentation. The first one is used for the determination of additive elements (boron, barium, calcium, copper, magnesium, sulfur, and zinc) in additive packages and unused lubricating oils, and the second one is used for lubricating oils, base oils, and used oils for a large number of elements, in addition to sulfur. In both methods a sample is diluted by mass with mixed xylene or other suitable solvent. An internal standard is mandatory in D4951 but optional in D5185. The solutions are introduced to the ICP instrument by free aspiration or an optional peristaltic pump. By comparing emission intensities of elements in the test sample with emission intensities measured with the calibration standards, and by applying appropriate internal standard correction, the concentrations of elements in the sample are calculated.

Interferences—There are no known spectral interferences between elements determined by these test methods when using the recommended spectral lines (180.73, 182.04, or 182.62 nm for sulfur). However, if spectral interferences do exist because of other interfering elements or selection of other spectral lines, the interference can be corrected for by using the technique described in test method D5185.

A second serious interference is from viscosity index improvers that may be present in the multigrade lubricating oils, which can bias the results. However, these biases can be reduced to negligible proportion by using the specified solvent-to-sample dilution and an internal standard such as cobalt [8].

D7039 – MWD-XRF

This modern method determines sulfur in gasolines, diesels, and refinery process streams used to blend gasolines and diesels, at concentrations from 2 to 500 mg/kg. Samples above this level may be analyzed after dilution with sulfur-free appropriate solvent. A monochromatic X-ray beam with a wavelength suitable to excite the K-shell electrons of sulfur is focused onto a sample contained in a sample cell. The fluorescent K alpha radiation at 0.5373 nm emitted by sulfur is collected by a fixed monochromator (analyzer). The intensity (count rate) of the sulfur X-rays is measured using a suitable detector and converted to the sulfur concentration using a calibration equation. Excitation by monochromatic X-rays reduces background, simplifies matrix correction, and increases the signal-to-background ratio compared to polychromatic excitation used in conventional WD-XRF techniques.

Interferences—When the elemental compositions of the samples differ significantly from the calibration standards used to prepare the calibration curve, biased results can occur. The only important elements contributing to bias resulting from differences in the matrixes of calibrants and test samples are hydrogen, carbon, and oxygen. A matrix correction factor is used to correct this bias. When the calculated correction factor C is within 0.98 to 1.04, no matrix correction is required. For most of the testing, matrix correction can be avoided with a proper choice of calibrants. Gasoline samples containing oxygenates may be analyzed with this test method if the matrix of the calibration standards is either matched to the sample matrices or a matrix correction given in the method is applied to the results [9].

D5453 – UV-Fl

This is one of the widely used techniques for low levels of sulfur determination in a variety of petroleum products. It is based on an oxidative combustion at 1100°C of the sample in an oxygen-enriched environment which converts sulfur compounds to sulfur dioxide (SO_2) gas, which is excited to higher state with ultraviolet light. When the excited molecule comes back to normal state, the light emitted is measured with a photomultiplier tube. The hydrocarbon sample is either directly injected or placed in a sample boat, and subjected to high temperature combustion in an oxygen-rich environment. Water produced in the sample combustion is removed and the sample combustion gases are next exposed to ultraviolet light. The SO_2 absorbs the energy from the UV light and is converted to excited SO_2*. The fluorescence emitted from the excited SO_2* molecule as it returns to a stable state, SO_2, is detected by a photomultiplier tube and the resulting signal is a measure of the sulfur present in the sample.

$$R - S + O_2@1100^\circ C \rightarrow SO_2 + \text{combustion products}$$
$$SO_2 + hv \rightarrow SO_2 + hv'$$

Its range of analysis is from low ppb to 40 % of sulfur. Typical sample size used is 1 to 20 μL, and a typical analysis time is less than a minute. Liquid hydrocarbons boiling in the range from approximately 25 to 400°C, and with viscosities between approximately 0.2 and 20 cSt at room temperature can be analyzed by this method. These products include naphthas, distillates, engine oils, ethanol, fatty acid methyl esters (FAME), and engine fuel such as gasoline, oxygen enriched gasoline, E-85, M-85, reformulated gasoline (RFG), diesel, biodiesel, and jet fuel. Samples should contain less than 0.35 m % of halogens in them. A number of studies have been conducted in ASTM for determining the precision of various matrices using this method.

In one study, several organic compounds containing sulfur-oxygen bonds were analyzed at about 100 mg/kg sulfur concentration in aqueous solution, and analyzed in five replicates. Results and recoveries are reported in Table 6 [10].

Separately, sulfonate compounds were studied for their recovery in a hydrocarbon solution prepared in isopropyl alcohol and *iso*-octane using dibenzothiophene in *iso*-octane as standard. The results in Table 7 are essentially identical to the results obtained in aqueous solutions, in that about 80 % of the sulfur is recovered [10].

TABLE 6—Recovery of S-O Compounds

Compound	Expected Concentration (ppm)	Concentration Achieved (ppm)	Recovery (%)
2-Thiophene carboxylic acid	125	110	88
Sodium sulfate	105	99	94
Benzene sulfinic acid	124	110	89
2-Methyl-2-propene-1-sulfonic acid	115	113	98
Benzene sulfonic acid	108	86	80

TABLE 7—Sulfonate Recovery using D5453 Method			
Compound	Expected Concentration (ppm)	Concentration Achieved (ppm)	Recovery (%)
Dodecylbenzenesulfonate	10.1	7.9	78
Dodecylbenzenesulfonate	25.3	19.2	76
Dodecylbenzenesulfonate	50.4	38.3	76

D6667 – UV-FL

A method based on the same technology as D5453 is used for sulfur determination in gaseous hydrocarbons and liquefied petroleum gases (LPG) in test method D6667 in the sulfur concentration range of 1 to 100 mg/kg. The method may not detect sulfur compounds that do not volatilize under the conditions of the test. The samples should also contain less than 0.35 m % of halogens in them to avoid interference.

OTHER XRF METHODS

Several other XRF methods have been reported in the last few years; instruments for all of them are available from the vendors. However, their usage so far has been limited. These methods include:

D6334 is a WD-XRF method similar to D2622. It is applicable in the sulfur range 15 to 940 mg/kg. Method protocol, interferences, and instrumentation required are similar to those in D2622 test method.

D6443 is a WD-XRF method with mathematical correction routine used for the determination of sulfur and several metals (calcium, chlorine, copper, magnesium, phosphorus, and zinc) in unused lubricating oils and additives. Thus, it is similar to D4927 method discussed previously. The spectral and matrix effects in both methods are similar.

D6445 is another ED-XRF method for the determination of sulfur in the range 48 to 1000 mg/kg in unleaded gasoline and gasoline-oxygenate blends. It uses X-ray tube with energy above 2.5 keV. Interferences are similar to those in other XRF methods for sulfur.

D7212 is an ED-XRF method that uses a low-background proportional counter for measurements. The instrument uses a titanium target and primary filtration so that excitation is by essentially monochromatic radiation of 4.51 keV and virtually no background at 2.3 keV. The scope of the method is between 7 to 50 mg/kg of sulfur.

If chlorine is expected to be present in samples, then other regions of the spectrum must be measured to provide compensation for spectral overlap. The chlorine interference is most likely to happen in biodiesel samples derived from recycled waste vegetable oil. Spectral interferences by overlapping peaks may be by lead alkyls, silicon, phosphorus, calcium, potassium, and halides if their total concentration is more than 10 mg/kg. The presence of oxygenates or water alters the sensitivity for sulfur.

D7220 uses polarization X-ray fluorescence spectrometry for the determination of sulfur in automotive fuels in the sulfur range of 6 to 50 mg/kg. The

sample is placed in a polarized X-ray beam, and the peak area of the sulfur K alpha line at 2.307 keV is measured. The background spectrum measured with a sulfur-free white oil or other matrix matching blank sample is adapted to the measured spectrum using adjustment regions following the instrument manufacturer's instructions, and then subtracted from the measured spectrum. A typical analysis time is 200 to 300 s per sample. The interferences in this method are very similar to those observed in other XRF test methods, and adequate corrections need to be performed to obtain accurate results.

The precisions obtainable by the methods discussed above are summarized in Table 8.

TABLE 8—Precision of Spectroscopic Methods for Sulfur Determination in Petroleum Products

ASTM #	Technique	Range	Repeatability (mg/kg)	Reproducibility (mg/kg)	BIAS
D2622	WD-XRF	3 mg/kg to 4.6 m %	$0.1462\ X^{0.8015}$	$0.4273\ X^{0.8015}$	None
D4294	ED-XRF	1 mg/kg to 4.6 m %	$0.4347\ X^{0.6446}$	$1.9182\ X^{0.6446}$	None
D4927	WD-XRF-IS WD-XRF-MC	0.1–4.0 m %	0.03966 X m % 0.05335 (X + 0.001) m %	0.2098 X m % 0.1669 (X + 0.001) m %	N/A
D4951	ICP-AES -Oil -Additive	 0.3–0.8 m % 3.0–3.2 m %	 0.016 m % 0.14 m %	 0.061 m % 0.372 m %	N/A
D5185	ICP-AES	900–6000 mg/kg	$0.49\ X^{0.81}$	$1.2\ X^{0.75}$	None
D5453	UV-FL	< 400 mg/kg > 400 mg/kg	$0.1788\ X^{0.75}$ 0.02902 X	$0.5797\ X^{0.75}$ 0.1267 X	None
D6334	WD-XRF	15–940 mg/kg	0.0400 (X + 97.29)	0.1182 (X + 54.69)	None
D6443	WD-XRF -Oil -Additive	 0.03–0.8 m % 1–5 m %	 $0.02371\ X^{0.9}$ m % $0.02783\ X^{0.8}$ m %	 $0.1623\ X^{0.9}$ m % $0.1744\ X^{0.8}$ m %	N/A
D6445	ED-XRF	48–1000 mg/kg	$12.30\ (X + 10)^{0.1}$	$36.26\ (X + 10)^{0.1}$	N/A
D6667	UV-FL	1–100 mg/kg	0.1152 X	0.3130 X	None
D7039	MWD-XRF	2–500 mg/kg -Gasoline -Diesel	 $0.555\ X^{0.5}$ $0.54\ X^{0.496}$	N/A	N/A
D7212	ED-XRF	7–50 mg/kg	$1.6196\ X^{0.1}$	$3.7668\ X^{0.1}$	None
D7220	ED-XRF	6–50 mg/kg	$1.0348\ X^{0.25}$	$2.0591\ X^{0.25}$	None

X is the average of two determinations.
N/A: Not available.

INTERLABORATORY STUDIES

Given this variety of sulfur test methods available and high interest from both producers and regulatory agencies, it is no surprise that a large number of interlaboratory studies (ILSs) have been conducted over the last few years. This is in addition to the original ILSs done to establish the precision and bias statements given in the individual test methods. Some of the important studies of the last few years are described next.

ASTM Research Report RR-DO2-1456

In work done at SouthWest Research Institute (SWRI), San Antonio, TX, three sulfur methods were compared for fitness of use: D2622, D4294, and D5453 [11]. All three were found to be equivalent for measurements in the 150 to 500 mg/kg range of sulfur. D2622 and D5453 demonstrated equivalent fitness for use down to 20 mg/kg. Strong evidence was found that the D5453 method can be fit for use in multilaboratory situations down to the 1 mg/kg sulfur level. A single *iso*-octane matrix was used to minimize the carbon-to-hydrogen ratio interference in the XRF test methods used in this study. All three test methods were then evaluated for any bias with respect to 24 commonly occurring organosulfur compounds. No bias was found and the accuracy was within the precision limits for each of the test methods. Of the three methods, D2622 and D5453 had the best precision and accuracy for low-level sulfur. Of these two, D5453 was found to generate better data, in the 50 mg/kg sulfur range.

Council of European Nations (CEN) Interlaboratory Study

In a large European study conducted by TC 19 / WG 27 [12], sixty-nine laboratories from nine countries participated in sulfur determination between 5 and 500 mg/kg in eight gasoline and seven diesel samples. The spectroscopic methods that were tested included D2622, D4294, and D5453 in their European versions. At the levels tested, all methods were found to produce essentially equivalent results, but the precision of different methods varied considerably. The best reproducibility found was for D2622 and D5453 methods. Only the latter method was considered suitable for the determination of sulfur in less than 10 mg/kg content required in the European commercial fuels. Thus, the conclusions of SWRI and CEN reports are very similar regarding the capability of spectroscopic methods for sulfur.

ASTM Research Report RR-DO2-1547

At one time, the U.S. Environmental Protection Agency (EPA) had mandated the D2622 WD-XRF method as a mandatory method for regulatory compliance for sulfur in gasoline [13]. It has been shown that this method was inadequate in accuracy at 20 mg/kg levels of sulfur. EPA later withdrew that mandate, replacing it with D6428, a combustion-electrochemical detection technique, as the compliance method for sulfur in diesel fuels of the future [14]. At that time no one in the oil industry had any experience with this method, and the published method showed poorly calculated precision based on a small study in the vendor's laboratory that did not meet ASTM D02 statistical requirements of an ILS. Hence, a major effort was undertaken to study the precisions and applicability of four main test methods for the low-level analysis of sulfur in gasolines and diesels. Eventually, this study, colloquially called the "mother of all ASTM cross checks," involved more than 6,000 data points from about 70

TABLE 9—Results of CEN TC 19 Sulfur Round Robin			
Test Method	**D2622**	**D4294**	**D5453**
Repeatability	0.0293 (X + 0.0003)	N/A	0.0285 (X + 0.0002)
Reproducibility	0.0725 (X + 0.0005)	0.0289 (X + 0.0016)	0.1088 (X + 0.0002)
Sulfur Range, 50 mg/kg	50 ± 9	50 ± 37	50 ± 7
Sulfur Range, 350 mg/kg	350 ± 30	343 ± 50	359 ± 40

worldwide laboratories, 4 test methods–D2622, D3120, D5453, and D6428, and 16 samples each of gasolines and diesels containing less than 100 mg/kg sulfur.

The results of this study are summarized in Table 10, and they clearly showed that the test method D6428 mandated by EPA was the least precise method, in both its repeatability and reproducibility for both gasoline and diesel at the sulfur levels of compliance interest, and was not useful for the precise determination of low levels of sulfur in the fuels of the future. Only D2622 and D5453 would be appropriate for industry and regulatory use [15]. As a result of this benchmark study, EPA withdrew the mandatory method D6428 and replaced it with the industry choice of D2622 or D5453, or other equivalent methods (later on, D7039). California Air Resources Board (CARB) has also approved these two methods for regulatory compliance in California. Also, ASTM D02 Committee revised the precisions of three methods to reflect the new precisions found and issued a new standard D6920 equivalent to D6428 method mandated earlier by EPA.

ASTM PROFICIENCY TESTING

For over a decade, ASTM Committee D02 has conducted proficiency testing through its CS 92 subcommittee. At present, these Interlaboratory Crosscheck Programs (ILCP) cover 23 petroleum products and involve more than 2,300 laboratories worldwide [16]. This program has proved highly successful in the

TABLE 10—Results of a Benchmark ASTM Study on Sulfur Analysis[a]

			30 mg/kg Gasoline		15 mg/kg Diesel	
Test Method	**Technique**	**Sulfur Range**	**r**	**R**	**r**	**R**
D2622	WD-XRF	3 mg/kg – 5.3 m%	3.8	7.4	3.4	6.7
D3120	Microcoulometry	3 to 100 mg/kg	3.85	17.7	7.33	8.07
D5453	UV fluorescence	1 to 800 mg/kg	1.95	11.7	1.20	6.26
D6428 (D6920)	Electrochemical	1 to 100 mg/kg	4.7	22.8	3.1	15.6

[a]Excerpted from Ref [15].

oil industry. Most products are analyzed three times a year, with some more frequently, e.g., a monthly program for RFG and ultra-low sulfur diesel (ULSD) because of regulatory interest. As can be imagined, a vast amount of data exists through these projects. At least for sulfur analysis, there appears to be good agreement between the average results obtained by alternative methods used for this analysis. However, there is sometimes considerable difference between the precision obtained through this program and that given in the standard test methods. Perhaps a lack of strict adherence to the details of the test method, inadequate calibration practice, and probably lack of quality control in the laboratory are the suspected reasons for this discrepancy between the two sets of precisions sometimes observed.

Various test methods used for sulfur determination in these ILCP crosschecks are tabulated in Table 11. A majority of results obtained in these crosschecks are mainly from the most widely used spectroscopic methods such as D2622, D4294, D5453, and D7039. A survey done in 2004 among 910 ILCP laboratories analyzing motor gasoline, # 2 diesel fuel, reformulated gasoline, and aviation fuel revealed that only three major methods were used for sulfur determination: D2622 (27 %), D4294 (39 %), and D5453 (16 %). Four other methods–D1266, D3120, D4045, and D6344–were used by fewer than 18 % of the laboratories.

ASTM ULSD ILCP PROGRAM

The EPA had historically designated specific test methods for fuel certification (e.g., see previous discussion on mandatory use of D2622 and later D6428 for ULSD certification). Only a limited number of alternative test methods were allowed if they were correlated to the designated method. This status changed in 2005 when EPA adopted a performance based management system (PBMS). Any national standard or nonstandard method can be used if it meets the set criteria of precision and accuracy. The requirement also includes a laboratory quality-control criterion. A laboratory has to qualify each method it wants to use on a laboratory-specific basis. The industry has preferred the PBMS protocol over mandatory methods. To meet the EPA qualification criteria, 20 repeat tests spread over 20 days must meet a standard deviation of 0.72 mg/kg for 15 mg/kg sulfur diesel fuel and 9.68 mg/kg for 500 mg/kg sulfur in diesel fuel. For establishing accuracy, two continuous series of ten replicates on two gravimetric standards have to be carried out. The mean of these results may not deviate from the accepted reference value (ARV) by more than 0.54 for 15 mg/kg sulfur diesel fuel and 7.26 for 500 mg/kg sulfur diesel fuel. Ten tests are required on each of two sulfur levels: 1 to 10 and 10 to 20 mg/kg for 15 mg/kg sulfur diesel fuel, and 100 to 200 and 400 to 500 mg/kg for 500 mg/kg sulfur diesel fuel [17].

Since at one time most industry laboratories did not have much experience in measuring sulfur at 15 mg/kg levels in fuels, ASTM D02.CS 92 initiated a new proficiency testing program to respond to EPA's Tier 2 sulfur limits and for the laboratories to prove to EPA that they can meet the requirements of < 10 or 15 mg/kg sulfur levels in diesel. This is a monthly testing program, and generally only five test methods are allowed to be used: D2622 WD-XRF, D3120 microcoulometry, D5453 UV-fluorescence, D6920 electrochemical, and D7039 MWD-XRF. Of these, because of a lack of participation, tests D3120 and D6920 were deleted from the program. A certified reference material has to be used with each set of analysis. Usually, National Institute of Standards and

TABLE 11—Sulfur Test Methods Used in ASTM ILCP Programs		
Product Type	**Spectroscopic Method**	**Other Methods**
#2 diesel fuel	D2622; D4294; D5453; D7039	D129
#6 fuel oil	D2622; D4294	D1552
ATF	. . .	D1552
Lubricant additives	D4927; D4951; D5185	D1552
Aviation turbine oil	D2622; D4294; D5453	D1266; D1275
Base oil	D2622; D4294	D3120
Biodiesel	D5453; D6428	D1266
Crude oil	D2622; D4294	. . .
Lubricating oil	D5453; D4927; D4951; D5185; D6481	D129; D1552
Fuel ethanol blend	D5453	. . .
Gear oil	D4294	. . .
General gas oil	D2622; D4294	. . .
Hydraulic fluid oils	D4951; D5185	. . .
Used oils (ISDO)	D5185; D6595	. . .
Mogas	D2622; D4294; D5453; D7039	D1266; D3120
Reformulated gasoline	D2622; D4294; D5453	D3120
Ultra-low sulfur diesel	D2622; D5453; D7039; D7212	D3120

Technology (NIST) standard reference material (SRM) 2723a with a certified sulfur value of 11 ± 1.1 mg/kg is used by many laboratories. Each sample has to be analyzed and reported in duplicate, unlike in any other ILCP program. Thus, not only reproducibility between the participating laboratories but also the repeatability of each laboratory can be estimated. In the short time that this program has been offered, it has been a significant success, meeting the needs of the industry and regulatory bodies. By now more than 200 laboratories worldwide are participating in this program. Some of the data from the 2007 program are summarized in Table 12.

A majority of laboratories are using D2622 or D5453 methods. Generally, the results by alternative methods are equivalent. The reproducibility obtained in these crosschecks is similar to that given in the standard methods. When the operator and equipment are prepared for the 10 mg/kg and below range with appropriate calibration and quality control, laboratories can produce better precision. This is, of course, true of any analytical test. Ideally, the calibration range and the analyte concentration in the sample as well as the matrices of standards and samples should closely match each other to produce the best results.

TABLE 12—Results of 2007/2008 ULSD ASTM ILCP Crosschecks				
ASTM #	D2622	D3120	D5453	D7039
ULSD 0701	9.08 ± 0.92 (86)	8.72 ± 0.44 (12)	8.95 ± 0.57 (210)	8.69 ± 0.57 (65)
ULSD 0702	5.73 ± 0.87 (88)	5.26 ± 0.50 (10)	5.49 ± 0.48 (206)	5.54 ± 0.49 (63)
ULSD 0703	5.41 ± 0.87 (89)	4.75 ± 0.52 (12)	5.04 ± 0.49 (215)	5.20 ± 0.43 (66)
ULSD 0704	8.79 ± 0.80 (95)	8.18 ± 0.45 (11)	8.88 ± 0.54 (225)	. . .
ULSD 0705	5.00 ± 0.87 (82)	4.33 ±0.26 (10)	4.64 ± 0.43 (209)	4.88 ± 0.54 (60)
ULSD 0706	5.37 ± 0.84 (88)	4.74 ± 0.46 (10)	4.97 ± 0.46 (220)	5.03 ± 0.42 (72)
ULSD 0707	8.71 ± 0.85 (85)	8.16 ± 1.31 (10)	8.89 ± 0.66 (233)	8.71 ± 0.70 (75)
ULSD 0708	4.91 ± 0.88 (89)	4.62 ± 0.22 (244)	4.84 ± 0.45 (85)	. . .
ULSD 0709	5.52 ± 0.80 (81)	5.10 ± 0.54 (6)	5.95 ± 0.51 (241)	5.38 ± 0.42 (75)
ULSD 0710	8.63 ± 0.81 (74)	8.52 ± 0.23 (8)	8.79 ± 0.61 (228)	8.83 ± 0.59 (74)
ULSD 0711	4.99 ± 0.95 (65)	4.37 ± 0.72 (10)	4.57 ± 0.43 (207)	4.89 ± 0.43 (79)
ULSD 0712	5.72 ± 1.05 (68)	5.14 ± 0.48 (10)	5.99 ± 0.52 (208)	5.44 ± 0.45 (72)
ULSD 0801	10.94 ± 1.16 (62)	9.73 ± 0.97 (6)	10.98 ± 0.74 (180)	10.98 ± 0.58 (74)
ULSD 0802	5.15 ± 0.73 (68)	4.59 ± 0.14 (4)	4.63 ± 0.49 (194)	4.91 ± 0.48 (81)
ULSD 0803	8.93 ±1.06 (83)	. . .	8.87 ± 0.69 (245)	8.83 ± 0.51 (88)
ULSD 0805	8.54 ± 1.00 (103)	. . .	8.93 ± 0.66 (249)	8.78 ± 0.59 (91)
ULSD 0806	5.06 ± 1.20 (102)	. . .	5.31 ± 0.49 (244)	5.56 ± 0.44 (98)
ULSD 0807	10.44 ± 1.62 (116)	. . .	10.93 ± 0.76 (253)	10.99 ± 0.47 (97)

All results are given as sulfur robust mean ± robust standard deviation mg/kg (number of results), excerpted from full ASTM crosscheck reports issued monthly. Generally, the average values from all four methods are comparable, although the precision is somewhat different for different test methods. The most widely used method is D5453, followed by D2622 and D7039. Method D3120 is used only by a limited number of labs (about ten or fewer).

U.S. EPA and CARB also participate in the ULSD programs, and their identities are not kept anonymous like those of all other laboratories. EPA uses the D2622 WD-XRF method and CARB uses the D5453 UV-Fl method. The results from both regulatory agencies are within the range of those provided by the industry laboratories.

Reproducibility of the data is somewhat more important than repeatability in intercompany commerce as well as regulatory compliance in assessing the compatibility of the certificates of analysis with the specification limits. In Table 13, reproducibility of recent ULSD crosschecks is compared with those given in the standards. Both repeatability and reproducibility of these crosschecks for all four test methods are mostly equal or better than the ones

TABLE 13—Reproducibilities of 2007/2008 ULSD Crosschecks versus Standard Test Methods

ULSD #	Sulfur Level, ~mg/kg	D2622		D3120		D5453		D7039	
		CC.	TM	CC.	TM	CC.	TM	CC.	TM
0701	9	2.56	6.90	1.28	4.83	1.58	4.05	1.58	N/A
0702	6	2.42	5.98	1.47	3.05	1.33	2.78	1.36	N/A
0703	5	2.42	5.88	1.51	2.79	1.36	2.62	1.19	N/A
0704	9	2.23	6.83	1.31	4.55	1.50	4.02	...	
0705	5	2.43	5.74	0.76	2.57	1.19	2.47	1.50	N/A
0706	5	2.34	5.86	1.35	2.78	1.28	2.59	1.17	1.12
0707	9	2.37	6.81	3.85	4.54	1.83	4.02	1.95	1.48
0708	5	2.45	5.71	0.68	2.72	1.19	2.46	1.25	1.10
0709	5	2.23	5.91	1.67	2.97	1.42	2.95	1.17	1.16
0710	9	2.26	3.31	0.69	4.73	1.69	3.99	1.65	1.49
0711	5	2.65	2.92	2.11	2.59	1.19	2.44	1.20	1.11
0712	6	2.93	3.00	1.41	2.99	1.44	2.96	1.26	1.17
0801	11	3.24	3.56	3.00	5.35	2.06	4.79	1.62	1.66
0802	5	2.04	2.94	0.47	2.70	1.36	2.47	1.34	1.11
0803	8	2.96	2.47	...	...	1.92	2.98	1.42	1.49
0805	8	2.79	2.38	...	...	1.83	1.03	1.64	0.68
0806	5	3.34	1.57	...	...	1.36	2.03	1.23	1.18
0807	11	4.51	2.80	...	...	2.11	3.48	1.31	1.66

suggested in the ASTM standard test methods. Precision over the years has generally remained constant for all four test methods.

A statistical analysis of 2004 ULSD ILCP data by Stanley and Schaefer [18] showed that for D5453 the ASTM ULSD reproducibility is better than the published reproducibility. The reproducibility increases with concentration, but the reproducibility remained essentially constant over the course of the year. Not all laboratories were alike with respect to outliers; 16 % of the labs contributed 11 % of the results but were responsible for 57 % of all outliers. Laboratory biases contributed significantly to reproducibility. Several laboratories had excessive bias. A linear (slope plus intercept) bias correction gave the largest reduction in reproducibility. Very similar conclusions were reached on analyzing the data from laboratories using the D2622 XRF method for sulfur determination. Some possible reasons for laboratory-specific bias could be that:

1. Check standard is outside the range of analysis;
2. Check standard has aged;

3. Check standard does not match the sample matrix; or
4. Instrument calibration is not correct.

An ILS conducted by the Alberta Research Council in 2005 showed that for motor gasoline, aviation gasoline, fuel oils, biodiesel, and aviation turbine diesel samples (a total of 28) using the D5453 and D7039 methods, there was no evidence that the two methods are biased above 100 mg/kg if results from one calibration curve are used. It was recommended that the D5453 and D7039 methods should be considered as practically equivalent over all sample types studied between 0 and 100 mg/kg sulfur range [19].

ON-LINE SULFUR DETERMINATION

For many operations, measuring sulfur on-line or at-line is a better option than waiting for the off-line analysis in a laboratory. High-speed real-time data on sulfur are critical for decisions in refineries, blend plants, and pipelines regarding sulfur levels in the fuels being shipped. This decision is particularly critical when diverse fuel streams use the same pipeline, to prevent contamination of low-level sulfur streams by one with high sulfur. It is of economic interest for the pipelines to keep the transmix region to a minimum. At present, the U.S. Environmental Protection Agency (EPA) has not allowed on-line methods to be used for fuel products certification. Historically, on-line sulfur analysis methods have used American Petroleum Institute (API) gravity or lead acetate paper tape tests. There is, however, not necessarily a correlation between gravity and sulfur content of the fuels. The lead acetate tape method may not be sensitive enough for very low levels of sulfur. Many proposed on-line methods are extensions of established laboratory test methods such as D2622, D4045, D4294, D5453, or D7039. Some others were developed specifically for on-line analysis.

A method based on combustion followed by gas chromatographic separation of sulfur species and flame photometric detection of SO_2 produced has been widely used in the field. This method based on a commercial instrument was issued as ASTM standard D7041.

A method based on hydrogeneolysis and rateometric colorimetry method D4045 is being developed; so is an ED-XRF method based on the D4294 method. The latter, however, may not have enough sensitivity to be used for the analysis of ultra low sulfur fuels.

A more promising commercially available technology is based on the D5453 UV-fluorescence method. Its on-line version instrument has a fast analysis time of less than a minute. A 5 μL sample is injected through a valve and pushed through the injection port into the combustion chamber. By optimizing the injected sample size, using innovative combustion tube design and an alternative way for removing moisture vapor produced, the instrument reduces the analysis time to less than a minute with precision of analysis better than 1 % of full scale. Linearity is better than 1 % at full scale at less than 1 mg/kg sulfur level. Recovery time is less than 15 minutes when switching from high (100 mg/kg) to low (15 mg/kg) sulfur samples. A possible interference from nitric oxide produced during sample combustion is not considered a serious bias. Similarly, presence of chlorine and carbon dioxide can have a quenching effect on the fluorescence, but the rejection ratio of heteroatoms to sulfur is very high to realistically matter. As a demonstration of the instrument's

stability, a 78 mg/kg sulfur in gasoline sample was run for 79 hours, and a 11.8 mg/kg sulfur sample was injected 3,048 times over a period of 10 days. In both cases, a % RSD of better than 1 % was obtained. An ASTM standard based on this methodology is being developed and is awaiting the completion of an ILS. Meanwhile, it is reported that a number of these units are operating in fields satisfactorily [20].

Fess describes an X-ray transmission (XRT) instrumentation applicable to on-line analysis for sulfur in 0.1 to 3.3 m % in crude oils. In the XRT method, sulfur absorbs X-rays transmitted between an X-ray source and detector. The technique compensates for the density changes in the crude oil and minimizes the effect of variations in the carbon/hydrogen ratio of the oil. The instrument can produce sulfur results in the high-pressure flow conditions required to pump crude oil, typically 800 psig in pipelines [21].

Finally, another XRF method that is being developed for on-line analysis is based on monochromatic WD-XRF method D7039. The limit of detection at 0.3 mg/kg and limit of quantitation at 1 mg/kg are estimated based on counting statistics. At 15 min measurement time, the precision of replicate analysis is about 1 to 2 % RSD.

Doubtless, given the importance of accurate determination of sulfur whether in the laboratory or on-line, efforts are going to continue to find better and better technology to improve the precision and the analysis time in the future.

SULFUR IN BIOFUELS PRODUCTS

As the production and usage of biofuels increase for its use as a blend component of gasoline and diesel for automotive vehicles, existing test methods need to be modified, if necessary, to fit the matrix of ethanol- and methanol-based fuels. Generally, it is expected that spectrometric methods such WD- and ED-XRF for sulfur will have appreciable problems because of the presence of oxygenates in such fuels, and consequently corrections need to be made to the results to account for oxygenates and different carbon/hydrogen ratios of biofuels and normally used XRF calibration standards.

Fortunately, this problem does not seem to plague the industry popular spectrometric method D5453 UV fluorescence and monochromatic WD-XRF method D7039. Data show both to be applicable to gasohols and similar biofuels based on the experiments done during interlaboratory studies [10,15,19] as well as ILCP crosschecks for biodiesels and ethanol blends carried out so far. In both ethanol-fuel blend and biodiesel ILCP programs, D5453 test method is used for sulfur determination. However, since no other sulfur method is used in these cross-checks, it is not possible to verify whether the D5453 values are correct or not.

In one study, ASTM ILCP sample 0607 (containing 45.4 mg/kg sulfur average value from ILS) was blended with varying amounts of ethanol and analyzed for sulfur using D5453 test method. They showed essentially quantitative recovery from the blended samples [10].

% Ethanol	0	5	10	50	70	100
Sulfur Found, mg/kg	33.7	32.5	30.6	18.3	11.5	3.4
Sulfur Expected, mg/kg	0	32	30.3	16.9	10.1	0.0

In the earlier 1992 ASTM ILS, two biodiesel samples were analyzed by D5453, D3120, and D6428 test methods. Results shown below agree among each method within the repeatability of each. The D2622 XRF method was not used in this comparison because of the interference from oxygenates and the carbon/hydrogen ratio [15].

Sample	D 11	D 12
D5453 mg/kg	11.0 ± 2.3 (40)	29.0 ± 4.4 (40)
D3120, mg/kg	11.9 ± 3.3	27.5 ± 4.3
D6428, mg/kg	9.18 ± 2.92	26.1 ± 6.9

In the Alberta Research Council study, biodiesel and ethanol-blended gasoline samples were analyzed by D5453 and D7039 each in duplicate. The results below show excellent agreement between the two sets of results [19].

Sample	D5453	D7039
Soybean Oil Ester B100 Biodiesel	1.1; 0.7	0.9; 1.0
Ethanol Blended Gasoline	23.1; 23.9	24.0; 23.1
Ethanol Blended Gasoline	36.3; 38.7	35.6; 35.4
BIOD B20/ULSD Canola FAME	5.3; 5.0	5.8; 5.8
BIOD B 100 Canola FAME	2.7; 2.0	2.6; 3.0
(All values are in milligrams per kilogram of sulfur).		

Thus, these and other ILCP data clearly show the applicability of at least D5453 and D7039 test methods for the analysis of biofuels without any method modifications.

D3120—Although not strictly a spectroscopic method, this oxidation microcoulometric method can also be used for the determination of trace amounts of sulfur in biofuels such as gasoline-ethanol blends. Examples of such analyses are given in Table 14. A ruggedness study for using this method for biofuels was conducted in one laboratory. Samples of gasoline, gasoline with 10 % ethanol, pure ethanol, and ethanol spiked with sulfur at two levels were analyzed multiple times using a Mitsubishi TOX-100 instrument [22].

The instrument was calibrated in the range of 0.000 to 1.515 mg/L of sulfur prepared from a stock solution of 101 mg/L of sulfur. The calibration was done at four levels of sulfur concentration: 0.252, 0.505, 1.010, and 1.515 ng of sulfur. Each measurement was repeated three times. A correlation R^2 of 0.9994 with a y of $0.8117x + 0.0067$ was found. The following results on gasoline-ethanol samples analyzed were obtained.

TABLE 14—Analysis of Gasoline-Ethanol Blends for Sulfur Using D3120

Sample	n	Sulfur Found, mg/kg	Std. Dev.	% RSD	Repeatability (SD X 2.77)
Gasoline EM 87	18	17.75	0.358	2.02	0.991
Gasoline EM 87 + 10 % ethanol	18	15.40	0.176	1.014	0.487
Ethanol	20	0.192	0.156	81.3	0.433
Ethanol + spike 1.42	10	1.37[a]	0.06	4.39	0.167
Ethanol + spike 2.25	15	2.18[a]	0.09	4.13	0.248

[a] % Recovery is 96.5 and 97.0, respectively.

CERTIFIED REFERENCE MATERIALS FOR SULFUR DETERMINATION

It was mentioned previously in this chapter that one of the reasons for poor agreement between different laboratories or between different test method results could be improper calibration or inadequate quality control of the analyses. This is true of any analysis but is particularly acute when trying to analyze trace amounts of sulfur in fuels. One proven way of minimizing such variation in data is to use certified reference materials as calibrants or quality control samples, or both. Fortunately, in the case of sulfur analyses a number of SRMs are available from NIST, in Gaithersburg, MD. A partial list of these is given in Table 15. We strongly recommend the use of such SRMs for calibration or quality control or both. There is some evidence that the laboratories using NIST SRMs as a check standard in the ULSD ILCP program produce more accurate results. As part of a laboratory's total quality management program, we cannot recommend more highly than that these SRMs be used as a part of routine laboratory quality control.

TABLE 15—Sulfur SRMs from NIST

Product	NIST SRM No.	Sulfur Concentration
Crude oils	2721	1.5832 ± 0.0044 m %
	2722	0.21037 ± 0.00084 m %
Di-n-butyl sulfide in base oil	2720	1.583 m %
Diesel fuels	1624d	0.3882 ± 0.0020 m %
	2723a	11.0 ± 1.1 mg/kg
	2724b	426.5 ± 5.7 mg/kg
	2770	41.57 ± 0.39 mg/kg
	8771	

(*Continued*)

TABLE 15—Sulfur SRMs from NIST (Continued)		
Product	**NIST SRM No.**	**Sulfur Concentration**
Fuel oil, distillate	1624c	0.4 m %
Gasolines – RFG	2294	40.9 ± 1.0 mg/kg
	2295	308 ± 2 mg/kg
	2296	40.0 ± 0.4 mg/kg
	2297	303.7 ± 1.5 mg/kg
	2299	13.6 ± 1.5 mg/kg
Gasolines – high octane	2298	4.7 ± 1.3 mg/kg
High gas oil feed	8590	
Kerosines	1616a	146.2 mg/kg
	1616b	8.41 ± 0.12 mg/kg
	1617a	0.17307 ± 0.00034 m %
Lubricating oil (X 5)	1819a	0.04235–0.6135 m %
Lubricating oil additive	1848	2.327 ± 0.0043 m %
Petroleum coke	2718	4.7032 ± 0.0079 m %
	2719	0.8877 ± 0.0010 m %
Reformulated gasoline	2299	13.6 mg/kg
- 10 % Ethanol	2297	303.7 mg/kg
- 13 % ETBE	2296	40.0 mg/kg
- 15 % MTBE	2295	308 mg/kg
- 11 % MTBE	2294	40.9 mg/kg
Residual fuel oils	1619b	0.6960 ± 0.0077 m %
	1620c	4.561 ± 0.015 m %
	1621e	0.9480 ± 0.0057 m %
	1622e	2.1468 ± 0.0041 m %
	1623c	0.3806 ± 0.0024 m %
	1634c	(2 m %)
	2717a	2.9957 ± 0.0032 m %
Used oils	1083	(980 mg/kg)
	1084a	(1,700 mg/kg)
	1085a	(4,500 mg/kg)

TABLE 15—Sulfur SRMs from NIST (Continued)		
Product	**NIST SRM No.**	**Sulfur Concentration**
Wear metals in base oils	1083	980 mg/kg
	1084a	1,700 mg/kg
	1085a	4,500 mg/kg

References

[1] Nadkarni, R. A., "Elemental Analysis," in *Fuels and Lubricants Handbook*, G. E. Totten, S. R. Westbrook, and R. J. Shah, Eds. ASTM International, West Conshohocken, PA, Chapter 26, 2003, pp. 707–716.

[2] Nadkarni, R. A., "Advances in Elemental Analysis of Hydrocarbon Products," in *Analytical Advances for Hydrocarbon Research*, C. S. Hsu, Ed., Kluwer/Academic/Plenum Publishers, New York, 2003, Chapter 2, pp. 27–56.

[3] Nadkarni, R. A., "Determination of Trace Amounts of Sulfur in Petroleum Products," *World Refining*, Vol. 10, No. 5, June 2000, pp. 5–14.

[4] Nadkarni, R. A., "Detecting Sulfur in Diesel," *Today's Refinery*, August 2000.

[5] Nadkarni, R. A., "The Challenge of Sulfur Analysis in the Fuels of the Future," *ASTM Standardization News*, June 2004, pp. 32–35.

[6] Nadkarni, R. A., "Determination of Trace Amounts of Sulfur in Petroleum Products and Lubricants: A Critical Review of Test Performance," *American Laboratory*, Vol. 32, No. 22, 2000, pp. 16–25.

[7] Nadkarni, R. A., *Guide to ASTM Test Methods for the Analysis of Petroleum Products and Lubricants*, MNL4, 2nd ed., ASTM International, West Conshohocken, PA, 2007.

[8] Bansal, J. G. and McElroy, F. C., "Accurate Elemental Analysis of Multigrade Lubricating Oils by ICP Method: Effect of Viscosity Modifiers," SAE Technical Series Paper 932694, Society for Automotive Engineers, Warrendale, PA, 1993.

[9] Chen, Z. W., Wei, F., Radley, I. and Beumer, B. "Low Level Sulfur in Fuel Determination using Monochromatic WDXRF-ASTM D 7039-04," *Elemental Analysis of Fuels and Lubricants: Recent Advances and Future Prospects*, *ASTM STP 1468*, R. A. Nadkarni, Ed., ASTM International, W. Conshohocken, PA, 2004, pp. 116–127.

[10] Nadkarni, R. A. and Crnko, J., "Report in Support of 2007 Revision of D5453-06 Test Method," ASTM RR-DO2-1633, ASTM International, West Conshohocken, PA, 2007.

[11] Kohl, K., "Fitness for Use Study of D5453," ASTM RR-DO2-1456, ASTM International, West Conshohocken, PA, 1999.

[12] Tittarelli, P., "Round Robin Exercise for Sulfur Test Methods for EN 228 and EN 590 Fuel Specifications," CEN/TC 19 / WG 27 (April 2000).

[13] U.S. Environmental Protection Agency, *Federal Register*, Vol. 65, No. 28, 2000, pp. 6752–6774.

[14] U.S. Environmental Protection Agency, *Federal Register*, Vol. 66, No. 12, 2001, pp. 5002–5146.

[15] Nadkarni, R. A. and Bly, K. J., "The Report of the Interlaboratory Study for Low Level Sulfur Determination in Gasoline and Diesel Fuels," ASTM RR-DO2-1547, ASTM International, West Conshohocken, PA, 2003.

[16] Nadkarni, R. A. and Bover, W. J., "Bias Management and Continuous Quality Improvements through Committee D02's Proficiency Testing," *ASTM Standardization News*, June 2004, pp. 36–40.

[17] Schaefer, R., "Ultra Low Sulfur Diesel Measurement Challenges," *OPIS Ultra Low Sulfur Diesel Summit*, Washington, DC, April 2005.

[18] Stanley, R. and Schaefer, R., "Statistical Performance of Methods for Measuring Sulfur Concentrations in Ultra Low Sulfur Diesel – Report from the 2004 Inter-Laboratory Crosscheck Program," *J. ASTM Intl.*, Vol. 15, ASTM International, West Conshohocken, PA, 2006, Paper ID 100294.

[19] Wispinski, D., "Statistical Comparison of Sulfur in Motor Gasoline, Aviation Gasoline, and Diesel using ASTM D5453 and D7039," ARC Project GO-2005-1026, Alberta Research Council, Edmonton, Alberta, Canada,

[20] Tarkanic, S. and Crnko, J., "Rapid Determination of Sulfur in Liquid Hydrocarbons for At-Line Process Applications Using Combustion/Oxidation and UV-Fluorescence Detection," *Elemental Analysis of Fuels and Lubricants: Recent Advances and Future Prospects*, ASTM STP 1468, R. A. Nadkarni, Ed., ASTM International, West Conshohocken, PA, 2004, pp. 137–151.

[21] Fess, S., "Determination of Sulfur Content in Crude Oils Using On-Line X-ray Transmission Technology," in *Elemental Analysis of Fuels and Lubricants: Recent Advances and Future Prospects*, ASTM STP 1468, R. A. Nadkarni, Ed., ASTM International, West Conshohocken, PA, 2004.

[22] Manahan, M., "ASTM Research Report on Application of D3120 Sulfur Test Method for Biofuels," ASTM RR-D02-1547, ASTM International, West Conshohocken, PA, 2008.

21

Atomic Spectroscopic Determination of Mercury in Fossil Fuels

R. A. Kishore Nadkarni[1]

MERCURY MENACE

The debilitating effects of mercury on humans and ecosystems have long been known, and they were brought to the attention of the world after the outbreak of diseases among the Japanese fishermen in Minamata Bay in the early seventies. Since then it has been recognized that the mercury contamination in fish is a worldwide human health threat because mercury is globally distributed through atmospheric transport. The methyl mercury present in fish is particularly toxic to humans, particularly pregnant women and children.

According to the U.S. Food and Drug Administration (FDA) and the U.S. Environmental Protection Agency (EPA), humans are exposed to more mercury from eating fish, marine mammals, and crustaceans than from any other source. Nearly all fish contain at least traces of methyl mercury in them, although the amount of mercury present and the latent time span from exposure to harmful effects are variable and unpredictable [1]. More than 40 U.S. state governments have warnings against eating lake fish because they are contaminated with mercury [2]. Mercury is neurologically toxic, particularly for children. EPA estimates that some 630,000 U.S. children are born each year with learning deficits caused by mercury exposure [2].

Coal and crude oil (particularly from the Pacific basin) are the main natural sources of mercury entering the ecosphere. Coal generally contains about <1 ppm of mercury, mostly concentrated in the pyrite mineral as mercury sulfide (HgS) in coal.

In the United States, federal authorities are working toward reducing the mercury emissions from coal-fired power plants, oil refineries, and chlor-alkali plants. Of these, it is estimated that power plants emit about 50 tons and chlor-alkali plants about 5 tons of mercury to the atmosphere each year [3]. EPA has designed a rule to cut the current annual mercury emissions of 48 tons from power plants by 21 % in 2010 and by 69 % after 2018, perhaps as late as 2025 [4]. An EPA proposal of "cap and trade" has been heavily criticized by the environmental groups as inadequate and ineffective in controlling the spread of mercury from coal-fired power plant emissions into the atmosphere and eventually in the aquatic system. The U.S. Congress is also considering banning the exports of mercury to foreign countries. EPA has issued guidelines on mercury emission levels from various industries [5].

Some of the species of mercury present in fish are more toxic than elemental mercury itself. Wilhelm and Bloom reviewed the speciation and occurrence of mercury in petroleum products [6].

[1] *Millennium Analytics, Inc., East Brunswick, NJ*

In an extensive study, Wilhelm et al. [24] determined mercury concentrations of 170 separate crude oil streams sampled repetitively to obtain 328 individual samples. Two separate test methods were employed:

- Procedure A used a two-stage combustion process, the first vaporizing the hydrocarbons and mercury compounds, and the second combusting the hydrocarbons. Mercury vapor in the combustion product gas exiting the combustion chamber was filtered to remove partially combusted hydrocarbons, and then collected by amalgamation on a gold trap. The mercury on the gold trap was released by heating inflowing argon that passed to the atomic fluorescence detector.
- Procedure B used a digestion–atomic fluorescence method in which the sample was decomposed with nitric acid in a sealed quartz vial at 300°C under approximately 130 bar pressure in an autoclave. The sample was then diluted with water and transferred into a bubbler to which stannous chloride solution was then added. Argon was passed sequentially through the bubbler, through soda-lime traps, and finally through a gold sand amalgam trap. The adsorbed mercury was released by heating and then adsorbed on a second gold trap, from which it was later released by heating and passed into an atomic fluorescence detector.

The arithmetic mean and median of 170 oil streams were 7.3 and 1.5 μg/kg of total mercury, respectively. The total mercury concentration of oil produced in the United States in 2004, including all species and both dissolved and suspended forms, expressed as a volume-weighted mean was calculated to be 3.5 ± 0.6 μg/kg. The range of measured concentrations extended from below the analytical detection limit (0.5 μg/kg) to approximately 600 μg/kg [24].

Mercury levels found in some major oil-producing nations and U.S. states are summarized in Table 1. These are averages, and levels vary widely from location to location in a country [24].

The data obtained by Wilhelm et al. [24] are consistent with other recent studies. Magaw et al. [25] reported data on 26 crude oils spanning major U.S. west coast crude streams. He reported mercury concentration below 10 μg/kg

TABLE 1—Mercury Concentrations in Some Major Oil Fields

Country	Mercury, μg/kg	U.S. State	Mercury, μg/kg
Algeria	13.3	Arkansas	3.7
Canada	2.1	California	11.3
Columbia	3.4	Louisiana	9.9
Iraq	0.7	Montana	3.1
Kuwait	0.8	Oklahoma	1.4
Mexico	1.3	Texas	3.4
Norway	19.5	Utah	2.2
Saudi Arabia	0.9	Wyoming	2.7
Venezuela	4.2		

for all oils except one. The New Jersey Department of Environmental Protection reported total mercury concentrations in oil delivered to U.S. east coast refineries [26]. In about 25 oil streams analyzed, the total mercury concentration was 0.1 to 12.3 μg/kg. The mean and median were reported as 3.5 and 2.7 μg/kg, respectively. Environment Canada has reported mercury levels in crude oils refined in Canada [27]. The volume-weighted average for Canadian refined oils is reported preliminarily as less than 4 μg/kg. In all these three studies, the analysis methods were similar–decomposition and atomic absorption spectrometry (AAS) or atomic fluorescence spectrometry (AFS) determination.

SAMPLING, STORAGE, AND HANDLING OF LIQUID HYDROCARBONS FOR MERCURY

Given the chemical tendency of mercury and its various organo-species to interact with container materials, it is important to consider this aspect before considering the actual procedures for analytical measurement of mercury. Bloom has shown that the organo-mercury species are stable for at least 30 days in all containers tested except those made of polyethylene; and Hg^0 was stable in all containers except those made of stainless steel or polyethylene. Mercury (II) was rapidly lost from all containers except those made of aluminum, which rapidly converted it to Hg^0, which was stable [7].

Bloom [7] showed storage experiments to indicate that two key species, Hg(II) and Hg^0, are relatively unstable in most commonly used shipping containers. This suggests that specimen analysis is best conducted at the point of production, or if that is impractical, the samples should be sent to a laboratory as soon as possible in completely full glass bottles. Metal sample containers used by the petroleum industry were found to introduce serious speciation artifacts or losses of analyte on the walls of containers, and should not be used for mercury samples.

In a standard guide prepared for ASTM, Hwang has described a procedure for sampling, storage, and handling of hydrocarbons for mercury determination [8]. This procedure was developed for sampling streams where the mercury speciation is predominantly Hg^0 present as a mixture of dissolved Hg^0 atoms, adsorbed Hg^0 on particulates, and suspended droplets of metallic mercury. The latter form, often called "colloidal" mercury because the droplet size can be very small, makes obtaining a representative sample very difficult. There could be several reasons for this: nonisokinetic sampling of the liquid can result in over- or undercollection of suspended droplets, or collection of mercury that has accumulated in dense larger drops and pools at the bottom of piping and in sample taps, and so on. Sampling should be directly done into the EPA-designated volatile organic analysis (VOA) vials, if possible. The sample taps should be purged sufficiently immediately before sampling to remove any elemental mercury droplets that may have accumulated in the piping, valves, or crevices. Since mercury can be readily absorbed on many metal surfaces, the sample taps should not contain process-contact materials composed of copper, zinc, tin, aluminum, brass, bronze, Monel, or other alloys containing these metals. Sometimes capping the vials while slowly purging under a flow of nitrogen was found to be beneficial in preventing the oxidation of elemental mercury during shipping.

Hwang cautions that a single droplet of metallic mercury can skew a mercury measurement by several orders of magnitude [8]. To avoid accumulation of mercury or mercury compounds such as mercury sulfide precipitates,

sample taps should not be located at the bottom of the piping but rather angle upward from the top or upper half of the piping. To further reduce the potential for contamination, sample lines should be thoroughly purged before use. Additional contamination issues arise from the use of improper sample containers, which can bias the sample results either high (if a container has been previously used and the adsorbed mercury on the container walls not removed) or low (by using an uncoated steel or tin-lined steel, which adsorbs mercury from the samples). In general, the sample containers for mercury should not be reused unless specially cleaned and tested as a blank before use. Uncoated metal containers should not be used for any sampling steps, even for short-term holding before transfer to the VOA vials. Stainless steel containers may be used, but must be cleaned and rinsed with a mild acid rinse and thoroughly dried before use. Epoxy-lined steel containers may also be used and are preferred for larger volumes (> 1 L).

The same issue is expressed by Shepherd regarding the storage containers used for mercury sampling [30]. Borosilicate glass with PTFE-lined closures is probably the best choice for sample storage. However, alternative containers even for short-term sample capture is likely to compromise sample integrity. Any material prone to adsorb mercury can reduce mercury levels in a sample, or contaminate it through re-release of any mercury previously accumulated on the surfaces. Experience shows that even stainless steel is problematic as a storage material for liquefied petroleum gas (LPG). For LPG sampling, stainless steel gas cylinders are typically a requirement and are often necessarily reused. So, confirmation of cleaning for subsequent use in mercury sampling is paramount. It has been found that both stainless steel and PTFE-lined containers become contaminated with mercury and cannot be adequately cleansed despite multiple rinses with polar and nonpolar organic solvents, overnight soak with mineral acids, nitrogen purge, heating at 120°C in vacuum, and so on. The subsequent polar solvent rinses consistently showed that trace mercury still remained on the container walls.

ANALYTICAL METHODOLOGY

Over the years, a number of different instrumental methods have been used to quantitatively determine total mercury as well as its species in a variety of fossil fuel matrices. Some of the methods that have been standardized by ASTM are summarized in Table 2. A number of other techniques besides those mentioned in Table 2 are described later in this chapter.

As a part of its program to accurately determine mercury concentrations in fossil fuels and emissions, U.S. Environmental Protection Agency (EPA) issued the following methods in Chapter SW-846 of RCRA.

6800	Elemental and speciated isotope dilution mass spectrometry
7471B	Mercury in solid or semisolid waste (manual cold vapor technique)
7473	Mercury in solids and solutions by thermal decomposition, amalgamation, and AAS
7474	Mercury in sediment and tissue samples by AFS.

TABLE 2—ASTM Standard Test Methods for Determination of Mercury in Fossil Fuels

ASTM No.	Matrix Analyzed	Analytical Technique
D5954	Natural gas	Gold amalgamation + CVAAS
D6350	Natural gas	Gold amalgamation + AFS
D3684	Coal	Oxygen bomb combustion + AAS
D6414	Coal	Acid extraction or wet oxidation + CVAAS
D6722	Coal	Combustion + gold amalgamation + CVAAS
D7482	Crude oil	Sampling, storage, and handling of mercury samples
D7623	Crude oil	Gold amalgamation + CVAAS (NIC)
D7622	Crude oil	Zeeman AAS (Lumex)
*	Crude oil	AFS

*In ASTM standardization process.
CVAAS, cold vapor atomic absorption spectrometry; AFS, atomic fluorescence spectrometry; AAS, atomic absorption spectrometry; NIC, Nippon Instrument Corporation.

Mercury in Natural Gas

Elemental mercury in natural gas may cause embrittlement of aluminum vessels and heat exchangers. The potential for catastrophic equipment failure could be a direct outcome of processing mercury-containing liquid natural gas. Mercury in natural gas is determined by sample combustion–gold amalgamation and final measurements with cold vapor atomic absorption spectrometry (CVAAS) or atomic fluorescence spectrometry (AFS). In ASTM standard test method D5954, the mercury in the gas stream is adsorbed onto gold-coated silica beads and subsequently directly desorbed by heat into a long-path-length quartz cell connected to an atomic absorption spectrophotometer. The mercury atoms are detected by measuring their absorbance of light from a mercury source lamp at 253.652-nm wavelength. The mercury concentration in the sample is calculated from the absorbance peak area by comparison to the mercury standards prepared at the time of the analysis. Adsorption of mercury on gold-coated beads can remove interference associated with the direct measurement of mercury in natural gas. It preconcentrates the mercury before analysis, thereby offering measurement of ultra-low average concentration in a natural gas stream over a long span of time. It avoids the cumbersome use of liquid spargers with in-site sampling, and eliminates contamination problems associated with the use of potassium permanganate solutions. The procedure detects both inorganic and organic forms of mercury and is capable of determining mercury down to 1 ng/m^3. Detection sensitivity may vary considerably depending on the type of spectrophotometer and its accessories used. Calibrations can be done using either aqueous or gaseous mercury standards.

The other method for mercury determination in natural gas–ASTM D6350–uses AFS. The sample preparation is very similar to the one in D5954.

Mercury is adsorbed onto a gold-coated silica sand trap, and the analyte from it is desorbed by raising the temperature of the trap. A flow of inert gas carries the mercury atoms into the cell assembly of an AFS spectrometer. The cell is irradiated by a low-pressure mercury vapor lamp at 253.652 nm. Excitation of the mercury atoms produces resonance fluorescence, which re-radiates at the excitation wavelength. The fluorescence radiation is detected by a photomultiplier tube and is directly proportional to the amount of mercury present in the cell. The concentration of mercury in the original sample is then calculated by comparing with the fluorescence of previously prepared mercury standards. This method can be used to determine the total mercury concentration of a natural gas stream down to 0.001 $\mu g/m^3$. Based on the analysis of mercury standards, a relative standard deviation of about 5 % can be obtained in the mercury concentration range of 0.056 to 0.226 ng.

Mercury in Coal and Coal Combustion Residues

The mass of coal burned in the United States annually ($\sim 10^{12}$ kg/y) is approximately the same as the mass of oil refined in the United States annually. The concentration of mercury in all U.S. coal is approximately 100 μg/kg. From the measured mean concentration for total mercury in oil and total annual volume (2004), oil that passes through U.S. refineries contains approximately 3 metric tons of mercury. The maximum amount of mercury released to the atmosphere from oil processed in the United States is, therefore, approximately less than 5 % of that which may be derived from burning coal in any given year [24].

There are at least three test methods standardized for the determination of mercury in coal and related materials. This field was active long before it became apparent that the mercury level in crude oils is also an environmental concern.

In the ASTM standard test method D3684 a sample is combusted in an oxygen bomb containing dilute nitric acid absorbing the mercury vapors. The bomb is rinsed into a reduction vessel with dilute nitric acid, and the mercury is determined by flameless CVAAS. Small amounts of potassium permanganate, hydroxylamine hydrochloride, and stannous chloride are added to the reduction vessel as reduction aids. Because mercury and its salts can be volatilized at relatively low temperatures, precautions should be taken against inadvertent loss of mercury when using this method.

The ASTM standard test method D6414 consists of two procedures. In procedure A, a sample is solubilized by heating at a specified temperature in a mixture of nitric and hydrochloric acids. In procedure B, the sample is solubilized in a mixture of nitric and sulfuric acids with vanadium pentoxide. In both cases the acid solutions so produced are transferred into a vessel in which the mercury is reduced to elemental mercury and is determined by the CVAAS technique.

In the third ASTM standard test method, D6722, which is similar to the EPA method 7473, controlled heating of the sample in oxygen is used to liberate mercury. The sample is heated to dryness in the instrument and then thermally and chemically decomposed. The decomposition products are carried by flowing oxygen to the catalytic section of the furnace, where oxidation is completed and halogens as well as nitrogen and sulfur oxides are trapped. The remaining decomposition products are carried to a gold amalgamator that

TABLE 3—Precision of Mercury Analysis in Coal			
ASTM Method	Mercury Concentration, ppm	Repeatability	Reproducibility
D3684	0.042–0.192	0.036	0.054
D6414	0.032–0.585	0.012 + 0.11X	0.003 + 0.25X
D6722	0.017–0.586	0.008 + 0.06X	0.007 + 0.13X
X is the average of results.			

selectively traps mercury. After the system is flushed with oxygen to remove any remaining decomposition products, the amalgamator is rapidly heated, releasing the mercury vapor. Flowing oxygen carries the mercury vapor through absorbance cells positioned in the light path of a single wavelength atomic absorption spectrophotometer. Absorbance peak height or peak area, as a function of mercury concentration, is measured at 253.7-nm wavelength.

The precision of these three methods for the determination of mercury in coal is shown in Table 3.

U.S. EPA draft method 30B has been approved as a referee method for relative accuracy testing audits in coal-fired utilities. The method measures total vapor phase mercury emissions from coal-fired combustion sources using an extractive or thermal analysis technique and ultraviolet–atomic absorption (UV-AA) or ultraviolet–atomic fluorescence (UV-AF) cold vapor analyzers. An example of such a system is the DMA-80 analyzer supplied by Milestone, Inc. [23]. This instrument uses thermal decomposition and AAS determination of mercury. The total analysis time is less than 10 minutes and the dynamic range of analysis is 0.005 to 1000 ng/sample boat. Controlled heating is used to first dry the sample and then thermally decompose it in a quartz decomposition chamber. A flow of oxygen carries the decomposition products through a catalytic section where halogens, nitrogen, and sulfur oxides are absorbed. All mercury species are reduced to Hg^0 and carried through a gold amalgamation, where mercury is selectively trapped. A purging step flushes all nonmercury vapors and decomposition products out of the system. The amalgamator is rapidly heated, releasing the mercury vapors to a single-beam fixed wavelength AA spectrometer. The absorbance is measured at 253.7 nm as a function of the mercury content. Results by this technique are shown in Table 4 [23].

Mercury in Crude Oil

In the last two decades, the interest in the mercury content of crude oil has increased, particularly when it was observed that the concentration of mercury in crude oils from the Pacific basin fields is much higher than that of crude oils from other sources. The most likely reason for this higher mercury concentration in Pacific basin oil is the volcanic activity in that part of the ocean floor. A number of mercury species have been identified in crude oil: Hg^0, mercury chloride ($HgCl_2$), HgS, CH_3HgCl, and $(CH_3)_2Hg$ [9]. Some evidence exists that other species may also be present in crude oil. Of those listed, elemental mercury and mercury sulfide are the major components of the mercury present in crude oils. Some examples of the mercury levels in various crude oils are given in Table 5.

TABLE 4—Determination of Mercury in NIST Coal and Fly Ash SRMs

NIST SRM	Hg Found, ppm	Hg, Certified ppm
1630a Coal	0.098 ± 0.004	0.0938 ± 0.0037
1633b Coal Fly Ash	0.143 ± 0.003	0.141 ± 0.019

SRM, standard reference material.

Crude oil is known to contain volatile mercury because mercury is found concentrated in the LPG and naphtha fractions of the atmospheric distillation when crude oil is refined. It is known conclusively that elemental mercury is at least one of the volatile mercury species in crude oil because it is sometimes found in trays in refinery distillation towers and condensed in cryogenic heat exchangers that liquefy petroleum gases [9]. In addition to the corrosion problems, exposure to accumulated mercury can pose a health hazard to refinery workers during turnaround operations of process units. Mercury may also find its way into fuel gas and wastewater streams, with subsequent release to the environment [10].

In a large study conducted at Chevron Research and Development Center, Hwang analyzed 2 crude oils, 5 organic fractions, and 5 water samples among 16 participating laboratories using 10 mercury analyzers available in the marketplace (Table 6). Most laboratories and instruments produced acceptable results (Table 7). The consensus values were consistently less than the reference values for the organic samples. For aqueous samples, the consensus values are quite close to the reference values.

Filby et al. [11,12] used neutron activation analysis for the determination of mercury and other trace metals in crude oils. Bloom [7] used extraction/CVAFS; Liang [13] used combustion–CVAFS, and Kelly et al. [14] used isotope dilution.

INAA

In instrumental neutron activation analysis (INAA), a sample in a sealed quartz vial is irradiated in a nuclear reactor and the resultant radioactive isotope produced is measured for its characteristics gamma ray emission. In this particular case, mercury measurement suffers from interferences caused by nickel and

TABLE 5—Mercury Levels in Some Crude Oils

Crude Oil Type	Mercury Concentration, ng/g	Reference
Crude oils (all)	1505 ± 3278	6
Crude oils	0.3–82	10
Light distillates	1.32 ± 2.81	6
Utility fuel oil	0.67 ± 0.96	6
Asphalt	0.27 ± 0.32	6
Condensates	51–450	10

TABLE 6—Some Mercury Analyzers on the Market[a]

Instrument Company	Model	Technique Used	Relevant Test Method
Leco	AMA 254	Pyrolysis and AAS	ASTM D6722; EPA 7473
PS Analytical	Merlin; Galahad	AFS	EPA 1631
Nippon	SP3D	Pyrolysis, gold amalgamation, CVAAS	UOP 938-95
Lumex	RA 915, etc.	Pyrolysis, CVAAS	
Milestone	DMA 80	Pyrolysis, CVAAS	EPA 7473
Cetac	QuickTrace	CV-AFS or AAS	
Teledyne Leeman	Hydra	Thermal decomposition, gold amalgamation, AFS or AAS	EPA 7473; EPA 245.7
Brooks Rand			EPA 1631; EPA 245.7
Tekran		CV-AFS, gold amalgamation	
AIT		SID-MS	EPA 6800
Frontier Geosciences		On-line analyzer	

[a] David Hwang, Chevron, personal communication.

selenium; however, a correction can be done for this bias [11]. The principal gamma ray photopeak of Hg^{203} overlaps the gamma ray photopeak of Se^{75}. Nickel in crude oil has similar interference in the mercury determination. The combination of the presence of selenium and nickel in crude oil samples even after correcting for them substantially elevates the mercury detection limits, and thus the method is not highly useful for the determination of low levels of mercury. Moreover, virtually no refinery laboratory has easy access to a nuclear reactor. Thus, although possible in principle, the INAA method is not practical in the field [9].

The analytical methods for mercury determination are based on basically the same principle as the test methods for coal and natural gas analysis. None of the three possible methods for crude oil analysis has yet been approved by ASTM; they are at various stages of standardization and balloting process in ASTM. Nevertheless, some details of these methods are described here because they are not likely to change in eventual ASTM approval. The methods are based on gold amalgamation and mercury measurement using either CVAAS or AFS technologies.

NIC METHOD

The UOP 938-00 method, which is similar to ASTM D7623, is based on the use of Nippon Instrument Corporation's (NIC) mercury analyzer, which is capable of

TABLE 7—Consensus Values Found in Chevron Interlaboratory Study[a]

Sample	Reference Value	Mean	2 Std. Dev.
Crude oil 1		22.80	3.79
Crude oil 2		2.86	0.34
Organic sample 1	520	492.8	30.7
Organic sample 2	720	696.4	42.9
Organic sample 3 (duplicate of 1)	520	494.9	27.8
Organic sample 5	920	889.7	53.0
Organic sample 6	320	309.8	17.8
Water sample 1	28	28.61	2.42
Water sample 2	98	98.95	6.95
Water sample 4	58	59.24	4.40
Water sample 5	78	78.17	6.22
Water sample 6 (duplicate of 4)	58	59.73	3.88

[a] David Hwang, Chevron, personal communication.

measuring from 0.1 to 10,000 ng Hg/mL. In this method, a sample is decomposed by heating at about 700°C and collecting the mercury vapors as gold amalgam. After collection, the amalgam is heated and the mercury is re-amalgamated on a second collector. Upon completion of this two-step gold amalgamation procedure, the mercury is liberated by heating the collector to 700°C. The vaporized mercury is carried to an absorption cell with a pure carrier gas and detected by the CVAAS technique. Aqueous mercury chloride standards are used. Based on the limited data available, a repeatability of 0.2 and 3 ng/mL was obtained at mercury levels of 0.8 and 47 ng/mL.

A modification of the method based on the work of Furuta et al. [15] allows the separation and determination of soluble mercury species in hydrocarbons: elemental mercury, organic nonionic mercury compounds, and ionic (both organic and inorganic) mercury compounds. This procedure can be applied to samples containing 15 to 4,000 ng/mL of mercury. In this procedure, any insoluble materials are first removed by pressure filtration. The particulate-free hydrocarbon sample is first analyzed for total soluble mercury content. It is then placed in an ice bath and purged with helium. The difference in the mercury concentration between the original and the purged sample represents the elemental mercury content. The purged sample is then extracted with a 1 % solution of L-cysteine to transfer the ionic species into an aqueous phase. The remaining purged, aqueous-extracted hydrocarbon sample is then analyzed for organic mercury. The elapsed time for the analysis of a single sample is 6 hours.

Fox et al. [10] used this NIC procedure for the analysis of several crude oils and NIST coal and crude oil standard reference materials (SRMs) for mercury. A precision of about 2 to 12 % RSD was obtained. A method similar to UOP 938-00, EPA 7473 [16], and ASTM D6722 has been proposed by Nadkarni and Fox for the analysis of crude oils for mercury using gold amalgamation and CVAAS. An interlaboratory study (ILS) was conducted in 2009. Overall repeatability and reproducibility have been established, and the method is used in many individual laboratories.

In the latest model of the NIC PE-1 instrument, a sensitivity of 0.01 ppb is claimed. An automatic sampler can analyze up to 110 samples. The method is applicable to naphtha, paraffin oil, kerosine, light and heavy oils, crude oil, condensate, LPG, LNG, and so on.

LUMEX METHOD

A method similar to the NIC method but without using the gold amalgamation procedure and using Zeeman AAS instead of CVAAS is proposed by Ohio Lumex for their instrument and is described in ASTM D7622. The use of Zeeman correction obviates the need for amalgamation by avoiding the matrix-induced interferences. There are other differences between the NIC and Ohio Lumex instruments.

In the Zeeman AAS method proposed by Ohio Lumex and used in many laboratories, controlled heating following thermal decomposition of the analysis sample in air is used to liberate the mercury. The sample is placed into the sample boat, which is inserted in the first chamber of the atomizer, where the sample is heated at a controlled temperature of 300 to 500°C. The mercury compounds are evaporated and partially dissociated, forming elemental mercury vapor. Mercury and all decomposition products are carried to the second chamber of the atomizer and heated to about 700 to 750°C. Mercury reduction takes place on the surface of the heating nichrome coil, and thus no catalyst is needed. In this step, mercury compounds are totally dissociated and the organic matrix of the sample is burnt out. Continuously flowing air carries mercury and other combustion products through an absorbance cell heated up to 750°C positioned in the light path of a double-wave, cold-vapor Zeeman AAS instrument. The mercury resonance line at 253.7 nm is split into several components, one of those falling within the mercury absorbance line (analytical line) profile and another one lying outside (reference line). The difference between the intensities of these compounds is proportional to the number of mercury atoms in the analytical cell. Absorbance peak area or peak height is a function of the mercury concentration in the original sample being analyzed.

Similar to the proposed draft method using the NIC analyzer, a separate draft method using Ohio Lumex instrument has also been prepared. An ILS has been completed and the precisions obtained are given in ASTM Standard Test Method D7622. Many laboratories around the world are using this instrument. The same set of crude oil samples was used in both ILSs using these two instrument models.

PSA METHOD

A third method also used in many laboratories is based on the AFS technique. Stockwell has used vapor generation and AFS [17]. This technique overcomes

the majority of matrix interference effects and benefits from the sensitivity and linearity of AFS technique. The sensitivity gained is equivalent to or better than that achieved in inductively coupled plasma–mass spectrometry (ICP-MS), and two orders of magnitude better than those obtained by AAS. The European standard EN 13506 uses vapor generation coupled with direct AFS measurement. U.S. EPA standard 1631 uses an additional gold amalgamation step. The amalgamation provides an additional order of sensitivity but also requires considerable attention to detail and cleanliness to avoid contamination.

The automated on-line AFS technique has been used for the determination of mercury in natural gas, coal, stack emissions, and so on [17]. Fully automated instrument systems have been installed in a number of countries [18,19].

Instruments have been built around meeting the EN 13506 and EPA 1631, 245.1, and 245.7 protocols, all based on the AFS technique with additional steps of gold amalgamation, vapor generation, or both. These vendors include PS Analytical [18,19], Teledyne [20,21], among others.

A draft of the method based on gold amalgamation plus AFS has been prepared for use by ASTM Committee D02 on Petroleum Products and Lubricants. In this proposed standard, mercury from the liquid samples is first vaporized in a stream of transfer gas into a heated chamber held above 400°C. The vaporized sample is then passed over a gold-coated silica trap that is held at a temperature of 170 to 200°C. After a preset time, the carrier gas flow is switched to a flow of clean (mercury-free) argon and the trap flushed for a short period. The analyte is then desorbed by raising the temperature of the trap. The argon flow carries the mercury vapor into the atomic fluorescence spectrometer. A low-pressure mercury vapor lamp emitting light at 256.652 nm excites the mercury atoms to produce resonance fluorescence and irradiation of the excitation wavelength. The latter is detected by a photomultiplier tube and is directly proportional to the amount of mercury in the cell. The concentration of mercury in the original sample is obtained by comparison with freshly prepared standards, which are analyzed by direct injection of mercury vapor into the instrument at a specified temperature on supported gold traps. Interferences such as from hydrogen sulfide can be avoided by the use of air as the active transfer gas before vaporizing into an argon stream.

At the moment, the precision of this proposed method is not known and an ILS involving multiple laboratories and multiple crude oil samples is necessary.

In addition to the three methods described for consideration as new ASTM standards, at least two other methods have been shown to produce satisfactory results in research environment.

Bloom [7] has studied a large number of crude oils and spiking studies for the quantitation of mercury speciation. The method is based on relatively simple chemical extraction that can be performed by any laboratory with a gold amalgamation/atomic spectroscopy based mercury analysis system. Although CVAFS affords the lowest detection limits and the most interference-free operation; the extractions are also suitable for analysis by CVAAS, with detection limits sufficient for most needs. The application of this technique to field samples indicates that total mercury concentrations in petroleum range over five orders of magnitude from 0.5 to 50,000 ng/g, and that most of the mercury is in the particulate and inorganic forms. The analytical figures of merit obtained for spike studies are given in Table 8.

TABLE 8—Analytical Figures of Merit for Species-Specific Mercury Extractions in Petroleum Samples [7]

Parameter	Mercury Concentration, ng/g			
	Total	Hg(II)	Hg^0	CH_3Hg
Method blank (@ n = 4)	0.10 ± 0.02	0.007 ± 0.003	0.16 ± 0.01	0.08 ± 0.06
Measured MDL	0.17	0.10	0.09	0.25
Mean spike recovery, %	100.3	93.1	98.7	105.5
Range of % recovery	98–102	76–101	94–103	99–106

Examples of complete mercury speciation in several petroleum samples are given in Table 9.

ID-CV-ICP-MS METHOD

NIST developed a research method for the determination of ultra-low levels of mercury in crude oil [14] and coal [22]. Based on the isotope dilution-cold vapor-inductively coupled plasma-mass spectrometry (ID-CV-ICP-MS technique, the method has been tested on coal and crude oil reference materials and is used for certifying SRMs for mercury issued by NIST. The method involves a closed system digestion process employing a Carius tube to completely oxidize the sample and chemically equilibrate the mercury in the sample with a ^{201}Hg isotopic spike. The digestates are diluted with high-purity quartz-distilled water, and the mercury is released as a vapor by reduction with tin chloride. Measurements of $^{201}Hg/^{202}Hg$ isotope ratios are made using a quadrupole ICP-MS system in time-resolved analysis mode. The new method has some significant advantages over the existing methods. The instrument detection limit is less

TABLE 9—Complete Mercury Speciation in Petroleum Samples [7]

Sample	Unfiltered Mercury, ng/g		0.8μ Filtered Mercury, ng/g		
	Total	Hg^0	Dissolved	Hg(II)	CH_3Hg
Condensate 1	20,700	3060	5210	2150	3.74
Condensate 2	49,400	34,500	36,800	237	6.24
Crude oil #1	1990	408	821	291	0.25
Crude oil #2	4750	1120	1470	433	0.26
Crude oil #3	4610	536	1680	377	0.27
Crude oil #4	4100	1250	1770	506	0.62
Crude oil #5	15,200	2930	3110	489	0.45
Crude oil #6	1.51	0.09	1.01	0.39	0.15
Crude oil #7	0.42	0.17	0.41	0.02	0.11

than 1 pg/mL. The average blank (n = 17) is 30 pg, which is roughly one order of magnitude lower than the equivalent microwave digestion procedure. Memory effects are very low. The relative reproducibility of the analytical measurements is ~0.5 % for mercury concentrations in the range of 10 to 150 ng/g.

U.S. EPA IDMS AND SIDMS METHODS

EPA method 6800 consists of two approaches: isotope dilution mass spectrometry (IDMS) for the total metals and elements and speciated isotope dilution mass spectrometry (SIDMS) for the determination of elemental and molecular species. The methods are applicable at μg/g and sub-μg/L levels in water samples, in solid samples, and in extracts or digests.

IDMS is based on the addition of a known amount of enriched isotopes to a sample. Equilibration of spiked isotope with the natural element/molecule/species in the sample alters the isotope ratio that is measured. With the known isotopic abundances of both spike and sample, the amount of the spike added to the known amount of sample, concentration of the spike added, and the altered isotope ratio, the concentration of the element/molecule/species in the sample can be calculated.

IDMS has several advantages over conventional calibration methodologies. Partial loss of the analyte after equilibration of the spike and the sample will not influence the accuracy of the determination. Fewer chemical and physical interferences influence the determination because they have similar effects on each isotope of the same element. The isotope ratio used for quantification can be measured with very high precision, typically RSD of better than 0.25 %.

SIDMS labels each species with a different isotope-enriched spike in the corresponding species form. Thus, the interconversions that occur after spiking are traceable and can be corrected. Although SIDMS maintains the advantages of IDMS, it is capable of correcting for the degradation of the species or the interconversion between the species.

Both IDMS and SIDMS require the equilibration of the spike isotopes and the natural isotopes. For IDMS, the spike and samples can be in different chemical forms; only total elemental composition will result. In general, IDMS equilibration of the spike and the sample isotopes occurs as a result of decomposition, which also destroys all species-specific information when the isotopes of an element are oxidized or reduced to the same oxidation state. For SIDMS, spikes and samples must be in the same speciated form. This requires the chemical conversion of the elements in spikes to be in the same molecular form as those in the sample.

Mercury levels in various environmental and biological samples determined by these two mass spectrometric methods are summarized in Table 10.

STANDARD REFERENCE MATERIALS FROM NIST

Over the years a number of SRMs have been issued by NIST for coal, fly ash, and crude oil matrices for mercury. These materials are highly useful in validating methods and laboratory capability to accurately analyze such materials. A list of these is given in Table 11. It is strongly recommended that use of these be made by all laboratories striving for precision and accuracy of their results.

TABLE 10—Mercury Concentrations Determined by Mass Spectrometry Methods

Material	Methyl Mercury (as Hg)		Total Mercury	
	Certified	Found[a]	Certified	Found[b]
Tuna fish BCR-464	5.12 ± 0.16	5.60 ± 0.30	5.24 ± 0.10	5.71 ± 0.42
Human hair IAEA-085	22.9 ± 1.4	23.65 ± 1.42	23.2 ± 0.8	24.24 ± 1.44

[a]EPA method 6800 used [28].
[b]EPA method 3200 used [29].

TABLE 11—NIST SRMs for Mercury in Fossil Fuels

SRM No.	Material	Mercury Concentration, μg/kg
1619b	Residual fuel oil	0.00346 ± 0.00074
1632b	Bituminous coal	70
1632c	Bituminous coal	93.8 ± 3.7
1633a	Coal fly ash	160
1633b	Bituminous coal fly ash	143.1 ± 1.8
1635	Subbituminous coal	10.9 ± 1.0
2682b	Subbituminous coal	108.8 ± 2.9
2683b	Bituminous coal	90.0 ± 3.6
2684b	Bituminous coal	97.4 ± 4.7
2685b	Bituminous coal	146.2 ± 10.6
2689	Coal fly ash	18
2690	Coal fly ash	0.5
2691	Coal fly ash	59
2692b	Coal	133.3 ± 4.1
2693	Bituminous coal	37.3 ± 7.7
2721	Light-sour crude oil	0.0417 ± 0.0057
2722	Heavy-sweet crude oil	0.129 ± 0.013
2724b	Diesel	0.000034 ± 0.000026

Note: Some of these SRMs are also certified for other elements. See NIST individual certificates of analyses.

CONCLUSION

Based on the expected increasing government regulations on mercury emissions during the use of fossil fuels, it is to be expected that analytical methods which are accurate, precise, and capable of measurement at nanogram levels are going to be in use in the laboratories. Among the test methods sponsored by regulatory bodies and international standards writing bodies, the leading candidates are gold amalgamation or extraction techniques followed by CVAAS or CVAFS. Several companies provide instrumentation for such analysis. More elaborate techniques such as INAA or ID-CV-ICP-MS are better suited for mercury analysis in research laboratories and are unlikely to be used for routine mercury determinations in fossil fuels because of their expense, time lag for analysis, and high technical expertise needed to establish and conduct such advanced technologies.

References

[1] Dalton, L. W., "Methyl Mercury Toxicology Probed," *Chem. Engin. News*, January 19, 2004, pp. 70–71.

[2] Johnson, J., "Grappling with Mercury," *Chem. & Engin. News,* July 12, 2004, pp. 19–20.

[3] Johnson, J., "Where Goes the Missing Mercury?" *Chem. Engin. News,* March 15, 2004, pp. 31–32.

[4] Hogue, C., "Mercury Battle," *Chem. & Engin. News,* April 2, 2007, pp. 52–55.

[5] U.S. EPA, "Guidance for Reporting Toxic Chemicals: Mercury and Mercury Compounds Category," EPA 260-B-01-004, U.S. Environmental Protection Agency, Washington, DC, August 2001.

[6] Wilhelm, S. M. and Bloom, N., "Mercury in Petroleum," *Fuel Process. Technol.,* Vol. 63, 2000, pp. 1–127.

[7] Bloom, N. S., "Analysis and Stability of Mercury Speciation in Petroleum Hydrocarbons," *Fresenius J. Anal. Chem.,* Vol. 366, 2000, pp. 438–443.

[8] Hwang, J. D., "Standard Practice for Sampling, Storage, and Handling of Liquid Hydrocarbons for Mercury," in ASTM ballot process.

[9] Wilhelm, S. M., Kirchgessner, D. A., Liang, L. and Kariher, P. H., "Sampling and Analysis of Mercury in Crude Oil," *J. ASTM Intl.,* Vol. 2, No. 9, 2005, ASTM International, West Conshohocken, PA, Paper ID 12985.

[10] Fox, B. S., Mason, K. J. and McElroy, F. C., "Determination of Total Mercury in Crude Oil by Combustion Cold Vapor Atomic Absorption Spectrometry," *J. ASTM Intl.,* Vol. 2, No. 9, 2005, ASTM International, West Conshohocken, PA, Paper ID 13089.

[11] Shah, K. R., Filby, R. H. and Heller, W. A., "Metals in Crude Oil by Neutron Activation Analysis," *J. Radioanal. Chem.,* Vol. 6, 1970, p. 413.

[12] Filby, R. H. and Shah, K. R., "Neutron Activation Methods for Trace Metal Analysis of Crude Oil," in *The Role of Trace Metals in Petroleum*, T. F. Yen Ed., Ann Arbor Science Publishers, Ann Arbor, MI, 1975.

[13] Liang, L., Horvat, M., Fajon, V., Proscnc, N., Li, H. and Pang, P., "Comparison of Improved Combustion/Trap Technique to Wet Extraction Methods for the Determination of Mercury in Crude Oil and Related Products by Atomic Fluorescence," *Energy & Fuels,* Vol. 17, No. 5, 2003, pp. 1175–1179.

[14] Kelly, W. R., Long, S. E. and Mann, J. L., "Determination of Mercury in Standard Reference Material Crude Oils and Refined Products by ID-CV-ICP-MS Using Closed System Combustion," *Anal. Bioanal. Chem.,* Vol. 376, 2003, pp. 753–758.

[15] Furuta, A., Sato. K., and Takabashi, K., "Trace Analysis of Mercury Compounds in Natural Gas Condensates," *Proc. Intl. Trace Anal. Symp.,* 1990, pp. 449–454.

[16] U.S. Environmental Protection Agency Method 7473, "Mercury in Solids and Solutions by Thermal Decomposition, Amalgamation, and Atomic Absorption Spectrometry."

[17] Stockwell, P. B., Corns, W. T. and Bryce, D. W., "Mercury Measurements in Fossil Fuels, Particularly Petrochemicals," *J. ASTM Intl.,* Vol. 3, No. 1, 2006, ASTM International, West Conshohocken, PA, Paper ID 12988.

[18] Stockwell, P. B., Corns, W. T. and Bryce, D. W., "Mercury Measurements: Overcoming Contamination and Interference to Enable the Correct Measurements for Valued Judgments," *Amer. Lab.,* December 2005, pp. 20–22.

[19] Stockwell, P. B., "Monitoring the Mercury Menace," *Today's Chemist at Work,* November 2003, pp. 27–28.

[20] Pfeil, D., "When U.S. EPA Method 245.7 (Determination of Mercury by Atomic Fluorescence) Is Approved, Will You Be Ready?" *Amer. Lab.,* August 2005, pp. 26–31.

[21] Pfeil, D. L., "Approval of U.S. EPA Method 245.7 for Mercury: A Simple Cost-Effective Method for Mercury at National Water Quality Criteria," *Amer. Lab.,* August 2007, p. 38.

[22] Long, S. E. and Kelly, W. R., "Determination of Mercury in Coal by Isotope Dilution Cold-Vapor Generation Inductively Coupled Plasma Mass Spectrometry," *Anal. Chem.,* Vol. 74, 2002, pp. 1477–1483.

[23] Nortje, J., "Determination of Total Mercury in Sorbent Tubes Using Direct Mercury Analysis," *Amer. Lab.,* Vol. 40, No. 4, 2008, pp. 22–23.

[24] Wilhelm, S. M., Liang, L., Cussen, D. and Kirchgessner, D. A., "Mercury in Crude Oil Processed in the United States (2004)," *Environ. Sci. Technol.,* Vol. 41, No. 13, 2007, p. 4509.

[25] Magaw, R., McMillen, S., Gala, W., Trefry, J. and Trocine, R., "Risk Evaluation of Metals in Crude Oils," SPE Paper 52725, *SPE/EPA Exploration & Production Environmental Conference,* Austin, TX, 1999.

[26] Morris, R., "New TRI Reporting Rules on Mercury," Proceedings, *National Petroleum Refiners Association Meeting,* San Antonio, TX, 2000.

[27] Hollebone, B. P., Yang, C., Lean, D., Nwobu, O. and Belletrutti, J., "Mercury in Canadian Crude Oil," *Arctic and Marine Oilspill Technical Seminar,* Vancouver, B.C., Canada, June 2006.

[28] Rahman, G. M. M., Fahrenholz, T. and Kingston, H. M., "Speciated Isotope Dilution Determination of Methyl Mercury in Fish Tissue," Preprint.

[29] Rahman, G. M. M., Fahrenholz, T. and Kingston, H. M., "Application of Speciated Isotope Dilution Mass Spectrometry to Evaluate Different Literature Methods for Mercury Speciation in Human Hair (IAEA-085)," Preprint.

[30] Shepherd, M., Shell, private communication, 2008.

22

Spectroscopic Analysis of Used Oils

R. A. Kishore Nadkarni[1]

INTRODUCTION

Usually all automobile users keep an eye on the gasoline gauge, but few pay much attention to the oil gauge until a warning light comes on the dashboard indicating that it is time to change the oil and filter. The time intervals between successive oil changes have increased from the usual 3,000 miles to nearly 10,000 miles per some manufacturers' warranties, and up to 25,000 miles for the synthetic oils.

Motor oil is about 90 % paraffinic heavy hydrocarbon base stock distilled from crude oil with the remainder being an additive package added to enhance the oil performance. Oil grades are based on a viscosity range at a standard temperature. High-molecular weight polymers (viscosity index improvers) such as polymethyl methacrylate and ethylene-propylene copolymers are added to a low-viscosity oil base stock to create multigrade oils. Advances have also been made in base stock catalytic processes that have gone a long way in improving the base stock quality, and these improved base stock qualities are in very much greater abundance. Usually oil additives are metal phenoxides. They play several roles, including acting as bases to neutralize acids that form from sulfur compounds in the oil and preventing hydrocarbon oxidation, which can lead to sludge formation. The phenoxides and their sulfates and carboxylates also serve as detergents to help solubilize or suspend soot and to carry particulates to the oil filter to be removed from the oil stream. Another key additive is antiwear agents such as zinc dialkyldithiophosphates. The zinc compounds and various amines such as diphenylamine also serve as corrosion inhibitors and antioxidants. In internal combustion engines, motor oil gets sprayed on the moving parts of the engine, forming a thin film coating on the metal surfaces. The primary role of motor oil is to reduce friction and prevent corrosion. Oil also helps dissipate heat and hold in suspension the micrometer-sized by-products of engine wear (metallic particles), soot from combustion, and oil degradation products [1–4].

Typical wear elements present in used engine oils and the engine wear they indicate are summarized in Table 1. In a normally running engine, wear metal content of the oil slowly increases due to normal wear. Trace metal analysis of such oils helps indicate mechanical wear from oil-wetted components of an engine or as a contaminant from air, fuel, and liquid coolant. Generally, these metals are present as particulates rather than in true solutions. The presence of specific metals in used oils is indicative of wearing of specific metal components in the engine. A sudden increase in the metal content of the oil sampled from an engine on a regular frequency indicates failure or

[1] *Millennium Analytics, Inc. East Brunswick, NJ*

TABLE 1—Wear Metals in Used Lubricating Oils	
Metal	**Wear Indication**
Aluminum	Piston and bearings wear, push rods, air cooler, pump housings, oil pumps, gear castings, box castings
Antimony	Crankshaft and camshaft bearings
Barium	Detergent additive, grease additive
Boron	Coolant leakage in system, coolant and grease additive
Cadmium	Bearings
Calcium	Hard water, detergent additive, oxidation inhibitor, road salt
Chlorine	Antiwear additive, extreme pressure additive
Chromium	Ring wear, cooling system leakage, chromium-plated parts in aircraft engines, cylinder liners, seal rings
Copper	Wear in bushings, injector shields, coolant core tubes, thrust washers, valve guides, connecting rods, piston rings, bearings, sleeves, bearing cages
Iron	Wear from engine block, cylinders, gears, cylinder liners, valve guides, wrist pins, rings, camshaft, oil pump, crankshaft, ball and roller bearings, rust
Lead	Bearings, fuel blowby, thrust bearings, bearing cages, bearing retainers
Magnesium	Cylinder liner, gear box housings in aircraft engines, hard water, lube oil additive
Molybdenum	Wear in bearing alloys and in oil coolers, various molybdenum-alloyed components in aircraft engines, piston rings
Nickel	Bearings, valves, gear platings, stainless steel component
Phosphorus	Antiwear additive, extreme pressure additive
Potassium	Coolant additive leakage
Silicon	Dirt intrusion from improper air cleaner, seal materials, antifoamant leakage
Silver	Wrist pin bearings in railroad and auto engines, silver-plated spline lubricating pump, solder
Sodium	Antifreeze leakage, road salt, grease additive
Tin	Bearings and coatings of connecting rods and iron pistons
Titanium	Various titanium-alloyed components in aircraft engines
Tungsten	Bearings
Vanadium	Surface coatings on piston rings, turbine impeller beds, valves
Zinc	Neoprene seals, galvanized piping, antiwear additive

excessive wear of an engine part. Such early diagnosis helps prevent catastrophic engine failure [2–4].

An area of particular interest in oil analysis is the analysis of used oils, also called in-service engine oils or condition monitoring. Engine oils analyzed on a regular basis help predict likely occurrence of engine failure, thus reducing the high cost of major overhaul and repairs of costly engines, be they in heavy duty trucks, railroad engines, bus fleets, or airplanes. Several articles describe the role engine oil analyses play in such preventive maintenance [5–7].

Usually, used oil analysis consists of determining several parameters: base number, acid number, viscosity, water, sediment, FT-IR, particle count, ferrography, metals, and so on. Despite this array of testing done on a sample, the cost of such multiparameter analysis remains at about $20 per sample! It is estimated that there are hundreds of commercial laboratories offering such services. The users are spending between $250 million and $300 million annually on the analysis of perhaps 50 million samples from some 15 million machines. The U.S. military alone spends at least $40 million a year on such analyses [8].

SAMPLING

Given the heterogeneous nature of the used oils, it is important to have a homogenous and representative sample before commencing the analysis. Otherwise the results may not be meaningful. This is particularly true for metals analysis using atomic absorption spectrometry (AAS) or inductively coupled plasma-atomic emission spectrometry (ICP-AES) techniques. Since the used oil analyses are used mainly to follow trends of oil degradation, it is not of utmost importance to obtain absolutely accurate and precise results, but only to look for sudden increase in an analyte. Because the metals are present as discrete particles of different sizes, sampling is of paramount importance to obtain accurate results.

It is important to make the sample as homogenous as possible before analysis. This can be achieved by shaking either by mechanical means or by hand for sufficient period of time (recommended 20 minutes). After this operation, aliquots should be taken out for individual analysis as soon as possible to prevent settling of suspended particulates. Inhomogeneous sampling, due to the effect of particle size of wear metals, is a big concern particularly in atomic spectroscopic analysis. Severely worn engines produce large particulates. It is more important to analyze the large particles than the small ones in such cases. An appreciable fraction of suspended metallic particles, especially large ones, may not reach the atomization source; rather they collect on the chamber walls and are washed down the drain, resulting in low biased results. It is reported that the analysis of oils containing particle sizes larger than 3 to 10 μm is not quantitative [9]. In one study, a 90 to 100 % recovery of <8-μm particles and a 70 to 100 % recovery of 9-μm particles were found [10]. Also, particulates that reach the source may not be "totally" atomized. To overcome this particle size effect, the so-called particle size independent methods have been developed; these consist of heating the oil in a small amount of mineral acids and then diluting with an appropriate organic solvent [11]. These include:

- Heating oil at 40°C for 5 min with HF + HCl while ultrasonicating and then diluting with kerosene + Neodol 91-6 mixture [12].

- Shaking the oil with HF + HNO_3 for 2 min and then diluting with MIBK [13].
- Heating the oil at 65°C for 45 min with HF + aqua regia while ultrasonicating and then diluting with MIBK + IPA [14].
- Heating the oil at 40°C for 5 min with HF + aqua regia while ultrasonicating and then diluting with MIBK + Neodol 91-6 [11].

A direct AAS or ICP-AES analysis will tend to give metal results biased low because larger metal particles will not be aspirated in the flame or plasma. Wet ashing with mineral acids as well as dry ashing has been used before converting the used oil sample into aqueous solution. However, given the extremely low price charged for such analyses, it is inconceivable that such sample preparations are used in commercial laboratories today. The dilution of samples with an organic solvent such as xylenes, MIBK, and kerosine is the most commonly used procedure.

USED OIL TESTING

Principal tests conducted on used oils are acid number, base number, viscosity, water, FT-IR, and metals by AAS or ICP-AES. Of these, only the last two categories are discussed here because they are the spectroscopic methods of analysis. At present, in the ASTM Committee D02, the only available spectroscopic methods for the analysis of used oils are the following:

- D5185 Wear metals by ICP-AES
- D6595 Wear metals by rotating disc electrode (rotrode) AES
- D7214 Oxidation by FT-IR.

Atomic Spectroscopy

Atomic spectroscopy is the main tool used for metals determination in used oils. Although for decades AAS was the main tool for such analyses, because of their simultaneous multielement detection capability, ICP-AES and rotating disc electrode emission spectrometry are now carrying out the bulk of such analyses.

The U.S. Air Force for a number of years conducted this kind of analysis on their jet engine oils under the acronym SOAP (Spectrometric Oil Analysis Program) [5]. As a result of the success of this program, the U.S. Air Force, Army, and Navy established a Joint Oil Analysis Program (JOAP) in 1976. More than 100 laboratories throughout the world are involved in these analyses using AAS, ICP-AES, and rotating disk electrode emission spectrometry. As part of the JOAP, U.S. armed forces use rotating disk electrode atomic emission spectrometry to determine iron, silver, chromium, copper, magnesium, nickel, and silicon in milligram per kilogram concentrations to diagnose an aircraft engine system, including turbine engine, compressor, transmission, and gear box. The used oil samples, of course, have to be sent back to the home bases from aircraft deployed elsewhere. To be able to perform this analysis in the field, a portable graphite furnace–atomic absorption spectrometry (GF-AAS) analyzer has been developed which determines the nine trace metals. A special sample introduction device, an air cooled furnace, compact furnace power supply, and a multielement scheme were developed to successfully use this instrument in the field by the U.S. Air Force and Navy [15].

ATOMIC ABSORPTION SPECTROMETRY

At one time AAS was the most widely used metal analysis technique throughout the world. Its ease of operation and simple instrumentation made it a quite popular technique in the oil and used oil industry. Samples and standards could be diluted with methyl isobutyl ketone (MIBK) or xylene to suitable concentration range, and simply nebulized in the flame atomic absorption spectrometer. When employing direct analysis, oil-soluble organometallic standards can be used. However, when the metals in the sample are solubilized with mineral acid digestion, aqueous standards must be used. The use of nitrous oxide plus air flame made it easier to determine more refractory elements than using air plus acetylene flame. Usual elements determined in this technique are silver, aluminum, chromium, copper, iron, magnesium, sodium, nickel, lead, silicon, tin, titanium, and zinc.

A list of analytical parameters for AAS determination of wear metals in used oils is given in Table 2, which is excerpted from Refs [2] and [16].

To overcome the drawback of a single element measurement in AAS, a new sequential AAS capable of rapid multielement measurement for up to 24 elements per sample in a single run was developed. The instrument can change the hollow cathode lamps and other instrumental parameters automatically within 2 seconds, thus allowing ten elements to be determined per minute. A sample is completely analyzed for all elements before the next sample is aspirated [17].

A thorough review of pre-1980 literature on used oil analysis using atomic spectroscopy is summarized by Sychra et al. [16].

Three sample preparation methods were compared for wear metals analysis by AAS: dry ashing, ashing with mineral acids and silica gel, and direct dilution with an organic solvent. The use of porous silica improves the dry ashing preparation and shortens the time required [18].

ROTATING DISC ELECTRODE EMISSION SPECTROMETRY

This technique with either a single spark technique or an ashing rotrode technique has been shown to rapidly provide multielement analysis of used oils. By analyzing two aliquots, one directly and one after acid dissolution, differentiation can be made between large and small wear particles [19]. A correlation has been shown to exist between ICP-AES and rotrode emission techniques. Results suggest that rotrode is somewhat more effective in sampling particulates than ICP-AES [20]. Nygaard et al. [20] and Lukas and Anderson [19] demonstrated the application of rotrode AES for wear metal analysis of used oils. Nygaard et al. found inconsistencies between ICP-AES and rotrode results attributable to differences of sample viscosities and particulates size in the used oils [20].

ASTM standard D6595 covers the determination of wear metals and contaminants in used lubricating oils or used hydraulic fluids by rotrode AES. The method is useful for a quick indication of abnormal wear and the presence of contaminants in new or used lubricants and hydraulic fluids. The method uses oil-soluble metals for calibration. It does not necessarily relate quantitatively to the values determined as insoluble particles to the dissolved metals. Low results may be obtained for those elements present as large particles. The method, however, can determine elements from dissolved materials to particles of approximately 10 μm in size.

TABLE 2—AAS Parameters for Wear Metals Determination

Element	Concentration Range, mg/kg	Wavelength, nm	Flame Used	Detection Limit, mg/kg
Aluminum	0–60	309.2	Nitrous oxide + acetylene	0.02
Barium	0–10	553.6	Nitrous oxide + acetylene	0.01
Boron	1–10	249.8	Nitrous oxide + acetylene	2
Chromium	0–8 10–40 25–100	357.9 425.4 428.9	Air + acetylene	0.005
Copper	0–8 6–25 15–60 20–80	324.7 327.4 217.9 218.2	Air + acetylene	0.001
Iron	0–10 25–100	248.3 372.0	Air + acetylene	0.01
Lead	0–20 10–40	217.0 283.0	Air + acetylene	0.02
Magnesium	0–1 5–20	285.2 202.5	Air + acetylene	0.0001
Manganese	0–10	279.2	Air + acetylene	0.005
Molybdenum	0–60	313.3	Air + acetylene	0.02
Nickel	0–12 15–60 35–140	232.0 341.5; 352.4 351.5	Air + acetylene	0.02
Silicon	5–400	251.6	Nitrous oxide + acetylene	0.2
Silver	0–10	328.1	Air + acetylene	0.002
Sodium	0–2	589.6	Air + acetylene	0.001
Tin	0–200	235.5	Nitrous oxide + acetylene	0.02
Titanium	0–350	364.3	Nitrous oxide + acetylene	0.08
Vanadium	0–20	318.5	Nitrous oxide + acetylene	0.08
Zinc	0–2	398.8; 213.9	Air + acetylene	0.003

In this test, wear metals and contaminants in the used oil sample are evaporated and excited by a controlled arc discharge using the rotating disk technique. A comparison of the emitted intensities of the elements in the sample with those of calibration standards gives the concentration of the elements in the samples. There are no spectral interferences in the analysis but there may be viscosity and particle size effects leading to biased results. The

precision given in Table 3 should be expected with the application of this method.

A similar standard based on rotrode technology is described in ASTM D6728 for the determination of contaminants in gas turbine and diesel engine fuels.

INDUCTIVELY COUPLED PLASMA – ATOMIC EMISSION SPECTROMETRY

Perhaps the widest used technology in the oil industry for metal analysis today is ICP-AES followed by X-ray fluorescence (XRF). XRF, however, is not really suitable for wear metals determination because particulate material present in the used oil sample will thoroughly bias the results. Thus, ICP-AES remains the most popular metal analysis technique today. The AAS methods described earlier have been replaced to a large extent with the ICP-AES instruments.

The wavelengths used and the detection limits achievable are summarized in Table 4 for most commonly determined elements in the used oils. Other alternate interference free wavelengths may also be used.

Almeida has described a high-throughput, high-performance ICP-AES system that can do an analysis every 30 seconds. A V-groove nebulizer made of inert polymer resistant to the solvents used and designed to handle the large particles present in the used oil samples without clogging was employed [21]. Garavaglia et al. used butanol as a diluent for the determination of boron and phosphorus in used lubricating oils by ICP-AES [22]. Ekanem et al. used sulfanilic acid as an ashing agent in the sample preparation for wear metals analysis by AAS [23]. Humphrey used energy dispersive–X-ray fluorescence (ED-XRF) to measure wear metals in the lubricant of the F104 engine on board an F-18 weapon system [24]. Prabhakaran and Jagga have compared ferrography, ICP-AES, scanning electron microscopy (SEM), and ED-XRF for their capability to study the wear particles in the lubricant of a steam turbine generator [25].

Anderau et al. showed the applicability of ICP-AES to analyze about 15 elements in NIST SRM 1085 for wear metals in lubricating oils. No special care was taken other than to dilute the oil sample with kerosine [26]. Similarly, Merryfield and Lloyd used dilution with mixed xylenes to determine about 20 elements in the used oils with an average relative standard deviation of 3.8 % [27]. These data are summarized in Table 5.

All three sets of analyses in Table 5 show excellent agreement between the NIST-certified values for these oils and the results found using ICP-AES by three different laboratories.

Table 6 shows analysis of NIST SRM 1848, a lubricant additive supplied to NIST by this author. The same material was also used in an ASTM Interlaboratory Crosscheck Program (ILCP) crosscheck ALA 9610, and in one company's internal crosschecks. The results show excellent agreement between the NIST-certified values and those obtained by using AAS (D4628), ICP-AES (D4951 and D5185), and wavelength dispersive–X-ray fluorescence (D4927) methods, a much larger number of both by laboratories in the ASTM crosscheck but a much smaller number of laboratories in the company circuit. It is interesting that a company's laboratory analyzed the same sample 6 months apart and obtained virtually the same results. The laboratories analyzed the sample the first time knowing that it was their company product. The second time they

TABLE 3—Rotrode Analysis of Wear Metals in Used Oils				
Element	**Wavelength, nm**	**Range, mg/kg**	**Repeatability, mg/kg**	**Reproducibility, mg/kg**
Aluminum	308.21	0.25–100	$0.5419\ (X + 0.57)^{0.45}$	$1.457\ (X + 0.57)^{0.45}$
Barium	230.48; 455.40	28–115	$0.0694\ X^{1.18}$	$0.1317\ X^{1.18}$
Boron	249.67	0.14–120	$0.4280\ (X + 0.1028)^{0.56}$	$0.9726\ (X + 0.1028)^{0.56}$
Calcium	393.37; 455.48	3.7–11,460	$0.1106\ (X + 2.184)$	$0.2951\ (X + 2.184)$
Chromium	425.43	0.18–152	$0.7285\ (X + 0.0557)^{0.41}$	$1.232\ (X + 0.0557)^{0.41}$
Copper	324.75; 224.26	0.47–100	$0.1631\ (X + 0.3459)^{0.85}$	$0.4386\ (X + 0.3459)^{0.85}$
Iron	259.94	4.8–210	$0.3159\ (X + 0.0141)^{0.73}$	$0.8323\ (X + 0.0141)^{0.73}$
Lead	283.31	0.43–101	$1.062\ (X + 0.6015)^{0.34}$	$1.814\ (X + 0.6015)^{0.34}$
Manganese	403.07; 294.92	0.3–117	$0.7017\ (X + 0.3534)^{0.34}$	$0.2272\ (X + 0.3534)^{0.34}$
Magnesium	280.20; 518.36	4.9–1,360	$0.1049\ X$	$0.3535\ X$
Molybdenum	281.60	0.21–100	$0.9978\ (X + 0.4795)^{0.34}$	$2.089\ (X + 0.4795)^{0.34}$
Nickel	341.48	0.35–100	$0.7142\ (X + 0.3238)^{0.40}$	$1.261\ (X + 0.3238)^{0.40}$

(*Continued*)

TABLE 3—Rotrode Analysis of Wear Metals in Used Oils (Continued)

Element	Wavelength, nm	Range, mg/kg	Repeatability, mg/kg	Reproducibility, mg/kg
Phosphorus	255.32; 214.91	52–2,572	$0.0761\ (X + 14.76)$	$0.3016\ (X + 14.76)$
Potassium	766.49	0.35–247	$0.4075\ (X + 0.1154)^{0.63}$	$1.023\ (X + 0.1154)^{0.63}$
Silicon	251.60	3.2–142	$0.4015\ (X + 0.1692)^{0.63}$	$0.8796\ (X + 0.1692)^{0.63}$
Silver	328.07; 243.78	31–102	$0.1523\ (X + 1.2)^{0.88}$	$0.4439\ (X + 1.2)^{0.88}$
Sodium	588.89; 589.59	3.6–99.6	$0.1231\ (X - 2.674)$	$0.1075\ (X + 26.36)$
Tin	317.51	30–139	$0.6777\ (X + 0.6578)^{0.45}$	$0.7967\ (X + 0.6578)^{0.45}$
Titanium	334.94	6.8–103	$0.5831(X + 0.9304)^{0.5}$	$0.9682\ (X + 0.9304)^{0.5}$
Vanadium	290.88; 437.92	2.1–101	$0.6389\ (X + 0.8418)^{0.41}$	$1.983\ (X + 0.8418)^{0.41}$
Zinc	213.86	5.3–1,345	$0.2031\ (X + 1.553)^{0.87}$	$0.5881\ (X + 1.553)^{0.87}$

Note: X is the mean concentration in milligrams per kilogram.

TABLE 4—Analytical Parameters Used for Used Oil Analysis by ICP-AES

Element	Wavelength Used, nm	Detection Limit, mg/L
Aluminum	308.215; 396.15; 309.27	0.021
Barium	233.53; 455.40; 493.41	0.01
Boron	208.959; 249.77	0.04
Calcium	422.673; 315.89; 317.93; 364.44	0.026
Chromium	267.716; 205.55	0.003
Copper	324.754	0.0021
Iron	259.940; 238.20	0.018
Lead	220.353	0.086
Magnesium	279.079; 279.55; 285.21	0.05
Manganese	204.920; 257.61; 293.31; 293.93	0.002
Molybdenum	204.598; 202.03; 281.62	0.043
Nickel	341.476; 231.60; 227.02; 221.65	0.07
Phosphorus	214.914; 177.51; 178.29; 213.62; 253.40	0.07
Potassium	766.49	0.030
Silicon	212.412; 288.16; 251.61	0.027
Silver	328.07	0.002
Sodium	589.59	0.001
Sulfur	180.73; 182.04; 182.62	0.0030
Tin	283.999; 189.99; 142.95	0.04
Titanium	337.28; 350.50; 334.94	0.03
Vanadium	292.40; 309.31; 310.23; 311.07	0.06
Zinc	213.856; 202.55; 206.20; 334.58; 481.05	0.0036

analyzed it as an ASTM ILCP sample not knowing that it was the same material as before. They did not know that it was the same sample as the one analyzed 6 months earlier, that it was their company product that many of these plant laboratories routinely analyzed. Thus, overall it is an excellent example of repeating the original results 6 months later as a blind crosscheck. It is a testimony to the fact that well-managed laboratories with active calibration and quality control practices can obtain results better than other laboratories [28]. Thus, all four spectroscopic techniques can be used with confidence for such metal analysis in fresh and used oils.

TABLE 5—Analysis of NIST SRMs by ICP-AES for Wear Metals

	SRM 1085 (mg/kg)		SRM 1634 (mg/kg)		SRM 1848 (m%)	
Element	Certified	Found (26)	Certified	Found (27)	Certified	Found (28)
Al	(289)	290 ± 3.2				
B					0.136 ± 0.013	0.137 ± 0.016
Ca					0.345 ± 0.011	0.355 ± 0.070
Cr	296.3 ± 3.3	289 ± 1.6				
Cu	295.1 ± 6.8	303 ± 3.8				
Fe	296.8 ± 2.7	304 ± 2.2	13.5 ± 1.0	13.0		
Mg	296.0 ± 3.1	296 ± 3.1			0.821± 0.058	0.818 ± 0.081
Mn			(0.12)	< 0.3		
Mo	293 ± 2.5	299 ± 2.2				
Ni	302.9 ± 6.8	302 ± 2.3	36 ± 4	36.7		
P					0.779 ± 0.036	0.794 ± 0.016
Pb	297.4 ± 9.6	302 ± 9.0	0.041 ± 0.005	<0.5		
S					2.327 ± 0.0043	2.28 ± 0.02
Si	(322)	295 ± 7.1			50 ± 2	52 ± 5 (mg/kg)
Sn	296.0 ± 13.4	293 ± 3.0				
V			320 ± 15	314		
Zn			0.23 ± 0.05	<0.6	0.866 ± 0.034	0.859 ± 0.081

Several papers have compared ICP-AES with AAS [29–31] or spark rotating disk electrode [30,31] methods for wear metals analysis and have found them to produce equivalent results. A round robin between 27 laboratories using these 3 methods found excellent data agreement between them [31]. Generally, xylene, MIBK, or kerosine dilutions have been employed in ICP-AES [32,33]. Smith cautions that wear metal oil samples diluted in xylene should be analyzed within 4 h [34]. After 24 h, a decrease of ~10 % is observed in the wear metals concentrations.

ASTM test method D5185-09 is the primary ICP-AES method for a large number of wear metals in used (as well as fresh) lubricating oils. It can also be used to determine contaminants in these and base oils. The method D5185 is very similar in technology to the other ASTM ICP-AES method D4951 used for the determination of additive elements in fresh oils. The oils are diluted tenfold with an organic solvent such as mixed xylenes or other appropriate hydrocarbon solvents and nebulized in the plasma. Oil-soluble organometallic elemental standards are used for calibration of the instrument. An optional internal

TABLE 6—Multielement Multitechnique Analysis of NIST SRM 1848 Lube Oil

ELEMENT, m %	NIST VALUE (METHOD)	D4628 (AAS)	D4927 (WD-XRF)	D4951 (ICP-AES)	D5185 (ICP-AES)	COMPANY 4/1996	COMPANY 10/1996
Boron	0.136 ± 0.013 (PGAA; ICP-AES)				0.1333 ± 0.0067	0.137 ± 0.061 (36)	0.1330 ± 0.003 (4)
Calcium	0.345 ± 0.011 (XRF; ICP-AES)	0.3584 ± 0.0152	0.3515 ± 0.0057	0.3569 ± 0.0112		0.355 ± 0/009 (52)	0.356 ± 0.009 (4)
Magnesium	0.821 ± 0.058 (XRF; ICP-AES)	0.8197 ± 0.027		0.8255 ± 0.025	0.8379 ± 0.022	0.818 ± 0.013 (48)	0.826 ± 0.011 (12)
Phosphorus	0.779 ± 0.036 (XRF; ICP-AES)		0.7813 ± 0.0141	0.7785 ± 0.0179	0.7873 ± 0.024	0.794 ± 0.015 (32)	0.776 ± 0.011 (9)
Sulfur	2.327 ± 0.0043 (IDTMS)		2.354 ± 0.0412	2.358 ± 0.0793	2.394 ± 0.1104	2.28 ± 0.07 (24)	2.34 ± 0.04 (6)
Silicon, mg/kg	50 ± 2 (XRF)				47 ± 9	52 ± 12 (28)	48 ± 6 (3)
Zinc	0.866 ± 0.034 PGAA; ICP-AES	0.8471 ± 0.0232	0.8585 ± 0.0722	0.8422 ± 0.0154	0.8467 ± 0.0203	0.859 ± 0.012 (52)	0.842 ± 0.021 (12)

Results are given in mean value ± standard deviation (number of valid results). The results of D4628, D4927, D4951, and D5185 are excerpted from ASTM ILCP report of ALA 9610.

standard may be used to compensate for the variations in the sample introduction efficiency. Earlier discussion about the particle size of wear metals is very true for these test methods, and the presence of large particles in the sample can lead to low biased results. Use of a high-solids nebulizer can help minimize this effect. The precision of analysis using D5185 test method is given in Table 7.

D6595-00(05) uses rotrode AES to determine a number of wear metals and contaminants in the used lubricating oils or hydraulic fluids.

ICP-mass spectrometry has been proposed as a sensitive tool for the determination of environmentally important elements in used oils. The technique has detection limits of parts per billion and needs no sample preparation other than solvent dilution. However, because of the matrix interference and formation of polyatomic species, it lacks the precision and accuracy of other atomic spectroscopy techniques [35].

Finally, a comparison of four atomic spectroscopic techniques for wear metals determination of used oils is given in Table 8. It is clear that despite its higher price tag, from a capability point of view, ICP-AES is a faster, more precise, and better technique than AAS or rotrode.

Fourier-Transform Infrared Spectroscopy

Chemical analysis by FT-IR is a powerful tool in petrochemicals research and quality control. This topic is described in detail in a separate chapter in this monograph by Dr. James M. Brown. Here only the applications of this technique to used oil analysis are described. FT-IR has been used in two areas of interest in characterizing the used oils: determination of chemical transformations in the sample and as an alternative method for acid or base-number determinations in oils.

A number of chemical entities in the sample can be identified with FT-IR. These moieties and their characteristic wavelengths are as follows:

- Fuel dilution, 815 to 805 cm^{-1}
- Glycol, 1,130 to 1,099 cm^{-1}
- Nitration, 1,650 to 1,600 cm^{-1}
- Oxidation, 1,798 to 1,670 cm^{-1}
- Soot loading, 2,000 cm^{-1}
- Sulfation, 1,180 to 1,120 cm^{-1}
- Water, 3,500 to 3,150 cm^{-1}

In a method for determining oxidation of used lubricants by FT-IR using peak area increase (PAI) calculation, the technique measures the concentration change of constituents containing a carbonyl function that have formed during the oxidation of the lubricant. The method, designated as ASTM D7214 standard, was developed for transmission oils that have been degraded either in service or in a laboratory test. It can also be used for other in-service oils. The PAI is representative of the quantity of all the compounds containing a carbonyl function that have formed by the oxidation of the lubricant (e.g., aldehydes, ketones, carboxylic acids, esters, anhydrides).

The results of this test can be affected by the presence of other compounds with an absorption band in the zone of 1,600 to 1,800 cm^{-1}. Low PAI values may be difficult to determine in such cases. Some specific cases (very viscous oil, use of ester as base stock, high soot content) may require a dilution of the

TABLE 7—Precision of ASTM D5185 Test Method for Wear Metals in Used Oils by ICP-AES

Element	Concentration Range, mg/kg	Repeatability, μg/g	Reproducibility, μg/g
Aluminum	6–40	$0.71\ X^{0.41}$	$3.8\ X^{0.26}$
Barium	0.5–4	$0.24\ X^{0.66}$	$0.59\ X^{0.92}$
Boron	4–30	0.26 X	$13\ X^{0.01}$
Calcium	4−9,000	$0.0020\ X^{1.4}$	$0.015\ X^{1.3}$
Chromium	1–40	$0.17\ X^{0.75}$	$0.81\ X^{0.61}$
Copper	2–160	$0.12\ X^{0.91}$	0.24 X
Iron	2–140	$0.13\ X^{0.80}$	$0.52\ X^{0.80}$
Lead	10–160	$1.6\ X^{0.32}$	$3.0\ X^{0.36}$
Magnesium	5–1700	$0.16\ X^{0.86}$	$0.72\ X^{0.77}$
Manganese	5–700	$0.010\ X^{1.3}$	$0.13\ X^{1.2}$
Molybdenum	5–200	$0.29\ X^{0.70}$	$0.64\ X^{0.71}$
Nickel	5–40	$0.52\ X^{0.49}$	$1.5\ X^{0.50}$
Phosphorus	10–1,000	$1.3\ X^{0.58}$	$4.3\ X^{0.50}$
Potassium	40–1,200	$3.8\ X^{0.33}$	$6.6\ X^{2.9}$
Silicon	8–50	$1.3\ X^{0.26}$	$2.9\ X^{0.39}$
Silver	0.5–50	$0.15\ X^{0.83}$	0.35 X
Sodium	7–70	$0.49\ X^{0.66}$	$1.1\ X^{0.71}$
Sulfur	900–6,000	$0.49\ X^{0.81}$	$1.2\ X^{0.75}$
Tin	10–40	$2.4\ X^{0.17}$	$2.1\ X^{0.62}$
Titanium	5–40	$0.54\ X^{0.37}$	$2.5\ X^{0.47}$
Vanadium	1–50	0.061 X	$0.28\ X^{1.1}$
Zinc	60–1,600	$0.15\ X^{0.88}$	$0.083\ X^{1.1}$

Note: X is the mean concentration in micrograms per gram.

sample and a specific area calculation. The presence of soot degrades the spectra by decreasing the transmittance level. This may require a dilution in order to obtain an absorbance lower than 1.5. The presence of esters may also require a dilution and use of a smaller path length (0.05 mm maximum).

FT-IR spectra of the fresh and of used oils are recorded in a transmission cell of known path length. Both spectra are converted to absorbance mode and then subtracted. Using this resulting differential spectrum, a baseline is set under the peak corresponding to the carbonyl region around 1,650 cm^{-1} and

TABLE 8—Atomic Spectrometric Methods for Elemental Analysis of Used Oils

Method	Scope	Elements Analyzed	Advantages	Drawbacks	Other
AAS	Lube oils & additives	Ba, Ca, Mg, Zn	Simple single-element	One element at a time	
D4951 ICP-AES	Lube oils & additives	B, Ba, Ca, Cu, Mg, Mo, P, S, Zn	– Multielement simultaneous determination – No spectral interference – Minimal sample preparation	– Viscosity index improver effect – Must match viscosities – Cost	Use of internal standard mandatory
D5185 ICP-AES	Used lube oils & base oils	Ag, Al, B, Ba, Ca, Cr, Cu, Fe, K, Pb, Mg, Mn, Mo, Ni, P, S, Si, Sn, Ti, V, Zn	– Multielement simultaneous determination – No spectral interference – Minimal sample preparation	– Viscosity index improver effect – Must match viscosities – Particulate bias – Cost	– Use of internal standard optional – Babington type high solids nebulizer useful
D6595 Rotrode	Used lube oils & hydraulic fluids/oils	Ag, Al, B, Ba, Ca, Cr, Cu, Fe, K, Li, Mg, Mn, Mo, Na, Ni, P, Pb, Si, Sn, Ti, W, V, Zn	– Multielement simultaneous determination – No spectral interferences	– Must match viscosities	

1,820 cm^{-1}, and the area created by this baseline and the carbonyl peak is calculated. The area of the carbonyl region is divided by the cell path length in millimetres, and this result is reported as the PAI.

This method has been found to have a repeatability of 0.029 (X + 9) and a reproducibility of 0.26 (X + 35), where X is the average of two results.

In work done at McGill University in Quebec, Canada, an FT-IR method has been proposed as an alternative to ASTM acid and base number methods D664, D974, D2896, D4739 [36–39]. It allows the determination of acid number (up to 5 mg KOH/g oil) and base number (up to 20 mg KOH/g oil) in lubricating oils. The cornerstone of the methodology is the use of a signal transduction reagent, which allows the various acids or bases present in the sample to be quantitated by measurement of a single IR signal associated with the added reagent, and the use of differential spectroscopy to eliminate the spectral features of the oil that could interfere with the measurement of the signal.

The signal transduction is effected through acid/base reactions, a suitable signal transduction reagent being a species whose un-ionized and ionized forms can be clearly distinguished and accurately quantitated in the 2,100 to 1,600 cm^{-1} region of the mid-IR spectrum (trifluoroacetic acid and potassium phthalimide). The latter region corresponds to a spectral window that is free of intense oil absorptions, except for ester-based fluids.

The precision of FT-IR acid and base number methods has been shown to be comparable to or better than that of the standard ASTM potentiometric and colorimetric methods. The validation results obtained in the study for a wide variety of new and used oils, including both hydrocarbon- and ester-based oils, trended titrimetric acid and base number values relatively well. The FT-IR methods use small amounts of an innocuous solvent iso-propanol and minimal amounts of reagent, sample preparation requires no special skills, and the time required is about 5 min/sample; once prepared, approximately 50 samples/h can be analyzed with the use of an autosampler [36–39].

In a recently prepared document based on ASTM Standard Practice E2412, Standard Practice for Condition Monitoring of Used Lubricants by Trend Analysis Using FT-IR Spectrometry, the D02 standard D7418 provides specific instrument settings and FT-IR spectral acquisition protocols to be used for various in-service oil conditioning monitoring parameter test methods.

The measurement and data interpretation parameters are standardized to allow operators of different FT-IR spectrometers to obtain comparable results by employing the same techniques. Two approaches can be used to monitor in-service oil samples by FT-IR spectrometry:

1. Direct trend analysis involving measurements made directly on in-service oil samples without reference to the base oil formulation, and
2. Differential (spectral subtraction) trend analysis involving measurements obtained after the spectrum of a reference oil has been subtracted from the spectrum of the in-service oil being analyzed.

Either of these two approaches may be used as appropriate for determining parameters such as oxidation, nitration, soot, water, ethylene glycol, fuel dilution, gasoline dilution, sulfate by-products, and phosphate antiwear additives. Changes in the values of these parameters over operating time can then be used to help diagnose the operational condition of various machinery and equipment and to indicate when an oil change should take place. This practice

is intended to give a standardized configuration for FT-IR instrumentation and operating parameters employed in in-service oil condition monitoring to obtain comparable between-instrument and between-laboratory data. Other work in this area can be found in Refs [40] through [44].

INTERLABORATORY CROSSCHECK PROGRAMS

There are probably hundreds of small and large laboratories in the industry which are engaged in analysis of used oil samples. Although absolute values are not required in this type of analyses, but only the relative trends in concentrations of the parameters determined, to bring some consistency in this business, several years back ASTM Committee D02 initiated a Proficiency Testing Program (PTP). Details of this project are described elsewhere [45]. There are two programs in the used oil area: an In-Service Diesel Oil (ISDO) analysis interlaboratory crosscheck program for several analytes normally determined in the used oils, and a similar In-Service Hydraulic Fluids and Oils (ISHF) program. Each program is conducted three times a year, with each participating laboratory being supplied with a 250 mL sample and a set of tests to be performed. The current tests included in these programs are listed in Table 9.

TABLE 9—ASTM Interlaboratory Crosscheck Programs for Used Oils

Analysis	ISDO	ISHF
Acid number	D664; D974	D664
Additive elements[a]	D6481	...
Houillion viscosity	D7279	...
Wear metals[a]	D5185; D6595	D4951; D5185; D6595
Base number	D974; D2896	D974; D2896; D4739
Fuel dilutions	D3524	...
Flash point	D92; D93; D3828	D92; D93; D6450
FT-IR[a]	Fuel dilution; glycol, insolubles; nitration; oxidation; sulfation; soot loading; water	...
Glycol	D2982; D4291	D2982; D4291
Insolubles	D893; D4055	
Particle count	Any method	Any method
Kinematic viscosity	D445	
Water	D95; D1744; D6304	D95; D1744; D6304
Boiling point distribution	...	D2887

[a]Spectroscopic method.

TABLE 10—Elemental Analysis of Used Oil ILCP Samples by Spectroscopic Methods

Analysis	Test Method	IHFO 0711	ISDO 0707	ISDO 0711
Aluminum	D5185	0.04 ± 0.06 (10)	4.12 ± 2.65 (49)	1.58 ± 0.45 (37)
Boron	D5185	3.90 ± 2.66 (9)	103.4 ± 11.6 (36)	1.10 ± 0.97 (31)
Boron	D6595		98.0 ± 9.9 (16)	
Calcium	D5185	2.72 ± 2.40 (10)	3261 ± 202 (42)	1196 ± 58 (37)
Calcium	D6595	4.8 ± 0.9 (2)	3235 ± 365 (19)	1153 ± 134 (17)
Chromium	D5185	0.10 ± 0.11 (12)	0.55 ± 0.46 (41)	0.39 ± 0.34 (34)
Copper	D5185	0.45 ± 0.47 (12)	1.07 ± 0.11 (39)	0.69 ± 0.42 (37)
Iron	D5185	0.17 ± 0.24 (11)	21.7 ± 1.9 (47)	13.5 ± 0.95 (41)
Iron	D6595		25.2 ± 2.6 (19)	16.1 ± 1.5 (16)
Magnesium	D5185		54.3 ± 6.6 (42)	823 ± 46 (38)
Magnesium	D6595		69.2 ± 9.3 (18)	774 ± 79 (15)
Molybdenum	D6595		194.7 ± 31.6(19)	1.65 ± 1.80 (8)
Molybdenum	D5185		201.4 ± 15.5(44)	0.32 ± 0.39 (31)
Phosphorus	D4951	590 ± 10 (3)		
Phosphorus	D5185	596.5 ± 33.9 (11)	1216 ± 85 (42)	1083 ± 70 (38)
Phosphorus	D6595	672 ± 113 (2)	1254 ± 93 (17)	1147 ± 62 (16)
Potassium	D5185	0.77 ± 0.90 (10)	1.83 ± 1.13 (29)	0.65 ± 0.84 (25)
Sulfur	D5185		4678 ± 542 (16)	3101 ± 430 (13)
Zinc	D4951	13 ± 5 (3)		
Zinc	D5185	13.1 ± 2.7 (9)	1436 ± 86 (42)	1231 ± 88 (39)
Zinc	D6595		1474 ± 120 (20)	1265 ± 91 (17)

All results are in mg/kg and are expressed as robust mean value ± robust standard deviation (number of results).

Since many/most commercial laboratories, to remain cost-effective, do not strictly follow the ASTM standard test methods or the required calibration and quality control practices, it would be interesting to see how well different laboratories agree with each other, or how well the precision obtained in these crosschecks compares with those given in the ASTM test methods. Examples of the data obtained by spectroscopic methods in these crosschecks are given in Table 10. Since at present there is no standardized procedure for chemical state quantitation by FT-IR, data on such analysis are collected in these programs but are not statistically analyzed. Hence, Table 10 contains data only on the metal analysis using ICP test methods D4951 and D5185, and rotrode test

method D6595. Coordinating Subcommittee D02.CS 96 has initiated work on the use of FT-IR technique for the determination of a number of properties in used oils or in-service oils. These new test methods include:

D7214	Determination of Oxidation of Used Lubricants by FT-IR Using Peak Area Increase Calculation
D7371	Determination of Biodiesel (Fatty Acid Methyl Esters) Content in Diesel Fuel Oil Using Mid Infrared Spectroscopy
D7412	Condition Monitoring of Phosphate Antiwear Additives in In-Service Petroleum and Hydrocarbon Based Lubricants by Trend Analysis Using FT-IR Spectrometry
D7414	Condition Monitoring of Oxidation in In-Service Petroleum and Hydrocarbon Based Lubricants by Trend Analysis Using FT-IR Spectrometry
D7415	Condition Monitoring of Sulfate By-Products in In-Service Petroleum and Hydrocarbon Based Lubricants by Trend Analysis Using FT-IR Spectrometry
D7417	Analysis of In-Service Lubricants Using Particular Four-Part Integradted Tester (AES, IR, Viscosity, and Laser Particle Counter)
D7418	Practice for Setup and Operation of FT-IR Spectrometers for In-Service Oil Condition Monitoring
D7624	Condition Monitoring of Nitration in In-Service Petroleum and Hydrocarbon Based Lubricants by Trend Analysis Using FT-IR Spectrometry, and
E2412	Practice for Condirion Monitoring of In-Service Lubricants by Trend Analysis Using FT-IR Spectrometry

However, in the area of other molecular species in used oils, ASTM D02.CS 96 has recently developed several new standard test methods based on FT-IR technology. Of these, D7214 test method has been discussed above.

Test Method D7371 determines biodiesel (fatty ester methyl esters) in diesel fuel oils. It is applicable to concentrations from 1.00 to 20 v %. This procedure is applicable only to FAME. Biodiesel in the form of fatty acid ethyl ester (FAEE) will cause a negative bias. In this method, a sample of diesel fuel, biodiesel, or biodiesel blend is introduced into a liquid attenuated total reflectance (ATR) sample cell. A beam of infrared light is imaged through the sample onto a detector, and the detector response is determined. Wavelengths of the absorption spectrum that correlate highly with biodiesel or interferences are selected for analysis. A multivariate mathematical analysis converts the detector response for the selected areas of the spectrum from an unknown to a concentration of biodiesel. This test method uses Fourier transform mid-IR spectrometer with an ATR sample cell. The absorption spectrum is used to calculate the partial least square (PLS) calibration algorithm. The hydrocarbon composition of diesel fuel has a significant impact on the calibration model. Therefore, for a robust calibration model, it is important that the diesel fuel in the biodiesel fuel blend is represented in the calibration set. This test method can have interferences from water vapor, FAEE, or undissolved water. Proper choice of instrument, design of calibration matrix, utilization of multivariate calibration

techniques, and evaluation routines as described in the test method standard can minimize interferences. The precision of this test method is as follows:

Repeatability	0.01505 (X + 14.905) v %
Reproducibility	0.04770 (X + 14.905) v %
Where X is the biodiesel concentration determined.	

Test Method D7412 determines phosphate antiwear additives in-service lubricants using FT-IR spectrometry. Typical phosphate antiwear additives include zinc dialkyldithiophosphates, trialkyl phosphates, and triaryl phosphates. This test method is based on trending of spectral changes associated with phosphate antiwear additives in in-service lubricants. Warnings of alarm limits can be set on the basis of a fixed minimum value for a single measurement or, alternatively, can be based on a rate of change of the response measured. High levels of glycol and ester based additives or contaminants, or both, can interfere with the measurement of phosphate antiwear additives.

Test Method D7414 determines oxidation in in-service lubricants using FT-IR spectrometry. It measures build-up of oxidation products in the oils produced as a result of normal machinery operation.

Test Method D7415 determines sulfate by-products in in-service lubricants using FT-IR spectrometry. Sulfate by-products can result from the introduction of sulfur from combustion or from the oxidation of sulfur-containing base oil additives. There can be a number of interferences from other additive packages added, contaminants, and other oxidation by-products.

Test Method D7417 covers the quantitative analysis of in-service lubricants using an automatic testing device that integrates these varied technologies: atomic emission spectrometry, infrared spectrometry, viscosity, and particle counting. Up to nineteen trace elements in the range 5 to 1,000 ppm, as well as water, glycol, soot, fuel dilution, oxidation, nitration, and base number can be determined by this test method.

Standard Practice D7418 describes the instrument set-up and operation parameters for using FT-IR spectrometers for in-service oil condition monitoring for both direct trend analysis and differential trend analysis approaches. The following parameters are typically monitored for petroleum and hydrocarbon based lubricants: water, soot, oxidation, nitration, phosphate anti-wear additives, fuel dilution, sulfate by-products and ethylene glycol.

Test Method D7590 describes a method for measuring remaining primary antioxidant content in in-service industrial lubricating oils by linear sweep voltametry.

Test Method D7624 describes condition monitoring of nitration in in-service lubricants by trend analysis using FT-IR. Direct trend analysis or differential trend analysis can be used.

Standard Practice E2412 describes condition monitoring of used lubricants by trend analysis using FT-IR spectrometry. Periodic samples are acquired from the engine or machine being monitored. An IR absorbance spectrum of the sample is acquired, typically covering the range of 4,000 to 550 cm^{-1}, with sufficient signal-to-noise ratio to measure absorbance areas of interest.

The precision obtainable for various FT-IR test methods described above is summarized in Table 11.

TABLE 11—Precision for FT-IR Methods for Used Oil Analysis			
Test Method Standard	**Repeatability**	**Reproducibility**	**Research Report**
D7412 A	0.53	NA	RR-DO2-1667
D7412 B	0.57	NA	RR-D02-1667
D7414 A	0.68	NA	RR-D02-1668
D7414 B	0.70	NA	RR-D02-1668
D7415 A	0.30	NA	RR-D02-1669
D7415 B	0.31	NA	RR-D02-1669
D7417	See the test method		RR-D02-1702
D7624	0.078	NA	
All vales are in absorbance units/0.100 nm. Procedure A is for direct trend analysis. Procedure B is for differential trend analysis			

SUMMARY

Analysis of used oil to identify metal contaminants and other species in the used lubricating oils is a thriving business. A number of alternate techniques are employed for this task. Often it is not the precision of the analysis but the trend that successive used oil samples obtained from the same source that is of interest to the oil producers as well as the users of the machinery equipment.

References

[1] Ritter, S., "Motor Oil," *Chem. Engin. News*, March 13, 2006, pp. 38.

[2] Nadkarni, R. A., "Occurrence and Significance of Trace Metals in Petroleum and Lubricants," in *Modern Instrumental Methods of Elemental Analysis of Petroleum Products and Lubricants*, *ASTM STP 1109*, R. A. Nadkarni, Ed., STP 1109 ASTM International, West Conshohocken, PA, 1989.

[3] Nadkarni, R. A., "Elemental Analysis," in *Fuels and Lubricants Handbook*, G. E. Totten, S. R. Westbrook, and R. J. Shah, Eds., ASTM International, West Conshohocken, PA, 2003, Chapter 26, p. 707.

[4] Nadkarni, R. A., "Advances in Elemental Analysis of Hydrocarbon Products," in *Analytical Advances for Hydrocarbon Research*, C. S. Hsu, Ed., Kluwer Academic/Plenum Publishers, New York, Chapter 2, 2003, pp. 1-27.

[5] Eisentraut, K. J., Newman, R. W., Saba, C. C., Kauffman, R. E. and Rhine, W. E., "Spectrometric Oil Analysis: Detecting Engine Failures before They Occur," *Anal. Chem.*, Vol. 56, 1984, p. 1086A.

[6] Leugner, L., "Putting Used Oil Analysis to Work," *Lubes 'N' Greases*, May 1997, p. 20.

[7] Thomas, R. J., "Oil Analysis Prevents Paralysis," *Today's Chemist at Work*, Vol. 9, No. 10, 2000, p. 53.

[8] Carnes, K., "Measure by Measure," *Lubricants World,* June 2001, p. 13.

[9] Saba, C. S., Rhine, W. E. and Eisentraut, K. J., *Anal. Chem.,* Vol. 53, 1981, p. 1099.

[10] Klentschi, N., *Mater. Technol.,* Vol. 12, 1984, p. 3.
[11] Kauffman, R. E., Saba, C. S., Rhine, W. E. and Eisentraut, K. J., *Anal. Chem.,* Vol. 54, 1982, p. 975.
[12] Nygaard, D. D., Chase, D. S. and Leighty, D. A., *Instrumentation Lab Applic. Note,* AID 183.
[13] Saba, C. S. and Eisentraut, K. J., *Anal. Chem.,* Vol. 51, 1979, p. 1927.
[14] Brown, J. R., Saba, C. S., Rhine, W. E. and Eisentraut, K. J., "Particle Size Independent Spectrometric Determination of Wear Metals in Aircraft Lubricating Oils," *Anal. Chem.,* Vol. 52, 1980, p. 2365.
[15] Niu, W., Haring, R. and Newman, R., "A Multielement Furnace AA Spectrometer for Wear Metals Analysis," *Amer. Lab.,* Vol. 19, No. 11, 1987, p. 40.
[16] Sychra, V., Lang, I. and Sebor, G., "Used Lubricating Oil Analysis," *Progr. Anal. At. Spectr.,* Vol. 4, 1981, p. 381.
[17] Carter, J. M., Batie, W. and Bernhard, A. E., "Automated Rapid Multielement Analysis of Oils for Wear Metals by Flame Atomic Absorption Using a Single Aspiration per Sample," *Modern Instrumental Methods of Elemental Analysis of Petroleum Products and Lubricants*, *ASTM STP 1109*, R. A. Nadkarni, Ed., ASTM International, West Conshohocken, PA, 1991, p. 70.
[18] Barbooti, M. M., Zaki, N. S., Baha-Uddin, S. S. and Hassan, E. B., "Use of Silica Gel in the Preparation of Used Lubricating Oil Samples for the Determination of Wear Metals by Flame Atomic Absorption Spectrometry," *Analyst,* Vol. 115, 1990, p. 1059.
[19] Lukas, M. and Anderson, D. P., "Techniques to Improve the Ability of Spectroscopy to Detect Large Wear Particles in Lubricating Oils," *Modern Instrumental Methods of Elemental Analysis of Petroleum Products and Lubricants*, *ASTM STP 1109,* R. A. Nadkarni, Ed., ASTM International, West Conshohocken, PA, 1991, p. 83.
[20] Nygaard, D., Bulman, F. and Alvosus, T., "Correlation Between Inductively Coupled Plasma and Rotating Disk Electrode Spark Emission Spectrometry for Used Diesel Engine Oils," *Modern Instrumental Methods of Elemental Analysis of Petroleum Products and Lubricants*, *ASTM STP 1109,* R. A. Nadkarni, Ed., ASTM International, West Conshohocken, PA, 1991, p. 77.
[21] Almeida, M., "High-Throughput/High-Performance Wear Metal Analysis Using ICP," *Amer. Lab.,* Vol. 32, No. 16, 2000, p. 52.
[22] Garvaglia, R. N., Rodriguez, R. E. and Bastioni, D. A., *Fresneius' J. Anal. Chem.,* Vol. 360, 1998, p. 683.
[23] Ekanem, E. J., Lori, J. A. and Thomas, S. A., *Talanta*, Vol. 44, 1997, p. 2103.
[24] Humphrey, G. R., *Lubr. Engr.,* Vol. 55, No. 10, 1999, p. 19.
[25] Prabhakaran, A. and Jagga, C. R., *Tribol. Int.,* Vol. 32, No. 3, 1999, p. 145.
[26] Anderau, C., Fredeen, K., Thomsen, M. and Yates, D., "Analysis of Wear Metals in Oil," ICP Application Studies 65, Perkin Elmer, Norwalk, CT, 1992.
[27] Merryfield, R. N. and Lloyd, R. C., "Simultaneous Determination of Metals in Oil by ICP-AES," *Anal. Chem.,* Vol. 51, 1979, pp. 1965–1968.
[28] Nadkarni, R. A., "Zen and the Art (or Is It Science) of a Perfect Analysis," *J. ASTM Intl.,* Vol. 2, No. 3, West Conshohocken, PA, 2005, Paper ID JAI12964.
[29] Mckenzie, T., "Atomic Absorption Spectrophotometry for the Analysis of Wear Metals in Oil Samples," Varian AA 10 Note, Varian Techtron, Palo Alto, CA, January 1981.
[30] Varnes, A. W. and Andrews, T. E., *Jarrell-Ash Olasma Newsletter,* Vol. 1, No. 1, 1978, p. 12.
[31] Allied Analytical Systems, ICP Application Note, 1985.
[32] Fassel, V. A., Peterson, C. A., Abercrombie, F. N. and Kniseley, R. A., *Anal. Chem.,* Vol. 48, 1976, p. 516.
[33] Ward, A. F. and Marciello, L., "Analysis of Energy Resources by ICAP Spectroscopy: Part II Petroleum Products," *Jarrell-Ash Plasma Newsletter*, Vol. 1, No. 4, 1978, p. 10.

[34] Smith, J. C., *Jarrell-Ash Plasma Newsletter,* Vol. 2, No. 3, 1979, p. 4.

[35] Williams, M. C., "Elemental Analysis of Waste Oils by Inductively Coupled Plasma Mass Spectrometry," *Modern Instrumental Methods of Elemental Analysis of Petroleum Products and Lubricants*, *ASTM STP 1109*, R. A. Nadkarni, Ed., ASTM International, West Conshohocken, PA, 1991, p. 96.

[36] Dong, J., Van de Voort, F. R., Yaylayan, V., Ismail, A. A., Pinchuk, D. and Taghizadeh, A., "Determination of TBN in Lubricating Oils by Mid-FTIR Spectroscopy," *Lubr. Engin.*, November 2001, pp. 24–30.

[37] Van de Voort, F. R., Pinchuk, D., Davies, M. and Taghizadeh, A., "FTIR Acid and Base Number Analysis: Their Potential to Replace ASTM Methods," *JOAP Conf.*, Mobile, AL, April 2002.

[38] Van de Voort, F. R., Sedman, J. and Pinchuk, D., "Acid and Base Number Analysis by FT-IR Spectroscopy," ASTM D02.CS 76 Meeting, June 18, 2002.

[39] Van de Voort, F. R., Sedman, J., Yaylayan, V. and Saint Laurent, C., "Determination of Acid Number and Base Number in Lubricants by FT-IR Spectroscopy," *Appl. Spec.*, Vol. 57, No. 11, 2003, pp. 1425–1431.

[40] ASTM D7371, "Test Method for Determination of Biodiesel (Fatty Acid Methyl Esters) Content in Diesel Fuel Oil Using Mid Infra-Red Spectroscopy," *Annual Book of ASTM Standards*, ASTM International, West Conshohocken, PA, 2007.

[41] ASTM D7412, "Test Method for Condition Monitoring of Phosphate Antiwear Additives in In-Service Petroleum and Hydrocarbon Based Lubricants by Trend Analysis Using Fourier Transform Infrared Spectrometry," *Annual Book of ASTM Standards*, ASTM International, West Conshohocken, PA, 2009.

[42] ASTM D7414, "Test Method for Condition Monitoring of Oxidation in In-Service Petroleum and Hydrocarbon Based Lubricants by Trend Analysis Using Fourier Transform Infrared Spectrometry," *Annual Book of ASTM Standards*, ASTM International, West Conshohocken, PA, 2009.

[43] ASTM D7415, "Test Method for Condition Monitoring of Sulfate By-Products in In-Service Petroleum and Hydrocarbon Based Lubricants by Trend Analysis Using Fourier Transform Infrared Spectrometry," *Annual Book of ASTM Standards*, ASTM International, West Conshohocken, PA, 2009.

[44] ASTM D7418, "Practice for Set-up and Operation of Fourier Transform Infrared Spectrometers for In-Service Oil Condition Monitoring," *Annual Book of ASTM Standards*, ASTM International, West Conshohocken, PA, 2007.

[45] ASTM D7590, "Guide for Measurement of Remaining Primary Antioxident Content in In-Service Lubricant Oils by Linear Sweep Voltametry," *Annual Book of ASTM Standards*, ASTM International, West Conshohocken, PA, 2009.

[46] ASTM D7624, "Test Method for Condition Monitoring of Nitration in In-Service Petroleum and Hydrocarbon Based Lubricants by Trend Analysis Using Fourier Transform Infrared Spectrometry," *Annual Book of ASTM Standards*, ASTM International, West Conshohocken, PA, 2010.

[47] ASTM E2412, "Practice for Condition Monitoring of In-Service Lubricants by Trend Analysis Using Fourier Transform Infrared Spectrometry," *Annual Book of ASTM Standards*, ASTM International, West Conshohocken, PA, 2010.

[48] Nadkarni, R. A. and Bover, W. J., "Bias Management and Continuous Quality Improvements through Committee D02's Proficiency Testing," *ASTM Standardization News,* June 2004, pp. 36–40.

23

Elemental Analysis of Crude Oils Using Spectroscopic Methods

R. A. Kishore Nadkarni[1]

SIGNIFICANCE

Crude oils are highly complex hydrocarbon samples with some organometallic compounds, inorganic sediment, and water. Nearly 300 individual hydrocarbons and more than 200 separate sulfur compounds have been identified in crude oils [1]. A number of trace elements have been found in crude oils, but other than vanadium and nickel, which are most abundant in crude oils, other metals present have not received much work. There is also interest in the sodium content of crude oil as an indicator of sea-water contamination during transport. Many of these trace elements are present in milligram per kilogram (parts per million, ppm) or sub-ppm levels and thus, only sophisticated analytical techniques will be able to quantify them accurately.

Generally it is believed that the source of petroleum is marine animal and vegetative life deposited with sediment in the coastal waters in prehistoric times. Over eons, with bacterial action along with intense heat and pressure, some percentages of sulfur, oxygen, nitrogen, and volatile compounds originally present evolved out of this material. The end product was a mixture of hydrocarbons containing varying amounts of sulfur, oxygen, nitrogen, and some trace metals.

Sulfur over 6 % and nitrogen over 1 % mass fractions have been reported in some crude oil samples. More than 40 other trace elements have been reported in crude oil at trace levels (<1000 mg/kg). Most common are vanadium, nickel, and iron. Arsenic, beryllium, barium, cadmium, mercury, selenium, copper, antimony, chromium, lead, manganese, molybdenum, tellurium, and tin have been found in lesser quantities. Extensive data on elemental composition of crude oils can be found in Ref [2]. Elemental analyses of crude oils from some giant oil fields of the world are summarized in Table 1.

Ratios such as vanadium to vanadium plus nickel and iron to vanadium are suggested as being useful for oil type characterization [3]. Because organometallic compounds are concentrated in the heavy ends of petroleum, transition element concentrations and ratios can serve as excellent oil–oil correlation parameters. Generally, vanadium and nickel contents increase with aliphatic content of crude oil (American Petroleum Institute [API] gravity is an indicator). The lighter oils contain less metal [4].

The metals present in crude oils can be porphyrins or nonporphyrins. The former have been the most extensively studied. Porphyrins are a class of tetrapyrrole macrocyclics with a basic structural unit consisting of four pyrrol rings linked consecutively at the alpha position by means of methane bridges.

[1] *Millennium Analytics, Inc., East Brunswick, NJ*

TABLE 1—Elemental Content of Crude Oils from Some Giant Oil Fields[a]

Country	V, mg/kg	Ni, mg/kg	Fe, mg/kg
Abu Dhabi	1	0.43	...
Algeria	0.2–1.5	...	...
Canada	<1–220	1–60	<1–629
Colombia	59–135	9–14	2–18
Egypt	15–120	7–72	58
Indonesia	...	7–33	...
Iran	11–151	3–39	...
Iraq	6–95	4–15	...
Kuwait	23–43	6–9	0.3–0.7
Libya	1–28	1–35	...
Nigeria	1–4	1–13	...
Saudi Arabia	6–80	1–20	...
United States			
– Alaska (N. Slope)	16–30	4–13	...
– Arkansas	12–19	4–23	1–6
– California	1–403	2–174	2–125
– Louisiana	0–4	0–6	...
– Oklahoma	0–148	0–71	1–51
– Texas	0–23	0–5	...
– Wyoming	1–144	1–102	1–23

[a]Excerpted from Reference 2.

The principal porphyrins in petroleum are Ni(II) and VO(II), although Cu(II) porphyrins may be found in the early stages of sediment digenesis [5]. Filby has shown that iron, cobalt, copper, zinc, mercury, and part of nickel occur as nonporphyrin complexes. Arsenic and antimony appear to be present as low molecular weight compounds such as alkyl or aryl arsines or stibines [6].

Knowledge of trace elements in crude oils is important because these elements can have an adverse effect on the refining process and quality of the products produced. Elements such as iron, arsenic, and lead are catalyst poisons. When the fuels are combusted, vanadium present in the fuel can form corrosive compounds. Sodium compounds have been known to cause superficial fusion on fire brick. Volatile organometallic compounds can cause contamination of distillate fractions [1]. The value of crude oil is determined, in

part, by the concentrations of nickel, vanadium, and iron. The first two elements, present at trace levels in petroleum fractions, can deactivate or poison catalysts during processing. Trace elements in crude oils can have potential impacts on the environment resulting from atmospheric emissions when fuels are burned. Two sources of information about the trace elements in crude oils are Refs [2] and [3].

SAMPLING

A most critical part of total analytical sequence is representative sampling, which if not done properly can have far-reaching effects on the quality of final results, whether physical or chemical. Maintaining compositional integrity of the samples from the time of collection until they are analyzed requires planning, care, and effort. Moreover, the sampling procedure should not introduce any contaminants into the sample or otherwise alter the sample composition so that the final test results are not compromised. Two ASTM procedures give protocols for manual and automatic sampling: D4057 and D4177, respectively. In many manual liquid sampling applications, a heavy component such as free water may tend to separate from the main component. A third ASTM standard, D5854, covers the mixing and handling of liquid samples. It also provides a guide for selecting suitable containers for crude oil samples for various analyses (Table 2).

ANALYSIS OF CRUDE OILS

A number of analytical techniques have been employed for the determination of metals and elements in crude oils. Of these elements, sulfur is perhaps most important because of its impact on environment pollution during utilization of crude oil and petroleum. This issue will not be discussed here further because the necessary information can be found in Chapter 20 of this monograph.

Among the more widely used elemental analytical techniques are neutron activation analysis (see Chapter 15) and X-ray fluorescence (see Chapters 12,

TABLE 2—Recommended Sample Containers for Crude Oil Storage[a]

Container Material	For Immediate Use	For Storage for 6 Months	Reuse
Hard borosilicate glass	Preferred	Preferred	Suitable
Stainless steel	Suitable	Suitable	Suitable
Epoxy lined steel	Suitable	Suitable	Suitable
Tin-plated soldered steel	Not Recommended	Not recommended	Not recommended
Polytetrafluoro-ethylene propylene	Preferred	Not recommended	Suitable
High density linear polyethylene	Preferred	Not recommended	Not recommended

[a]Excerpted from ASTM standard D5854.

13, and 14). Determination of mercury in crude oil is also the subject of Chapter 21. Thus, only the truly atomic spectroscopic techniques [atomic absorption spectrometry (AAS), graphite furnace atomic absorption spectrometry (GFAAS), inductively coupled plasma atomic emission spectrometry (ICP-AES), and inductively coupled plasma mass spectrometry (ICP-MS)] as they are applied to crude oils are discussed in the current chapter. The ASTM analytical standards mentioned in this chapter are listed in Table 3.

SAMPLE PREPARATION

Two principal ways to analyze a crude oil sample are either to decompose it with a mixture of acids and bring it into dilute aqueous solution or to dilute the sample with an organic solvent such as kerosine, xylene, toluene, or tetralin and directly aspirate the solution into a nebulizer of an AAS, ICP-AES, or ICP-MS instrument.

Decomposition of crude oil sample by dry ashing (such as in ASTM Test Method D482) is generally not preferred if the ash needs to be analyzed for trace elements because there is a likelihood of loss of elements with high volatility for elements such as arsenic, cadmium, mercury, lead, and selenium. Wet ashing involves the use of various mineral acids–sulfuric, nitric, fuming nitric, and perchloric–either alone or in mixtures. Of these, wet ashing with sulfuric acid is the basis of ASTM Test Method D874. This digestion tends to minimize volatilization losses.

TABLE 3—ASTM Standards Referred to in This Chapter

ASTM Standard	Description
D482	Ash from Petroleum Products
D874	Sulfated Ash from Lubricating Oils and Additives
D4057	Practice for Manual Sampling of Petroleum and Petroleum Products
D4177	Practice for Automatic Sampling of Petroleum and Petroleum Products
D5185	Determination of Additive Elements, Wear Metals, and Contaminants in Used Lubricating Oils and Determination of Selected Elements in Base Oils by Inductively Coupled Plasma – Atomic Emission Spectrometry
D5708	Determination of Nickel, Vanadium and Iron in Crude Oils and Residual Fuels by ICP-AES
D5854	Practice for Mixing and Handling of Liquid Samples of Petroleum and Petroleum Products
D5863	Determination of Nickel, Vanadium, Iron, and Sodium in Crude Oils and Residual Fuels by Flame Atomic Absorption Spectrometry
D7372	Guide for Analysis and Interpretation of Proficiency Test Program Results
D7691	Multielement Analysis of Crude Oils Using ICP-AES

In ASTM Test Methods D5708B and D5863A, up to 20 g of sample are decomposed with concentrated sulfuric acid by heating to dryness. Residual carbon is burned off by heating at 525°C in a muffle furnace. The resultant inorganic residue is digested with nitric acid, evaporated to incipient dryness, dissolved in dilute nitric acid, and made up to volume. In Test Method D5708 B, ICP-AES is used for final elemental measurements and in Test Method D5863A, AAS is used. Aqueous matrix matched calibration standards are used in both cases. See Table 4 for a comparison of these two methods.

TABLE 4—ASTM Test Methods for Metals in Crude Oils

Test Method	D5708	D5863	D7691
Elements analyzed	Ni, V, Fe	Ni, V, Fe, Na	Ni, V, Fe, S
Sample preparation	A – Organic solvent dilution	A – Acid decomposition	Organic solvent dilution
	B – Acid decomposition	B – Organic solvent dilution	
Measurement technique	ICP-AES	Flame AAS	ICP-AES
Concentration range, mg/kg	Ni: 10 to 100	Ni: 10 to 100	Ni: 1 to 100
	V: 50 to 500	V: 50 to 55	V: 1 to 1000
	Fe: 1 to 10	Fe: 3 to 10	Fe: 10 to 40
		Na: 1 to 20	
Repeatability, mg/kg Ni	A – 0.01 $X^{1.3}$	A – 0.20 $X^{0.65}$	0.1754 $X^{1.0168}$
	B – 0.02 $X^{1.2}$	B – 0.005 $X^{1.4}$	
V	A – 0.07 $X^{0.88}$	A – 1.1 $X^{0.50}$	0.0392 $(X + 0.7485)^{0.8668}$
	B – 0.02 $X^{1.1}$	B – 0.13 $X^{0.92}$	
Fe	A – 0.22 $X^{0.30}$	A – 0.98	0.1885 $X^{0.9145}$
	B – 0.23 $X^{0.67}$		
Na	. . .	B – 0.12 X	
Reproducibility, mg/kg Ni	A – 0.41 $X^{0.78}$	A – 1.3 $X^{0.53}$	1.1389 $X^{0.7085}$
	B – 0.05 $X^{1.3}$	B – 0.06 $X^{1.2}$	
V	A – 0.12 $X^{1.1}$	A – 0.33 $X^{0.90}$	0.8628 $(X + 0.7485)^{0.8668}$
	B – 0.10 $X^{1.1}$	B – 1.2 $X^{0.80}$	
Fe	A – 0.68 $X^{0.35}$	A – 1.45 $X^{0.46}$	0.5649 $X^{0.9145}$
	B – 0.91 $X^{0.51}$		
Na	. . .	B – 0.69 X	

Atomic Absorption Spectrometry

The AAS technique is often preferred in oil analysis because of its cost-effectiveness, simplicity of operation, good detection limits, and freedom from interference. Its main drawback is that it is a single-element method, meaning that only one element can be determined at a time. Thus, if data on multiple elements are required, it will proportionally take longer time to analyze the sample. Some examples of applications of AAS to crude oil analysis include Venezuela crude oil for cadmium, lead, and nickel [7], and crude oils for copper, magnesium, sodium, tin, cadmium, zinc, and aluminum [8].

Details of the actual AAS technique are not discussed here because it has been adequately dealt with in Chapter 6 of this monograph. AAS is truly a "cook-book" type of analysis. A large number of publications have appeared on using the AAS technique for the determination of metals in petroleum products. ASTM Test Method D5863 uses flame AAS for the determination of nickel, vanadium, iron, and sodium in crude oils. Detection limits of some selected elements are given in Table 5.

Graphite Furnace Atomic Absorption Spectrometry

GFAAS is a technique that differs from flame AAS in that it uses a graphite furnace instead of a flame for the volatilization of metals. The technique is also called carbon rod atomization or electrothermal vaporization. Its sensitivity is several orders of magnitude better than the flame AAS methods. Even though it is capable of determining all elements doable by AAS, its forte lies in the determination of elements in petroleum products that are in sub-ppm range and are difficult to measure by AAS. Detailed technical discussion of GFAAS technique is given in Chapter 7 of this monograph, and is not be repeated here. Some examples of application of GFAAS to crude oil analysis can be found in Refs [10] and [11], which determine vanadium and lead, respectively.

Inductively Coupled Plasma–Atomic Emission Spectrometry

One of the most sensitive atomic spectroscopic techniques to come along in a long time is ICP-AES. It has several advantages over conventional AAS: large dynamic range, very good detection limits, freedom from chemical or matrix interferences, multielement capability, applicability to a large number of metals and some nonmetals, and high temperature of the plasma, enabling atomization of refractory metals. Technical aspects of this technique have been discussed in detail in Chapter 8 and hence will not be repeated here.

TABLE 5—Parameters Used in AAS Measurements

Element	Concentration Range, μg/mL	Wavelength, nm	Flame Used	Detection Limits, μg/mL
Nickel	0.5–20	232.0; 341.5	Air + C_2H_2	0.02
Vanadium	0.5–20	318.4	N_2O + C_2H_2	0.08
Iron	3.0–10	248.3; 372.0	Air + C_2H_2	0.01
Sodium	0.1–5	589.0	Air + C_2H_2	0.001

Wavelengths employed for detecting the elements in ICP-AES spectra are listed in Table 6. In several ICP-AES analyses, internal standards are employed to compensate for matrix and viscosity effects between the samples and calibration standards. These are listed in Table 7. The detection limits for some elements using ICP-AES are compared in Table 8.

A large amount of literature exists on the applications of ICP-AES in the oil industry. Particularly for the lubricating oils, it is the workhorse of metal analysis. ASTM has issued several ICP-AES methods, and D5708 is used for the determination of nickel, vanadium, and iron in crude oils. Procedure A of this standard uses organic solvent dilution and procedure B employs acid decomposition of the matrix before ICP-AES measurements. A summary of the two procedures is given in Table 4.

Table 9 illustrates the precision possible for AAS and ICP-AES procedures at various concentration levels of vanadium, nickel, iron, and sodium in crude oils based on ASTM standards D5708 and D5863.

Gonzales and Lynch used dilution with kerosine and scandium as an internal standard to determine 18 trace elements in crude oils by ICP-AES [12].

TABLE 6—Wavelengths Used in ICP-AES Measurements

Element	Wavelength,[a] nm
Aluminum	308.215; 396.153; 309.271; 237.01
Barium	233.53; 455.403; 494.410
Calcium	315.887; 317.933; 364.44; 422.67
Chromium	205.552; 267.716; 298.92; 283.563
Copper	324.754; 219.226
Iron	259.94; 238.204; 271.44; 259.837
Magnesium	279.079; 279.553; 285.21; 293.65
Manganese	257.61; 293.31; 293.93; 294.92
Nickel	231.604; 227.02; 221.648; 216.56; 341.476
Phosphorus	177.51; 178.289; 213.62; 214.914; 253.40
Potassium	766.491; 769.896
Sodium	588.995; 330.29; 589.3; 589.592
Silicon	288.159; 251.611; 212.412; 282.851
Sulfur	180.731; 182.04; 182.62
Vanadium	292.403; 309.31; 310.23; 311.07
Zinc	202.551; 206.209; 213.856; 334.58; 481.05; 202.48

[a]These wavelengths are suggested and do not represent all possible choices.

TABLE 7—Internal Standards Used in ICP-AES Analysis		
Element	**Concentration, mg/kg**	**Wavelengths, nm[a]**
Cadmium	10	214.438; 228.802; 226.502
Cobalt	10	228.616; 238.892; 237.662
Lanthanum	10	379.48; 379.08
Scandium	10	255.237; 361.384; 357.253
Yttrium	10	371.030; 324.228; 360.073
[a]These wavelengths are only suggested and do not represent all possible choices.		

A new standard test method for multielement ICP-AES analysis of crude oil after dilution with an organic solvent has been recently issued. This is based on a similar test method, D5185, which is widely used in the industry for the analysis of lube oils, base oils, and used oils. An interlaboratory study was completed and a new Standard Test Method D7691 was published in 2010. One point in this context is whether direct dilution of crude oils can account for some inorganic solids present in the sample. This is a legitimate question. Because of the particulates present in crude oil samples, if they do not dissolve in the organic solvents used or if they do not get aspirated in the nebulizer, low elemental values may result, particularly for iron and sodium. This can also occur if the elements are associated with water, which can drop out of solution when diluted with an organic solvent. It is also possible that, particularly in the case of silicon, low results may be obtained irrespective of whether organic dilution or acid decomposition is used. Silicones are present as oil field additives and

TABLE 8—Detection Limits of Atomic Spectroscopic Techniques				
Element	**AAS (μg/mL)**	**GFAAS (pg)**	**ICP-AES (ng/mL)**	**ICP-MS (ng/mL)**
Aluminum	0.02	4	0.2	0.5
Calcium	0.002	2	0.0001	100
Chromium	0.005	1	0.08	0.5
Copper	0.001	1	0.04	0.6
Iron	0.01	2	0.09	10
Magnesium	0.0001	0.5	0.003	1.0
Nickel	0.02	10	0.2	0.4
Potassium	0.004	. . .	15	20
Silicon	0.2	40	2	15
Sodium	0.001	. . .	0.1	20
Vanadium	0.08	20	0.06	0.5
Zinc	0.003	0.1	0.1	0.7

TABLE 9—Calculated Precision of Alternative Methods for Metals in Crude Oils

		1 mg/kg		10 mg/kg		50 mg/kg		100 mg/kg	
Element	Test Method	r	R	r	R	r	R	r	R
Vanadium	D5708A			. . .		2.2	8.9	4.0	19
	D5708B	. . .				1.5	7.4	3.2	16
	D5863A					7.8	11.0	11.0	21.0
	D5863B					4.8	27.0	9.0	48.0
	D7691	–	–	–	–	1.14	23.5	2.14	47.0
Nickel	D5708A	. . .		0.20		1.6		4.0	
	D5708B			2.5		2.2	8.7	5.0	15
	D5863A			0.32		2.5	10.0	4.0	15.0
	D5863B			0.89	4.4	1.2	6.6	3.2	15.0
	D7691	–	–	1.83	5.8	9.4	18.2	19.1	29.8
Iron	D5708A	0.22	0.68	0.44	1.5	. . .		. . .	
	D5708B	0.23	0.91	1.08	2.9				
	D5863A			0.98	4.1				
	D769	0.19	0.57	1.11	3.35				
Sodium	D5863B	0.12	0.69	1.2	6.9	. . .		. . .	

can be lost in ashing. Silicates should be retained, but unless hydrofluoric acid or alkali fusion is used for sample dissolution, they may not be accounted for.

Based on the ASTM Interlaboratory Crosscheck Program (ILCP) on crude oils, it is not clear that the organic solvent dilution technique will necessarily give lower results than those obtained using the acid decomposition technique. Crude oil ASTM ILCP results for metals for 2008 and 2009 are summarized in Table 10. Test Methods D5708A and D5863B use acid decomposition before ICP-AES and AAS measurements, respectively. Test methods D5708B and D5863A use organic solvent dilution before ICP-AES and AAS measurements. Compared to the method reproducibility, it would be difficult to conclude that the two sample preparation techniques give any significantly different results for any of the four elements measured in crude oils in these six crosschecks.

Table 11 compares the reproducibility obtained in these ILCPs with those expected in the ASTM Standard Test Methods D5708 and D5863 for crude oils. The precision is expressed as test performance indices (TPIs), which are defined in ASTM Guide D7372 as ratios of ASTM reproducibility to site precision. The standard guide suggests that TPI values of less than 1.2 indicate that the laboratory performance is marginal relative to ASTM published precision. This appears to be the case in Table 11 for a majority of analyses. In this

TABLE 10—Metals in Crude Oils Determined with and without Acid Decomposition[a]

ILCP Sample	Metal, mg/kg	D5708 A	D5708 B	D5863 A	D5863 B
CO 0907	Iron	6.55 ± 2.11 (27)	13.06 ± 7.28 (18)	11.91 ± 6.05 (15)	. . .
	Nickel	1.44 ± 0.50 (26)	1.29 ± 0.64 (18)	1.24 ± 0.39 (12)	2.31 ± 1.17 (11)
	Vanadium	0.29 ± 0.11 (21)	0.30 ± 0.30 (15)	0.4 ± 0.5 (8)	0.8 ± 0.8 (8)
CO 0903	Iron	6.43 ± 2.39 (30)	9.67 ± 3.16 (19)	9.07 ± 3.11 (17)	. . .
	Nickel	6.19 ± 0.99 (30)	5.93 ± 0.76 (18)	5.88 ± 1.01 (16)	7.04 ± 1.57 (13)
	Vanadium	13.9 ± 2.05 (31)	12.9 ± 1.06 (17)	12.9 ± 2.6 (18)	14.7 ± 3.4 (14)
CO 0811	Iron	1.36 ± 0.26 (24)	1.78 ± 0.73 (19)	2.18 ± 0.56 (13)	. . .
	Nickel	10.5 ± 1.18 (25)	9.83 ± 1.42 (21)	9.24 ± 0.83 (14)	8.12 ± 2.98 (9)
	Vanadium	24.1 ± 2.98 (26)	22.1 ± 3.24 (21)	21.3 ± 3.4 (14)	21.8 ± 7.0 (11)
CO 0807	Iron	1.097 ± 0.28 (22)	2.25 ± 0.98 (16)	2.16 ± 0.95 (11)	. . .
	Nickel	10.2 ± 1.13 (22)	9.79 ± 1.40 (16)	10.2 ± 0.6 (11)	11.0 ± 2.0 (9)
	Vanadium	39.0 ± 3.48 (24)	34.8 ± 4.73 (17)	33.5 ± 4.1 (12)	42.2 ± 9.1 (8)
CO 0803	Iron	0.102 ± 0.093 (13)	1.30 ± 0.54 (13)	1.09 ± 0.32 (9)	. . .
	Nickel	0.056 ± 0.059 (13)	0.093 ± 0.021 (9)	. . .	0.197 ± 0.18 (8)
	Vanadium	0.097 ± 0.085 (15)	0.09 ± 0.019 (10)		0.56 ± 0.60 (6)
CO 0911	Iron	1.70 ± 0.32 (20)	3.66 ± 0.93 (14)	4.00 ± 0.52 (6)	–
	Nickel	24.2 ± 1.88 (22)	23.03 ± 1.45 (14)	15.88 ± 9.5 (7)	22.8 ± 3.2 (9)
	Vanadium	234.2 ± 17 (23)	217.3 ± 19.4 (14)	202.2 ± 45.1 (7)	228.8 ± 24.5 (9)
CO 1003	Iron	0.624 ± 0.109 (22)	0.822 ± 0.479 (15)	1.07 ± 0.52 (13)	–
	Nickel	8.26 ± 1.11 (26)	8.72 ± 1.36 (18)	7.85 ± 0.84 (13)	8.84 ± 2.01 (9)
	Vanadium	19.53 ± 1.59 (26)	19.74 ±1.56 (18)	17.7 ± 3.6 (14)	20.9 ± 1.8 (10)
CO 1011	Iron	5.31 ± 0.68 (27)	6.20 ± 1.31 (16)	7.28 ± 2.36 (11)	–
	Nickel	63.37 ± 7.64 (27)	57.31 ± 9.0 (18)	62.53 ± 14.94 (11)	66.61 ± 7.55 (11)
	Vanadium	265.7 ± 30.5 (27)	250.2 ± 31.9 (17)	237.1 ± 43.6 (11)	265.7 ± 43.6 (11)

[a]All values are expressed as robust mean ± robust standard deviation (# valid results).

particular case it may be a combination of low concentration levels of metals determined, a method not based on a robust interlaboratory study, or the laboratories not adhering to the test method details as required.

TABLE 11—Precision of ILCP of Crude Oils Compared to ASTM Test Methods										
Metal / ILCP	**Test Method**	**ASTM R**	**CO0907**	**CO0903**	**CO0811**	**CO0807**	**CO0803**	**CO0911**	**CO1003**	**CO1011**
Iron	D5708A	$0.68X^{0.35}$	0.22	0.20	1.06	0.90	NA	0.873	0.302	1.895
	D5708B	$0.91X^{0.51}$	NA	0.33	0.61	0.51	0.70	2.582	1.33	3.62
	D5863A	$1.45X^{0.46}$	NA	0.45	NA	NA	NA	1.44	1.44	6.54
	D5863B						NA	–	–	–
Nickel	D5708A	$0.41X^{0.78}$	NA	NA	0.78	0.80	NA	5.21	3.07	21.2
	D5708B	$0.05X^{1.3}$	NA	NA	NA	NA	NA	4.01	3.75	24.9
	D5863A	$1.3X^{0.53}$	NA	NA	NA	2.65	NA	26.2	2.33	41.4
	D5863B	$0.06X^{1.2}$		NA	NA	0.20	NA	8.92	5.57	20.9
Vanadium	D5708A	$0.12X^{1.1}$	NA	NA	NA	NA	NA	46.98	4.40	84.6
	D5708B	$0.10X^{1.1}$	NA	NA	NA	NA	NA	53.8	4.32	88.5
	D5863A	$0.33X^{0.90}$	NA	NA	NA	NA	NA	124.9	10.0	71.5
	D5863B	$1.2X^{0.80}$	NA	NA	NA	NA	NA	67.9	5.0	120.8
NA – Not applicable because < 4 Z-scores calculated from the crosscheck.										

Inductively Coupled Plasma – Mass Spectrometry

The ICP-MS technique combines the power of ICP for atomizing and ionizing the sample with the sensitivity and selectivity of mass spectrometric detection. Coupled together, ICP-MS offers an efficient ion source, a less complex background spectrum, the capability of simultaneous determination of more than 70 elements, a wide dynamic range, and detection limits down to 10 ng/kg (parts per trillion) in solution for most elements. Detailed technical discussion of this important technique is described in Chapter 9, and is not be repeated here.

At present, the technique is more adapted to oil company R&D laboratories than to routine testing laboratories because of the cost and sophistication of the equipment. Because of that, at present no ICP-MS test methods related to crude oil analysis have been published by ASTM. Some examples of use of ICP-MS in crude oil analysis are listed in Table 12. This is by no means a comprehensive list, but includes only randomly selected examples of applications of ICP-MS to crude oil analysis.

McElroy et al. compared the use of ICP-AES and ICP-MS for the determination of nickel and vanadium in NIST SRM 1618 fuel oil and an Arab heavy resid [14]. In both cases, direct aspiration and sample preparation after acid decomposition (i.e., Test Method D874) were used. Both sample preparation methods as well as two measurement techniques showed comparable results (Table 13).

TABLE 12—Applications of ICP-MS to Crude Oil Analysis

Author	Reference #	Subject
Dreyfus, et al.	15	Trace elements in crude oils after toluene dilution
Duyck, et al.	16	Trace elements in crude oils after toluene dilution
Dreyfus et al.	17	Lead isotopes in crude oils
Dreyfus et al.	18	Oil-in-water microemulsion
Al-Swaidan et al.	13	Microemulsion ICP-MS
Al-Swaidan et al.	19	Pb and Cd in Saudi Arabian crude oils
Akinlua et al.	20	Rare earth elements in Niger crude oils
Yasnygina et al.	21	Rare earth elements in Baikal crude oils
Hwang et al.	22	Microwave digestion and ICP-MS
Xie et al.	23	Microwave digestion and ICP-MS
Nakamoto et al.	24	Oxygen bomb combustion and ICP-MS for Cd and Se
Botto	25	Trace elements in crude oils
Kelly et al.	26	Hg in crude oils by ID-CV-ICP-MS
Osborne	27	Hg by ETV-ICP-MS
Duyck et al.	28	Trace elements in crude oils

Excerpted from Chapter 9 in this monograph.

TABLE 13—Comparison of ICP-AES and ICP-MS Techniques[a]

Sample	Element	Method	Mean, mg/kg	% RSD	Certified Value, mg/kg
NIST SRM 1618	Ni	Sash-ICP-AES	76.2	1.7	75.2 ± 0.4
		Direct ICP-MS	75.9	1.5	
	V	Sash-ICP-AES	426	1.3	423.1 ± 3.4
		Direct ICP-MS	424	1.9	
Arab Heavy Resid	Ni	Sash-ICP-AES	57.8	2.1	
		Direct ICP-MS	58	1.0	
	V	Sash-ICP-AES	183	1.9	
		Direct ICP-MS	182	1.3	

[a]Excerpted from Ref [14].

Neutron Activation Analysis (NAA)

The NAA technique, though highly precise and accurate, is usually not used in oil industry laboratories because it requires a nuclear reactor for irradiation of samples. In many academic and national research laboratories throughout the world, however, this technique is used extensively for multielement characterization of crude oils and its fractions.

In this technique, a small amount of oil sample sealed in a quartz ampoule is irradiated for various periods of time in a high neutron flux in a nuclear reactor. The resultant radioactive isotopes of the elements present in the sample are measured by their gamma spectroscopy over a period of time and quantitated using elemental calibration standards also irradiated along with the samples. Differentiation between different isotopes is achieved by their decay times and their gamma ray energies. The main interference in this technique is overlapping of gamma ray energies of individual isotopes. Further operating details of this technique will not be described here because they have been adequately covered in Chapter 15 of this monograph.

A large number of elements can be determined by this technique, some useful, others more exotic, the latter done simply because they have good sensitivity for NAA. Some examples of applications of NAA in petroleum field are given in Table 14.

X-ray Fluorescence

Along with atomic spectrometric techniques such as AAS and ICP-AES just described, X-ray fluorescence (XRF) serves as a workhorse of petrochemicals analysis. Crude oils in particular are analyzed for their sulfur content very easily and nondestructively using the XRF technique. Both wavelength-dispersive (WD-XRF) and energy-dispersive (ED-XRF) modes are used with different instrumentation. Both these techniques are described in detail in this monograph in Chapters 12 and 13, and will not be described here again.

TABLE 14—Applications of NAA to Analysis of Crude Oils		
Author	**Reference**	**Comments**
Al-Shahristani	29	29 trace elements in crude oils
Guinn et al.	30	Trace elements in crude oils
Filby et al.	31	Elements in crude oils
Lukens	32	V in crude oils using a Californium ^{252} source
Veal	33	As and five other trace elements in crude oils
Filby and Shah	34	Trace elements in crude oils for spill source identification
Mandler et al.	35	Trace elements in crude oils by charged particle activation for spill source identification

The technique requires only a small amount of liquid sample, and the analysis is rapid and nondestructive, and has very good precision. It is one of the primary methods chosen by U.S. Environmental Protection Agency for sulfur surveillance of U.S. refinery products such as gasoline and diesel. There are, however, some well-recognized interferences in the technique:

1. A fundamental assumption in XRF analysis is that the standard and sample matrices are well matched, or that the matrix differences are accounted for. Matrix mismatch can be caused by carbon/hydrocarbon ratio differences between samples and standards or by the presence of other interfering heteroatoms or species.
2. A second source is spectral interference caused by the closeness of the X-ray characteristic lines of the elements present in a sample and the detector's limited ability to completely resolve them. As a result, the lines produce spectral peaks that overlap with each other. Spectral interferences may arise from samples containing silicon, phosphorus, calcium, potassium, halides, and so on if present at concentrations greater than 0.1 times the measured sulfur concentration, or more than a few hundred milligrams per kilogram.
3. Matrix effects are caused by concentration variations of the elements in a sample. These variations directly influence X-ray absorption and change the measured intensity of each element.

These interferences may be compensated for in modern XRF instruments with the use of built-in software for spectra deconvolution or overlap correction and interelement correction by multiple regression or by other mathematical methods.

For samples such as crude oils that may contain suspended water, it is recommended that the water be removed before testing or that the sample be thoroughly homogenized and immediately tested. The interference is greatest if the water creates a layer over the transparent film because it will attenuate the X-ray intensity for the elements. One way to remove water is to centrifuge the sample first under ambient sealed conditions.

ASTM has issued a number of standard test methods using this technique. Those of interest to crude oil analyses are:

TABLE 15—Precision of XRF Test Methods for Sulfur in Crude Oils			
Test Method	**Repeatability**	**Reproducibility**	**Bias**
D2622	$0.1462\ X^{0.8015}$	$0.4273\ X^{0.8015}$	No significant bias detected
D4294	$0.4347\ X^{0.6446}$	$1.9182\ X^{o.6446}$	No significant bias detected

- D2622 – Sulfur in Petroleum Products by Wavelength Dispersive X-ray Fluorescence Spectrometry
- D4294 – Sulfur in Petroleum and Petroleum Products by Energy-Dispersive X-ray Fluorescence Spectrometry

Precision data for these two test methods are summarized in Table 15. Calculated precisions at various levels of sulfur are given in Table 16 for both test methods. Clearly, the precision is superior for D2622 at lower levels of sulfur concentration compared to that of D4294. Comparative data for sulfur in crude oils obtained from the ASTM ILCP programs in 2008 through 2010 are summarized in Table 17. Both test methods have given equivalent results for crude oils. It is apparent that a much larger number of laboratories are using the D4294 ED-XRF method rather than the D2622 WD-XRF method. The obvious reason for this is the significantly lower cost and ease of operation of ED-XRF instruments compared to the WD-XRF ones. Additional data based on the two interlaboratory studies conducted by ASTM to establish precisions of these two methods are summarized in Table 20 for crude oils. The study included ten National Institute of Standards and Technology (NIST)

TABLE 16—Calculated Precision of XRF Test Methods for Sulfur				
S, mg/kg	**D2622 Repeatability**	**D2622 Reproducibility**	**D4294 Repeatability**	**D4294 Reproducibility**
3	0.4	1.0	. . .	. . .
5	0.5	1.6	. . .	. . .
10	0.9	2.7	. . .	. . .
25	1.9	5.6	3.4	15
50	3.4	9.8	5.4	24
100	5.9	17.1	8.5	37
500	21	62	24	105
1000	37	108	37	165
5000	135	394	105	465
10,000	235	687	165	727
46,000	798	2333	440	1943

TABLE 17—Determination of Sulfur in Crude Oil ILCP Samples		
ASTM ILCP	**D2622 Results**	**D4294 Results**
CO 0711	0.1978 ± 0.0072 (18)	0.202 ± 0.010 (73)
CO 0803	0.2003 ± 0.0092 (23)	0.2025 ± 0.0065 (82)
CO 0807	2.722 ± 0.126 (19)	2.832 ± 0.098 (89)
CO 0811	0.9319 ± 0.0363 (25)	0.9487 ± 0.0324 (89)
CO 0903	0.4227 ± 0.0152 (27)	0.4237 ± 0.0132 (92)
CO 0907	0.0645 ± 0.0314 (21)	0.0864 ± 0.0159 (70)
CO 0911	1.76 ± 0.089 (19)	1.797 ± 0.055 (68)
CO 1003	0.737 ± 0.041 (26)	0.773 ± 0.03 (86)
CO 1011	2.625 ± 0.086 (25)	2.721 ± 0.084 (84)
All results are expressed in m fraction %. All results are expressed as robust mean ± robust standard deviation (number of valid results).		

standard reference materials (SRM), including two crude oils [36,37]. See Table 18 for analysis of NIST crude oil SRMs by these two XRF test methods.

Crude Oil Reference Materials

To ensure that a laboratory is producing reliable and reproducible results it is important to include a sample of reference material of the same matrix as the samples. Based on the certified values of such reference materials the laboratory can satisfy itself and its customers that the results are precise and accurate. There are some crude oil certified reference materials that are commercially available. In addition, NIST currently provides two crude oil SRMs that serve as the definitive source of measurement traceability in the United States for the elements certified. NIST also provides a crude oil reference material (RM) with one reference value. These are listed in Table 19. All three of these have been included in the interlaboratory study mentioned earlier for an ICP-AES method for trace elements. It is expected that NIST will use

TABLE 18—Analysis of NIST Crude Oil SRMs for Sulfur by XRF Test Methods			
NIST SRM	**Certified Sulfur, mg/kg**	**ILS Sulfur Results**	**Relative Bias %**
2721	15833	(WD-XRF) 15884	0.33
		(ED-XRF) 16118	1.81
2722	2103.7	(WD-XRF) 2105	0.06
		(ED-XRF) 2082	–1.03

TABLE 19—NIST Standard Reference Materials for Crude Oils		
NIST	**Certification**	**Concentration**
SRM 2721 Light-sour crude oil	Sulfur	1.5832 ± 0.0044 m %
SRM 2722 Heavy-sweet crude oil	Sulfur	0.21037 ± 0.00084 m %
RM 8505 Crude oil	Vanadium (noncertified reference value)	390 ± 10 mg/kg

these data to identify additional elements to certify and to better characterize the matrices beyond their current certifications.

Another source of reference materials is the residual quantities of crude oils from the ASTM Interlaboratory Crosscheck Program. Once the crosscheck is over, ASTM publishes the report of analysis based on the data from a large number of laboratories. Unfortunately, only limited quantities of these materials are available for a short period of time. They are more suited as quality control materials rather than as reference standards.

TABLE 20—Comparison of Spectroscopic Methods						
Criteria	**AAS**	**GFAAS**	**ICP-AES**	**ICP-MS**	**XRF**	**NAA**
Cost	Moderate	Moderate	High	Very high	High	Very high
Maintenance	Moderate	Moderate	High	Very high	High	High
Dynamic Range	Narrow	Narrow	Wide	Wide	Moderate	Moderate
Element	Single	Single	Multi	Multi	Multi	Multi
No. of Elements	~ 70	~70	~ 70	>100	~ 65	~ 60
Detection Limits	ppm	ppb	Sub-ppm	Sub-ppm	ppm	ppm
Analysis Time	Few minutes	> AAS	Few minutes	Few minutes	Few minutes	Few minutes to several days
Interferences	Chemical, ionization	Chemical, physical	Spectral, matrix	Molecular, matrix	Matrix	Matrix, spectral
Sample Volume	Few mL	μL	Few mL	Few mL	Few mL	Few mL
Precision, %	1 to 2	5	5	5	1 to 2	1-2
Usage in Oil Industry	Wide	Limited	Wide	R&D laboratories	Wide	Limited
Speciation	No	No	No	Yes	No	No

TABLE 21—Spectroscopic Methods Versus an Ideal Method of Analysis

Criteria	Ideal Method	AAS	GFAAS	ICP-AES	ICP-MS	XRF	NAA
Sensitivity	High	Good	High	High	High	High	High
Dynamic Range	Broad	Narrow	Narrow	Broad	Broad	Broad	Broad
Precision	High	High	< AAS	< AAS	< AAS	High	High
Interferences	None	Some	Some	Few	Few	Some	Some
Sample Preparation	None	Some	Some	Some	Some	None	None
Price	Low	X	X+	5 X	10 X	X – 10X	100 X
Maintenance	Low	Low	Low	High	High	Moderate	High
Applications						Extensive	Extensive
Moderate						Extensive	Few
Extensive						Extensive	
Elements	All	Most	Most	Most	All	Most	Most
Multielement Capability	Yes	No	No	Yes	Yes	Yes	Yes
Turnaround	Fast	5 min	10 min	5 min	5 min	10 min	Min – days
Nondestructive	Yes	No	No	No	No	Yes	Yes

CONCLUSIONS

AAS, GFAAS, ICP-AES, ICP-MS, XRF, and NAA are all mature spectroscopic techniques widely used for the determination of trace elements in crude oils. Table 20 summarizes the advantages and drawbacks of these techniques. For lower cost, AAS and GFAAS are well suited. For best sensitivities, all except AAS are suitable. For multielement capability and wide dynamic range, ICP-AES and ICP-MS are unsurpassed. Speciation of inorganic molecules can only be done with ICP-MS. XRF may do a lesser number of elements than AAS or ICP-AES, but ease of operation and precision of the latter technique are superior to that of former ones. Because of the necessity of a nuclear reactor, NAA has not found much favor in industrial laboratories.

Table 21 compares the properties of each spectroscopic method against an "ideal" method. The properties attributed for an "ideal" method may be arguable. But it has to be admitted that most of them come close to meeting the ideal. XRF may be applicable to fewer elements than AAS or ICP-AES but ease of operation and precision of the former technique are superior. Thus, atomic spectroscopic methods, in particular, AAS, ICP-AES, and XRF, remain the methods of choice in the industry for trace element analysis of crude oil and other petroleum products.

References

[1] Giles, H. N., "Crude Oils," *Significance of Tests for Petroleum Products*, 7th ed., S. J. Rand, Ed., ASTM Manual 1, ASTM International Inc., West Conshohocken, PA, 2003.

[2] Magee, E. M., Hall, H. J. and Varga, G. M., "Potential Pollutants in Fossil Fuels," EPA R2-73-249, National Technical Information Service Publication PB 225-039, Washington, DC, 1973.

[3] Bailey, E. H., Snavely, P. D. and White D. E., USGS Paper 424D, U.S. Geological Survey, Reston, VA, 1961.

[4] Yen, T. F., Ed. *Role of Trace Elements in Petroleum*, Ann Arbor Science Publishers, Ann Arbor, MI, 1975.

[5] Filby, R. H. and Van Berkel, G. J., *Metal Complexes in Fossil Fuels*, R. H. Filby, and J. F. Branthaver, Eds., ACS Symposium Series. No. 344, American Chemical Society, Washington, D. C., 1987.

[6] Filby, R. H., "Elemental Analysis of Crude Oils Using Neutron Activation Analysis," Preprint No. 630, Petroleum Division, American Chemical Society, Washington, DC, 1973.

[7] Valkovic, V., *Trace Elements in Petroleum*, The Petroleum Publishing Co., Tulsa, OK, 1978.

[8] Sheldon, J., Lee, Y. I., Noble, C. O., Beck, J. N. and Profit, C. E., "Determination of Selected Metals by Simultaneous Flame AAS in Burned and Unburned Venezuelan Crude Oil," *Amer. Environ. Lab.,* Vol. 10, No. 6, 1998, p. 4.

[9] Arakting, Y. E., Chakrabarti, C. L. and Maines, I. S., "Determination of Cobalt, Magnesium, Sodium, Tin, Cadmium, Zinc, and Aluminum in Crude Oils," *Spectroscopy Lett.*, Vol. 7, 1974, p. 97.

[10] Lepri, F. G., Welz, B., Borges, D. L. G., Vale, M. G. R. and Heitmann, U., "Speciation Analysis of Volatile and Non-Volatile Vanadium Compounds in Brazilian Crude Oils Using High-Resolution Continuum Source Graphite Furnace Atomic Absorption Spectrometry," *Anal. Chim. Acta*, Vol. 558, 2006, pp. 195–200.

[11] Kowaleswska, Z., Bulska, E. and Hulanicki, A., "Organic Palladium and Palladium-Magnesium Chemical Modifiers in Direct Determination of Lead in Fractions from Distillation of Crude Oil by Electrothermal Atomic Absorption Analysis," *Spectrochim. Acta Part B,* Vol. 54, 1999, pp. 835–843.

[12] Gonzales, M. and Lynch, A. W., "Methods Development for Trace Metal Characterization of Crude Oil by ICP-AES," *Modern Instrumental Methods of Elemental Analysis of Petroleum Products and Lubricants, ASTM STP 1109*, R. A. Nadkarni, Ed., ASTM International, West Conshohocken, PA, 1991.

[13] Al-Awaidan, H. M., "Neutron Activation Analysis of Iraqui Crude Oils," *Anal. Lett.,* Vol. 21, 1988, p. 1487.

[14] McElroy, F. C., Mennito, A., Debrah, E. and Thomas, R., "Uses and Applications of ICP-MS in the Petrochemical Industry," *Spectroscopy,* Vol. 13, No. 2, 1998, pp. 42–53.

[15] Dreyfus, S., Pecheyran, C., Mangier, C., Prinzhofer, A., Lienemann, C. P. and Donard, O. F. X., "Direct Trace and Ultra-Trace Metals Determination in Crude Oils and Fractions by ICP-MS," *ASTM STP 1468*, ASTM International, West Conshohocken, PA, 2005, pp. 51–58.

[16] Duyck, C., Miekeley, N., Porto, S., Carmem, L. and Szatmari, P., "Trace Element Determination in Crude Oils and its Fractions by ICP-MS Using Ultrasonic Nebulization of Toluene Solutions," *Spectrochim. Acta,* Vol. 57B, No. 12, 2002, pp. 1979–1990.

[17] Dreyfus, S., Pecheyran, C., Lienemann, C. P., Magnier, C, Prinzhofer, A. and Donard, O. F. X., "Determination of Lead Isotope Ratios in Crude Oils with Q-ICP/MS," *J. Anal. At. Spectrom.,* Vol. 22, No. 4, 2007, pp. 351–360.

[18] Dreyfus, S., Pecheyran, C., Lienemann, C. P., Magnier, C., Prinzhofer, A. and Donard, O. F. X., "Determination of Trace Metals in Crude Oil by ICP-MS with Micro-Emulsion Sample Introduction," *Anal. Chem.,* Vol. 63, No. 15, 1991, pp. 1594–1599.

[19] Al-Swaidan, H. M., "Microemulsion Determination of Lead and Cadmium in Saudi Arabian Petroleum Products by ICP-MS," *Sci. Total Environ.,* Vol. 145, No. 1–2, 1994, pp. 157–161.

[20] Akinlua, A., Torto, N. and Ajayi, T. R., "Determination of Rare Earth Elements in Niger Delta Crude Oils by ICP-MS," *Fuel,* Vol. 87, No. 8-9, 2008, pp. 1469–1477.

[21] Yasnygina, T. A., Malykh, Yu. M., Rasskazov, S. V., Primina, S. P., Zemskaya, T. I. and Khlystov, O. M., "ICP-MS Determination of Rare Earth and Other Metals in Baikal Crude Oil: Comparison with Crude Oils in Siberia and the Russian Far East," *Dokl. Earth Sci.,* Vol. 41–198, 2006, pp. 1237–1240.

[22] Hwang, J. D., Horton, M. and Leong, D., "Elemental Analysis of Fuels and Lubricants: Recent Advances and Future Prospects," *The Use of Microwave Digestion and ICP-MS to Determine Elements in Petroleum Samples, ASTM STP 1468*, ASTM International, West Conshohocken, PA, 2005, pp. 33–41.

[23] Xie, H., Li, L., Hu, H. and Li, A., "Determination of Trace Metal Elements in Crude Oil by ICP-MS," *Shiyou Xuebao, Shiyou Jiagong,* Vol. 21, No. 4, 2005, pp. 86–90.

[24] Nakamoto, Y. and Tomiyama, T., "Highly Sensitive Determination of Sb and Se in Crude Oils by Oxygen Bomb Combustion/ICP-MS," *Bunseki Kagaku*, Vol. 46, No. 8, 1997, pp. 665–668.

[25] Botto, R. I., "Analysis of Heavy Oils for Trace Metals Using Plasma Spectrochemistry," *Winter Conf. on Plasma Spectrochem.,* San Diego, CA, paper S02, 2008.

[26] Kelly, W. R., Long, S. E. and Mann, J. L., "Determination of Mercury in SRM Crude Oils and Refined Products by ID-CV-ICP-MS Using Closed System Combustion," *Anal. Bioanal. Chem.,* Vol. 376, No. 5, 2003, pp. 753–758.

[27] Osborne, S. P., "Quantitation of Mercury in Petroleum by ETV-ICP-MS," *Appl. Spectrosc.,* Vol. 44, No. 6, 1990, pp. 1044–1046.

[28] Duyck, C., Miekeley, N., Porto, S., Carmem, L., Aucelio, R. Q., Campos, R. C., Grinberg, P., Brandao, P. and Geisamanda, P., "Determination of Trace Elements in Crude Oils and its Heavy Fractions by Atomic Spectrometry," *Spectrochim. Acta,* Vol. 62B, 2007, pp. 939–951.

[29] Al-Shahristani, H. and Al-Atyia, M. J., "Analysis of Crude Oils Using Neutron Activation Analysis," *J. Radioanal. Chem.,* Vol. 14, 1973, p. 401.

[30] Guinn, V. P., Lukens, H. R. and Steele, E. L., "The Role of Small Accelerators and Nuclear Reactors in Neutron Activation Analysis of Petroleum," *Proc. Amer. Petrol. Institute,* Vol. 44-III, 1964, p. 234.

[31] Shah, K. R., Filby, R. H. and Haller, W. A., "Trace Element Analysis of Crude Oils Using Instrumental Neutron Activation Analysis," *J. Radioanal. Chem.,* Vol. 6, 1970, p. 413.

[32] Lukens, H. R., Company Report Gilf-RT-A-10973, Gulf Research, San Diego, CA, 1972.

[33] Veal, D. J., "Nondestructive Activation Analysis of Crude Oils for Arsenic to One ppb and the Simultaneous Determination of Five Other Trace Elements," *Anal. Chem.,* Vol. 38, 1966, p. 1080.

[34] Filby, R. H. and Shah, K. R., "Mode of Occurrence of Trace Elements in Petroleum, and Relationship to Oil-Spill Identification Methods," in *Nuclear Methods in Environmental Research*, University of Missouri, Columbia, MO, 1971, p. 86.

[35] Mandle, J. W., Reed, J. H. and Moler, R. B., "Oil Slick Identification Utilizing Charged Particle Activation Techniques," in *Nuclear Methods in Environmental Research*, University of Missouri, Columbia, MO, 1971, p. 111.

[36] ASTM RR-D02-1622, "Interlaboratory Study for Determination of Sulfur in Petroleum Products Using D2622 Test Method."

[37] ASTM RR-DO2-1635, "Interlaboratory Study for Determination of Sulfur in Petroleum Products Using D4294 Test Method."

24

Spectroscopic Analysis of Biofuels and Biolubes

R. A. Kishore Nadkarni[1]

INTRODUCTION

As crude oil stocks around the world slowly dwindle and the prices of crude oil and gasoline at the pump skyrocket, serious attention is being given to developing alternative fuels for the internal combustion engines. The more prominent among these alternative fuels is one derived from biomass, which a majority of oil-consuming countries have an abundance of. Whether biofuels will truly deliver the consumers from dependence on foreign oils is a matter of debate. The United States went through a similar scenario in the 1980s after Arab oil embargos, when concentrated efforts were dedicated by all major oil companies and nations to produce synthetic oil from coal and oil shale. Although technically successful, those efforts came to nothing when the crude oil price tumbled to about $5 a barrel in 1985 and all research and development efforts on synthetic fuels were abandoned. But at least at the moment, with encouragement from state and federal governments, a big push is on the way to commercialize biofuels. Worldwide investment in biofuels rose from $5 billion in 1995 to $38 billion in 2005 and is expected to top $100 billion by 2010. ASTM International is working toward standardizing or developing test methods for the characterization of these biofuels and biolubes.

President George W. Bush signed the Energy Policy Act of 2005 (PL 109-58), which set minimum use requirements for renewable fuels such as ethanol and biodiesel. It established a renewable fuels standard (RFS) and mandated 4 billion gallons of renewable fuels (ethanol and biodiesel) in 2006, increasing to 7.5 billion gallons by 2012. The U.S. Environmental Protection Agency (EPA) issued a final rule implementing the RFS on May 1, 2007. President Bush has called for the scope of the RFS to be expanded to an alternative fuels standard (AFS) to include not only corn-based and cellulose-based ethanol and biodiesel but also methanol, butanol, and other alternative fuels. It is likely that at least 15 % of the president's target for a 10 % reduction in the U.S. gasoline usage by 2017 will be met by the AFS. An energy bill signed by President Bush in December 2007 required 500 million gallons of biomass-based diesels to be introduced into the diesel pool by 2009, with a phased increase to 1 billion gallons by 2012 and 36 billion gallons by 2022.

The original RFS targets are surpassed by increased use of biofuels. Ethanol is currently blended into 46 % of the nation's gasoline. In his January 23, 2007 State of the Union address, President Bush called for a 20 % reduction in gasoline consumption by 2017 (the so-called "twenty in ten" plan). This plan would increase the use of renewable and alternative fuels to 35 billion gallons by 2017, nearly five times the 2012 level required under the Energy Policy Act

[1] *Millennium Analytics, Inc., East Brunswick, NJ*

of 2005. Several bills have been introduced in the U.S. Congress to increase biofuels production and consumption. Several states and even some cities have adopted ethanol or biodiesel mandates. State and federal governments are adopting ASTM specifications and standards for these biofuels. By late 2005, U.S. ethanol production increased to 5 billion gallons, a 1 billion gallon increase since the beginning of the year. As ethanol capacity nears 12 billion gallons, the "food-versus-fuel" debate has intensified.

There were about 6 million E85 capable vehicles in the United States, and original equipment manufacturers (OEMs) have announced that by the end of 2012, about 50 % of U.S. automobiles will be flex-fuels E85 capable. To bring production more in line with capacity and biofuels targets, the ethanol industry would like to see the current 10 % limit in gasoline (for non-E85 vehicles) doubled to 20 % for all cars and trucks, a suggestion that U.S. OEMs strongly oppose [1].

SOURCES OF BIOFUELS

The majority of ethanol in the United States is made from corn, but it can also be produced from a variety of other feedstocks. Ethanol can be produced by a dry mill process or a wet mill process. The first one is the most widely used process, and in it the starch portion of the corn is fermented into sugar and then distilled into ethanol. For producing biodiesels, a fat or oil is reacted with an alcohol (e.g., methanol) in the presence of a catalyst to produce glycerin and methyl esters, or biodiesel. The methanol is charged in excess to help in quick conversion, and is recovered for reuse. The catalyst used in the process is usually sodium or potassium hydroxides which are pre-mixed with methanol [2].

The term biodiesel refers to mono-alkyl esters of fatty acids, typically fatty acids methyl esters that are produced from vegetable oil, animal fat, or waste cooking oil in a chemical reaction known as trans-esterification. In the United States, soybean oil is the major feedstock; rapeseed oil is used in Europe and palm oil is a large player in other regions of the world. Although there are some users of 100 % biodiesel, or B100, as a fuel, the properties of B100 are considerably different from those of conventional diesel fuel or heating oil. It is not clear that diesel engines or boilers are fully compatible with B100. Therefore, it is much more common to use biodiesel as a blend with petroleum diesel at levels ranging from 2 % (B2) to 20 % (B20) by volume [3]. Biodiesel is produced from a variety of vegetable oils and animal fats, with soy being the predominant source in the United States. However, as demand increases, it is likely that a variety of other sources, including canola, palm, jatropha, and used kitchen oil, will be used. This brings increased quality concerns over parameters including oxidative stability, low temperature handling and operability, resistance to phase separation, batch-to-batch consistency, biological growth, and additive response [1].

ECONOMICS OF BIOFUELS USAGE

Some critics believe that replacing the conventional gasoline with ethanol-based fuels is uneconomic and not sustainable in practice. Many doubt that ethanol will ever take hold in a big way because it costs the same as gasoline on a per gallon basis but delivers only about two thirds of the energy. Even if the United States produces 9 billion gallons in a year or two from now, the United States uses 140 billion gallons of gasoline per year. Thus, nine billion gallons of

ethanol will replace only about 6 billion gallons of gasoline or about 4.3 % of the U.S. total consumption. Production of that much ethanol, however, would require more than 20 million acres of corn or about one fourth of the U.S. total corn acreage. This will increase the corn prices, used for human and animal consumption, in turn increasing the meat and other product prices for the consumers [4]. The scenario can dramatically worsen if the current federal subsidy of 51 cents per gallon of ethanol is reduced or eliminated. Soaring corn prices have sparked tortilla riots in Mexico City, and skyrocketing flour prices have made that staple of diet impossible to purchase for many poor Pakistanis.

With 113 ethanol plants currently operating and 78 more under construction in the United States producing ethanol from corn requires expending energy–plowing, planting, fertilizing, and harvesting–all require machinery that burns fossil fuels. Because ethanol is more corrosive than gasoline, it cannot be pumped through relatively efficient existing pipelines, but must be transported by rail or tanker trucks. In the end, it is estimated that it takes the energy equivalent of 3 gallons of ethanol to produce 4 gallons of it. The environmental benefits of corn ethanol are also limited. In 2006 the ethanol production used 12 % of the U.S. corn harvest, but it replaced only 2.8 % of the nation's gasoline consumption. One alternative to corn ethanol is cellulosic ethanol from a wide variety of plants such as poplar trees, switchgrass, corn stalks, municipal waste, and used cooking oil. But it may take 10 to 15 years before cellulosic ethanol becomes competitive [5]. Perhaps sugar cane used in Brazil is a better choice instead of corn for ethanol production. Twenty-eight percent of the cars in Brazil run on ethanol produced from sugar cane.

In a recent lead article in *Time* magazine, Grunwald [6] discusses the environmental and economic implications of biofuels produced from corn, sugar cane, and soy beans. Using land to grow fuel leads to the destruction of forests, wetlands and grasslands that store enormous amounts of carbon. Indonesia and Malaysia have bulldozed and cleared large swaths of forests to plant palm oil trees for biodiesel. One fifth of the U.S. corn crop is diverted to more than 100 ethanol refineries. The increased demand has boosted the price of corn to record levels. Many U.S. soybean growers have switched to planting corn which is pricier, thus raising the prices of soybeans as supplies shrink. To meet global demands for soybeans, farmers in Brazil are expanding into fields previously used as cattle pasture lands. Sugarcane provides 45 % of Brazil's fuels but uses only 1% of its arable land. Only sugarcane based ethanol is efficient enough to cut emissions by more than it takes to produce the fuel. All cars in that country are able to run on ethanol.

In the United States, Iowa is the heart of biofuel production via corn, with 53,000 jobs and $1.8 billion income dependent on this industry. In 2007, Iowa produced nearly 2 billion gallons of ethanol, 30% of the U.S. total. In 2007 fewer than 2 % of U.S. gas stations offered ethanol, and the country produced 7 billion gallons of biofuel, which cost U.S. taxpayers at least $8 billion in subsidies. The United States leads the world in corn and soybean production, but even if 100 % of both crops were turned into fuel, it would be enough to offset just 20 % of the on-road fuel consumption [6].

It is quite possible, given the political and economic climate in the United States, that the above discussion about the economic feasibility of biofuels can change in the future. Considerable changes in legislation over the next few

years will impact this industry. The current downturn in the stock markets and worldwide economy has probably already impacted some of the above statements about demand and supply. None of the economic aspects, however, affect the analytical methods discussed here.

BIOFUELS TEST METHODS

Unfortunately, many of the test methods required in ASTM specification D4814, D4806, D5798, or D6751 were written before oxygenates were introduced in the fuels. Thus, certain test methods either do not address or are unclear as to whether they are applicable to ethanol and at what concentrations. A majority of the test methods quoted in these biofuels specifications will have to be updated in their scopes and precision statements to cover biofuels and biolubes. This will involve conducting several interlaboratory studies (ILS) to arrive at the precision of these methods and to evaluate if modifications to the original methods are necessary. A suggested plan (which has not yet been launched) is to carry out a major ILS covering all appropriate test methods at all appropriate alcohol concentration levels. That way in one attempt all necessary data to update the test methods will become available.

Additionally, some of the test methods required in the fuel specifications are outdated or are not used in the laboratories in the industry today. Some are not under the jurisdiction of ASTM Committee D02 on Petroleum Products and Lubricants. These ancient methods need to be replaced with newly developed methods wherever appropriate. Examples of this situation include replacing old methods for chloride, phosphorus, lead and copper with modern methods using ICP-AES and ion chromatography.

Specifications governing biofuels are summarized in Table 1. Only the parameters determined by spectroscopic methods are excerpted from the ASTM specifications here.

Standard D4814 specification covers automotive fuels used in spark ignition engines. Examples of these are gasolines and their blends with oxygenates including gasoline containing up to 10 v % ethanol (E10).

Standard D4806 specification covers nominally anhydrous denatured fuel ethanol intended to be blended with gasoline at 1 to 10 v % ethanol for use as spark ignition engine fuel.

Standard D5798 specification covers nominally 75 to 85 v % denatured fuel ethanol and 15 to 25 additional v % hydrocarbons for use in ground vehicles with automotive spark ignition engines (E85).

Standard D6751 specification covers biodiesel B100 grades S15 and S500 for use as a blend component with diesel fuel oils defined by Specification D 975 Grade 1-D, 2-D, and low sulfur 1-D and 2-D.

TEST METHODOLOGY

Discussion on the spectroscopic methods listed in biofuel specifications and experience on them is given here.

Copper D1688A–This is an atomic absorption spectrometry method used for trace amounts of copper in aqueous solutions. A better choice for this would be the multi-element technique such as ICP-AES. As a matter of fact the copper level in biofuel is almost below the detection limit; in the ETOH 0708 crosscheck no copper could be detected using the test method D1688A. Thus,

TABLE 1—Spectroscopic Tests Required in Biofuels Specifications					
Analysis	**ASTM Test Method**	**D4806-07 (Denatured Fuel Ethanol)**	**D4814-06 (Gasoline)**	**D5798-07 (Ethanol Ed 75-85)**	**D6751-07a (B100 Biodiesel Fuel Blend)**
Copper, mg/kg	D1688A[a]	0.1 mg/kg max.	...	0.07 mg/kg max.	...
Sulfur, mg/kg	D2622 or D5453[a]	30 mg/kg max.	350 mg/kg max for unleaded; 1500 mg/kg max for leaded.	210 – 300 mg/kg	0.0015 to 0.05 max.
Sulfate, mg/kg	D7319 or D7328	4 mg/kg max.	...	...	...
Ethanol, v%	D5501	92.1 min.	70 – 79	...	...
Inorganic Chloride, mg/kg	D512[a]	40 mg/kg max.	...	1 mg/kg	...
Lead, mg/kg	D3341	...	0.013 in unleaded; 1.1 in leaded	...	...
	D5059, or D3237[a]				
Oxygenates	D4815	...	...	...	...
	D5845 or D5599				
Phosphorus, m%	D4951[a]	...	...	...	0.001 max.
Calcium + Magnesium, mg/kg	EN 14538 or UOP 389[a]	...	...	...	5 max.
Sodium + Potassium, mg/kg	EN 14538 or UOP 391[a]	...	...	...	5 max.

[a]Alternative test methods proposed for these tests include a new ICP-AES method for copper, lead, and phosphorus as well as Ca + Mg + Na + K, additional test D7039 for sulfur, and inorganic chloride by D7319 or D7328.

the specified method may not be sensitive enough for this analysis. There is little point in keeping this requirement in the specification. It is apparently a carryover from earlier days when copper pipes were used in synthesis, which is not the case now.

Phosphorus D4951–This is an ICP-AES method used for lubricating additives and oils. As such it is not appropriate for use in analyzing aqueous ethanol samples. Nor is its precision for such matrices known at present.

(Ca + Mg) + (Na + K)–EN 14538–This is an ICP-AES method, not widely used in the United States at present. The method determines these four elements in fatty acid methyl ester (FAME) at levels of about 1 to 10 mg/kg. The samples are diluted in 1:1 ratio with kerosine and analyzed by ICP-AES. The sums of calcium plus magnesium and sodium plus potassium are reported. The following wavelengths are recommended:

Calcium	422.673; 317.933; 393.366; or 396.847 nm
Magnesium	279.553 or 285.213 nm
Sodium	588.995 or 589.592 nm
Potassium	769.897 or 766.490 nm

The following precisions have been obtained by this test method:

Analysis	Repeatability	Reproducibility
Ca + Mg	0.023 X + 0.271	0.149 X + 1.186
Na + K	0.020 X + 0.193	0.191 X + 0.941
Where X is the average of two determinations.		

To replace the currently specified methods for metals analysis (calcium, phosphorus, copper, magnesium, potassium, and sodium) a new method has been drafted that uses aqueous medium ICP-AES after conversion of the organic matrix into an acidic aqueous solution. However, an ILS needs to be completed before the proposed test method can be used in the specifications.

Sulfur D2622–This standard is widely used in the oil industry for sulfur determination in a variety of matrices, and is suitable for biofuels analysis if proper precautions are taken to eliminate the interferences from the presence of oxygenates and different carbon/hydrogen ratios in the sample and standard, problems inherent in the XRF technology.

The method uses a wavelength dispersive X-ray fluorescence spectrometer equipped for X-ray detection in the wavelength range from about 0.52 nm to about 0.55 nm. Usually, X-ray tubes with anodes made up of rhodium, chromium, or scandium are used although other anodes can be used. Calibration standards made from mass dilution of certified di-n-butyl sulfide with sulfur-free white oil or other suitable base material are used. Alternate calibration standards can also be made from mixing of certified reference materials or by mass serial dilution of polysulfide oils with sulfur-free white oil.

This method is applicable to liquid petroleum products such as diesel fuel, jet fuel, kerosine, other distillate oils, naphtha, residual oil, lubricating base oil, hydraulic oil, crude oil, unleaded gasoline, gasohol, and biodiesel. The range of this test method is between the PLOQ (pooled limit of quantitation as defined in ASTM D6259 standard) of 3 mg/kg total sulfur and at least up to 4.6 m % total sulfur. Samples containing more than 4.6 m % sulfur can be diluted to bring the sulfur concentration of the diluted material within the scope of this method. The samples that are diluted can have higher errors than indicated precision of undiluted samples. Volatile samples (such as high vapor pressure gasolines or light hydrocarbons) may also not meet the precision stated in the method because of the selective loss of light materials during the analysis. A fundamental assumption of this test method is that the calibration standard and the sample matrices are well matched, or that the matrix differences are accounted for. Matrix mismatches can be caused by carbon/hydrogen ratio differences between samples and standards, or by the presence of other interfering heteroatoms or species. The values of the limits of quantitation and method precision for a specific laboratory's instrument depends on the instrument source power (low or high power), sample type, and the practice established by the laboratory to perform the method.

In this method, a sample is placed in the X-ray beam of the XRF instrument, and the peak intensity of the sulfur K alpha line at 0.5373 nm is measured. The background intensity measured at a recommended wavelength of 0.5190 nm (0.5437 nm for a rhodium target tube) is subtracted from the peak intensity. The resultant net counting rate is then compared to a previously prepared calibration curve or equation to obtain the concentration of sulfur.

Although the equipment for this method tends to be more expensive than that required for alternative test methods, such as ASTM D4294 ED-XRF method, this method provides a rapid and precise measurement of total sulfur in a variety of petroleum products with a minimum of sample preparation. A typical analysis time is 1 to 2 minutes per sample.

Interferences—When the element composition (excluding sulfur) of samples differs significantly from the standards, errors in the sulfur determination can result. Differences in the carbon/hydrogen ratio of samples and calibration standards introduce errors in the determination. Some other interferences and their concentration in m % tolerated include:

Phosphorus	0.3	Zinc	0.6	Barium	0.8	Lead	0.9
Calcium	1	Chlorine	3	Oxygen	2.8	FAME	25
Ethanol	8.6	Methanol	6				

One way of minimizing or eliminating such interferences is to dilute the sample with blank sulfur solvent to reduce the interferent concentration below the values given above to mitigate the effect of interference.

Fuels containing large amounts of ethanol or methanol have a high oxygen content leading to significant absorption of sulfur K alpha radiation and low

sulfur results. Such fuels can, however, be analyzed using this test method provided either that correction factors are applied to the results (when calibrating with white oils) or that the calibration standards are prepared to match the matrix of the sample. In general, petroleum products with compositions that vary from white oils can be analyzed with standards made from base materials that are of the same or similar composition. Thus, a gasoline may be mimicked by mixing *iso*-octane and toluene in a ratio that approximates the expected aromatic content of the samples to be analyzed. Standards made from such simulated gasoline can produce results that are more accurate than the results obtained using white oil standards.

In a recently completed ILS to reevaluate test method D2622 for determination of sulfur in fuels, one sample each of B5, B100 biodiesels, E85 gasohol, gasoline with 13 % ETBE, and gasoline with 5 % ethanol were analyzed with satisfactory results. These samples contained sulfur levels between 18 and 232 mg/kg [7]. An earlier study, conducted in 2002, also included two biodiesels and one soy biodiesel that were analyzed by various test methods for sulfur [8]. Both these studies clearly showed that with proper interference calibration, test method D2622 is capable of determining sulfur in biofuels.

Sulfur D5453–This is one of the widely used techniques for low levels of sulfur determination in a variety of petroleum products. It is based on oxidative combustion at 1100°C of the sample in an oxygen stream which converts sulfur compounds to SO_2 gas which is excited to higher state with ultraviolet light. When the excited molecule comes back to normal state the light emitted is measured with a photomultiplier tube. The hydrocarbon sample is either directly injected or placed in a sample boat, and subjected to high temperature combustion in an oxygen rich environment. Water produced in the sample combustion is removed and the sample combustion gases are then exposed to ultraviolet light. The SO_2 absorbs the energy from the UV light and is converted to excited SO_2*. The fluorescence emitted from the excited SO_2* molecule as it returns to a stable state, SO_2, is detected by a photomultiplier tube and the resulting signal is a measure of the sulfur present in the sample.

$$R - S + O_2@100^{\circ}C \rightarrow SO_2 + \text{combustion products}$$
$$SO_2 + hv \rightarrow SO_2 + hv'$$

Its range of analysis is from low ppb to 40 % of sulfur. Typical sample size used is 1 to 20 μL and a typical analysis time is less than a minute. Liquid hydrocarbons boiling in the range from approximately 25 to 400°C, and with viscosities between approximately 0.2 and 20 cSt at room temperature can be analyzed by this method. These products include naphthas, distillates, engine oils, ethanol, FAME, and engine fuel such as gasoline, oxygenate enriched gasoline, E85, M85, RFG, diesel, biodiesel, and jet fuel. Samples should contain less than 0.35 m % of halogens in them. A number of studies have been conducted in ASTM for determining the precision of various matrices using this method.

In a separate study, several organic compounds containing sulfur-oxygen bonds were analyzed at about 100 mg/kg sulfur concentration in aqueous solution, and analyzed in five replicates. Results and recoveries are reported in Table 2 [9].

TABLE 2—Recovery of S-O Compounds			
Compound	**Expected Concentration (ppm)**	**Observed Concentration (ppm)**	**Recovery (%)**
2-Thiophene carboxylic acid	125	110	88
Sodium sulfate	105	99	94
Benzene sulfinic acid	124	110	89
2-Methyl-2-propene-1-sulfonic acid	115	113	98
Benzene sulfonic acid	108	86	80

Separately sulfonate compounds were studied for their recovery in a hydrocarbon solution prepared in iso-propyl alcohol and *iso*-octane using dibenzothiophene in iso-octane as standard. The results in Table 3 are essentially identical to the results obtained in aqueous solutions, in that about 80 % of the sulfur is recovered [9].

In another study, sulfur was determined in ASTM Interlaboratory Crosscheck Program (ILCP) sample of reformulated gasoline (RFG) 0607 blended with 0 to 90 % of varying amounts of ethanol. The data show close agreement between the average measured and expected sulfur values.

Sulfur D7039–This recent and popular method determines sulfur in gasolines, diesels, and refinery process streams used to blend gasolines and diesels, at concentrations from 2 to 500 mg/kg. Samples above this level may be analyzed after dilution with sulfur-free appropriate solvent. A monochromatic X-ray beam with a wavelength suitable to excite the K-shell electrons of sulfur is focused onto a sample contained in a sample cell. The fluorescent K alpha radiation at 0.5373 nm emitted by sulfur is collected by a fixed monochromator (analyzer). The intensity (count rate) of the sulfur X-rays is measured using a suitable detector and converted to the sulfur concentration using a calibration equation. Excitation by monochromatic X-rays reduces background, simplifies matrix correction, and increases the signal to background ratio compared to polychromatic excitation used in conventional WD-XRF techniques.

Interferences–When the elemental composition of the samples differ significantly from the calibration standards used to prepare the calibration curve, biased results can occur. The only important elements contributing to bias

TABLE 3—Sulfonate Recovery Using D5453 Method			
Compound	**Expected Concentration (ppm)**	**Observed Concentration (ppm)**	**Recovery (%)**
Dodecylbenzenesulfonate	10.1	7.9	78
Dodecylbenzenesulfonate	25.3	19.2	76
Dodecylbenzenesulfonate	50.4	38.3	76

TABLE 4—Sulfur Determination in Gasoline/Ethanol Mixtures Using Test Method D5453

% ETOH	Average Measured Sulfur, mg/kg	Expected Sulfur Value, mg/kg
0	33.7	
2	33.4	33.0
5	32.5	32.0
10	30.6	30.3
20	27.9	27.0
30	24.7	23.6
40	21.4	20.2
50	18.3	16.9
60	15.2	13.5
70	11.5	10.1
80	9.1	6.7
90	5.7	3.4
100	3.4	0.0

resulting from differences in the matrixes of calibrants and test samples are hydrogen, carbon, and oxygen. A matrix correction factor is used to correct this bias. When the calculated correction factor C is within 0.98 to 1.04, no matrix correction is required. For most testing, matrix correction can be avoided with a proper choice of calibrants. Gasoline samples containing oxygenates may be analyzed with this test method if the matrix of the calibration standards is either matched to the sample matrices or a matrix correction given in the method is applied to the results. In a limited study conducted by Alberta Research Council in 2007, a sample of fuel ethanol was analyzed by 31 laboratories to obtain a value of 1.6879 ± 0.4837 mg/kg to demonstrate the ability of test method D7039 to analyze ethanol samples [10].

Precision of Sulfur Test Methods–Table 5 is based on the existing ILSs used in establishing the precision of these three test methods for determination of sulfur in petroleum products. A new ILS just for biofuels is planned; that time this information on precision of sulfur test methods may have to be revised.

Inorganic Chloride and Sulfate–Test methods D7319 and D7328 based on ion chromatography were developed specifically for biofuel application. The difference between the two ion chromatographic methods is that the first one is based on direct injection suppressed ion chromatography and the second one uses aqueous sample injection. The D7319 method is intended for ethanol samples that contain between 1 to 20 mg/kg total or potential inorganic sulfate and 1 to 50 mg/kg of inorganic chloride.

TABLE 5—Precision of Sulfur Test Methods

ASTM Test Method	Sulfur Concentration, mg/kg	Repeatability[a]	Reproducibility[a]
D2622-08	3 mg/kg – 4.6 m %	$0.1462\ X^{0.8015}$	$0.4273\ X^{0.8015}$
D5453-08a	$<$ 400 mg/kg $>$ 400 mg/kg	$0.1788\ X^{0.75}$ 0.02902 X	$0.5797\ X^{0.75}$ 0.1267 X
D7039-07-Gasoline-Diesel	$<$ 500 mg/kg 4 – 17 mg/kg 17 – 500 mg/kg	$0.555\ X^{0.5}$ $0.23\ X^{0.5}$ $0.55\ X^{0.5}$	N/A $0.5\ X^{0.5}$ N/A

[a]X is the average of two results.
N/A – Not available.

The D7328 method can measure between 0.55 and 20 mg/kg of total inorganic sulfate, 4 to 20 mg/kg of potential inorganic sulfate, and 0.75 to 50 mg/kg of total inorganic chloride.

In the D7319 method for the total sulfate and chloride, a small volume of an ethanol sample is directly injected into a suitable configured ion chromatograph in accordance with manufacturer's recommendations for this test method. For potential sulfate, 0.5 mL of 30 % hydrogen peroxide solution is added to 9.5 mL of the ethanol sample, and then injected into the ion chromatograph. Ions are separated based on their affinity for exchange sites of the resin with respect to the resin's affinity for the eluent. The suppressor increases the sensitivity of the test method by both increasing the conductivity of the analyte and decreasing the conductivity of the eluent. It also converts the eluent and analytes to corresponding hydrogen forms of anions. Anions are quantified by integrating their responses compared with an external calibration curve. The calibration standards are prepared in an aqueous matrix.

Interferences—These can be caused by substances with similar ion chromatographic retention times, especially if they are in high concentration compared to the analyte of interest. Sample dilution can be used to minimize or resolve most interference problems.

A water dip (system void or negative peak) can cause interference with some integrators. Usually for chloride and sulfate determinations, water dip should not be a problem since their peaks are far away from the water dip. Given the trace amounts of chloride and sulfate determined in this test method, interferences can be caused by contamination of glassware, eluent, reagents, etc. Hence, great care should be kept to ensure that the contamination is kept to a minimum.

Table 6 gives the precision for D7319 obtained during an ILS in 2006. Since there is no generally accepted reference material for this analysis, no statement regarding the bias of this method can be made.

In the D7328 method for total inorganic sulfate and chloride, a small volume of a sample is evaporated to dryness and reconstituted to the initial sample volume with deionized water, and injected into an ion chromatograph consisting of appropriate ion exchange columns, suppressor, and a conductivity detector. For potential sulfate, the dried residue is reconstituted with 0.90 % hydrogen peroxide solution in water, and injected into an ion chromatograph.

TABLE 6—Precision of Ion Chromatographic Method D7319			
Determination	**Mode**	**Repeatability[a]**	**Reproducibility[a]**
Chloride	–	$6.851^{-2}\ X^{0.7000}$	$0.4172\ X^{0.7000}$
Total Sulfate	Trichamber Suppression Regeneration	$8.604^{-2}\ X\ (X + 1.00^{-4})^{0.6175}$	$1.2160\ (X + 1.00^{-4})^{0.6175}$
Potential Sulfate	Trichamber Suppression Regeneration	$0.1266\ X^{0.6940}$	$0.9749\ X^{0.6940}$
Total Sulfate	Continuous Suppressor Membrane Regeneration	$0.2451\ (X + 1.00^{-4})^{0.6593}$	$1.6015\ (X + 1.00^{-4})^{0.6593}$
Potential Sulfate	Continuous Suppressor Membrane Regeneration	$0.2741\ X^{0.6897}$	$1.4334\ X^{0.6897}$
[a]X is the average of two determinations.			

The interferences are similar to those found in test method D7319. The following precision has been found based on an ILS conducted in 2006 (Table 7).

Similar methods for chloride and sulfate determinations can be found in Test Method D5827 for engine coolant and for ethanol in ISO/CEN 15492.

Since no generally accepted reference materials are available for this analysis, no statement regarding the bias of this test method can be made.

Ethanol—Methanol D5501–This test method covers the determination of ethanol content of denatured fuel ethanol by gas chromatography. Ethanol is determined from 93 to 97 mass %, and methanol from 0.1 to 0.6 mass %. The test method does identify and quantify methanol but does not purport to identify all individual components that make up the denaturant. Water cannot be measured by this test method, but can be measured by a procedure such as D1364. The result is used to correct the chromatographic values. This method is inappropriate for impurities that boil at temperatures above 225°C, or for impurities that cause poor or no response in a flame ionization detector, such as water.

In this method a fuel ethanol sample is injected into a gas chromatograph equipped with a methyl silicon bonded phase fused silica capillary column. Helium carrier gas transports the vaporized aliquot through the column where

TABLE 7—Precision of Ion Chromatographic Method D7328		
Analysis	**Repeatability[a]**	**Reproducibility[a]**
Total chloride	$0.02078\ (X + 10.0709)$	$0.1173\ (X + 10.0709)$
Total sulfate	$0.2319\ (X + 1.00^{-04})^{0.5000}$	$1.0963\ (X + 1.00^{-04})^{0.5000}$
Potential sulfate	$0.1763\ X^{0.4000}$	$1.0505\ X^{0.4000}$
[a]X is the average of two determinations.		

the compounds are separated. They are then detected by a flame ionization detector they elute from the column. The detector signal is processed by an electronic data acquisition system. The identification of all components is done by comparing their retention times with those of standards, and concentration is calculated by using normalized peak areas. No significant difference was found between the ethanol or methanol content obtained by this test method and the expected content based on their concentrations added to the samples. The precision of the method is as follows:

Component	Range	Repeatability	Reproducibility
Ethanol	93–97 m%	0.21	0.53
Methanol	0.01–0.6 m%	$0.01859 \times X^{0.5}$	$0.01172 \times X^{0.5}$

To replace the currently specified methods for metal analysis (copper, phosphorus, calcium, magnesium, potassium, and sodium) a new method has been drafted that uses aqueous medium ICP-AES. However, an ILS needs to be completed before the new method could be used in the specifications.

INTERLABORATORY CROSSCHECK PROGRAMS FOR BIOFUELS

Based on the heightened interest in standardized analysis of biofuels in the ethanol industry, ASTM Committee D02.CS 92 has offered two biofuels ILCPs to biofuels laboratories which need a statistical quality assurance program that will enable them to improve and maintain a high level of performance in

TABLE 8—Typical Spectroscopic Analysis of ILCP Biofuel Samples

Analysis	Test Method	ASTM BIOD0711	ASTM ETOH 0712
Phosphorus, mg/kg	D4951	N/D (25)	...
Sulfur, mg/kg	D5453	1.70 ± 0.62 (44)	3.49 ± 0.76 (23)
Ca/Mg, mg/kg	EN 14538	0.07 ± 0.07 (18)	...
Na/K, mg/kg	EN 14538	0.51 ± 0.54 (21)	...
Ethanol, v%	D5501	...	96.1 ± 0.45 (29)
Methanol, v%	D5501	...	0.011 ± 0.010 (22)
Inorganic chloride, mg/kg	D7319	...	0.03 ± 0.06 (6)
Inorganic chloride, mg/kg	D7328	...	0.03 ± 0.048 (2)
Inorganic sulfate, mg/kg	D7319	...	1.13 ± 0.27 (9)
Inorganic sulfate, mg/kg	D7328	...	0.895 ± 0.785 (4)

All results are expressed as robust mean ± robust standard deviation (number of results).
N/D: Not detected.

conducting routine ASTM specification tests. The program will enable the participating laboratories to compare their results with other program laboratories worldwide doing the same testing. The program helps a laboratory monitor its strengths and areas for improvement and demonstrate a laboratory's testing capability for regulatory purposes [11].

The two ILCP crosschecks for biodiesel and E85 ethanol are conducted three times a year each. Out of several tests offered on these products, results from the tests pertaining to spectroscopy are summarized in Table 8.

References

[1] "Understanding Clean Diesel and Biofuels," *Insight,* March 2008.

[2] "Biofuels Production," *NABL Advocate,* Spring 2007.

[3] McCormick, R. L. and Westbrook, S. R. "Biodiesel and Biodiesel Blends," *ASTM Standardization News,* 35(4), 1–3 (April 2007).

[4] Johnson, J., "Ethanol: Is it Worth it?" *Chemical and Engineering News,* pp. 19–21, January 1, 2007.

[5] Crenson, M., "The Truth about Ethanol," *Newark Star Ledger,* March 17, 2007.

[6] Grunwald, M., "The Clean Energy Scam," *Time*, pp. 40–45, April 7, 2008.

[7] Dahnke, K., ASTM RR-DO2-1622, 2007.

[8] Nadkarni, R. A. and Bly, K. J., ASTM RR-DO2-1547, 2003.

[9] Nadkarni, R. A. and Crnko, J., ASTM RR-DO2-1633, 2007.

[10] Wispenski, D., "Statistical Comparison of Sulfur in Motor Gasoline, Aviation Gasoline and Diesel using ASTM D5453 and D7039," Alberta Research Council Project GO-2005-1026.

[11] Nadkarni, R. A. and Bover, W. J. "Bias Management and Continuous Quality Improvements through Committee D02's Proficiency Testing," *ASTM Standardization News,* pp. 36–40, June 2004.

Index

A

B

C

D

E

F

G

H

I

J

K

L

M

N

O

P

Q

R

S

T

Z

About the Author

DR. R. A. KISHORE NADKARNI received his Ph.D. in analytical Chemistry at the University of Bombay. Since then he has worked as a Research Associate at the University of Kentucky, Manager of the Materials Science Center Analytical Facility at Cornell University, and analytical Leader in the ExxonMobil Company. In his last position he was responsible for technical quality management of the Paramis Division's global plant laboratories.

He has authored over 100 technical publications in the area of analytical chemistry and quality management. He is a member of the American Chemical Society, ASTM, and the American Society for Quality. He is very active in ASTM and ISO in the petroleum products and lubricant field, holding the position of immediate Past Chairman of ISO/TC28, Chairman of ASTM's D02.SC3 on Elemental Analysis, Vice-Chairman of D02.CS 92 on Interlaboratory Cross-Check Programs, D02.CS 94 on Quality and Statistics, and Editor of the D02.CS.92 Newsletter.

He has received the Award for Appreciation (1991) and Awards for Excellence (1998 and 1999) from ASTM's D02 Committee for his contribution to the oil industry, the Award of Merit (2005), and the George Dyroff Award of Honorary D02 membership (2006).

www.astm.org

ISBN 978-0-8031-7020-9
Stock #: MONO9